Mechanisms of Acute Inflammatory Control by Phagocytes

by

Aja M. Rieger

A thesis submitted in partial fulfillment of the requirements for the degree of

Doctor of Philosophy

in
Physiology, Cell and Developmental Biology

Department of Biological Sciences
University of Alberta

© Aja M. Rieger, 2014

Abstract

Phagocytosis is an important, evolutionarily conserved mechanism integral to immune defense and homeostasis. Phagocytosis is initiated by the interaction of receptors on the surface of phagocytes with ligands on large particles, generally over 1 μm. Receptor ligation results in actin polymerization, which subsequently leads to particle internalization. The main objective of my thesis research was to characterize functional phagocytic responses at inflammatory sites, where various responses are involved in the clearance of pathogens, dying or senescent cells, and in tissue repair/ wound healing. While this balance is well understood in mammals, much less is known in lower vertebrates.

In accordance with mammals, I found that differentiation along the macrophage pathway resulted in increases in phagocytic capacity, with mature macrophage having the greatest capacity. Interestingly, activation resulted in differential regulation of phagocytosis in monocytes and mature macrophages. Within these subsets there was also differential regulation of phagolysosome fusion and the production of reactive oxygen species (ROS). The activation of specific phagocytic responses at distinct stages of differentiation suggests that these responses may allow specialization of host immunity requirements within specialized niches.

When phagocytic responses to inflammatory or homeostatic responses were studied, I found that teleost fish displayed divergent responses following phagocytosis, which is consistent with observations in mice. However, I found significant differences between these species with regards to the level of

responsiveness to zymosan and apoptotic bodies, the identity of infiltrating leukocytes, their rate of infiltration, and the kinetics and strength of resulting antimicrobial responses. The primary differences were noted in the neutrophilic responses. Importantly, I found that activated murine, but not teleost, neutrophils possess the capacity to internalize apoptotic cells, resulting in decreased neutrophil ROS production. This may play an important part in the recently identified anti-inflammatory activity that mammalian neutrophils display during the resolution phase of inflammation.

Goldfish responses were partially regulated by soluble factors. However, no changes were noted in canonical mammalian factors, leading to identification of a novel role for a unique teleost receptor- soluble colony stimulating factor-1 receptor (sCSF-1R). Soluble CSF-1 receptor was originally described as a regulator of macrophage proliferation. Soluble CSF-1R is highly upregulated following interaction with apoptotic cells, resulting in reduced cellular infiltration, phagocytosis, ROS production, expression of pro-inflammatory factors, and downstream antimicrobial responses. The effects sCSF-1R mirrored several of those induced by apoptotic cells, suggesting that sCSF-1R may be a central player in the regulation of anti-inflammatory responses induced by apoptotic cells.

These observations were then applied to the study of an *Aeromonas* infection. *Aeromonas* is a highly virulent fish pathogen with devastating effects on the fish farming industry. It has been previously shown that increases in the production of reactive intermediates by host immune cells cause significant cytotoxicity at the infection site, but have limited protective effects against this catalase-producing

bacterium. I found that *Aeromonas veronii* infection promotes systemic expression of sCSF-1R. However, unlike other pathogen models, sCSF-1R was unable to inhibit inflammation at the *A. veronii* challenge site and had no impact on the production of ROS *in vitro* or *in vivo*. Importantly though, I found that the increased systemic expression of sCSF-1R in *A. veronii* infected fish appears to decrease proliferative activity among cells in the hematopoietic compartment, which is further coupled to a decrease in CSF-1 expression in kidney hematopoietic tissues.

Overall, the data presented here places the CSF-1 system and its regulator sCSF-1R at the center of both the induction and regulation of inflammation in teleost fish, with the effects of this system impacting the macrophage-lineage cells as well as the neutrophilic and potentially lymphocytic cells.

Preface

This thesis is an original work by Aja M. Rieger. The research project, of which this thesis is a part, received research ethics approval from the University of Alberta Research Ethics Board as part of an NSERC Discovery Grant entitled "Comparative biology of phagocytic antimicrobial responses" awarded to Dr. Daniel R. Barreda, held from 2008-2013 and 2013-2018:

1. Comparative biology of fish phagocytic antimicrobial responses; Protocol # 706.
2. Comparative biology of phagocytic antimicrobial responses in mice; Protocol # 760.

Some of the research conducted in this thesis was part of collaborations with local and international groups, leading to publication. Details for each chapter are outlined below:

Chapter 1: Portions of this chapter have been previously published in: Rieger AM and Barreda DR. 2011. Antimicrobial mechanisms of fish leukocytes. *Dev Comp Immunol* 35: 1238-45. And Rieger AM, Hanington PC, Belosevic M and Barreda DR. 2014. Control of CSF-1 induced inflammation in teleost fish by a soluble form of the CSF-1 receptor. *Fish Shellfish Immunol* pii: S1050-4648(14)00105-3. For both manuscripts, I contributed to the design of the review, manuscript composition, and figure design. P.C. Hanington contributed to a portion of the manuscript composition. M. Belosevic contributed to manuscript editing. D.R. Barreda was the supervisory author, and assisted in manuscripts composition

and editing.

Chapter 3: A version of this chapter has been previously published in: Rieger AM, Hall BE and Barreda DR. 2010. Macrophage activation differentially modulates particle binding, phagocytosis and downstream antimicrobial mechanisms. *Dev Comp Immunol* 34: 1144-59. I was responsible for the experimental design, data collection and analysis, and manuscript composition. B.E. Hall (Amnis Corporation, part of EMD Millipore) assisted in design of analysis templates and contributed to manuscript editing. D.R. Barreda was the supervisory author, and assisted in experimental design and manuscript composition.

Chapter 4: A version of this chapter has been previously published in: Rieger AM, Konowalchuk JD, Grayfer L, Katzenback BA, Havixbeck JJ, Kiemele MD, Belosevic M, Barreda DR. 2012. Fish and mammalian phagocytes differentially regulate pro-inflammatory and homeostatic responses *in vivo*. *PLoS One* 7: e47070. I was responsible for experimental design, data collection and analysis, and manuscript composition. J.D. Konowalchuk assisted with data collection from murine experiments. L. Grayfer assisted with Q-PCR experimental design. B.A. Katzenback assisted with neutrophil identification and analysis. J.J. Havixbeck assisted with manuscript editing. M.D. Kiemele assisted in flow cytometry staining. M. Belosevic and D.R. Barreda were supervisory authors, and assisted in experimental design and manuscript editing.

Chapters 5 and 6: Portions of these chapters has been previously published

in: Rieger AM, Konowalchuk JD, Havixbeck JJ, Robbins JS, Smith MK, Lund JM, Barreda DR. 2013. A soluble form of the CSF-1 receptor contributes to the inhibition of inflammation in a teleost fish. *Dev Comp Immunol* 39: 438-46. I was responsible for experimental design, data collection and analysis, portions of the manuscript composition, and manuscript editing. J.D. Konowalchuk and J.J. Havixbeck were involved in data collection and manuscript editing. J.S. Robbins was responsible for the generation of recombinant sCSF-1R. M.K. Smith assisted in sample processing and manuscript editing. J.M. Lund provided preliminary data that guided this line of research and assisted in manuscript editing. D.R. Barreda was the supervisory author, and assisted in experimental design, manuscript composition, and manuscript editing.

Chapter 8: A portion of this chapter has been previously published in: Rieger AM, Hanington PC, Belosevic M and Barreda DR. 2014. Control of CSF-1 induced inflammation in teleost fish by a soluble form of the CSF-1 receptor. *Fish Shellfish Immunol* pii: S1050-4648(14)00105-3. I contributed to the design of the review, manuscript composition, and figure design. P.C. Hanington contributed to a portion of the manuscript composition. M. Belosevic contributed to manuscript editing. D.R. Barreda was the supervisory author, and assisted in manuscripts composition and editing.

Appendix I: A version of this chapter has been previously published in: Rieger AM, Hall BE, Luong Le T, Schang LM, Barreda DR. 2010. Conventional apoptosis assays using propidium iodide generate a significant number of false positives that prevent accurate assessment of cell death. *J Immunol Methods* 358:

81-92. And Rieger AM, Nelson KL, Konowalchuk JD, Barreda DR. 2011. Modified AnnexinV/Propidium Iodide apoptosis assay for accurate assessment of cell death. *J Vis Exp* 50: pii: 2597. I was responsible for experimental design, data collection and analysis, video performance, and manuscript composition for both papers. B.E. Hall (Amnis Corporation, part of EMD Millipore) assisted in design of analysis templates and contributed to manuscript editing. T. Luong Le preformed all viral infections. L.M. Schang assisted in experimental design of viral work and participated in manuscript editing. K.L. Nelson assisted in compiling figures for the JoVE publication and assisted in manuscript editing. J.D. Konowalchuk assisted in data collection, manuscript editing, and video performance. D.R. Barreda was the supervisory author for both papers, and assisted in experimental design and manuscript editing.

Acknowledgements

This journey has been a fantastic and rewarding experience that would not have been possible without the guidance, support, and encouragement of many individuals. I appreciate everything you have done for me over the past 5 and a bit years and would not be where I am today without you.

Firstly, I would like to thank my supervisor Dr. Dan Barreda. Dan, you have provided me with excellent advice, suggestions, and opportunities, while allowing me to grow as a scientist. Thank you for always being there to bounce ideas off of and supporting (and funding) my research ideas, even when they sounded crazy at the start. I have been spoiled in your lab and will be hard pressed to find another lab with the same resources, mentorship, and atmosphere. It has truly been a pleasure to work with you.

I would also like to thank my committee members, Dr. Mike (Miodrag) Belosevic and Dr. Luis Schang. Your guidance, comments, and input have been integral to the shaping of my research. I would also like to extend an extra thanks to Mike for being like a co-supervisor, always being available for pop-ins from across the hall or a beer at the Faculty Club. The science chats we have had inspired me to be creative in my research and your curiosity and love of science is truly infectious. I would also like to thank my defense and candidacy examination members: Dr. Lisa Cameron, Dr. Christine Szymanski, Dr. Ben Willing, and Dr. Jesús Lamas for thought-provoking and interesting discussions and challenging questions. Finally, Dr. Allen Shostak, thank you for providing highly valuable statistical advice.

To my lab mates throughout my degree: you kept it real! My Ph.D. experience would not have been nearly as much fun without having you at my side. A special thanks to Moira Kiemele, Matthew Smith, Jeffrey Konowalchuk, Jeffrey Havixbeck, and Mike Wong, as well as to my colleagues from the center wing gang- you've all been a pleasure to work closely with, talk science with, and for being fantastic friends in and out of the lab. Thank you for making Bio Sci a magical place.

I have also had the opportunity to collaborate with a number of scientists throughout the course of my degree. Dr. J. Oriol Sunyer, Dr. David Parra, and Dr. Fumio Takizawa (UPenn); Dr. Miki Nakao and Takahiro Nagasawa (Kyushu University); Dr. John Chang and Joshua Pemberton (U of A); Dr. A. Dean Befus and Dr. Tae Chul Moon (U of A); Dr. Mike Belosevic and Belosevic lab members (Dr. Leon Grayfer, Dr. Barbara Katzenback, Dr. Fumihiko Katakura; U of A); Dr. Luis Schang (U of A), you have all provided me with the opportunity to broaden my research and understanding of other research areas.

Finally, to my family and friends, especially my parents, thank you for your undying support and encouragement, for keeping me sane and levelheaded, and for helping wherever possible. I'd like to give a special thank you to Keith Heslinga- your engineering logic helped me to think outside of the box and inspired some truly imaginative ideas and solutions throughout my degree, and your constant cheer-leading pushed me to be the best scientist I could be. To Azalia and Quince- your smiles make even the longest, most frustrating days better.

Table of Contents

Chapter 1: Introduction and Literature Review

Chapter 2: Materials and Methods

Chapter 4: Goldfish phagocytes display divergent responses to pro-inflammatory and homeostatic stimuli *in vivo*

Chapter 5: Apoptotic cells induce expression of non-classical soluble factors in goldfish macrophages

List of Tables

List of Figures

List of abbreviations

AC	apoptotic cell
Aero	*Aeromonas*
AMP	antimicrobial peptides
ANOVA	analysis of variance
AnxV	Annexin V
APC	allophycocyanin
ATP	adenosine tri-phosphate
AVG	*Aeromonas veronii* group
BrdU	bromolated deoxyuridine triphosphate nucleotides
cAMP	cyclic adenosine mono-phosphate
CCM	cell-conditioned media
CD	cluster of differentiation
cDNA	complementary DNA
CFU	colony forming units
ChK	chemokinesis
CHX	cycloheximide
CSF-1	colony stimulating factor-1
CSF-1R	colony stimulating factor-1 receptor
DAMPs	damage-associated molecular patterns
DAPI	4’,6-diamidino-2-phenylidole
DC	dendritic cell
DHR	dihydrorhodamine
DMEM	Dulbecco’s modified Eagle media
DNA	deoxyribonucleic acid
dsRNA	double stranded ribonucleic acid
FACS	fluorescence activated cell sorter
FBS	fetal calf serum
FITC	fluorescein isothiocyanate
Flow-FISH	flow cytometry-based fluorescence *in situ* hybridization
G-CSF	granulocyte colony stimulating factor
G-CSFR	granulocyte-colony stimulating factor receptor
GM-CSF	granulocyte-macrophage colony stimulating factor
HBSS	Hank’s balanced salt solution
HG	hybridization group
HSP	heat shock protein
ICAM	intracellular adhesion molecule
ICE	caspase-1/IL-1β converting enzyme
IFN	interferon

IL	interleukin
iNOS	inducible nitric oxide synthase
kDa	kilo-Dalton
LB	Luria-Bertani
LDL	low density lipoprotein
LPS	lipopolysaccharide
LTBP	latent TGF binding protein
M-CSF	macrophage-colony stimulating factor
MAPK	mitogen-activated protein kinase
MAF	macrophage activating factors
MGFL-15	modified goldfish Leibovitz-15
mRNA	messenger ribonucleic acid
NETs	neutrophil extracellular traps
NF-κB	nuclear factor-κB
NK	natural killer
NLRs	Nod-like receptors
NO	nitric oxide
PAMPs	pathogen-associated molecular patterns
PBS	phosphate buffered saline
PCR	polymerase chain reaction
PE	phycoerythrin
PG	prostaglandin
PI	propidium iodide
PKC	protein kinase C
PKM	primary kidney macrophages
PMA	phorbol myristate acetate
polyI:C	polyinosinic:polycytidylic acid
PRR	pattern recognition receptor
Q-PCR	quantitative polymerase chain reaction
RNA	ribonucleic acid
ROS	reactive oxygen species
rsCSF-1R	recombinant soluble colony stimulating-1 receptor
SAS	saturated ammonium sulfate
sCSF-1R	soluble colony stimulating factor-1 receptor
SOCS	suppressor of cytokine signaling
SSC	saline sodium-citrate
T3SS	type III secretion system
TACE	TNF-α converting enzyme
TGF	transforming growth factor
Th	helper T cell

TLRs	Toll-like receptors
TMS	tricaine methane sulfonate
TNF	tumor necrosis factor
TSA	tryptic soy agar
TSB	tryptic soy broth
VCAM	vascular cell adhesion molecule
VEGF	vascular endothelial growth factor
VHSV	viral haemorrhagic septicemia virus
Zy	zymosan

Chapter 1. Introduction and Literature Review[1]

1.1. Introduction

Since Metchnikoff's seminal discovery of phagocytosis in 1882, phagocytes have become widely appreciated for their critical role in immune defenses. Phagocytic cells are found in all branches of the animal kingdom. Professional phagocytes are integral to the maintenance of tissue homeostasis and turnover, embryogenesis and organogenesis, recognition and clearance of pathogens, initiation and resolution of inflammatory processes, and activation of immune cells through the production of bioactive molecules and presentation of antigens.

The initiation and resolution of inflammation by phagocytes is central to both wound healing and defense against pathogens. In mammalian immunology, it is widely accepted that phagocytes, macrophages in particular, are capable of internalizing pathogenic and homeostatic self particles, leading to induction of divergent macrophage responses. Following internalization of pathogens, phagocytes produce an array of inflammatory mediators that activate pro-inflammatory immune processes. Internalization of pathogens also increases

---

[1] Portions of this chapter have been previously published:

Rieger AM and Barreda DR. 2011. Antimicrobial mechanisms of fish leukocytes. *Dev Comp Immunol* 35: 1238-45.

Rieger AM, Hanington PC, Belosevic M and Barreda DR. 2014. Control of CSF-1 induced inflammation in teleost fish by a soluble form of the CSF-1 receptor. *Fish Shellfish Immunol* pii: S1050-4648(14)00105-3.

production of microbicidal products, which is integral to preventing pathogen dissemination. Conversely, phagocytosis of homeostatic, self particles (eg. apoptotic cells) results in activation of anti-inflammatory processes. This involves changes in the types of soluble factors produced and, generally, a decrease in phagocytic and microbicidal activities. Further, phagocytosis of apoptotic cells induces a switch in macrophage activity, which is important to resolving inflammatory processes and promoting wound healing. While this process is well understood in mammalian models, little is known about responses in lower vertebrates.

Non-classical immune models have been particularly important in informing the evolution of immune responses and in identifying novel immune responses/ pathways/ molecules. This is highlighted by the discovery of phagocytosis in starfish larva (Elie Metchnikoff; 1908 Nobel Prize in physiology or medicine), Toll receptors in *Drosophila* (Jules Hoffman; 2011 Nobel Prize in physiology or medicine), and phagocytic B cells in fish and amphibians. All of these discoveries lead to the identification of these novel activities in mammalian immune defenses. In my thesis, I employ a comparative approach to dissecting roles of phagocytes in the initiation and resolution of inflammation. Teleosts (bony fish) are one of the earliest vertebrate classes that possess functional innate and adaptive immune components similar to those found in mammals. Teleosts are part of an large family, containing over 30,000 identified species. Most teleost immune studies, however, have focused on gene identification and expression. Using a goldfish model system, my thesis work focused on the characterization of the functional

responses of phagocytes and their antimicrobial defenses in the initiation and resolution of inflammatory processes.

1.2. Objectives of thesis

The main objective of my thesis research was to characterize functional phagocyte responses that occur at inflammatory sites, where various responses are involved in the clearance of pathogens, dying or senescent cells, and in tissue repair/ wound healing. The specific aims of my research were (1) investigate the responses of goldfish and murine phagocytes to pathogenic vs. homeostatic stimuli; (2) characterize the contributions of sCSF-1R as a homeostatic stimulus; and (3) elucidate the role of sCSF-1R in an *in vivo* model of *Aeromonas veronii* infection.

1.2.1. Outline of thesis

This thesis is comprised of 8 chapters. The first chapter is a literature review focusing on the antimicrobial defenses of phagocytes and the roles these have in an inflammatory response. Specifically, this chapter will outline important steps of an acute inflammatory response (from induction to resolution) and the roles of phagocytes in the various stages. Chapter 2 provides detailed descriptions of the methodologies employed throughout this thesis. In Chapter 3, I examine the phagocytic responses of teleost macrophages to pathogenic stimuli and the impact on the induction of antimicrobial defenses. Chapter 4 describes the responses of goldfish and murine phagocytes (macrophages and neutrophils) to pathogenic and homeostatic stimuli *in vivo*. Chapter 5 identifies soluble colony stimulating factor-1

receptor (sCSF-1R) as a potential soluble homeostatic mediator in goldfish and examines expression of this receptor. In Chapter 6, I investigate the role of sCSF-1R in regulating acute inflammatory responses *in vivo*. Chapter 7 examines in importance of sCSF-1R in the context of an *Aeromonas veronii* infection. Finally, in Chapter 8, I provide an overview of my findings and describe a model of inflammatory control in bony fish. This chapter also suggests future directions for this work and describes the relevance of my findings.

1.3. Literature review: The role of phagocytes in the induction and resolution of acute inflammatory responses

1.3.1. Introduction

Inflammation is a tightly regulated process that occurs following tissue injury or pathogenic insult. It is a complex biological process involved in the repair of damaged tissue or clearing infection. The end goal of inflammation is the restoration of tissue homeostasis. The classical signs of acute inflammation are redness, heat, swelling, pain, and loss of function.

A hallmark of inflammation is the clustering of monocytes, macrophages, neutrophils, and dendritic cells at inflammatory foci, initiated by the production of inflammatory cytokines and chemokines (1). These foci maintain immune cells in close contact and promote the crosstalk necessary for tight regulation and integration of immune responses. Within these foci, antimicrobial products are important mediators of immune cell function and contribute to the promotion and resolution of inflammation at distinct stages of the antimicrobial response.

Antimicrobial responses are critical components of the innate immune system. Many of these responses are conserved through evolution, pointing to the importance of these responses in providing protection against infection and in limiting dissemination of pathogens. The phagocytic leukocytes in fish are armed with an array of intracellular and extracellular antimicrobial defenses that are generally induced by the internalization of pathogens or by the presence of pro-inflammatory immune products or pathogen products and provide protection against diverse pathogens. Further, products of antimicrobial responses are also integral in shaping protective immune responses and in resolution of inflammatory processes through their concentration dependent, divergent effects on immune cells.

1.3.2. Antimicrobial defense mechanisms of fish leukocytes

The innate immune system provides a critical first line of defense against invading pathogens. Multi-parametric recognition of pathogen associated molecular patterns (PAMPs) based on well-established receptor families (e.g. TLRs, NLRs) effectively defines microbial intruders and ultimately leads to activation of cell armamentarium designed to kill infiltrating pathogens. Antimicrobial responses are tailored to the type of pathogen, as well as to the location of the pathogen (internalized or external to the cell). Because of their potency and efficiency, these primordial immune defenses have been largely conserved through evolution. For lower vertebrate species like the teleost fish, these innate antimicrobial responses are particularly critical for host survival in

light of the reduced repertoire of classical adaptive responses compared to those of mammalian species.

Antimicrobial defenses can be divided into two main categories: intracellular and extracellular. Intracellular defense mechanisms are designed to provide protection against pathogens found within membrane-enclosed structures. These defenses are not limited to killing pathogens that have been internalized (e.g. though phagocytosis), but also provide protection against pathogens that actively enter immune cells as a mechanism of protection from humoral defense mechanisms. In the following section, I highlight the role of mechanisms based on superoxide and nitric oxide production, as well as phagolysosome fusion for the effective establishment of a toxic degradative environment within teleost fish leukocytes. These soluble products are efficient antimicrobial agents, but their modes of action are generally non-specific (2-4). As such, they can be highly toxic to host cells as well. Targeted production and release of these antimicrobial molecules into membrane-enclosed structures ensures reduced damage to host phagocytes, while also sequestering the pathogen within a specialized degradative environment.

Extracellular defense mechanisms provide complementary strategies to those described above. Extracellular defenses are targeted towards pathogens within the extracellular space, providing a means for the innate immune system to effectively clear pathogens that have escaped internalization or those that are too large to be internalized. These responses are generally activated by the presence of microbial products or inflammatory mediators and result in the release of antimicrobial

factors into the extracellular space. While reactive oxygen and nitrogen intermediates can also be produced extracellularly and thus be considered extracellular defense mechanisms, this chapter will focus on the antimicrobial contributions provided by degranulation of neutrophilic granules, formation of neutrophil extracellular traps, and antimicrobial peptides as representative strategies for the effective defenses against extracellular pathogens. Unlike intracellular defenses, products in neutrophilic granules and antimicrobial peptides are more specifically targeted towards microorganisms and cause little damage to healthy host cells (5, 6).

The mechanisms and effectiveness of teleost cellular responses against microbial challenge are well documented for classical professional phagocytes such as monocytes, macrophages, and neutrophils. These provide clear examples of the potent intracellular (7-9) and extracellular (10-13) antimicrobial strategies available to the teleost host. There is also increasing evidence that non-classical cells such as B-lymphocytes may fill important roles in early teleost antimicrobial defenses. B cells have recently been described to be phagocytic and to effectively mediate killing of phagocytosed bacteria (14-16). Furthermore, phagocytic B cells appear to represent a significant proportion of the phagocytic blood leukocytes in trout, suggesting significant contributions for phagocytic B cells in teleost host defense (14). It remains unclear whether the presence of phagocytic B cells reflects a requirement for specialization from a lower vertebrate group that relies heavily on innate defense mechanisms for pathogen clearance. Alternatively, this may point to

novel innate mechanisms that have remained conserved within specialized niches in higher vertebrates (17).

1.3.2.1. *Intracellular mechanisms*

1.3.2.1.1. Respiratory burst

The respiratory burst was first described in mammalian leukocytes in the 1930's when it was noted that phagocytosis was associated with increased oxygen consumption (18). It was subsequently found that this increased oxygen consumption- or respiratory burst- resulted in the formation of superoxide anion (19) and that this process was catalyzed by NADPH-oxidase, a multi-component enzyme that assembled on the inner surface of the plasma membrane following appropriate activation (20). In mammalian phagocytes, the NADPH-oxidase consists of the catalytic membrane-associated flavocytochrome b_{588}, which is a heterodimer $gp91^{phox}$ (also known as Nox2; phox for phagocyte oxidase) and $p22^{phox}$ (21, 22). The remaining three components of NADPH-oxidase – $p40^{phox}$, $p47^{phox}$, and $p67^{phox}$ remain complexed in the cytosol until appropriate stimulation is received (22), thereby providing an important control strategy for NADPH-oxidase activation in resting cells.

Phagocyte NADPH-oxidase has only begun to be characterized in teleost fish. Cloning, sequencing and phylogenetic analysis NADPH-oxidase has been described in several teleost fish species, including rainbow trout (23), Japanese pufferfish (24), carp (25), Atlantic salmon (26), zebrafish, medaka, and pufferfish (27, 28). Phylogenetic analysis indicates that the radiation of NADPH-oxidase

components occurred in a common teleost/ mammalian ancestor (25) and have evolved separately, leading to a clustering of all fish components separate from mammals (26).

Although the evolutionary divergence observed for NADPH-oxidase has led to a relatively low sequence homology between fish and mammals, the functional domains remain highly homologous (23-26). Fish phox subunits contain all essential interaction and activation domains required for correct assembly and function of the mammalian NADPH-oxidase complex, as well as the motifs required for the production of reactive oxygen intermediates (ROI) (23-25). Importantly, fish NADPH-oxidase components have been shown to have a similar expression pattern to that of mammals, suggesting that fish and mammal NADPH-oxidase may have similar modes of activation and functional activities (24-26).

Recent studies on the functional induction of the respiratory burst response suggest an important role for inflammatory cytokines (7, 29). These include inflammatory cytokines such as tumor necrosis factor (TNF) α-1 and -2 (30, 31), interferon (IFN) γ (32-35), colony stimulating factor-1 (CSF-1) (36) and interleukin (IL)-8 (37). Interestingly, recent reports suggest that in some teleost fish TNF-α does not directly activate phagocytes but instead activates endothelial cells, leading to an indirect activation of phagocytes (38, 39). For example, direct stimulation of gilthead seabream (39) or carp (38) phagocytes with either TNF-α 1 or 2 fails to induce the respiratory burst.

Respiratory burst responses in fish can also be strongly activated by PAMPs. Most of these studies have focused on LPS, which has been shown to induce

respiratory burst in goldfish (7, 40), rainbow trout (23, 41), Atlantic salmon, and gilthead seabream (42). Other PAMPs that have been shown to induce respiratory burst, including CpG ODN in gilthead seabream (42, 43), poly I:C in rainbow trout (23), flagellin in gilthead seabream (42), MDP in gilthead seabream (42) and β-glucans including zymosan in rainbow trout (23) and *Saccharomyces cerevisiae* in gilthead seabream (8). Important pathogens of teleost fish have also been shown to induce potent respiratory burst responses, including *Aeromonas* spp. in goldfish (44) and carp (45), and *Vibrio anguillarum* in gilthead seabream (46) infections. Following stimulation, NADPH-oxidase is activated through three sequential steps: [1.] activation of protein kinase C (PKC), [2.] phosphorylation of $p47^{phox}$, which likely results in its translocation to the cell membrane, and [3.] the production of reactive oxygen intermediates by NADPH-oxidase (26). While activation pathways are conserved across teleost fish species, the kinetics and strength of respiratory burst show differences across those fish species studied. For example, a report by Nikoskelainen *et al*. (2006) (47) showed that the magnitude of respiratory burst in Atlantic cod blood leukocytes following activation with opsonized or non-opsonized zymosan was at least double that of rainbow trout blood cells, and has faster induction kinetics. Another study that compared respiratory burst responses of carp and ayu neutrophils found that ayu neutrophils spontaneously activated respiratory burst that was not further enhanced by priming (48). In contrast, carp neutrophils displayed low levels of respiratory burst in resting cells that was enhanced in the presence of inflammatory stimuli (48). Despite a high level of conservation in NADPH-oxidase components and similarities in the stimulatory

factors that induce this response cross teleost fish, disparate responses exist. It will be interesting to determine if these observations point to divergent responses between various fish species and reflect a differential dependence on this mechanism for host defenses. Alternatively, these observations may highlight a differential level of responsiveness across fish that is partially driven through the specific requirements and challenges that face each species within its chosen ecological niche.

Significant heterogeneity can also be observed across leukocyte populations within a single fish species. Recent work has examined the activation of respiratory burst in goldfish primary kidney macrophage (PKM) cultures (7, 29). These *in vitro* derived cells have been previously shown to contain three distinct subpopulations that correspond to progressively more differentiated stages across the macrophage lineage (early progenitors, monocytes and mature macrophages) (7, 29). Interestingly, these three cellular subpopulations have distinct kinetics in the priming of respiratory burst reflecting potential differences in the intrinsic regulatory mechanisms among these cell types (7, 29). Early progenitors in sorted and mixed populations showed a limited capacity for respiratory burst response that was not affected by activation. In contrast, monocytes have an early induction of respiratory burst that was not maintained with prolonged activation with MAF/LPS. TNF-α-2 appears to be a key factor in activating respiratory burst in PKM monocytes populations (31). In contrast to PKM monocytes, PKM mature macrophages have a low early induction of respiratory burst that is greatly enhanced by prolonged activation. Interestingly, in the mature macrophage

populations but not the monocyte population, the kinetics of respiratory burst induction parallel the kinetics of phagocytosis. This suggests that in goldfish PKM, similar to mammalian monocytes and macrophages (49-52), phagocytosis and respiratory burst may be complementary but not interdependent antimicrobial mechanisms. Further demonstration of the heterogeneity of respiratory burst responses within a single species comes from zebrafish studies. Production of reactive oxygen species in zebrafish leukocytes was found to vary significantly throughout the day, with the highest levels being produced at dawn, suggesting that respiratory burst in zebrafish may be at least partially regulated by circadian rhythms (53). Thus, much remains to be defined, despite our improved understanding of respiratory burst responses in teleost fish in recent years. In light of the available results, it will be particularly interesting to go beyond the intrinsic mechanisms that regulate these responses at the cellular level, and assess the differential cross-talk that exists between respiratory burst mechanisms and other antimicrobial host responses across distinct cellular niches.

1.3.2.1.2. Nitric oxide

Nitric oxide (NO) is an important molecule involved in diverse physiological processes, including vasorelaxation, neuronal communications, inhibition of cell proliferation, and intracellular signaling. NO also has potent toxic effects and, as such, is an important component of the arsenal available to animal hosts for effective antimicrobial defenses. NO is formed by the oxidation of l-arginine to l-citrulline by NO synthase (NOS) (54). Three forms of NOS have been

identified in mammals: neuronal (nNOS), endothelial (eNOS) and inducible (iNOS) (55). Of these three, only iNOS has been shown to be involved in immune defense.

Within fishes, iNOS was first identified in the goldfish (56) and has been further characterized in carp (57) and rainbow trout (58). iNOS sequences have also been identified in zebrafish (59), small spotted catshark (60), and scup (61). The identified carp iNOS protein has 57% similarity with human iNOS and contains putative binding sites for heme, tetrahydobiopterin calmodulin, flavine mononucleotide, flavine adenine dinucleotide and NADPH, all of which represent important sites in mammalian iNOS (57). In addition to iNOS gene expression, its activity has been demonstrated in teleost phagocytes, including heterophillic granulocytes, neutrophils and macrophages (57, 62).

Induction of teleost *iNOS* transcription appears to involve NF-κB (57) and, similar to mammalian iNOS, is induced mainly after stimuli with cytokines or PAMPs. iNOS transcription is only induced in activated cells and results in the production of NO. Studies in goldfish, carp and turbot have identified IFN-γ, TNF-α, CSF-1, and the IL-6 family member M17 as the major pro-inflammatory cytokines inducing iNOS expression and contributing to NO production (30-32, 35, 36, 63-66). Many of these cytokines synergize with LPS to induce high levels of NO. However, as noted previously, the effects of some cytokines may be indirect, as studies in carp have shown that TNF-α does not induce nitric oxide production in carp head kidney leukocytes but again activates epithelial cells (38).

In addition to inflammatory cytokines, modified transferrin, a non-cytokine

serum protein, also potently induces NO responses in macrophages. Modified transferrin or transferrin-like proteins have been identified in many species and may constitute a highly conserved pathway for activating NO responses (67). Furthermore, transferrin and transferrin-derived synthetic proteins have been shown to induce highly conserved responses in murine and fish macrophages, pointing to an important conserved antimicrobial role of modified transferrin in both lower and higher vertebrates (68, 69). Full-length transferrin does not appear to be immunologically active and must be cleaved in order to induce NO responses in fish (67). Transferrin is cleaved by enzymes, such as elastase, released from cellular damage and/or necrosis at the inflammatory site, resulting in a truncated transferrin that significantly enhances the ability of macrophages to produce NO in response to pathogens or pathogen products (70). In several fish species, including salmon (71), goldfish, (72) and carp (73), several transferrin variants are expressed that may have differential abilities to induce NO production (74). These results, combined with earlier observations, suggest that polymorphisms in transferrin may be linked to resistance against pathogens.

Nitric oxide has been shown to have potent antimicrobial effects against a number of relevant fish pathogens (75-77). For example, nitric oxide was found to significantly impact the replication of viral haemorrhagic septicemia virus (VHSV) when examined *in vitro* using a turbot fibroblast cell line (TV-1) and kidney macrophages (75). However, similar to products from respiratory burst responses, NO is not specifically targeted to microorganisms and also has the potential to be toxic to host tissues in high concentrations. Because of this, the production of NO

must be tightly regulated. One of the primary mechanisms for controlling NO production is through the production of anti-inflammatory cytokines such as transforming growth factor (TGF)-β (78). Recent work has also shown that increased cyclic AMP (cAMP) levels leads to reduced NO production (79, 80), pointing to an important role of this second messenger in modulating fish antimicrobial responses. The antioxidant glutathione has also been shown to play a protective role against nitrosative stress, especially in carp phagocytes that contain higher levels of glutathione compared to other peripheral blood leukocytes (81). In addition, carp neutrophils have been shown to upregulate gene expression of the enzymes involved in the glutathione redox cycle following stimulation with LPS, which results in further protection against the detrimental effects of NO products following immune challenge (81).

1.3.2.1.3. Phagolysosome fusion

Phagolysosome fusion is a critical component for the degradation of phagocytosed microorganisms (82). Following internalization, lysosomes migrate towards and fuse with the phagosome resulting in the release of acidic and enzymatic lysosomal contents into the phagosome and subsequent degradation of phagolysosome contents. Phagolysosome fusion has been shown to occur in rainbow trout B cells, (14) as well as in goldfish monocytes and mature macrophages (7). I have recently reported that both monocytes and mature macrophages acquire the capacity for phagolysosome fusion that parallels their capacity for phagocytosis (7). Importantly, although I found increased

phagolysosome fusion in activated monocytes/macrophages, I observed a direct correlation between these phagocytosis and phagolysosome fusion processes. In other words, within cellular groups mediating phagocytosis there was no relative increase in phagolysosome fusion as a result of cellular activation (7). Interestingly, monocytes displayed a greater capacity for phagolysosome fusion compared to mature macrophages (7). It is possible that terminal differentiation into macrophages leads to a decreased intracellular degradative capacity that allows for increased efficiency during antigen presentation events. This would be consistent with observations on mammalian dendritic cells, which have a decreased capacity for lysosomal proteolysis but an increased ability for antigen presentation following maturation (83).

1.3.2.2. *Extracellular mechanisms*

1.3.2.2.1. Neutrophil degranulation and extracellular traps

As one of the first cells at sites of inflammation, neutrophils are armed with a wide arsenal of intracellular and extracellular antimicrobial tools that are integral to the early defenses against pathogens. Of all the phagocytic leukocytes, they possess the greatest repertoire of extracellular antimicrobial mechanisms and, as such, highlight the important contributions of extracellular mechanisms to host defenses.

One of the primary extracellular defense mechanisms of neutrophils is the targeted degranulation of cytoplasmic granules containing preformed mediators. Mammalian neutrophilic granules have been shown to contain a variety of

antimicrobial products that include enzymes such as myeloperoxidase, acidic hydrolases, metalloproteinase, proteinase-3, cathepsin G and elastase, and antimicrobial peptides such as lactoferrin and cathlicidin (5). While granular contents of teleost neutrophils have not been as thoroughly described, an assay has been recently developed to quantitate myeloperoxidase degranulation in fish neutrophils (84). Using this assay, teleost neutrophils have been shown to degranulate in response to various mitogens, zymosan, and *Aeromonas salmonicida* (12, 44, 84). These responses are not affected by the presence of cytochalasin B suggesting that potent degranulation does not require prior phagocytic events. Though protein analysis and functional studies are only starting to dissect these mechanisms, teleost fish have been shown to express homologues of proteinase-3, cathepsin G, elastase and azurocidin, suggesting that teleost neutrophils possess the potential to produce these classical granule contents (85). However, more work must be done to confirm that these enzymes are expressed at the protein level within the neutrophil granules, to confirm that these enzymes are functional, and to determine their relative contributions to the effector mechanisms mounted against invading pathogens.

Degranulation in mammalian neutrophils has recently been shown to also result in the release of chromatin, and is associated with the formation of extracellular fibers that trap bacteria (86). These mammalian neutrophil extracellular traps, or NETs, bind microorganisms, degrade virulence factors, prevent dissemination and kill bacteria by maintaining a high local concentration of antimicrobial granule components (86). The production of NETs by teleost

neutrophils has been recently described in both zebrafish and fathead minnows (10, 87). Similar to mammalian NETs, fish NETs are composed of neutrophil granule proteins associated with DNA fibers, but not cytoskeleton (10, 86, 87). However, much remains to be learned about the contribution of different neutrophilic granule classes to the composition of teleost NETs, as well as the ability of these NETs to prevent pathogen spread, to contain the diffusion of potentially tissue damaging factors, and to kill invading microorganisms.

1.3.2.2.2. Antimicrobial peptides

Antimicrobial peptides (AMPs) are an important innate immune defense because of their broad-spectrum antimicrobial activity (88). AMPs are one of the most primordial antimicrobial defense mechanisms, having been isolated from microorganisms, insects and other invertebrates, plants, amphibians, birds, fish, and mammals (89). Teleost fish express a number of AMPs in tissues that are important for immune defenses including kidney, spleen, intestine, gills, skin and epidermal mucous, blood, reproductive organs, and eyes. The recent identification of AMP expression in professional phagocytes and other leukocytes is of particular interest (11, 13). Head kidney primary leukocytes from rainbow trout, for example, express beta-defensins omDB-1 and omDB-3 following stimulation with poly I:C (90), suggesting a role for beta-defensins in leukocyte antimicrobial defenses. Further, two potent AMPs, hepcidin and piscidin, were found to be highly expressed in acidophilic granulocytes (functionally equivalent to neutrophils) but not monocytes/macrophages or lymphocytes of gilthead seabream (11, 13).

Expression of AMPs by granulocytes is upregulated after treatment with mitogens, PAMPs or particulate antigens both *in vitro* and *in vivo* (11), suggesting that neutrophil activation also increases antimicrobial killing potential through AMP production. Intriguingly, it appears that piscidins may play a role in both intracellular and extracellular killing of bacteria as piscidins are also delivered to bacteria-containing phagosomes (13). Though relatively little work has been done in this area, it appears that immune cell expression of AMPs may represent an important innate antimicrobial defense in teleost fish.

1.3.2.3. *The phagocytes: neutrophils, monocytes, macrophages, and B cells*

Neutrophils are one of the first cell types to arrive in inflammatory sites and are a critical component of teleost innate immune defenses. Neutrophils are armed with an impressive antimicrobial armamentarium that looks to limit dissemination of a broad range of pathogens. They also display a broad repertoire of intracellular and extracellular antimicrobial defenses. Interestingly, many antimicrobial mechanisms of fish neutrophils are utilized both as intracellular and extracellular defenses. A prime example is the strong respiratory burst (25, 91) and nitric oxide (12, 92) responses of teleost neutrophils. Unlike the predominantly intracellular responses in macrophages, ROS and NO responses in neutrophils can occur potently both intracellularly and extracellularly (12, 93), providing protection against both phagocytosed and extracellular pathogens. Another example of overlapping intracellular and extracellular defenses lies in the antimicrobial and cytotoxic substances stored in neutrophilic granules (5, 11, 13). Granular contents

can either be degranulated into the extracellular space, as described above, or released within the phagosome, where they exert potent antimicrobial actions. The dual roles of neutrophil antimicrobial mechanisms provide neutrophils with potent killing capabilities against a wide range of pathogens, both intracellular and extracellular, without requiring numerous distinct mechanisms.

Monocytes/ macrophages of teleost fish are highly phagocytic cells and, as such, possess potent intracellular antimicrobial defenses. Both cell types have been shown to be variably capable of producing reactive oxygen and nitrogen intermediates and phagolysosome fusion, and appear to rely on distinct antimicrobial defenses. Monocytes have been shown to have a relatively short respiratory burst response following activation (7, 29) and lack a nitric oxide response (29), which may be compensated for by having greater capacity of phagolysosome fusion than do macrophages (7). This is unlike mature macrophages, which have a prolonged respiratory burst (7, 29) and potent nitric oxide responses (40, 64, 65) following activation, but a more limited capacity for phagolysosome fusion. Based on this, it appears that macrophages may rely predominantly on ROS and NO for antimicrobial defenses, while monocytes may kill predominantly through phagolysosome fusion. These differences may reflect segregation of function between monocytes and macrophages in immune defense (antigen presentation vs. pathogen killing) or differences in developmental stage. These differences may also make monocytes and macrophages variably susceptible to pathogen infection/ escape and may lead to preferential targeting of one cellular subset by pathogens.

B cells are the most recently described phagocytic cells in teleost fish and, consequently, relatively little work has been done on antimicrobial defenses of B cells. However, it is evident that B cells phagocytosis leads to phagolysosome fusion and results in killing of phagocytosed microorganisms (14). Additional work is needed to characterize downstream antimicrobial responses in these potentially central contributors to fish innate antimicrobial defenses.

1.3.3. Phagocytes and acute inflammatory responses

This section of the literature review will focus on our current understanding of inflammatory processes in mammalian systems. This is overviewed in Figure 1.1. These processes in fish will be discussed in the data chapters of this thesis.

1.3.3.1. *Phase I: Resident macrophages recruit inflammatory neutrophils*

The initiation of inflammatory responses starts with the recognition of molecular alarm signals that are generated by tissue damage or pathogens being recognized by antigen presenting cells such as resident tissue macrophages and dendritic cells. These signals include damage-associated molecular patterns (DAMPs) and pathogen-associated molecular patterns (PAMPs) (94-98). Tissue damage and/or infection generally cause disruption of cell membranes or necrotic cell death, leading to release of intracellular components= the DAMPs (99). Common DAMPs include HMGB1 (100-104), DNA/ chromatin/ nucleosomes (105-108), heat shock proteins (109-113), and adenosine and ATP (114-118). DAMPs can also be generated by the breakdown of extracellular components caused by the release of intracellular proteases and hydrolases. Similar to the

recognition of PAMPs, DAMPs are recognized by pattern recognition receptors such as Toll-like receptors (TLRs; see inserted Table 1.1 below) (99, 119-121). These signals are received by patrolling, steady-state non-classical monocytes, found on the luminal side of the endothelium (122), resulting in a rapid entry into the damaged site. It is thought currently that these cells are important for the subsequent initiation of the inflammatory cascade, as their entry into the site coincides with an increase in their expression of antimicrobial peptides, pattern recognition receptors, scavenger receptors, antigen presentation receptors, cytokines, and chemokines, all important components of pathogen/injury detection and immune activation (123). DAMP, PAMP, and monocyte-derived signals also activate the resident tissue macrophages.

Activation of resident macrophages and patrolling monocytes results in the production of an array of neutrophil-recruiting chemokines, importantly CXCL1, CXCL2, CXCL5, and CXCL8 (124-128). Interestingly, macrophage production of chemokines can also be induced by the presence of ROS, in the absence of any receptor ligation (129). This may be an important signal for macrophages that there is currently tissue injury/ pathogenic insult that they have not yet detected by pattern recognition receptors. Neutrophils are also strongly chemotactic to other agents such as complement component C5a, leukotriene B4, and platelet activating factor, largely derived from tissue resident cells (130). Adhesion and entry of neutrophils into the inflammatory site is dependent on endothelial expression of P-selectin, intercellular adhesion molecule 1 (ICAM1) and ICAM2 (131). These receptors are bound by CD11b-CD18 expressed by neutrophils (131).

Table 1.1. Mammalian Toll-like receptors and major ligands

TLR	PAMP	DAMP
TLR 1/2	Triacylated lipoproteins	
TLR 2	Diacylated lipoproteins, zymosan	Heat-shock proteins, HMGB1
TLR 3	dsRNA	mRNA, tRNA
TLR 4	Lipopolysaccharide	Heat-shock proteins, HMGB1
TLR 5	Flagellin	
TLR 2/6	Diacylated lipopeptides	
TLR 7	ssRNA, guanosine analogs	ssRNA
TLR 8	ssRNA	ssRNA
TLR 9	Unmethylated CpG DNA	Chromatin IgG complex
TLR 10/11/12	Profillin and profillin-like proteins	

1.3.3.2. *Phase II: Recruitment of classical monocytes*

Upon entering an inflammatory site, neutrophils release preformed granule contents in a sequential manner (132). Neutrophil antimicrobial defenses are covered in an earlier section of this chapter. Some of the first mediators released have antimicrobial and matrix-degrading activities that allow neutrophils (and also potentially leukocytes recruited in the future) to navigate through the tissue (5, 133, 134). In addition to antimicrobial effects, some of the early mediators (eg. cathelicidin, α-defensins, cathepsin G, azurocidin) are also important recruiters of

monocytes (135-137). These mediators are particularly important for the rapid recruitment of classical monocytes (138-140). Monocytes extravasate into the site of inflammation following interaction with endothelial cell-expressed E-selectin, vascular cell adhesion molecule 1 (VCAM1), and CCL2 (131).

While neutrophilic granule proteins begin initial recruitment of classical inflammatory monocytes, many monocyte chemoattractants require *de novo* synthesis. An important mediator in the switch from neutrophil recruitment to monocyte recruitment is IL-6. Activation of neutrophils results in shedding of IL-6Rα, a soluble receptor that binds IL-6 produced by macrophages and endothelial cells (130). The IL-6-IL-6Rα complex is then bound by gp130 on endothelial cells (141), resulting in IL-6-trans-signalling and upregulation of VCAM1 and CCL2 on endothelial cells (142, 143).

Neutrophil granule products also activate cells within close proximity, such as resident macrophages, to produce factors that promote recruitment of monocytes. CCL3, CCL6, CCL9, CCL15, and CCL23 produced by macrophages are all known chemoattractants for monocytes (130). Expression of these chemokines, especially CCL3, have been shown to be induced by azurocidin, a neutrophil granule component (144). However, many of the chemokines are produced by macrophages in a pro-form and require processing by neutrophil proteases to become fully active (145). Finally, appropriately activated neutrophils are also able to produce CCL3, CCL4, and CCL20 (146-148).

1.3.3.3. *Phase III: Termination of neutrophil recruitment by phagocyte signals*

Within the site of injury/infection, macrophages, neutrophil, and monocytes collaborate to remove the noxious stimuli (ie. pathogen). The mechanisms used for this are described in Section 1.3.2 of this chapter. After the inflammatory stimulus has been cleared, the process of resolution must begin to prevent excess tissue damage and initiate wound healing, the initial steps towards a return to homeostasis. This process is not merely a termination of inflammation but is an active process that occurs through several steps.

1. Decrease neutrophil recruitment

Lipid mediators are important to both the initiation of inflammation and the induction of resolution, and the change between these two states appears to involve a "switch" in the lipid mediators found within an inflammatory site (coined 'lipid-mediator class switch') (149). During the initiation of inflammation, endothelial cells, monocytes, macrophages and neutrophils generate prostaglandins and leukotrienes that increase inflammation (150). The switch between inflammation and resolution occurs as prostaglandin E_2 (PGE_2) and PGD_2 promote the synthesis of pro-resolution molecules such as lipoxins (151, 152). Neutrophils play an important role in lipid-mediator class switching through interactions with platelets and epithelial cells (151, 152). One such lipoxin, lipoxin A4, is involved in inhibiting neutrophil entry (153) and decreasing neutrophil ROS production, NF-κB translocation, and inflammatory cytokine and chemokine synthesis (154). Resolvins and protectins, other important pro-resolution mediators (155), have been shown to increase expression of CCR5 on spent neutrophils (156), thereby

promoting the clearance of pro-inflammatory chemoattractants CCL3 and CCL5, and terminating inflammatory cell influx.

2. Induction of apoptosis

Neutrophils are naturally short-lived cells. Signals within an inflammatory site play a large role in instructing neutrophil apoptosis. Upon entering an inflammatory site, neutrophils receive survival signals such as IL-1β, granulocyte-colony stimulating factor (G-CSF) and granulocyte-macrophage colony stimulating factor (GM-CSF) from macrophages, delaying the onset of apoptosis (157). Macrophages, however, also produce signals that reduce neutrophil lifespan, such as tumor necrosis factor, which induces neutrophil apoptosis at high levels of expression (158). Monocytes and macrophages also have membrane-bound TNF on their surface that similarly induces neutrophil apoptosis, promoting the resolution of inflammation (159, 160).

During an inflammatory response, there is also the generation of a large pool of inflammatory macrophages, thought to be derived from inflammatory monocytes (161). Unlike resident tissue macrophages, these cells do not remain within the site for long spans of time. However, these cells do not undergo apoptosis within the inflammatory site, but instead emigrate to the draining lymph node quickly during the resolution process (162). It is thought that this emigration and subsequent antigen presentation within the lymph node is an important component in activating downstream adaptive responses towards antigens from the inflamed site (162).

3. Phagocytosis of apoptotic neutrophils

During apoptotic cell death, neutrophils release a series of "find me" signals including S19 ribosomal protein, split tyrosyl-tRNA synthetase, thrombospondin 1, lysophosphatidylcholine, ATP and UTP, and CX_3CL1 (130, 163-165). Apoptotic cells also have changes in membrane composition, including negative surface charges, which also recruit scavenging cells to the apoptotic cells (166). A critical component of resolution is the clearance of apoptotic cells; inefficient clearance may lead to loss of cellular integrity, leakage of cellular contents, and activation of immune responses to antigens derived from apoptotic cells (167). Within an inflammatory site, this is largely accomplished by professional phagocytes-macrophages and immature dendritic cells (167).

Unlike "find me" signals, which are diffusible soluble factors, "eat me" signals are displayed on the surface of apoptotic cells early in the apoptotic cascade and signal phagocytes to clear that cell (168, 169). The most well recognized "eat me" signal is exposure phosphatidylserine from the inner membrane leaflet to the outer membrane surface (170, 171). Other common "eat me" signals include changes in the charge of surface glycoproteins and lipids from the addition of sugars, binding of thrombospondin or complement component C1q to the apoptotic cell surface, expression of ICAM3, and expression of oxidized low-density lipoprotein (LDL)-like moiety (171-173). These "eat me" signals are recognized by various receptors on the phagocyte: lectins (bind altered sugars) (174), vitronectin receptor (thrombospondin) (175), scavenger receptors (oxidized LDL-like

moieties) (174), CD14 (ICAM3) (176), CD91/LRP1 (C1q) (177, 178) are some examples. Internalization of apoptotic cells appears to depend on the type of cell about to be engulfed, the combination of signals the phagocyte receives, and the activation state of the phagocyte (169, 179-181). Once the phagocyte receives the appropriate collection of signals, the phagocytic process ensues as with pathogens: pseudopods are extended around the apoptotic cell, the apoptotic cell is internalized into a phagosome, and the contents of the phagosome are broken down (167).

1.3.3.4. *Phase IV: Return to homeostasis*

Phagocytosis of apoptotic cells was originally thought to be immunologically "silent" (182) because there was no induction of inflammatory responses. As such, to differentiate phagocytosis of apoptotic cells from pathogens, this process has been occasionally termed 'efferocytosis' (meaning "carrying the corpse to the grave") (183). While there is no induction of inflammatory processes following apoptotic cell phagocytosis, there is a well-documented increase in anti-inflammatory cytokines transforming growth factor β (TGF-β) and IL-10 (162, 184, 185). This occurs in combination with a decrease in pro-inflammatory mediators (TNFα, IL-6, CXCL-8, IL-12, IL-23, PGE_2, leukotriene C4, thromboxane B2) and antimicrobial factors (ROS and NO) (162, 184-193). In addition to anti-inflammatory factors, resolution processes also trigger the release of vascular endothelial growth factor (VEGF) and other growth factors that are critical to repair (130). However, many of the soluble mediators of resolution also decrease antimicrobial defenses of phagocytes, which may promote pathogen

persistence (194, 195). Consequently, the timing of resolution events is crucial for the outcome: initiation too early may prolong infection and delayed initiation may cause excess damage to host tissues.

1.3.4. Soluble mediators of acute inflammation and resolution

Cytokines are small, soluble immune mediators that are important in cell signaling. Broadly, these mediators can be classified into interleukins (lymphokines and monokines), interferons, colony stimulating factors and chemokines, each with specific roles within an immune response. A wide range of cells produce cytokines, including leukocytes, endothelial cells, fibroblasts, and stromal cells. While numerous cytokines are involved in mediating acute inflammatory and subsequent resolution responses, for the purposes of this chapter, I will review the mediators that are studied throughout this thesis. I will also highlight the fish species these cytokines have been currently identified in. This does not exclude existence of the cytokines in other species.

1.3.4.1. *Chemokines*

Chemokines are a class of around 50 polypeptides that have a conserved tertiary structure (196). They are separated into 4 main classes, depending on the location of key cysteine residues that participate in disulfide binding: C, CC, CXC, CX_3C (196). Chemokines are also identified based on their capacity to promote chemotaxis of leukocytes (197).

1.3.4.1.1. CCL-1

CCL-1 is a small glycoprotein. It is a strong chemoattractant, primarily for monocytes, NK cells, immature B cells and dendritic cells, depending on the expression of its cognate receptor CCR8 (198-200). This chemokine has been linked to several important diseases, including neuropathic pain (201, 202), atopic dermatitis (203), allergy/ allergic asthma (204, 205), and type I diabetes (206)

In goldfish, CCL-1 is stimulated by the presence of recombinant *Trypanosoma carassii* heat-shock protein (HSP) 70 (207), recombinant CSF-1 (36), and recombinant interferon (IFN)-γ (32). The expression patterns of CCL-1 are also affected by seasonal changes and human chorionic gonadotrophin (208).

1.3.4.1.2. CXCL-8 (IL-8)

CXCL-8 (IL-8) was the first chemokine described. It is known for an ability to attract neutrophils (209, 210). CXCL-8 is generated following cleavage of a 20 amino acid leader sequence from a 99 amino acid precursor (211, 212). This protein is then processed extracellularly, resulting in increased activity (211, 212). CXCL-8 and the other CXCL chemokines, in addition to be strong attractants for neutrophils, also induce neutrophil shape change, transient increases in neutrophil intracellular free Ca^{2+} concentration, upregulation of adhesion molecules, formation of bioactive lipids, and respiratory burst induction (213). *In vivo*, this chemokine induces exudation of neutrophils from the plasma and a large accumulation of neutrophils in the injection site (214). Interestingly, the effects of CXCL-8 are unusually long *in vivo*, thought to be due to resistance of inactivation

and binding to matrix glycosaminoglycans (215). CXCL-8 has also been described to be weakly chemotactic for basophils *in vitro*, but not for eosinophils or monocytes (210, 216, 217). While some reports have suggested that CXCL-8 may also attract lymphocytes (218), this has been disputed (219) and is not supported by human studies (220). Binding studies have revealed that there are two receptors for CXCL-8: IL-8R1 (or IL-8RA) and IL-8R2 (or IL-8RB) (127, 221, 222). IL-8R1, the IL-8 selective receptor, is detectable in a variety of cells types, including leukocytes, lymphocytes, and fibroblasts (223). IL-8R2 is restricted to monocytes and myeloid cell lines (223).

CXCL-8 was originally found in culture supernatants of human blood monocytes (209). It has since been found that endothelial cells, fibroblasts, keratinocytes, synovial cells, chondrocytes, epithelial cells, tumor cells, and even neutrophils can produce active CXCL-8 (215, 222). Within these cell types, IL-1 and TNF induce CXCL-8 expression (215, 222). In monocytes and macrophages, CXCL-8 expression can be induced by IL-7, GM-CSF, IL-3, lectins, immune complexes and bacteria, adherence, and changes in oxygen partial pressure (215, 222).

CXCL-8 has been identified in multiple fish species (224-228). Like mammalian CXCL-8, piscine CXCL-8 is a potent chemoattractant for neutrophils (37, 229). Some fish species also express multiple isoforms of CXCL-8. For example, carp have two identified isoforms that have distinct expression patterns; both are chemotactic (230). Rainbow trout have recently been shown to have at least 10 variants (231). In goldfish, similar to CCL-1, CXCL-8 expression is

induced by recombinant *Trypanosoma carassii* heat-shock protein (HSP) 70 (207), recombinant CSF-1 (36), recombinant interferon (IFN)-γ (32), and seasonal changes (208). Expression is reduced by recombinant IL-10 (232). In Arctic char, CXCL-8 expression is induced by *Aeromonas salmonicida* subsp. *achromogenes* (233).

1.3.4.2. *Pro-inflammatory mediators*

1.3.4.2.1. TNF-α

Tumor necrosis factor (TNF)-α is a potent inflammatory cytokine with pleiotropic effects. TNF-α plays a major role in host defense and the initiation of acute inflammation (234) and is largely produced by activated macrophages. TNF-α was originally discovered in 1975 as a cytotoxic factor produced by macrophages (235, 236). In the original descriptions, TNF-α expression was induced by the presence of endotoxin (LPS), resulting in the induction of necrosis in tumor cells (hence the name tumor necrosis factor) (235, 236). TNF-α is primarily produced as a homo-trimeric trans-membrane protein (237, 238). To produce soluble TNF-α, the membrane-bound version is cleaved by the metalloproteinase TNF-α converting enzyme (TACE, also known as ADAM17) (239). Both versions are biologically active (240).

TNF-α expression is induced in response to LPS and other bacterial products, and IL-1. While this cytokine has broad physiological effects, in the immune system it is known to promote chemotaxis of neutrophils, monocytes and macrophages (241, 242), enhance phagocytosis (243-245), and prime cells for ROS

and NO production (246, 247). TNF-α has two cognate receptors- TNFR1 and TNFR2- that trimerize around the ligand (248, 249). TNFR1 is expressed in most tissues and appears to be activated by either the soluble or membrane bound forms of TNF-α (250, 251). TNFR2 is found on immune cells and appears to largely respond to membrane-bound TNF-α (250, 251). While there has been some controversy involving the roles of these two receptors, the prevailing thought is that TNFR1 is the central receptor for signal propagation while TNFR2 plays a smaller role in binding but is involved in redistribution of TNF-α ligand (252-254). However, it has also been reported that ligation of TNFR1 results in apoptosis while TNFR2 ligation results in survival and induction of proliferation (255). There is also evidence that TNFR2 may be involved in activation of T cells (256, 257) and in tumor suppression (258).

Ligation of TNFR results in the recruitment of the adaptor protein TRADD, ultimately resulting in the initiation of 3 potential pathways: activation of NF-κB, activation of MAPK pathways, or activation of apoptotic pathways (253, 259). The NF-κB pathway mediates transcription of proteins involved in cell survival and proliferation, inflammation, and anti-apoptotic factors (260, 261). The MAPK pathways generally promote cell differentiation and proliferation (262). Activation of apoptotic pathways involves signaling through death-domain-containing membrane proteins, resulting in caspase activation (263).

TNF-α has been found in several fish species, including Japanese flounder (264), rainbow trout (265), catfish (266), carp (267), and goldfish (31). In trout, carp and goldfish, multiple isoforms of TNF-α have been reported (31, 267-269).

In fish, TNF-α has been reported to upregulate expression of immune genes including IL-1β and CXCL-8, rapid recruitment of phagocytes, increased phagocytosis, and priming of ROS and NO responses (31, 270, 271).

1.3.4.2.2. IL-1β

The interleukin-1 family consists of 11 cytokines, which are central of the regulation of immune and inflammatory processes (272). Discovery of this family started with studies on fever, leading IL-1 to initially be called "endogenous pyrogen" (273). I will focus solely on IL-1β.

IL-1β is produced largely by myeloid cells (monocytes, macrophages, dendritic cells) (274) and is important in mediating inflammatory responses (275). IL-1β is produced as a pro-peptide that must be cleaved in order to become biologically active. It is currently believed that myeloid cells, following activation by pathogens or pathogen derived factors (ie. PAMPs), induce the expression of pro-IL-1β (276). The pro-form is then cleaved by caspase-1/ IL-1β converting enzyme (ICE), leading to release of active IL-1β (277, 278). Release may be accomplished through a variety of mechanisms, including exocytosis, microvesicular budding, export through specific transporters, or cellular lysis (279). IL-1β is recognized by its cognate receptor IL-1R. The receptor is structurally related to TLR structure and employs similar downstream signaling pathways (280). Binding of IL-1β to IL-1R is competitively inhibited by IL-1 receptor antagonist (IL-1Ra) (281).

IL-1β has a very broad range of physiological effects and targets most cell types in the body (extensively reviewed (272, 274-276)). In terms of inflammatory effects, IL-1β is known to in induce synthesis of lipid mediators such as PGE_2, induce synthesis of thromboxane, promote chemotaxis of T and B cells, enhance basophil histamine release and eosinophil degranulation, upregulate synthesis of type I interferons, and increase expression of leukocyte adherence receptors on endothelial surfaces (272, 274-276, 282). Given its wide range of effects and target cells, it in not surprising that IL-1β has been implicated in a number of pathological conditions, including autoimmune/ auto-inflammatory disease (282, 283), cardiac disease (284), neurodegenerative diseases (285), rheumatoid arthritis (282), and type 2 diabetes (282). It has also become a therapeutic target for various inflammatory conditions.

In fish, IL-1β has been found in various species (286-291). Similar to mammalian IL-1β, fish IL-1β also contributes to inflammatory processes by enhancing antibody responses to *Aeromonas hydrophila* (292) and resistance to *Aeromonas salmonicida* and *Aeromonas hydrophila* (293, 294), enhancing MHCII β chain expression (295), increasing COX-2 expression (295), promoting proliferation (295), and increasing phagocytic responses (294, 295). Other studies have also shown increases in ROS production (294). Similar to other cytokines, certain species of fish possess multiple isoforms of IL-1β. In carp, these transcripts have been termed IL-1β1 and IL-1β2 (286). Both IL-1β1 and 2 are expressed following immune challenge, thought IL-1β1 tends to be more greatly expressed (286).

1.3.4.2.3. IL-12

IL-12 is an important pro-inflammatory involved in both innate and adaptive immune responses (296). The IL-12 family consists of 4 cytokines: IL-12, IL-23, IL-27, and IL-35 (297, 298). Each IL-12 member is a heterodimeric cytokine composed of two separate subunits: an α-chain (p19, p28, and p35) and a β-chain (p40) (297, 299). This section will focus solely on IL-12p70, formed by IL-12p35 and IL-12p40 (300-302).

Macrophages and dendritic cells are the primary producers of IL-12 following activation with PAMPs (296, 303). This signal is further augmented by secondary pro-inflammatory stimuli (ie. TNF- α, IL-6) (302, 304, 305). IL-12 is important for the differentiation of T cell to Th1 cells (298, 303, 306) and also enhances NK responses (307). In addition to activating Th1 and NK responses, IL-12 stimulates the production of TNF-α (308) and reduces the suppression of IFN-γ responses (301).

In fish, IL-12 has received relatively less attention than other cytokines and remains poorly elucidated. Genes for p35 (single gene) and p40 (multiple genes: p40a, p40b, p40c) have been identified in some fish species (309-315). Functional analyses has shown that IL-12 can induce IFN-γ production by rainbow trout head kidney leukocytes (315). More work is still needed to determine the role of fish IL-12 in T cell development.

1.3.4.2.4. IFN-γ

Interferon gamma (IFN-γ) is a pro-inflammatory pleiotropic cytokine with anti-viral properties (316). IFN-γ is an important activator of macrophages, leading to its moniker of 'macrophage activating factor'. The primary producers of IFN-γ are activated Th1 CD4+ cells, CD8+ T cells, and NK cells (317-319), though myeloid cells can also secrete IFN-γ. Activation of cells by IFN-γ produces a variety of effects, including increased antigen presentation and lysosome activity in macrophages, activation of iNOS, differentiation of Th1 cells, promotion of cytotoxic CD8+ and NK activity, promotion of leukocyte extravasation, and induction of increased expression of MHCI and MHCII (320). IFN-γ also augments host defense against a variety of intracellular pathogens besides viruses (*Listeria monocytogenes*, and *Leishmania major*, for example) (321-326). The biological effects of IFN-γ are exerted following binding to its cognate receptor, a heterodimer of IFNGR1 and IFNGR2 (327).

It was first suspected that fish possess IFN-γ after experiments demonstrated the presence of a macrophage activating factor with actions similar to mammalian IFN-γ (328). Since then, IFN-γ has been sequenced in various fish species (32, 35, 329). In goldfish, recombinant IFN-γ has been shown to induce ROS and NO responses, enhance macrophage phagocytosis, and increase expression of pro-inflammatory cytokines (32).

In addition to IFN-γ, goldfish also express another isoform, called IFN-γrel (for IFN-γ related) (34). Similar to IFN-γ, IFN-γrel increases ROS production, though the priming was much shorter in duration than that achieved with IFN-γ (34). Further, IFN-γrel induces a much more potent increase in phagocytosis, iNOS

expression and NO production than IFN-γ does (34). Both IFN-γ and IFN-γrel also increase expression of a number of pro-inflammatory cytokines, though the gene expression patterns of monocytes activated with IFN-γ or IFN-γrel were quite different (34).

1.3.4.2.5. CSF-1

Colony-stimulating factor -1 (CSF-1) or macrophage colony-stimulating factor (M-CSF) is the principal regulator of the survival, proliferation, and differentiation of macrophages and their precursors (330-332). As such, macrophages are the main target for this protein (333-336). Outside of the female reproductive tract, where CSF-1 expression is governed through a separate promoter, the high affinity tyrosine kinase CSF-1 receptor (CSF-1R) is exclusively found in cells of the macrophage lineage (337, 338). As such, CSF-1R expression is an excellent marker for the identification of macrophages and their hematopoietic progenitors (337, 338). Further, it has also been shown that the level of CSF-1R progressively increases from primitive hematopoietic precursors to monocytes and further increases upon terminal maturation to macrophages (335).

Ligation of CSF-1R by CSF-1 promotes proliferation of macrophage progenitor populations and increases expression of several other macrophage differentiation antigens (339-341). In addition, CSF-1 is also a central regulator of macrophage function. It promotes monocyte and macrophage activation through contributions to chemotactic, phagocytic, and killing activities (342-348). Further, it increases production of plasminogen activator (349, 350), prostaglandin E_2 (351),

reactive oxygen (348, 352, 353) and reactive nitrogen intermediates (354, 355), in addition to several cytokines including G-CSF, GM-CSF, IL-1, IL-6, IL-8, IL-18, TNF-α, and interferon (356-363).

In addition to its primary role in the maintenance of macrophage populations and their function, CSF-1 activity is also relevant to other cells and tissues. This has been illuminated by studies of CSF-1R knockout (KO) and $CSf1^{op}/CSf1^{op}$ mice. The latter lacks active CSF-1 production due to a null mutation in the CSF-1 gene-coding region, which results in the generation of a biologically inactive truncated form of the cytokine (364, 365). $CSf1^{op}/CSf1^{op}$ mice have a severe deficiency of tissue macrophages, as well as deficiency in bone-resorbing osteoclasts, absence of teeth, abnormal bone remodeling, and osteopetrosis (364, 365). They also exhibit abnormal breast development, decreased fertility, low body weight, and shortened life-span, which can be largely reversed through expression of CSF-1 or injections with recombinant CSF-1 early during development (364, 365). Importantly, unlike CSF-1R KO models, the $CSf1^{op}/CSf1^{op}$ mouse does not suffer from the confounding effects based on inhibition of IL-34, a ligand that has been recently shown to bind similar regions on the CSF-1R as CSF-1 with similar binding affinity (334). Together, these studies identify CSF-1 contributions to immunity and inflammation, bone metabolism, atherogenesis, lipoprotein clearance, development, and reproduction (331, 334, 335, 366-369).

Because of the broad range of CSF-1 activity, it has served as the basis for several clinical trials aimed at therapeutic antimicrobial applications, and amelioration of autoimmune disorders, cancer and inflammatory diseases (370).

Recombinant human CSF-1 (rh-CSF-1) treatment alone or in combination with other cytokines effectively increased the numbers and activation of monocytes and macrophages, enhanced antibody-dependent cellular cytotoxicity (ADCC) and antibody-independent tumor cell cytolysis, promoted macrophage antimicrobial phagocytic and killing activities, and lowered platelet numbers and cholesterol levels (355, 366, 370). Further, administration of rh-CSF-1also proved effective in the control of invasive fungal infections in patients undergoing bone marrow transplantation, through significant reduction in mortality rates when given in combination with standard antifungal treatments (371). Acute myeloid leukemia (AML) patients have also benefited from CSF-1 treatment, as shown by reduced incidence and shortened duration of febrile neutropenia and thrombopenia following chemotherapy, as well as shortening the period required to finish three courses of intensive consolidation therapy (355).

1.3.4.2.5.a. Evolutionary conservation of CSF-1 and CSF-1R

The CSF-1 / CSF-1R axis has been well conserved across evolution. Among mammals, homologs for CSF-1 have been described in humans, chimpanzees, rhesus monkeys, cattle, dogs, mice, and rats. CSF-1R is also well conserved among higher vertebrates. Homologs for CSF-1R have been described in humans, chimpanzees, rhesus monkeys, cattle, dogs, mice, and rats.

Transcripts for CSF-1 have been identified in birds (372), amphibians (373) and fish (374, 375). CSF-1R has been identified in birds (372) and a number of fish species including zebrafish (376), goldfish (377), rainbow trout (378), Atlantic

salmon (379), pufferfish (380) and the gilthead sea bream (347). Functional characterization of CSF-1 activity has shown similar effects on macrophage systems. In chicken and Xenopus, CSF-1 promoted growth and survival of primary bone marrow-derived cultures (372, 373). In goldfish, CSF-1 macrophage expression was positively modulated by TNFα-2, rgIFNγ but not rgTGFβ (31, 32, 34, 78). *In vitro* macrophage treatment with CSF-1, in turn, increased the expression of IL-8, CCL-1, TNFα-1, TNFα-2, IL-1β1, IL-1β2, IL-12-p35, IL-12-p40, IFN, IL-10, and iNOS A and B (36). It also led to expression of TGF-β at later time points (36). Functionally, goldfish CSF-1 enhances macrophage proliferation and differentiation from hematopoietic precursors, chemotaxis, phagocytosis and production of antimicrobial reactive oxygen and nitrogen intermediates (36, 65, 374). *In vivo*, goldfish CSF-1 administration led to an increase in the number of circulating monocytes in the bloodstream (379).

Despite the functional similarities observed when comparing goldfish CSF-1 with mammalian CSF-1 (36), goldfish CSF-1 varies from its mammalian counterpart in a number of ways. Goldfish CSF-1 is composed of 199 amino acids making it significantly smaller than the secreted glycoprotein or the secreted/matrix bound proteoglycan form of mammalian CSF-1, and most similar to the membrane bound glycosylated form of the molecule (381). Interestingly, all mammalian CSF-1 isoforms were shown to be functional as long as they possessed the first 150 amino acids found in the N-terminal of the CSF-1 protein, the region shown to be required for proper folding (382). This region has the most similarity to goldfish CSF-1.

Non-immunological roles have also been described for CSF-1 in lower vertebrates. In chickens, CSF-1 activity has been linked to the promotion of embryo development (383). In zebrafish, the presence of the *c-fms* gene, which encodes the CSF-1R, contributes to postembryonic pigment patterning through neural crest xanthophore precursor maintenance and development of a population of adult melanocytes (376, 384).

1.3.4.2.5.b. Control of CSF-1 activity

CSF-1 is synthesized by a variety of cell types including endothelial cells, bone marrow stromal cells, osteoblasts, fibroblasts, keratinocytes, thymic epithelial cells, astrocytes, myoblasts, endothelial cells, mesothelial cells, endometrial gland cells and the placenta-trophoblast decidual stroma (335, 366, 385). The normal range for serum CSF-1 concentration is between 150-500 U/mL or 3-8 ng/mL (381, 386-389). Maximum stimulation of CSF-1-mediated proliferation can be observed at 250 pM, but proliferation can be detected at concentrations as low as 1 pM, as is the case for bone-marrow colony-forming cells (390). CSF-1 activity is also well known to increase during inflammatory conditions. Inflammatory cytokines including TNF-α (391), IL-1 (341, 392), IFN-γ (393, 394), and GM-CSF (395) have been shown to up-regulate expression of CSF-1. Activation of endothelial cells, T- and B-lymphocytes, fibroblasts, chondrocytes, and mesangial cells also leads to increased CSF-1 production. Thus, unlike other colony-stimulating factors like G-CSF and GM-CSF, which are primarily expressed during periods of crisis, CSF-1 is ubiquitously expressed under steady state conditions,

can be upregulated dramatically within local microenvironments based on unique physiological requirements, and also serves a critical role during infection and injury. Thus, a number of mechanisms have evolved to effectively control the magnitude and duration of CSF-1 activity.

As with other cytokines, CSF-1 can be regulated though its expression and that of its cognate receptor. Its mRNA also contains AU- rich sequences in the 3' non-coding region that confers transcript instability (396-398). CSF-1 protein has a short half-life and can be effectively cleared through internalization and degradation of ligand-receptor complexes, where CSF-1 receptor-mediated internalization is followed by intracellular destruction of the growth factor (333, 399). The degradation process is partially mediated through the action of the ubiquitin-protein ligase c-Cbl, which is recruited to the plasma membrane upon receptor activation (400-402). Association of c-Cbl with the receptor then leads to ubiquitination, followed by ligand:receptor complex internalization and degradation. Removal of circulating CSF-1 is accomplished primarily through the action of liver and splenic macrophages, which efficiently remove over 90% of the circulating CSF-1, much of the remaining circulating CSF-1 is filtered through the kidney (333, 399).

1.3.4.2.5.c. Identification of a soluble CSF-1 receptor in teleost fish

Insights from the mammalian models described above indicate that CSF-1 activity is tightly controlled through mechanisms regulating gene expression of CSF-1 and its receptor, metabolic processing, receptor-mediated endocytosis, as

well as inhibition of CSF-1R signaling. The original studies into the mechanisms that control the growth of self-renewing macrophage populations in goldfish identified an additional mechanism for the regulation of CSF-1 activity - through the production of a novel soluble form of the CSF-1 receptor (377). In short, goldfish primary macrophages derived from kidney hematopoietic tissues (PKM) had been observed to grow spontaneously *in vitro* in response to endogenous macrophage growth factors (29, 403, 404). Preliminary examinations suggested the presence of a CSF-1-like molecule in culture supernatants. Analysis of 26,000 clones from two PKM cDNA libraries yielded the CSF-1 membrane-bound receptor transcript (377). Interestingly, we also identified a unique transcript encoding only for the ligand-binding portion of the CSF-1R. Sequence analysis revealed that this unique transcript was derived from a full-length mRNA species containing a start codon, signal peptide, stop codon, poly-adenylation signals, and a poly-A tail. This short transcript was preferentially expressed during a period of PKM development associated with a decrease in proliferation and differentiation events, decreased growth factor activity in culture supernatants, and marked phenotypic changes that culminated in apoptotic cell death (the senescence phase of PKM development) (377, 403).

Protein expression of the unique transcript in an insect-based system confirmed that it encoded for a soluble form of the CSF-1R (sCSF-1R), which inhibited PKM proliferation at nanomolar concentrations. Moreover, generation of antibodies against recombinant sCSF-1R identified native sCSF-1R in supernatants of PKM senescent phase cultures, suggesting the presence of an endogenous

mechanism temporally regulating sCSF-1R release during goldfish macrophage development. Further, the native protein was detected in goldfish serum (377), which suggested that this protein might also play a role in systemic regulation in addition to its role in regulating proliferation within the hematopoietic compartment.

1.3.4.2.5.d. Molecular characterization of CSF-1-sCSF-1R interactions

Unlike mammalian macrophages which rely on other cells to produce CSF-1 (405), goldfish monocytes and macrophages are capable of producing CSF-1 themselves. CSF-1 then acts in an autocrine fashion, inducing further proliferation and differentiation of myeloid cells (374). The teleost approach to myeloid proliferation and differentiation implies that a unique regulatory process must exist in fish to properly control myelopoiesis. This regulatory role was the initial function hypothesized for the soluble CSF-1 receptor (sCSF-1R). As described above, functional assessments supported the idea that sCSF-1R negatively regulated myelopoiesis. Addition of the soluble receptor to early myeloid cultures abrogated proliferation and differentiation of monocytes and macrophages induced by cell conditioned medium-induced or recombinant goldfish CSF-1 *in vitro* (377). Furthermore, this inhibitory effect on myelopoiesis was also observed when recombinant goldfish CSF-1 (rgfCSF-1) action was blocked using an anti-gfCSF-1 polyclonal antibody (374). Both of these myelopoiesis-blocking mechanisms derive from a prevention of proper CSF-1 function.

Cross-linking studies demonstrated that goldfish CSF-1 forms a dimer under native conditions, and that this dimer is recognized by the soluble CSF-1 receptor (374). Although the mechanism by which CSF-1 function is prevented by sCSF-1R is currently unknown, the soluble receptor possesses the relevant binding regions for CSF-1 interaction. Thus, the current working hypothesis describes a competitive model where sCSF-1R interacts with CSF-1, preventing CSF-1 from properly engaging the cell surface form of the CSF-1R, thereby disrupting CSF-1 signaling and downstream effects on teleost macrophages. Overall, the presence of CSF-1, CSF-1R, and sCSF-1R in goldfish provides an opportunity for the establishment of a control loop for the regulation of macrophage numbers (Figure 1.2).

1.3.4.3. *Anti-inflammatory/ resolution mediators*

1.3.4.3.1. TGF-β

TGF-β is a member of a cytokine/ growth factor superfamily with at least 40 members (406). There are currently 3 known isoforms in mammals: TGF-β1, TGF-β2, and TGF-β3. While these three isoforms have partially overlapping functions, they are produced within distinct tissues by different cells types (407). TGF-β is secreted in a latent form, complexed with latent TGF-β binding protein (LTBP) and latency-associated protein (LAP) (407). LAP is necessary for TGF-β secretion, prevents engagement of TGF-β with its cognate receptors, and maintains a readily accessible extracellular store of TGF-β (408). LTBPs are thought to maintain proper folding of TGF-β and target it to extracellular structures (407). Dissociation

of TGF-β from the latency complex is thought to involve proteolytic and non-proteolytic processes and interactions with various cells (408-411). TGF-β binds a complex of multiple TGF-β serine/threonine kinase receptor chains (412-414), leading to signaling through the SMAD pathway (415). This pathway is complex and likely varies across cell types and activation states, allowing the wide array of TGF-β responses to occur.

In the immune system, TGF-β has a complex role, dependent on concentration, target cell type, activation/ differentiation state of the target cell, and the milieu of soluble factors. TGF-β has been shown to inhibit proliferation and induce apoptosis in lymphocytes (407, 416). It is also important in downregulating NK cell activity and IFN-γ production (417, 418). Further, TGF-β inhibits naïve T cell responses, while inhibiting functions of only Th1 memory T cells (419). Another potential mechanism by which TGF-β decreases Th1 responses is through the enhancement of CD4+Foxp3+ T-regulatory cells (420). TGF-β also induces antibody class switching and maturation of B cells (421).

TGF-β also has numerous roles on phagocytes. In dendritic cells, it has been shown to affect antigen presentation ability, decrease MHC class II expression, affect differentiation, and reduce IL-1β and TNF-α expression (422). In monocytes, TGF-β is thought to drive cells towards an alternatively activated/M2/ myeloid suppressor cell state of activation (423). In the macrophage populations, TGF-β ablates ROS and NO production, reduces binding of TNF-α and IFN-γ by decreasing receptor expression, and reduces antimicrobial responses (246, 424, 425). Finally, TGF-β1 knockout mice have an excessive inflammatory response,

extensive organ infiltration by macrophages and lymphocytes, and cardiopulmonary complications (426-429). In addition, these mice also tend to develop severe autoimmune diseases (430, 431), pointing to the importance of this cytokine. TGF-β2 and TGF-β3 knockout mice have severe developmental defects that result in death (432).

Interestingly, TGF-β also has some pro-inflammatory functions, especially at low concentrations. Resting monocytes have been shown to upregulate expression of IL-1β, TNF-α, and IL-6 following treatment with TGF-β (433-435). However, the addition of LPS diminishes these responses (436, 437). TGF-β has also been shown to be chemotactic at low doses to both monocytes and neutrophils (434, 435, 438, 439), and has been shown to not affect phagocytic responses (440).

In fish, TGF-β was first identified in trout (288, 441, 442), and has subsequently been found in other species, including carp (443), sea bream (444), striped bass and hybrid tilapia (445), and goldfish (78). In goldfish, recombinant TGF-β has been shown to decrease NO responses in macrophages and induce proliferation of a fibroblast cell line (78).

1.3.4.3.2. IL-10

IL-10 is an anti-inflammatory cytokine that is central to preventing pathologies due to inflammation and autoimmune diseases (446-448). This includes inflammatory-induced pathologies caused by a variety of infections (ie. *Mycobacterium*, *Toxoplasma gondii*, and viral infections) (449-457). Because of its potent effects on inflammatory responses, several pathogens induce IL-10 as an

immune evasion mechanism (456, 458-460), which generally leads to increased pathogen accumulation, decreased killing, and enhanced growth of infiltrating pathogens (461-463). IL-10 knockout mice highlight the importance of this cytokine in regulating immunity; these mice develop inflammatory bowel disease in response to their natural flora and have an exaggerated response to microbial challenges (464).

IL-10 production is induced in macrophages and dendritic cells *in vitro* following activation with certain PAMPs (465-468). *In vivo*, it has been shown that dendritic cells, macrophages, neutrophils and various lymphocytes (Th1,Th2, Th17, Treg, B cell) populations can produce IL-10 (457, 469-473). Eosinophils, epithelial cells, keratinocytes, mesangial cells, NK cells and tumor cells can also produce IL-10 (474). It is generally thought that IL-10 acts predominantly on monocyte lineage cells, which then alter responses of other cells (ie. lymphocytes) through changing expression patterns of various monocyte lineage-derived cytokines, primarily TNF-α (465, 475-478). IL-10 has also been shown to decrease macrophage ROS and, to a lower extent, NO responses (475, 478) and decrease expression of MHCII (479). To induce signaling, IL-10 forms a homodimer (480, 481) that binds to a receptor complex consisting of a ligand binding (IL10R1) and accessory receptor subunit (IL10R2) (482-485). This results in signaling through the Jak-Stat pathway (486).

In fish, IL-10 has been identified in puffer fish (487), trout (488), zebrafish (489), carp (490), goldfish (232), sea bass (491), and cod (492). In goldfish, recombinant IL-10 has been shown to decrease gene expression of TNF-α1, TNF-

α2, IL-1β1, IL-10, CXCL-8, and NADPH oxidase component p47 in activated monocytes, combined with a large increase in suppressor of cytokine signaling-3 (SOCS3) gene expression (232). In splenocytes, recombinant IL-10 reduced IFN-γ expression (232). Finally, pre-treatment with IL-10 diminished monocyte ROS responses to *Aeromonas salmonicida* (232).

1.3.4.3.3. Vascular endothelial growth factor (VEGF)

Vascular endothelial growth factor (VEGF) is one of the most potent inducers of angiogenesis (493). This family contains multiple members: VEGF-A, VEGF-B, VEGF-C, VEGF-D, and placenta growth factor. VEGF-A is the most well known of the family and will be the focus of this section. VEGF-B is important in preventing apoptotic cell death, maintaining newly formed blood vessels (494-496). VEGF-C and VEGF-D are important for lymphangiogenesis (the process by which new lymphatic vessels are formed) (497-499). Placenta growth factor is important to embryogenesis (500, 501).

VEGF-A is produced by macrophages following activation with pro-inflammatory agonists (502-505). This protein increases vascular permeability, stimulates angiogenesis, and enhances neutrophil and monocyte recruitment (506-509). Because of these properties, VEGF may be considered a mediator of inflammation, and increased expression is linked to a number of diseases including obesity, autoimmunity, and cancer (510). However, in spite of its involvement in inflammatory processes, it is included in this section because it is an integral part of wound healing (511). Binding of VEGF-A to its cognate receptor VEGFR1 or

VEGFR2 causes receptor dimerization, resulting in trans-phosphorylation and signaling (512, 513).

In fish, VEGF-A has been found in zebrafish (514), where it is also important for angiogenesis (515). A sequence has also been identified in trout, though this has not yet been published (Raino, J., unpublished; gene accession number AJ17301).

1.3.4.3.4. Suppressor of cytokine signaling 3 (SOCS3)

Tight control of cytokine release and responses is necessary for immune defenses, appropriate activation and differentiation of immune cells, and prevention of inflammation-induced pathologies (516). Members of the suppressor of cytokine signaling (SOCS) family are key to this process through their regulation of STAT signaling pathways (517). This family consists of 8 members (SOCS1, SOCS2, SOCS3, SOCS4, SOCS5, SOCS6, SOCS7, and CIS (cytokine-inducible SH2 protein) (517). There are four main mechanisms by which SOCS can inhibit signaling: [1.] block recruitment of STATs to the cytokine receptor by masking STAT binding sites; [2.] target proteins for degradation via ubiquitination; [3.] bind JAKs, inhibiting their kinase; and [4.] target JAKs for degradation (518).

In vivo, loss of SOCS3 has dramatic effects on placental development and inflammation. SOCS3 knockout mice are embryonic lethal, due to increased STAT and MAP kinase activity (519, 520). As such, various Cre models have been employed to study this gene *in vivo* (reviewed in (516)). These studies have shown that loss of SOCS3 results in severe inflammatory disease (521).

In fish, SOCS3 has been identified in zebrafish (522), fugu (522), trout (523), three-spined stickleback (524), Japanese medaka (524), channel catfish (525), and carp (526). While studies still need to be done on the function of SOCS3 in regulating inflammatory responses in fish, in zebrafish SOCS3 has been shown to be important in nerve regeneration (527, 528) and in the modulation of the somatotrophic axis (529).

1.3.5. *Aeromonas* spp.

1.3.5.1. *Aeromonas* species: overview of genus

Aeromonads are ubiquitous pathogens known to cause disease in poikilothermic and homeothermic animals (530). From 1943, when the genus *Aeromonas* was created, to the mid-1970's, aeromonads were classified into two main groups based on growth characteristics and biochemical features (531). The fist group, the mesophilic group, contained motile isolates that grew well between 35-37^{o}C and caused disease in humans. The second group, the psychrophilic group, contained non-motile isolates that grew optimally between 22-25^{o}C and caused disease in fish. From the mid-1970's to mid-1980's, there was significant interest to redefine the groups based on DNA relatedness, leading to the creation DNA hybridization groups (HG) (532). These hybridization groups were represented by reference strains and each was given a number (eg. *A. hydrophila*= HG1). This lead to the creation of 12 HG's, containing both defined and unnamed species of *Aeromonas* (532), which were then separated by phenotypic markers leading to the proposal of new species (533).

Since the advent of DNA sequencing in the 1980's, there has been a 450% increase in the number of published, valid bacterial species (534). A similar trend in growth has occurred within the *Aeromonas* family, with 7 new species being described since 2002. Currently, there at 24 published *Aeromonas* species, though not all of these are recognized in 'Bergey's Manual of Systemic Bacteriology' (535). Of these, this chapter will focus on diseases caused by *A. salmonicida*, *A. hydrophila*, and *A. veronii*. All three of these species are known to cause disease in fish, with *A. salmonicida* being the predominant isolate from fish infections (535). Further, *A. hydrophila* and *A. veronii* bv. *sobria*, with *A. caviae*, cause the majority of human diseases, found in greater than 85% of human diseases attributed to aeromonads (536).

1.3.5.2. *Aeromonas* infections in fish

Of the identified *Aeromonas* species, several have been isolated from fish. The most common reported are *A. veronii* bv. *sobria*, *A. bestarium*, *A. salmonicida*, *A. hydrophila*, *A. sobria*, *A. encheleia*, *A. allosaccharophila*, and *A. jandaei* (537). Of these isolates, all *A. hydrophila* and *A. bestarium* isolates, and most *A. salmonicida* and *A. veronii* isolates were found to be pathogenic in carp, causing septicemia (537). Furthermore, the dominant isolate found in carp (*A. veronii* bv. *sobria*) was isolated from both healthy and diseased fish (537). *Aeromonas* has been shown to be the causative agent of furunculosis in fish, a worldwide disease (reported in Scotland, France, Norway, Iceland, Spain, United States of America, Canada, Japan, Chile, and Australia) (538-542). *Aeromonas* infections in fish have

caused large economic losses to the aquaculture sector due to mass fish death (538-542).

Furunculosis is one of the oldest documented fish diseases, first described in 1894 by Emmerich and Weibel (originally named *Bacillus salmonicida, Bacterium salmonicida, Bacterium trutta*) (543, 544). Further, it was the first fish disease that demonstrated Koch's postulates (540, 542). While furunculosis was originally thought to only affect salmonids, it has since been characterized in a variety of fish species including Atlantic cod, halibut, turbot, Artic char, lamprey, carp, goldfish, and eel (539-542, 545-547). Common early symptoms of *Aeromonas* infection include lethargy, decreased appetite, and skin hyperpigmentation. As the infection progresses, fish may then develop furuncules or ulcers, exophthalmia, septicaemia, petequia, anemia, ascites, and haemorrhages in the muscle, gills, fins, nares, vent and internal organs (540-542). However, not all infected fish develop furuncles and may not even show clinical signs of infection (539). Healthy carrier fish can pose particular problems in aquaculture, as they are able to shed *Aeromonas* into the water at a high level (10^5-10^6 CFU/fish/hour) (539, 541, 542). It is estimated that up to 80% of farmed trout carry *Aeromonas* (548). Outbreaks of furunculosis tend to occur under stressful conditions (change in water temperature, poor water quality, improper handling) or during spawning season (539, 541, 542, 548).

In goldfish, *Aeromonas* infections are known as 'goldfish ulcer disease', with the dominant species studied being *Aeromonas salmonicida* subsp. *salmonicida* (543, 544). This disease was first described in 1969 (549). It has been shown that *A. salmonicida* preferentially binds to mucus and dead/damaged cells of the dermis

(543, 544). As the infection progresses, the infected area begins to appear white, followed by hemorrhages beneath the scales (543, 544). This is followed by sloughing of the scales, necrosis of the dermis, and degeneration of the muscles (543, 544). There is also a marked infiltration of leukocytes to the site if infection (acidophilic, basophilic, and heterophylic granulocytes, lymphocytes, monocytes and macrophages) that is maintained for at least 21 days (543, 544). Septicemia is most likely to occur in fish with well-developed lesions (543, 544). Finally, the causative bacteria are most easily isolated from the peripheral margins of the lesions (543, 544).

1.3.5.2.1. Transmission of Aeromonas

Aeromonas infections are generally transmitted horizontally either through physical contact or the shedding of bacteria into the water column (550, 551). Large aggregations of fish in pools, including in fish farms, may aid in transmission of the bacteria (552). Furunculosis can also be transmitted through ingestion of salmon (543, 544). There is also evidence of perbranchial and percutaneous routes of infection (553, 554). Goldfish developed ulcers following exposure to *Aeromonas* in the water or after scarification (removal of a patch of scales and swabbing exposed dermis) (543, 544). Removal of mucus also aids in infection (543, 544). The importance of these steps if highlighted by Takahashi *et al* (1975) (555) who showed that the most severe goldfish ulcerative disease occurred in fish whose dermis had been eroded by ectoparasites or handling.

Aeromonas can also be dispersed at least 100 cm in aerosolized droplets, allowing spread between nearby bodies of water (556). While *Aeromonas* is present within the ovaries and testes of infected fish, there is currently no evidence supporting vertical transmission of this pathogen.

1.3.5.2.2. Identification of Aeromona*s species*

Correct identification of causative agents of ichthyopathology is essential for determining the etiology of disease and for establishing appropriate treatment. In *Aeromonas* outbreaks, it is essential that this process be fast and reliable to minimize the impact of the infection. Phenotypic and biochemical methods of identification allow discrimination between three main groups: the "Aeromonas hydrophila complex" (*A. hydrophila, A. bestarium, A. salmonicida, A. popoffii*), the "Aeromonas caviae complex" (*A. caviae, A. media, A. eucrenophila*), and the "Aeromonas sobria complex" (*A. sobria, A. veronii, A. jandaei, A. trota*) (557-562). Generally, *Aeromonas* species are characterized phenotypically as a Gram-negative bacilli that can grow at 0% sodium chloride but not 6%; they are generally cytochrome oxidase positive, ferment glucose, and do not produce acid from inositol (557-562). For a comprehensive review of biochemical and phenotypical properties of *Aeromonas* species, please reference Abbott, S.L. *et al* (2003) (558).

Most identification is now done by PCR and sequence analysis, with 16S rRNA, *gyrB*, and *rpoD* most commonly used in these analyses. Importantly, these techniques can be used to identify *Aeromonas* species in bacterial cultures, from

various fish tissues (kidney, spleen, blood, feces, skin, liver, intestine), and from the water (537, 538, 546, 548, 562-564).

1.3.5.2.3. Control of Aeromonas *infections in fish*

Since aeromonads are able to infect a wide variety of hosts from diverse habitats, this pathogen is found ubiquitously throughout the environment. In aquaculture, the most significant risks of infection are associated with migration of anadromous fish into aquaculture water supplies, infected fish culture stations near uncontaminated stations, and sharing of equipment or personnel between stations (565). Main mechanisms to prevent disease include ultraviolet irradiation or ozonation of incoming water, fallowing of net pen sites, and education of personnel (566-568). Topical disinfections and antibiotic regimens have also been shown to prevent or minimize disease (569). Intraperitoneal immunization with *Aeromonas salmonicida* emulsified in oil adjuvants or water has been shown to provide long-lasting protection and may induce immunity in water temperatures as low as 2^{o}C (570, 571). This is of particular importance to fisheries in colder climates. However, the mineral oil vaccine may produce an increased degree of adhesions between internal organs and the abdominal wall near the site of injection, which may decrease growth rate (572). While vaccination is only currently done with *A. salmonicida*, it is thought that immunization of fishes with other *Aeromonas* strains may also be realistic (573). There is also a range of treatment options available, depending on the species of fish.

1.3.5.3. *Aeromonas* in other organisms

In humans, *Aeromonas* infections fall into four broad categories: [1.] gastrointestinal tract disorders; [2.] wound and soft tissue infections; [3.] blood-borne disease; and [4.] a miscellaneous category of the less frequently encountered syndromes (535). The scope of the infections in humans caused by aeromonads is quite broad, ranging from mild disorders such as acute gastroenteritis, to life-threatening disorders like septicemia, necrotizing fasciitis, and myonecrosis (574). Other, less frequent infections include intra-abdominal problems (peritonitis), ocular disease, bone and joint infections, respiratory infections, and urogenital infections (535). Spikes in *Aeromonas* infections are common following natural disasters. For example, following the 2004 tsunami in Thailand, of the 305 survivors with skin and soft tissue infections, *Aeromonas* was the most commonly identified pathogen, making up over 20% of the 614 isolates identified (575). There are also increases in *Aeromonas* infections that coincide with warmer times of year (spring, summer) when water temperatures elevate, likely allowing increased concentrations of *Aeromonas* in freshwater environments and domestic water supplies (576, 577). It has been noted that 40-67% of extra-intestinal *Aeromonas* infections (ie. septicemia) occur in the summer season (578-580). However, immune-compromised individuals and trauma patients are at the greatest risk for *Aeromonas* infections, with healthy individuals having a comparatively low infection and mortality rate (535).

In addition to fish and humans, aeromonads are commonly isolated from other vertebrate and invertebrate hosts. For example, a recent study found

Aeromonas within the gastrointestinal tracts of 5-10% of healthy sheep, cattle and horses (581). Infections in other animals range from ulcerative stomatitis in snakes and lizards, 'red leg' disease in frogs, septicemia in dogs, septic arthritis in calves, seminal vesiculitis in bulls, and a variety of diseases in seals (582-584).

It has recently been found that *Aeromonas* is one of two microbial species found within the intestinal tract of medicinal leeches (585, 586). Using this model, several classes of genes involved in intestinal colonization have been identified, including bacterial cell surface modifications, regulatory factors, amino acid and phosphate transporters, and genes involved in a type III secretion system (T3SS) (586). Further, genetic manipulations of *Aeromonas veronii* have identified genes encoding Braun's major outer membrane lipoprotein or a gene encoding a cytoplasmic membrane component of a T3SS result in a 10,000- to 25,000-fold decrease in colonization (586, 587). Seven other colonization mutants have also been identified, though the genes involved resulting in this phenotype are currently unknown (586), and may potentially allow the uncovering of other genes involved in colonization of gastrointestinal tracts of susceptible hosts.

1.3.5.4. Immune evasion and infection strategies of *Aeromonas* species

Murine studies have shown that most *Aeromonas* strains are poorly phagocytosed by a macrophage cell line (588). Of the 26 strains studied, *A. veronii* and *A. hydrophila* were among the least efficiently phagocytosed (588), even though aeromonads induce high levels of pro-inflammatory cytokines known to increase phagocytic responses, namely TNF-α, IL-1β, and IL-6 (589). When the

internalized bacteria were studied using a killing assay, it was found that internalized bacteria replicate within the macrophage cells for 3 hours post-infection in 31% of strains studied, suggesting aeromonads possess evasion mechanisms against intracellular killing processes (588). This may be due to the expression of catalase genes, which protect against reactive oxygen killing mechanisms and are necessary for proliferation and persistence within the intestinal tract of the medicinal leech (590). Further, *Aeromonas veronii* is known to induce apoptosis in murine macrophages (591), which may be another evasion mechanism.

Through studies of human wound infections, it is currently thought that infection requires local attachment, followed by degradation of tissues, and invasion into deeper tissues (535). This process may be aided by severe inflammation at the site of infection. *Aeromonas* species have been shown to have an elaborate range of microbial proteases, such as metalloproteases, serine proteases, and aminopeptidases, that can degrade proteins found in serum and connective tissues (ie. albumin, fibrinogen, elastin, collagen) (592-595). While this degradation promotes tissue invasion, it also provides essential energy sources for replication (535). Depletion of nutrients within a local area creates a protein density gradient, with protein concentration increasing away from the area of colonization. Most aeromonads are extremely chemotactic towards amino acids, proteins, and mucins (595), and such chemotactic responses trigger rapid migration into subcutaneous tissues in motile aeromonads.

Aeromonads also posses a wide range of enterotoxigenic factors that fall into

broad categories of cytolytic toxins with hemolytic activity and cytotonic enterotoxins (596, 597). The best characterized is the pore forming toxin β-hemolysin, also called Bernheimer's aerolysin, found in *A. hydrophila*, *A. veronii*, and other species (598, 599). A second family of β-hemolysins, similar to HlyA hemolysin of *Vibrio cholerae*, has been found ubiquitously expressed in *A. hydrophila*, as well as in *A. veronii* (12%) (599, 600). Finally, *Aeromonas* also express Act, a cytotoxic enterotoxin. This toxin is a type II secreted pore-forming toxin with hemolytic activity (601). Act has also been shown to induce elevated levels of TNF-α, IL-1β, and IL-6 (602). In terms of cytotonic enterotoxins, at least two have been identified: heat-labile Alt and heat-stable Ast (601). In *Aeromonas veronii*, a vacuolating toxin has been identified that appears to be a non-hemolytic serine protease that induces apoptosis (603). *Aeromonas* species have also been reported to express invasins, though only a fraction of strains are characterized as invasive within the intestinal system (604). Finally, *A. veronii* possess a type III secretion system (T3SS) that aids in colonization in the medicinal leech (586). The *A. veronii* T3SS has been shown to inactivate innate immune cells in a highly localized manner (587). It is thought that AexU and AexT, two ADP-ribosylating toxins and effectors of the T3SS, impart these effects (605, 606). Both these toxins have been shown to be necessary for virulence in mice and fish, respectively. Both these effectors have been identified in *A. veronii* (607).

When isolates from human septicemia were further analyzed, it was discovered that 90% of infections are caused by a small subset of genospecies (608). Studies have shown that bacteria most associated with blood-borne disease

belong to specific sero-groups: O:11, O:16, O:18, and O:34, implying LPS structure and O-antigens are important to systemic disease (608). Further, the most bacteremic *Aeromonas* isolates are resistant to the lytic effects of complement (608-610). This may be due to the LPS architecture or the possession of S layers (608-610). Resistance to complement lysis has been linked to rapid degradation of complement component C3b, preventing formation of the membrane attack complex (609, 610).

1.4. Summary

Inflammation is an important part of host defense, necessary for wound healing and defense against pathogens. This process, however, must be tightly regulated in order to prevent immune-mediated injury to host tissues while still permitting clearance of pathogenic insults. Phagocytes are central to this process and are involved in both the initiation and resolution of inflammatory processes. Depending on the encountered stimuli, phagocytes interface with leukocytes, directing responses through a variety of mechanisms, including the production of soluble mediators. While this process is fairly well understood in mammalian models, there is currently limited knowledge on these responses in lower vertebrates. By examining unique mechanisms of inflammatory control employed by teleost macrophages, we will gain important knowledge on the evolution of host defenses. Further, utilizing these models may allow us to discover novel mechanisms that may be unique to teleosts or not yet identified in mammals, allowing a deeper understanding of the immune system.

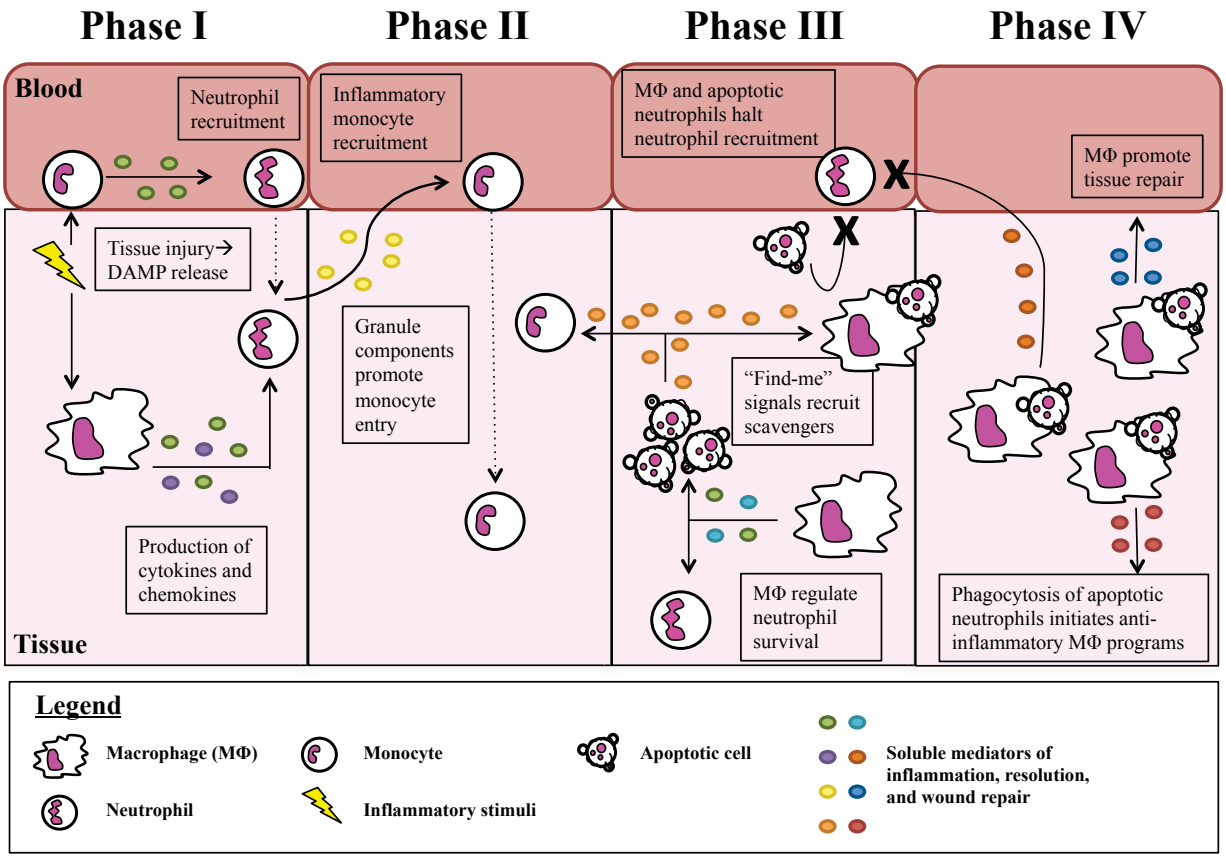

Figure 1.1. Roles of phagocytes in the acute inflammatory response.

Partnerships between phagocytes are integral to the proper initiation and resolution of an acute inflammatory response. Reponses are initiated following the sensing of damage or danger by resident tissue macrophages and patrolling monocytes in the blood. Soluble factors produced by these cells recruit and promote extravasation of neutrophils. Activation of the neutrophil armamentarium leads to release of granule contents, promoting recruitment of inflammatory monocytes. Macrophages, neutrophils, and monocytes all work to control the infection/ remove the cause of tissue damage. As the process beings to resolve, macrophages induce neutrophil apoptosis. Apoptotic neutrophils produce "find me" signals that recruit monocytes and macrophages, leading to recognition of "eat me" signals and subsequent phagocytosis of apoptotic neutrophils. This initiates anti-inflammatory and tissue/wound repair programs that promote resolution of inflammation and a return to homeostasis.

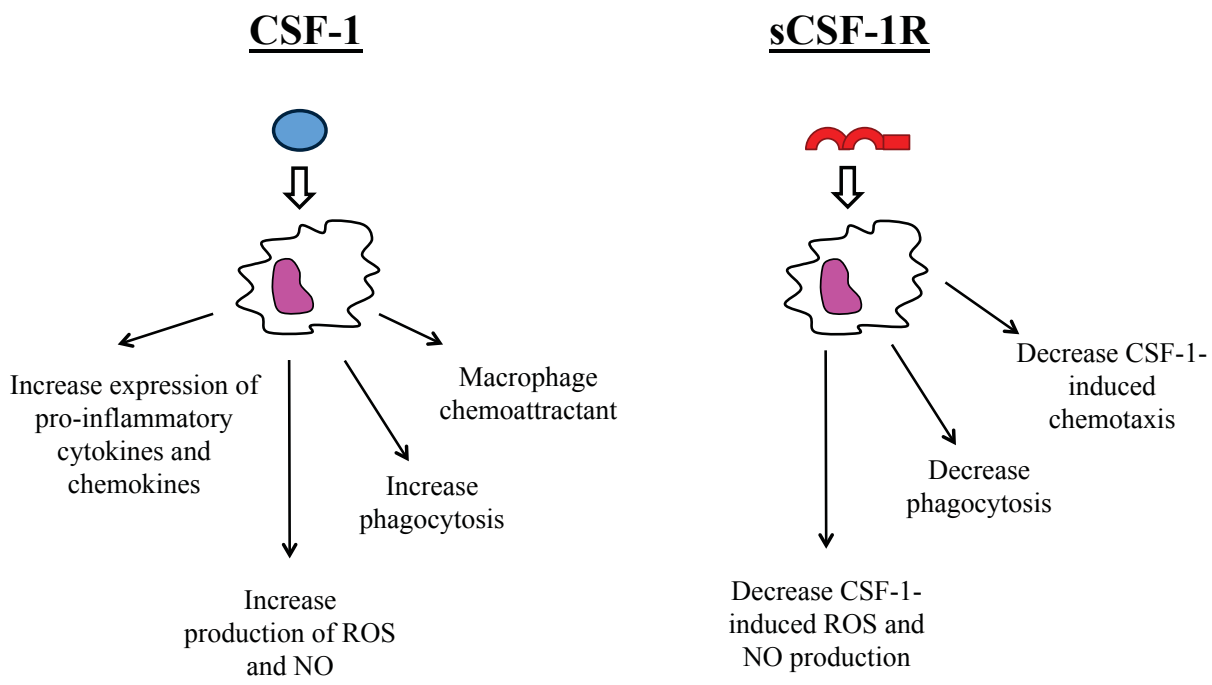

Figure 1.2. Known effects of CSF-1 and sCSF-1R on goldfish macrophage inflammatory responses.

CSF-1 is known to be an important regulator of macrophage survival, proliferation, and differentiation. This figure highlights the effects of CSF-1 and a novel teleost receptor- soluble CSF-1R- on the regulation of inflammatory processes in cultured goldfish macrophages.

1.5. References

1. Silva, M.T. 2009. When two is better than one: macrophages and neutrophils work in concert in innate immunity as complementary and cooperative partners of a myeloid phagocyte system. *J Leukoc Biol*.
2. Morel, F., Doussiere, J., and Vignais, P.V. 1991. The superoxide-generating oxidase of phagocytic cells. Physiological, molecular and pathological aspects. *Eur J Biochem* 201:523-546.
3. Nathan, C.F., and Hibbs, J.B., Jr. 1991. Role of nitric oxide synthesis in macrophage antimicrobial activity. *Curr Opin Immunol* 3:65-70.
4. Stuart, L.M., and Ezekowitz, R.A. 2005. Phagocytosis: elegant complexity. *Immunity* 22:539-550.
5. Faurschou, M., and Borregaard, N. 2003. Neutrophil granules and secretory vesicles in inflammation. *Microbes Infect* 5:1317-1327.
6. Zasloff, M. 1992. Antibiotic peptides as mediators of innate immunity. *Curr Opin Immunol* 4:3-7.
7. Rieger, A.M., Hall, B.E., and Barreda, D.R. 2010. Macrophage activation differentially modulates particle binding, phagocytosis and downstream antimicrobial mechanisms. *Dev Comp Immunol* 34:1144-1159.
8. Cuesta, A., Rodriguez, A., Salinas, I., Meseguer, J., and Esteban, M.A. 2007. Early local and systemic innate immune responses in the teleost gilthead seabream after intraperitoneal injection of whole yeast cells. *Fish Shellfish Immunol* 22:242-251.
9. do Vale, A., Afonso, A., and Silva, M.T. 2002. The professional phagocytes of sea bass (Dicentrarchus labrax L.): cytochemical characterisation of neutrophils and macrophages in the normal and inflamed peritoneal cavity. *Fish Shellfish Immunol* 13:183-198.
10. Palic, D., Ostojic, J., Andreasen, C.B., and Roth, J.A. 2007. Fish cast NETs: neutrophil extracellular traps are released from fish neutrophils. *Dev Comp Immunol* 31:805-816.
11. Cuesta, A., Meseguer, J., and Esteban, M.A. 2008. The antimicrobial peptide hepcidin exerts an important role in the innate immunity against bacteria in the bony fish gilthead seabream. *Mol Immunol* 45:2333-2342.
12. Forlenza, M., Scharsack, J.P., Kachamakova, N.M., Taverne-Thiele, A.J., Rombout, J.H., and Wiegertjes, G.F. 2008. Differential contribution of neutrophilic granulocytes and macrophages to nitrosative stress in a host-parasite animal model. *Mol Immunol* 45:3178-3189.
13. Mulero, I., Noga, E.J., Meseguer, J., Garcia-Ayala, A., and Mulero, V. 2008. The antimicrobial peptides piscidins are stored in the granules of professional phagocytic granulocytes of fish and are delivered to the bacteria-containing phagosome upon phagocytosis. *Dev Comp Immunol* 32:1531-1538.
14. Li, J., Barreda, D.R., Zhang, Y.A., Boshra, H., Gelman, A.E., Lapatra, S., Tort, L., and Sunyer, J.O. 2006. B lymphocytes from early vertebrates have potent phagocytic and microbicidal abilities. *Nat Immunol* 7:1116-1124.

15. Overland, H.S., Pettersen, E.F., Ronneseth, A., and Wergeland, H.I. 2010. Phagocytosis by B-cells and neutrophils in Atlantic salmon (Salmo salar L.) and Atlantic cod (Gadus morhua L.). *Fish Shellfish Immunol* 28:193-204.
16. Zhang, Y.A., Salinas, I., Li, J., Parra, D., Bjork, S., Xu, Z., LaPatra, S.E., Bartholomew, J., and Sunyer, J.O. 2010. IgT, a primitive immunoglobulin class specialized in mucosal immunity. *Nat Immunol* 11:827-835.
17. Parra, D., Rieger, A.M., Li, J., Zhang, Y.A., Randall, L.M., Hunter, C.A., Barreda, D.R., and Sunyer, J.O. 2012. Pivotal advance: peritoneal cavity B-1 B cells have phagocytic and microbicidal capacities and present phagocytosed antigen to CD4+ T cells. *J Leukoc Biol* 91:525-536.
18. Baldridge, C.W., and Gerard, R.W. 1933. The extra respiration of phagocytosis. *Am J Physiol* 103:235-236.
19. Babior, B.M., Kipnes, R.S., and Curnutte, J.T. 1973. Biological defense mechanisms. The production by leukocytes of superoxide, a potential bactericidal agent. *J Clin Invest* 52:741-744.
20. Briggs, R.T., Drath, D.B., Karnovsky, M.L., and Karnovsky, M.J. 1975. Localization of NADH oxidase on the surface of human polymorphonuclear leukocytes by a new cytochemical method. *J Cell Biol* 67:566-586.
21. Robinson, J.M. 2009. Phagocytic leukocytes and reactive oxygen species. *Histochem Cell Biol* 131:465-469.
22. Babior, B.M. 1999. NADPH oxidase: an update. *Blood* 93:1464-1476.
23. Boltana, S., Donate, C., Goetz, F.W., MacKenzie, S., and Balasch, J.C. 2009. Characterization and expression of NADPH oxidase in LPS-, poly(I:C)- and zymosan-stimulated trout (Oncorhynchus mykiss W.) macrophages. *Fish Shellfish Immunol* 26:651-661.
24. Inoue, Y., Suenaga, Y., Yoshiura, Y., Moritomo, T., Ototake, M., and Nakanishi, T. 2004. Molecular cloning and sequencing of Japanese pufferfish (Takifugu rubripes) NADPH oxidase cDNAs. *Dev Comp Immunol* 28:911-925.
25. Mayumi, M., Takeda, Y., Hoshiko, M., Serada, K., Murata, M., Moritomo, T., Takizawa, F., Kobayashi, I., Araki, K., Nakanishi, T., et al. 2008. Characterization of teleost phagocyte NADPH oxidase: molecular cloning and expression analysis of carp (Cyprinus carpio) phagocyte NADPH oxidase. *Mol Immunol* 45:1720-1731.
26. Olavarria, V.H., Gallardo, L., Figueroa, J.E., and Mulero, V. 2010. Lipopolysaccharide primes the respiratory burst of Atlantic salmon SHK-1 cells through protein kinase C-mediated phosphorylation of p47phox. *Dev Comp Immunol*.
27. Kawahara, T., and Lambeth, J.D. 2007. Molecular evolution of Phox-related regulatory subunits for NADPH oxidase enzymes. *BMC Evol Biol* 7:178.
28. Kawahara, T., Quinn, M.T., and Lambeth, J.D. 2007. Molecular evolution of the reactive oxygen-generating NADPH oxidase (Nox/Duox) family of enzymes. *BMC Evol Biol* 7:109.

29. Neumann, N.F., Barreda, D.R., and Belosevic, M. 2000. Generation and functional analysis of distinct macrophage sub-populations from goldfish (Carassius auratus L.) kidney leukocyte cultures. *Fish Shellfish Immunol* 10:1-20.
30. Grayfer, L., and Belosevic, M. 2009. Molecular characterization of tumor necrosis factor receptors 1 and 2 of the goldfish (Carassius aurutus L.). *Mol Immunol* 46:2190-2199.
31. Grayfer, L., Walsh, J.G., and Belosevic, M. 2008. Characterization and functional analysis of goldfish (Carassius auratus L.) tumor necrosis factor-alpha. *Dev Comp Immunol* 32:532-543.
32. Grayfer, L., and Belosevic, M. 2009. Molecular characterization, expression and functional analysis of goldfish (Carassius aurutus L.) interferon gamma. *Dev Comp Immunol* 33:235-246.
33. Zou, J., Carrington, A., Collet, B., Dijkstra, J.M., Yoshiura, Y., Bols, N., and Secombes, C. 2005. Identification and bioactivities of IFN-gamma in rainbow trout Oncorhynchus mykiss: the first Th1-type cytokine characterized functionally in fish. *J Immunol* 175:2484-2494.
34. Grayfer, L., Garcia, E.G., and Belosevic, M. 2010. Comparison of macrophage antimicrobial responses induced by type II interferons of the goldfish (Carassius auratus L.). *J Biol Chem* 285:23537-23547.
35. Arts, J.A., Tijhaar, E.J., Chadzinska, M., Savelkoul, H.F., and Verburg-van Kemenade, B.M. 2010. Functional analysis of carp interferon-gamma: evolutionary conservation of classical phagocyte activation. *Fish Shellfish Immunol* 29:793-802.
36. Grayfer, L., Hanington, P.C., and Belosevic, M. 2009. Macrophage colony-stimulating factor (CSF-1) induces pro-inflammatory gene expression and enhances antimicrobial responses of goldfish (Carassius auratus L.) macrophages. *Fish Shellfish Immunol* 26:406-413.
37. Harun, N.O., Zou, J., Zhang, Y.A., Nie, P., and Secombes, C.J. 2008. The biological effects of rainbow trout (Oncorhynchus mykiss) recombinant interleukin-8. *Dev Comp Immunol* 32:673-681.
38. Forlenza, M., Magez, S., Scharsack, J.P., Westphal, A., Savelkoul, H.F., and Wiegertjes, G.F. 2009. Receptor-mediated and lectin-like activities of carp (Cyprinus carpio) TNF-alpha. *J Immunol* 183:5319-5332.
39. Roca, F.J., Mulero, I., Lopez-Munoz, A., Sepulcre, M.P., Renshaw, S.A., Meseguer, J., and Mulero, V. 2008. Evolution of the inflammatory response in vertebrates: fish TNF-alpha is a powerful activator of endothelial cells but hardly activates phagocytes. *J Immunol* 181:5071-5081.
40. Stafford, J.L., Galvez, F., Goss, G.G., and Belosevic, M. 2002. Induction of nitric oxide and respiratory burst response in activated goldfish macrophages requires potassium channel activity. *Dev Comp Immunol* 26:445-459.
41. Nya, E.J., and Austin, B. 2010. Use of bacterial lipopolysaccharide (LPS) as an immunostimulant for the control of Aeromonas hydrophila infections in rainbow trout Oncorhynchus mykiss (Walbaum). *J Appl Microbiol* 108:686-694.

42. Sepulcre, M.P., Lopez-Castejon, G., Meseguer, J., and Mulero, V. 2007. The activation of gilthead seabream professional phagocytes by different PAMPs underlines the behavioural diversity of the main innate immune cells of bony fish. *Mol Immunol* 44:2009-2016.
43. Cuesta, A., Salinas, I., Esteban, M.A., and Meseguer, J. 2008. Unmethylated CpG motifs mimicking bacterial DNA triggers the local and systemic innate immune parameters and expression of immune-relevant genes in gilthead seabream. *Fish Shellfish Immunol* 25:617-624.
44. Katzenback, B.A., and Belosevic, M. 2009. Isolation and functional characterization of neutrophil-like cells, from goldfish (Carassius auratus L.) kidney. *Dev Comp Immunol* 33:601-611.
45. Ardo, L., Jeney, Z., Adams, A., and Jeney, G. 2010. Immune responses of resistant and sensitive common carp families following experimental challenge with Aeromonas hydrophila. *Fish Shellfish Immunol* 29:111-116.
46. Chaves-Pozo, E., Munoz, P., Lopez-Munoz, A., Pelegrin, P., Garcia Ayala, A., Mulero, V., and Meseguer, J. 2005. Early innate immune response and redistribution of inflammatory cells in the bony fish gilthead seabream experimentally infected with Vibrio anguillarum. *Cell Tissue Res* 320:61-68.
47. Nikoskelainen, S., Kjellsen, O., Lilius, E.M., and Schroder, M.B. 2006. Respiratory burst activity of Atlantic cod (Gadus morhua L.) blood phagocytes differs markedly from that of rainbow trout. *Fish Shellfish Immunol* 21:199-208.
48. Serada, K., Moritomo, T., Teshirogi, K., Itou, T., Shibashi, T., Inoue, Y., and Nakanishi, T. 2005. Comparison of respiratory burst activity of inflammatory neutrophils in ayu (Plecoglossus altivelis) and carp (Cyprinus carpio). *Fish Shellfish Immunol* 19:363-373.
49. Sasada, M., and Johnston, R.B., Jr. 1980. Macrophage microbicidal activity. Correlation between phagocytosis-associated oxidative metabolism and the killing of Candida by macrophages. *J Exp Med* 152:85-98.
50. Nakagawara, A., DeSantis, N.M., Nogueira, N., and Nathan, C.F. 1982. Lymphokines enhance the capacity of human monocytes to secret reactive oxygen intermediates. *J Clin Invest* 70:1042-1048.
51. Watson, R.W., Redmond, H.P., and Bouchier-Hayes, D. 1994. Role of endotoxin in mononuclear phagocyte-mediated inflammatory responses. *J Leukoc Biol* 56:95-103.
52. Landmann, R., Scherer, F., Schumann, R., Link, S., Sansano, S., and Zimmerli, W. 1995. LPS directly induces oxygen radical production in human monocytes via LPS binding protein and CD14. *J Leukoc Biol* 57:440-449.
53. Kaplan, J.E., Chrenek, R.D., Morash, J.G., Ruksznis, C.M., and Hannum, L.G. 2008. Rhythmic patterns in phagocytosis and the production of reactive oxygen species by zebrafish leukocytes. *Comp Biochem Physiol A Mol Integr Physiol* 151:726-730.
54. MacMicking, J., Xie, Q.W., and Nathan, C. 1997. Nitric oxide and macrophage function. *Annu Rev Immunol* 15:323-350.

55. Knowles, R.G., and Moncada, S. 1994. Nitric oxide synthases in mammals. *Biochem J* 298 (Pt 2):249-258.
56. Laing, K.J., Grabowski, P.S., Belosevic, M., and Secombes, C.J. 1996. A partial sequence for nitric oxide synthase from a goldfish (Carassius auratus) macrophage cell line. *Immunol Cell Biol* 74:374-379.
57. Saeij, J.P., Stet, R.J., Groeneveld, A., Verburg-van Kemenade, L.B., van Muiswinkel, W.B., and Wiegertjes, G.F. 2000. Molecular and functional characterization of a fish inducible-type nitric oxide synthase. *Immunogenetics* 51:339-346.
58. Wang, T., Ward, M., Grabowski, P., and Secombes, C.J. 2001. Molecular cloning, gene organization and expression of rainbow trout (Oncorhynchus mykiss) inducible nitric oxide synthase (iNOS) gene. *Biochem J* 358:747-755.
59. Lepiller, S., Franche, N., Solary, E., Chluba, J., and Laurens, V. 2009. Comparative analysis of zebrafish nos2a and nos2b genes. *Gene* 445:58-65.
60. Reddick, J.I., Goostrey, A., and Secombes, C.J. 2006. Cloning of iNOS in the small spotted catshark (Scyliorhinus canicula). *Dev Comp Immunol* 30:1009-1022.
61. Cox, R.L., Mariano, T., Heck, D.E., Laskin, J.D., and Stegeman, J.J. 2001. Nitric oxide synthase sequences in the marine fish Stenotomus chrysops and the sea urchin Arbacia punctulata, and phylogenetic analysis of nitric oxide synthase calmodulin-binding domains. *Comp Biochem Physiol B Biochem Mol Biol* 130:479-491.
62. Barroso, J.B., Carreras, A., Esteban, F.J., Peinado, M.A., Martinez-Lara, E., Valderrama, R., Jimenez, A., Rodrigo, J., and Lupianez, J.A. 2000. Molecular and kinetic characterization and cell type location of inducible nitric oxide synthase in fish. *Am J Physiol Regul Integr Comp Physiol* 279:R650-656.
63. Ordas, M.C., Costa, M.M., Roca, F.J., Lopez-Castejon, G., Mulero, V., Meseguer, J., Figueras, A., and Novoa, B. 2007. Turbot TNFalpha gene: molecular characterization and biological activity of the recombinant protein. *Mol Immunol* 44:389-400.
64. Hanington, P.C., and Belosevic, M. 2007. Interleukin-6 family cytokine M17 induces differentiation and nitric oxide response of goldfish (Carassius auratus L.) macrophages. *Dev Comp Immunol* 31:817-829.
65. Hanington, P.C., Hitchen, S.J., Beamish, L.A., and Belosevic, M. 2009. Macrophage colony stimulating factor (CSF-1) is a central growth factor of goldfish macrophages. *Fish Shellfish Immunol* 26:1-9.
66. Tafalla, C., and Novoa, B. 2000. Requirements for nitric oxide production by turbot (Scophthalmus maximus) head kidney macrophages. *Dev Comp Immunol* 24:623-631.
67. Stafford, J.L., Neumann, N.F., and Belosevic, M. 2001. Products of proteolytic cleavage of transferrin induce nitric oxide response of goldfish macrophages. *Dev Comp Immunol* 25:101-115.

68. Stafford, J.L., Wilson, E.C., and Belosevic, M. 2004. Recombinant transferrin induces nitric oxide response in goldfish and murine macrophages. *Fish Shellfish Immunol* 17:171-185.
69. Haddad, G., and Belosevic, M. 2009. Transferrin-derived synthetic peptide induces highly conserved pro-inflammatory responses of macrophages. *Mol Immunol* 46:576-586.
70. Stafford, J.L., and Belosevic, M. 2003. Transferrin and the innate immune response of fish: identification of a novel mechanism of macrophage activation. *Dev Comp Immunol* 27:539-554.
71. Ford, M.J. 2001. Molecular evolution of transferrin: evidence for positive selection in salmonids. *Mol Biol Evol* 18:639-647.
72. Yang, L., Zhou, L., and Gui, J.F. 2004. Molecular basis of transferrin polymorphism in goldfish (Carassius auratus). *Genetica* 121:303-313.
73. Valenta, M., Stratil, A., Slechtova, V., Kalal, L., and Slechta, V. 1976. Polymorphism of transferrin in carp (Cyprinus carpio L.): genetic determination, isolation, and partial characterization. *Biochem Genet* 14:27-45.
74. Jurecka, P., Irnazarow, I., Stafford, J.L., Ruszczyk, A., Taverne, N., Belosevic, M., Savelkoul, H.F., and Wiegertjes, G.F. 2009. The induction of nitric oxide response of carp macrophages by transferrin is influenced by the allelic diversity of the molecule. *Fish Shellfish Immunol* 26:632-638.
75. Tafalla, C., Figueras, A., and Novoa, B. 1999. Role of nitric oxide on the replication of viral haemorrhagic septicemia virus (VHSV), a fish rhabdovirus. *Vet Immunol Immunopathol* 72:249-256.
76. Campos-Perez, J.J., Ellis, A.E., and Secombes, C.J. 2000. Toxicity of nitric oxide and peroxynitrite to bacterial pathogens of fish. *Dis Aquat Organ* 43:109-115.
77. Forlenza, M., Nakao, M., Wibowo, I., Joerink, M., Arts, J.A., Savelkoul, H.F., and Wiegertjes, G.F. 2009. Nitric oxide hinders antibody clearance from the surface of Trypanoplasma borreli and increases susceptibility to complement-mediated lysis. *Mol Immunol* 46:3188-3197.
78. Haddad, G., Hanington, P.C., Wilson, E.C., Grayfer, L., and Belosevic, M. 2008. Molecular and functional characterization of goldfish (Carassius auratus L.) transforming growth factor beta. *Dev Comp Immunol* 32:654-663.
79. Pietsch, C., Vogt, R., Neumann, N., and Kloas, W. 2008. Production of nitric oxide by carp (Cyprinus carpio L.) kidney leukocytes is regulated by cyclic 3',5'-adenosine monophosphate. *Comp Biochem Physiol A Mol Integr Physiol* 150:58-65.
80. Joerink, M., Savelkoul, H.F., and Wiegertjes, G.F. 2006. Evolutionary conservation of alternative activation of macrophages: structural and functional characterization of arginase 1 and 2 in carp (Cyprinus carpio L.). *Mol Immunol* 43:1116-1128.
81. Saeij, J.P., van Muiswinkel, W.B., van de Meent, M., Amaral, C., and Wiegertjes, G.F. 2003. Different capacities of carp leukocytes to encounter

nitric oxide-mediated stress: a role for the intracellular reduced glutathione pool. *Dev Comp Immunol* 27:555-568.

82. Jutras, I., and Desjardins, M. 2005. Phagocytosis: at the crossroads of innate and adaptive immunity. *Annu Rev Cell Dev Biol* 21:511-527.
83. Delamarre, L., Pack, M., Chang, H., Mellman, I., and Trombetta, E.S. 2005. Differential lysosomal proteolysis in antigen-presenting cells determines antigen fate. *Science* 307:1630-1634.
84. Palic, D., Andreasen, C.B., Menzel, B.W., and Roth, J.A. 2005. A rapid, direct assay to measure degranulation of primary granules in neutrophils from kidney of fathead minnow (Pimephales promelas Rafinesque, 1820). *Fish Shellfish Immunol* 19:217-227.
85. Wernersson, S., Reimer, J.M., Poorafshar, M., Karlson, U., Wermenstam, N., Bengten, E., Wilson, M., Pilstrom, L., and Hellman, L. 2006. Granzyme-like sequences in bony fish shed light on the emergence of hematopoietic serine proteases during vertebrate evolution. *Dev Comp Immunol* 30:901-918.
86. Brinkmann, V., Reichard, U., Goosmann, C., Fauler, B., Uhlemann, Y., Weiss, D.S., Weinrauch, Y., and Zychlinsky, A. 2004. Neutrophil extracellular traps kill bacteria. *Science* 303:1532-1535.
87. Palic, D., Andreasen, C.B., Ostojic, J., Tell, R.M., and Roth, J.A. 2007. Zebrafish (Danio rerio) whole kidney assays to measure neutrophil extracellular trap release and degranulation of primary granules. *J Immunol Methods* 319:87-97.
88. Noga, E.J., Silphaduang, U., Park, N.G., Seo, J.K., Stephenson, J., and Kozlowicz, S. 2009. Piscidin 4, a novel member of the piscidin family of antimicrobial peptides. *Comp Biochem Physiol B Biochem Mol Biol* 152:299-305.
89. Jenssen, H., Hamill, P., and Hancock, R.E. 2006. Peptide antimicrobial agents. *Clin Microbiol Rev* 19:491-511.
90. Casadei, E., Wang, T., Zou, J., Gonzalez Vecino, J.L., Wadsworth, S., and Secombes, C.J. 2009. Characterization of three novel beta-defensin antimicrobial peptides in rainbow trout (Oncorhynchus mykiss). *Mol Immunol* 46:3358-3366.
91. Moritomo, T., Serata, K., Teshirogi, K., Aikawa, H., Inoue, Y., Itou, T., and Nakanishi, T. 2003. Flow cytometric analysis of the neutrophil respiratory burst of ayu, Plecoglossus altivelis: comparison with other fresh water fish. *Fish Shellfish Immunol* 15:29-38.
92. Scharsack, J.P., Steinhagen, D., Kleczka, C., Schmidt, J.O., Korting, W., Michael, R.D., Leibold, W., and Schuberth, H.J. 2003. Head kidney neutrophils of carp (Cyprinus carpio L.) are functionally modulated by the haemoflagellateTrypanoplasma borreli. *Fish Shellfish Immunol* 14:389-403.
93. Leiro, J., Iglesias, R., Parama, A., Sanmartin, M.L., and Ubeira, F.M. 2001. Effect of Tetramicra brevifilum (Microspora) infection on respiratory-burst responses of turbot (Scophthalmus maximus L.) phagocytes. *Fish Shellfish Immunol* 11:639-652.

94. Janeway, C.A., Jr. 1989. Approaching the asymptote? Evolution and revolution in immunology. *Cold Spring Harb Symp Quant Biol* 54 Pt 1:1-13.
95. Matzinger, P. 2002. An innate sense of danger. *Ann N Y Acad Sci* 961:341-342.
96. Matzinger, P. 2002. The danger model: a renewed sense of self. *Science* 296:301-305.
97. Matzinger, P. 2007. Friendly and dangerous signals: is the tissue in control? *Nat Immunol* 8:11-13.
98. Matzinger, P. 2012. The evolution of the danger theory. Interview by Lauren Constable, Commissioning Editor. *Expert Rev Clin Immunol* 8:311-317.
99. Kono, H., and Rock, K.L. 2008. How dying cells alert the immune system to danger. *Nat Rev Immunol* 8:279-289.
100. Lotze, M.T., and Tracey, K.J. 2005. High-mobility group box 1 protein (HMGB1): nuclear weapon in the immune arsenal. *Nat Rev Immunol* 5:331-342.
101. Scaffidi, P., Misteli, T., and Bianchi, M.E. 2002. Release of chromatin protein HMGB1 by necrotic cells triggers inflammation. *Nature* 418:191-195.
102. Rovere-Querini, P., Capobianco, A., Scaffidi, P., Valentinis, B., Catalanotti, F., Giazzon, M., Dumitriu, I.E., Muller, S., Iannacone, M., Traversari, C., et al. 2004. HMGB1 is an endogenous immune adjuvant released by necrotic cells. *EMBO Rep* 5:825-830.
103. Andersson, U., Wang, H., Palmblad, K., Aveberger, A.C., Bloom, O., Erlandsson-Harris, H., Janson, A., Kokkola, R., Zhang, M., Yang, H., et al. 2000. High mobility group 1 protein (HMG-1) stimulates proinflammatory cytokine synthesis in human monocytes. *J Exp Med* 192:565-570.
104. Orlova, V.V., Choi, E.Y., Xie, C., Chavakis, E., Bierhaus, A., Ihanus, E., Ballantyne, C.M., Gahmberg, C.G., Bianchi, M.E., Nawroth, P.P., et al. 2007. A novel pathway of HMGB1-mediated inflammatory cell recruitment that requires Mac-1-integrin. *EMBO J* 26:1129-1139.
105. Ishii, K.J., Suzuki, K., Coban, C., Takeshita, F., Itoh, Y., Matoba, H., Kohn, L.D., and Klinman, D.M. 2001. Genomic DNA released by dying cells induces the maturation of APCs. *J Immunol* 167:2602-2607.
106. Decker, P., Singh-Jasuja, H., Haager, S., Kotter, I., and Rammensee, H.G. 2005. Nucleosome, the main autoantigen in systemic lupus erythematosus, induces direct dendritic cell activation via a MyD88-independent pathway: consequences on inflammation. *J Immunol* 174:3326-3334.
107. Ronnefarth, V.M., Erbacher, A.I., Lamkemeyer, T., Madlung, J., Nordheim, A., Rammensee, H.G., and Decker, P. 2006. TLR2/TLR4-independent neutrophil activation and recruitment upon endocytosis of nucleosomes reveals a new pathway of innate immunity in systemic lupus erythematosus. *J Immunol* 177:7740-7749.
108. Boule, M.W., Broughton, C., Mackay, F., Akira, S., Marshak-Rothstein, A., and Rifkin, I.R. 2004. Toll-like receptor 9-dependent and -independent

dendritic cell activation by chromatin-immunoglobulin G complexes. *J Exp Med* 199:1631-1640.

109. Feng, H., Zeng, Y., Graner, M.W., Likhacheva, A., and Katsanis, E. 2003. Exogenous stress proteins enhance the immunogenicity of apoptotic tumor cells and stimulate antitumor immunity. *Blood* 101:245-252.
110. Basu, S., and Srivastava, P.K. 2000. Heat shock proteins: the fountainhead of innate and adaptive immune responses. *Cell Stress Chaperones* 5:443-451.
111. Asea, A., Kabingu, E., Stevenson, M.A., and Calderwood, S.K. 2000. HSP70 peptidembearing and peptide-negative preparations act as chaperokines. *Cell Stress Chaperones* 5:425-431.
112. Wallin, R.P., Lundqvist, A., More, S.H., von Bonin, A., Kiessling, R., and Ljunggren, H.G. 2002. Heat-shock proteins as activators of the innate immune system. *Trends Immunol* 23:130-135.
113. Schmitt, E., Gehrmann, M., Brunet, M., Multhoff, G., and Garrido, C. 2007. Intracellular and extracellular functions of heat shock proteins: repercussions in cancer therapy. *J Leukoc Biol* 81:15-27.
114. Cronstein, B.N., Daguma, L., Nichols, D., Hutchison, A.J., and Williams, M. 1990. The adenosine/neutrophil paradox resolved: human neutrophils possess both A1 and A2 receptors that promote chemotaxis and inhibit O2 generation, respectively. *J Clin Invest* 85:1150-1157.
115. Poelstra, K., Heynen, E.R., Baller, J.F., Hardonk, M.J., and Bakker, W.W. 1992. Modulation of anti-Thy1 nephritis in the rat by adenine nucleotides. Evidence for an anti-inflammatory role for nucleotidases. *Lab Invest* 66:555-563.
116. Bours, M.J., Swennen, E.L., Di Virgilio, F., Cronstein, B.N., and Dagnelie, P.C. 2006. Adenosine 5'-triphosphate and adenosine as endogenous signaling molecules in immunity and inflammation. *Pharmacol Ther* 112:358-404.
117. Fredholm, B.B. 2007. Adenosine, an endogenous distress signal, modulates tissue damage and repair. *Cell Death Differ* 14:1315-1323.
118. la Sala, A., Ferrari, D., Corinti, S., Cavani, A., Di Virgilio, F., and Girolomoni, G. 2001. Extracellular ATP induces a distorted maturation of dendritic cells and inhibits their capacity to initiate Th1 responses. *J Immunol* 166:1611-1617.
119. Medzhitov, R., Preston-Hurlburt, P., and Janeway, C.A., Jr. 1997. A human homologue of the Drosophila Toll protein signals activation of adaptive immunity. *Nature* 388:394-397.
120. Medzhitov, R. 2007. Recognition of microorganisms and activation of the immune response. *Nature* 449:819-826.
121. Medzhitov, R. 2007. TLR-mediated innate immune recognition. *Semin Immunol* 19:1-2.
122. Auffray, C., Fogg, D., Garfa, M., Elain, G., Join-Lambert, O., Kayal, S., Sarnacki, S., Cumano, A., Lauvau, G., and Geissmann, F. 2007. Monitoring of blood vessels and tissues by a population of monocytes with patrolling behavior. *Science* 317:666-670.

123. Auffray, C., Sieweke, M.H., and Geissmann, F. 2009. Blood monocytes: development, heterogeneity, and relationship with dendritic cells. *Annu Rev Immunol* 27:669-692.
124. Lin, M., Carlson, E., Diaconu, E., and Pearlman, E. 2007. CXCL1/KC and CXCL5/LIX are selectively produced by corneal fibroblasts and mediate neutrophil infiltration to the corneal stroma in LPS keratitis. *J Leukoc Biol* 81:786-792.
125. Scapini, P., Morini, M., Tecchio, C., Minghelli, S., Di Carlo, E., Tanghetti, E., Albini, A., Lowell, C., Berton, G., Noonan, D.M., et al. 2004. CXCL1/macrophage inflammatory protein-2-induced angiogenesis in vivo is mediated by neutrophil-derived vascular endothelial growth factor-A. *J Immunol* 172:5034-5040.
126. Moser, B., Clark-Lewis, I., Zwahlen, R., and Baggiolini, M. 1990. Neutrophil-activating properties of the melanoma growth-stimulatory activity. *J Exp Med* 171:1797-1802.
127. Schumacher, C., Clark-Lewis, I., Baggiolini, M., and Moser, B. 1992. High- and low-affinity binding of GRO alpha and neutrophil-activating peptide 2 to interleukin 8 receptors on human neutrophils. *Proc Natl Acad Sci U S A* 89:10542-10546.
128. de Oliveira, S., Reyes-Aldasoro, C.C., Candel, S., Renshaw, S.A., Mulero, V., and Calado, A. 2013. Cxcl8 (IL-8) mediates neutrophil recruitment and behavior in the zebrafish inflammatory response. *J Immunol* 190:4349-4359.
129. Yamamoto, S., Shimizu, S., Kiyonaka, S., Takahashi, N., Wajima, T., Hara, Y., Negoro, T., Hiroi, T., Kiuchi, Y., Okada, T., et al. 2008. TRPM2-mediated Ca2+influx induces chemokine production in monocytes that aggravates inflammatory neutrophil infiltration. *Nat Med* 14:738-747.
130. Soehnlein, O., and Lindbom, L. 2010. Phagocyte partnership during the onset and resolution of inflammation. *Nat Rev Immunol* 10:427-439.
131. Ley, K., Laudanna, C., Cybulsky, M.I., and Nourshargh, S. 2007. Getting to the site of inflammation: the leukocyte adhesion cascade updated. *Nat Rev Immunol* 7:678-689.
132. Lacy, P., and Eitzen, G. 2008. Control of granule exocytosis in neutrophils. *Front Biosci* 13:5559-5570.
133. Borregaard, N., and Cowland, J.B. 1997. Granules of the human neutrophilic polymorphonuclear leukocyte. *Blood* 89:3503-3521.
134. Borregaard, N. 1997. Development of neutrophil granule diversity. *Ann N Y Acad Sci* 832:62-68.
135. Yang, D., de la Rosa, G., Tewary, P., and Oppenheim, J.J. 2009. Alarmins link neutrophils and dendritic cells. *Trends Immunol* 30:531-537.
136. Yang, D., Chen, Q., Chertov, O., and Oppenheim, J.J. 2000. Human neutrophil defensins selectively chemoattract naive T and immature dendritic cells. *J Leukoc Biol* 68:9-14.
137. Chertov, O., Ueda, H., Xu, L.L., Tani, K., Murphy, W.J., Wang, J.M., Howard, O.M., Sayers, T.J., and Oppenheim, J.J. 1997. Identification of human neutrophil-derived cathepsin G and azurocidin/CAP37 as

chemoattractants for mononuclear cells and neutrophils. *J Exp Med* 186:739-747.

138. Soehnlein, O., Zernecke, A., Eriksson, E.E., Rothfuchs, A.G., Pham, C.T., Herwald, H., Bidzhekov, K., Rottenberg, M.E., Weber, C., and Lindbom, L. 2008. Neutrophil secretion products pave the way for inflammatory monocytes. *Blood* 112:1461-1471.
139. Soehnlein, O. 2009. An elegant defense: how neutrophils shape the immune response. *Trends Immunol* 30:511-512.
140. Soehnlein, O., Lindbom, L., and Weber, C. 2009. Mechanisms underlying neutrophil-mediated monocyte recruitment. *Blood* 114:4613-4623.
141. Taga, T., Hibi, M., Hirata, Y., Yamasaki, K., Yasukawa, K., Matsuda, T., Hirano, T., and Kishimoto, T. 1989. Interleukin-6 triggers the association of its receptor with a possible signal transducer, gp130. *Cell* 58:573-581.
142. Romano, M., Sironi, M., Toniatti, C., Polentarutti, N., Fruscella, P., Ghezzi, P., Faggioni, R., Luini, W., van Hinsbergh, V., Sozzani, S., et al. 1997. Role of IL-6 and its soluble receptor in induction of chemokines and leukocyte recruitment. *Immunity* 6:315-325.
143. Hurst, S.M., Wilkinson, T.S., McLoughlin, R.M., Jones, S., Horiuchi, S., Yamamoto, N., Rose-John, S., Fuller, G.M., Topley, N., and Jones, S.A. 2001. Il-6 and its soluble receptor orchestrate a temporal switch in the pattern of leukocyte recruitment seen during acute inflammation. *Immunity* 14:705-714.
144. Pahlman, L.I., Morgelin, M., Eckert, J., Johansson, L., Russell, W., Riesbeck, K., Soehnlein, O., Lindbom, L., Norrby-Teglund, A., Schumann, R.R., et al. 2006. Streptococcal M protein: a multipotent and powerful inducer of inflammation. *J Immunol* 177:1221-1228.
145. Berahovich, R.D., Miao, Z., Wang, Y., Premack, B., Howard, M.C., and Schall, T.J. 2005. Proteolytic activation of alternative CCR1 ligands in inflammation. *J Immunol* 174:7341-7351.
146. Kasama, T., Strieter, R.M., Standiford, T.J., Burdick, M.D., and Kunkel, S.L. 1993. Expression and regulation of human neutrophil-derived macrophage inflammatory protein 1 alpha. *J Exp Med* 178:63-72.
147. Pelletier, M., Maggi, L., Micheletti, A., Lazzeri, E., Tamassia, N., Costantini, C., Cosmi, L., Lunardi, C., Annunziato, F., Romagnani, S., et al. 2010. Evidence for a cross-talk between human neutrophils and Th17 cells. *Blood* 115:335-343.
148. Scapini, P., Laudanna, C., Pinardi, C., Allavena, P., Mantovani, A., Sozzani, S., and Cassatella, M.A. 2001. Neutrophils produce biologically active macrophage inflammatory protein-3alpha (MIP-3alpha)/CCL20 and MIP-3beta/CCL19. *Eur J Immunol* 31:1981-1988.
149. Levy, B.D., Clish, C.B., Schmidt, B., Gronert, K., and Serhan, C.N. 2001. Lipid mediator class switching during acute inflammation: signals in resolution. *Nat Immunol* 2:612-619.
150. Funk, C.D. 2001. Prostaglandins and leukotrienes: advances in eicosanoid biology. *Science* 294:1871-1875.

151. Serhan, C.N., Chiang, N., and Van Dyke, T.E. 2008. Resolving inflammation: dual anti-inflammatory and pro-resolution lipid mediators. *Nat Rev Immunol* 8:349-361.
152. Serhan, C.N., Yacoubian, S., and Yang, R. 2008. Anti-inflammatory and proresolving lipid mediators. *Annu Rev Pathol* 3:279-312.
153. Maddox, J.F., Hachicha, M., Takano, T., Petasis, N.A., Fokin, V.V., and Serhan, C.N. 1997. Lipoxin A4 stable analogs are potent mimetics that stimulate human monocytes and THP-1 cells via a G-protein-linked lipoxin A4 receptor. *J Biol Chem* 272:6972-6978.
154. Chiang, N., Serhan, C.N., Dahlen, S.E., Drazen, J.M., Hay, D.W., Rovati, G.E., Shimizu, T., Yokomizo, T., and Brink, C. 2006. The lipoxin receptor ALX: potent ligand-specific and stereoselective actions in vivo. *Pharmacol Rev* 58:463-487.
155. Schwab, J.M., Chiang, N., Arita, M., and Serhan, C.N. 2007. Resolvin E1 and protectin D1 activate inflammation-resolution programmes. *Nature* 447:869-874.
156. Ariel, A., Fredman, G., Sun, Y.P., Kantarci, A., Van Dyke, T.E., Luster, A.D., and Serhan, C.N. 2006. Apoptotic neutrophils and T cells sequester chemokines during immune response resolution through modulation of CCR5 expression. *Nat Immunol* 7:1209-1216.
157. Kantari, C., Pederzoli-Ribeil, M., and Witko-Sarsat, V. 2008. The role of neutrophils and monocytes in innate immunity. *Contrib Microbiol* 15:118-146.
158. van den Berg, J.M., Weyer, S., Weening, J.J., Roos, D., and Kuijpers, T.W. 2001. Divergent effects of tumor necrosis factor alpha on apoptosis of human neutrophils. *J Leukoc Biol* 69:467-473.
159. Allenbach, C., Zufferey, C., Perez, C., Launois, P., Mueller, C., and Tacchini-Cottier, F. 2006. Macrophages induce neutrophil apoptosis through membrane TNF, a process amplified by Leishmania major. *J Immunol* 176:6656-6664.
160. Meszaros, A.J., Reichner, J.S., and Albina, J.E. 2000. Macrophage-induced neutrophil apoptosis. *J Immunol* 165:435-441.
161. Rosen, H., and Gordon, S. 1990. Adoptive transfer of fluorescence-labeled cells shows that resident peritoneal macrophages are able to migrate into specialized lymphoid organs and inflammatory sites in the mouse. *Eur J Immunol* 20:1251-1258.
162. Bellingan, G.J., Caldwell, H., Howie, S.E., Dransfield, I., and Haslett, C. 1996. In vivo fate of the inflammatory macrophage during the resolution of inflammation: inflammatory macrophages do not die locally, but emigrate to the draining lymph nodes. *J Immunol* 157:2577-2585.
163. Lauber, K., Bohn, E., Krober, S.M., Xiao, Y.J., Blumenthal, S.G., Lindemann, R.K., Marini, P., Wiedig, C., Zobywalski, A., Baksh, S., et al. 2003. Apoptotic cells induce migration of phagocytes via caspase-3-mediated release of a lipid attraction signal. *Cell* 113:717-730.
164. Elliott, M.R., Chekeni, F.B., Trampont, P.C., Lazarowski, E.R., Kadl, A., Walk, S.F., Park, D., Woodson, R.I., Ostankovich, M., Sharma, P., et al.

2009. Nucleotides released by apoptotic cells act as a find-me signal to promote phagocytic clearance. *Nature* 461:282-286.

165. Truman, L.A., Ford, C.A., Pasikowska, M., Pound, J.D., Wilkinson, S.J., Dumitriu, I.E., Melville, L., Melrose, L.A., Ogden, C.A., Nibbs, R., et al. 2008. CX3CL1/fractalkine is released from apoptotic lymphocytes to stimulate macrophage chemotaxis. *Blood* 112:5026-5036.
166. Zhao, M., Song, B., Pu, J., Wada, T., Reid, B., Tai, G., Wang, F., Guo, A., Walczysko, P., Gu, Y., et al. 2006. Electrical signals control wound healing through phosphatidylinositol-3-OH kinase-gamma and PTEN. *Nature* 442:457-460.
167. Ravichandran, K.S., and Lorenz, U. 2007. Engulfment of apoptotic cells: signals for a good meal. *Nat Rev Immunol* 7:964-974.
168. Henson, P.M., Bratton, D.L., and Fadok, V.A. 2001. Apoptotic cell removal. *Curr Biol* 11:R795-805.
169. Savill, J., Dransfield, I., Gregory, C., and Haslett, C. 2002. A blast from the past: clearance of apoptotic cells regulates immune responses. *Nat Rev Immunol* 2:965-975.
170. Fadok, V.A., Bratton, D.L., Frasch, S.C., Warner, M.L., and Henson, P.M. 1998. The role of phosphatidylserine in recognition of apoptotic cells by phagocytes. *Cell Death Differ* 5:551-562.
171. Fadok, V.A., Warner, M.L., Bratton, D.L., and Henson, P.M. 1998. CD36 is required for phagocytosis of apoptotic cells by human macrophages that use either a phosphatidylserine receptor or the vitronectin receptor (alpha v beta 3). *J Immunol* 161:6250-6257.
172. Devitt, A., Moffatt, O.D., Raykundalia, C., Capra, J.D., Simmons, D.L., and Gregory, C.D. 1998. Human CD14 mediates recognition and phagocytosis of apoptotic cells. *Nature* 392:505-509.
173. Schlegel, R.A., Krahling, S., Callahan, M.K., and Williamson, P. 1999. CD14 is a component of multiple recognition systems used by macrophages to phagocytose apoptotic lymphocytes. *Cell Death Differ* 6:583-592.
174. Ezekowitz, R.A., Sastry, K., Bailly, P., and Warner, A. 1990. Molecular characterization of the human macrophage mannose receptor: demonstration of multiple carbohydrate recognition-like domains and phagocytosis of yeasts in Cos-1 cells. *J Exp Med* 172:1785-1794.
175. Savill, J., Dransfield, I., Hogg, N., and Haslett, C. 1990. Vitronectin receptor-mediated phagocytosis of cells undergoing apoptosis. *Nature* 343:170-173.
176. Gregory, C.D., Devitt, A., and Moffatt, O. 1998. Roles of ICAM-3 and CD14 in the recognition and phagocytosis of apoptotic cells by macrophages. *Biochem Soc Trans* 26:644-649.
177. Gardai, S.J., McPhillips, K.A., Frasch, S.C., Janssen, W.J., Starefeldt, A., Murphy-Ullrich, J.E., Bratton, D.L., Oldenborg, P.A., Michalak, M., and Henson, P.M. 2005. Cell-surface calreticulin initiates clearance of viable or apoptotic cells through trans-activation of LRP on the phagocyte. *Cell* 123:321-334.

178. Ogden, C.A., deCathelineau, A., Hoffmann, P.R., Bratton, D., Ghebrehiwet, B., Fadok, V.A., and Henson, P.M. 2001. C1q and mannose binding lectin engagement of cell surface calreticulin and CD91 initiates macropinocytosis and uptake of apoptotic cells. *J Exp Med* 194:781-795.
179. Fadok, V.A., Savill, J.S., Haslett, C., Bratton, D.L., Doherty, D.E., Campbell, P.A., and Henson, P.M. 1992. Different populations of macrophages use either the vitronectin receptor or the phosphatidylserine receptor to recognize and remove apoptotic cells. *J Immunol* 149:4029-4035.
180. Fadok, V.A., Voelker, D.R., Campbell, P.A., Cohen, J.J., Bratton, D.L., and Henson, P.M. 1992. Exposure of phosphatidylserine on the surface of apoptotic lymphocytes triggers specific recognition and removal by macrophages. *J Immunol* 148:2207-2216.
181. Pradhan, D., Krahling, S., Williamson, P., and Schlegel, R.A. 1997. Multiple systems for recognition of apoptotic lymphocytes by macrophages. *Mol Biol Cell* 8:767-778.
182. Henson, P.M. 2005. Dampening inflammation. *Nat Immunol* 6:1179-1181.
183. Vandivier, R.W., Henson, P.M., and Douglas, I.S. 2006. Burying the dead: the impact of failed apoptotic cell removal (efferocytosis) on chronic inflammatory lung disease. *Chest* 129:1673-1682.
184. Voll, R.E., Herrmann, M., Roth, E.A., Stach, C., Kalden, J.R., and Girkontaite, I. 1997. Immunosuppressive effects of apoptotic cells. *Nature* 390:350-351.
185. Fadok, V.A., Bratton, D.L., Konowal, A., Freed, P.W., Westcott, J.Y., and Henson, P.M. 1998. Macrophages that have ingested apoptotic cells in vitro inhibit proinflammatory cytokine production through autocrine/paracrine mechanisms involving TGF-beta, PGE2, and PAF. *J Clin Invest* 101:890-898.
186. Maderna, P., and Godson, C. 2003. Phagocytosis of apoptotic cells and the resolution of inflammation. *Biochim Biophys Acta* 1639:141-151.
187. Weigert, A., Jennewein, C., and Brune, B. 2009. The liaison between apoptotic cells and macrophages--the end programs the beginning. *Biol Chem* 390:379-390.
188. Tassiulas, I., Park-Min, K.H., Hu, Y., Kellerman, L., Mevorach, D., and Ivashkiv, L.B. 2007. Apoptotic cells inhibit LPS-induced cytokine and chemokine production and IFN responses in macrophages. *Hum Immunol* 68:156-164.
189. Bianchi, S.M., Prince, L.R., McPhillips, K., Allen, L., Marriott, H.M., Taylor, G.W., Hellewell, P.G., Sabroe, I., Dockrell, D.H., Henson, P.W., et al. 2008. Impairment of apoptotic cell engulfment by pyocyanin, a toxic metabolite of Pseudomonas aeruginosa. *Am J Respir Crit Care Med* 177:35-43.
190. Anderson, H.A., Englert, R., Gursel, I., and Shacter, E. 2002. Oxidative stress inhibits the phagocytosis of apoptotic cells that have externalized phosphatidylserine. *Cell Death Differ* 9:616-625.

191. Serinkan, B.F., Gambelli, F., Potapovich, A.I., Babu, H., Di Giuseppe, M., Ortiz, L.A., Fabisiak, J.P., and Kagan, V.E. 2005. Apoptotic cells quench reactive oxygen and nitrogen species and modulate TNF-alpha/TGF-beta1 balance in activated macrophages: involvement of phosphatidylserine-dependent and -independent pathways. *Cell Death Differ* 12:1141-1144.
192. Kim, S., Elkon, K.B., and Ma, X. 2004. Transcriptional suppression of interleukin-12 gene expression following phagocytosis of apoptotic cells. *Immunity* 21:643-653.
193. Stark, M.A., Huo, Y., Burcin, T.L., Morris, M.A., Olson, T.S., and Ley, K. 2005. Phagocytosis of apoptotic neutrophils regulates granulopoiesis via IL-23 and IL-17. *Immunity* 22:285-294.
194. Freire-de-Lima, C.G., Nascimento, D.O., Soares, M.B., Bozza, P.T., Castro-Faria-Neto, H.C., de Mello, F.G., DosReis, G.A., and Lopes, M.F. 2000. Uptake of apoptotic cells drives the growth of a pathogenic trypanosome in macrophages. *Nature* 403:199-203.
195. Medeiros, A.I., Serezani, C.H., Lee, S.P., and Peters-Golden, M. 2009. Efferocytosis impairs pulmonary macrophage and lung antibacterial function via PGE2/EP2 signaling. *J Exp Med* 206:61-68.
196. White, G.E., Iqbal, A.J., and Greaves, D.R. 2013. CC chemokine receptors and chronic inflammation--therapeutic opportunities and pharmacological challenges. *Pharmacol Rev* 65:47-89.
197. Baggiolini, M., Dewald, B., and Moser, B. 1994. Interleukin-8 and related chemotactic cytokines--CXC and CC chemokines. *Adv Immunol* 55:97-179.
198. Miller, M.D., and Krangel, M.S. 1992. The human cytokine I-309 is a monocyte chemoattractant. *Proc Natl Acad Sci U S A* 89:2950-2954.
199. Roos, R.S., Loetscher, M., Legler, D.F., Clark-Lewis, I., Baggiolini, M., and Moser, B. 1997. Identification of CCR8, the receptor for the human CC chemokine I-309. *J Biol Chem* 272:17251-17254.
200. Luo, Y., Laning, J., Devi, S., Mak, J., Schall, T.J., and Dorf, M.E. 1994. Biologic activities of the murine beta-chemokine TCA3. *J Immunol* 153:4616-4624.
201. Akimoto, N., Honda, K., Uta, D., Beppu, K., Ushijima, Y., Matsuzaki, Y., Nakashima, S., Kido, M.A., Imoto, K., Takano, Y., et al. 2013. CCL-1 in the spinal cord contributes to neuropathic pain induced by nerve injury. *Cell Death Dis* 4:e679.
202. Akimoto, N., Ifuku, M., Mori, Y., and Noda, M. 2013. Effects of chemokine (C-C motif) ligand 1 on microglial function. *Biochem Biophys Res Commun* 436:455-461.
203. Kim, H.O., Cho, S.I., Chung, B.Y., Ahn, H.K., Park, C.W., and Lee, C.H. 2012. Expression of CCL1 and CCL18 in atopic dermatitis and psoriasis. *Clin Exp Dermatol* 37:521-526.
204. Bishop, B., and Lloyd, C.M. 2003. CC chemokine ligand 1 promotes recruitment of eosinophils but not Th2 cells during the development of allergic airways disease. *J Immunol* 170:4810-4817.

205. Montes-Vizuet, R., Vega-Miranda, A., Valencia-Maqueda, E., Negrete-Garcia, M.C., Velasquez, J.R., and Teran, L.M. 2006. CC chemokine ligand 1 is released into the airways of atopic asthmatics. *Eur Respir J* 28:59-67.
206. Cantor, J., and Haskins, K. 2007. Recruitment and activation of macrophages by pathogenic CD4 T cells in type 1 diabetes: evidence for involvement of CCR8 and CCL1. *J Immunol* 179:5760-5767.
207. Oladiran, A., and Belosevic, M. 2009. Trypanosoma carassii hsp70 increases expression of inflammatory cytokines and chemokines in macrophages of the goldfish (Carassius auratus L.). *Dev Comp Immunol* 33:1128-1136.
208. Zhong, H., Zhou, Y., Yu, F., Xiao, J., Gan, X., and Zhang, M. 2014. Seasonal changes and human chorionic gonadotrophin (hCG) effects on innate immune genes expression in goldfish (Carassius auratus). *Fish Shellfish Immunol* 38:303-310.
209. Yoshimura, T., Matsushima, K., Tanaka, S., Robinson, E.A., Appella, E., Oppenheim, J.J., and Leonard, E.J. 1987. Purification of a human monocyte-derived neutrophil chemotactic factor that has peptide sequence similarity to other host defense cytokines. *Proc Natl Acad Sci U S A* 84:9233-9237.
210. Yoshimura, T., Matsushima, K., Oppenheim, J.J., and Leonard, E.J. 1987. Neutrophil chemotactic factor produced by lipopolysaccharide (LPS)-stimulated human blood mononuclear leukocytes: partial characterization and separation from interleukin 1 (IL 1). *J Immunol* 139:788-793.
211. Clark-Lewis, I., Schumacher, C., Baggiolini, M., and Moser, B. 1991. Structure-activity relationships of interleukin-8 determined using chemically synthesized analogs. Critical role of NH2-terminal residues and evidence for uncoupling of neutrophil chemotaxis, exocytosis, and receptor binding activities. *J Biol Chem* 266:23128-23134.
212. Clark-Lewis, I., Moser, B., Walz, A., Baggiolini, M., Scott, G.J., and Aebersold, R. 1991. Chemical synthesis, purification, and characterization of two inflammatory proteins, neutrophil activating peptide 1 (interleukin-8) and neutrophil activating peptide. *Biochemistry* 30:3128-3135.
213. Baggiolini, M., Imboden, P., and Detmers, P. 1992. Neutrophil activation and the effects of interleukin-8/neutrophil-activating peptide 1 (IL-8/NAP-1). *Cytokines* 4:1-17.
214. Colditz, I., Zwahlen, R., Dewald, B., and Baggiolini, M. 1989. In vivo inflammatory activity of neutrophil-activating factor, a novel chemotactic peptide derived from human monocytes. *Am J Pathol* 134:755-760.
215. Baggiolini, M., Loetscher, P., and Moser, B. 1995. Interleukin-8 and the chemokine family. *Int J Immunopharmacol* 17:103-108.
216. Leonard, E.J., Skeel, A., Yoshimura, T., Noer, K., Kutvirt, S., and Van Epps, D. 1990. Leukocyte specificity and binding of human neutrophil attractant/activation protein-1. *J Immunol* 144:1323-1330.
217. Krieger, M., Brunner, T., Bischoff, S.C., von Tscharner, V., Walz, A., Moser, B., Baggiolini, M., and Dahinden, C.A. 1992. Activation of human basophils through the IL-8 receptor. *J Immunol* 149:2662-2667.

218. Larsen, C.G., Anderson, A.O., Appella, E., Oppenheim, J.J., and Matsushima, K. 1989. The neutrophil-activating protein (NAP-1) is also chemotactic for T lymphocytes. *Science* 243:1464-1466.
219. Taub, D.D., Conlon, K., Lloyd, A.R., Oppenheim, J.J., and Kelvin, D.J. 1993. Preferential migration of activated CD4+ and CD8+ T cells in response to MIP-1 alpha and MIP-1 beta. *Science* 260:355-358.
220. Leonard, E.J., Yoshimura, T., Tanaka, S., and Raffeld, M. 1991. Neutrophil recruitment by intradermally injected neutrophil attractant/activation protein-1. *J Invest Dermatol* 96:690-694.
221. Moser, B., Schumacher, C., von Tscharner, V., Clark-Lewis, I., and Baggiolini, M. 1991. Neutrophil-activating peptide 2 and gro/melanoma growth-stimulatory activity interact with neutrophil-activating peptide 1/interleukin 8 receptors on human neutrophils. *J Biol Chem* 266:10666-10671.
222. Baggiolini, M., and Dahinden, C.A. 1994. CC chemokines in allergic inflammation. *Immunol Today* 15:127-133.
223. Moser, B., Barella, L., Mattei, S., Schumacher, C., Boulay, F., Colombo, M.P., and Baggiolini, M. 1993. Expression of transcripts for two interleukin 8 receptors in human phagocytes, lymphocytes and melanoma cells. *Biochem J* 294 (Pt 1):285-292.
224. Corripio-Miyar, Y., Bird, S., Tsamopoulos, K., and Secombes, C.J. 2007. Cloning and expression analysis of two pro-inflammatory cytokines, IL-1 beta and IL-8, in haddock (Melanogrammus aeglefinus). *Mol Immunol* 44:1361-1373.
225. Huising, M.O., Stolte, E., Flik, G., Savelkoul, H.F., and Verburg-van Kemenade, B.M. 2003. CXC chemokines and leukocyte chemotaxis in common carp (Cyprinus carpio L.). *Dev Comp Immunol* 27:875-888.
226. Laing, K.J., Bols, N., and Secombes, C.J. 2002. A CXC chemokine sequence isolated from the rainbow trout Oncorhynchus mykiss resembles the closely related interferon-gamma-inducible chemokines CXCL9, CXCL10 and CXCL11. *Eur Cytokine Netw* 13:462-473.
227. Laing, K.J., Zou, J.J., Wang, T., Bols, N., Hirono, I., Aoki, T., and Secombes, C.J. 2002. Identification and analysis of an interleukin 8-like molecule in rainbow trout Oncorhynchus mykiss. *Dev Comp Immunol* 26:433-444.
228. Lee, E.Y., Park, H.H., Kim, Y.T., and Choi, T.J. 2001. Cloning and sequence analysis of the interleukin-8 gene from flounder (Paralichthys olivaceous). *Gene* 274:237-243.
229. Zhonghua, C., Chunpin, G., Yong, Z., Kezhi, X., and Yaou, Z. 2008. Cloning and bioactivity analysis of a CXC ligand in black seabream Acanthopagrus schlegeli: the evolutionary clues of ELR+CXC chemokines. *BMC Immunol* 9:66.
230. van der Aa, L.M., Chadzinska, M., Tijhaar, E., Boudinot, P., and Verburg-van Kemenade, B.M. 2010. CXCL8 chemokines in teleost fish: two lineages with distinct expression profiles during early phases of inflammation. *PLoS One* 5:e12384.

231. Rebl, A., Rebl, H., Korytar, T., Goldammer, T., and Seyfert, H.M. 2014. The proximal promoter of a novel interleukin-8-encoding gene in rainbow trout (Oncorhynchus mykiss) is strongly induced by CEBPA, but not NF-kappaB p65. *Dev Comp Immunol*.
232. Grayfer, L., Hodgkinson, J.W., Hitchen, S.J., and Belosevic, M. 2011. Characterization and functional analysis of goldfish (Carassius auratus L.) interleukin-10. *Mol Immunol* 48:563-571.
233. Schwenteit, J.M., Breithaupt, A., Teifke, J.P., Koppang, E.O., Bornscheuer, U.T., Fischer, U., and Gudmundsdottir, B.K. 2013. Innate and adaptive immune responses of Arctic charr (Salvelinus alpinus, L.) during infection with Aeromonas salmonicida subsp. achromogenes and the effect of the AsaP1 toxin. *Fish Shellfish Immunol* 35:866-873.
234. Tracey, D., Klareskog, L., Sasso, E.H., Salfeld, J.G., and Tak, P.P. 2008. Tumor necrosis factor antagonist mechanisms of action: a comprehensive review. *Pharmacol Ther* 117:244-279.
235. Helson, L., Green, S., Carswell, E., and Old, L.J. 1975. Effect of tumour necrosis factor on cultured human melanoma cells. *Nature* 258:731-732.
236. Carswell, E.A., Old, L.J., Kassel, R.L., Green, S., Fiore, N., and Williamson, B. 1975. An endotoxin-induced serum factor that causes necrosis of tumors. *Proc Natl Acad Sci U S A* 72:3666-3670.
237. Kriegler, M., Perez, C., DeFay, K., Albert, I., and Lu, S.D. 1988. A novel form of TNF/cachectin is a cell surface cytotoxic transmembrane protein: ramifications for the complex physiology of TNF. *Cell* 53:45-53.
238. Tang, P., Hung, M.C., and Klostergaard, J. 1996. Human pro-tumor necrosis factor is a homotrimer. *Biochemistry* 35:8216-8225.
239. Black, R.A., Rauch, C.T., Kozlosky, C.J., Peschon, J.J., Slack, J.L., Wolfson, M.F., Castner, B.J., Stocking, K.L., Reddy, P., Srinivasan, S., et al. 1997. A metalloproteinase disintegrin that releases tumour-necrosis factor-alpha from cells. *Nature* 385:729-733.
240. Palladino, M.A., Bahjat, F.R., Theodorakis, E.A., and Moldawer, L.L. 2003. Anti-TNF-alpha therapies: the next generation. *Nat Rev Drug Discov* 2:736-746.
241. Ming, W.J., Bersani, L., and Mantovani, A. 1987. Tumor necrosis factor is chemotactic for monocytes and polymorphonuclear leukocytes. *J Immunol* 138:1469-1474.
242. Yonemaru, M., Stephens, K.E., Ishizaka, A., Zheng, H., Hogue, R.S., Crowley, J.J., Hatherill, J.R., and Raffin, T.A. 1989. Effects of tumor necrosis factor on PMN chemotaxis, chemiluminescence, and elastase activity. *J Lab Clin Med* 114:674-681.
243. Klebanoff, S.J., Vadas, M.A., Harlan, J.M., Sparks, L.H., Gamble, J.R., Agosti, J.M., and Waltersdorph, A.M. 1986. Stimulation of neutrophils by tumor necrosis factor. *J Immunol* 136:4220-4225.
244. Lohmann-Matthes, M.L., Luttig, B., and Hockertz, S. 1991. Involvement of membrane-associated TNF in the killing of Leishmania donovani parasites by macrophages. *Behring Inst Mitt*:125-132.

245. van Strijp, J.A., van der Tol, M.E., Miltenburg, L.A., van Kessel, K.P., and Verhoef, J. 1991. Tumour necrosis factor triggers granulocytes to internalize complement-coated virus particles. *Immunology* 73:77-82.
246. Ding, A.H., Nathan, C.F., and Stuehr, D.J. 1988. Release of reactive nitrogen intermediates and reactive oxygen intermediates from mouse peritoneal macrophages. Comparison of activating cytokines and evidence for independent production. *J Immunol* 141:2407-2412.
247. Neumann, M., and Kownatzki, E. 1989. The effect of adherence on the generation of reactive oxygen species by human neutrophilic granulocytes. *Agents Actions* 26:183-185.
248. Banner, D.W., D'Arcy, A., Janes, W., Gentz, R., Schoenfeld, H.J., Broger, C., Loetscher, H., and Lesslauer, W. 1993. Crystal structure of the soluble human 55 kd TNF receptor-human TNF beta complex: implications for TNF receptor activation. *Cell* 73:431-445.
249. Eck, M.J., Beutler, B., Kuo, G., Merryweather, J.P., and Sprang, S.R. 1988. Crystallization of trimeric recombinant human tumor necrosis factor (cachectin). *J Biol Chem* 263:12816-12819.
250. Grell, M., Douni, E., Wajant, H., Lohden, M., Clauss, M., Maxeiner, B., Georgopoulos, S., Lesslauer, W., Kollias, G., Pfizenmaier, K., et al. 1995. The transmembrane form of tumor necrosis factor is the prime activating ligand of the 80 kDa tumor necrosis factor receptor. *Cell* 83:793-802.
251. Grell, M. 1995. Tumor necrosis factor (TNF) receptors in cellular signaling of soluble and membrane-expressed TNF. *J Inflamm* 47:8-17.
252. Dranoff, G. 2004. Cytokines in cancer pathogenesis and cancer therapy. *Nat Rev Cancer* 4:11-22.
253. Chen, G., and Goeddel, D.V. 2002. TNF-R1 signaling: a beautiful pathway. *Science* 296:1634-1635.
254. Wallach, D., Varfolomeev, E.E., Malinin, N.L., Goltsev, Y.V., Kovalenko, A.V., and Boldin, M.P. 1999. Tumor necrosis factor receptor and Fas signaling mechanisms. *Annu Rev Immunol* 17:331-367.
255. Mukhopadhyay, A., Suttles, J., Stout, R.D., and Aggarwal, B.B. 2001. Genetic deletion of the tumor necrosis factor receptor p60 or p80 abrogates ligand-mediated activation of nuclear factor-kappa B and of mitogen-activated protein kinases in macrophages. *J Biol Chem* 276:31906-31912.
256. Kim, E.Y., and Teh, H.S. 2004. Critical role of TNF receptor type-2 (p75) as a costimulator for IL-2 induction and T cell survival: a functional link to CD28. *J Immunol* 173:4500-4509.
257. Kim, E.Y., Priatel, J.J., Teh, S.J., and Teh, H.S. 2006. TNF receptor type 2 (p75) functions as a costimulator for antigen-driven T cell responses in vivo. *J Immunol* 176:1026-1035.
258. Zhao, X., Mohaupt, M., Jiang, J., Liu, S., Li, B., and Qin, Z. 2007. Tumor necrosis factor receptor 2-mediated tumor suppression is nitric oxide dependent and involves angiostasis. *Cancer Res* 67:4443-4450.
259. Wajant, H., Pfizenmaier, K., and Scheurich, P. 2003. Tumor necrosis factor signaling. *Cell Death Differ* 10:45-65.
260. Baltimore, D. 2011. NF-kappaB is 25. *Nat Immunol* 12:683-685.

261. Smale, S.T. 2011. Hierarchies of NF-kappaB target-gene regulation. *Nat Immunol* 12:689-694.
262. McCubrey, J.A., Steelman, L.S., Chappell, W.H., Abrams, S.L., Wong, E.W., Chang, F., Lehmann, B., Terrian, D.M., Milella, M., Tafuri, A., et al. 2007. Roles of the Raf/MEK/ERK pathway in cell growth, malignant transformation and drug resistance. *Biochim Biophys Acta* 1773:1263-1284.
263. Gaur, U., and Aggarwal, B.B. 2003. Regulation of proliferation, survival and apoptosis by members of the TNF superfamily. *Biochem Pharmacol* 66:1403-1408.
264. Hirono, I., Nam, B.H., Kurobe, T., and Aoki, T. 2000. Molecular cloning, characterization, and expression of TNF cDNA and gene from Japanese flounder Paralychthys olivaceus. *J Immunol* 165:4423-4427.
265. Laing, K.J., Wang, T., Zou, J., Holland, J., Hong, S., Bols, N., Hirono, I., Aoki, T., and Secombes, C.J. 2001. Cloning and expression analysis of rainbow trout Oncorhynchus mykiss tumour necrosis factor-alpha. *Eur J Biochem* 268:1315-1322.
266. Zou, J., Secombes, C.J., Long, S., Miller, N., Clem, L.W., and Chinchar, V.G. 2003. Molecular identification and expression analysis of tumor necrosis factor in channel catfish (Ictalurus punctatus). *Dev Comp Immunol* 27:845-858.
267. Saeij, J.P., Stet, R.J., de Vries, B.J., van Muiswinkel, W.B., and Wiegertjes, G.F. 2003. Molecular and functional characterization of carp TNF: a link between TNF polymorphism and trypanotolerance? *Dev Comp Immunol* 27:29-41.
268. Zou, J., Wang, T., Hirono, I., Aoki, T., Inagawa, H., Honda, T., Soma, G.I., Ototake, M., Nakanishi, T., Ellis, A.E., et al. 2002. Differential expression of two tumor necrosis factor genes in rainbow trout, Oncorhynchus mykiss. *Dev Comp Immunol* 26:161-172.
269. Savan, R., and Sakai, M. 2004. Presence of multiple isoforms of TNF alpha in carp (Cyprinus carpio L.): genomic and expression analysis. *Fish Shellfish Immunol* 17:87-94.
270. Zou, J., Peddie, S., Scapigliati, G., Zhang, Y., Bols, N.C., Ellis, A.E., and Secombes, C.J. 2003. Functional characterisation of the recombinant tumor necrosis factors in rainbow trout, Oncorhynchus mykiss. *Dev Comp Immunol* 27:813-822.
271. Garcia-Castillo, J., Chaves-Pozo, E., Olivares, P., Pelegrin, P., Meseguer, J., and Mulero, V. 2004. The tumor necrosis factor alpha of the bony fish seabream exhibits the in vivo proinflammatory and proliferative activities of its mammalian counterparts, yet it functions in a species-specific manner. *Cell Mol Life Sci* 61:1331-1340.
272. Dinarello, C.A. 1994. The interleukin-1 family: 10 years of discovery. *FASEB J* 8:1314-1325.
273. Auron, P.E., Webb, A.C., Rosenwasser, L.J., Mucci, S.F., Rich, A., Wolff, S.M., and Dinarello, C.A. 1984. Nucleotide sequence of human monocyte interleukin 1 precursor cDNA. *Proc Natl Acad Sci U S A* 81:7907-7911.
274. Dinarello, C.A. 1988. Biology of interleukin 1. *FASEB J* 2:108-115.

275. Dinarello, C.A. 1996. Biologic basis for interleukin-1 in disease. *Blood* 87:2095-2147.
276. Dinarello, C.A. 1998. Interleukin-1 beta, interleukin-18, and the interleukin-1 beta converting enzyme. *Ann N Y Acad Sci* 856:1-11.
277. Contassot, E., Beer, H.D., and French, L.E. 2012. Interleukin-1, inflammasomes, autoinflammation and the skin. *Swiss Med Wkly* 142:w13590.
278. Sahoo, M., Ceballos-Olvera, I., del Barrio, L., and Re, F. 2011. Role of the inflammasome, IL-1beta, and IL-18 in bacterial infections. *ScientificWorldJournal* 11:2037-2050.
279. Eder, C. 2009. Mechanisms of interleukin-1beta release. *Immunobiology* 214:543-553.
280. O'Neill, L.A. 2000. The interleukin-1 receptor/Toll-like receptor superfamily: signal transduction during inflammation and host defense. *Sci STKE* 2000:re1.
281. Colotta, F., Re, F., Muzio, M., Bertini, R., Polentarutti, N., Sironi, M., Giri, J.G., Dower, S.K., Sims, J.E., and Mantovani, A. 1993. Interleukin-1 type II receptor: a decoy target for IL-1 that is regulated by IL-4. *Science* 261:472-475.
282. Dinarello, C.A. 2011. Interleukin-1 in the pathogenesis and treatment of inflammatory diseases. *Blood* 117:3720-3732.
283. Masters, S.L., Simon, A., Aksentijevich, I., and Kastner, D.L. 2009. Horror autoinflammaticus: the molecular pathophysiology of autoinflammatory disease (*). *Annu Rev Immunol* 27:621-668.
284. Bujak, M., and Frangogiannis, N.G. 2009. The role of IL-1 in the pathogenesis of heart disease. *Arch Immunol Ther Exp (Warsz)* 57:165-176.
285. Griffin, W.S., Sheng, J.G., Royston, M.C., Gentleman, S.M., McKenzie, J.E., Graham, D.I., Roberts, G.W., and Mrak, R.E. 1998. Glial-neuronal interactions in Alzheimer's disease: the potential role of a 'cytokine cycle' in disease progression. *Brain Pathol* 8:65-72.
286. Engelsma, M.Y., Stet, R.J., Saeij, J.P., and Verburg-van Kemenade, B.M. 2003. Differential expression and haplotypic variation of two interleukin-1beta genes in the common carp (Cyprinus carpio L.). *Cytokine* 22:21-32.
287. Ellsaesser, C.F., and Clem, L.W. 1994. Functionally distinct high and low molecular weight species of channel catfish and mouse IL-1. *Cytokine* 6:10-20.
288. Secombes, C., Zou, J., Daniels, G., Cunningham, C., Koussounadis, A., and Kemp, G. 1998. Rainbow trout cytokine and cytokine receptor genes. *Immunol Rev* 166:333-340.
289. Sigel, M.M., Hamby, B.A., and Huggins, E.M., Jr. 1986. Phylogenetic studies on lymphokines. Fish lymphocytes respond to human IL-1 and epithelial cells produce an IL-1 like factor. *Vet Immunol Immunopathol* 12:47-58.
290. Hamby, B.A., Huggins, E.M., Jr., Lachman, L.B., Dinarello, C.A., and Sigel, M.M. 1986. Fish lymphocytes respond to human IL-1. *Lymphokine Res* 5:157-162.

291. Verburg-van Kemenade, B.M., Weyts, F.A., Debets, R., and Flik, G. 1995. Carp macrophages and neutrophilic granulocytes secrete an interleukin-1-like factor. *Dev Comp Immunol* 19:59-70.
292. Yin, Z., and Kwang, J. 2000. Carp interleukin-1 beta in the role of an immuno-adjuvant. *Fish Shellfish Immunol* 10:375-378.
293. Hong, S., Peddie, S., Campos-Perez, J.J., Zou, J., and Secombes, C.J. 2003. The effect of intraperitoneally administered recombinant IL-1beta on immune parameters and resistance to Aeromonas salmonicida in the rainbow trout (Oncorhynchus mykiss). *Dev Comp Immunol* 27:801-812.
294. Kono, T., Fujiki, K., Nakao, M., Yano, T., Endo, M., and Sakai, M. 2002. The immune responses of common carp, Cyprinus carpio L., injected with carp interleukin-1beta gene. *J Interferon Cytokine Res* 22:413-419.
295. Hong, S., Zou, J., Crampe, M., Peddie, S., Scapigliati, G., Bols, N., Cunningham, C., and Secombes, C.J. 2001. The production and bioactivity of rainbow trout (Oncorhynchus mykiss) recombinant IL-1 beta. *Vet Immunol Immunopathol* 81:1-14.
296. Liu, J., Cao, S., Herman, L.M., and Ma, X. 2003. Differential regulation of interleukin (IL)-12 p35 and p40 gene expression and interferon (IFN)-gamma-primed IL-12 production by IFN regulatory factor 1. *J Exp Med* 198:1265-1276.
297. Watford, W.T., Moriguchi, M., Morinobu, A., and O'Shea, J.J. 2003. The biology of IL-12: coordinating innate and adaptive immune responses. *Cytokine Growth Factor Rev* 14:361-368.
298. Vignali, D.A., and Kuchroo, V.K. 2012. IL-12 family cytokines: immunological playmakers. *Nat Immunol* 13:722-728.
299. van Wanrooij, R.L., Zwiers, A., Kraal, G., and Bouma, G. 2012. Genetic variations in interleukin-12 related genes in immune-mediated diseases. *J Autoimmun* 39:359-368.
300. Sieburth, D., Jabs, E.W., Warrington, J.A., Li, X., Lasota, J., LaForgia, S., Kelleher, K., Huebner, K., Wasmuth, J.J., and Wolf, S.F. 1992. Assignment of genes encoding a unique cytokine (IL12) composed of two unrelated subunits to chromosomes 3 and 5. *Genomics* 14:59-62.
301. Gately, M.K., Renzetti, L.M., Magram, J., Stern, A.S., Adorini, L., Gubler, U., and Presky, D.H. 1998. The interleukin-12/interleukin-12-receptor system: role in normal and pathologic immune responses. *Annu Rev Immunol* 16:495-521.
302. Zhang, S., and Wang, Q. 2008. Factors determining the formation and release of bioactive IL-12: regulatory mechanisms for IL-12p70 synthesis and inhibition. *Biochem Biophys Res Commun* 372:509-512.
303. Macatonia, S.E., Hsieh, C.S., Murphy, K.M., and O'Garra, A. 1993. Dendritic cells and macrophages are required for Th1 development of CD4+ T cells from alpha beta TCR transgenic mice: IL-12 substitution for macrophages to stimulate IFN-gamma production is IFN-gamma-dependent. *Int Immunol* 5:1119-1128.

304. Kang, B.Y., Kim, E., and Kim, T.S. 2005. Regulatory mechanisms and their therapeutic implications of interleukin-12 production in immune cells. *Cell Signal* 17:665-673.
305. Gee, K., Guzzo, C., Che Mat, N.F., Ma, W., and Kumar, A. 2009. The IL-12 family of cytokines in infection, inflammation and autoimmune disorders. *Inflamm Allergy Drug Targets* 8:40-52.
306. Hsieh, C.S., Macatonia, S.E., Tripp, C.S., Wolf, S.F., O'Garra, A., and Murphy, K.M. 1993. Development of TH1 CD4+ T cells through IL-12 produced by Listeria-induced macrophages. *Science* 260:547-549.
307. Wang, K.S., Frank, D.A., and Ritz, J. 2000. Interleukin-2 enhances the response of natural killer cells to interleukin-12 through up-regulation of the interleukin-12 receptor and STAT4. *Blood* 95:3183-3190.
308. Jana, M., Dasgupta, S., Saha, R.N., Liu, X., and Pahan, K. 2003. Induction of tumor necrosis factor-alpha (TNF-alpha) by interleukin-12 p40 monomer and homodimer in microglia and macrophages. *J Neurochem* 86:519-528.
309. Yoshiura, Y., Kiryu, I., Fujiwara, A., Suetake, H., Suzuki, Y., Nakanishi, T., and Ototake, M. 2003. Identification and characterization of Fugu orthologues of mammalian interleukin-12 subunits. *Immunogenetics* 55:296-306.
310. Huising, M.O., van Schijndel, J.E., Kruiswijk, C.P., Nabuurs, S.B., Savelkoul, H.F., Flik, G., and Verburg-van Kemenade, B.M. 2006. The presence of multiple and differentially regulated interleukin-12p40 genes in bony fishes signifies an expansion of the vertebrate heterodimeric cytokine family. *Mol Immunol* 43:1519-1533.
311. Nascimento, D.S., do Vale, A., Tomas, A.M., Zou, J., Secombes, C.J., and dos Santos, N.M. 2007. Cloning, promoter analysis and expression in response to bacterial exposure of sea bass (Dicentrarchus labrax L.) interleukin-12 p40 and p35 subunits. *Mol Immunol* 44:2277-2291.
312. Overgard, A.C., Nepstad, I., Nerland, A.H., and Patel, S. 2012. Characterisation and expression analysis of the Atlantic halibut (Hippoglossus hippoglossus L.) cytokines: IL-1beta, IL-6, IL-11, IL-12beta and IFNgamma. *Mol Biol Rep* 39:2201-2213.
313. Tsai, J.L., Priya, T.A., Hu, K.Y., Yan, H.Y., Shen, S.T., and Song, Y.L. 2014. Grouper interleukin-12, linked by an ancient disulfide-bond architecture, exhibits cytokine and chemokine activities. *Fish Shellfish Immunol* 36:27-37.
314. Wang, T., and Husain, M. 2014. The expanding repertoire of the IL-12 cytokine family in teleost fish: Identification of three paralogues each of the p35 and p40 genes in salmonids, and comparative analysis of their expression and modulation in Atlantic salmon Salmo salar. *Dev Comp Immunol*.
315. Wang, T., Husain, M., Hong, S., and Holland, J.W. 2014. Differential expression, modulation and bioactivity of distinct fish IL-12 isoforms: Implication towards the evolution of Th1-like immune responses. *Eur J Immunol* 44:1541-1551.

316. Wheelock, E.F. 1965. Interferon-Like Virus-Inhibitor Induced in Human Leukocytes by Phytohemagglutinin. *Science* 149:310-311.
317. Mosmann, T.R., and Coffman, R.L. 1989. TH1 and TH2 cells: different patterns of lymphokine secretion lead to different functional properties. *Annu Rev Immunol* 7:145-173.
318. Sad, S., Marcotte, R., and Mosmann, T.R. 1995. Cytokine-induced differentiation of precursor mouse CD8+ T cells into cytotoxic CD8+ T cells secreting Th1 or Th2 cytokines. *Immunity* 2:271-279.
319. Perussia, B. 1991. Lymphokine-activated killer cells, natural killer cells and cytokines. *Curr Opin Immunol* 3:49-55.
320. Schroder, K., Hertzog, P.J., Ravasi, T., and Hume, D.A. 2004. Interferon-gamma: an overview of signals, mechanisms and functions. *J Leukoc Biol* 75:163-189.
321. Belosevic, M., Davis, C.E., Meltzer, M.S., and Nacy, C.A. 1988. Regulation of activated macrophage antimicrobial activities. Identification of lymphokines that cooperate with IFN-gamma for induction of resistance to infection. *J Immunol* 141:890-896.
322. Kerr, I.M., and Stark, G.R. 1992. The antiviral effects of the interferons and their inhibition. *J Interferon Res* 12:237-240.
323. Krishnan, L., Guilbert, L.J., Wegmann, T.G., Belosevic, M., and Mosmann, T.R. 1996. T helper 1 response against Leishmania major in pregnant C57BL/6 mice increases implantation failure and fetal resorptions. Correlation with increased IFN-gamma and TNF and reduced IL-10 production by placental cells. *J Immunol* 156:653-662.
324. Staeheli, P. 1990. Interferon-induced proteins and the antiviral state. *Adv Virus Res* 38:147-200.
325. Stevenson, M.M., Tam, M.F., Belosevic, M., van der Meide, P.H., and Podoba, J.E. 1990. Role of endogenous gamma interferon in host response to infection with blood-stage Plasmodium chabaudi AS. *Infect Immun* 58:3225-3232.
326. Stevenson, M.M., Tam, M.F., and Nowotarski, M. 1990. Role of interferon-gamma and tumor necrosis factor in host resistance to Plasmodium chabaudi AS. *Immunol Lett* 25:115-121.
327. Ihle, J.N., and Kerr, I.M. 1995. Jaks and Stats in signaling by the cytokine receptor superfamily. *Trends Genet* 11:69-74.
328. Graham, S., and Secombes, C.J. 1988. The production of a macrophage-activating factor from rainbow trout Salmo gairdneri leucocytes. *Immunology* 65:293-297.
329. Zou, J., Yoshiura, Y., Dijkstra, J.M., Sakai, M., Ototake, M., and Secombes, C. 2004. Identification of an interferon gamma homologue in Fugu, Takifugu rubripes. *Fish Shellfish Immunol* 17:403-409.
330. Chitu, V., and Stanley, E.R. 2006. Colony-stimulating factor-1 in immunity and inflammation. *Curr Opin Immunol* 18:39-48.
331. Fixe, P., and Praloran, V. 1997. Macrophage colony-stimulating-factor (M-CSF or CSF-1) and its receptor: structure-function relationships. *Eur Cytokine Netw* 8:125-136.

332. Mossadegh-Keller, N., Sarrazin, S., Kandalla, P.K., Espinosa, L., Stanley, E.R., Nutt, S.L., Moore, J., and Sieweke, M.H. 2013. M-CSF instructs myeloid lineage fate in single haematopoietic stem cells. *Nature* 497:239-243.
333. Bartocci, A., Mastrogiannis, D.S., Migliorati, G., Stockert, R.J., Wolkoff, A.W., and Stanley, E.R. 1987. Macrophages specifically regulate the concentration of their own growth factor in the circulation. *Proceedings of the National Academy of Sciences (USA)* 84:6179-6183.
334. Hamilton, J.A., and Achuthan, A. 2013. Colony stimulating factors and myeloid cell biology in health and disease. *Trends Immunol* 34:81-89.
335. Stanley, E.R., Berg, K.L., Einstein, D.B., Lee, P.S., Pixley, F.J., Wang, Y., and Yeung, Y.G. 1997. Biology and action of colony--stimulating factor-1. *Mol Reprod Dev* 46:4-10.
336. Stanley, E.R., Guilbert, L.J., Tushinski, R.J., and Bartelmez, S.H. 1983. CSF-1--a mononuclear phagocyte lineage-specific hemopoietic growth factor. *J Cell Biochem* 21:151-159.
337. Barreda, D.R., Hanington, P.C., and Belosevic, M. 2004. Regulation of myeloid development and function by colony stimulating factors. *Developmental and Comparative Immunology* 28:509-554.
338. Ryan, G.R., Dai, X.M., Dominguez, M.G., Tong, W., Chuan, F., Chisholm, O., Russell, R.G., Pollard, J.W., and Stanley, E.R. 2001. Rescue of the colony-stimulating factor 1 (CSF-1)-nullizygous mouse (Csf1(op)/Csf1(op)) phenotype with a CSF-1 transgene and identification of sites of local CSF-1 synthesis. *Blood* 98:74-84.
339. Bot, F.J., van Eijk, L., Broeders, L., Aarden, L.A., and Lowenberg, B. 1989. Interleukin-6 synergizes with M-CSF in the formation of macrophage colonies from purified human marrow progenitor cells. *Blood* 73:435-437.
340. Bot, F.J., van Eijk, L., Schipper, P., Backx, B., and Lowenberg, B. 1990. Synergistic effects between GM-CSF and G-CSF or M-CSF on highly enriched human marrow progenitor cells. *Leukemia* 4:325-328.
341. Sweet, M.J., and Hume, D.A. 2003. CSF-1 as a regulator of macrophage activation and immune responses. *Arch Immunol Ther Exp (Warsz)* 51:169-177.
342. Bober, L.A., Grace, M.J., Pugliese-Sivo, C., Rojas-Triana, A., Sullivan, L.M., and Narula, S.K. 1995. The effects of colony stimulating factors on human monocyte cell function. *Int J Immunopharmacol* 17:385-392.
343. Karbassi, A., Becker, J.M., Foster, J.S., and Moore, R.N. 1987. Enhanced killing of Candida albicans by murine macrophages treated with macrophage colony-stimulating factor: evidence for augmented expression of mannose receptors. *J Immunol* 139:417-421.
344. Munn, D.H., and Cheung, N.K. 1990. Phagocytosis of tumor cells by human monocytes cultured in recombinant macrophage colony-stimulating factor. *J Exp Med* 172:231-237.
345. Munn, D.H., and Cheung, N.K. 1995. Antibody-independent phagocytosis of tumor cells by human monocyte-derived macrophages cultured in

recombinant macrophage colony-stimulating factor. *Cancer Immunol Immunother* 41:46-52.

346. Ralph, P., Warren, M.K., Nakoinz, I., Lee, M.T., Brindley, L., Sampson-Johannes, A., Kawasaki, E.S., Ladner, M.B., Strickler, J.E., Boosman, A., et al. 1986. Biological properties and molecular biology of the human macrophage growth factor, CSF-1. *Immunobiology* 172:194-204.
347. Roca, F.J., Sepulcre, M.A., Lopez-Castejon, G., Meseguer, J., and Mulero, V. 2006. The colony-stimulating factor-1 receptor is a specific marker of macrophages from the bony fish gilthead seabream. *Mol Immunol* 43:1418-1423.
348. Wing, E.J., Ampel, N.M., Waheed, A., and Shadduck, R.K. 1985. Macrophage colony-stimulating factor (M-CSF) enhances the capacity of murine macrophages to secrete oxygen reduction products. *J Immunol* 135:2052-2056.
349. Hamilton, J.A., Stanley, E.R., Burgess, A.W., and Shadduck, R.K. 1980. Stimulation of macrophage plasminogen activator activity by colony-stimulating factors. *J Cell Physiol* 103:435-445.
350. Lin, H.S., and Gordon, S. 1979. Secretion of plasminogen activator by bone marrow-derived mononuclear phagocytes and its enhancement by colony-stimulating factor. *J Exp Med* 150:231-245.
351. Kurland, J.I., Pelus, L.M., Ralph, P., Bockman, R.S., and Moore, M.A. 1979. Induction of prostaglandin E synthesis in normal and neoplastic macrophages: role for colony-stimulating factor(s) distinct from effects on myeloid progenitor cell proliferation. *Proc Natl Acad Sci U S A* 76:2326-2330.
352. Desai, G., Nassar, F., Brummer, E., and Stevens, D.A. 1995. Killing of Histoplasma capsulatum by macrophage colony stimulating factor-treated human monocyte-derived macrophages: role for reactive oxygen intermediates. *J Med Microbiol* 43:224-229.
353. Garcia Lloret, M.I., Rocha Ramirez, L.M., Ramirez, A., and Santos Preciado, J.I. 1992. Macrophage colony-stimulating factor enhances the respiratory burst of human monocytes in response to Entamoeba histolytica. *Arch Med Res* 23:139-141.
354. Meager, A. 1991. *Cytokines*. Englewood Cliffs, New Jersey: Prentice Hall.
355. Motoyoshi, K. 1998. Biological activities and clinical application of M-CSF. *Int J Hematol* 67:109-122.
356. Curley, S.A., Roh, M.S., Kleinerman, E., and Klostergaard, J. 1990. Human recombinant macrophage colony stimulating factor activates murine Kupffer cells to a cytotoxic state. *Lymphokine Res* 9:355-363.
357. James, S.L., Cook, K.W., and Lazdins, J.K. 1990. Activation of human monocyte-derived macrophages to kill schistosomula of Schistosoma mansoni in vitro. *J Immunol* 145:2686-2690.
358. Metcalf, D., and Nicola, N.A. 1985. Synthesis by mouse peritoneal cells of G-CSF, the differentiation inducer for myeloid leukemia cells: stimulation by endotoxin, M-CSF and multi-CSF. *Leuk Res* 9:35-50.

359. Moore, R.N., Oppenheim, J.J., Farrar, J.J., Carter, C.S., Jr., Waheed, A., and Shadduck, R.K. 1980. Production of lymphocyte-activating factor (Interleukin 1) by macrophages activated with colony-stimulating factors. *J Immunol* 125:1302-1305.
360. Motoyoshi, K., Suda, T., Kusumoto, K., Takaku, F., and Miura, Y. 1982. Granulocyte-macrophage colony-stimulating and binding activities of purified human urinary colony-stimulating factor to murine and human bone marrow cells. *Blood* 60:1378-1386.
361. Oster, W., Brach, M.A., Gruss, H.J., Mertelsmann, R., and Herrmann, F. 1992. Interleukin-1 beta (IL-1 beta) expression in human blood mononuclear phagocytes is differentially regulated by granulocyte-macrophage colony-stimulating factor (GM-CSF), M-CSF, and IL-3. *Blood* 79:1260-1265.
362. Warren, M.K., and Ralph, P. 1986. Macrophage growth factor CSF-1 stimulates human monocyte production of interferon, tumor necrosis factor, and colony stimulating activity. *J Immunol* 137:2281-2285.
363. Evans, R., Kamdar, S.J., Fuller, J.A., and Krupke, D.M. 1995. The potential role of the macrophage colony-stimulating factor, CSF-1, in inflammatory responses: characterization of macrophage cytokine gene expression. *J Leukoc Biol* 58:99-107.
364. Ogiku, M., Kono, H., Ishii, K., Hosomura, N., and Fujii, H. 2011. Role of macrophage colony-stimulating factor in polymicrobial sepsis according to studies using osteopetrotic (op/op) mice. *J Surg Res* 169:106-116.
365. Wiktor-Jedrzejczak, W., and Gordon, S. 1996. Cytokine regulation of the macrophage system using the colony stimulating factor-1 deficient op/op mouse. *Physiological Reviews* 76:927-947.
366. Moore, M.A.S. 1997. Macrophage colony-stimulating factor. In *Colony-stimulating factors: Molecular and cellular biology*. J.M. Garland, P.J. Quesenberry, and D.J. Hilton, editors. New York, N.Y.: Marcell Dekker. 255-289.
367. Fixe, P., and Praloran, V. 1998. M-CSF: haematopoietic growth factor or inflammatory cytokine? *Cytokine* 10:32-37.
368. Aharinejad, S., Salama, M., Paulus, P., Zins, K., Berger, A., and Singer, C.F. 2013. Elevated CSF1 serum concentration predicts poor overall survival in women with early breast cancer. *Endocr Relat Cancer* 20:777-783.
369. Pollard, J.W. 2009. Trophic macrophages in development and disease. *Nat Rev Immunol* 9:259-270.
370. Hume, D.A., and MacDonald, K.P. 2012. Therapeutic applications of macrophage colony-stimulating factor-1 (CSF-1) and antagonists of CSF-1 receptor (CSF-1R) signaling. *Blood* 119:1810-1820.
371. Nemunaitis, J. 1998. Use of macrophage colony-stimulating factor in the treatment of fungal infections. *Clin Infect Dis* 26:1279-1281.
372. Garceau, V., Smith, J., Paton, I.R., Davey, M., Fares, M.A., Sester, D.P., Burt, D.W., and Hume, D.A. 2010. Pivotal Advance: Avian colony-

stimulating factor 1 (CSF-1), interleukin-34 (IL-34), and CSF-1 receptor genes and gene products. *J Leukoc Biol* 87:753-764.

373. Grayfer, L., and Robert, J. 2013. Colony-stimulating factor-1-responsive macrophage precursors reside in the amphibian (Xenopus laevis) bone marrow rather than the hematopoietic subcapsular liver. *J Innate Immun* 5:531-542.
374. Hanington, P.C., Wang, T., Secombes, C.J., and Belosevic, M. 2007. Growth factors of lower vertebrates: characterization of goldfish (Carassius auratus L.) macrophage colony-stimulating factor-1. *J Biol Chem* 282:31865-31872.
375. Wang, T., Kono, T., Monte, M.M., Kuse, H., Costa, M.M., Korenaga, H., Maehr, T., Husain, M., Sakai, M., and Secombes, C.J. 2013. Identification of IL-34 in teleost fish: differential expression of rainbow trout IL-34, MCSF1 and MCSF2, ligands of the MCSF receptor. *Mol Immunol* 53:398-409.
376. Parichy, D.M., Ransom, D.G., Paw, B., Zon, L.I., and Johnson, S.L. 2000. An orthologue of the kit-related gene fms is required for development of neural crest-derived xanthophores and a subpopulation of adult melanocytes in the zebrafish, Danio rerio. *Development* 127:3031-3044.
377. Barreda, D.R., Hanington, P.C., Stafford, J.L., and Belosevic, M. 2005. A novel soluble form of the CSF-1 receptor inhibits proliferation of self-renewing macrophages of goldfish (Carassius auratus L.). *Dev Comp Immunol* 29:879-894.
378. Honda, T., Nishizawa, T., Uenobe, M., Kohchi, C., Kuroda, A., Ototake, M., Nakanishi, T., Yokomizo, Y., Takahashi, Y., Inagawa, H., et al. 2005. Molecular cloning and expression analysis of a macrophage-colony stimulating factor receptor-like gene from rainbow trout, Oncorhynchus mykiss. *Mol Immunol* 42:1-8.
379. !!! INVALID CITATION !!!
380. Pettersen, E.F., Ingerslev, H.C., Stavang, V., Egenberg, M., and Wergeland, H.I. 2008. A highly phagocytic cell line TO from Atlantic salmon is CD83 positive and M-CSFR negative, indicating a dendritic-like cell type. *Fish Shellfish Immunol* 25:809-819.
381. Shadle, P.J., Allen, J.I., Geier, M.D., and Koths, K. 1989. Detection of endogenous macrophage colony-stimulating factor (M-CSF) in human blood. *Exp Hematol* 17:154-159.
382. Koths, K. 1997. Structure-function studies on human macrophage colony-stimulating factor (M-CSF). *Mol Reprod Dev* 46:31-37; discussion 37-38.
383. Shao, X., Kikuchi, K., Watari, E., Norose, Y., Araki, T., and Yokomuro, K. 1996. Changes in M-CSF-like activity during chicken embryonic development. *Reprod Fertil Dev* 8:103-109.
384. Parichy, D.M., and Turner, J.M. 2003. Temporal and cellular requirements for Fms signaling during zebrafish adult pigment pattern development. *Development* 130:817-833.
385. Callard, R.E., and A.J.H., G., editors. 1994. *The Cytokine FactsBook*. San Diego: Academic Press. 265 pp.

386. Das, S.K., Stanley, E.R., Guilbert, L.J., and Forman, L.W. 1981. Human colony-stimulating factor (CSF-1) radioimmunoassay: resolution of three subclasses of human colony-stimulating factors. *Blood* 58:630-641.
387. Gilbert, H.S., Praloran, V., and Stanley, E.R. 1989. Increased circulating CSF-1 (M-CSF) in myeloproliferative disease: association with myeloid metaplasia and peripheral bone marrow extension. *Blood* 74:1231-1234.
388. Hanamura, T., Motoyoshi, K., Yoshida, K., Saito, M., Miura, Y., Kawashima, T., Nishida, M., and Takaku, F. 1988. Quantitation and identification of human monocytic colony-stimulating factor in human serum by enzyme-linked immunosorbent assay. *Blood* 72:886-892.
389. Praloran, V. 1991. Structure, biosynthesis and biological roles of monocyte-macrophage colony stimulating factor (CSF-1 or M-CSF). *Nouv Rev Fr Hematol* 33:323-333.
390. Stanley, E.R., and Guilbert, L.J. 1981. Methods for the purification assay, characterization, and target cell binding of a colony stimulating factor (CSF-1). *Journal of Immunological Methods* 42:253-284.
391. Oster, W., Lindemann, A., Horn, S., Mertelsmann, R., and Herrmann, F. 1987. Tumor necrosis factor (TNF)-alpha but not TNF-beta induces secretion of colony stimulating factor for macrophages (CSF-1) by human monocytes. *Blood* 70:1700-1703.
392. Gruber, M.F., Webb, D.S., and Gerrard, T.L. 1992. Stimulation of human monocytes via CD45, CD44, and LFA-3 triggers macrophage-colony-stimulating factor production. Synergism with lipopolysaccharide and IL-1 beta. *J Immunol* 148:1113-1118.
393. Horiguchi, J., Warren, M.K., Ralph, P., and Kufe, D. 1986. Expression of the macrophage specific colony-stimulating factor (CSF-1) during human monocytic differentiation. *Biochem Biophys Res Commun* 141:924-930.
394. Oster, W., Lindemann, A., Mertelsmann, R., and Herrmann, F. 1988. Regulation of gene expression of M-, G-, GM-, and multi-CSF in normal and malignant hematopoietic cells. *Blood Cells* 14:443-462.
395. Horiguchi, J., Warren, M.K., and Kufe, D. 1987. Expression of the macrophage-specific colony-stimulating factor in human monocytes treated with granulocyte-macrophage colony-stimulating factor. *Blood* 69:1259-1261.
396. Bakheet, T., Frevel, M., Williams, B.R., Greer, W., and Khabar, K.S. 2001. ARED: human AU-rich element-containing mRNA database reveals an unexpectedly diverse functional repertoire of encoded proteins. *Nucleic Acids Res* 29:246-254.
397. Shaw, G., and Kamen, R. 1986. A conserved AU sequence from the 3' untranslated region of GM-CSF mRNA mediates selective mRNA degradation. *Cell* 46:659-667.
398. Woo, H.H., Baker, T., Laszlo, C., and Chambers, S.K. 2013. Nucleolin mediates microRNA-directed CSF-1 mRNA deadenylation but increases translation of CSF-1 mRNA. *Mol Cell Proteomics* 12:1661-1677.
399. Tushinski, R.J., Oliver, I.T., Guilbert, L.J., Tynan, P.W., Warner, J.R., and Stanley, E.R. 1982. Survival of mononuclear phagocytes depends of a

lineage specific growth factor that the differentiated cells selectively destroy. *Cell* 28:71-81.

400. Mancini, A., Koch, A., Wilms, R., and Tamura, T. 2002. c-Cbl associates directly with the C-terminal tail of the receptor for the macrophage colony-stimulating factor, c-Fms, and down-modulates this receptor but not the viral oncogene v-Fms. *J Biol Chem* 277:14635-14640.
401. Wang, Y., Yeung, Y.G., and Stanley, E.R. 1999. CSF-1 stimulated multiubiquitination of the CSF-1 receptor and of Cbl follows their tyrosine phosphorylation and association with other signaling proteins. *Journal of Cellular Biochemistry* 72:119-134.
402. Wilhelmsen, K., Burkhalter, S., and van der Geer, P. 2002. C-Cbl binds the CSF-1 receptor at tyrosine 973, a novel phosphorylation site in the receptor's carboxy-terminus. *Oncogene* 21:1079-1089.
403. Barreda, D.R., and Belosevic, M. 2001. Characterisation of growth enhancing factor production in different phases of *in vitro* fish macrophage development. *Fish and Shellfish Immunology* 11:169-185.
404. Neumann, N.F., Barreda, D., and Belosevic, M. 1998. Production of a macrophage growth factor(s) by a goldfish macrophage cell line and macrophages derived from goldfish kidney leukocytes. *Dev Comp Immunol* 22:417-432.
405. Pixley, F.J., and Stanley, E.R. 2004. CSF-1 regulation of the wandering macrophage: complexity in action. *Trends Cell Biol* 14:628-638.
406. Herpin, A., Lelong, C., and Favrel, P. 2004. Transforming growth factor-beta-related proteins: an ancestral and widespread superfamily of cytokines in metazoans. *Dev Comp Immunol* 28:461-485.
407. Govinden, R., and Bhoola, K.D. 2003. Genealogy, expression, and cellular function of transforming growth factor-beta. *Pharmacol Ther* 98:257-265.
408. Khalil, N. 1999. TGF-beta: from latent to active. *Microbes Infect* 1:1255-1263.
409. Gleizes, P.E., Munger, J.S., Nunes, I., Harpel, J.G., Mazzieri, R., Noguera, I., and Rifkin, D.B. 1997. TGF-beta latency: biological significance and mechanisms of activation. *Stem Cells* 15:190-197.
410. Munger, J.S., Harpel, J.G., Gleizes, P.E., Mazzieri, R., Nunes, I., and Rifkin, D.B. 1997. Latent transforming growth factor-beta: structural features and mechanisms of activation. *Kidney Int* 51:1376-1382.
411. Nunes, I., Gleizes, P.E., Metz, C.N., and Rifkin, D.B. 1997. Latent transforming growth factor-beta binding protein domains involved in activation and transglutaminase-dependent cross-linking of latent transforming growth factor-beta. *J Cell Biol* 136:1151-1163.
412. Hata, A., Shi, Y., and Massague, J. 1998. TGF-beta signaling and cancer: structural and functional consequences of mutations in Smads. *Mol Med Today* 4:257-262.
413. Massague, J. 1998. TGF-beta signal transduction. *Annu Rev Biochem* 67:753-791.

414. Massague, J., and Weis-Garcia, F. 1996. Serine/threonine kinase receptors: mediators of transforming growth factor beta family signals. *Cancer Surv* 27:41-64.
415. Kretzschmar, M., and Massague, J. 1998. SMADs: mediators and regulators of TGF-beta signaling. *Curr Opin Genet Dev* 8:103-111.
416. Sillett, H.K., Cruickshank, S.M., Southgate, J., and Trejdosiewicz, L.K. 2001. Transforming growth factor-beta promotes 'death by neglect' in post-activated human T cells. *Immunology* 102:310-316.
417. Bellone, G., Aste-Amezaga, M., Trinchieri, G., and Rodeck, U. 1995. Regulation of NK cell functions by TGF-beta 1. *J Immunol* 155:1066-1073.
418. Rook, A.H., Kehrl, J.H., Wakefield, L.M., Roberts, A.B., Sporn, M.B., Burlington, D.B., Lane, H.C., and Fauci, A.S. 1986. Effects of transforming growth factor beta on the functions of natural killer cells: depressed cytolytic activity and blunting of interferon responsiveness. *J Immunol* 136:3916-3920.
419. Ludviksson, B.R., Seegers, D., Resnick, A.S., and Strober, W. 2000. The effect of TGF-beta1 on immune responses of naive versus memory CD4+ Th1/Th2 T cells. *Eur J Immunol* 30:2101-2111.
420. Sica, A., and Bronte, V. 2007. Altered macrophage differentiation and immune dysfunction in tumor development. *J Clin Invest* 117:1155-1166.
421. Letterio, J.J., and Roberts, A.B. 1998. Regulation of immune responses by TGF-beta. *Annu Rev Immunol* 16:137-161.
422. Geissmann, F., Revy, P., Regnault, A., Lepelletier, Y., Dy, M., Brousse, N., Amigorena, S., Hermine, O., and Durandy, A. 1999. TGF-beta 1 prevents the noncognate maturation of human dendritic Langerhans cells. *J Immunol* 162:4567-4575.
423. Martinez, F.O., Sica, A., Mantovani, A., and Locati, M. 2008. Macrophage activation and polarization. *Front Biosci* 13:453-461.
424. Pinson, D.M., LeClaire, R.D., Lorsbach, R.B., Parmely, M.J., and Russell, S.W. 1992. Regulation by transforming growth factor-beta 1 of expression and function of the receptor for IFN-gamma on mouse macrophages. *J Immunol* 149:2028-2034.
425. Ding, A.H., and Porteu, F. 1992. Regulation of tumor necrosis factor receptors on phagocytes. *Proc Soc Exp Biol Med* 200:458-465.
426. Shull, M.M., Ormsby, I., Kier, A.B., Pawlowski, S., Diebold, R.J., Yin, M., Allen, R., Sidman, C., Proetzel, G., Calvin, D., et al. 1992. Targeted disruption of the mouse transforming growth factor-beta 1 gene results in multifocal inflammatory disease. *Nature* 359:693-699.
427. Kulkarni, A.B., and Karlsson, S. 1993. Transforming growth factor-beta 1 knockout mice. A mutation in one cytokine gene causes a dramatic inflammatory disease. *Am J Pathol* 143:3-9.
428. Kulkarni, A.B., Huh, C.G., Becker, D., Geiser, A., Lyght, M., Flanders, K.C., Roberts, A.B., Sporn, M.B., Ward, J.M., and Karlsson, S. 1993. Transforming growth factor beta 1 null mutation in mice causes excessive inflammatory response and early death. *Proc Natl Acad Sci U S A* 90:770-774.

429. Geiser, A.G., Letterio, J.J., Kulkarni, A.B., Karlsson, S., Roberts, A.B., and Sporn, M.B. 1993. Transforming growth factor beta 1 (TGF-beta 1) controls expression of major histocompatibility genes in the postnatal mouse: aberrant histocompatibility antigen expression in the pathogenesis of the TGF-beta 1 null mouse phenotype. *Proc Natl Acad Sci U S A* 90:9944-9948.
430. Yaswen, L., Kulkarni, A.B., Fredrickson, T., Mittleman, B., Schiffman, R., Payne, S., Longenecker, G., Mozes, E., and Karlsson, S. 1996. Autoimmune manifestations in the transforming growth factor-beta 1 knockout mouse. *Blood* 87:1439-1445.
431. Christ, M., McCartney-Francis, N.L., Kulkarni, A.B., Ward, J.M., Mizel, D.E., Mackall, C.L., Gress, R.E., Hines, K.L., Tian, H., Karlsson, S., et al. 1994. Immune dysregulation in TGF-beta 1-deficient mice. *J Immunol* 153:1936-1946.
432. Goumans, M.J., and Mummery, C. 2000. Functional analysis of the TGFbeta receptor/Smad pathway through gene ablation in mice. *Int J Dev Biol* 44:253-265.
433. McCartney-Francis, N., Mizel, D., Wong, H., Wahl, L., and Wahl, S. 1990. TGF-beta regulates production of growth factors and TGF-beta by human peripheral blood monocytes. *Growth Factors* 4:27-35.
434. Wahl, S.M., McCartney-Francis, N., Allen, J.B., Dougherty, E.B., and Dougherty, S.F. 1990. Macrophage production of TGF-beta and regulation by TGF-beta. *Ann N Y Acad Sci* 593:188-196.
435. Wiseman, D.M., Polverini, P.J., Kamp, D.W., and Leibovich, S.J. 1988. Transforming growth factor-beta (TGF beta) is chemotactic for human monocytes and induces their expression of angiogenic activity. *Biochem Biophys Res Commun* 157:793-800.
436. Chantry, D., Turner, M., Abney, E., and Feldmann, M. 1989. Modulation of cytokine production by transforming growth factor-beta. *J Immunol* 142:4295-4300.
437. Bogdan, C., Paik, J., Vodovotz, Y., and Nathan, C. 1992. Contrasting mechanisms for suppression of macrophage cytokine release by transforming growth factor-beta and interleukin-10. *J Biol Chem* 267:23301-23308.
438. Parekh, T., Saxena, B., Reibman, J., Cronstein, B.N., and Gold, L.I. 1994. Neutrophil chemotaxis in response to TGF-beta isoforms (TGF-beta 1, TGF-beta 2, TGF-beta 3) is mediated by fibronectin. *J Immunol* 152:2456-2466.
439. Reibman, J., Meixler, S., Lee, T.C., Gold, L.I., Cronstein, B.N., Haines, K.A., Kolasinski, S.L., and Weissmann, G. 1991. Transforming growth factor beta 1, a potent chemoattractant for human neutrophils, bypasses classic signal-transduction pathways. *Proc Natl Acad Sci U S A* 88:6805-6809.
440. Tsunawaki, S., Sporn, M., Ding, A., and Nathan, C. 1988. Deactivation of macrophages by transforming growth factor-beta. *Nature* 334:260-262.

441. Hardie, L.J., Laing, K.J., Daniels, G.D., Grabowski, P.S., Cunningham, C., and Secombes, C.J. 1998. Isolation of the first piscine transforming growth factor beta gene: analysis reveals tissue specific expression and a potential regulatory sequence in rainbow trout (Oncorhynchus mykiss). *Cytokine* 10:555-563.
442. Daniels, G.D., and Secombes, C.J. 1999. Genomic organisation of rainbow trout, Oncorhynchus mykiss TGF-beta. *Dev Comp Immunol* 23:139-147.
443. Zhan, Y., and Jimmy, K. 2000. Molecular isolation and characterisation of carp transforming growth factor beta 1 from activated leucocytes. *Fish Shellfish Immunol* 10:309-318.
444. Tafalla, C., Aranguren, R., Secombes, C.J., Castrillo, J.L., Novoa, B., and Figueras, A. 2003. Molecular characterisation of sea bream (Sparus aurata) transforming growth factor beta1. *Fish Shellfish Immunol* 14:405-421.
445. Harms, C.A., Howard, K.E., Wolf, J.C., Smith, S.A., and Kennedy-Stoskopf, S. 2003. Transforming growth factor-beta response to mycobacterial infection in striped bass Morone saxatilis and hybrid tilapia Oreochromis spp. *Vet Immunol Immunopathol* 95:155-163.
446. Hawrylowicz, C.M., and O'Garra, A. 2005. Potential role of interleukin-10-secreting regulatory T cells in allergy and asthma. *Nat Rev Immunol* 5:271-283.
447. O'Garra, A., Barrat, F.J., Castro, A.G., Vicari, A., and Hawrylowicz, C. 2008. Strategies for use of IL-10 or its antagonists in human disease. *Immunol Rev* 223:114-131.
448. Moore, K.W., de Waal Malefyt, R., Coffman, R.L., and O'Garra, A. 2001. Interleukin-10 and the interleukin-10 receptor. *Annu Rev Immunol* 19:683-765.
449. Bekker, L.G., Maartens, G., Steyn, L., and Kaplan, G. 1998. Selective increase in plasma tumor necrosis factor-alpha and concomitant clinical deterioration after initiating therapy in patients with severe tuberculosis. *J Infect Dis* 178:580-584.
450. Gazzinelli, R.T., Wysocka, M., Hieny, S., Scharton-Kersten, T., Cheever, A., Kuhn, R., Muller, W., Trinchieri, G., and Sher, A. 1996. In the absence of endogenous IL-10, mice acutely infected with Toxoplasma gondii succumb to a lethal immune response dependent on CD4+ T cells and accompanied by overproduction of IL-12, IFN-gamma and TNF-alpha. *J Immunol* 157:798-805.
451. Grau, G.E., Fajardo, L.F., Piguet, P.F., Allet, B., Lambert, P.H., and Vassalli, P. 1987. Tumor necrosis factor (cachectin) as an essential mediator in murine cerebral malaria. *Science* 237:1210-1212.
452. Magez, S., Stijlemans, B., Caljon, G., Eugster, H.P., and De Baetselier, P. 2002. Control of experimental Trypanosoma brucei infections occurs independently of lymphotoxin-alpha induction. *Infect Immun* 70:1342-1351.
453. Robinson, N., Wolke, M., Ernestus, K., and Plum, G. 2007. A mycobacterial gene involved in synthesis of an outer cell envelope lipid is a

key factor in prevention of phagosome maturation. *Infect Immun* 75:581-591.

454. Suvas, S., Azkur, A.K., Kim, B.S., Kumaraguru, U., and Rouse, B.T. 2004. CD4+CD25+ regulatory T cells control the severity of viral immunoinflammatory lesions. *J Immunol* 172:4123-4132.
455. Wilson, E.H., Wille-Reece, U., Dzierszinski, F., and Hunter, C.A. 2005. A critical role for IL-10 in limiting inflammation during toxoplasmic encephalitis. *J Neuroimmunol* 165:63-74.
456. Wu, Y., Wang, Q.H., Zheng, L., Feng, H., Liu, J., Ma, S.H., and Cao, Y.M. 2007. Plasmodium yoelii: distinct CD4(+)CD25(+) regulatory T cell responses during the early stages of infection in susceptible and resistant mice. *Exp Parasitol* 115:301-304.
457. McGuirk, P., McCann, C., and Mills, K.H. 2002. Pathogen-specific T regulatory 1 cells induced in the respiratory tract by a bacterial molecule that stimulates interleukin 10 production by dendritic cells: a novel strategy for evasion of protective T helper type 1 responses by Bordetella pertussis. *J Exp Med* 195:221-231.
458. Anderson, C.F., Mendez, S., and Sacks, D.L. 2005. Nonhealing infection despite Th1 polarization produced by a strain of Leishmania major in C57BL/6 mice. *J Immunol* 174:2934-2941.
459. Belkaid, Y., Hoffmann, K.F., Mendez, S., Kamhawi, S., Udey, M.C., Wynn, T.A., and Sacks, D.L. 2001. The role of interleukin (IL)-10 in the persistence of Leishmania major in the skin after healing and the therapeutic potential of anti-IL-10 receptor antibody for sterile cure. *J Exp Med* 194:1497-1506.
460. Roque, S., Nobrega, C., Appelberg, R., and Correia-Neves, M. 2007. IL-10 underlies distinct susceptibility of BALB/c and C57BL/6 mice to Mycobacterium avium infection and influences efficacy of antibiotic therapy. *J Immunol* 178:8028-8035.
461. Feng, C.G., Kullberg, M.C., Jankovic, D., Cheever, A.W., Caspar, P., Coffman, R.L., and Sher, A. 2002. Transgenic mice expressing human interleukin-10 in the antigen-presenting cell compartment show increased susceptibility to infection with Mycobacterium avium associated with decreased macrophage effector function and apoptosis. *Infect Immun* 70:6672-6679.
462. Groux, H., Cottrez, F., Rouleau, M., Mauze, S., Antonenko, S., Hurst, S., McNeil, T., Bigler, M., Roncarolo, M.G., and Coffman, R.L. 1999. A transgenic model to analyze the immunoregulatory role of IL-10 secreted by antigen-presenting cells. *J Immunol* 162:1723-1729.
463. Reed, S.G., Brownell, C.E., Russo, D.M., Silva, J.S., Grabstein, K.H., and Morrissey, P.J. 1994. IL-10 mediates susceptibility to Trypanosoma cruzi infection. *J Immunol* 153:3135-3140.
464. Sellon, R.K., Tonkonogy, S., Schultz, M., Dieleman, L.A., Grenther, W., Balish, E., Rennick, D.M., and Sartor, R.B. 1998. Resident enteric bacteria are necessary for development of spontaneous colitis and immune system activation in interleukin-10-deficient mice. *Infect Immun* 66:5224-5231.

465. Fiorentino, D.F., Zlotnik, A., Mosmann, T.R., Howard, M., and O'Garra, A. 1991. IL-10 inhibits cytokine production by activated macrophages. *J Immunol* 147:3815-3822.
466. de Waal Malefyt, R., Abrams, J., Bennett, B., Figdor, C.G., and de Vries, J.E. 1991. Interleukin 10(IL-10) inhibits cytokine synthesis by human monocytes: an autoregulatory role of IL-10 produced by monocytes. *J Exp Med* 174:1209-1220.
467. Boonstra, A., Rajsbaum, R., Holman, M., Marques, R., Asselin-Paturel, C., Pereira, J.P., Bates, E.E., Akira, S., Vieira, P., Liu, Y.J., et al. 2006. Macrophages and myeloid dendritic cells, but not plasmacytoid dendritic cells, produce IL-10 in response to MyD88- and TRIF-dependent TLR signals, and TLR-independent signals. *J Immunol* 177:7551-7558.
468. Chang, E.Y., Guo, B., Doyle, S.E., and Cheng, G. 2007. Cutting edge: involvement of the type I IFN production and signaling pathway in lipopolysaccharide-induced IL-10 production. *J Immunol* 178:6705-6709.
469. Rieger, A., and Bar-Or, A. 2008. B-cell-derived interleukin-10 in autoimmune disease: regulating the regulators. *Nat Rev Immunol* 8:486-487.
470. Akbari, O., DeKruyff, R.H., and Umetsu, D.T. 2001. Pulmonary dendritic cells producing IL-10 mediate tolerance induced by respiratory exposure to antigen. *Nat Immunol* 2:725-731.
471. Siewe, L., Bollati-Fogolin, M., Wickenhauser, C., Krieg, T., Muller, W., and Roers, A. 2006. Interleukin-10 derived from macrophages and/or neutrophils regulates the inflammatory response to LPS but not the response to CpG DNA. *Eur J Immunol* 36:3248-3255.
472. Fiorentino, D.F., Bond, M.W., and Mosmann, T.R. 1989. Two types of mouse T helper cell. IV. Th2 clones secrete a factor that inhibits cytokine production by Th1 clones. *J Exp Med* 170:2081-2095.
473. Saraiva, M., Christensen, J.R., Veldhoen, M., Murphy, T.L., Murphy, K.M., and O'Garra, A. 2009. Interleukin-10 production by Th1 cells requires interleukin-12-induced STAT4 transcription factor and ERK MAP kinase activation by high antigen dose. *Immunity* 31:209-219.
474. Saraiva, M., and O'Garra, A. 2010. The regulation of IL-10 production by immune cells. *Nat Rev Immunol* 10:170-181.
475. Oswald, I.P., Wynn, T.A., Sher, A., and James, S.L. 1992. Interleukin 10 inhibits macrophage microbicidal activity by blocking the endogenous production of tumor necrosis factor alpha required as a costimulatory factor for interferon gamma-induced activation. *Proc Natl Acad Sci U S A* 89:8676-8680.
476. Fiorentino, D.F., Zlotnik, A., Vieira, P., Mosmann, T.R., Howard, M., Moore, K.W., and O'Garra, A. 1991. IL-10 acts on the antigen-presenting cell to inhibit cytokine production by Th1 cells. *J Immunol* 146:3444-3451.
477. Ding, L., and Shevach, E.M. 1992. IL-10 inhibits mitogen-induced T cell proliferation by selectively inhibiting macrophage costimulatory function. *J Immunol* 148:3133-3139.

478. Bogdan, C., Vodovotz, Y., and Nathan, C. 1991. Macrophage deactivation by interleukin 10. *J Exp Med* 174:1549-1555.
479. de Waal Malefyt, R., Haanen, J., Spits, H., Roncarolo, M.G., te Velde, A., Figdor, C., Johnson, K., Kastelein, R., Yssel, H., and de Vries, J.E. 1991. Interleukin 10 (IL-10) and viral IL-10 strongly reduce antigen-specific human T cell proliferation by diminishing the antigen-presenting capacity of monocytes via downregulation of class II major histocompatibility complex expression. *J Exp Med* 174:915-924.
480. Walter, M.R., and Nagabhushan, T.L. 1995. Crystal structure of interleukin 10 reveals an interferon gamma-like fold. *Biochemistry* 34:12118-12125.
481. Syto, R., Murgolo, N.J., Braswell, E.H., Mui, P., Huang, E., and Windsor, W.T. 1998. Structural and biological stability of the human interleukin 10 homodimer. *Biochemistry* 37:16943-16951.
482. Kotenko, S.V., Krause, C.D., Izotova, L.S., Pollack, B.P., Wu, W., and Pestka, S. 1997. Identification and functional characterization of a second chain of the interleukin-10 receptor complex. *EMBO J* 16:5894-5903.
483. Liu, Y., Wei, S.H., Ho, A.S., de Waal Malefyt, R., and Moore, K.W. 1994. Expression cloning and characterization of a human IL-10 receptor. *J Immunol* 152:1821-1829.
484. Spencer, S.D., Di Marco, F., Hooley, J., Pitts-Meek, S., Bauer, M., Ryan, A.M., Sordat, B., Gibbs, V.C., and Aguet, M. 1998. The orphan receptor CRF2-4 is an essential subunit of the interleukin 10 receptor. *J Exp Med* 187:571-578.
485. Tan, J.C., Indelicato, S.R., Narula, S.K., Zavodny, P.J., and Chou, C.C. 1993. Characterization of interleukin-10 receptors on human and mouse cells. *J Biol Chem* 268:21053-21059.
486. Weber-Nordt, R.M., Riley, J.K., Greenlund, A.C., Moore, K.W., Darnell, J.E., and Schreiber, R.D. 1996. Stat3 recruitment by two distinct ligand-induced, tyrosine-phosphorylated docking sites in the interleukin-10 receptor intracellular domain. *J Biol Chem* 271:27954-27961.
487. Zou, J., Clark, M.S., and Secombes, C.J. 2003. Characterisation, expression and promoter analysis of an interleukin 10 homologue in the puffer fish, Fugu rubripes. *Immunogenetics* 55:325-335.
488. Inoue, Y., Kamota, S., Ito, K., Yoshiura, Y., Ototake, M., Moritomo, T., and Nakanishi, T. 2005. Molecular cloning and expression analysis of rainbow trout (Oncorhynchus mykiss) interleukin-10 cDNAs. *Fish Shellfish Immunol* 18:335-344.
489. Zhang, D.C., Shao, Y.Q., Huang, Y.Q., and Jiang, S.G. 2005. Cloning, characterization and expression analysis of interleukin-10 from the zebrafish (Danio rerion). *J Biochem Mol Biol* 38:571-576.
490. Savan, R., Igawa, D., and Sakai, M. 2003. Cloning, characterization and expression analysis of interleukin-10 from the common carp, Cyprinus carpio L. *Eur J Biochem* 270:4647-4654.
491. Pinto, R.D., Nascimento, D.S., Reis, M.I., do Vale, A., and Dos Santos, N.M. 2007. Molecular characterization, 3D modelling and expression

analysis of sea bass (Dicentrarchus labrax L.) interleukin-10. *Mol Immunol* 44:2056-2065.

492. Seppola, M., Larsen, A.N., Steiro, K., Robertsen, B., and Jensen, I. 2008. Characterisation and expression analysis of the interleukin genes, IL-1beta, IL-8 and IL-10, in Atlantic cod (Gadus morhua L.). *Mol Immunol* 45:887-897.
493. Cursiefen, C., Chen, L., Borges, L.P., Jackson, D., Cao, J., Radziejewski, C., D'Amore, P.A., Dana, M.R., Wiegand, S.J., and Streilein, J.W. 2004. VEGF-A stimulates lymphangiogenesis and hemangiogenesis in inflammatory neovascularization via macrophage recruitment. *J Clin Invest* 113:1040-1050.
494. Li, X., Lee, C., Tang, Z., Zhang, F., Arjunan, P., Li, Y., Hou, X., Kumar, A., and Dong, L. 2009. VEGF-B: a survival, or an angiogenic factor? *Cell Adh Migr* 3:322-327.
495. Zhang, F., Tang, Z., Hou, X., Lennartsson, J., Li, Y., Koch, A.W., Scotney, P., Lee, C., Arjunan, P., Dong, L., et al. 2009. VEGF-B is dispensable for blood vessel growth but critical for their survival, and VEGF-B targeting inhibits pathological angiogenesis. *Proc Natl Acad Sci U S A* 106:6152-6157.
496. Li, Y., Zhang, F., Nagai, N., Tang, Z., Zhang, S., Scotney, P., Lennartsson, J., Zhu, C., Qu, Y., Fang, C., et al. 2008. VEGF-B inhibits apoptosis via VEGFR-1-mediated suppression of the expression of BH3-only protein genes in mice and rats. *J Clin Invest* 118:913-923.
497. Kataru, R.P., Jung, K., Jang, C., Yang, H., Schwendener, R.A., Baik, J.E., Han, S.H., Alitalo, K., and Koh, G.Y. 2009. Critical role of CD11b+ macrophages and VEGF in inflammatory lymphangiogenesis, antigen clearance, and inflammation resolution. *Blood* 113:5650-5659.
498. Orlandini, M., Marconcini, L., Ferruzzi, R., and Oliviero, S. 1996. Identification of a c-fos-induced gene that is related to the platelet-derived growth factor/vascular endothelial growth factor family. *Proc Natl Acad Sci U S A* 93:11675-11680.
499. Yamada, Y., Nezu, J., Shimane, M., and Hirata, Y. 1997. Molecular cloning of a novel vascular endothelial growth factor, VEGF-D. *Genomics* 42:483-488.
500. Maglione, D., Guerriero, V., Viglietto, G., Ferraro, M.G., Aprelikova, O., Alitalo, K., Del Vecchio, S., Lei, K.J., Chou, J.Y., and Persico, M.G. 1993. Two alternative mRNAs coding for the angiogenic factor, placenta growth factor (PlGF), are transcribed from a single gene of chromosome 14. *Oncogene* 8:925-931.
501. Maglione, D., Guerriero, V., Rambaldi, M., Russo, G., and Persico, M.G. 1993. Translation of the placenta growth factor mRNA is severely affected by a small open reading frame localized in the 5' untranslated region. *Growth Factors* 8:141-152.
502. Kerjaschki, D. 2005. The crucial role of macrophages in lymphangiogenesis. *J Clin Invest* 115:2316-2319.

503. Maruyama, K., Asai, J., Ii, M., Thorne, T., Losordo, D.W., and D'Amore, P.A. 2007. Decreased macrophage number and activation lead to reduced lymphatic vessel formation and contribute to impaired diabetic wound healing. *Am J Pathol* 170:1178-1191.
504. Xiong, M., Elson, G., Legarda, D., and Leibovich, S.J. 1998. Production of vascular endothelial growth factor by murine macrophages: regulation by hypoxia, lactate, and the inducible nitric oxide synthase pathway. *Am J Pathol* 153:587-598.
505. Ramanathan, M., Giladi, A., and Leibovich, S.J. 2003. Regulation of vascular endothelial growth factor gene expression in murine macrophages by nitric oxide and hypoxia. *Exp Biol Med (Maywood)* 228:697-705.
506. Ferrara, N., and Davis-Smyth, T. 1997. The biology of vascular endothelial growth factor. *Endocr Rev* 18:4-25.
507. Ferrara, N., and Keyt, B. 1997. Vascular endothelial growth factor: basic biology and clinical implications. *EXS* 79:209-232.
508. Weis, S.M., and Cheresh, D.A. 2005. Pathophysiological consequences of VEGF-induced vascular permeability. *Nature* 437:497-504.
509. Zittermann, S.I., and Issekutz, A.C. 2006. Endothelial growth factors VEGF and bFGF differentially enhance monocyte and neutrophil recruitment to inflammation. *J Leukoc Biol* 80:247-257.
510. Shaik-Dasthagirisaheb, Y.B., Varvara, G., Murmura, G., Saggini, A., Potalivo, G., Caraffa, A., Antinolfi, P., Tete, S., Tripodi, D., Conti, F., et al. 2013. Vascular endothelial growth factor (VEGF), mast cells and inflammation. *Int J Immunopathol Pharmacol* 26:327-335.
511. Martino, M.M., Briquez, P.S., Guc, E., Tortelli, F., Kilarski, W.W., Metzger, S., Rice, J.J., Kuhn, G.A., Muller, R., Swartz, M.A., et al. 2014. Growth factors engineered for super-affinity to the extracellular matrix enhance tissue healing. *Science* 343:885-888.
512. Holmes, K., Roberts, O.L., Thomas, A.M., and Cross, M.J. 2007. Vascular endothelial growth factor receptor-2: structure, function, intracellular signalling and therapeutic inhibition. *Cell Signal* 19:2003-2012.
513. Karkkainen, M.J., and Petrova, T.V. 2000. Vascular endothelial growth factor receptors in the regulation of angiogenesis and lymphangiogenesis. *Oncogene* 19:5598-5605.
514. Nasevicius, A., Larson, J., and Ekker, S.C. 2000. Distinct requirements for zebrafish angiogenesis revealed by a VEGF-A morphant. *Yeast* 17:294-301.
515. Goishi, K., and Klagsbrun, M. 2004. Vascular endothelial growth factor and its receptors in embryonic zebrafish blood vessel development. *Curr Top Dev Biol* 62:127-152.
516. Carow, B., and Rottenberg, M.E. 2014. SOCS3, a Major Regulator of Infection and Inflammation. *Front Immunol* 5:58.
517. White, C.A., and Nicola, N.A. 2013. SOCS3: An essential physiological inhibitor of signaling by interleukin-6 and G-CSF family cytokines. *JAKSTAT* 2:e25045.
518. Yoshimura, A., Suzuki, M., Sakaguchi, R., Hanada, T., and Yasukawa, H. 2012. SOCS, Inflammation, and Autoimmunity. *Front Immunol* 3:20.

519. Marine, J.C., McKay, C., Wang, D., Topham, D.J., Parganas, E., Nakajima, H., Pendeville, H., Yasukawa, H., Sasaki, A., Yoshimura, A., et al. 1999. SOCS3 is essential in the regulation of fetal liver erythropoiesis. *Cell* 98:617-627.
520. Roberts, A.W., Robb, L., Rakar, S., Hartley, L., Cluse, L., Nicola, N.A., Metcalf, D., Hilton, D.J., and Alexander, W.S. 2001. Placental defects and embryonic lethality in mice lacking suppressor of cytokine signaling 3. *Proc Natl Acad Sci U S A* 98:9324-9329.
521. Croker, B.A., Metcalf, D., Robb, L., Wei, W., Mifsud, S., DiRago, L., Cluse, L.A., Sutherland, K.D., Hartley, L., Williams, E., et al. 2004. SOCS3 is a critical physiological negative regulator of G-CSF signaling and emergency granulopoiesis. *Immunity* 20:153-165.
522. Jin, H.J., Shao, J.Z., and Xiang, L.X. 2007. Identification and characterization of suppressor of cytokine signaling 3 (SOCS-3) homologues in teleost fish. *Mol Immunol* 44:1042-1051.
523. Wang, T., and Secombes, C.J. 2008. Rainbow trout suppressor of cytokine signalling (SOCS)-1, 2 and 3: molecular identification, expression and modulation. *Mol Immunol* 45:1449-1457.
524. Jin, H.J., Shao, J.Z., Xiang, L.X., Wang, H., and Sun, L.L. 2008. Global identification and comparative analysis of SOCS genes in fish: insights into the molecular evolution of SOCS family. *Mol Immunol* 45:1258-1268.
525. Chen, F., Lee, Y., Jiang, Y., Wang, S., Peatman, E., Abernathy, J., Liu, H., Liu, S., Kucuktas, H., Ke, C., et al. 2010. Identification and characterization of full-length cDNAs in channel catfish (Ictalurus punctatus) and blue catfish (Ictalurus furcatus). *PLoS One* 5:e11546.
526. Xiao, Z.G., Liu, H., Fu, J.P., Hu, W., Wang, Y.P., and Guo, Q.L. 2010. Cloning of common carp SOCS-3 gene and its expression during embryogenesis, GH-transgene and viral infection. *Fish Shellfish Immunol* 28:362-371.
527. Elsaeidi, F., Bemben, M.A., Zhao, X.F., and Goldman, D. 2014. Jak/Stat signaling stimulates zebrafish optic nerve regeneration and overcomes the inhibitory actions of Socs3 and Sfpq. *J Neurosci* 34:2632-2644.
528. Liang, J., Wang, D., Renaud, G., Wolfsberg, T.G., Wilson, A.F., and Burgess, S.M. 2012. The stat3/socs3a pathway is a key regulator of hair cell regeneration in zebrafish. [corrected]. *J Neurosci* 32:10662-10673.
529. Studzinski, A.L., Almeida, D.V., Lanes, C.F., Figueiredo Mde, A., and Marins, L.F. 2009. SOCS1 and SOCS3 are the main negative modulators of the somatotrophic axis in liver of homozygous GH-transgenic zebrafish (Danio rerio). *Gen Comp Endocrinol* 161:67-72.
530. Joseph, S.W., and Carnahan, A.M. 2000. Update on the genus Aeromonas. *ASM News* 66:218-223.
531. Janda, J.M., and Duffey, P.S. 1988. Mesophilic aeromonads in human disease: current taxonomy, laboratory identification, and infectious disease spectrum. *Rev Infect Dis* 10:980-997.

532. Popoff, M.Y., Coynault, C., Kiredjian, M., and Lemelin, M. 1981. Polynucleotide sequence relatedness among motile *Aeromonas* species. *Curr. Microbiol.* 5:109-114.
533. Carnahan, A.M. 1993. Aeromonas taxonomy: a sea of change. *Med. Microbiol. Lett.* 2:206-211.
534. Janda, J.M., and Abbott, S.L. 2007. 16S rRNA gene sequencing for bacterial identification in the diagnostic laboratory: pluses, perils, and pitfalls. *J Clin Microbiol* 45:2761-2764.
535. Janda, J.M., and Abbott, S.L. 2010. The genus Aeromonas: taxonomy, pathogenicity, and infection. *Clin Microbiol Rev* 23:35-73.
536. Janda, J.M., and Abbott, S.L. 1998. Evolving concepts regarding the genus Aeromonas: an expanding Panorama of species, disease presentations, and unanswered questions. *Clin Infect Dis* 27:332-344.
537. Kozinska, A. 2007. Dominant pathogenic species of mesophilic aeromonads isolated from diseased and healthy fish cultured in Poland. *J Fish Dis* 30:293-301.
538. Beaz-Hidalgo, R., Alperi, A., Bujan, N., Romalde, J.L., and Figueras, M.J. 2010. Comparison of phenotypical and genetic identification of Aeromonas strains isolated from diseased fish. *Syst Appl Microbiol* 33:149-153.
539. Noga, E. 2010. *Fish disease*: Willey-Blackwell.
540. Austin, B., and Autin, D. 2007. *Bacterial fish pathogens, disease of farmed and wild fish*: Springer-Praxis.
541. Wiklund, T., and Dalsgaard, I. 1998. Occurrence and significance of atypical Aeromonas salmonicida in non-salmonid and salmonid fish species: a review. *Dis Aquat Organ* 32:49-69.
542. Bernoth, E., Ellis, A., Midtlyng, P., Olivier, G., and Smith, P. 1997. *Furunculosis Multidisciplinary Fish Disease Research*: Academic Press.
543. Bullock, G.L., Cipriano, R.C., Snieszko, S.F., and United States. Division of Fishery Ecology Research. 1983. *Furunculosis and other diseases caused by aeromonas salmonicida*. Washington, D.C.: U.S. Dept. of the Interior, Fish and Wildlife Service, Division of Fishery Ecology Research. 29 p. pp.
544. Bullock, G.L., and U.S. Fish and Wildlife Service. 1990. *Furunculosis and other diseases caused by Aeromonas salmonicida*. Washington, DC: Dept. of the Interior Available from Publications Unit, U.S. Fish and Wildlife Service. 1 folded sheet (6 p.) pp.
545. Dalsgaard, I., Gudmundsdottir, B.K., Helgason, S., Hoie, S., Thoresen, O.F., Wichardt, U.P., and Wiklund, T. 1998. Identification of atypical Aeromonas salmonicida: inter-laboratory evaluation and harmonization of methods. *J Appl Microbiol* 84:999-1006.
546. Godoy, M., Gherardelli, V., Heisinger, A., Fernandez, J., Olmos, P., Ovalle, L., Ilardi, P., and Avendano-Herrera, R. 2010. First description of atypical furunculosis in freshwater farmed Atlantic salmon, Salmo salar L., in Chile. *J Fish Dis* 33:441-449.
547. Goldschmidt-Clermont, E., Hochwartner, O., Demarta, A., Caminada, A.P., and Frey, J. 2009. Outbreaks of an ulcerative and haemorrhagic disease in

Arctic char Salvelinus alpinus caused by Aeromonas salmonicida subsp. smithia. *Dis Aquat Organ* 86:81-86.
548. Gustafson, C.E., Thomas, C.J., and Trust, T.J. 1992. Detection of Aeromonas salmonicida from fish by using polymerase chain reaction amplification of the virulence surface array protein gene. *Appl Environ Microbiol* 58:3816-3825.
549. Mawdesley-Thomas, L.E. 1969. Furunculosis in the goldfish, Carassius auratus (L.). *J Fish Biol* 1.
550. Horne, J.H. 1928. Furunculosis in Trout and the Importance of Carriers in the Spread of the Disease. *J Hyg (Lond)* 28:67-78.
551. Scott, M. 1968. The pathogenicity of Aeromonas salmonicida (Griffin) in sea and brackish waters. *J Gen Microbiol* 50:321-327.
552. Johnsen, B.O., and Jensen, A.J. 1994. The spread of furunculosis in salmonids in Norwegian rivers. *J Fish Biol* 45.
553. Miyazaki, T. 1975. Histopathological studies on the furunculosis of the Amago. – II. Perbranchial infection. *Fish Pathol* 9:203-212.
554. Miyazaki, T. 1975. Histopathological studies on the furunculosis of the Amago. – III. Perbcutaneous infection. *Fish Pathol* 9:213-218.
555. Takahashi, K., Kawana, T., and Nakamura, T. 1975. Studies on ulcer disease in goldfish - III. Infection experiments. *Fish Pathol* 9:187-192.
556. Wooster, G.A., and Bowser, P.R. 1996. The aerobiological pathway of a fish pathogen: survival and dissemination of Aeromonas salmonicida in aerosols and its implications in fish health management. *J World Aquaculture Soc* 27:7-14.
557. Abbott, S.L., Seli, L.S., Catino, M., Jr., Hartley, M.A., and Janda, J.M. 1998. Misidentification of unusual Aeromonas species as members of the genus Vibrio: a continuing problem. *J Clin Microbiol* 36:1103-1104.
558. Abbott, S.L., Cheung, W.K., and Janda, J.M. 2003. The genus Aeromonas: biochemical characteristics, atypical reactions, and phenotypic identification schemes. *J Clin Microbiol* 41:2348-2357.
559. Abbott, S.L., Cheung, W.K., Kroske-Bystrom, S., Malekzadeh, T., and Janda, J.M. 1992. Identification of Aeromonas strains to the genospecies level in the clinical laboratory. *J Clin Microbiol* 30:1262-1266.
560. Borrell, N., Figueras, M.J., and Guarro, J. 1998. Phenotypic identification of Aeromonas genomospecies from clinical and environmental sources. *Can J Microbiol* 44:103-108.
561. Kozinska, A., Figueras, M.J., Chacon, M.R., and Soler, L. 2002. Phenotypic characteristics and pathogenicity of Aeromonas genomospecies isolated from common carp (Cyprinus carpio L.). *J Appl Microbiol* 93:1034-1041.
562. Martinez-Murcia, A.J., Soler, L., Saavedra, M.J., Chacon, M.R., Guarro, J., Stackebrandt, E., and Figueras, M.J. 2005. Phenotypic, genotypic, and phylogenetic discrepancies to differentiate Aeromonas salmonicida from Aeromonas bestiarum. *Int Microbiol* 8:259-269.
563. O'Brien, D., Mooney, J., Ryan, D., Powell, E., Hiney, M., Smith, P.R., and Powell, R. 1994. Detection of Aeromonas salmonicida, causal agent of

furunculosis in salmonid fish, from the tank effluent of hatchery-reared Atlantic salmon smolts. *Appl Environ Microbiol* 60:3874-3877.
564. Morgan, J.A., Rhodes, G., and Pickup, R.W. 1993. Survival of nonculturable Aeromonas salmonicida in lake water. *Appl Environ Microbiol* 59:874-880.
565. Jarp, J., Tangen, K., Willumsen, F.V., Djupvik, H.O., and Tveit, A.M. 1993. Risk factors for infections with *Aeromonas salmonicida* in Norwegian fresh water hatcheries. *Dis Aquat Organ* 17:81-86.
566. Bullock, G.L., and Stuckey, H.M. 1977. Ultraviolet treatment of water for destruction of five gram-negative bacteria pathogenic to fishes. *J Fisheries Res Board Can* 34:1244-1249.
567. Colberg, P.J., and Lingg, A.J. 1978. Effect of ozonation on microbial fish pathogens, ammonia, nitrate, nitrite, and BOD in simulated reuse hatchery water. . *J Fisheries Rev Board Can* 35:1290-1296.
568. Wedemeyer, G.A., and Nelson, N.C. 1977. Survival of two bacterial fish pathogens (Aeromonas salmonicida and the enteric redmouth bacterium) in ozonated, chlorinated, and untreated water. *J Fisheries Res Board Can* 34:429-432.
569. Cipriano, R.C., Ford, L.A., Smith, D.R., Schachte, J.H., and Petrie, C.J. 1997. Differences in detection of Aeromonas salmonicida in covertly infected salmonid fishes by the stress-inducible furunculosis test and culture-based assays. *J Aqua Animal Health* 9:108-113.
570. Lillehaug, A., Lunder, T., and Poppe, T.T. 1992. Field testing of adjuvanted furunculosis vaccines in Atlantic salmon, *Salmo salar* L. *J Fish Dis* 15:485-496.
571. Ellis, A.E. 1997. Immunization with bacterial antigens: furunculosis. *Dev Biol Standards* 90:107-116.
572. Midtlyng, P.J., and Lillehaug, A. 1998. Growth of Atlantic salmon Salmo salar after intraperitoneal administration of vaccines containing adjuvants. *Dis Aquat Organ* 32:91-97.
573. Paterson, W.D., Douey, D., and Desautels, D. 1980. Relationships between selected strains of typical and atypical Aeromonas salmonicida, Aeromonas hydrophila, and Haemophilus piscium. *Can J Microbiol* 26:588-598.
574. Janda, J.M., and Abbott, S.L. 1996. *Human pathogens*. West Sussex, England.: John Wiley & Sons Ltd.
575. Dixon, B. 2008. Natural disaster microbiology. *Microbe* 3:312-313.
576. Edberg, S.C., Browne, F.A., and Allen, M.J. 2007. Issues for microbial regulation: Aeromonas as a model. *Crit Rev Microbiol* 33:89-100.
577. Khardori, N., and Fainstein, V. 1988. Aeromonas and Plesiomonas as etiological agents. *Annu Rev Microbiol* 42:395-419.
578. Kelly, K.A., Koehler, J.M., and Ashdown, L.R. 1993. Spectrum of extraintestinal disease due to Aeromonas species in tropical Queensland, Australia. *Clin Infect Dis* 16:574-579.
579. Llopis, F., Grau, I., Tubau, F., Cisnal, M., and Pallares, R. 2004. Epidemiological and clinical characteristics of bacteraemia caused by

Aeromonas spp. as compared with Escherichia coli and Pseudomonas aeruginosa. *Scand J Infect Dis* 36:335-341.

580. Tsai, M.S., Kuo, C.Y., Wang, M.C., Wu, H.C., Chien, C.C., and Liu, J.W. 2006. Clinical features and risk factors for mortality in Aeromonas bacteremic adults with hematologic malignancies. *J Microbiol Immunol Infect* 39:150-154.
581. Ceylan, E., Berktas, M., and Agaoglu, Z. 2009. The occurrence and antibiotic resistance of motile Aeromonas in livestock. *Trop Anim Health Prod* 41:199-204.
582. Thorton, S.M., Nolan, S., and Gulland, F.M. 1998. Bacterial isolates from California sea lions (Zalophus californicus), harbor seals (Phoca vitulina), and northern elephant seals (Mirounga angustirostris) admitted to a reha-bilitation center along the central California coast, 1994–1995. *J. Zool. Wildl. Med.* 29:171-176.
583. Moro, E.M., Weiss, R.D., Friedrich, R.S., de Vargas, A.C., Weiss, L.H., and Nunes, M.P. 1999. Aeromonas hydrophila isolated from cases of bovine seminal vesiculitis in south Brazil. *J Vet Diagn Invest* 11:189-191.
584. Gosling, P.J. 1996. *Aeromonas species in disease of animals*. West Sussex, England.: John Wiley & Sons Ltd.
585. Graf, J. 2000. Symbiosis of Aeromonas and Hirudo medicinalis, the medicinal leech. *ASM News* 66:147-153.
586. Silver, A.C., Rabinowitz, N.M., Kuffer, S., and Graf, J. 2007. Identification of Aeromonas veronii genes required for colonization of the medicinal leech, Hirudo verbana. *J Bacteriol* 189:6763-6772.
587. Silver, A.C., Kikuchi, Y., Fadl, A.A., Sha, J., Chopra, A.K., and Graf, J. 2007. Interaction between innate immune cells and a bacterial type III secretion system in mutualistic and pathogenic associations. *Proc Natl Acad Sci U S A* 104:9481-9486.
588. Krzyminska, S., Kaznowski, A., and Puk, M. 2008. Interaction of Aeromonas spp. human isolates with murine macrophages. *New Microbiol* 31:481-488.
589. Ko, W.C., Chiang, S.R., Yan, J.J., and Chuang, Y.C. 2005. Comparative pathogenicity of bacteraemic isolates of Aeromonas hydrophila and Klebsiella pneumoniae. *Clin Microbiol Infect* 11:553-558.
590. Rio, R.V., Anderegg, M., and Graf, J. 2007. Characterization of a catalase gene from Aeromonas veronii, the digestive-tract symbiont of the medicinal leech. *Microbiology* 153:1897-1906.
591. Krzyminska, S., Kaznowski, A., and Chodysz, M. 2009. Aeromonas spp. human isolates induce apoptosis of murine macrophages. *Curr Microbiol* 58:252-257.
592. Han, H.J., Taki, T., Kondo, H., Hirono, I., and Aoki, T. 2008. Pathogenic potential of a collagenase gene from Aeromonas veronii. *Can J Microbiol* 54:1-10.
593. Nitta, H., Imamura, T., Wada, Y., Irie, A., Kobayashi, H., Okamoto, K., and Baba, H. 2008. Production of C5a by ASP, a serine protease released from Aeromonas sobria. *J Immunol* 181:3602-3608.

594. Imamura, T., Nitta, H., Wada, Y., Kobayashi, H., and Okamoto, K. 2008. Impaired plasma clottability induction through fibrinogen degradation by ASP, a serine protease released from Aeromonas sobria. *FEMS Microbiol Lett* 284:35-42.
595. Janda, J.M. 1985. Biochemical and exoenzymatic properties of Aeromonas species. *Diagn Microbiol Infect Dis* 3:223-232.
596. Chopra, A.K., and Houston, C.W. 1999. Enterotoxins in Aeromonas-associated gastroenteritis. *Microbes Infect* 1:1129-1137.
597. Albert, M.J., Ansaruzzaman, M., Talukder, K.A., Chopra, A.K., Kuhn, I., Rahman, M., Faruque, A.S., Islam, M.S., Sack, R.B., and Mollby, R. 2000. Prevalence of enterotoxin genes in Aeromonas spp. isolated from children with diarrhea, healthy controls, and the environment. *J Clin Microbiol* 38:3785-3790.
598. Fujii, Y., Nomura, T., Yokoyama, R., Shinoda, S., and Okamoto, K. 2003. Studies of the mechanism of action of the aerolysin-like hemolysin of Aeromonas sobria in stimulating T84 cells to produce cyclic AMP. *Infect Immun* 71:1557-1560.
599. Heuzenroeder, M.W., Wong, C.Y., and Flower, R.L. 1999. Distribution of two hemolytic toxin genes in clinical and environmental isolates of Aeromonas spp.: correlation with virulence in a suckling mouse model. *FEMS Microbiol Lett* 174:131-136.
600. Wang, G., Clark, C.G., Liu, C., Pucknell, C., Munro, C.K., Kruk, T.M., Caldeira, R., Woodward, D.L., and Rodgers, F.G. 2003. Detection and characterization of the hemolysin genes in Aeromonas hydrophila and Aeromonas sobria by multiplex PCR. *J Clin Microbiol* 41:1048-1054.
601. Sha, J., Kozlova, E.V., and Chopra, A.K. 2002. Role of various enterotoxins in Aeromonas hydrophila-induced gastroenteritis: generation of enterotoxin gene-deficient mutants and evaluation of their enterotoxic activity. *Infect Immun* 70:1924-1935.
602. Chopra, A.K., Xu, X., Ribardo, D., Gonzalez, M., Kuhl, K., Peterson, J.W., and Houston, C.W. 2000. The cytotoxic enterotoxin of Aeromonas hydrophila induces proinflammatory cytokine production and activates arachidonic acid metabolism in macrophages. *Infect Immun* 68:2808-2818.
603. Martins, L.M., Catani, C.F., Falcon, R.M., Carbonell, G.V., Azzoni, A.A., and Yano, T. 2007. Induction of apoptosis in Vero cells by Aeromonas veronii biovar sobria vacuolating cytotoxic factor. *FEMS Immunol Med Microbiol* 49:197-204.
604. Couto, C.R., Oliveira, S.S., Queiroz, M.L., and Freitas-Almeida, A.C. 2007. Interactions of clinical and environmental Aeromonas isolates with Caco-2 and HT29 intestinal epithelial cells. *Lett Appl Microbiol* 45:405-410.
605. Sha, J., Wang, S.F., Suarez, G., Sierra, J.C., Fadl, A.A., Erova, T.E., Foltz, S.M., Khajanchi, B.K., Silver, A., Graf, J., et al. 2007. Further characterization of a type III secretion system (T3SS) and of a new effector protein from a clinical isolate of Aeromonas hydrophila--part I. *Microb Pathog* 43:127-146.

606. Braun, M., Stuber, K., Schlatter, Y., Wahli, T., Kuhnert, P., and Frey, J. 2002. Characterization of an ADP-ribosyltransferase toxin (AexT) from Aeromonas salmonicida subsp. salmonicida. *J Bacteriol* 184:1851-1858.
607. Silver, A.C., and Graf, J. 2009. Prevalence of genes encoding the type three secretion system and the effectors AexT and AexU in the Aeromonas veronii group. *DNA Cell Biol* 28:383-388.
608. Janda, J.M., Guthertz, L.S., Kokka, R.P., and Shimada, T. 1994. Aeromonas species in septicemia: laboratory characteristics and clinical observations. *Clin Infect Dis* 19:77-83.
609. Janda, J.M., Kokka, R.P., and Guthertz, L.S. 1994. The susceptibility of S-layer-positive and S-layer-negative Aeromonas strains to complement-mediated lysis. *Microbiology* 140 (Pt 10):2899-2905.
610. Merino, S., Rubires, X., Aguilar, A., Alberti, S., Hernandez-Alles, S., Benedi, V.J., and Tomas, J.M. 1996. Mesophilic Aeromonas sp. serogroup O:11 resistance to complement-mediated killing. *Infect Immun* 64:5302-5309.

Chapter 2. Materials and Methods

2.1 Animals

2.1.1 Fish

Goldfish (*Carassius auratus* L.) 10–15 cm in length were purchased from Mount Parnell (Mercersburg, PA) and obtained through Aquatic Imports (Calgary, AB). Fish were maintained in the Aquatic Facility of the Department of Biological Sciences, University of Alberta. The fish were held at 20^{o}C in a continuous flow-through water system on a simulated natural photoperiod. Fish were fed daily and were acclimated for at least two weeks prior to use in the experiments. Fish were monitored daily for any signs of disease and only fish that appeared to be healthy were used, unless otherwise noted. Prior to handling, fish were sedated using tricaine methane sulfonate (TMS) solution of 40-50 mg/L of water. When necessary, individual fish were marked by fin clipping. Goldfish were terminated via cervical dislocations using approved procedures. All efforts were made to minimize animal stress and to ensure that termination procedures were efficiently performed.

2.1.2 Mice

Five-to-nine week old C57BL/6 female mice (*Mus musculus*) were maintained in a P-2-specific pathogen-free facility in the Biosciences Animal Services Centre at the University of Alberta. The mice were held on a simulated natural photoperiod, fed daily, and acclimated for at least 10 days before use.

All animals were maintained according to the guidelines of the Canadian Council on Animal Care, and the University of Alberta Animal Care and Use

Committee approved protocols. Information on animal protocols and ethics approvals can be found within the Preface. C57BL/6 mice were terminated via cervical dislocations using approved procedures. All efforts were made to minimize animal stress and to ensure that termination procedures were efficiently performed.

2.2 Fish serum

Carp (*Cyprinus carpio*) were bled from the caudal vein every 4-6 weeks using a 21-gauge needle attached to a 1 or 3 mL syringe, depending on fish size. Blood was pooled and clotted overnight at 4^{o}C. The next day, blood was centrifuged for 30 minutes at 1000 x *g* at 4^{o}C. Serum was collected and heat inactivated at 56^{o}C for 30 minutes. Serum was then filter sterilized using a 0.22 μm filter, and frozen at -20^{o}C until use in the experiments. Carp serum was used for the cultivation of goldfish primary kidney macrophage (PKM) cultures.

Goldfish serum was collected from the caudal vein using a 23-gauge needle attached to a 1 mL syringe into BD Vacutainer tubes with clot activator and gel for serum separation (BD Biosciences, yellow cap tube). Following collection, tubes were rested at room temperature for 10 minutes then spun at 485 x *g* for 10 minutes at 4^{o}C. Serum was collected and frozen at -20^{o}C until use in the experiments.

2.3 Generation of specific reagents

2.3.1 Macrophage activating factor (MAF)

Goldfish total kidney leukocytes were seeded at a density of 2x10^{6}/mL in complete MGFL-15 media (containing serum and antibiotics; Table 2.3) with 10

μg/mL concanavlin A, 10 ng/mL phorbol myristate acetate (PMA) and 100 ng/mL calcium ionophore (all from Sigma) for 6 hours at 20°C. Cells were then washed three times with 1xPBS$^{-/-}$ (Table 2.1) and 20 mL of incomplete MGFL-15 media (no serum, no antibiotics) was added to each T75 flask. Cells were incubated for 72 hours at 20°C. Supernatants were then collected, filtered with a 0.22 μm filter and stored at -20°C for up to 6 months.

2.3.2 Labeled zymosan particles

2.3.2.1 FITC

Unlabeled zymosan particles (Molecular Probes) were labeled overnight with 1 mg/mL fluorescein isothiocyanate (FITC, Sigma) with continuous shaking on an electronic rocker at a low speed at 4°C in 500 μL carbonate buffer (Table 2.2). After staining, zymosan-FITC was washed twice with 1xPBS$^{-/-}$ at 863 x *g* for 10 minutes at room temperature. Particles were stored at 4°C in the dark until used and added directly to samples as needed. Stain was stable for 1 month.

2.3.2.2 APC

Unlabeled zymosan particles (Molecular Probes) were labeled overnight with 75 μg /mL allophycocyanin (APC, Sigma) with continuous shaking at 4°C in 1x PBS$^{-/-}$ (no magnesium, no calcium). To retain APC signal, zymosan had to be stored in the APC solution. Prior to use, zymosan particles were washed twice with 1xPBS$^{-/-}$ at 863 x *g* for 10 minutes at room temperature.

2.3.3 Apoptotic cells

Apoptotic cells were generated by incubating cells for 24 hours in the presence of 10 μg/mL cycloheximide. Incubation temperature depended on the species from which apoptotic cells were derived- 20°C for fish, 37°C/5% CO_2 for mouse. Treated cells were harvested, washed twice in 1x $PBS^{-/-}$ (spin at 311 x *g* for 10 minutes at 4°C) and stained overnight with 1.5 μg/mL wheat germ agglutinin AlexaFluor 555 (Molecular Probes). Apoptotic cells were then washed twice in 1x $PBS^{-/-}$ (spin at 393 x *g* for 10 minutes at 4°C). For murine experiments, apoptotic cells were generated from primary total splenocytes. For goldfish experiments, apoptotic cells were generated from catfish 3B11 B cells or primary goldfish kidney leukocytes, as indicated. Catfish 3B11 B cells were selected in order to maintain consistency across experiments, as clonal goldfish leukocytes are not available. No difference was found in PKM responses when 3B11 cells were compared with apoptotic cells derived from primary goldfish kidney leukocytes (Figure 4.2). Catfish 3B11 cells were a gift from Dr. Melanie Wilson (University of Mississippi Medical Center) and were generated following *in vitro* lipopolysaccharide stimulation of catfish peripheral blood leukocytes with LPS (1, 2).

2.3.4 Recombinant sCSF-1R

Sf9 and KC1 insect cells were grown in serum free ESF 921 media (Expression Systems). Cells were transfected at 95% confluency using Cellfectin

(Invitrogen) and 1 μg of the sCSF-1R expression plasmid, according to the manufacturers specifications. After 24 hours, transfected cells were transferred to T-25 flasks containing 10 μg/mL blasticidin (Invitrogen) and incubated for 4 days to select for transfectants. Transfected cells were maintained in media containing 10 μg/mL of blasticidin throughout the experiments.

The recombinant protein was purified from the cell supernatants using the MagneHis™ Protein Purification System (Promega). Transfected KC1 cells were grown in T-75 flasks 1 day past confluency and supernatants were collected. One mL of Ni-NTA particles was added to 50 mL of the collected supernatant and mixed by inversion, followed by incubation at room temperature for 2 minutes. Particles were then captured using a magnetic stand and the supernatant was discarded. The particles were then washed 5 times with 3 mL of the wash buffer (40 mM imidazole and 100 mM HEPES) containing 1 M sodium chloride to reduce nonspecific binding. The bound protein was then eluted from the paramagnetic particles using an imidazole gradient (25, 50, 100, 250 and 500 mM). Weakly interacting proteins and other contaminating proteins were eluted at lower concentrations of imidazole whereas the recombinant soluble CSF-1R eluted at 250-500 mM concentration of imidazole. Protein concentrators with a 3K MW cut off (Thermo Scientific) were used following the manufacturers specifications. This was effective at removing residual imidazole in addition to concentrating the protein. Concentration of the rsCSF-1R was determined at 562 nm using a BCA protein assay kit (Thermo Scientific) based on the manufacturers specifications. Figure 2.1 shows a serial dilution of sCSF-1R as detected by Western blotting.

2.3.5 Polyclonal anti-CSF-1R antibody

The identification, expression and purification of a recombinant sCSF-1R and the production of a rabbit polyclonal antibody against the sCSF-1R were performed as previously described in (3). To purify antibodies from rabbit serum, ice-cold saturated ammonium sulphate (SAS) was added to rabbit serum through a drop-wise addition with continuous, gentle manual agitation to a final percentage of 45% (v/v) SAS and incubated overnight at 4^{o}C with rocking. Following incubation, the solution was centrifuged at 10 000 x *g* for 30 minutes at 4^{o}C, the supernatant was aspirated and the pellet re- suspended in 20 mM sodium phosphate buffer, pH 7.2. This solution was dialyzed against 4 L of 20 mM sodium phosphate buffer pH 7.2 overnight to remove excess salts. The collected solution was then applied to a Protein A column (GE Healthcare) following manufacturers instructions. Briefly, the solution was applied to the column and allowed to pass through. The column was then washed with 10 column volumes of 20 mM sodium phosphate buffer, pH 7.2. Citric acid buffers of decreasing pH were applied to the column to elute the bound IgG from the column. The addition of 1M Tris, pH 9 was added to each elution fraction to neutralize the acidity of the solution and prevent antibody denaturation. IgG-containing fractions were pooled and dialyzed for 72 hours in 1xPBS$^{-/-}$ at 4^{o}C with constant mixing. Following dialysis, protein concentration was measured by BCA assay (Pierce) according to manufacturers specifications. Antibodies were filter sterilized (0.22 μm), and stored at -20^{o}C until use.

2.4 Pathogens and pathogen mimics

2.4.1 *Aeromonas veronii*

Aeromonas veronii was isolated from a naturally infected goldfish in the Department of Biological Sciences Aquatic Facilities by swabbing a body furuncle with a cotton swab and inoculating a tryptic soy agar (TSA) plate. Single colonies were grown up and typed using the indicated primers (Table 2.11). Each tested colony was identified to be *Aeromonas veronii* based on sequence analysis. A single colony was used to inoculate tryptic soy broth to create a clonal glycerol stock. The growth curve for *A. veronii* can be found in Figure 2.2. Heat killed *A. veronii* was generated by incubating at 60^{o}C for 45 minutes. Heat inactivated cultures were spun down at 2640 x *g* for 10 minutes at 4^{o}C. Ten mL of 1XPBS$^{-/-}$ was then added to wash, and heat killed cultures were spun down again at 2640 x *g* for 10 minutes at 4^{o}C. Following heat inactivation, an aliquot of bacteria was plated onto TSA plates to ensure that cultures had been adequately killed and no cultures typically developed. Heat killed bacteria was stored at 4^{o}C until use, for no longer than 1 month.

2.4.2 *Aeromonas salmonicida* A449

Aeromonas salmonicida A449 was a gift from Dr. Miodrag Belosevic, originally given by Dr. Jessica Boyd (NRC Institute, Halifax, Canada). Glycerol stocks of *A. salmonicida* A449 stored at -80^{o}C were used to streak tryptic soy agar (TSA) + 20 μg/mL chloramphenicol (Sigma) plates and incubated at 18^{o}C for 72

hours. Tryptic soy broth (TSB) + 20 μg/mL chloramphenicol was inoculated with a single colony and grown at 18°C with rotation into log phase growth. Heat killed *A. salmonicida* A449 was generated by incubating at 60°C for 45 minutes and washed as described above. Following heat inactivation, an aliquot of bacteria was plated onto TSA+ 20 μg/mL chloramphenicol plates to ensure that cultures had been adequately killed and no cultures typically developed. Heat killed bacteria was stored at 4°C until use, for no longer than 1 month. Bacteria were enumerated based on the growth curve generated by Dr. Barbara Katzenback (Katzenback, B.A., Ph.D. thesis).

2.4.3 Zymosan

Zymosan was used to induce acute, self-resolving peritonitis. Injectable (not a particle) zymosan was purchased from Sigma and resuspended at a concentration of 50 mg/mL in 1xPBS$^{-/-}$. To resuspend, 4 mL of 1xPBS$^{-/-}$ was added to the lyophilized stock. This was then vortexed for several minutes at a high speed. Once bubbles had dissipated, another 1 mL of 1xPBS$^{-/-}$ was added to reach the final concentration. Resuspended zymosan was stored at 4°C for no longer than 1 month.

2.4.4 Lipopolysaccharide

Lipopolysaccharide (LPS) is known to be a potent stimulator of immune processes and was used in *in vitro* leukocyte activation assays. Murine cells were activated with *E. coli* Ultrapure LPS (InVivogen) at 100 ng/mL. Goldfish cells were activated with *E. coli* LPS (Sigma) at a concentration of 1 μg/mL. A higher

concentration was needed for goldfish assays as goldfish leukocytes are less sensitive to LPS stimulation than murine cells (4). In order to adequately activate goldfish cells, all LPS stimulations were also done in the presence of 25% MAF.

2.5 Intraperitoneal injections

Goldfish were lightly anesthetized with TMS. Goldfish were then removed from water and placed on bench-coat. Intraperitoneal injections were done in the soft area under the left pectoral fin. Goldfish were then returned to water and allowed to recover. Goldfish were subsequently returned to tank with oxygenation. Fish were monitored closely during and post all injection procedures.

Mice were ventrally injected in the lower left quadrant. In order to prevent puncturing of the intestines with the needle, mice were inverted at a 45^{o} angle during injections. Following injection, mice were returned to cages and monitored closely during and post all injection procedures.

2.5.1 Zymosan

Injectable zymosan was vortexed well prior to removal from vial. Zymosan stock (5 mg/mL) was diluted 1:2 with $1xPBS^{-/-}$ to create a 2.5 mg/mL diluted stock. One hundred μL of diluted stock was aspirated in 25-gauge 1mL needles and all bubbles were removed.

2.5.2 Apoptotic cells

Apoptotic cells were washed thoroughly and counted by haemacytometer. Cells were resuspended at a concentration of $5x10^7$ cells/mL in $1xPBS^{-/-}$. One hundred μL of apoptotic cell stock was aspirated in 25-gauge 1mL needles and all bubbles were removed. Apoptotic cells were made fresh for each experiment.

2.5.3 Recombinant sCSF-1R

Recombinant sCSF-1R was stored at -20°C until use. Protein concentrations were determined prior to freezing. Soluble CSF-1R was diluted in $1xPBS^{-/-}$ in order to have the required concentration in 100 μL of diluted stock. One hundred μL was aspirated in 25-gauge 1mL needles and all bubbles were removed.

2.6 Isolation of primary fish cells

2.6.1 Primary kidney leukocytes

Goldfish were anesthetized with TMS and sacrificed by cervical dislocation. The entire body kidney tissue was dissected and placed into a Petri dish containing 10 mL of cold incomplete medium (without serum). The kidney tissue was gently homogenized using a wire mesh screen and collected by washing the screen with incomplete MGFL-15. The cell suspension sat for 5 minutes to allow debris to settle and the cells were collected into a new conical tube. Cells were spun at 311 x *g* for 10 minutes at 4°C and the supernatant was decanted off. The pellets were resuspended in 1-3 mL ACK Lysis buffer (Lonza), depending on kidney size, and incubated at room temperature for 3 minutes. Ten mL incomplete MGFL-15 was then added and cells were centrifuged at 311 x *g* for 10 minutes at 4°C. Cells were

then resuspended in complete MGFL-15 (with serum and antibiotics), counted using a haemocytometer and used for various assays.

2.6.1.1 Mononuclear cells

Kidneys were homogenized as described above, in incomplete MGFL-15 containing heparin. As above, debris was settled out and cells were layered over a 51% Percoll solution (51 mL Percoll, 10 mL 10 x HBSS, 39 mL incomplete MGFL-15 medium) and centrifuged for 25 minutes at 400 x *g* at 4^{o}C. Cells at the 51% Percoll/medium interface were collected and transferred into a new conical tube and washed twice with incomplete MGFL-15 media (centrifuge 311 x *g* at 4^{o}C for 10 minutes).

2.6.1.2 Neutrophils

Goldfish kidney leukocytes were isolated as described above and layered onto 51% Percoll and centrifuged at 400 x *g* for 25 minutes at 4^{o}C. All the liquid was decanted, leaving behind the red blood cell/neutrophil pellet found at the bottom of the tube. The red blood cells were lysed using ACK Lysis buffer as described above. Neutrophils were then washed twice (centrifuge 311 x *g* at 4^{o}C for 10 minutes) and used in downstream assays.

2.6.2 Peritoneal lavage

As with kidney isolations, goldfish were anesthetized with TMS and sacrificed by cervical dislocation. A square incision was made around the left

pectoral fin, approximately 1 cm x 1 cm x 1cm, to create a flap. Ten mL of ice-cold 1xPBS$^{-/-}$ was injected into fish, 2 scales above the center-line approximately 2/3 of the length of the fish using a blunted 18-gauge needle. Lavages were collected from the pectoral fin flap into a 50 mL conical tube. To exclude changes in relative adherence of resident peritoneal leukocytes following injections, control lavages were performed using trypsin-EDTA added to the lavage medium. While no differences were found in terms of cellular counts, cells lavaged using the trypsin-EDTA displayed weaker DHR staining due to decreased functionality and, thus, this was omitted in subsequent experiments.

To isolate subpopulations from lavage exudate, lavages were run over a 51% Percoll gradient, as described above. Following centrifugation, buffy coats containing mononuclear cells were collected into a separate tube. These cells and the neutrophil pellets were washed once with serum-free media (centrifuge 311 x *g* at 4^{o}C for 10 minutes). Cells were then resuspended in complete MGFL-15 media and used in downstream assays.

2.7 Fish primary cell culture

2.7.1 Culture media

The culture medium used for cultivation of goldfish primary kidney macrophages- modified goldfish Lebovitz-15 (MGFL-15) has been previously described (5). The composition of MGFL-15 is shown in Table 2.3. The composition of the additives to the media is shown in Table 2.4 (nucleic acid precursor solution) and Table 2.5 (10x Hanks Balanced Salt Solution). MEM non-

essential amino acid solution, MEM amino acid solution and MEM vitamin solution were purchased from Gibco. Bovine insulin was purchased from Sigma. Complete MGFL-15 medium contained 10% heat-inactivated fetal calf serum, 5% heat-inactivated carp serum, 100 U/mL penicillin/100 µg/mL streptomycin and 100 µg/mL gentamicin.

2.7.2 Primary kidney macrophages

Kidneys were homogenized as described above, in incomplete MGFL-15 containing heparin. As above, debris was settled out and cells were layered over a 51% Percoll solution (51 mL Percoll, 10 mL 10 x HBSS, 39 mL incomplete MGFL-15 medium) and centrifuged for 25 minutes at 400 x *g* at 4^{o}C. Cells at the 51% Percoll/medium interface were collected and transferred into a new conical tube and washed twice with incomplete MGFL-15 media. Primary kidney macrophages (PKM) were generated by seeding isolated leukocytes and culturing in 15 mL complete MGFL-15 media (MGFL-15 supplemented with 100 U/mL penicillin, 100 µg/mL streptomycin, 100 µg/mL gentamicin, 10% newborn calf serum (Gibco) and 5% carp serum) with 5 mL cell-conditioned media from previous experiments and incubated for 6-9 days at 20^{o}C (5, 6), until cultures reached proliferative phase of growth. This growth phase is dominated by significant proliferation of macrophage progenitors (typically 6-8 generations) and differentiation into mature macrophages (7).

2.8 Fish cell lines

2.8.1 Catfish 3B11 cells

Catfish 3B11 B-cells were maintained in complete MGFL-15 at 27^{o}C without CO_2. This cell line is non-adherent. Cells were passed upon reaching confluency, generally every 2-3 days, at a 1:40 dilution in fresh complete MGFL-15 media.

2.9 Isolation of primary mammalian cells

2.9.1 Peritoneal lavage

Mice were sacrificed by cervical dislocation. Skin surrounding the peritoneal cavity was removed, ensuring the peritoneal cavity remained intact. Ten mL of ice-cold 1xPBS$^{-/-}$ was then injected using a blunt end 18-gauge needle. Peritoneal cavity was massaged gently to detach cells and PBS was sucked back into the needle.

To isolate cell subpopulations, murine lavages were run over a Ficoll (Histo-Paque) gradient. This was centrifuged at 400 x *g* for 30 minutes at 4^{o}C. Following centrifugation, buffy coats containing mononuclear cells were collected into a separate tube. These cells and the neutrophil pellets were washed with once with serum-free media (centrifuge 311 x *g* at 4^{o}C for 10 minutes). Cells were then resuspended in complete media and plated in 6-well plates with 1x10^{6} cells in 2 mL in each condition (responding cells).

2.9.2 Splenocytes

Mice were sacrificed by cervical dislocation. Spleens were removed and homogenized using a wire mesh screen using ice cold incomplete DMEM (no serum or antibiotics). As with goldfish kidneys, debris was settled and cells were collected and spun down at 311 x *g* for 10 minutes at 4^{o}C. Pellets were resuspended in 1 mL ACK Lysis buffer for 1 minute and washed with incomplete 10 mL DMEM. Cells were then centrifuged at 311 x *g* for 10 minutes at 4^{o}C and were then resuspended in complete DMEM and used to make apoptotic cells.

2.10 Mammalian cell lines

2.10.1 Jurkat T cells

Jurkat T cells were cultured in RPMI 1640 supplemented with 100 U/mL penicillin/ 100 μg/mL streptomycin, 10% fetal calf serum, 1 mM sodium pyruvate, and 1x non-essential amino acids (all from Gibco). These cells are non-adherent. Cells were passaged every 2-3 days at a 1:10 dilution in complete RPMI 1640.

2.10.2 RAW 264.7 macrophages

RAW 264.7 macrophage cells were cultured in complete DMEM media (DMEM with 10% fetal calf serum and 100 U/mL penicillin/ 100 μg/mL streptomycin). Cell lines were cultured at 37^{o}C/5% CO_2 and passaged every 3-4 days, prior to reaching confluence. This is an adherent cell line. To pass cells, media was decanted and the flask was washed thoroughly with 10 mL 1x $PBS^{-/-}$ to remove remaining serum. One mL of trypsin-EDTA was then added and incubated at 37^{o}C/5% CO_2 for 3 minutes. Cells were then detached by gently banging flask.

To inactivate trypsin, 10 mL of complete DMEM was added. Cells were then collected into a 15 mL tube and centrifuged at 311 x *g* for 10 minutes at 4^{o}C. Pelleted cells were resuspended in 10 mL of fresh complete DMEM. One mL of resuspended cells was added to a culture flask containing fresh complete DMEM.

2.11 Cytochemical staining

2.11.1 Hema3

One hundred thousand cells were spun onto glass slides at 55 x *g* for 6 minutes at room temperature using a cytocentrifuge (Shandon Instruments). Cells were fixed by incubation in 70% methanol for 5 seconds. Cells were stained with hematoxylin for 5 seconds and counter-stained with eosin for 1 second (all components from Fisher Scientific). Slides were then rinsed with tap water and air-dried prior observation using bright field microscopy. Photomicrographs were generated using a DM1000 microscope (Leica) using a bright field 100x objective (1000x magnification). Images were acquired using QCapture software.

2.11.2 Sudan Black

One hundred thousand cells were spun onto glass slides at 55 x *g* for 6 minutes at room temperature using a cytocentrifuge (Shandon Instruments). For Sudan Black staining (Sigma), cells were fixed with a 75% gluteraldehyde: 25% acetone fixative solution for one minute at 4^{o}C. Slides were then rinsed well with distilled water and stained with Sudan Black for 5 minutes with continuous, gentle rocking. Slides were thoroughly rinsed with 70% ethanol to remove excess Sudan

Black staining and further rinsed in distilled water. Cells were counterstained with Gill's 3 solution (Sigma) for 5 minutes and rinsed with tap water for 2 minutes. Slides were air-dried prior to observation using bright field microscopy. Photomicrographs were generated using a DM1000 microscope (Leica) using a bright field 100x objective (1000x magnification). Images were acquired using QCapture software.

2.12 Flow cytometric staining

2.12.1 Antibody labeling

To distinguish murine leukocyte populations, cells were stained with a combination of: CD11b-FITC/ Gr1-PE/ F4/80-APC or CD11b-PE-Cy7/ CD3-FITC/ B220-PE/ NK1.1-APC (all from BD Biosciences). Prior to staining, cells were blocked for 20 minutes with a solution of 1x $PBS^{-/-}$ with 10% calf serum. All staining was done in a solution of 1x $PBS^{-/-}$ with 2% calf serum for 30 minutes at room temperature in the dark. Antibodies were added according to the manufacturer's protocols. Goldfish leukocytes were stained with a polyclonal anti-CSF-1R antibody that was produced and validated by the Belosevic lab (University of Alberta) (8). Cells were stained with 1x $PBS^{-/-}$ with 2% calf serum and 0.05% sodium azide. Following primary stain, goldfish cells were washed and stained with an anti-rabbit-FITC secondary (Jackson ImmunoResearch).

2.12.2 Flow cytometry-based fluorescent *in situ* hybridization

A detailed description of this procedure, related data, and a full protocol can be found in Appendix II. Briefly, desired genes were amplified by PCR and cloned into TOPO TA plasmid (Invitrogen). Primer sequences for gene inserts can be found in Table 2.12. Competent DH5α were transformed and plasmids were isolated using a Miniprep kit (Qiagen). Plasmids were linearized with BamHI (Invitrogen) for 1 hour at 37^{o}C followed by purification with a PCR purification kit (Qiagen). RNA probes were generated from linearized plasmids using T7 RNA polymerase (Invitrogen), and labeled nucleotides (biotin-14-CTP (Invitrogen) or fluorescein-12-UTP (Roche)) were used to distinguish between specific probes.

For hybridization, cells were fixed overnight in 2% formaldehyde at 4^{o}C, washed in incomplete media, and re-fixed in 70% ethanol at room temperature. Cells were then spun down at 393 x *g* for 10 minutes at 4^{o}C and all liquid was decanted. Membranes were digested with proteinase K for 7 minutes at room temperature. To stop the digestion, 1 mL of 2% formaldehyde was added for 10 minutes at 4^{o}C. RNA probes were added to cells in hybridization buffer (Table 2.6) and incubated at 60^{o}C for 4 hours. Tubes were inverted every 30-60 minutes. Excess hybridization buffer without probe was added and cells were incubated for a further 45 minutes at 60^{o}C. Cells were then washed using 2xSSC (Table 2.7), 0.1xSSC, and 1xPBS$^{-/-}$ (all centrifugations at 393 x *g* for 10 minutes at 4^{o}C), and subsequently stored in 2% formaldehyde O/N at 4^{o}C. Staining with secondary antibodies allowed detection of RNA probes (streptavidin-APC to detect biotin-14-CTP; BD BioSciences or anti-fluorescein DyLight 488 to detect fluorescein-12-UTP; Jackson ImmunoResearch). Levels of gene expression were then analyzed

using an ImageStream IS100 or mkII (Amnis Corporation, EMD Millipore) and a FACSCanto II flow cytometer (BD Biosciences).

2.13 Cell bioassays

2.13.1 Phagocytosis

2.13.1.1 Light microscopy

RAW 264.7 macrophages were plated in 6-well plates at a concentration of $5x10^5$ cells/mL. Cells were allowed to adhere overnight. Three μm latex beads (Polysciences) were added at a ratio of 5:1 (zymosan: cells) and incubated for the indicated times at $37^oC/5\%$ CO_2. Cells were then stained by Hema3 stain set as outlined above (Fisher Scientific) and counted by light microscopy. At least 200 cells were counted.

2.13.1.2 Confocal fluorescent microscopy

RAW 264.7 macrophages were seeded onto sterilized glass coverslips in a 6-well plate at a concentration of $5x10^5$ cells/mL. Cells were allowed to adhere overnight. Zymosan-FITC particles (Molecular Probes) were added at a ratio of 5:1 (zymosan: cells) and incubated for the indicated times at $37^oC/5\%$ CO_2. Cells were then fixed with 1% formaldehyde for 10 minutes on ice and washed 2 times with $1xPBS^{-/-}$ (centrifuge at 393 x *g* at 4^oC for 10 minutes). One hundred ng/mL 4', 6-diamidino-2-phenylindole (DAPI; Molecular Probes) was added to the mounting media and coverslips were mounted onto slides. Cells were

imaged using a Zeiss LSM 510 laser scanning confocal microscope. Images were acquired at 40x/1.3. At least 100 cells were counted.

2.13.1.3 Flow cytometry

In order to evaluate our capacity to differentiate between phagocytic and non-phagocytic cells in mixed populations, we took advantage of two well-characterized cellular models: RAW 264.7 cells and Jurkat cells. RAW 264.7 cells were mixed with Jurkat T cells at a ratio of 1:1. Zymosan-FITC was added to cells at a ratio of 3:1 or 5:1 (zymosan: total cells) and cells were incubated for the indicated times at 37^{o}C/5% CO_2. Following phagocytosis, cells were washed twice with 1xPBS$^{-/-}$ (no calcium, no magnesium) and labeled with anti-mouse CD45-PE (BD Biosciences) for 30 minutes on ice. Anti-mouse CD45 allows differentiation between RAW 264.7 macrophages (murine derived) and Jurkat T cells (human derived) based on specificity for the murine, but not human, CD45. Following staining, cells were washed twice with 1xPBS$^{-/-}$ (centrifuge at 311 x *g* for 10 minutes at 4^{o}C) and fixed with 1% formaldehyde for 10 minutes on ice and data was acquired on a FACSCalibur (BD Biosciences). At least 20,000 cellular events were analyzed.

2.13.1.4 ImageStream

FITC labeled zymosan-A particles were added at a ratio of 3:1 or 5:1 (zymosan: cell) to 2x10^{6} cells. Mammalian cells were incubated for 2 hours at 37^{o}C/5% CO_2 in complete DMEM media. Teleost phagocytosis assays were

performed in incomplete MGFL-15 media (no serum) at 20^{o}C. Following phagocytosis, cells were fixed with 1% formaldehyde overnight at 4^{o}C. Data was acquired on an ImageStream IS100 or mkII (Amnis Corporation, EMD Millipore). At least 10,000 cells were acquired.

2.13.2 Respiratory burst

This assay was performed as previously described (9, 10). Briefly, following activation, cells were harvested and collected into 5 mL polystyrene round bottom tubes (BD Falcon). Cells were washed twice with 1xPBS$^{-/-}$ (centrifuge at 311 x *g* for 10 minutes at 4^{o}C) then resuspended in 100 μL 1xPBS$^{-/-}$. Dihydrorhodamine (DHR, Molecular Probes) was added to cells at a final concentration of 10 μM and incubated for 5 minutes to allow cells to take up the DHR. Phorbol 12-myristate 13-acetate (PMA; Sigma) was then added at a final concentration of 100 ng/mL. This concentration of PMA has been shown to trigger ROS production in primed fish cells (11). Cells were incubated for a further 30 minutes to allow oxidation of DHR. For all murine experiments, incubations were done at 37^{o}C/5%CO_2. For all goldfish experiments, incubations were done at 20^{o}C. All samples were properly staggered with respect to time to accommodate for the transient state of oxidized DHR fluorescence. DHR fluorescence was not quenched by the presence of other fluorochromes, including the wheat germ agglutinin or APC labels on phagocytosed particles.

2.13.3 Nitric oxide production

Nitric oxide production was determined indirectly by the Griess reaction (12). Ten thousand cells in 50 μL of complete MGFL-15 medium were added to individual wells of a 96-well plate, followed by 50 μL of treatments also in complete MGFL-15 medium. For all goldfish macrophage assays, plates were incubated for 72 hours at 20°C. Following incubation, plates were centrifuged at 230 x *g* and 75 μL of cell media transferred to new wells of a 96-well plate. One hundred μL of 1% sulfanilamide (dissolved in 2.5% H_3PO_4) was added to each well, followed by 100 μL of 0.1% N-naphthyl-ethylenediamine (dissolved in 2.5% H_3PO_4). The reaction was allowed to proceed for 2 minutes before plates were read using a micro plate reader at a wavelength of 540 nm. The concentration of nitrate produced by individual samples was determined using a standard curve that was generated using sodium nitrate standard curve.

2.13.4 Phagolysosome fusion

In order to study fusion of lysosomes to phagosomes, cells were loaded with 0.25 μg dextran-FITC (Molecular Probes) for 45 minutes at 20°C (13). Cells were washed twice in incomplete MGFL-15 media (no serum; centrifuge at 311 x *g* for 10 minutes at 4°C) followed by incubation in serum-containing media for 45 minutes at 20°C to allow dextran localization to the lysosomes. After this, 'dextran-loaded' cells were incubated for 2 hours with 3 μm non-fluorescent latex beads (Polysciences) at a 3:1 ratio (bead: cell). A lower bead ratio compared to phagocytosis assays was used to reduce the number of beads internalized per cell to provide more accurate quantification of phagolysosome fusion. Following

phagocytosis, cells were washed with 1xPBS$^{-/-}$ and fixed for 10 minutes on ice with 1% formaldehyde. Cells were then analyzed by confocal microscopy or with an ImageStream IS100 (Amins Corportation, EMD Millipore).

2.13.5 Gentamicin protection assay

Bacteria (*Aeromonas veronii* for most assays) were grown into log phase growth in tryptic soy broth at room temperature. Bacteria was then washed thoroughly with 1xPBS$^{-/-}$ (centrifuge at 2640 x *g* for 10 minutes at room temperature) and added to cells at a ratio of 100:1. All assays were done in 5 mL round-bottom FACS tubes (BD Biosciences). Cells were incubated with bacteria for 30 minutes at 20^{o}C, then washed with incomplete MGFL-15 media (centrifuge at 311 x *g* for 10 minutes at 4^{o}C). Cells were then resuspended in 100 µL incomplete MGFL-15 media containing 200 µg/mL gentamicin, added to the 100 µL cell suspension and incubated for 30 minutes at 20^{o}C. After incubation, 2 mL of incomplete media was added to dilute the gentamicin. At required time points, cells were spun down at 311 x *g* for 10 minutes at 4^{o}C. To lyse cells, media was decanted and cells were resuspended in 90 µL MilliQ water with 0.1% Triton-X 100. Cells were vigorously flicked for 30 seconds then 10 µL of 10xPBS$^{-/-}$ was then added to return solution of isotonic levels. The lysate was plated onto square TSA plates following serial 10-fold dilutions. For each dilution, 10 µL was plated. Colony formation was counted after 48 hours.

2.13.6 Arginase assay

The arginase assay was completed as previously described (14-16). Briefly, macrophages were lysed in a 0.1% Triton X-100 buffer containing pepstain, aprotinin and antipain. Equivalent volume of 10 mM $MnCl_2$/ 50mM Tris-HCl/ pH 5.5 was added and samples were incubated for 7 minutes at 56^{o}C to activate the enzyme. One hundred µL of this solution was added to 100 µL of 0.5M arginine/pH 9.7 and incubated for 2 hours at 37^{o}C. The reaction was stopped by adding 800 µL of acid mix (H_3PO_4: H_2SO_4: H_2O, 1:3:7). Forty µL of α-isonitrosopropiophenone in 100% ethanol was added to all samples and concentration standards and incubated for 45 minutes at 100^{o}C. After cooling for 10 minutes, the A540 was measured using a plate reader. Arginase activity was calculated from the curve produced by concentration standards, generated with each experiment.

2.13.7 Survivability assay

To assess survival of cells under oxidative conditions, PKMs exposed to increasing concentration of rsCSF-1R were treated with 2 mM H_2O_2 for 2 hours. Viability was determined by AnnexinV/ propidium iodide staining, as previously described (17, 18). A thorough protocol can be found in Appendix I. In brief, cells were harvested and washed twice in 1xAnnexinV binding buffer (BD Biosciences). AnnexinV and PI were then added according to the manufacturers specifications and incubated in the dark for 30 minutes at room temperature. Cells were then washed well with 1xAnnexinV binding buffer and fixed with 1% formaldehyde for 10 minutes at 4^{o}C. Cells were then treated with RNase for 30 minutes and 37^{o}C,

washed twice with 1xPBS$^{-/-}$ (centrifuge at 393 x *g* for 10 minutes at 4^{o}C) and images were acquired using an ImageStream IS100 or mkII (Amnis Corporation, EMD Millipore). When cells were analyzed on a FACSCanto II flow cytometer (BD Biosciences), acquisition was done immediately following staining, without fixation and RNase digestion.

2.13.8 Trans-well assay

To determine the role of soluble factors in mediating responses, trans-wells (0.4 μm pore size, Corning) were used. These trans-wells permit free flow of soluble factors but prevent cell transmigration and physical interactions with cells across the barrier. Activator cells with various stimuli were added into the bottom of a 6-well plate in 1 mL of complete MGFL-15 media. The bottom was used for responding cells due to issues to trans-wells tearing during harvesting, resulting in poor recovery. Trans-wells were then placed and 1 mL of media containing responding cells was added into each trans-well. Cells were then incubated for 2 hours (at 18^{o}C for goldfish cells; 37^{o}C/5% CO_2 for murine cells). Five μg/mL zymosan was added to all murine cells during the incubation to maintain activation achieved *in vivo*. Following incubation, responding cells were harvested and ROS production was assayed with DHR. Since lymphocytes could not be efficiently removed from mononuclear cells preparations without affecting cellular responses, these cells were removed from the analysis through gating strategies. As such, analyzed populations are referred to as ‘neutrophils’ and ‘monocytes/macrophages’.

2.13.9 Cellular infiltration

Animals were sacrificed after indicated time points and cells were harvested by peritoneal lavage. To determine *in vivo* responses to apoptotic cells, goldfish and C57BL/6 mice were injected with either $5x10^6$ apoptotic cells (in 100 μL of 1x PBS $^{-/-}$) and/or 2.5 mg zymosan (Sigma) in 100 μL of 1x PBS $^{-/-}$for 24 hours. To study the effects of pre-injection of apoptotic cells, animals were injected with apoptotic cells at 0 hours, 2 hours, or 4 hours before zymosan (zymosan injection defined time 0). Cells were counted using a haemocytometer. Within these time points, changes in cellular numbers were largely associated with cellular infiltration. Sub-populations were defined by expression of specific markers (CD11c, Gr1, F4/80, CD3, B220, NK1.1; mice) or by a combination of size, complexity, morphology and cytochemical staining (goldfish).

2.13.10 Chemotaxis assay

Proliferative PKM cultures were incubated with zymosan +/- increasing concentrations of recombinant sCSF-1R or apoptotic cells (5:1 ratio) for 24 hours. Supernatants were collected fresh for each experiment, filtered through a 0.22 μm filter and 100 μL were applied to the bottom chamber of blind well leucite chemotaxis chambers (Nucleoprobe).

Goldfish were injected with 2.5 mg zymosan (Sigma) and cells were harvested after 24 hours. Neutrophils were isolated from peritoneal lavage cells by layering over 51% Percoll as previously described (19, 20) and outlined above. Red

blood cells were lysed by ACK Lysis buffer (Lonza), typically in 3 mL for 5 minutes. Cell viability was confirmed with AnnexinV/PI staining; functionality was confirmed by ROS production. Neutrophils ($1x10^6$) were applied to the top chamber of blind well leucite chemotaxis chambers. The top and bottom chambers were separated by a 5 μm pore polycarbonate membrane (NeuroProbe). The chemokinesis (ChK) control allowed for control of neutrophil chemotaxis to an inflammatory stimulus in the absence of a chemotactic gradient and consisted of zymosan-stimulated supernatants in both the upper and lower chambers of the chemotaxis apparatus. Cells were then incubated for 1 hour at 20^{o}C after which the cell suspensions were aspirated from the top chamber. The filters removed, fixed in methanol for 1 minute, stained with Gill's Solution 3 (Sigma) for 1 minute and then applied to a slide and fixed under a coverslip using Permount (Fisher Scientific). Chemotactic activity was measured by counting cells found on the underside of filters in 25 random fields of view (100x, oil immersion).

2.13.11 *In* vivo BrdU proliferation assay

Following treatment, goldfish were anesthetized and injected with 100 μL of BrdU solution. The final concentration was adjusted to be 1 mg/g of fish, as previously described (21). Goldfish were incubated for 1 hour in water from the fish facilities. Goldfish were then terminated and kidneys were harvested and processed as above. An aliquot of $1x10^6$ cells were then removed and fixed for a minimum of 24 hours in 1% formaldehyde at 4^{o}C. After fixation, cells were spun down at 393 x *g* for 10 minutes at 4^{o}C and resuspended in BrdU

fixation/permeabilization buffer according to the manufacturers' protocol (eBioscience) for 1 hour at 4°C. Cells were then washed once in FACS buffer at (centrifuge at 393 x *g* for 10 minutes at 4°C) and resuspended in 100 µL FACS buffer (1xPBS$^{-/-}$ supplemented with 2% calf serum) containing DNase I, followed by a 1 hour incubation at 37°C. Cells were then washed once and stained with 5 µL of anti-BrdU-FITC antibody (eBioscience) in 100 µL of FACS buffer for 1 hour at room temperature. Cells were then washed twice with 2 mL FACS buffer (centrifuge 393 x *g* for 10 minutes at 4°C) and acquired on a CANTO II (BD Biosciences).

2.14 Quantitative PCR

2.14.1 RNA isolation

2.14.1.1 Trizol method

RNA was isolated from goldfish tissues using Trizol (Invitrogen) according to the manufacturers specifications. Briefly, tissues were placed in 12 mL round-bottom tubes, flash frozen and stored at -80°C. The required amount of Trizol was then added, depending on tissue size (generally 1 mL for kidney and spleen; 2mL for furuncle tissue) and tissue was homogenized using blade disruption. Following homogenization, the Trizol mixture was incubated in ice for 10 minutes prior to addition of chloroform (0.1 mL/ 1mL Trizol) and volume was transferred into a 1.5 mL microcentrifuge tube. Tubes were vigorously vortexed, settled on ice for 5 minutes and then re-vortexed. Tubes were centrifuged at 10,800 x *g* for 30 minutes in a refrigerated microcentrifuge at

4°C. The aqueous (clear) layer was extracted and transferred to a new 1.5 mL microcentrifuge tube. One volume of isopropanol was added and tubes were gently inverted and incubated at -20°C overnight. Samples were then centrifuged at 10,800 x *g* for 60 minutes at 4°C to pellet the RNA. Supernatants were aspirated, and the RNA pellet washed with 1 mL of 75% reagent grade ethanol followed by centrifugation at 10,800 x *g* for 30 minutes at 4°C. Ethanol was aspirated and pellets allowed to air-dry for 5 minutes. Nuclease-free water was used to re-suspend the RNA pellet. The nucleic acid concentration was quantified using a Nanodrop apparatus at an absorbance of 260 nm. Samples were also read at absorbences of 230 nm and 280 nm to determine phenolic and protein contamination.

2.14.1.2 Qiagen RNeasy kit

RNA was isolated from peritoneal lavage cells using a Qiagen RNeasy kit (Qiagen) according to the manufacturers specifications. Briefly, cells were lysed in Buffer RLT. One volume of 70% ethanol was added to the lysate and applied to the spin column. Columns were spun at 8,000 x *g* for 15 seconds at room temperature and washed with Buffer RW1. Columns were spun at 8,000 x *g* for 15 seconds at room temperature. Columns were then washed with Buffer RPE and spun at 8,000 x *g* for 2 minutes at room temperature. The column was then placed into a new 1.5 mL microcentrifuge tube and 30-50 µL of nuclease-free water (Ambion) was added. To elute RNA, columns were spun at 8,000 x *g* for 1 minute room temperature. The nucleic acid concentration was quantified using

a Nanodrop apparatus at an absorbance of 260 nm. Samples were also read at absorbences of 230 nm and 280 nm to determine phenolic and protein contamination.

2.14.2 cDNA synthesis

cDNA synthesis performed using SMARTScribe Reverse Transcriptase (Clontech) according to the manufacturer's protocol using poly-dT. First strand synthesis was cycled at 72^{o}C for 3 minutes followed by 42^{o}C for 60 minutes. Second strand synthesis was completed as follows: 95^{o}C for 30 seconds; 55^{o}C for 30 seconds; 72^{o}C for 15 minutes. RNA levels were quantified and normalized prior to cDNA synthesis (2 mg for tissues; 200 ng for peritoneal lavages). Primers used in cDNA synthesis reactions can be found in Table 2.10.

2.14.3 Primers

All primers used had been previously validated for use in goldfish. Briefly, for Q-PCR, primers were validated by 1:2 serial dilutions of cDNA and creating a standard curve, used in determining in the R^2 value, y-intercept, and efficiency of the primer set using the 7500 Fast software. All primer sets were chosen with an R^2 value of 0.997 or higher, a y-intercept value of -3.0 to -3.2, and an efficiency of 85% or higher. Melt curves were analyzed to ensure a single melting peak, and qPCR products were run on a gel, excised, and sequenced to ensure the correct amplicon was being amplified. Q-PCR primers can be found in Table 2.14. For

RT-PCR, products were run on a gel, excised, and sequenced to ensure the correct amplicon was being amplified.

2.14.4 Quantitative PCR conditions

Quantitative PCR was performed using an Applied Biosystems 7500 Fast Real-Time PCR machine using SYBR green reagents. Elongation factor 1 alpha (EF1α) was used as the endogenous control for all experiments. Thermocycling conditions were: 95^{o}C for 10 minutes followed by 40 cycles of 95^{o}C for 15 seconds and 60^{o}C for 1 minute. A melting curve step was added to the end of this protocol. Data were analyzed using the 7500 fast software (Applied Biosciences) and is represented as the average of the samples with standard error shown. The RQ values were normalized against control fish.

2.15 Detection of sCSF-1R transcripts

Target mRNA transcripts were amplified by adding 1 µL of cDNA template to 40.3 µL of nuclease free water, 5 µL of Micah's 10xPCR buffer (1 mM Tris-HCl, pH 8.3, 500 mM KCl, 15 mM MgCl2, 0.01% w/v gelatin), 1.2 µL of 20 mM primer solution, 0.8 µL of 25 mM dNTPs, and 0.5 µL of Taq polymerase. Reactions were amplified in an Eppendorf Mastercycler Nexus Gradient thermocycler. The general thermocycling program consisted of an initial denaturation step of 94^{o}C for 3 minutes, followed by 40 cycles of 95^{o}C for 30 seconds; 55^{o}C for 1 minute and 30 seconds; 72^{o}C for 2 minutes, and a final extension of 72^{o}C for 5 minutes. Bands were visualized by running out on a 1%

agarose gel. Gels were then stained with an ethidium bromide solution for 30 minutes, followed by destaining in distilled water for 30 minutes. Gel images were acquired using an AlphaImager 2200 (Alpha Innotech). Primer sequences can be found in Table 2.13.

For densitometry analysis, files were uploaded in ImageJ and relative band intensity was determined for sCSF-1R and β-actin. The ratio of β-actin to sCSF-1R was determined for each set. RT-PCR was used for these assays, as selective Q-PCR primers could not be developed for this transcript.

2.16 Detection of sCSF-1R protein

Samples were diluted 1:1 in 2x Laemmli buffer (Table 2.8) and boiled for 10 minutes. Proteins were separated under denaturing and reducing conditions on a 10% polyacrylamide (PAGE) gel. Proteins were transferred to a 0.2 μm nitrocellulose membrane (BioRad) and blocked for 1 hour at room temperature in 5% milk/TBS-T. Membranes were then incubated with anti-CSF-1R (1:1000 in 5% milk/TBS-T) overnight at 4^{o}C with continuous rocking. Membranes were then washed 3 times and incubated with goat-anti-rabbit HRP (1:50 000 in 5% milk/TBS-T) for 1 hour at room temperature. Membranes were developed with WesternBrightECL (advansta) to detect horseradish peroxidase (HRP) conjugated antibodies according to the manufacturers specifications. Membranes were imaged with film (Kodak).

2.17 Analysis

All confocal data was analyzed using Zen 2012 lite software (Zeiss). Flow cytometry data was analyzed with FCS Express software v3 (DeNovo Software) or FACSDiva v6.1.3 (BD Biosciences). ImageStream data was analyzed using IDEAS v3 through v5 software (Amnis Corporation, EMD Millipore). Statistics were performed on Prism 4 software (GraphPad Prism). For statistics involving two comparisons a Students' t-test was preformed. For statistics involving more than two comparisons, a one-way ANOVA was used. For post-hoc analyses, a Tukey's test was used when all-pairwise analyses were desired. When only a comparison to control was desired a Dunnet's post-hoc test was used. For all one-way ANOVA tests, all values were transformed by square roots for ensure equal variance in all samples, fulfilling a requirement for the test to be preformed. For each assessment, each experiment was assessed for a Trial effect. For statistics involving more than two comparisons over time, a two-way ANOVA was used followed by a Bonferroni post-hoc test. Similar to one-way ANOVA tests, all values were transformed by square roots for ensure equal variance in all samples, fulfilling a requirement for the test to be preformed. In addition, each experiment also underwent an assessment for a Trial effect, a Time effect and a Trial X Time effect. No Trial X Time effect was noted for any experiment.

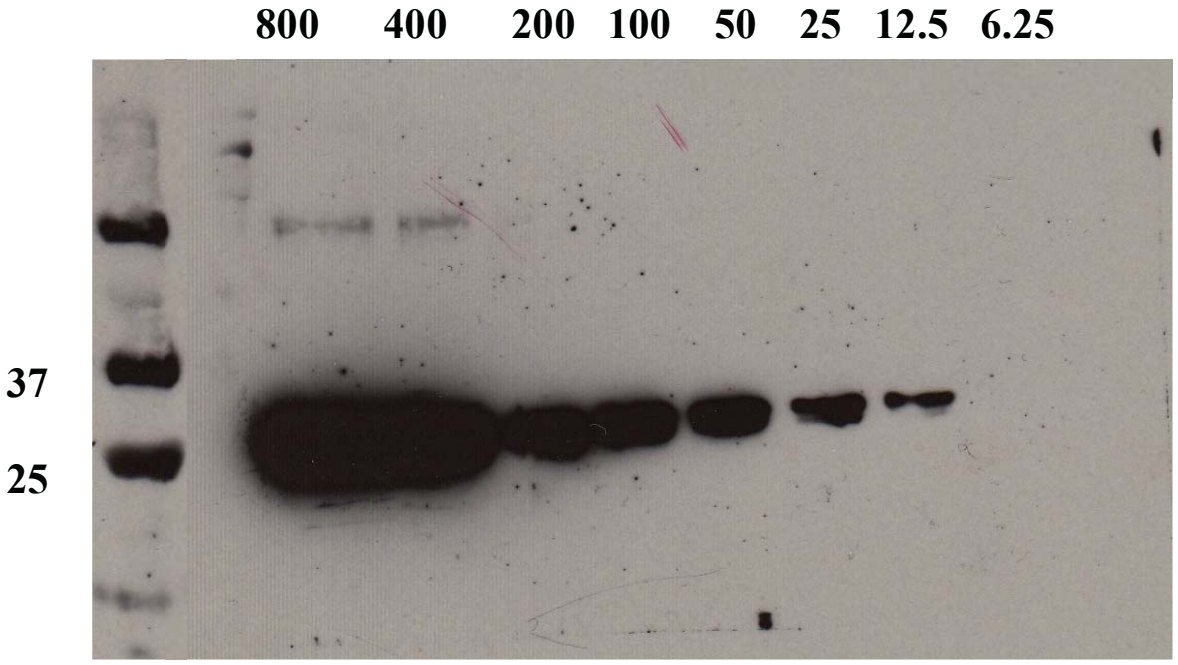

Figure 2.1. Serial dilutions of recombinant sCSF-1R.

Recombinant sCSF-1R was serially diluted 1:1. Samples were treated as described and run on a 10% PAGE gel. Protein was detected with polyclonal rabbit anti-goldfish CSF-1R. Concentrations indicated are in nanograms.

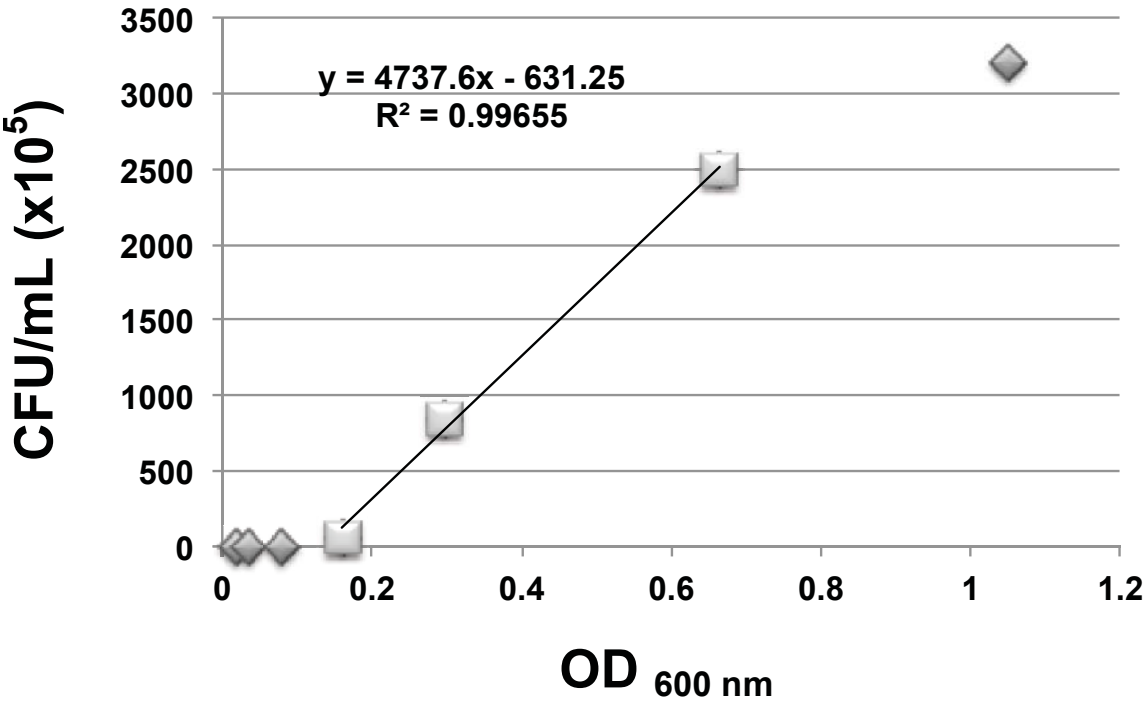

Figure 2.2. ***Aeromonas veronii*** **growth curve.**

Aeromonas veronii was grown at room temperature for 8 hours. Every hour, a 1 mL aliquot was removed. Optical density (OD) and colony forming units (CFU) were determined for each time point.

Table 2.1. Composition of 10xPBS$^{-/-}$.

COMPONENT	AMOUNT (g)
KCl	2.00
KH_2PO_4	2.00
NaCl	80.00
$Na_2HPO_4 \bullet 7H_20$	21.60
MilliQ water	top to 1 L

Table 2.2. Composition of carbonate buffer.

COMPONENT	AMOUNT (g)
0.5 M sodium carbonate buffer*	0.8 mL
0.5 M sodium bicarbonate buffer**	1.7 mL
MilliQ water	top to 10 mL

* Add 0.529 g of sodium carbonate to 10 mL MilliQ water.
** Add 0.42 g sodium bicarbonate to 10 mL MilliQ water.

pH final buffer to 9.6.

Table 2.3. Composition of incomplete MGFL-15 media.

COMPONENT	AMOUNT
HEPES	7.00 g
KH_2PO_4	0.688 g
K_2HPO_4	0.57 g
NaOH	0.75 g
$NaHCO_3$	0.34 g
10x Hanks Balanced Salt Solution	80 mL
MEM amino acid solution	25 mL
MEM non-essential amino acid solution	25 mL
Sodium pyruvate	25 mL
MEM vitamin solution	20 mL
Nucleic acid precursor solution	20 mL
L-glutamine	0.5844 g
Insulin	0.01 g
GFL-15*	1000 mL
β-mercaptoethanol	7 μL
MilliQ water	top to 2 L

*GFL-15 is made by mixing DMEM and Leibovitz-15 media powders in 2 L of MilliQ.

Table 2.4. Composition of nucleic acid precursor solution.

COMPONENT	AMOUNT (g)
Adenosine	0.067
Cytidine	0.061
Hypoxanthine	0.034
Thymidine	0.061
Uridine	0.061
MilliQ water	100 mL

Table 2.5. Composition of 10x Hank's Balanced Salt solution.

COMPONENT	AMOUNT (g)
KCl	2.00
KH_2PO_4	0.30
NaCl	40.00
$Na_2HPO_4 \bullet 7H_20$	0.45
D-glucose	5.00
Phenol red	0.05
MilliQ water	top to 500 mL

Table 2.6. Composition of hybridization buffer.

COMPONENT	AMOUNT
Sheared salmon sperm DNA	1 mL
Formamide	10 mL
20x SSC	5 mL
Tween-20	200 µL
SDS	0.1 g
Nuclease-free water	4 mL

Table 2.7. Composition of SSC buffer.

COMPONENT	AMOUNT (g)
NaCl	175.3
Sodium citrate	88.2
MilliQ water	1 L

pH solution to 7.0 and autoclave.

Table 2.8. Composition of 2x Laemmli buffer.

COMPONENT	AMOUNT
SDS	0.4 g
β-mercaptoethanol	1 mL
Glycerol	2 mL
0.5 M Tris	2.5 mL
Bromophenol blue	pinch
MilliQ water	10 mL

Table 2.9. Primers used in cDNA synthesis.

PRIMER	SEQUENCE (5'-3')
5' oligo	AAG CAG TGG TAT CAA CGC AGA GTA CG
3' CDS poly T	AAG CAG TGG TAT CAA CGC AGA GTA TT
5' PCR	AAG CAG TGG TAT CAA CGC AGA GT

Table 2.10. Primers used in *Aeromonas spp.* detection.

PRIMER	SEQUENCE (5'-3')
16S rRNA forward (26)	AGA GTT TGA TCA TGG CTC A
16S rRNA reverse (1391)	GTG TGA CGG GCG GTG TGT A
16S rRNA forward (308)	GCT GGT CTG AGA GGA TGA TC
16S rRNA reverse (556)	CTT TAC GCC CAG TAA TTC CG
gyrB UP3	ACT ACG AGA TCC TGG CCA AG
gyrB UP4	TCC TCC CAG ACC AAG GAC
gyrB UP5r	GCC TTC TTG CTG TAG TCC TCT
gyrB UP6r	GCA GAG TCC CCT TCC ACT ATG TA

Table 2.11. Primers used to design flow cytometry-based *in situ* hybridization probes.

PRIMER	SEQUENCE (5'-3')
M13 forward	GTA AAA CGA CGG CCA G
M13 reverse	ACC AGC TAT GAC CAT GAT TAC
G-CSFR forward	TGG CTC ACC CGT ATC AGT GT
G-CSFR reverse	CAT GTG TCC AAG CTG CCA GT
CSF-1R forward	TCC TGT TCG TCT GTG GGA TCC TTT
CSF-1R reverse	GTT GGA GTC ATT GAT GAT GTC
sCSF-1R forward	CGG TCG GTA CGG ATG TGA TTC
sCSF-1R reverse	CCT TCA GCA AAG TAA TGA ACT

Table 2.12. Primers used in reverse transcriptase PCR for sCSF-1R expression.

PRIMER	SEQUENCE (5'-3')
β-actin forward	GTA AAA CGA CGG CCA G
β-actin reverse	ACC AGC TAT GAC CAT GAT TAC
sCSF-1R forward	TCG CTG CCC TGG TCG TTG ATA
sCSF-1R reverse	GGC GGC GGT TCC CAT CTC

Table 2.13. Primers used in quantitative PCR analysis.

PRIMER	SEQUENCE (5'-3')
EF-1α forward	CCG TTG AGA TGC ACC ATG AGT
EF-1α reverse	TTG ACA GAC ACG TTC TTC ACG TT
CSF-1 forward	ACA CAC ATA ACA GCC CAC AAA GCC
CSF-1 reverse	AGC ACA GGA CAA GGA TGA AGC ACT
CXCL-8 forward	CTG AGA GTC GAC GCA TTG GAA
CXCL-8 reverse	TGG TGT CTT TAC AGT GTG AGT TTG G
IFNγ forward	GAA ACC CTA TGG GCG ATC AA
IFNγ reverse	GTA GAC ACG CTT CAG CTC AAA CA
IFNγrel forward	TGT CGG AGC CAG ACT TCC A
IFNγrel reverse	GAC TCG ATT TTT TCT CGT ACG TTC T
IL-1β-1 forward	GCG CTG CTC AAC TTC ATC TTG
IL-1β-1 reverse	GTG ACA CAT TAA GCG GCT TCA C
IL-1β-2 forward	GAT GCG CTG CTC AGC TTC T
IL-1β-2 reverse	AGT GGG TGC TAC ATT AAC CAT ACG
IL-10 forward	CAA GGA GCT CCG TTC TGC AT
IL-10 reverse	TCG AGT AAT GGT GCC AAG TCA TCA
IL-12 p35 forward	TGT TTT ACG TGC ATT CCT TTG G
IL-12 p35 reverse	GGC GCC TGA AAA AAA TAC GA
IL-12 p40 forward	CTT CAG AAG CAG CTT TGT TGT TG
IL-12 p40 reverse	CAG TTT TTG AGA GCT CACCGA TAT C
iNOS A forward	TTG GTA CAT GGG CAC TGA GAT T
iNOS A reverse	CCA ACC CGC TCA AGA ACA TT
iNOS B forward	CAT CTT CCA TCC GAC CCT AGT G
iNOS B reverse	AAA GCT ACG GAA GGG AGC AAT
SOCS-3 forward	CGA GTC GGG CAC CAA GAA
SOCS-3 reverse	AAG CTC TGG AGT CCG TCT GAA
TGFβ forward	GTA CAC TAC GGC GGA GGA TTG
TGFβ reverse	CGC TTC GAT TCG CTT TCT CT
TNFα1 forward	CAT TCC TAC GGA TGG CAT TTA CTT
TNFα1 reverse	CCT CAG GAA TGT CAG TCT TGC AT
TNFα2 forward	TCA TTC CTT ACG ACG GCA TTT
TNFα2 reverse	CAG TCA CGT CAG CCT TGC AG

2.18 References

1. Majji, S., Thodima, V., Arnizaut, A., Deng, Y., May, W., Sittman, D., Waldbieser, G.C., Hanson, L., Cuchens, M.A., Bengten, E., et al. 2009. Expression profiles of cloned channel catfish (Ictalurus punctatus) lymphoid cell lines and mixed lymphocyte cultures. *Dev Comp Immunol* 33:224-234.
2. Miller, N.W., Rycyzyn, M.A., Wilson, M.R., Warr, G.W., Naftel, J.P., and Clem, L.W. 1994. Development and characterization of channel catfish long term B cell lines. *J Immunol* 152:2180-2189.
3. Barreda, D.R., Hanington, P.C., Stafford, J.L., and Belosevic, M. 2005. A novel soluble form of the CSF-1 receptor inhibits proliferation of self-renewing macrophages of goldfish (Carassius auratus L.). *Dev Comp Immunol* 29:879-894.
4. Sepulcre, M.P., Alcaraz-Perez, F., Lopez-Munoz, A., Roca, F.J., Meseguer, J., Cayuela, M.L., and Mulero, V. 2009. Evolution of lipopolysaccharide (LPS) recognition and signaling: fish TLR4 does not recognize LPS and negatively regulates NF-kappaB activation. *J Immunol* 182:1836-1845.
5. Neumann, N.F., Barreda, D.R., and Belosevic, M. 2000. Generation and functional analysis of distinct macrophage sub-populations from goldfish (Carassius auratus L.) kidney leukocyte cultures. *Fish Shellfish Immunol* 10:1-20.
6. Neumann, N.F., Barreda, D., and Belosevic, M. 1998. Production of a macrophage growth factor(s) by a goldfish macrophage cell line and macrophages derived from goldfish kidney leukocytes. *Dev Comp Immunol* 22:417-432.
7. Barreda, D.R., and Belosevic, M. 2001. Characterisation of growth enhancing factor production in different phases of *in vitro* fish macrophage development. *Fish and Shellfish Immunology* 11:169-185.
8. Katzenback, B.A., and Belosevic, M. 2012. Colony-stimulating factor-1 receptor protein expression is a specific marker for goldfish (Carassius auratus L.) macrophage progenitors and their differentiated cell types. *Fish Shellfish Immunol* 32:434-445.
9. Stafford, J.L., McLauchlan, P.E., Secombes, C.J., Ellis, A.E., and Belosevic, M. 2001. Generation of primary monocyte-like cultures from rainbow trout head kidney leukocytes. *Dev Comp Immunol* 25:447-459.
10. Rieger, A.M., Hall, B.E., and Barreda, D.R. 2010. Macrophage activation differentially modulates particle binding, phagocytosis and downstream antimicrobial mechanisms. *Dev Comp Immunol* 34:1144-1159.
11. Rieger, A.M., Hall, B.E., and Barreda, D.R. 2010. Macrophage activation differentially modulates particle binding, phagocytosis and downstream antimicrobial mechanisms. *Dev Comp Immunol* 34:1144-1159.
12. Green, L.C., Wagner, D.A., Glogowski, J., Skipper, P.L., Wishnok, J.S., and Tannenbaum, S.R. 1982. Analysis of nitrate, nitrite, and [15N]nitrate in biological fluids. *Anal Biochem* 126:131-138.

13. Worth, R.G., Kim, M.K., Kindzelskii, A.L., Petty, H.R., and Schreiber, A.D. 2003. Signal sequence within Fc gamma RIIA controls calcium wave propagation patterns: apparent role in phagolysosome fusion. *Proc Natl Acad Sci U S A* 100:4533-4538.
14. Classen, A., Lloberas, J., and Celada, A. 2009. Macrophage activation: classical versus alternative. *Methods Mol Biol* 531:29-43.
15. Joerink, M., Forlenza, M., Ribeiro, C.M., de Vries, B.J., Savelkoul, H.F., and Wiegertjes, G.F. 2006. Differential macrophage polarisation during parasitic infections in common carp (Cyprinus carpio L.). *Fish Shellfish Immunol* 21:561-571.
16. Joerink, M., Savelkoul, H.F., and Wiegertjes, G.F. 2006. Evolutionary conservation of alternative activation of macrophages: structural and functional characterization of arginase 1 and 2 in carp (Cyprinus carpio L.). *Mol Immunol* 43:1116-1128.
17. Rieger, A.M., Hall, B.E., Luong le, T., Schang, L.M., and Barreda, D.R. 2010. Conventional apoptosis assays using propidium iodide generate a significant number of false positives that prevent accurate assessment of cell death. *J Immunol Methods* 358:81-92.
18. Rieger, A.M., Nelson, K.L., Konowalchuk, J.D., and Barreda, D.R. 2011. Modified annexin V/propidium iodide apoptosis assay for accurate assessment of cell death. *J Vis Exp*.
19. Rieger, A.M., Konowalchuk, J.D., Grayfer, L., Katzenback, B.A., Havixbeck, J.J., Kiemele, M.D., Belosevic, M., and Barreda, D.R. 2012. Fish and mammalian phagocytes differentially regulate pro-inflammatory and homeostatic responses in vivo. *PLoS One* 7:e47070.
20. Katzenback, B.A., and Belosevic, M. 2009. Isolation and functional characterization of neutrophil-like cells, from goldfish (Carassius auratus L.) kidney. *Dev Comp Immunol* 33:601-611.
21. Santamaria, J.A., Mari-Beffa, M., Santos-Ruiz, L., and Becerra, J. 1996. Incorporation of bromodeoxyuridine in regenerating fin tissue of the goldfish Carassius auratus. *J Exp Zool* 275:300-307.

Chapter 3. Goldfish macrophages possess potent phagocytic responses and antimicrobial defenses[1]

3.1 Introduction

Phagocytosis is an important, evolutionarily conserved mechanism that is integral to host defenses against invading microorganisms. Phagocytosis is initiated by the interaction of receptors on the surface of the phagocyte with ligands on large particles, generally over 1 μm. Receptor ligation results in actin polymerization, which subsequently leads to particle internalization (1-4). Once internalized, the phagosome that encloses the particle undergoes a series of maturation steps that culminate in phagolysosome fusion. In order for phagocytosis to be an effective immune defense mechanism, these two components- internalization and phagosomal maturation- must occur (5).

There are a number of methods available to study phagocytosis. Of these, three common ones are based on light microscopy, fluorescent microscopy, and flow cytometry techniques. Each of these assays allow for detection phagocytosis with varying levels of specificity. These techniques, however, also have caveats that limit the accurate quantification of phagocytosis and their widespread application (e.g. time, reproducibility of quenching steps to remove fluorescence

---

[1] A version of this chapter has been published:

Rieger AM, Hall BE and Barreda DR. 2010. Macrophage activation differentially modulates particle binding, phagocytosis and downstream antimicrobial mechanisms. *Dev Comp Immunol* 34: 1144-59.

from surface bound particles, and others) (6, 7). Microscopy-based assays are largely limited by time requirements and low populations counts, which prevent statistically robust evaluation of phagocytosis. Flow cytometry-based assays have become increasingly popular due to the ability to analyze much higher cell counts in a short period of time. These assays, however, lack the spatial resolution of microscopy-based assays, which limit accurate quantification of internalized particles.

Using an ImageStream multi-spectral imaging flow cytometer, a novel assay was developed that incorporates the strengths of the previous assays, while overcoming the weaknesses associated with both the microscopy and flow cytometry assays. Analysis of phagocytic responses can be further enhanced by incorporation of specific cellular markers, characterization of cellular morphology, and an increased capacity for multivariate analysis. Images can be acquired at over 100 images/second, allowing analysis of a large population of cells.

This chapter describes the phagocytic capacity of goldfish primary kidney macrophage (PKM) cells. While it has been previously reported that mixed populations of these cultures are phagocytic, it is unclear which of the sub-populations are responsible for this activity (8, 9). Further, it remains unclear if these myeloid cells may display a differential capacity for phagocytosis and downstream killing mechanisms during key steps along their differentiation pathways. This chapter examines these questions among mixed populations of cells to allow for cellular cross-talk and to minimize the need for isolation of individual subpopulations, which is often associated with higher levels of basal activation.

The main objectives of this chapter were to (1) determine the predominant phagocyte in PKM cultures, (2) assess the impact of activation on phagocytic responses, including induction of downstream antimicrobial defense mechanisms, and (3) quantify phagolysosome fusion within a mixed PKM culture.

3.2 Results

3.2.1 Current methods have limitations for detecting phagocytosis.

While a number of assays exist to study phagocytosis, each of these assays has important limitations stemming from time constraints, low sample numbers and/or lack of spatial resolution. I initially evaluated three phagocytosis assays based on three commonly used platforms: (i) light microscopy, (ii) fluorescent microscopy and (iii) conventional flow cytometry.

In a standard light microscopy phagocytosis assay, well-characterized phagocytic RAW 264.7 macrophages were adhered to plate and incubated with non-fluorescent 3 μm latex beads for 2 hours (Figure 3.1 A). Cells were subsequently stained and phagocytosis was assessed using a compound light microscope. While this assay is relatively easy to carry out, does not require specialized equipment, and can distinguish between cells with internalized and surface bound particles (this is limited to X-Y axis), two major limitations include the number of cells that can be quantified (usually 200-300 cells) and the time that it takes to manually count these cells and the particles within them.

Similarly to the light microscopy-based assay, in the fluorescence microscopy-based assay, RAW 264.7 macrophage cells were adhered to coverslips and incubated with zymosan-FITC for 3 hours (Figure 3.1 B). Zymosan particles

are composed of the cell wall of chemically or heat-killed *Saccharomyces cerevisiae*, which makes them a relevant model of pathogenicity. Dectin-1 appears to be the main receptor involved in the phagocytosis of these zymosan particles (10). Phagocytosis was analyzed with a confocal fluorescence microscope. As with the light microscopy-based assay, the fluorescence microscopy-based assay allowed for differentiation between internalized and surface bound particles (also limited to X-Y axis). This was further improved by use of the Z-stacking feature, which is useful in determining particles that may be surface bound along the Z-axis. However, this method requires more specialized equipment than the light microscopy method and care must be exercised to prevent fluorochrome bleaching of fluorescent particles and/or cells during analysis. Furthermore, because relatively few cells are quantified, both light and fluorescence microscopy-based methods lack the statistical robustness of assays that can analyze thousands of cells in a population.

Using a flow cytometry-based phagocytosis assay, phagocytosis can be studied in a statistically robust manner (over 10,000 cells can be analyzed in a few minutes) and can be assessed in the context of a mixed population of cells. For this study, phagocytic RAW 264.7 macrophages were co-incubated with Jurkat T cells, a non-phagocytic human T cell line, and FITC-labeled zymosan (Figure 3.1 C). Prior to acquisition, cells were stained with anti-mouse CD45-PE, which selectively labels murine-derived RAW 264.7 macrophage cells but not human-derived Jurkat cells. The level of phagocytosis in both the RAW 264.7 macrophage and Jurkat T cell populations was quantified. While this assay allows analysis of a

large number of cells, there is no differentiation between cells with surface bound particles and internalized particles because of the lack of spatial resolution available through conventional flow cytometry. As such, the phagocytic population encompasses cells with internalized particles as well as those with bound (non-internalized) particles (Figure 3.1 D). Importantly, binding and internalization can have drastically different immunity outcomes. For example, only internalized pathogens within the maturing phagosome will be subjected to the potent intracellular killing mechanisms that characterize the phagocytosis process.

3.2.2 Multi-spectral imaging flow cytometry can help to overcome the limits of previous assays, while maintaining their strengths.

The ImageStream 100 and mkII multi-spectral imaging flow cytometers combine features of both conventional flow cytometry and fluorescence microscopy, produces simultaneous images of each cell (four (IS100) or six (ISmkII) fluorescent channels, brightfield and side-scatter) and can image over 100 cells per second (11, 12). This allows for analysis of a population of cells in a statistically robust manner within a few minutes.

RAW 264.7 macrophage and Jurkat T cells lines were co-incubated with FITC-labeled zymosan for two hours, similarly to the flow cytometry-based method. Following the incubation, cells were stained with anti-mouse CD45, which selectively labels RAW 264.7 macrophages, as described above. Subsequently, RAW 264.7 macrophage (CD45+) and Jurkat T cell (CD45-) populations were analyzed for zymosan fluorescence and phagocytosis, and produced dot plot

profiles equivalent to those shown above (Figure 3.2 A). In conventional flow cytometry, all cells in the FITC+ population would be considered phagocytic. However, as shown in Figures 3.2 A and 3.1 D, this population includes cells with internalized zymosan and as well as those with surface bound (i.e. non-internalized) zymosan. Using IDEAS software, a mask was created to identify the cellular membrane. This mask allowed differentiation between internalized (degree of internalization greater than 0) and bound (degree of internalization less than 0) zymosan particles in the X-Y axis (Figure 3.2 B). By gating on the population with a positive degree of internalization, I was able to remove cells with surface-bound particles from subsequent analysis, which was not possible with conventional flow cytometry. The degree of focus of the zymosan particles was then analyzed to remove surface bound zymosan in the Z-axis (Figure 3.2 C), a feature absent even in microscopy-based assays, which only provide spatial resolution in the X-Y axis. Zymosan bound outside of the X-Y plane of the cell image appears out of focus relative to the stained nucleus (i.e. in front or behind the plasma membrane boundaries of the cell [Z-axis]). While not as accurate as a confocal microscopy Z-stack, this method still allows clear distinction between internalized and surface bound (non-internalized) particles on the Z-axis because of digital-based quantitation of relative object focus (particle versus cell nucleus). The population of cells remaining after these two gating steps (X-Y axis and Z-axis) encompasses those with “true” phagocytosis, as all particles are internalized (Figure 3.2 D). This provides a more reliable approach for analysis of phagocytosis and generates statistically robust analyses in a relatively short amount of time. There is minimal

fluorochrome bleaching when compared to fluorescent microcopy-based approaches (and even superior to that found in flow cytometry) because of the mechanics of signal acquisition within the flow cell. Once gates are defined, IDEAS software can easily differentiate between internalized and bound particles. Finally, this phagocytosis analysis can be coupled with evaluation of morphological markers provided through the ImageStream platform (over 150 potential markers including size, nuclear morphology, nuclear: cytoplasmic ratios, and others). This is particularly relevant for comparative animal model systems where reagent availability (e.g. antibodies against surface or intracellular markers) often lags significantly behind the availability for murine/human models. Importantly, particle-binding events can also be quantified, thus providing an additional important parameter for the characterization of phagocytic responses. For example, this can provide a functional indicator of phagocytic receptor expression at the cell surface. As such, this approach has the potential to allow for more detailed characterization of phagocytic responses and the role that these events have on host antimicrobial mechanisms.

3.2.3 RAW 264.7 macrophage activation preferentially enhances binding and not internalization of zymosan.

Activation of RAW 264.7 macrophages has previously been shown to increase phagocytosis (13, 14). As a first step in the validation of the ImageStream-based phagocytosis assay I sought to examine if this increase in phagocytosis may be partially due to an increased capacity for particle binding during the phagocytic

response. To this end, I studied the effect of LPS stimulation on surface binding and internalization of zymosan particles in RAW 264.7 macrophages. RAW 264.7 cells were activated for 24 hrs with 100 ng/mL ultrapure *E. coli* LPS. Cells were then incubated with either a 3:1 or 5:1 ratio of zymosan for 2 hours. Surface binding and internalization were analyzed as described above. As expected, I found that LPS stimulation resulted in an overall increase in the number zymosan-positive cells (Figure 3.3). However, this increase in zymosan positivity was not associated with "true" phagocytosis but a combinatorial effect of an increase in both binding and internalization. In fact, surface binding was the primary contributor to this increase following LPS-driven activation. The increase in surface-binding appeared to be independent of the cell: zymosan ratio (Figure 3.3). It is likely that increased binding was due to an upregulation of surface phagocytic receptors during cellular activation. Alternatively, it may reflect increased "stickiness" of cells following activation, largely due to the upregulation of receptors involved in the phagocytic process.

3.2.4 Goldfish PKMs differentially upregulate phagocytosis in response to activation with host and pathogen derived factors.

It has been previously shown that goldfish kidney-derived hematopoietic progenitors develop along the macrophage lineage *in vitro* through three well defined stages of differentiation: early progenitors, monocytes and mature macrophages (8, 15). Each of these three unique primary kidney macrophage (PKM) subpopulations displays unique forward- and side-scatter profiles,

morphological features, gene expression profiles and functional capacities (8, 15, 16). Based on conventional flow cytometry profiles these subpopulations are defined as early progenitor cells (R1-gate), monocytes (R3-gate) and mature macrophages (R2-gate) (15, 16). However, it was unknown the extent to which each subset contributed to the phagocytic response. As such, I decided to examine this antimicrobial response taking advantage of my novel imaging flow cytometer-based assay. Firstly, ImageStream analysis identified these three PKM subpopulations based on cellular area and side scatter intensity, consistent with previous conventional flow cytometry-based analyses (Figure 3.4 A). In addition, *in situ* morphological examination of cellular events in each of the ImageStream-defined gates showed morphological features that were consistent with those of FACS-sorted PKM subsets (15).

PKM cultures in the proliferative phase of growth were activated for 6- and 48-hours with macrophage activating factors (MAF) and 1 μg/mL *E. coli* LPS. Following activation, cells were incubated with zymosan-FITC at a ratio of 5:1 (zymosan: cells) for 2 hours at 20^{o}C. Phagocytosis was analyzed as described above. I focused on true particle internalization events since my goal was to correlate these with the activation of downstream intracellular antimicrobial responses. Under basal levels of activation, monocytes and mature macrophages were the predominant phagocytic populations, while early progenitor cells had very low levels of phagocytosis under both basal and activated conditions (Figure 3.4 B). Mature macrophages displayed greater basal capacity for phagocytosis when compared to the less differentiated monocytes (49% vs 34%, respectively).

Following 6-hours MAF/LPS activation, cells in the monocyte population significantly increased their phagocytic capacity. This was further increased after 48-hours of activation. In contrast to monocytes, 6-hour MAF/LPS activation did not significantly increase the capacity for phagocytosis among mature macrophages above basal levels. However, after 48 hours of MAF/LPS activation PKM mature macrophages significantly increased their phagocytic capacity by 136 percent. This increase was coupled with a significant increase in the phagocytic index, which was not observed among cells of the monocyte population (Figure 3.4 C). Phagocytic index was defined as the measure of the average number of particles ingested per phagocyte. As such, these results suggest a segregation of phagocytic antimicrobial responses along the teleost macrophage lineage, and highlight the potential for differential contributions of each of these macrophage differentiation stages to host-pathogen interactions.

3.2.5 PKM mature macrophages and not monocytes display an increased capacity for the production of reactive oxygen species following activation.

Reactive oxygen species (ROS) have long been recognized as a crucial component of host defense and provide a high degree of toxicity against phagocytosed microorganisms (17). ROS production during the respiratory burst can be detected using dihydrorhodamine (DHR), based on the oxidization of DHR into fluorescent rhodamine (18). This provides a useful tool for the characterization of the respiratory burst assays in phagocytic cells (e.g. mammalian neutrophils),

and has been shown to have a high degree of correlation with alternative approaches such as the nitrobluetetrazolium (NBT) assay (18). The DHR assay has also been successfully applied to study respiratory burst in teleost fish cells (19).

In control experiments, I examined the respiratory burst in mixed cultures of LPS activated RAW 264.7 macrophages and Jurkat T cells. As shown previously (20), I found that LPS activation led to an increased respiratory burst in RAW 264.7 macrophage, but not Jurkat T cells (Figure 3.5 A). Previous experiments showed that sorted monocytes and mature macrophages from PKM *in vitro* cultures had different kinetics of respiratory burst induction following activation (15). However, these analyses were limited to FACS-sorted populations of cells. In order to examine the potential for cross-talk among PKM subpopulations, I applied the DHR assay to study the induction of ROS production in mixed PKM cultures. Following activation with MAF/LPS for 6- or 48-hours, cells were loaded with DHR and respiratory burst was triggered with PMA. Similarly to previous reports on sorted populations (15), I found that monocytes in mixed PKM cultures had a strong early activation of respiratory burst that was significantly reduced with prolonged (48-hour) MAF/LPS stimulation (Figure 3.5 B). The original increase by 6 hours mirrored the relative capacity of this population to increase its phagocytic capacity in response to MAF/LPS (see above). The mature macrophage population had increased ROS production after 6-hour MAF/LPS stimulation that was further increased after 48-hour activation. Importantly, higher basal levels of phagocytosis among PKM mature macrophages were not associated with equivalent higher basal levels of ROS production (Figure 3.4 B versus 3.5 B). This suggests that non-

activated teleost mature macrophages have an increased capacity for phagocytosis compared to the less mature monocytes; however, this does not appear to be linked to an increased basal capacity for killing through ROS-mediated mechanisms. In contrast to PKM monocytes and mature macrophages, early progenitor cells had low levels of ROS production that were not affected by MAF/LPS activation.

The similarity in the kinetics of ROS induction in both sorted and mixed cell populations suggests that induction of protective anti-microbial responses in these fish are intrinsically regulated by each of these two macrophage subsets. There was no apparent crosstalk among these subsets under the conditions that were examined. Interestingly, for the mature macrophage subset, the induction of anti-microbial respiratory burst responses follows similar kinetics to that observed for phagocytosis. In contrast, monocytes see a decrease in respiratory burst capacity despite continued increase in phagocytosis from 6 to 48 hours. This suggests that phagocytosis and respiratory burst may represent complementary but not interdependent mechanisms among the antimicrobial armament available to cells of the macrophage lineage in these teleost fish, drawing parallels to previously defined phagocytic and antimicrobial responses of mammalian monocytes and macrophages (21-24). This points to a strong conservation of these responses across evolution.

3.2.6 PKM monocytes and mature macrophages display a differential capacity for phagolysosome fusion under basal and immune challenged conditions.

Phagolysosome fusion is a central contributor to the degradation of internalized particles during a phagocytic response. Classically, phagolysosome fusion has been studied by cell disruption followed by differential gradient centrifugation to isolate highly purified phagolysosomes (25) or by confocal microscopy (26). Recently, flow cytometry-based assays have been developed for quantification of phagolysosomes in cell lysates (27). While this flow cytometry-based approach can provide information on the composition and maturation of phagosomes based on differential expression of markers, there is currently no assay that allows quantitation of phagolysosomes within an intact cell. Herein, I show the development of such an assay, taking advantage of the speed, spatial resolution and detection sensitivity of the ImageStream multispectral imaging flow cytometry system. As with the approaches described above, this assay can take advantage of cellular markers (e.g. antibody, cytochemical, and/or morphological-based markers) to define specific cellular subsets. This opens the door for the examination of antimicrobial phagocytic events in mixed cell populations, and thereby allows for the identification and characterization of paracrine cross-talk events between defined cellular subsets.

Initial pulsing of cells with dextran-FITC allows detection of phagolysosomes based on the high affinity of this molecule for acidic lysosomes (28, 29). Briefly, in the absence of phagocytosis, lysosomes are distributed throughout the cell leading to a punctuate staining pattern based on this staining procedure. Upon internalization, lysosomes migrate towards the phagosome, fuse with the phagosome and form a degradative phagolysosome. My approach is based

on the detection of phagolysosomes made visible through the formation of a fluorescent dextran ‘ring’ around an internalized particle; those cells with a visible dextran ring are classified as positive for phagolysosome fusion (Figure 3.6 A). Those cells with no clear dextran ring, partial co-localization without ring formation, or no association of dextran-FITC with the particle are classified as negative. Based on this level of stringency, a fraction of the negative events may correspond to early events in the phagocytic process that have yet to culminate in phagolysosome fusion. As such, this provides a rapid, yet conservative approach, for the quantitation of phagolysosome fusion.

Phagolysosome ring formation examined through the ImageStream multispectral imaging flow cytometry platform was equivalent to that displayed by confocal microscopy-analyzed phagocytes (Figure 3.6 B and 3.6 C). As expected, bound (non-internalized particles) were not associated with fluorescent dextran, consistent with the requirement for internalization for the initiation of phagosome maturation events that lead to phagolysosome fusion (Figure 3.6 C). One current limitation of this assay is that phagocytosed particles must be at least 3 μm in diameter; detection of phagolysosome fusion among smaller particles is currently limited by the resolution provided by this platform (approximately 40x magnification). I applied this new technique to the study of phagolysosome fusion in the teleost PKM *in vitro* model of macrophage development. The goal was to determine if PKM monocytes and mature macrophages had a differential capacity for phagolysosome fusion following particle internalization. Importantly, I looked to examine phagolysosome fusion under basal and immune challenged conditions

to assess whether cellular activation may contribute differentially to phagolysosome fusion in these two unique macrophage subsets. Unlike the smaller zymosan particles utilized above, the 3 μm beads utilized during examination of phagolysosome fusion greatly increased cellular side-scatter characteristics and required re-optimization of the PKM subpopulation gating parameters for this assay (Figure 3.7 A). Thus, I developed an alternative method to differentiate between the three subpopulations, which took advantage of cellular diameter and nuclear area morphological parameters. Detection of phagolysosomes within intact cells was based on identification of green fluorescent dextran rings around brightfield-defined internalized particles (Figure 3.7 B).

Multivariate integration of phagocytosis and phagolysosome approaches allowed me to examine these biological events in mixed PKM cultures. I focused on PKM monocyte and mature macrophage subpopulations, as early progenitor cells did not show any significant capacity to internalize 3 μm beads. I found that PKM monocytes and mature macrophages phagocytosed 3 μm beads with kinetics similar to zymosan, though at reduced levels, as expected based on the relative increase in particle size (Figure 3.8 A). I found that the kinetics of phagolysosome fusion mirrored the kinetics of phagocytosis indicating that PKM were able to effectively initiate degradative pathways following particle internalization (Figure 3.8 B). Importantly, when analysis of phagolysosome formation focused on phagocytic cells (rather than total PKM population), I found that cellular activation did not result in a relative change in their formation (Figure 3.8 C). Correlation of phagolysosome fusion and phagocytosis indicated a direct relationship between

these two processes (R^2= 0.87). However, I found no change in response to cellular activation, in both monocyte and mature macrophage PKM subpopulations. Interestingly, the monocyte population had a greater capacity for phagolysosome formation compared to the mature macrophage subset, as phagocytic monocytes had a 1.5-fold greater incidence of phagolysosome fusion when compared to PKM mature macrophages.

3.3 Discussion

The wide conservation of phagocytosis in metazoans highlights its critical importance as a first line of defense against invading microbes. Pathogen engagement of a finite set of receptors on the phagocyte cell surface leads to the induction of phagocytic cascades, the activation of potent killing mechanisms, and the rapid expansion of pro-inflammatory programs. Despite the importance of these immune defense mechanisms to host integrity, current technologies have significant limitations in their ability to accurately quantitate receptor binding and particle internalization events during phagocytosis. This is particularly prominent in comparative model systems where reagent availability, such as cellular markers, has limited their characterization. In this chapter, I described a novel alternative for the characterization of phagocytosis and downstream intracellular events. My approach was based on a multi-spectral imaging flow cytometry platform and allowed for accurate discrimination between internalized and surface-bound particles. Rapid sample acquisition allowed the generation of robust data sets that brought forward discrete changes in particle binding and internalization. This

opens the door for multi-parametric analysis of phagocytosis and downstream anti-microbial responses within mixed cell populations and allows users to examine segregation of responses following both binding and internalization steps during the phagocytic cascade.

Macrophages provide a unique population of phagocytes known to efficiently mount phagocytic antimicrobial responses at distinct tissue sites. In teleost fish, macrophages have long been recognized as effective phagocytes (15, 30-37). However, it has remained unclear whether the heterogeneity displayed within these teleost macrophage populations may be a result of a differential capacity for induction of phagocytic responses as cells mature from early hematopoietic progenitors. To this end, I focused this chapter on a well-characterized goldfish primary kidney macrophage (PKM) model, whose distinct stages of macrophage maturation (early progenitors, monocytes, and mature macrophages) have been previously defined based on morphological, cytochemical, gene expression, and functional characteristics (15, 38-41). Utilizing my novel approach, I was able to examine discrete functional events along the phagocytic cascade in a mixed population of cells. This minimized the undesirable higher levels of basal activation that are often found in highly manipulated (e.g. mechanically sorted) populations of cells and allowed me to identify potential cross-talk between these three distinct macrophage subsets. I found that both monocyte and mature macrophage PKM subsets were highly phagocytic but had differential kinetics for induction of phagocytosis in response to activation by pathogen- and host-derived factors. Unlike the more differentiated subsets, early progenitors appeared to have a

very limited capacity for phagocytosis and induction of killing responses. This is consistent with macrophage phagocytic responses in higher vertebrates where phagocytosis appears to be associated with the more differentiated stages along the macrophage pathway (42-45). I found that the greatest capacity for phagocytosis displayed by the mature macrophage subset was most evident following examination of its phagocytic index, and not simply that of the percent of phagocytic cells.

The mature macrophage PKM subset displayed very good correlation between phagocytosis, the induction of phagolysosome fusion, and the production of reactive oxygen species (ROS). This was consistent with the induction of effective degradative and killing mechanisms following pathogen internalization, and likely reflects an increased impetus to tightly link antimicrobial mechanisms following immune challenge. Interestingly, in the absence of MAF/LPS, I found that mature macrophages had high basal levels of phagocytosis despite displaying a low capacity for phagolysosome formation and ROS production. As such, my results show the increased efficiency of PKM mature macrophages to couple phagocytosis and downstream degradative/killing responses upon cell activation. Unfortunately, these results also highlight intrinsic disadvantages to the original uncoupling of these mechanisms under basal conditions. One could envision situations in the early phases of pathogen infiltration where teleost tissue macrophages may be able to efficiently internalize incoming pathogens, but lack the capacity to initiate subsequent degradative and killing responses. This could lead to an increased incidence of pathogen spread, particularly in the case of those

that can thrive within macrophages, as well as a decreased capacity to process antigens required for effective antigen presentation (46, 47). Similar scenarios could stem from host- or pathogen-driven events that promote anti-inflammatory conditions. PKM monocytes also showed such disconnect between phagocytosis and downstream intracellular degradative/killing events. In the context of increased vulnerability to pathogen infiltration, however, this may be less relevant *in vivo* for this population as monocytes entering an inflammatory site should be pre-activated through growing interactions with chemokine gradients, activated vascular epithelium, and an inflammatory milieu at the infection site (48). An alternative hypothesis to the uncoupling of phagocytosis and downstream antimicrobial mechanisms may reflect a host-evolved compartmentalization of macrophage responses under basal and immune-challenged conditions. The low capacity to couple phagocytosis and downstream inflammatory mechanisms among PKM monocytes and mature macrophages may serve to promote homeostaticly relevant (rather than antimicrobial focused) phagocytic events under basal conditions. In one example, macrophages could effectively uptake spent host cells and contribute to normal tissue turnover under controlled conditions that do not promote inflammation and surrounding tissue damage (49, 50). This would provide a host-driven strategy for effective segregation of antimicrobial and homeostatic roles within the lower vertebrate macrophage compartment. It remains to be determined whether both positive and negative implications of this uncoupling observed under non-challenged conditions may be reflected *in vivo*.

The kinetics for phagocytosis and downstream degradative/killing responses also differed between monocyte and mature macrophage PKM subsets upon activation. This further suggests specialization within the macrophage lineage early in evolution and may contribute to meeting specific requirements for each of these populations within their specialized niches. The mature macrophage subset saw a progressive increase in its capacity for phagocytosis, phagolysosome fusion, and induction of the respiratory burst over a 48-hour activation period with MAF/LPS. In contrast, monocytes displayed examples of uncoupling between phagocytosis and downstream antimicrobial responses: although this PKM subset saw an increased capacity for zymosan internalization over a 48-hour period, it also showed a significant decrease in ROS production between 6 and 48 hours. Notably, my current results are consistent with previous observations based on FACS-sorted monocyte and mature macrophage PKM subpopulations (15). This study took advantage of the more traditional NBT method for examination of ROS production. It found that sorted monocytes displayed maximum ROS production after 6 hours of MAF/LPS stimulation followed by a significant subsequent decrease by 48 hours. This de-priming effect was most notable in monocytes stimulated with LPS only. In contrast, mature macrophages showed a progressive increase in ROS producing capacity over the prolonged 48-hour observation period. One possibility is that PKM monocytes have yet to develop the functional antimicrobial robustness exhibited by cells of the more differentiated mature macrophage PKM subset. Another possibility is that PKM monocytes may share some functional responses to LPS with mammalian monocytes destined for a myeloid dendritic cell (DC)

phenotype. In mammals, monocytes progressing towards the myeloid DC maturation path shift between a phagocytic internalization-focused phenotype in the absence of LPS, to one geared for effective antigen processing/presentation following LPS stimulation (51-54). It remains unclear whether such phenotype may be partially reflected in PKM cultures.

As with ROS responses, phagolysosome fusion provides an important mechanism for degradation of internalized pathogens (55, 56). In this chapter, I also examined the differential capacity of phagocyte subsets to form phagolysosomes following particle internalization. This novel approach also allows for quantification of phagolysosome fusion among mixed populations of cells. I found that both the monocyte and mature macrophage populations had an increased proportion of cells with fused phagolysosomes following activation, which followed the same proportional increase as phagocytosis in these populations. In this context, it is clear that teleost fish macrophages acquire the capacity to form phagolysosomes following activation, which parallels a progressive increase in their capacity for pathogen internalization. However, when the phagolysosome fusion was studied in the context of the phagocytic cells populations, I found that activation had no effect on phagolysosome fusion on a per cell basis. In other words, the increase in phagolysosome fusion following activation appeared to stem from an overall increase in phagocytosis and was not due to a greater capacity of individual activated phagocytic cells to form phagolysosomes. Further, I showed that monocytes have an increased capacity for phagolysosome fusion compared to mature macrophages. This is also in keeping with the idea that these monocytes

may be differentiating into antigen presenting cells following activation as they have high levels of phagocytosis combined with high antigen-processing capability. It is possible that terminal differentiation into macrophages or other myeloid cells could lead to decreased phagolysosomal fusion, similar to levels seen in the mature macrophage population. This phenotype has been linked to potent antigen presenting capability in mammalian antigen presenting cells, particularly dendritic cells, which have been shown to have a limited capacity for lysosomal proteolysis (57).

In this chapter, I have limited the analysis to the characterization of phagocytosis and downstream antimicrobial responses. However, on a broader sense, these approaches pave the way for characterization of non-microbicidal phagocytic responses in comparative model systems, including the study of the delicate balance that exists between pro- and anti-inflammatory responses at the inflammatory site, which is known to contain both positive (e.g. pathogens and PAMPs) and negative (e.g. apoptotic cells) regulatory signals. This is discussed in the next chapter.

In summary, I have shown here that monocytes and mature macrophages are the predominant phagocytes of teleost fish based on a goldfish PKM model. In response to activation by host and pathogen derived factors, these distinct cell types upregulate phagocytosis and downstream anti-microbial responses in a temporally regulated fashion that varies depending on the stage of macrophage differentiation. It appears that monocytes and mature macrophages may also rely on different killing mechanisms for degrading phagocytosed particles. Based on

current and previous results, monocytes appear be best able to kill through phagolysosome degradation, while mature macrophages may rely predominantly on the production of reactive oxygen and nitrogen intermediates for pathogen killing. Overall, I believe that the results highlight the intrinsic complexities that contribute to the regulation of phagocytic responses, and that these processes are already well developed in teleost fish. Segregation of inflammatory processes may provide an important mechanism for the maintenance of homeostasis through efficient tissue turnover under basal conditions and the capacity to efficiently mount synergistic and potent pathogen killing responses under immune challenged conditions. However, this may also create unique opportunities for pathogens that are able to devise clever immune evasion strategies as they enter the teleost host.

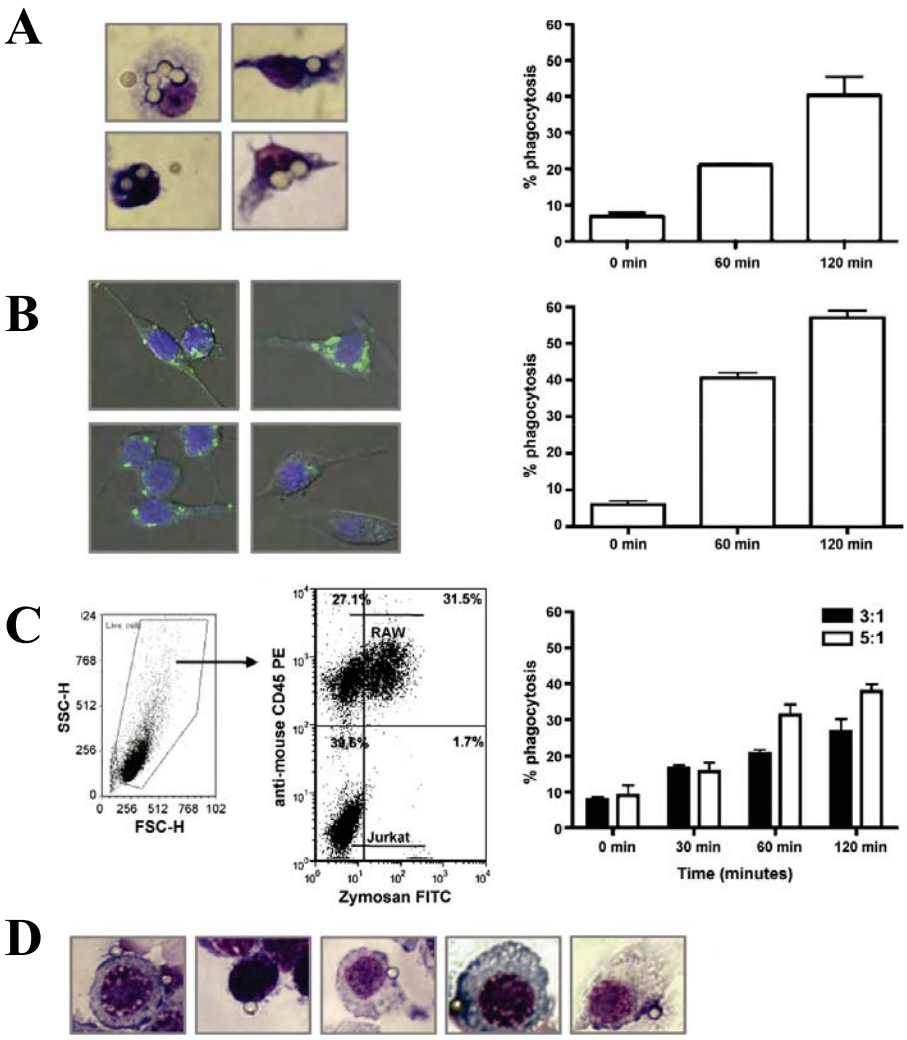

Figure 3.1. Current assays have caveats that limit accurate quantification of phagocytosis.

(A) RAW 264.7 macrophages were plated in a 6-well plate and allowed to adhere overnight. Cells were incubated with 3 μm beads for the times indicated and stained with HEMA3 stain set. Phagocytosis was quantified by light microscopy at 100X magnification. **(B)** RAW 264.7 macrophages were plated on glass coverslips and incubated with zymosan FITC for the times indicated. Cells were stained with anti-mouse CD45 PE and DAPI. Phagocytosis was quantified by confocal microscopy at 40X magnification. **(C)** RAW 264.7 macrophages and Jurkat T cells (1:1 ratio) were incubated with zymosan-FITC for the times indicated. Cells were then stained with anti-mouse CD45 PE to identify RAW 264.7 cells. Phagocytosis was quantified by flow cytometry. (**D**) Representative images of phagocytosis positive cells by flow cytometry (100X) shows that a proportion of these are surface-bound (non-internalized) particles. Results are derived from three independent experiments For A-C, n=3; error bars show SEM.

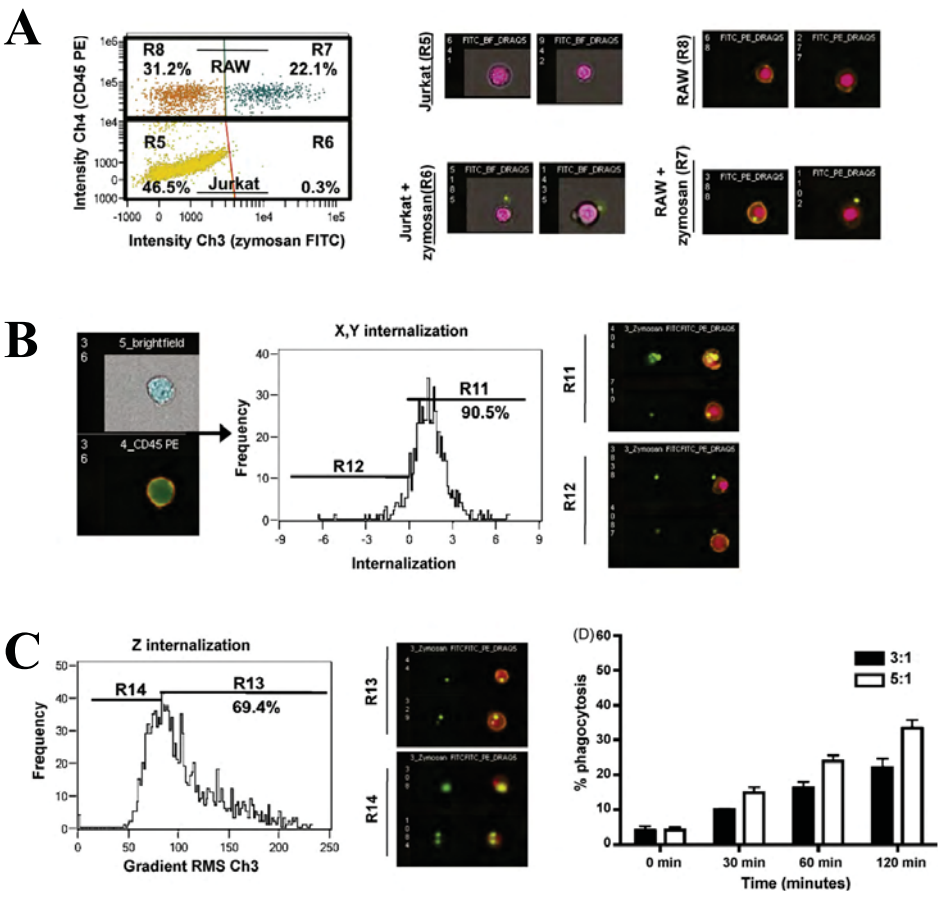

Figure 3.2. Novel assay overcomes caveats from current methods by providing spatial resolution and high throughput quantification of phagocytosis.

(A) RAW 264.7 macrophages and Jurkat T cells (1:1 ratio) were incubated with zymosan-FITC (5:1 ratio) for 120 minutes. Cells were then stained with anti-mouse CD45 PE to identify RAW 264.7 cells. Phagocytosis was quantified using an ImageStream multi-spectral imaging flow cytometer. Phagocytosis was measured by the intensity of zymosan-FITC. Representative images show that cells positive for phagocytosis have zymosan particles that are either internalized or surface bound. **(B)** Using IDEAS analysis software and the cellular plasma membrane as a boundary, a mask was applied to identify areas inside and outside the cell. This mask was used to calculate the degree of internalization of zymosan along the X and Y axes. (**C**) The gradient root mean square (RMS) feature was then applied to the population of cells with internalized particles (gate R11) to find cells with focused zymosan particles in the Z-axis (gate R13). Cells with zymosan out of focus on the Z-axis relative to the nuclear focus were included in the surface bound population. RAW 264.7 macrophages were incubated with a 3:1 or 5:1 ratio of zymosan-FITC for 2 hours. Using the above analysis strategy, the percent of true phagocytosis was determined based on RAW 264.7 macrophage cells with internalized zymosan particles. n=3; error bars show SEM.

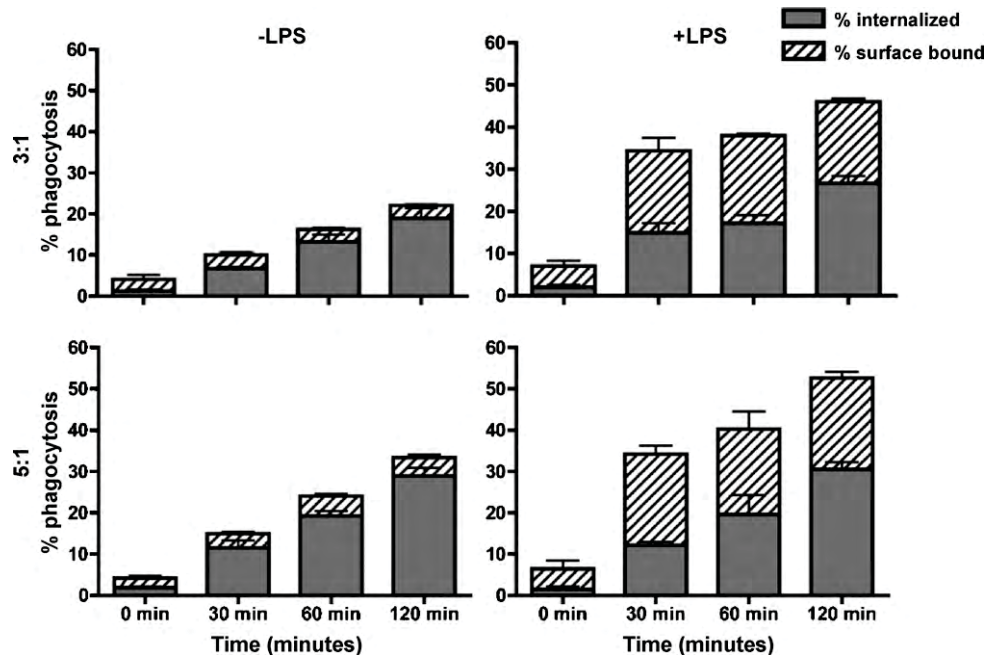

Figure 3.3. LPS activation increases surface binding, but not internalization, of zymosan particles.

RAW 264.7 macrophages were activated in the presence or absence of 100 ng/mL ultrapure *E. coli* LPS for 24 hours. Cells were then washed and incubated with zymosan FITC at a 3:1 or 5:1 (zymosan: RAW 264.7) ratio. Data was acquired using an ImageStream multi-spectral flow cytometer and analyzed as described. LPS activation increased the apparent phagocytosis in RAW 264.7 cells; however, the majority of the increase in phagocytosis is due to increased surface binding and not increased internalization. n=3; error bars show SEM.

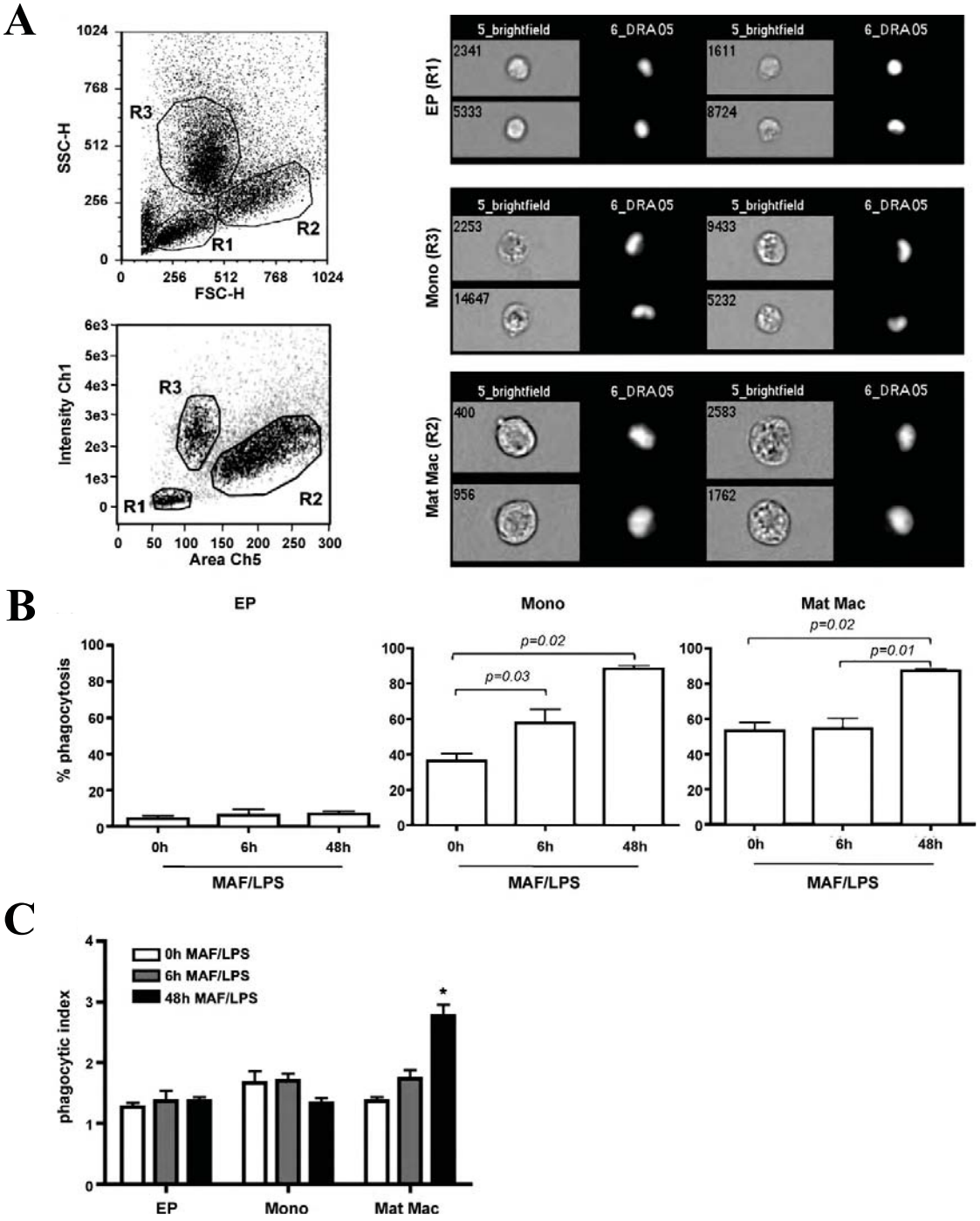
A
SSC-H
FSC-H
R1
R2
R3
Intensity Ch1
Area Ch5
5_brightfield
6_DRA05
EP (R1)
Mono (R3)
Mat Mac (R2)
2341
5333
1611
8724
2253
14647
9433
5232
400
956
2583
1762
B
EP
Mono
Mat Mac
% phagocytosis
p=0.02
p=0.03
p=0.01
0h
6h
48h
MAF/LPS
C
0h MAF/LPS
6h MAF/LPS
48h MAF/LPS
phagocytic index
*
EP
Mono
Mat Mac

Figure 3.4. Monocytes and mature macrophages are the predominant phagocytic populations in mixed PKM cultures and differentially upregulate phagocytosis in response to activation.

(**A**) Flow cytometric analysis of primary kidney macrophage (PKM) cultures has previously identified three distinct sub-populations based on forward- and side-scatter properties (size and internal complexity parameters, respectively). These three sub-populations (R1: early progenitor cells; R2: mature macrophages; R3: monocytes) can also be differentiated using an ImageStream multi-spectral flow cytometer based on cellular area (analogous to FSC-H in conventional flow cytometry) and side scatter intensity (analogous to SSC-H in conventional flow cytometry). Cells in each of these populations display similar cellular and nuclear morphology characteristics as previously described. (**B**) PKM cultures were harvested in the proliferative phase of growth and activated with MAF/LPS for 6 or 48 hours. Cells were then incubated with zymosan-FITC at a ratio of 5:1 (zymosan: cells) for 2 hours and analyzed for phagocytosis using the ImageStream-based approach. Bars represent internalized particles only. Monocyte and mature macrophage sub-populations are the predominantly phagocytic cells in a mixed PKM culture. (**C**) Phagocytic index was calculated for each population following activation. There was no significant difference in the phagocytic index of either early progenitor or monocyte populations. However, the phagocytic index of mature macrophages increased significantly after 48 hours of MAF/LPS activation. For B and C, n=8; * p=0.04 compared to non-activated cells (Student's t-test; error bars show SEM.

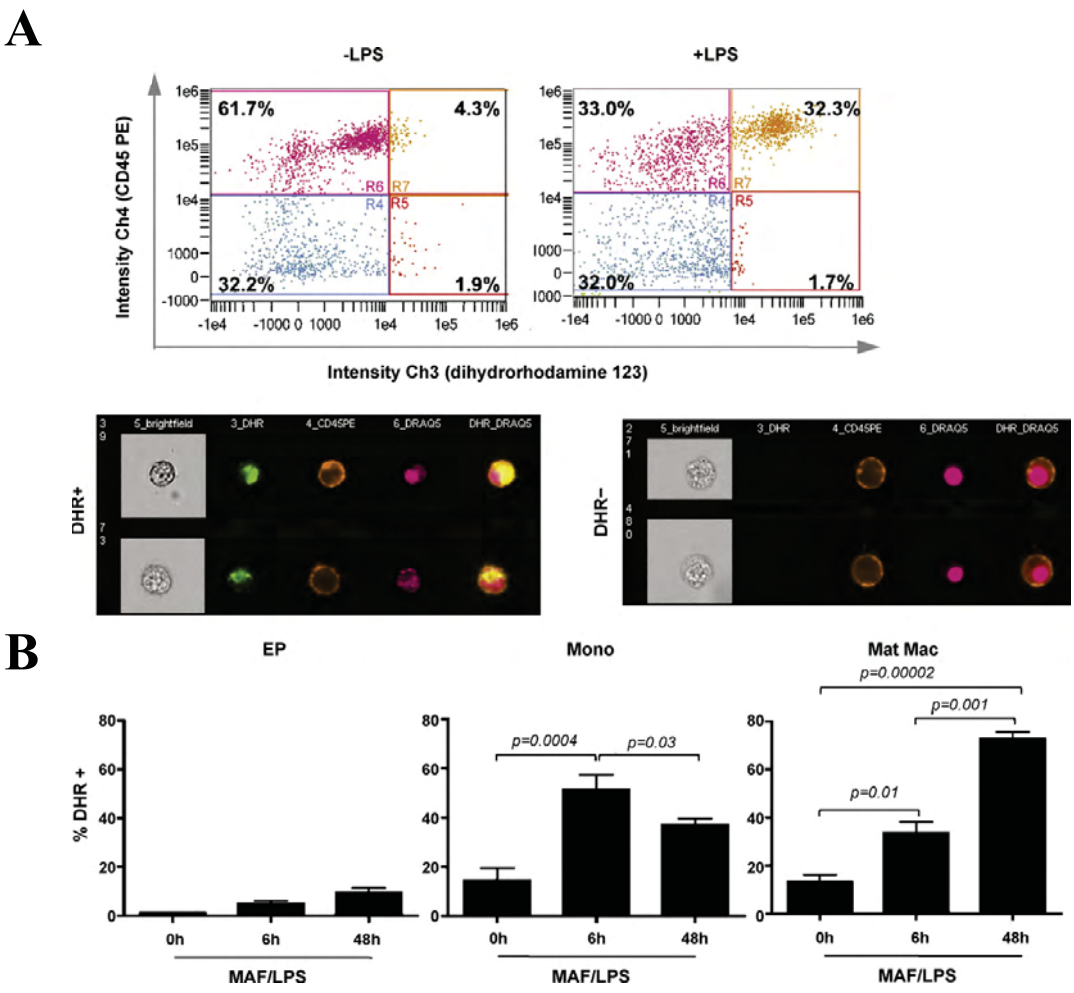

Figure 3.5. The kinetics of respiratory burst production in mixed PKM cultures parallels the increase in mature macrophage but not monocyte phagocytic responses.

(**A**) Control experiments show a mixed culture of RAW 264.7 macrophages and Jurkat T cells was stimulated for 24 hours with 100 ng/mL ultrapure *E. coli* LPS. Cells were then loaded with DHR and respiratory burst was triggered with PMA. As expected, LPS stimulation resulted in increased respiratory burst from the RAW 264.7 macrophage, but not Jurkat T cell, populations. Representative images show characteristic staining pattern of DHR+ and DHR- cells. (**B**) PKM cultures were harvested in the proliferative phase of growth and activated with MAF/LPS for 6 or 48 hours. Cultures were then loaded with DHR and triggered with PMA. Respiratory burst was measured by DHR positivity. Bars represent the percent of DHR+ cells in each sub-population. Monocytes show increased respiratory burst after 6-hour activation. This is followed by a significant decrease after 48 hours of activation. Mature macrophages showed a significant increase in respiratory burst by 6 hours that continued to increase following 48 hours of stimulation. Results are derived from eight independent experiments (n=8); error bars show SEM. Statistics by Student's t-test.

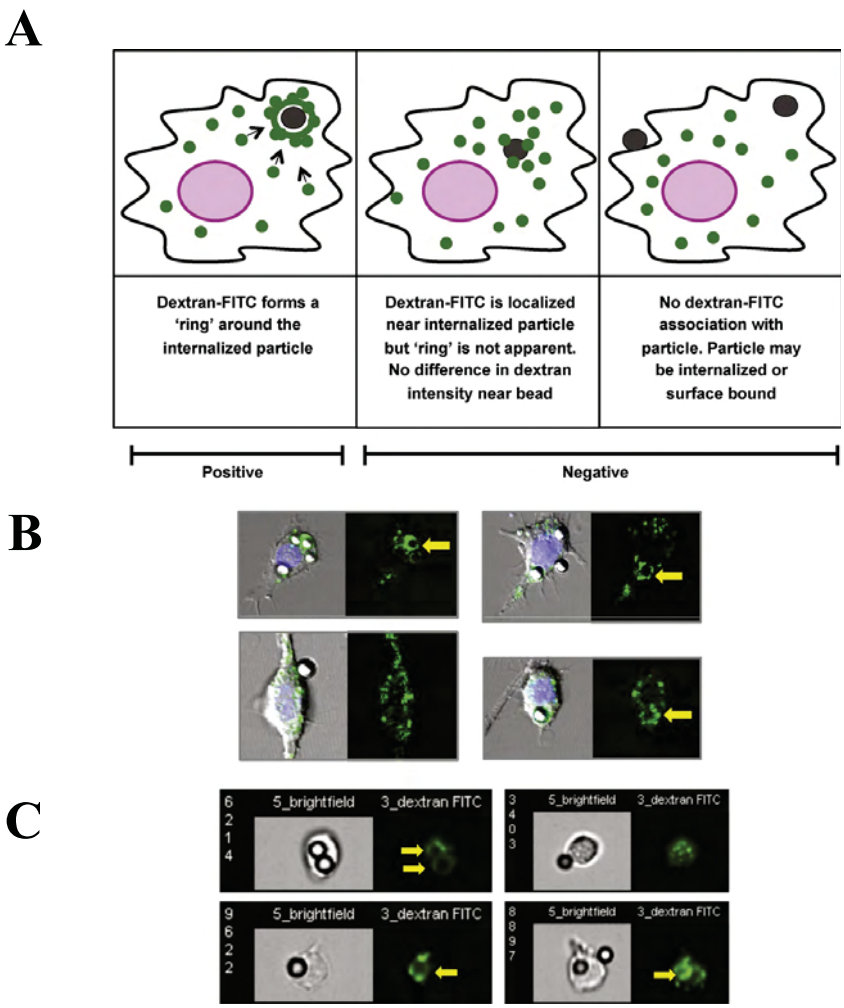

Figure 3.6. Evaluation of macrophage phagolysosome fusion using a novel imaging flow cytometry-based approach.

(**A**) Classification scheme for phagolysosome fusion. Phagolysosome fusion was measured by dextran-FITC. Cells were considered positive for phagolysosome fusion when the internalized particle had a visible dextran 'ring' around the particle or dextran stain overlapping with the entire area of the internalize particle (filled in ring). All other cells were classified as negative resulting in a robust yet conservative evaluation of phagolysosome fusion. (**B**) RAW 264.7 macrophages were grown overnight on glass coverslips. Cells were then pulsed with dextran-FITC, followed by incubation with 3 μm beads. Phagolysosome fusion was imaged using a Zeiss LSM 510 laser scanning confocal microscope. Images were acquired at 40x/1.3. (**C**) RAW 264.7 macrophages in suspension were pulsed with dextran-FITC. Cells were then incubated with 3 μm beads at a ratio of 3:1 (beads: cells). Phagolysosome fusion was analyzed using an ImageStream multi-spectral imaging flow cytometer and show equivalent identification of phagolysosome formation to confocal microscopy-based approach.

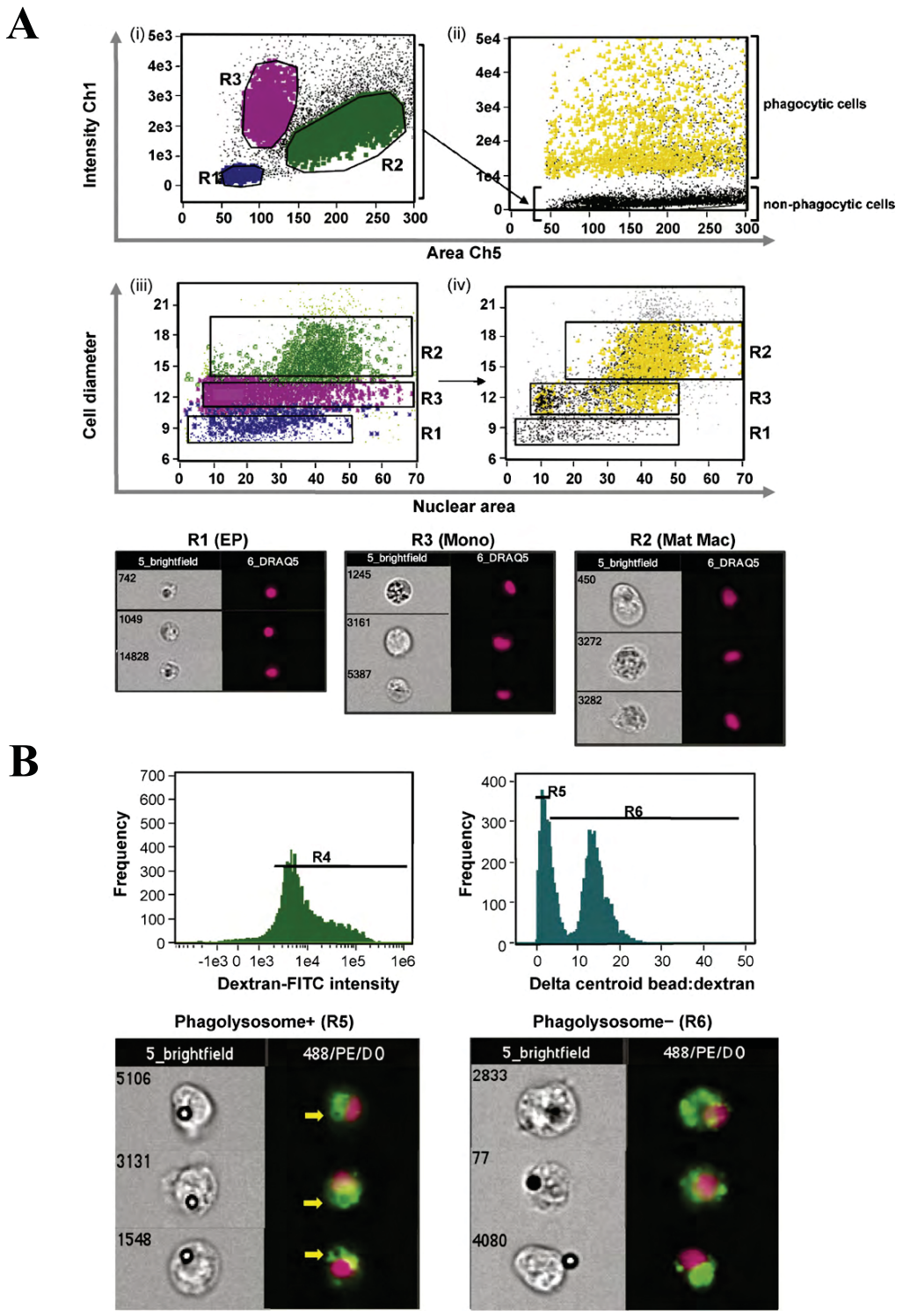
A
(i)
(ii)
Intensity Ch1
Area Ch5
R1
R2
R3
phagocytic cells
non-phagocytic cells
(iii)
(iv)
Cell diameter
Nuclear area
R1 (EP)
R3 (Mono)
R2 (Mat Mac)
5_brightfield
6_DRAQ5
B
Frequency
Dextran-FITC intensity
Delta centroid bead:dextran
R4
R5
R6
Phagolysosome+ (R5)
Phagolysosome− (R6)
488/PE/D0

Figure 3.7. Application of phagolysosome fusion evaluation approach to a comparative macrophage model system.

(**A**) Phagolysosome fusion was detected following ingestion of 3 μm particles. Under these conditions cellular side scatter properties changed significantly, preventing analysis of the three PKM sub-populations through the standard gating strategy. Expansion of y-axis demonstrates increased side-scatter (Intensity Ch1) characteristics for phagocytic cells (i, ii). To accommodate for this, I developed a new strategy based on cell diameter and nuclear area. Overlap between conventional and new gating strategies for PKM early progenitors (R1), monocytes (R3) and mature macrophages (R2) are shown by blue, purple, and green colors, respectively (i vs. iii). Overlap between conventional and new gating strategies for phagocytic and non-phagocytic cell populations is shown by black and yellow colors, respectively (ii vs. iv). Representative images from cells based on new gates are shown. Cell morphology analysis points to the effectiveness of this new gating strategy to differentiate between the three PKM subsets (early progenitors, monocytes and mature macrophages). (**B**) To quantify phagolysosome fusion, analysis was focused on those cells that stained with dextran-FITC. To identify and quantitate phagolysosome fusion, I developed a brightfield mask to identify beads and a green fluorescence mask to identify areas with high dextran-FITC intensity. Mathematical overlap between these two masks identified dextran-FITC rings around brightfield-defined beads. Representative images of positive and negative cells are shown. Note the capacity to differentiate between phagolysosome positive and negative events despite high FITC fluorescence in some phagolysosome negative cells.

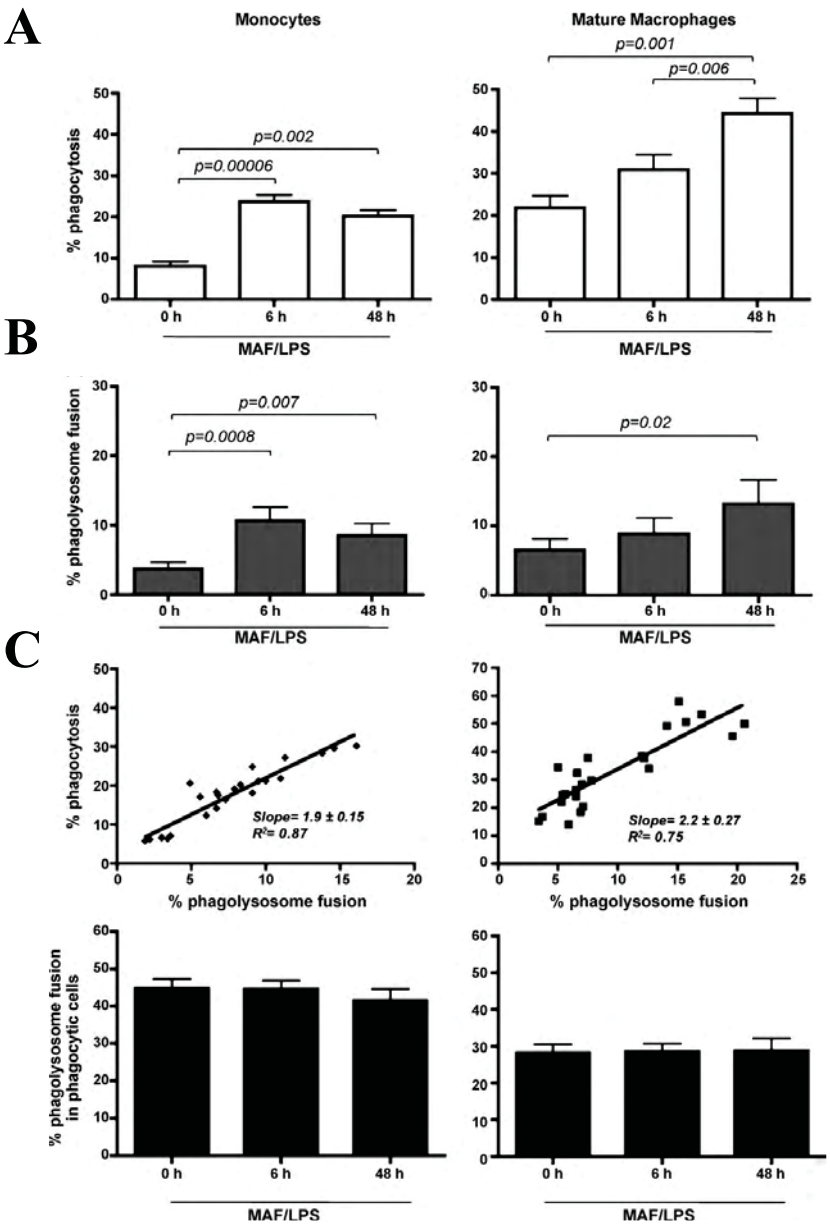

Figure 3.8. Phagolysosome fusion follows the kinetics of phagocytosis.

(**A**) PKM cultures activated with MAF/LPS for 0, 6 and 48 hours were pulsed with dextran-FITC for 45 minutes subsequently incubated with 3 μm beads at a ratio of 3:1 (beads: cells) for 2 hours. Phagocytosis of 3 μm beads followed similar kinetics to those seen with zymosan-FITC. (**B**) Phagolysosome fusion was analyzed as outline in Figure 8. Phagolysosome fusion followed the similar kinetics as phagocytosis. (**C**) Phagolysosome fusion was then focused on phagocytic monocyte and mature macrophage PKM subsets. Within the phagocytic cell subsets, phagolysosome fusion appeared unaffected by activation. Interestingly, monocytes displayed a 1.5 fold greater capacity for phagolysosome fusion when compared to mature macrophages. For A-C, n=6; error bars show SEM. Statistics by Student's t-test.

3.4 References

1. Zigmond, S.H., and Hirsch, J.G. 1972. Effects of cytochalasin B on polymorphonuclear leucocyte locomotion, phagocytosis and glycolysis. *Exp Cell Res* 73:383-393.
2. Axline, S.G., and Reaven, E.P. 1974. Inhibition of phagocytosis and plasma membrane mobility of the cultivated macrophage by cytochalasin B. Role of subplasmalemmal microfilaments. *J Cell Biol* 62:647-659.
3. Greenberg, S., el Khoury, J., di Virgilio, F., Kaplan, E.M., and Silverstein, S.C. 1991. Ca(2+)-independent F-actin assembly and disassembly during Fc receptor-mediated phagocytosis in mouse macrophages. *J Cell Biol* 113:757-767.
4. Aderem, A., and Underhill, D.M. 1999. Mechanisms of phagocytosis in macrophages. *Annu Rev Immunol* 17:593-623.
5. Flannagan, R.S., Cosio, G., and Grinstein, S. 2009. Antimicrobial mechanisms of phagocytes and bacterial evasion strategies. *Nat Rev Microbiol* 7:355-366.
6. Drevets, D.A., and Campbell, P.A. 1991. Macrophage phagocytosis: use of fluorescence microscopy to distinguish between extracellular and intracellular bacteria. *J Immunol Methods* 142:31-38.
7. Hampton, M.B., and Winterbourn, C.C. 1999. Methods for quantifying phagocytosis and bacterial killing by human neutrophils. *J Immunol Methods* 232:15-22.
8. Neumann, N.F., Barreda, D., and Belosevic, M. 1998. Production of a macrophage growth factor(s) by a goldfish macrophage cell line and macrophages derived from goldfish kidney leukocytes. *Dev Comp Immunol* 22:417-432.
9. Grayfer, L., Walsh, J.G., and Belosevic, M. 2008. Characterization and functional analysis of goldfish (Carassius auratus L.) tumor necrosis factor-alpha. *Dev Comp Immunol* 32:532-543.
10. Diniz, S.N., Nomizo, R., Cisalpino, P.S., Teixeira, M.M., Brown, G.D., Mantovani, A., Gordon, S., Reis, L.F., and Dias, A.A. 2004. PTX3 function as an opsonin for the dectin-1-dependent internalization of zymosan by macrophages. *J Leukoc Biol* 75:649-656.
11. Henery, S., George, T., Hall, B., Basiji, D., Ortyn, W., and Morrissey, P. 2008. Quantitative image based apoptotic index measurement using multispectral imaging flow cytometry: a comparison with standard photometric methods. *Apoptosis* 13:1054-1063.
12. Zuba-Surma, E.K., Kucia, M., Abdel-Latif, A., Lillard, J.W., Jr., and Ratajczak, M.Z. 2007. The ImageStream System: a key step to a new era in imaging. *Folia Histochem Cytobiol* 45:279-290.
13. Ralph, P., Ito, M., Broxmeyer, H.E., and Nakoinz, I. 1978. Corticosteroids block newly induced but not constitutive functions of macrophage cell lines: myeloid colony-stimulating activity production, latex phagocytosis, and antibody-dependent lysis of RBC and tumor targets. *J Immunol* 121:300-303.

14. Wu, T.T., Chen, T.L., and Chen, R.M. 2009. Lipopolysaccharide triggers macrophage activation of inflammatory cytokine expression, chemotaxis, phagocytosis, and oxidative ability via a toll-like receptor 4-dependent pathway: validated by RNA interference. *Toxicol Lett* 191:195-202.
15. Neumann, N.F., Barreda, D.R., and Belosevic, M. 2000. Generation and functional analysis of distinct macrophage sub-populations from goldfish (Carassius auratus L.) kidney leukocyte cultures. *Fish Shellfish Immunol* 10:1-20.
16. Belosevic, M., Hanington, P.C., and Barreda, D.R. 2006. Development of goldfish macrophages in vitro. *Fish Shellfish Immunol* 20:152-171.
17. Morel, F., Doussiere, J., and Vignais, P.V. 1991. The superoxide-generating oxidase of phagocytic cells. Physiological, molecular and pathological aspects. *Eur J Biochem* 201:523-546.
18. Richardson, M.P., Ayliffe, M.J., Helbert, M., and Davies, E.G. 1998. A simple flow cytometry assay using dihydrorhodamine for the measurement of the neutrophil respiratory burst in whole blood: comparison with the quantitative nitrobluetetrazolium test. *J Immunol Methods* 219:187-193.
19. Stafford, J.L., McLauchlan, P.E., Secombes, C.J., Ellis, A.E., and Belosevic, M. 2001. Generation of primary monocyte-like cultures from rainbow trout head kidney leukocytes. *Dev Comp Immunol* 25:447-459.
20. Zughaier, S.M., Shafer, W.M., and Stephens, D.S. 2005. Antimicrobial peptides and endotoxin inhibit cytokine and nitric oxide release but amplify respiratory burst response in human and murine macrophages. *Cell Microbiol* 7:1251-1262.
21. Landmann, R., Scherer, F., Schumann, R., Link, S., Sansano, S., and Zimmerli, W. 1995. LPS directly induces oxygen radical production in human monocytes via LPS binding protein and CD14. *J Leukoc Biol* 57:440-449.
22. Nakagawara, A., DeSantis, N.M., Nogueira, N., and Nathan, C.F. 1982. Lymphokines enhance the capacity of human monocytes to secret reactive oxygen intermediates. *J Clin Invest* 70:1042-1048.
23. Sasada, M., and Johnston, R.B., Jr. 1980. Macrophage microbicidal activity. Correlation between phagocytosis-associated oxidative metabolism and the killing of Candida by macrophages. *J Exp Med* 152:85-98.
24. Watson, R.W., Redmond, H.P., and Bouchier-Hayes, D. 1994. Role of endotoxin in mononuclear phagocyte-mediated inflammatory responses. *J Leukoc Biol* 56:95-103.
25. Chakraborty, P., Sturgill-Koszycki, S., and Russell, D.G. 1994. Isolation and characterization of pathogen-containing phagosomes. *Methods Cell Biol* 45:261-276.
26. Zimmerli, S., Majeed, M., Gustavsson, M., Stendahl, O., Sanan, D.A., and Ernst, J.D. 1996. Phagosome-lysosome fusion is a calcium-independent event in macrophages. *J Cell Biol* 132:49-61.
27. Hmama, Z., Sendide, K., Talal, A., Garcia, R., Dobos, K., and Reiner, N.E. 2004. Quantitative analysis of phagolysosome fusion in intact cells: inhibition by mycobacterial lipoarabinomannan and rescue by an 1alpha,25-

dihydroxyvitamin D3-phosphoinositide 3-kinase pathway. *J Cell Sci* 117:2131-2140.

28. Ohkuma, S., Moriyama, Y., and Takano, T. 1982. Identification and characterization of a proton pump on lysosomes by fluorescein-isothiocyanate-dextran fluorescence. *Proc Natl Acad Sci U S A* 79:2758-2762.
29. Ohkuma, S., and Poole, B. 1978. Fluorescence probe measurement of the intralysosomal pH in living cells and the perturbation of pH by various agents. *Proc Natl Acad Sci U S A* 75:3327-3331.
30. Barnes, A.C., Guyot, C., Hansen, B.G., Horn, M.T., and Ellis, A.E. 2002. Antibody increases phagocytosis and killing of Lactococcus garvieae by rainbow trout (Oncorhynchus mykiss, L.) macrophages. *Fish Shellfish Immunol* 12:181-186.
31. Montero, J., Coll, J., Sevilla, N., Cuesta, A., Bols, N.C., and Tafalla, C. 2008. Interleukin 8 and CK-6 chemokines specifically attract rainbow trout (Oncorhynchus mykiss) RTS11 monocyte-macrophage cells and have variable effects on their immune functions. *Dev Comp Immunol* 32:1374-1384.
32. Zou, J., Peddie, S., Scapigliati, G., Zhang, Y., Bols, N.C., Ellis, A.E., and Secombes, C.J. 2003. Functional characterisation of the recombinant tumor necrosis factors in rainbow trout, Oncorhynchus mykiss. *Dev Comp Immunol* 27:813-822.
33. Hong, S., Peddie, S., Campos-Perez, J.J., Zou, J., and Secombes, C.J. 2003. The effect of intraperitoneally administered recombinant IL-1beta on immune parameters and resistance to Aeromonas salmonicida in the rainbow trout (Oncorhynchus mykiss). *Dev Comp Immunol* 27:801-812.
34. McKinney, E.C., and Flajnik, M.F. 1997. IgM-mediated opsonization and cytotoxicity in the shark. *J Leukoc Biol* 61:141-146.
35. Joerink, M., Ribeiro, C.M., Stet, R.J., Hermsen, T., Savelkoul, H.F., and Wiegertjes, G.F. 2006. Head kidney-derived macrophages of common carp (Cyprinus carpio L.) show plasticity and functional polarization upon differential stimulation. *J Immunol* 177:61-69.
36. Brattgjerd, S., and Evensen, O. 1996. A sequential light microscopic and ultrastructural study on the uptake and handling of Vibrio salmonicida in phagocytes of the head kidney in experimentally infected Atlantic salmon (Salmo salar L.). *Vet Pathol* 33:55-65.
37. Cerezuela, R., Cuesta, A., Meseguer, J., and Angeles Esteban, M. 2009. Effects of dietary vitamin D3 administration on innate immune parameters of seabream (Sparus aurata L.). *Fish Shellfish Immunol* 26:243-248.
38. Barreda, D.R., Hanington, P.C., Stafford, J.L., and Belosevic, M. 2005. A novel soluble form of the CSF-1 receptor inhibits proliferation of self-renewing macrophages of goldfish (Carassius auratus L.). *Dev Comp Immunol* 29:879-894.
39. Barreda, D.R., Neumann, N.F., and Belosevic, M. 2000. Flow cytometric analysis of PKH26-labeled goldfish kidney-derived macrophages. *Dev Comp Immunol* 24:395-406.

40. Barreda, D.R., and Belosevic, M. 2001. Characterisation of growth enhancing factor production in different phases of in vitro fish macrophage development. *Fish Shellfish Immunol* 11:169-185.
41. Barreda, D.R., Hanington, P.C., Walsh, C.K., Wong, P., and Belosevic, M. 2004. Differentially expressed genes that encode potential markers of goldfish macrophage development in vitro. *Dev Comp Immunol* 28:727-746.
42. Gordon, M.A., Jack, D.L., Dockrell, D.H., Lee, M.E., and Read, R.C. 2005. Gamma interferon enhances internalization and early nonoxidative killing of Salmonella enterica serovar Typhimurium by human macrophages and modifies cytokine responses. *Infect Immun* 73:3445-3452.
43. Perri, D., Shabani, F., Ziaeian, G., and Denomme, G.A. 2008. IFN-gamma treated monocyte/macrophage phagocytosis of red cells sensitized with IgG1 and IgG3 Anti-D containing identical immunoglobulin variable region genes. *Transfus Apher Sci* 39:37-44.
44. Katsura, Y., Tsuru, S., Noritake, M., Shinomiya, N., Kayashima, S., Motoyoshi, K., and Rokutanda, M. 1992. Effects of macrophage colony-stimulating factor on the activities of murine monocytes and peritoneal macrophages in vivo. *Nat Immun* 11:167-176.
45. Sunderkotter, C., Nikolic, T., Dillon, M.J., Van Rooijen, N., Stehling, M., Drevets, D.A., and Leenen, P.J. 2004. Subpopulations of mouse blood monocytes differ in maturation stage and inflammatory response. *J Immunol* 172:4410-4417.
46. Alvarez, M., Burn, T., Luo, Y., Pirofski, L.A., and Casadevall, A. 2009. The outcome of Cryptococcus neoformans intracellular pathogenesis in human monocytes. *BMC Microbiol* 9:51.
47. Kubica, M., Guzik, K., Koziel, J., Zarebski, M., Richter, W., Gajkowska, B., Golda, A., Maciag-Gudowska, A., Brix, K., Shaw, L., et al. 2008. A potential new pathway for Staphylococcus aureus dissemination: the silent survival of S. aureus phagocytosed by human monocyte-derived macrophages. *PLoS One* 3:e1409.
48. Serbina, N.V., Jia, T., Hohl, T.M., and Pamer, E.G. 2008. Monocyte-mediated defense against microbial pathogens. *Annu Rev Immunol* 26:421-452.
49. Paidassi, H., Tacnet-Delorme, P., Arlaud, G.J., and Frachet, P. 2009. How phagocytes track down and respond to apoptotic cells. *Crit Rev Immunol* 29:111-130.
50. Nakanishi, Y., Henson, P.M., and Shiratsuchi, A. 2009. Pattern recognition in phagocytic clearance of altered self. *Adv Exp Med Biol* 653:129-138.
51. Nayak, J.V., Hokey, D.A., Larregina, A., He, Y., Salter, R.D., Watkins, S.C., and Falo, L.D., Jr. 2006. Phagocytosis induces lysosome remodeling and regulated presentation of particulate antigens by activated dendritic cells. *J Immunol* 177:8493-8503.
52. Salter, R.D., and Watkins, S.C. 2006. Dynamic properties of antigen uptake and communication between dendritic cells. *Immunol Res* 36:211-220.

53. Blander, J.M. 2007. Signalling and phagocytosis in the orchestration of host defence. *Cell Microbiol* 9:290-299.
54. Zhou, L.J., and Tedder, T.F. 1996. CD14+ blood monocytes can differentiate into functionally mature CD83+ dendritic cells. *Proc Natl Acad Sci U S A* 93:2588-2592.
55. Ricevuti, G., Mazzone, A., Fossati, G., Mazzucchelli, I., Cavigliano, P.M., Pasotti, D., and Notario, A. 1993. Assay of phagocytic cell functions. *Allerg Immunol (Paris)* 25:55-66.
56. Jutras, I., and Desjardins, M. 2005. Phagocytosis: at the crossroads of innate and adaptive immunity. *Annu Rev Cell Dev Biol* 21:511-527.
57. Delamarre, L., Pack, M., Chang, H., Mellman, I., and Trombetta, E.S. 2005. Differential lysosomal proteolysis in antigen-presenting cells determines antigen fate. *Science* 307:1630-1634.

Chapter 4: Goldfish phagocytes display divergent responses to pro-inflammatory and homeostatic stimuli *in vivo*[1]

4.1 Introduction

Inflammation is a complex and highly regulated response to pathogen infiltration and tissue damage. While this response is critical to pathogen clearance, inflammatory processes can lead to substantial tissue injury if unchecked (1-3). Thus, there has been a significant drive for co-evolution of regulatory programs to minimize deleterious effects on surrounding tissues (4).

As a mechanism to control tissue damage, inflammation-associated apoptosis triggers anti-inflammatory programs in mammals (4). *In vitro* studies have shown that phagocytosis of apoptotic cells drives a decrease in pro-inflammatory antimicrobial killing mechanisms (5-7). *In vivo*, apoptotic cells reduce thioglycollate-induced leukocyte infiltration and promote the resolution of thioglycollate or LPS-driven inflammation (8, 9). Further, *in vitro* and *in vivo* studies have shown that the clearance of apoptotic cells within an inflammatory site also promotes the production of anti-inflammatory immune mediators, notably

---

[1] A version of this chapter has been published:

Rieger AM, Konowalchuk JD, Grayfer L, Katzenback BA, Havixbeck JJ, Kiemele MD, Belosevic M, Barreda DR. 2012. Fish and mammalian phagocytes differentially regulate pro-inflammatory and homeostatic responses *in vivo*. *PLoS One* 7: e47070.

interleukin (IL)-10, transforming growth factor (TGF)-β, and platelet activating factor, as well as a decrease in pro-inflammatory cytokines, including tumor necrosis factor (TNF)-α, IL-6 IL-8, IL-12, IL-17, IL-23, prostaglandin E2, leukotriene C4 and thromboxane B2 (10-17). The shift in the balance between TNF-α and TGF-β contributes to the 'quenching' of reactive oxygen and nitrogen species (18). Removal of the oxidative stress associated with ROS production favors effective uptake of apoptotic cells and further promotes anti-inflammatory programs (19, 20). Importantly, although continued ROS production can lead to unnecessary tissue damage, premature neutrophilic apoptosis, and inhibition of apoptotic cell uptake, NADPH oxidase also appears to play an important role in the effective resolution of inflammation, by contributing to macrophage recognition and clearance of activated neutrophils at sites of inflammation (21).

Phagocytes contribute to both pro-inflammatory and anti-inflammatory (resolution) responses at infectious foci (11, 20-23). However, it remains unclear if this dichotomy is a recent evolutionary development or whether the capacity to balance between these two seemingly contradictory processes following phagocytosis is a feature already displayed by lower vertebrate phagocytes. Recent evolutionary developments may have provided novel strategies for the control of inflammation, but may contribute to the development of inflammation-associated diseases as new mechanisms look to integrate into existing immune regulatory networks. Importantly, phagocytes are known to internalize pathogens, apoptotic cells, or both at sites of inflammation, raising questions about the contributions of individual phagocytes to the inflammatory process *in vivo*.

In this chapter, I examine the effects of homeostatic phagocytosis on the regulation of pro-inflammatory antimicrobial responses. Using a comparative model of zymosan-induced peritonitis, the impact of apoptotic cells on reactive oxygen species (ROS) production was measured *in vivo* in both mice and fish. Zymosan is a commonly used pathogen mimic that induces self-resolving peritonitis *in vivo* (24-28). Previous *in vitro* and *in vivo* studies have shown that zymosan phagocytosis results in activation of pro-inflammatory responses that include induction of pro-inflammatory cytokines, production of reactive oxygen and nitrogen intermediates, and increased infiltration of leukocytes, predominantly neutrophils (28-34).

The main objectives of this chapter were (1) compare the kinetics of the induction of inflammatory processes in mice and goldfish, (2) determine goldfish macrophage responses to pathogenic and homeostatic particles and (3) examine the conservation of functional phagocyte responses in the induction and resolution stages of inflammation. Importantly, I chose to do these experiments using two potential phagocytic particles: zymosan and apoptotic cells. This allowed a closer examination of the balance of phagocyte responses within an inflammatory site that would not be possible in systems where inflammation is induced by a soluble/ non-particulate mediator (i.e. thioglycollate or LPS).

4.2 Results

4.2.1 Teleost phagocytes reduce pro-inflammatory responses following apoptotic cell internalization.

As a first step in the characterization of divergent pro-inflammatory and homeostatic responses in lower vertebrate phagocytes, I examined the impact of zymosan and apoptotic cell internalization in a well-characterized phagocyte model of teleosts that uses primary macrophages (PKM) derived from the hematopoietic compartment of goldfish (35, 36). Apoptotic cells were derived from treating cells with cycloheximide. Preparations were generally >70% AnnexinV+ with limited necrosis detected (Figure 4.1). No differences were noted in goldfish responses with apoptotic cell derived from either 3B11 cells or primary kidney leukocytes (Figure 4.2). Cellular respiratory burst was used as a marker for the induction of macrophage antimicrobial responses. This also provided important insights into NADPH activity, which is known to have key roles in both the induction and resolution of inflammation. As expected, internalization of zymosan induced a strong respiratory burst among phagocytes (Figure 4.3 A). Conversely, phagocytosis of apoptotic cells resulted in a significant decrease in the production of reactive oxygen species (ROS). Interestingly, zymosan selectively increased the respiratory burst in phagocytes internalizing zymosan, while the presence of apoptotic cells decreased the respiratory burst responses in both phagocytic and non-phagocytic cells (Figure 4.3 A). Internalization of apoptotic cells may induce soluble mediators in fish macrophages to globally reduce activation.

Within an inflammatory site, macrophages are exposed to both pro-inflammatory stimuli and dying cells. As such, I measured the effects on macrophage activation following combined stimulation with both apoptotic cells and zymosan. Individual goldfish PKM respiratory burst responses were analyzed

by imaging flow cytometry based on cells that had no particles internalized, cells that had only apoptotic cells internalized, cells that had only zymosan internalized, or cells that had internalized both apoptotic cells and zymosan (Figure 4.3 B). The same trends were observed as when cells were treated with a single stimulus despite the presence of four distinct phagocyte groups within these mixed populations - PKM that ingested apoptotic cells exhibited a significant decrease in respiratory burst while PKM with internalized zymosan had significantly increased respiratory burst (Figure 4.3 B; refer to 0h group). Together with results from Figure 4.3 A, this data indicates that the divergence of responses to pro-inflammatory and homeostatic signals at the level of the individual phagocyte is already present in teleost fish. This also extends to the production of nitric oxide (Figure 4.4). Further, these results indicate that regulation of pro- and anti-inflammatory phagocyte responses displays an important intrinsic level of regulation.

Pre-incubation with apoptotic cells for 2 hours or 4 hours prior to addition of zymosan resulted in reduced respiratory burst responses in those cells that were non-phagocytic, those that had only internalized zymosan or those that had internalized both zymosan and apoptotic cells (Figure 4.3 B, -2h and -4h groups), again suggesting the involvement of soluble factors for amelioration of pro-inflammatory responses. For the group that had only internalized apoptotic cells, pre-incubation did not lead to an added decrease in ROS production, suggesting that maximal down-regulation of respiratory burst responses was achieved by 2 hours. Together, these data show that internalization of apoptotic cells leads to

discrete cellular events that result in reduced macrophage activation in the presence or absence of stimulatory zymosan particles. The former indicates that this control mechanism(s) is sufficient to over-ride stimulatory signals that would otherwise lead to pro-inflammatory responses.

4.2.2 Zymosan differentially induces cellular infiltration in mice and teleost fish.

Cellular infiltration and induction of antimicrobial defenses are two of the hallmarks of inflammation at a site of infection (4). Using a commonly used zymosan-peritonitis model, it was determined that 24 hours following injection was the best time point for comparison of cellular infiltration and ROS responses between goldfish and mice; at this time point both had reached significant increases in the number of infiltrating leukocytes (Figure 4.5). However, examination of leukocyte exudates following intraperitoneal challenge with zymosan showed marked differences between mice and goldfish. Murine cellular infiltrates were defined based on surface expression of $Gr1^{+}$/ $CD11b^{+}$/ $F4/80^{-}$ for granulocytes, $Gr1^{+/-}$/ $CD11b^{+}$/ $F4/80^{mid/hi}$ for monocytes/ macrophages, and CD3, B220, and NK1.1 expression for lymphocytes (Figure 4.6). In the absence of the range of surface markers available for mice, goldfish leukocytes were first characterized based on imaging flow cytometry parameters. Because neutrophils displayed similar morphology to monocytes (37), cytochemical staining and surface receptor expression further defined the leukocyte subsets isolated from the goldfish peritoneum (Figure 4.7). Injected goldfish displayed increases in the total numbers

of infiltrating leukocytes, comprised of both myeloid and lymphoid cells (an overall 20-fold increase relative to saline controls; Figure 4.8). Increases were noted in neutrophils, monocytes/ macrophages, and lymphocytes (20-fold, 25-fold, and 15-fold increases relative to saline controls, respectively).

In contrast to goldfish, mice displayed a more moderate increase in the total number of infiltrating leukocytes compared to saline controls (1.5-fold increase; Figure 4.8), with the increase limited to cells in the neutrophil pool ($Gr1^{+}$/ $CD11b^{+}$/ $F4/80^{-}$). No significant changes were detected in the infiltration of monocyte/ macrophage ($Gr1^{+/-}$/ $CD11b^{+}$/ $F4/80^{mid/hi}$) or lymphocyte (based on CD3, B220, and NK1.1 expression) subsets. This data suggests that inflammatory responses in the murine peritoneum may depend to a greater extent on resident leukocytes and/or targeted infiltration by specific leukocyte subsets. Importantly, I also found significant differences in the kinetics of the leukocyte infiltration responses. Faster kinetics were observed in goldfish (rapid induction by 8 hours) compared to a delayed but sustained onset of leukocyte infiltration in mice from 24 to 48 hours (Figure 4.5).

4.2.3 Apoptotic cells differentially control cellular infiltration in mice and teleost fish.

In vivo peritoneal administration of apoptotic cells also led to significant differences in the modulation of leukocyte infiltration in the lower and higher vertebrate models. In goldfish, addition of apoptotic cells led to a 3.2-fold increase in total number of infiltrating leukocytes compared to saline controls (goldfish total

leukocyte panel; Figure 4.8). This was driven by increases in monocyte/ macrophage and lymphocyte populations. No change was detected in the neutrophil pool. In sharp contrast, administration of apoptotic cells to mice induced a significant decrease in leukocyte infiltration compared to saline controls, driven by a reduced number in monocyte/ macrophage and lymphocyte populations (Figure 4.8). No change was detected in the neutrophil pool. Thus, upon immune recognition of apoptotic cells, mice and goldfish differentially modulate the recruitment of individual leukocyte populations.

The presence of apoptotic cells also showed differential effects on cellular infiltration driven by zymosan in mice and goldfish. Overall, administration of apoptotic cells returned levels of leukocyte infiltration to those of saline controls in both goldfish and mice (Total: -4h versus PBS groups; Figure 4.8). However, significant differences were detected, particularly when focused on the neutrophil subset. Goldfish showed efficient down-modulation of neutrophil infiltration when apoptotic cells were administered to a zymosan-induced inflammatory site (neutrophil group; Figure 4.8). In contrast, parallel experiments in mice showed maintenance of neutrophil numbers (Figure 4.8). This may point to an increased role for infiltrating neutrophils in the control of inflammation in higher vertebrates, which goes beyond the initial induction and maintenance of early pro-inflammatory phases of the antimicrobial response. This is consistent with the resistance of transmigrated inflammatory neutrophils to pro-survival/anti-apoptotic signals, potentially to allow the mammalian host to better take advantage of apoptosis as an effective mechanism for the control of inflammation (38).

4.2.4 Apoptotic cells reduce teleost pro-inflammatory responses *in vivo* in a time dependent manner.

Consistent with *in vitro* measurements, injection of zymosan led to significant increases in respiratory burst in goldfish peritoneal cells (Figure 4.9). Co-injection of apoptotic cells significantly decreased the respiratory burst relative to the 'zymosan only' group. The respiratory burst response decreased in a time dependent manner, with respiratory burst being almost undetectable at the -4h time point despite the presence of zymosan. As expected, respiratory burst responses predominantly occurred in the myeloid, and not lymphoid population (Figure 4.10). Mean fluorescence intensity of myeloid cell DHR fluorescence shows a similar trend (Figure 4.11, top). Interestingly, the decrease in respiratory burst responses was more pronounced *in vivo* than *in vitro* (Figure 4.3B vs. Figure 4.9), suggesting that teleost cells at an inflammatory site other than macrophages contribute to the control of pro-inflammatory responses.

4.2.5 Apoptotic cells reduce pro-inflammatory responses in mice to a lesser extent than in goldfish.

Although *in vitro* and *in vivo* studies of murine immune responses to either zymosan (39, 40) or apoptotic cells (8, 10) have been examined independently, the combined effects have not been thoroughly investigated. To this end, I injected C57BL/6 mice intraperitoneally with zymosan and/or apoptotic cells. Similar to goldfish, zymosan injections of mice resulted in respiratory burst activity in

peritoneal cells (Figure 4.9); however, basal responses were higher and zymosan-induced responses were not as pronounced as those in goldfish (ie. relative increase in ROS production in response to zymosan was much less pronounced in mice). Mice injected with apoptotic cells also exhibited significantly reduced respiratory burst response compared to those in the zymosan-injected group (Figure 4.9). Again, the relative decrease was less pronounced than that observed in goldfish. Interestingly, murine neutrophil populations demonstrated the greatest decrease in ROS production, while the monocyte/macrophage subset showed mild reductions in the respiratory burst (Figure 4.12 A). This decrease was further associated with a shift in neutrophil ROS responses from 'high' levels to 'low'/ 'mid' levels, especially in neutrophils from mice injected with apoptotic cells 4 hours prior to zymosan (Figure 4.12 B). A similar shift was noted in the monocyte/macrophage population, although it was not as prominent as that of neutrophils. Mean fluorescence intensity of neutrophil and monocyte/macrophage DHR fluorescence shows a similar trend to these results (Figure 4.11, bottom).

4.2.6 Murine, but not teleost, neutrophils phagocytose apoptotic cells, which actively reduce pro-inflammatory ROS production in a contact dependent manner.

Mammalian macrophages are well known to internalize apoptotic cells and subsequently down-regulate their pro-inflammatory responses (5-7). Similarly, previous reports indicate that activated *ex vivo* human neutrophils possess the capacity to phagocytose apoptotic cells, which results in a decrease in pro-

inflammatory neutrophil functions, including production of ROS (41). This establishes macrophages and neutrophils as active contributors to homeostatic responses at a mammalian inflammatory site. However, classical neutrophils represent recent additions to the immune cell repertoire of metazoans and, therefore, may have only recently acquired the capacity to contribute to both pro-inflammatory and homeostatic responses in higher vertebrates. Therefore, I wished to compare the relative capacity of murine and teleost neutrophils to internalize apoptotic cells, and to determine if this subsequently decreased ROS production through either contact dependent or soluble factor-mediated mechanisms. To this end, goldfish and C57BL/6 mice were injected intraperitoneally with zymosan and cells were harvested by peritoneal lavages 24 hours later. Using density gradient centrifugation, isolated cells were separated into granulocyte and mononuclear fractions in a manner that has been shown to result in a high level of purity in the isolated populations (37). To determine the capacity of these leukocytes to internalize apoptotic cells, cells were incubated with labeled species-specific apoptotic cells for 2 hours and phagocytosis was analyzed. Consistent with murine results, goldfish monocytes/ macrophages were efficient at internalizing apoptotic cells (Figure 4.13 A). There was also limited surface binding capacity in both goldfish myeloid populations. In sharp contrast, goldfish neutrophils displayed a very limited capacity for their uptake (<0.6% phagocytosis) whereas murine neutrophils displayed efficient internalization of apoptotic cells, equivalent to that of murine monocytes/ macrophages.

To measure the effects of apoptotic cells on activated *ex vivo* neutrophils and monocyte/ macrophage populations, cells were stimulated *in vivo* and isolated as described above. Cells were then cultured for 2 hours in the presence of apoptotic cells. To determine if the effect was contact dependent or mediated through soluble factors, apoptotic cells were also added to 0.4 μm trans-wells alone or in combination with various cell populations (Figure 4.13 B; bracketed groups). In the trans-well conditions, only responding cells were present outside of the trans-well (ie. no other factors were added to these cells). In goldfish, neutrophil ROS production was unchanged in any of the experimental conditions, indicating that neither contact dependent factors nor soluble mediators were present and affected neutrophil responses (Figure 4.13 B, left panel). In contrast, direct contact with apoptotic cells significantly reduced monocyte/ macrophage ROS production. This suggests that the reduction in ROS production identified in the myeloid population of Figure 4.10 was associated with a selective decrease in monocyte/macrophage and not neutrophil ROS production. Interestingly, in spite of the limited ability of neutrophil to phagocytose apoptotic cells, activated goldfish neutrophils cultured in the presence of apoptotic cells produced soluble factor(s) that significantly decreased monocyte/ macrophage ROS responses (bracketed N+AB group in monocyte/macrophage analysis; Figure 4.13 B). This decrease is further enhanced when the total peritoneal isolate was used, suggesting an additive role of soluble factors from both neutrophils and mononuclear cells (bracketed Total+AB group in monocyte/macrophage analysis; Figure 4.13 B).

In sharp contrast, isolated murine neutrophils significantly downregulated their ROS responses in the presence of apoptotic cells (Figure 4.13 B, right panel), similar to the responses observed following *in vivo* injection of apoptotic cells. The downregulation of ROS was contact-dependent, as no changes in ROS were observed when apoptotic cells alone, monocyte/macrophages plus apoptotic cells, or total leukocytes plus apoptotic cells were added to the experimental trans-well. This suggests that the decreases in neutrophil ROS measured *in vivo* were due to direct contact between apoptotic cells and neutrophils within the peritoneum and not soluble factors produced by other leukocytes at the site.

4.3 Discussion

Phagocytosis is a well-conserved innate defense mechanism that has served as a robust platform for incorporation of novel layers of immunological control (11, 20, 22, 23). For inflammatory processes of higher vertebrates, phagocytosis represents a central node for the induction and resolution of inflammation. In this chapter, I studied murine and teleost fish *in vivo* and *in vitro* models to assess the evolutionary conservation of this inflammatory control axis.

Although I found some conservation of phagocyte functional responses, I also found significant differences in the level and control of these responses to pro-inflammatory and homeostatic internalization signals between goldfish and mice. Fish mounted very robust, quick responses to zymosan that led to the recruitment of several leukocyte populations. Addition of apoptotic cells resulted in a marked suppression of these responses. In contrast, mice displayed more subtle responses

to both zymosan and apoptotic cells with targeted cellular recruitment and appeared to rely more heavily on resident tissue subsets.

Two important characteristics of an inflammatory site are cellular infiltration and induction of antimicrobial defenses (4). Goldfish exhibited significantly higher cellular infiltration than mice following intraperitoneal challenge with zymosan (20-fold increase vs 1.5 fold increase). In goldfish, this infiltrate was composed of both lymphoid and myeloid cells, while murine leukocyte infiltration was dominated by neutrophils. Furthermore, apoptotic cells inhibited infiltration of both myeloid and lymphoid cells in goldfish. This is in sharp contrast to mice, where the infiltrating macrophage and lymphocyte populations modestly decreased while neutrophil infiltration was maintained in the presence of apoptotic cell stimuli.

Murine respiratory burst responses also displayed added cell specificity compared to the teleost model. In mice, apoptotic cells preferentially caused a decrease in neutrophil respiratory burst, whereas only a limited effect was evident in macrophage responses. Murine respiratory burst responses also displayed faster kinetics preceding the wave of leukocyte infiltration, suggesting a significant contribution from resident peritoneal leukocytes. These results are consistent with an evolutionary shift towards leukocyte specialization in mammals. This shift appears to favor targeted induction of leukocyte infiltration ($F4/80^{-}$/ $Gr1^{+}$/ $CD11b^{+}$ neutrophils in this model), and is increasingly reliant on local peritoneal leukocyte populations for early activation of innate antimicrobial effector mechanisms. This may be associated with evolving roles for specific leukocyte populations. For example, teleost circulating lymphocyte pools contribute directly to innate

phagocytic responses (42-44), whereas mammalian lymphocytes display increased specialization towards homeostatic tissue repair mechanisms (45-48) and adaptive mechanisms of immunity (49-51).

These results also point to changing roles for neutrophils across evolution. In both goldfish and mice, neutrophils are among the first leukocytes recruited to an inflammatory site (52) and their loss from an inflammatory site is often considered a key histological feature that signals the start to the resolution of inflammation (53). The evolutionary origins of neutrophils may lie in their roles as novel contributors for the induction of potent antimicrobial defenses. However, recent studies highlight another role for mammalian neutrophils as contributors to homeostatic responses at an inflammatory site. Within hours after entering an inflammatory site, infiltrating neutrophils actively produce protective molecules, such as lipoxins from arachidonic acid, which promote resolution of an inflammatory response (coined 'lipid mediator class- switching') (53). My results add to this paradigm and indicate that mammalian neutrophils display an increased capacity to participate in the down-regulation of inflammation though contact dependent interactions with apoptotic cells. This contact and subsequent internalization of apoptotic cells significantly reduces not only neutrophilic ROS production but also macrophage ROS production through a soluble factor-mediated mechanism. While it is currently unknown which soluble factor(s) contribute to this action, lipoxins have been shown to attenuate ROS production in a number of cells including microglia (54), endothelial cells (55), and aggregated peripheral blood leukocytes (56). Further, while the ability of neutrophils to internalize

apoptotic cells appears to have evolved recently, as teleost neutrophils do not display this capability, teleost neutrophils are able to produce soluble factor(s) that downregulate macrophage ROS production. As such, future studies should assess the potential differences between mammals and teleosts in the production of pro-resolution molecules such as lipoxins, resolvins, maresins, and protectins, and the role(s) these molecules may have in promoting the resolution of inflammation through neutrophil/apoptotic cell contact-dependent and independent mechanisms.

The balance between pathogen and homeostatic phagocytic responses is critical for the effective induction of pathogen clearance mechanisms that are efficiently controlled to prevent excessive tissue damage (57). Loss of this balance contributes to the development and exacerbation of autoimmune diseases that include systemic lupus erythematosus (58), adult respiratory distress syndrome and rheumatoid arthritis (59), and can also lead to incomplete pathogen clearance (4). The specific importance of homeostatic phagocytic responses is further highlighted by several recent studies. For example, injection of apoptotic cells prevents the development of experimental immune complex-mediated inflammatory arthritis (60), accelerates the resolution of acute inflammation (8), expands a pool of TGF-β tolerogenic T cells (61), non-specifically facilitates allogenic bone marrow engraftment (62), and interferes with graft rejection and the development of graft-versus-host disease (63). These effects appear to be linked to the capacity of exogenously administered apoptotic cells to promote an immunosuppressive environment, activate immunomodulatory cells, and decrease inflammatory immune cell infiltration (8). I have shown in this chapter that the presence of

apoptotic cells results in greatly diminished zymosan-induced ROS production. This provides added insights into the mechanisms by which apoptotic cells contribute to the control of inflammatory processes and may also highlight unique therapeutic opportunities for treatment of those disease states that possess a strong ROS component.

Together, my results demonstrate that the distinct polarization of immune cells in response to inflammatory or homeostatic stimuli are evolutionarily intact in bony fish. However, differences in the rate of leukocyte migration to the inflammatory site, increased selectivity for the leukocyte subsets recruitment to this site, increased participation of resident leukocyte pools, and changes to the kinetics and strength of the antimicrobial response highlight the significant honing that has developed for the control of inflammation across evolution.

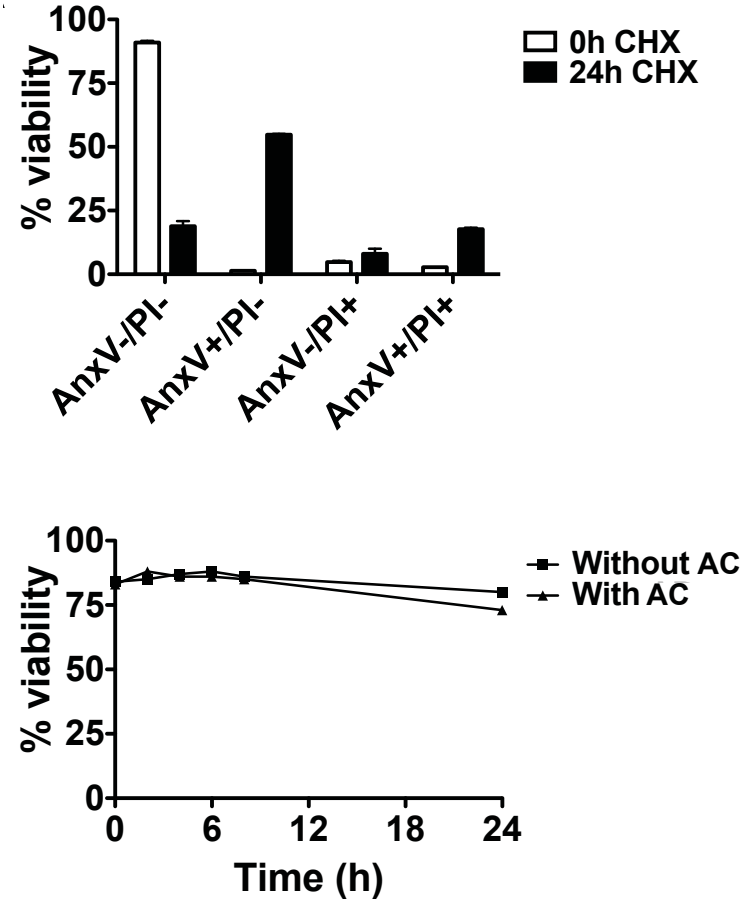

Figure 4.1. Cycloheximide primarily induces apoptosis in treated cells and can be effectively removed from apoptotic cell preparations.

Representative experiments show apoptotic cells generated for treatment of goldfish phagocytes. 3B11 catfish B cells were cultured for 24 hours in the presence of 10 μg/mL cycloheximide. Cells were subsequently harvested and stained with Annexin V/ propidium iodide to determine cell viability. Cycloheximide treatment primarily induced apoptotic cell death for effective generation of apoptotic cells, which were then labeled with wheat germ agglutinin-Alexa Fluor 555 overnight. To ensure that apoptotic cell preparations did not negatively impact phagocyte viability, apoptotic cell preparations were washed three times in 1x $PBS^{-/-}$ to remove remaining cycloheximide and added to goldfish PKM for the times indicated. At these time points, PKM cells were harvested and stained with Annexin V/ propidium iodide to assess viability status of these phagocytes. Apoptotic cells did not induce cell death in PKM cultures.

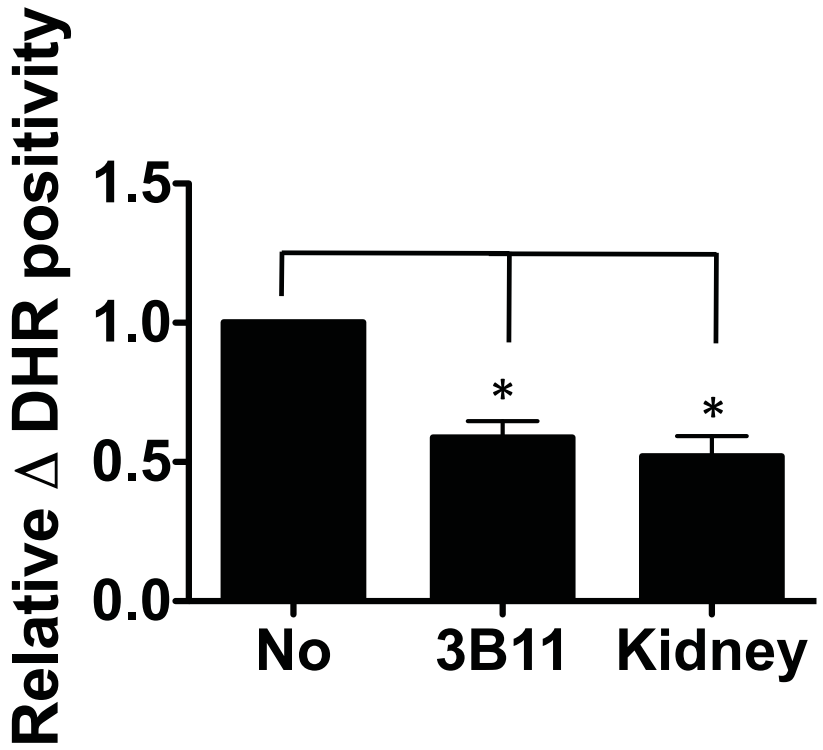

Figure 4.2. Two distinct sources of apoptotic cells repress goldfish macrophage respiratory burst to equivalent levels.

PKM cultures were incubated with apoptotic cells derived from 3B11 B cells or goldfish kidney leukocytes. Cells were incubated for 2 hours (5:1, particle: cell ratio) and respiratory burst was analyzed by DHR. There was no significant difference in PKM responses to 3B11-derived or kidney-derived apoptotic cells. n=4; *$p<0.05$ (One-way ANOVA; Tukey's post-hoc); error bars show SEM.

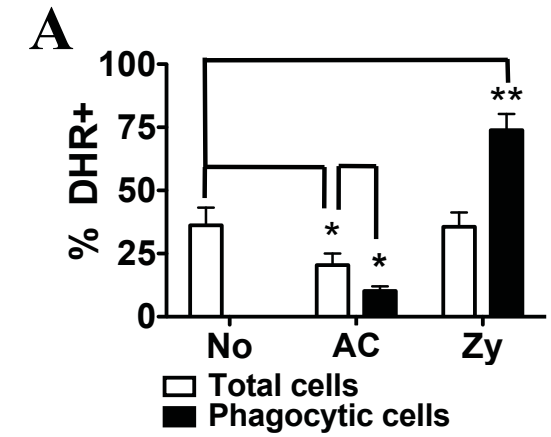
A
100
75
50
25
0
% DHR+
**
*
*
No
AC
Zy
Total cells
Phagocytic cells

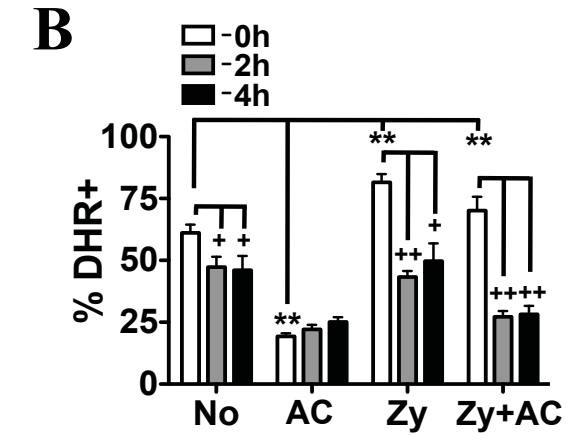
B
0h
2h
4h
100
75
50
25
0
% DHR+
**
**
**
+ +
++
+
++++
No
AC
Zy
Zy+AC

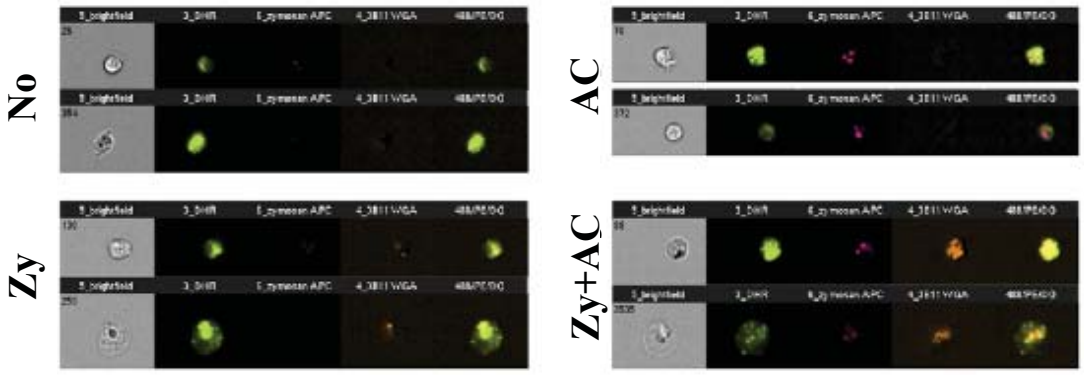
No
AC
Zy
Zy+AC

Figure 4.3. Apoptotic cells significantly reduce inflammatory respiratory burst responses of goldfish primary macrophages.

(**A**) Goldfish PKM were separately incubated with apoptotic cells or zymosan (5:1, particle: cell ratio) for 2 hours. Cells were then harvested and respiratory burst was assayed using DHR. n=3. (**B**) Goldfish PKM were cultured in the presence of both apoptotic cells and zymosan for 2 hours (5:1 ratio for both). Respiratory burst was then analyzed in cells based on phagocytic capacity as follows: non-phagocytic cells, cells containing only apoptotic cells, cells containing only zymosan or cells containing both apoptotic cells and zymosan (white bars). Representative images are shown for cells in each of these groups. To investigate the effects of pre-incubation with apoptotic cells, apoptotic cells were added to PKM simultaneously to zymosan ('-0h'), 2 hours before zymosan ('-2h') or 4 hours before zymosan ('-4h'). n=4. For all, * $p<0.05$; ** $p<0.01$ (compared to 'No'); + $p<0.05$ and ++ $p<0.01$ compared to ('-0h') (One-way ANOVA; Tukey's post-hoc); error bars show SEM. No- no internalized particle; AC- apoptotic cell; Zy- zymosan.

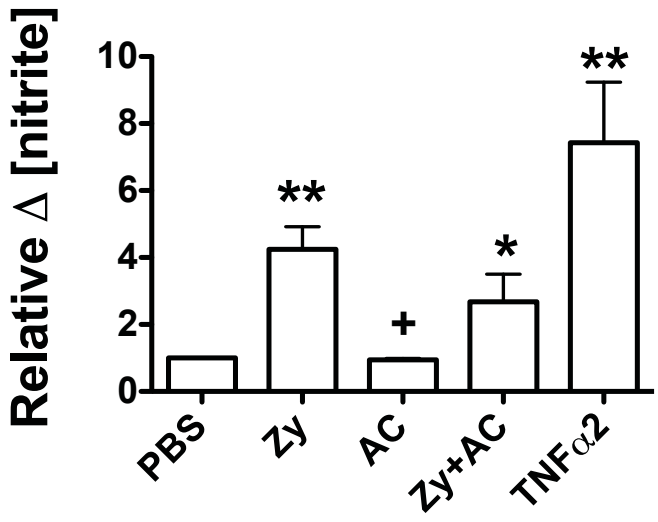

Figure 4.4. Apoptotic cells do not induce nitric oxide responses.

Goldfish PKM were separately incubated with apoptotic cells or zymosan (5:1, particle: cell ratio) for 72 hours. Cells were then harvested and nitric oxide was assayed using a Griess assay. n=4. * $p<0.05$; ** $p<0.01$ compared to PBS; + $p<0.05$ and ++ $p<0.01$ compared to zymosan (One-way ANOVA; Tukey's post-hoc); error bars show SEM. No- no internalized particle; AC- apoptotic cell; Zy- zymosan.

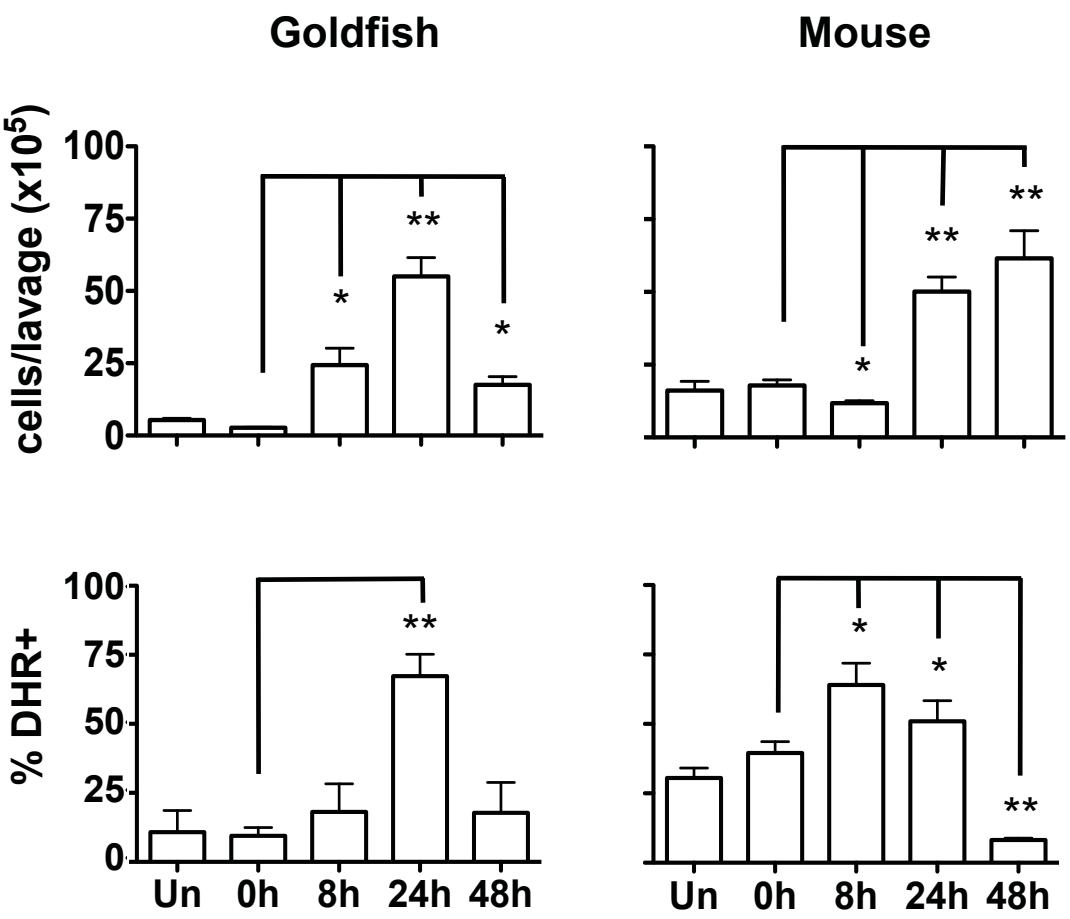

Figure 4.5. ***In vivo*** **administration of zymosan induces a marked infiltration of leukocytes that is linked to high levels of respiratory burst.**

Goldfish (left) and C57BL/6 mice (right) were injected intraperitoneally with 2.5 mg of zymosan. Cells were harvested by peritoneal lavage at 0 hours (saline alone), 8, 24 and 48 hours and counted (top row). Injection of zymosan resulted in a marked increase in cell numbers isolated from the peritoneum that peaked at 48 hours for mice and 24 hours for goldfish. Respiratory burst in isolated cells at these time points was determined with DHR (bottom row). n=4; * $p<0.05$; ** $p<0.01$ (One-way ANOVA; Tukey's post-hoc); error bars show SEM.

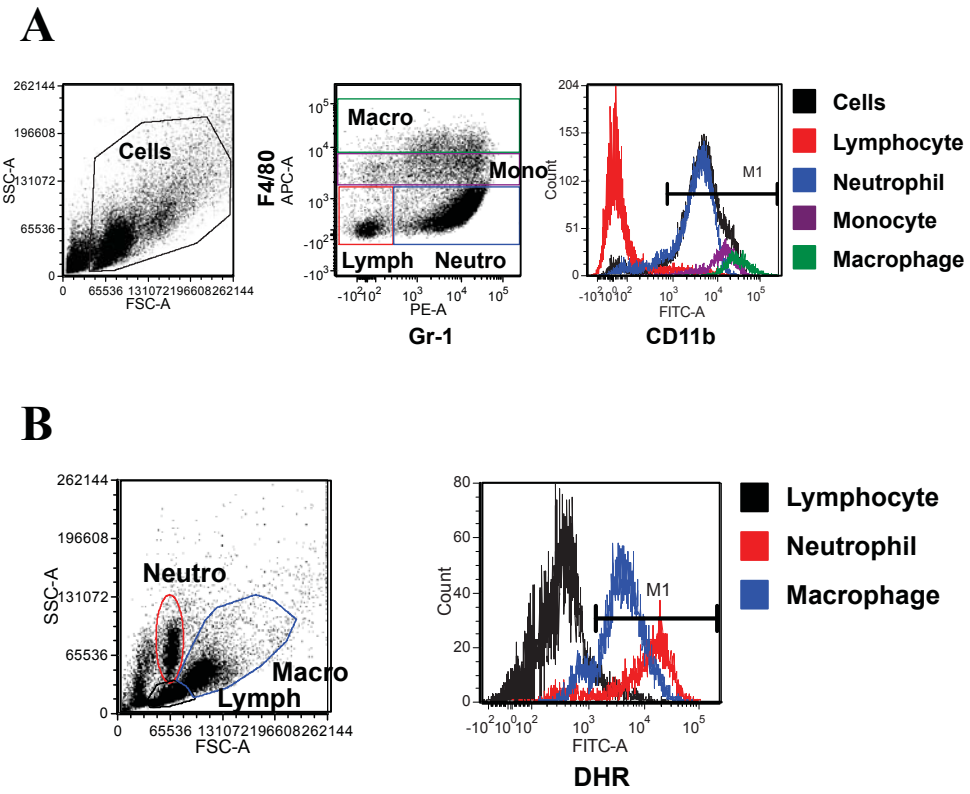

Figure 4.6. Gating strategy for cell subpopulations isolated from murine peritoneum.

(**A**) Peritoneal cells from C57BL/6 mice were stained with combination of CD11b-FITC/ Gr1-PE/ F4/80-APC or CD11b-PE-Cy7/ CD3-FITC/ B220-PE/ NK1.1-APC to determine the infiltration of granulocytes ($F4/80^-$/ $Gr1^+$/ $CD11b^+$), macrophages ($F4/80^{hi}$/ $Gr1^{+/-}$/ $CD11b^+$), monocytes ($F4/80^{lo}$/ $Gr1^{+/-}$/ $CD11b^+$) and lymphocytes ($F4/80^-/Gr1^-$). Lymphocyte populations were confirmed to contain T cells ($CD11b^-$ / $CD3^+$), B cells ($CD11b^{+/-}$/ $B220^+$) and NK cells ($CD11b^-$/ $NK1.1^+$). (**B**) Murine peritoneal cells were stained with DHR and analyzed using a FACSCanto II flow cytometer. Cell populations were determined based on forward (FSC-A) and side scatted (SSC-A) characteristics.

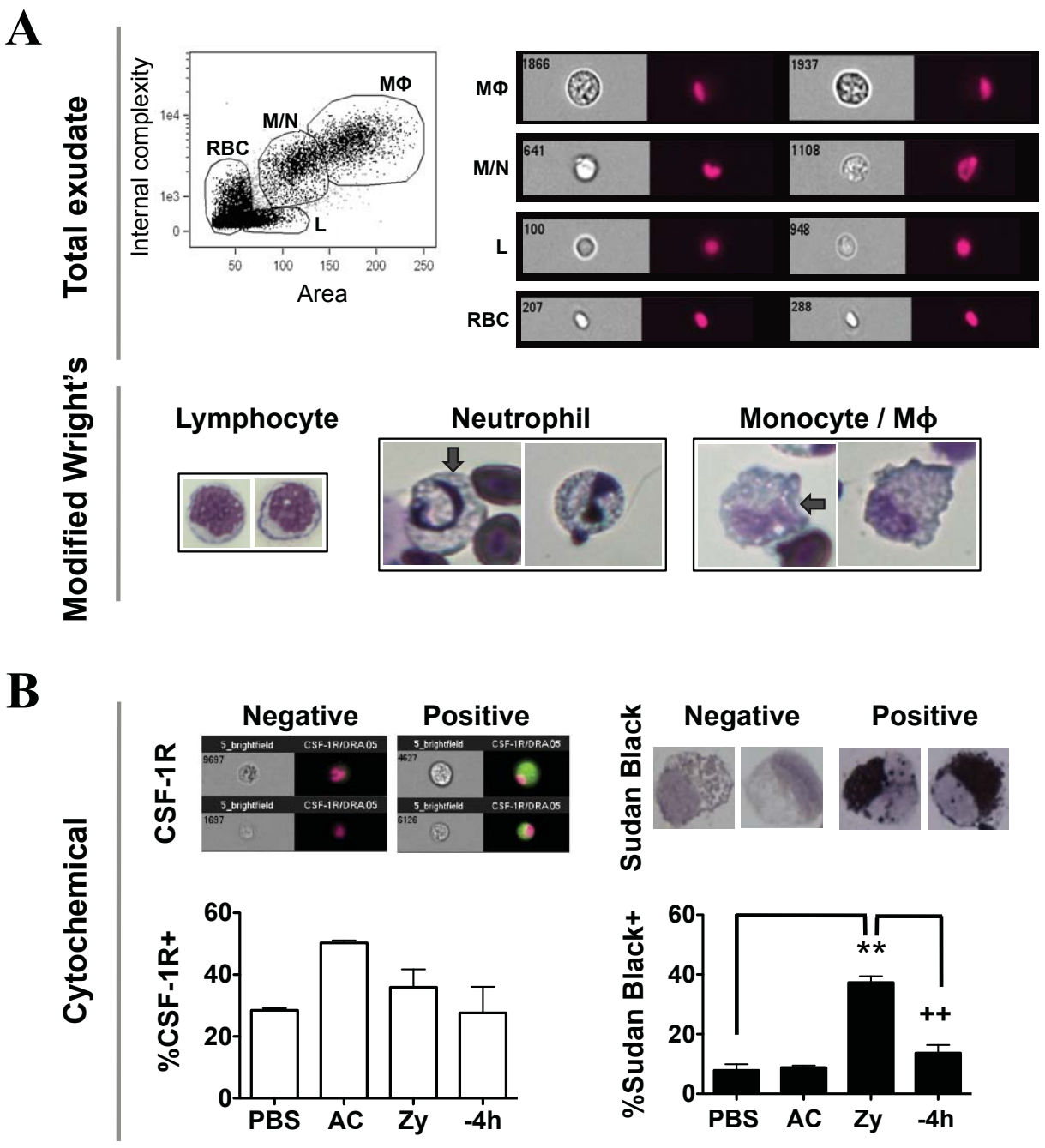
A
Total exudate
Internal complexity
Area
MΦ
M/N
RBC
L
1866
1937
641
1108
100
948
207
288
Modified Wright's
Lymphocyte
Neutrophil
Monocyte / Mϕ
B
Cytochemical
CSF-1R
Negative
Positive
5_brightfield
CSF-1R/DRA05
%CSF-1R+
PBS
AC
Zy
-4h
Sudan Black
%Sudan Black+
**
++

Figure 4.7. Characterization of goldfish peritoneal myeloid cells.

(**A**) Total peritoneal exudates were analyzed by imaging flow cytometry and four distinct cellular subsets characterized based on area, internal complexity, and morphology. Unlike macrophage and lymphocyte subsets, monocytes and neutrophils could not be subdivided into two distinct populations solely based on these parameters. Modified Wright's stain confirmed the presence of cells with classical lymphocyte, neutrophil, and monocyte / macrophage morphology. (**B**) To better differentiate between myeloid populations within the goldfish peritoneal exudate, cells were analyzed based on surface CSF-1R expression and Sudan Black cytochemical staining, which denote monocyte/macrophages and neutrophils, respectively. Representative cells stained with anti-CSF-1R antibodies or Sudan Black are shown. Goldfish were injected intraperitoneally with saline, apoptotic cells (AC; $5x10^6$) or zymosan (Zy; 2.5 mg) and incubated for 24 hours. Apoptotic cells were also pre-injected 4 hours (-4h) before zymosan injections to assess the contributions of kinetics to these responses. For flow cytometry, n=2; for cytochemical stains, n=4. * $p<0.05$ and ** $p<0.01$ compared to control; ++$p<0.01$ compared to zymosan (One-way ANOVA; Tukey's post-hoc); error bars show SEM.

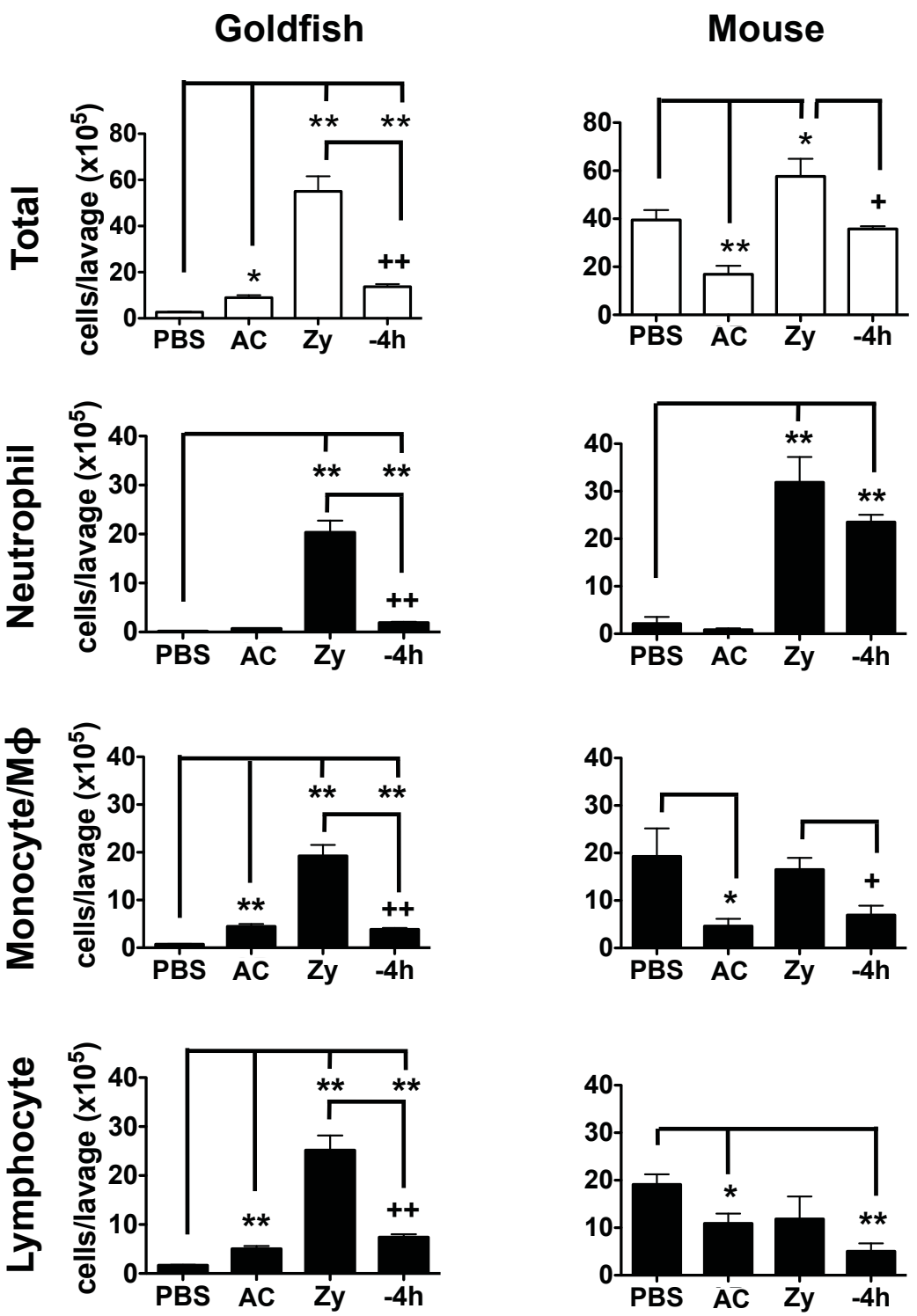
Goldfish
Mouse
Total
Neutrophil
Monocyte/Mφ
Lymphocyte
cells/lavage (x10^5)
PBS
AC
Zy
-4h
*
**
+
++

Figure 4.8. Pro-inflammatory (zymosan) and homeostatic (apoptotic cells) stimuli differentially impact leukocyte infiltration profiles in goldfish and mice.

Goldfish and C57BL/6 mice were injected intraperitoneally with saline, apoptotic cells ($5x10^6$) or zymosan (2.5 mg). Apoptotic cells were also pre-injected 4 hours before zymosan injections. Goldfish leukocyte populations were defined by imaging flow cytometry (area, internal complexity, and morphology) and staining patterns with Sudan Black and an anti-CSF-1R antibody. Murine cells were defined based on surface markers for neutrophils ($F4/80^-/ Gr1^+/ CD11b^+$), monocytes ($F4/80^{lo}/ Gr1^{+/-}/ CD11b^+$), macrophages ($F4/80^{hi}/ Gr1^{+/-}/ CD11b^+$) and lymphocytes ($F4/80^-/Gr1^-$; CD3, B220, NK1.1). n=4; * $p<0.05$ and ** $p<0.01$ compared to control; + $p<0.05$ and ++ $p<0.01$ compared to zymosan (One-way ANOVA; Tukey's post-hoc); error bars show SEM. No- no internalized particle; AB- apoptotic body; Zy- zymosan.

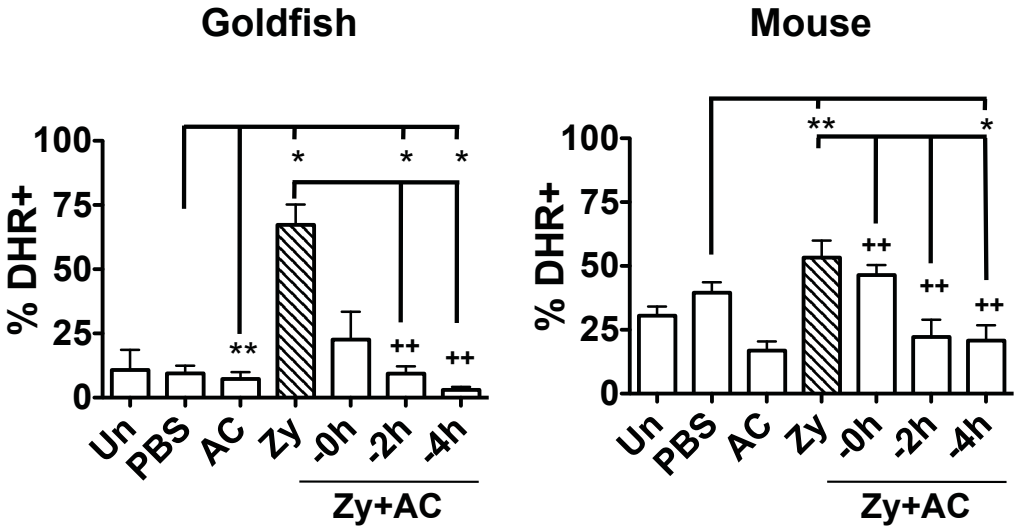

Figure 4.9. *In vivo* administration of apoptotic cells leads to a more dramatic reduction of pro-inflammatory respiratory burst responses in teleost fish compared to mice.

Goldfish and C57BL/6 mice were injected intraperitoneally with saline, apoptotic cells ($5x10^6$) or zymosan (2.5 mg) and incubated for 24 hours. Apoptotic cells were also pre-injected 0, 2, or 4 hours before zymosan injections to assess the contributions of kinetics to these responses. Cells from injected animals were harvested by peritoneal lavage and respiratory burst was assayed with DHR. n=4; * $p<0.05$ and ** $p<0.01$ compared to PBS (saline) control; + $p<0.05$ and ++ $p<0.01$ compared to zymosan (One-way ANOVA; Tukey's post-hoc); error bars show SEM. No- no internalized particle; AC- apoptotic cell; Zy- zymosan.

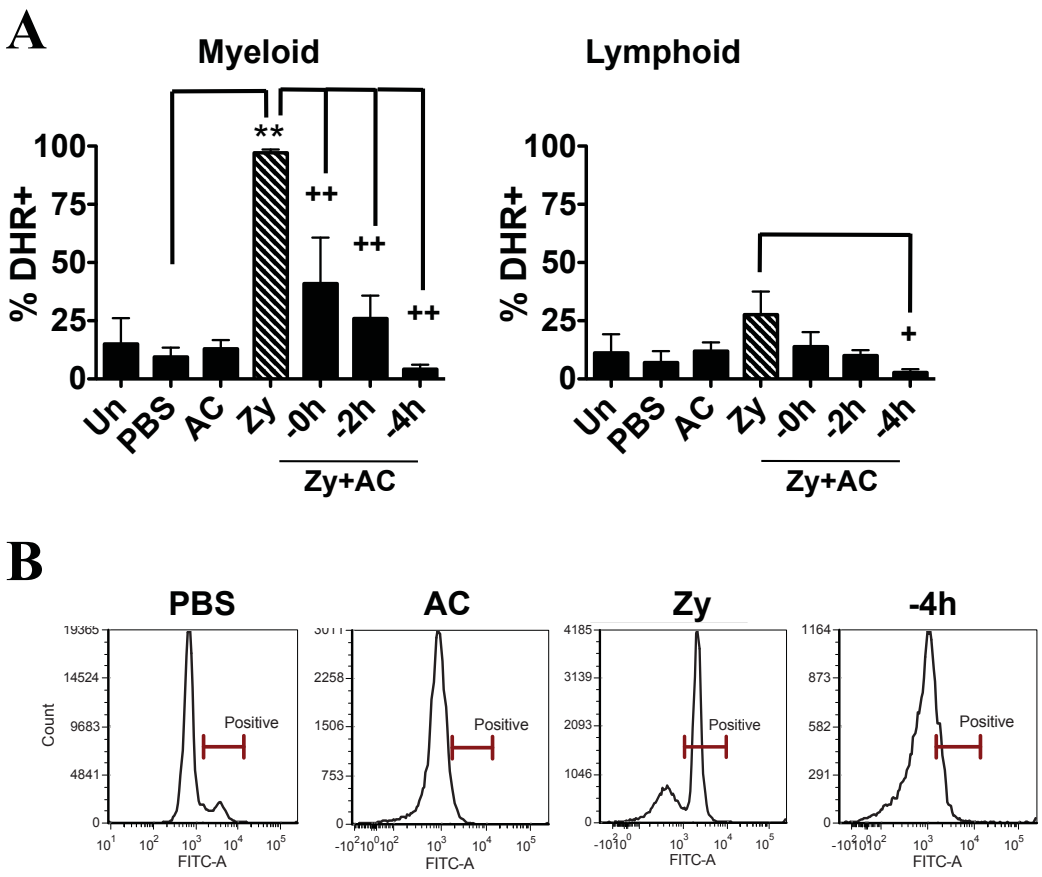

Figure 4.10. Goldfish myeloid cell respiratory burst responses are most affected by the presence of apoptotic cells.

(**A**) Goldfish were injected intraperitoneally with saline, apoptotic cells ($5x10^6$) or zymosan (2.5 mg). Apoptotic cells were also pre-injected 0, 2, or 4 hours before zymosan injections. Cells from injected goldfish were harvested by peritoneal lavage and respiratory burst was assayed with DHR in peritoneal cell subpopulations based on forward scatter and side scatter profiles. n=4; * $p<0.05$ and ** $p<0.01$ compared to control; + $p<0.05$ and ++ $p<0.01$ compared to zymosan (One-way ANOVA; Tukey's post-hoc); error bars show SEM. No- no internalized particle; AC- apoptotic cell; Zy- zymosan. (**B**) Representative histograms show a single peak in DHR responses.

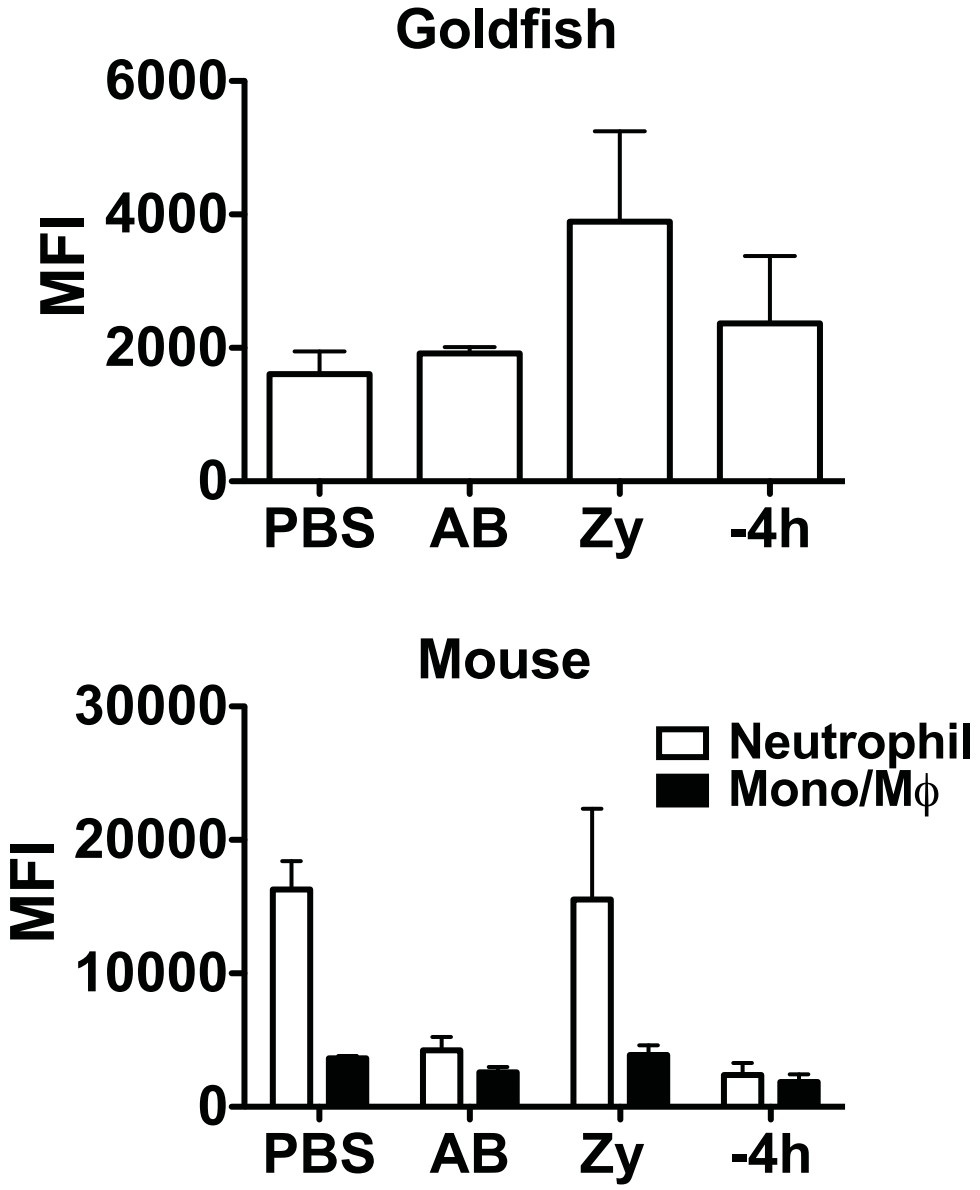

Figure 4.11. Mean fluorescence intensity of teleost and murine phagocytes.

Goldfish and mice were injected intraperitoneally with saline, species-specific apoptotic cells ($5x10^6$) or zymosan (2.5 mg). Apoptotic cells were also pre-injected 4 hours before zymosan injections. Cells from injected animals were harvested by peritoneal lavage and respiratory burst was assayed with DHR in peritoneal cell subpopulations based on forward scatter and side scatter profiles. The mean fluorescence intensity was calculated based on the mean DHR fluorescence in the entire population. For goldfish, myeloid cells are shown. For mice, phagocyte populations were further split into neutrophils and monocyte/ macrophages. Error bars show SEM.

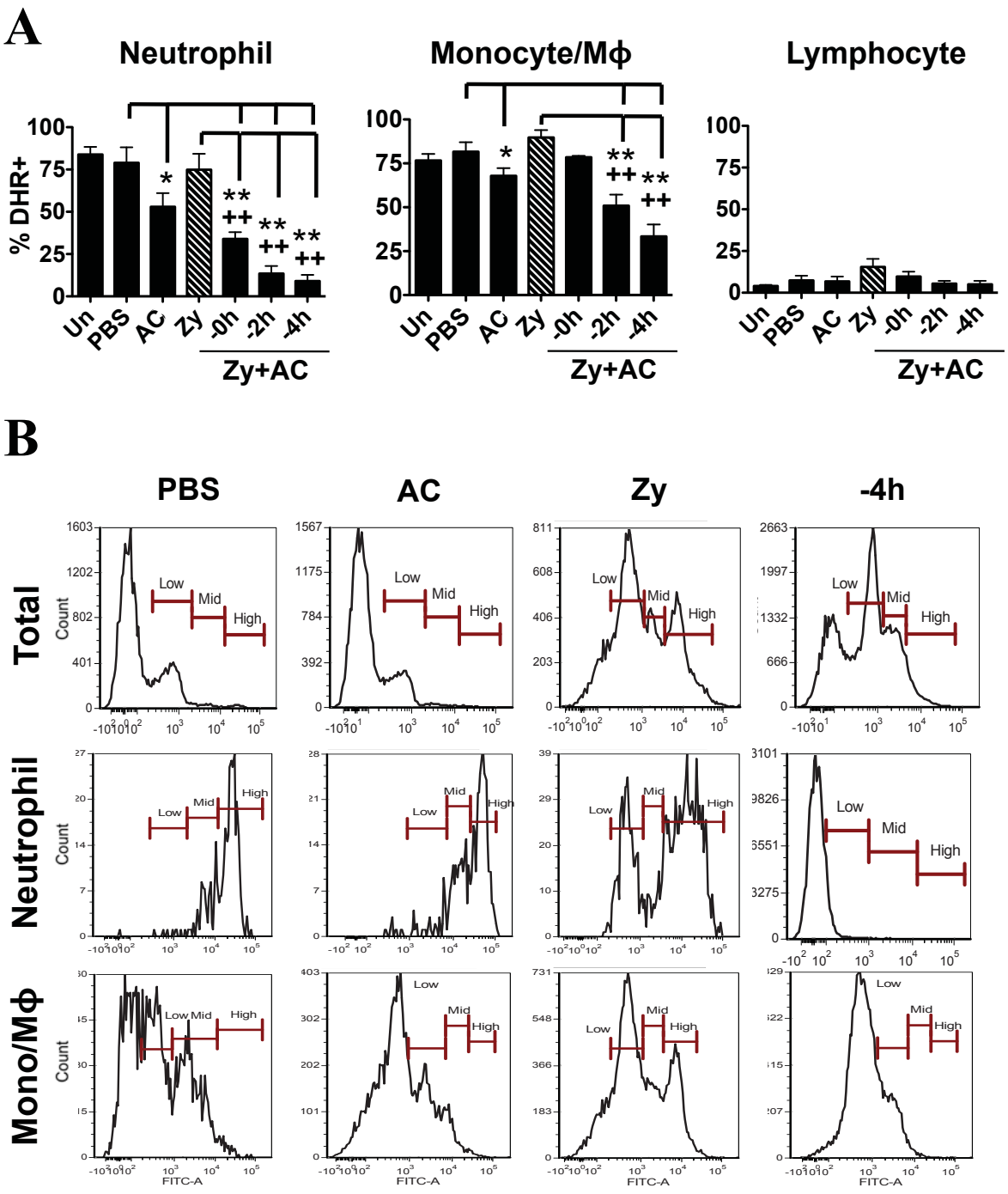
A
Neutrophil
Monocyte/Mϕ
Lymphocyte
% DHR+
100
75
50
25
0
Un
PBS
AC
Zy
-0h
-2h
-4h
Zy+AC
B
PBS
AC
Zy
-4h
Total
Neutrophil
Mono/Mϕ
Count
FITC-A
Low
Mid
High

Figure 4.12. Murine neutrophil respiratory burst antimicrobial responses are most greatly affected by the presence of apoptotic cells.

(**A**) C57BL/6 mice were injected intraperitoneally with saline, apoptotic cells ($5x10^6$) or zymosan (2.5 mg). Apoptotic cells were also pre-injected 0, 2, or 4 hours before zymosan injections. Cells from injected mice were harvested by peritoneal lavage and respiratory burst was assayed with DHR in peritoneal cell subpopulations based on forward scatter and side scatter profiles. n=4; * $p<0.05$ and ** $p<0.01$ compared to control; + $p<0.05$ and ++ $p<0.01$ compared to zymosan (One-way ANOVA; Tukey's post-hoc); error bars show SEM. No- no internalized particle; AC- apoptotic cell; Zy- zymosan. (**B**) Histograms show representative DHR responses for total leukocytes, neutrophils and monocytes/macrophages. We found that the high responders were predominantly neutrophils (>90%). Pre-incubation with apoptotic cells resulted in a preferential switch in the neutrophil population from high responders to mid/low responders.

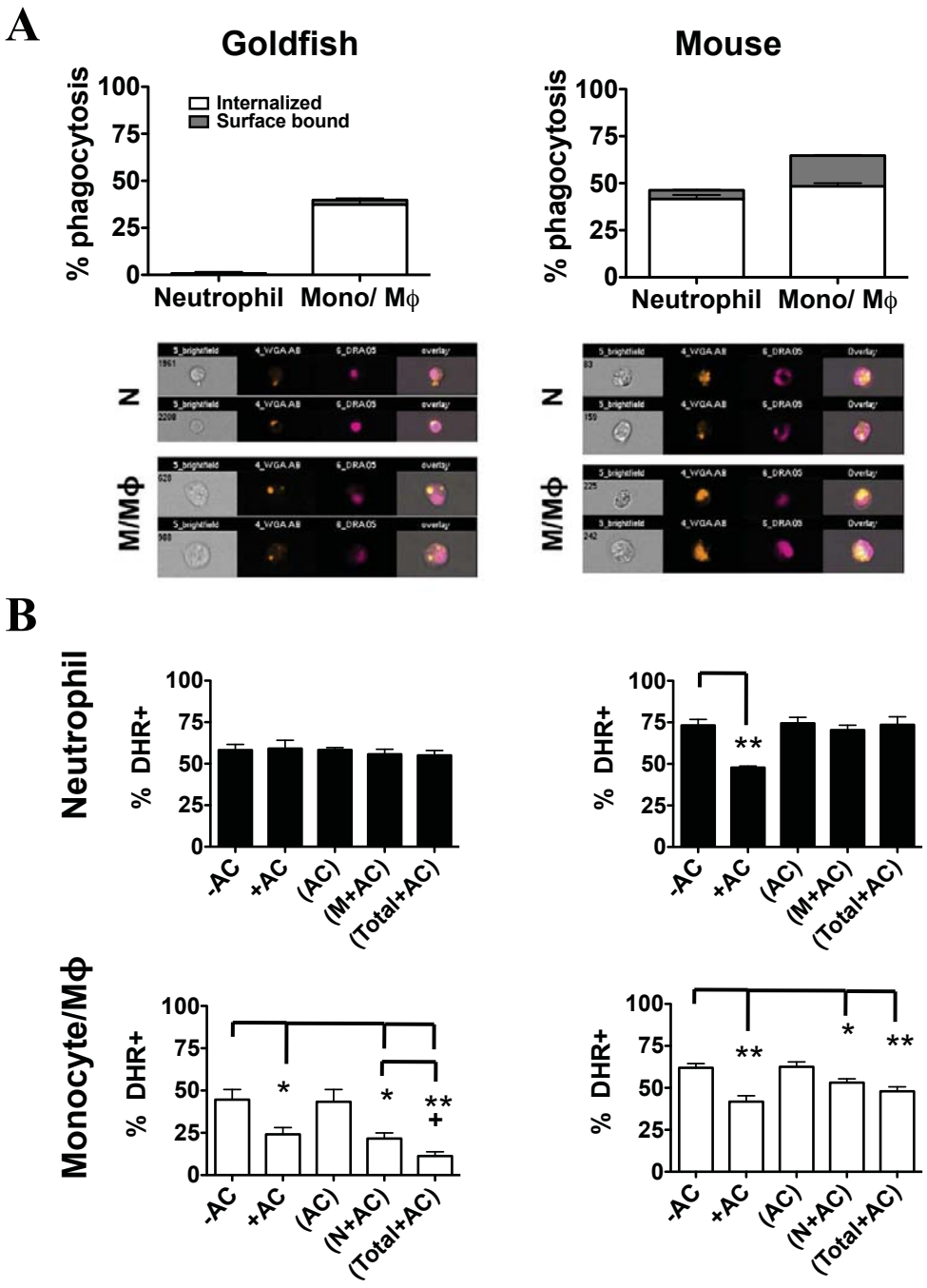
A
Goldfish
Mouse
% phagocytosis
100
75
50
25
0
Internalized
Surface bound
Neutrophil
Mono/ Mϕ
N
M/Mϕ
B
Neutrophil
Monocyte/Mϕ
% DHR+
-AC
+AC
(AC)
(M+AC)
(N+AC)
(Total+AC)
*
**
+

Figure 4.13. Apoptotic cells downregulate murine neutrophil ROS production in a contact dependent manner.

Goldfish (left) and C57BL/6 mice (right) were injected intraperitoneally with zymosan (2.5 mg). Activated peritoneal cells from were harvested by peritoneal lavage and subpopulations were isolated by density centrifugation. (**A**) Separated neutrophil or mononuclear populations were incubated with labeled apoptotic cells for 2 hours and internalization was analyzed. n=4; * $p<0.05$ and ** $p<0.01$ (One-way ANOVA; Tukey's post-hoc); error bars show SEM; Mono/Mϕ= monocytes/ macrophage. (**B**) Isolated populations were cultured for 2 hours in the presence of the indicated stimuli. Conditions denoted within brackets were contained within a 4 μm transwell. After 2 hours, responder cells outside the transwells were harvested and respiratory burst was assayed using DHR. n=4; * $p<0.05$ and ** $p<0.01$ (One-way ANOVA; Tukey's post-hoc); error bars show SEM; Mono/Mϕ= monocytes/ macrophage.

4.4 References

1. Poon, I.K.H., Hulett, M.D., and Parish, C.R. 2010. Molecular mechanisms of late apoptotic/necrotic cell clearance. *Cell Death Differ* 17:381-397.
2. Gregory, C.D., and Devitt, A. 2004. The macrophage and the apoptotic cell: an innate immune interaction viewed simplistically? *Immunology* 113:1-14.
3. Duffield, J.S. 2003. The inflammatory macrophage: a story of Jekyll and Hyde. *Clin Sci (Lond)* 104:27-38.
4. Soehnlein, O., and Lindbom, L. 2010. Phagocyte partnership during the onset and resolution of inflammation. *Nat Rev Immunol* 10:427-439.
5. Zamboni, D.S., and Rabinovitch, M. 2003. Nitric oxide partially controls Coxiella burnetii phase II infection in mouse primary macrophages. *Infect Immun* 71:1225-1233.
6. Johann, A.M., von Knethen, A., Lindemann, D., and Brune, B. 2006. Recognition of apoptotic cells by macrophages activates the peroxisome proliferator-activated receptor-gamma and attenuates the oxidative burst. *Cell Death Differ* 13:1533-1540.
7. Reiter, I., Krammer, B., and Schwamberger, G. 1999. Cutting edge: differential effect of apoptotic versus necrotic tumor cells on macrophage antitumor activities. *J Immunol* 163:1730-1732.
8. Huynh, M.L., Fadok, V.A., and Henson, P.M. 2002. Phosphatidylserine-dependent ingestion of apoptotic cells promotes TGF-beta1 secretion and the resolution of inflammation. *J Clin Invest* 109:41-50.
9. Potter, P.K., Cortes-Hernandez, J., Quartier, P., Botto, M., and Walport, M.J. 2003. Lupus-prone mice have an abnormal response to thioglycolate and an impaired clearance of apoptotic cells. *J Immunol* 170:3223-3232.
10. Fadok, V.A., Bratton, D.L., Konowal, A., Freed, P.W., Westcott, J.Y., and Henson, P.M. 1998. Macrophages that have ingested apoptotic cells in vitro inhibit proinflammatory cytokine production through autocrine/paracrine mechanisms involving TGF-beta, PGE2, and PAF. *J Clin Invest* 101:890-898.
11. Maderna, P., and Godson, C. 2003. Phagocytosis of apoptotic cells and the resolution of inflammation. *Biochim Biophys Acta* 1639:141-151.
12. Weigert, A., Jennewein, C., and Brune, B. 2009. The liaison between apoptotic cells and macrophages--the end programs the beginning. *Biol Chem* 390:379-390.
13. Voll, R.E., Herrmann, M., Roth, E.A., Stach, C., Kalden, J.R., and Girkontaite, I. 1997. Immunosuppressive effects of apoptotic cells. *Nature* 390:350-351.
14. Bellingan, G.J., Caldwell, H., Howie, S.E., Dransfield, I., and Haslett, C. 1996. In vivo fate of the inflammatory macrophage during the resolution of inflammation: inflammatory macrophages do not die locally, but emigrate to the draining lymph nodes. *J Immunol* 157:2577-2585.
15. Stark, M.A., Huo, Y., Burcin, T.L., Morris, M.A., Olson, T.S., and Ley, K. 2005. Phagocytosis of apoptotic neutrophils regulates granulopoiesis via IL-23 and IL-17. *Immunity* 22:285-294.

16. Tassiulas, I., Park-Min, K.H., Hu, Y., Kellerman, L., Mevorach, D., and Ivashkiv, L.B. 2007. Apoptotic cells inhibit LPS-induced cytokine and chemokine production and IFN responses in macrophages. *Hum Immunol* 68:156-164.
17. Kim, S., Elkon, K.B., and Ma, X. 2004. Transcriptional suppression of interleukin-12 gene expression following phagocytosis of apoptotic cells. *Immunity* 21:643-653.
18. Serinkan, B.F., Gambelli, F., Potapovich, A.I., Babu, H., Di Giuseppe, M., Ortiz, L.A., Fabisiak, J.P., and Kagan, V.E. 2005. Apoptotic cells quench reactive oxygen and nitrogen species and modulate TNF-alpha/TGF-beta1 balance in activated macrophages: involvement of phosphatidylserine-dependent and -independent pathways. *Cell Death Differ* 12:1141-1144.
19. Anderson, H.A., Englert, R., Gursel, I., and Shacter, E. 2002. Oxidative stress inhibits the phagocytosis of apoptotic cells that have externalized phosphatidylserine. *Cell Death Differ* 9:616-625.
20. Bianchi, S.M., Prince, L.R., McPhillips, K., Allen, L., Marriott, H.M., Taylor, G.W., Hellewell, P.G., Sabroe, I., Dockrell, D.H., Henson, P.W., et al. 2008. Impairment of apoptotic cell engulfment by pyocyanin, a toxic metabolite of Pseudomonas aeruginosa. *Am J Respir Crit Care Med* 177:35-43.
21. Fadeel, B., Xue, D., and Kagan, V. 2010. Programmed cell clearance: molecular regulation of the elimination of apoptotic cell corpses and its role in the resolution of inflammation. *Biochem Biophys Res Commun* 396:7-10.
22. Erwig, L.P., and Henson, P.M. 2007. Immunological consequences of apoptotic cell phagocytosis. *Am J Pathol* 171:2-8.
23. Fullard, J.F., Kale, A., and Baker, N.E. 2009. Clearance of apoptotic corpses. *Apoptosis* 14:1029-1037.
24. Bannenberg, G.L., Chiang, N., Ariel, A., Arita, M., Tjonahen, E., Gotlinger, K.H., Hong, S., and Serhan, C.N. 2005. Molecular circuits of resolution: formation and actions of resolvins and protectins. *J Immunol* 174:4345-4355.
25. Ariel, A., Fredman, G., Sun, Y.P., Kantarci, A., Van Dyke, T.E., Luster, A.D., and Serhan, C.N. 2006. Apoptotic neutrophils and T cells sequester chemokines during immune response resolution through modulation of CCR5 expression. *Nat Immunol* 7:1209-1216.
26. Schwab, J.M., Chiang, N., Arita, M., and Serhan, C.N. 2007. Resolvin E1 and protectin D1 activate inflammation-resolution programmes. *Nature* 447:869-874.
27. Chadzinska, M., Leon-Kloosterziel, K.M., Plytycz, B., and Lidy Verburg-van Kemenade, B.M. 2008. In vivo kinetics of cytokine expression during peritonitis in carp: evidence for innate and alternative macrophage polarization. *Dev Comp Immunol* 32:509-518.
28. Cash, J.L., White, G.E., and Greaves, D.R. 2009. Chapter 17. Zymosan-induced peritonitis as a simple experimental system for the study of inflammation. *Methods Enzymol* 461:379-396.

29. Kolaczkowska, E., Barteczko, M., Plytycz, B., and Arnold, B. 2008. Role of lymphocytes in the course of murine zymosan-induced peritonitis. *Inflamm Res* 57:272-278.
30. Vandivier, R.W., Fadok, V.A., Hoffmann, P.R., Bratton, D.L., Penvari, C., Brown, K.K., Brain, J.D., Accurso, F.J., and Henson, P.M. 2002. Elastase-mediated phosphatidylserine receptor cleavage impairs apoptotic cell clearance in cystic fibrosis and bronchiectasis. *J Clin Invest* 109:661-670.
31. Gantner, B.N., Simmons, R.M., Canavera, S.J., Akira, S., and Underhill, D.M. 2003. Collaborative induction of inflammatory responses by dectin-1 and Toll-like receptor 2. *J Exp Med* 197:1107-1117.
32. Herre, J., Marshall, A.S., Caron, E., Edwards, A.D., Williams, D.L., Schweighoffer, E., Tybulewicz, V., Reis e Sousa, C., Gordon, S., and Brown, G.D. 2004. Dectin-1 uses novel mechanisms for yeast phagocytosis in macrophages. *Blood* 104:4038-4045.
33. Pini, M., and Fantuzzi, G. 2010. Enhanced production of IL-17A during zymosan-induced peritonitis in obese mice. *J Leukoc Biol* 87:51-58.
34. Cuzzocrea, S., Zingarelli, B., Sautebin, L., Rizzo, A., Crisafulli, C., Campo, G.M., Costantino, G., Calapai, G., Nava, F., Di Rosa, M., et al. 1997. Multiple organ failure following zymosan-induced peritonitis is mediated by nitric oxide. *Shock* 8:268-275.
35. Neumann, N.F., Barreda, D.R., and Belosevic, M. 2000. Generation and functional analysis of distinct macrophage sub-populations from goldfish (Carassius auratus L.) kidney leukocyte cultures. *Fish Shellfish Immunol* 10:1-20.
36. Neumann, N.F., Barreda, D., and Belosevic, M. 1998. Production of a macrophage growth factor(s) by a goldfish macrophage cell line and macrophages derived from goldfish kidney leukocytes. *Dev Comp Immunol* 22:417-432.
37. Katzenback, B.A., and Belosevic, M. 2009. Isolation and functional characterization of neutrophil-like cells, from goldfish (Carassius auratus L.) kidney. *Dev Comp Immunol* 33:601-611.
38. Christenson, K., Bjorkman, L., Karlsson, J., Sundqvist, M., Movitz, C., Speert, D.P., Dahlgren, C., and Bylund, J. In vivo-transmigrated human neutrophils are resistant to antiapoptotic stimulation. *J Leukoc Biol* 90:1055-1063.
39. Goodridge, H.S., Simmons, R.M., and Underhill, D.M. 2007. Dectin-1 stimulation by Candida albicans yeast or zymosan triggers NFAT activation in macrophages and dendritic cells. *J Immunol* 178:3107-3115.
40. Underhill, D.M. 2003. Macrophage recognition of zymosan particles. *J Endotoxin Res* 9:176-180.
41. Esmann, L., Idel, C., Sarkar, A., Hellberg, L., Behnen, M., Moller, S., van Zandbergen, G., Klinger, M., Kohl, J., Bussmeyer, U., et al. 2009. Phagocytosis of apoptotic cells by neutrophil granulocytes: diminished proinflammatory neutrophil functions in the presence of apoptotic cells. *J Immunol* 184:391-400.

42. Li, J., Barreda, D.R., Zhang, Y.A., Boshra, H., Gelman, A.E., Lapatra, S., Tort, L., and Sunyer, J.O. 2006. B lymphocytes from early vertebrates have potent phagocytic and microbicidal abilities. *Nat Immunol* 7:1116-1124.
43. Zhang, Y.A., Salinas, I., Li, J., Parra, D., Bjork, S., Xu, Z., LaPatra, S.E., Bartholomew, J., and Sunyer, J.O. 2010. IgT, a primitive immunoglobulin class specialized in mucosal immunity. *Nat Immunol* 11:827-835.
44. Overland, H.S., Pettersen, E.F., Ronneseth, A., and Wergeland, H.I. 2010. Phagocytosis by B-cells and neutrophils in Atlantic salmon (Salmo salar L.) and Atlantic cod (Gadus morhua L.). *Fish Shellfish Immunol* 28:193-204.
45. Rieger, A., and Bar-Or, A. 2008. B-cell-derived interleukin-10 in autoimmune disease: regulating the regulators. *Nat Rev Immunol* 8:486-487.
46. Fillatreau, S., Gray, D., and Anderton, S.M. 2008. Not always the bad guys: B cells as regulators of autoimmune pathology. *Nat Rev Immunol* 8:391-397.
47. Zouali, M. 2008. B lymphocytes--chief players and therapeutic targets in autoimmune diseases. *Front Biosci* 13:4852-4861.
48. Keen, D. 2008. A review of research examining the regulatory role of lymphocytes in normal wound healing. *J Wound Care* 17:218-220, 222.
49. Martinez-Martin, N., Fernandez-Arenas, E., Cemerski, S., Delgado, P., Turner, M., Heuser, J., Irvine, D.J., Huang, B., Bustelo, X.R., Shaw, A., et al. 2011. T Cell Receptor Internalization from the Immunological Synapse Is Mediated by TC21 and RhoG GTPase-Dependent Phagocytosis. *Immunity* 35:208-222.
50. Parra, D., Rieger, A.M., Li, J., Zhang, Y.A., Randall, L.M., Hunter, C.A., Barreda, D.R., and Sunyer, J.O. Pivotal Advance: Peritoneal cavity B-1 B cells have phagocytic and microbicidal capacities and present phagocytosed antigen to CD4+ T cells. *J Leukoc Biol*.
51. Nakashima, M., Kinoshita, M., Nakashima, H., Habu, Y., Miyazaki, H., Shono, S., Hiroi, S., Shinomiya, N., Nakanishi, K., and Seki, S. Pivotal Advance: Characterization of mouse liver phagocytic B cells in innate immunity. *J Leukoc Biol*.
52. Leitch, A.E., Lucas, C.D., and Rossi, A.G. Editorial: Neutrophil apoptosis: hot on the TRAIL of inflammatory resolution. *J Leukoc Biol* 90:841-843.
53. Levy, B.D., Clish, C.B., Schmidt, B., Gronert, K., and Serhan, C.N. 2001. Lipid mediator class switching during acute inflammation: signals in resolution. *Nat Immunol* 2:612-619.
54. Wu, Y., Zhai, H., Wang, Y., Li, L., Wu, J., Wang, F., Sun, S., Yao, S., and Shang, Y. 2012. Aspirin-triggered lipoxin A(4) attenuates lipopolysaccharide-induced intracellular ROS in BV2 microglia cells by inhibiting the function of NADPH oxidase. *Neurochem Res* 37:1690-1696.
55. Nascimento-Silva, V., Arruda, M.A., Barja-Fidalgo, C., and Fierro, I.M. 2007. Aspirin-triggered lipoxin A4 blocks reactive oxygen species generation in endothelial cells: a novel antioxidative mechanism. *Thromb Haemost* 97:88-98.

56. Borgeson, E., Lonn, J., Bergstrom, I., Brodin, V.P., Ramstrom, S., Nayeri, F., Sarndahl, E., and Bengtsson, T. 2011. Lipoxin A(4) inhibits porphyromonas gingivalis-induced aggregation and reactive oxygen species production by modulating neutrophil-platelet interaction and CD11b expression. *Infect Immun* 79:1489-1497.
57. Medzhitov, R. 2007. Recognition of microorganisms and activation of the immune response. *Nature* 449:819-826.
58. Munoz, L.E., Janko, C., Schulze, C., Schorn, C., Sarter, K., Schett, G., and Herrmann, M. 2010. Autoimmunity and chronic inflammation - two clearance-related steps in the etiopathogenesis of SLE. *Autoimmun Rev* 10:38-42.
59. Weiss, S.J. 1989. Tissue destruction by neutrophils. *N Engl J Med* 320:365-376.
60. van Lent, P.L., Licht, R., Dijkman, H., Holthuysen, A.E., Berden, J.H., and van den Berg, W.B. 2001. Uptake of apoptotic leukocytes by synovial lining macrophages inhibits immune complex-mediated arthritis. *J Leukoc Biol* 70:708-714.
61. Kleinclauss, F., Perruche, S., Masson, E., de Carvalho Bittencourt, M., Biichle, S., Remy-Martin, J.P., Ferrand, C., Martin, M., Bittard, H., Chalopin, J.M., et al. 2006. Intravenous apoptotic spleen cell infusion induces a TGF-beta-dependent regulatory T-cell expansion. *Cell Death Differ* 13:41-52.
62. Bittencourt, M.C., Perruche, S., Contassot, E., Fresnay, S., Baron, M.H., Angonin, R., Aubin, F., Herve, P., Tiberghien, P., and Saas, P. 2001. Intravenous injection of apoptotic leukocytes enhances bone marrow engraftment across major histocompatibility barriers. *Blood* 98:224-230.
63. Saas, P., Bonnefoy, F., Kury-Paulin, S., Kleinclauss, F., and Perruche, S. 2007. Mediators involved in the immunomodulatory effects of apoptotic cells. *Transplantation* 84:S31-34.

Chapter 5: Apoptotic cells induce expression of non-classical soluble factors in goldfish macrophages[1]

5.1 Introduction

In mammals, inflammation-associated apoptosis triggers anti-inflammatory programs as an effective mechanism to control tissue damage and help regain homeostatic balance (1). *In vitro* studies have shown that internalization of apoptotic cells drives a decrease in pro-inflammatory antimicrobial killing mechanisms (2-4). *In vivo*, apoptotic cells decrease thioglycollate-induced leukocyte infiltration and promote the resolution of thioglycollate or LPS-driven inflammation (5, 6). Mechanisms for apoptotic cell clearance within an inflammatory site are associated with a decrease in the production of pro-inflammatory cytokines such as TNF-α, IL-6 IL-8, IL-12, IL-17, IL-23, leukotriene C4 and thromboxane B2, as well as an increase in the production of classical anti-inflammatory immune mediators such as transforming growth factor (TGF)-β and interleukin (IL)-10 (1, 7-12).

Macrophage colony-stimulating factor (CSF-1) is the primary regulator of the survival, proliferation, and differentiation of macrophages, and their precursors and is also highly involved in an array of inflammatory processes (13-15). Activation

---

[1] A portion of this chapter has been previously published in:

Rieger AM, Konowalchuk JD, Havixbeck JJ, Robbins JS, Smith MK, Lund JM, Barreda DR. 2013. A soluble form of the CSF-1 receptor contributes to the inhibition of inflammation in a teleost fish. *Dev Comp Immunol* 39: 438-46.

of tyrosine kinase activity in its cognate receptor, CSF-1R, results in the recruitment and activation of discrete signaling pathways that confer its biological activity. These events occur quickly in the presence of minute amounts of circulating CSF-1. Consequently, mechanisms have evolved to effectively control the magnitude and duration of CSF-1 biological function (13-15). CSF-1 activity is tightly controlled through receptor-mediated endocytosis, metabolic processing, and inhibition of downstream signaling, as well as through intracellular mechanisms regulating gene expression of CSF-1 and its membrane-bound receptor (CSF-1R). In addition, there is a recently identified a novel mechanism for the control of CSF-1 activity in teleosts- through the production of an inhibitory soluble form of the CSF-1 receptor (sCSF-1R) (16). Early characterization of the unique sCSF-1R mRNA transcript derived from goldfish PKM determined that it was a full-length species possessing a start codon, signal peptide, stop codon, polyadenylation signals, and a poly-A tail (16). The truncated transcript of the CSF-1 receptor encoded for the ligand binding extracellular domains of the goldfish membrane-associated CSF-1R but lacked both transmembrane and cytoplasmic signal-transducing domains (16). Soluble recombinant sCSF-1R effectively associated with its cognate ligand, CSF-1 (17). Interestingly, PKM selectively expressed sCSF-1R during the senescence phase of development, which corresponds to a defined stage of *in vitro* culture development where inhibition of macrophage proliferation and increases in apoptotic cell death is prominent (16, 18). In contrast, PKM cultures undergoing active proliferation displayed low levels of sCSF-1R expression. Addition of purified recombinant sCSF-1R to developing

PKM led to a dose-dependent decrease in macrophage proliferation; nanomolar concentrations of recombinant sCSF-1R were sufficient for this inhibition (16). Conversely, addition of antibodies generated against sCSF-1R prevented this decrease in macrophage proliferation (16). Notably, unlike mammalian macrophages, which rely heavily on other cells for production of cytokine growth factors, teleost fish macrophages are well established to produce endogenous growth factors (19-21). As such, the sCSF-1R represents an elegant mechanism for endogenous control of macrophage numbers in this lower vertebrate.

Native sCSF-1R protein was found in goldfish PKM culture supernatants, consistent with sCSF-1R mRNA expression by PKM (16). Interestingly, native sCSF-1R was also identified in goldfish serum, suggesting that this soluble protein may also play a systemic regulatory role that expands its role beyond the regulation of macrophage proliferative events within goldfish hematopoietic tissues.

As a first step to characterize the contributions of apoptotic cells to the resolution of inflammatory responses in lower vertebrates, the previous chapter examined their impact on the innate antimicrobial responses of goldfish phagocytes and compared them to those of a C57BL/6 murine system (22). I assessed the conservation of divergent pro-inflammatory and anti-inflammatory (resolution) responses at the level of the phagocyte and identified significant differences between goldfish and mice *in vivo* with regards to the level of responsiveness to zymosan and apoptotic cells, the identity of infiltrating leukocytes, their rate of infiltration, and the kinetics and strength of resulting antimicrobial responses. Interestingly, I also found that *in vitro* treatment of goldfish PKM with apoptotic

cells decreased the respiratory burst responses in both phagocytic and non-phagocytic cells (22). Further, pre-incubation of PKM with apoptotic cells prior to addition of zymosan resulted in reduced respiratory burst responses in those cells that were non-phagocytic, those that had only internalized zymosan and those that had internalized both zymosan and apoptotic cells (22). Together, these results suggested that internalization of apoptotic cells induced the production of soluble inhibitors of cell activation by goldfish primary macrophages. In this chapter, I examine the role of soluble factors in regulating macrophage responses to apoptotic cells.

The main objectives of this chapter are to (1) examine the role of soluble factors in response to apoptotic cells, (2) investigate the expression patterns of sCSF-1R, a putative mediator of responses to apoptotic cells, and (3) determine the kinetics of expression of sCSF-1R during an acute inflammatory process.

5.2 Results

5.2.1 Apoptotic cells contribute to the production of non-classical inhibitor(s) of macrophage antimicrobial responses by goldfish PKM.

I showed in the previous chapter that apoptotic cells contribute to the global reduction of macrophage ROS production in goldfish primary kidney macrophage (PKM) *in vitro* cultures (22). My results suggested the production of soluble inhibitors by PKM, which were released into culture supernatants and modulated the responses of those macrophages actively internalizing apoptotic cells as well as those of surrounding non-phagocytic PKM (22). Further, pre-incubation of PKM

with apoptotic cells for 2 hours or 4 hours prior to addition of stimulatory zymosan resulted in reduced respiratory burst responses in those cells that were non-phagocytic, those that had only internalized zymosan as well as those that had internalized both zymosan and apoptotic cells (22). As the next step to determine the identity of these soluble factor(s), apoptotic cells were generated from catfish 3B11 B cells or primary goldfish kidney leukocytes and added to PKM cultures. Trans-well experiments demonstrated the production of soluble inhibitor(s) of respiratory burst responses. Target PKM, incubated opposite 0.4 μm trans-well permeable supports containing PKM exposed to apoptotic cells, displayed a significant decrease in ROS production (Figure 5.1 A). These soluble inhibitor(s) were actively produced by PKM, which required direct contact with apoptotic cells for production; no decrease in respiratory burst activity was detected in the absence of direct contact between PKM and apoptotic cells (Figure 5.1 A). In similar experiments, supernatants collected from PKM treated with apoptotic cells for 24 hours inhibited respiratory burst responses of target PKM later assayed for ROS production (Figure 5.1 A).

Phagocytosis of apoptotic cells in mammals is well documented to result in reduced expression of classical pro-inflammatory factors like TNF-α, combined with an increase in production of anti-inflammatory factors like TGF-β and IL-10 (1, 8, 10, 12). Since goldfish macrophages displayed a similar decrease in ROS production as mammalian macrophages following internalization of apoptotic cells, I examined whether goldfish PKM displayed changes in immune gene expression similar to those previously described in mice. Using real-time PCR, I measured the

expression of interleukin (IL)-1β, IL-10, tumor necrosis factor (TNF)-α1 and 2, transforming growth factor (TGF)-β, and vascular endothelial growth factor (VEGF), as a marker of alternative macrophage activation (23, 24), following 4, 24, or 48 hours incubation with apoptotic cells or zymosan (Figure 5.1 B). Interestingly, while apoptotic cells contributed to a decrease in teleost pro-inflammatory TNF-α1 and 2 and decreased VEGF expression, no significant changes were found in the expression of the teleost anti-inflammatory cytokines IL-10 and TGF-β. I considered whether goldfish macrophages may take advantage of other novel soluble factors for inhibition of pro-inflammatory responses such as the respiratory burst.

A novel soluble form of the CSF-1 receptor (sCSF-1R) represented a viable candidate for my studies. This soluble factor was previously shown to be temporally produced by goldfish PKM during periods of *in vitro* senescence and to actively inhibit macrophage proliferation in a dose-dependent manner (16). Previous studies also identified native sCSF-1R in goldfish serum, suggesting that this soluble protein may also play a systemic regulatory role that expanded its role beyond the regulation of macrophage proliferative events within goldfish hematopoietic tissues. Examination of sCSF-1R gene expression in goldfish tissues via RT-PCR indicated wide expression of sCSF-1R beyond kidney and spleen hematopoietic tissues, consistent with this hypothesis (Figure 5.1 C). Finally, among the various roles of CSF-1 in macrophage function, there is also a direct link between CSF-1 activity and ROS production (25, 26). Thus, subsequent experiments looked to examine the potential link between this novel cytokine

receptor and the inhibition of pro-inflammatory antimicrobial responses like the respiratory burst by apoptotic cells in goldfish.

5.2.2 Apoptotic cells selectively induce expression of a soluble CSF-1R in goldfish macrophages *in vitro.*

In vitro characterization of sCSF-1R expression determined selective up-regulation of cytoplasmic mRNA expression upon exposure of PKM to apoptotic cells (Figure 5.2 A). In contrast, zymosan, a strong inducer of pro-inflammatory dectin-1 and TLR-2/6 responses (27, 28), did not induce up-regulation of sCSF-1R expression (Figure 5.2 A). Analysis was based on a novel flow-assisted fluorescent *in-situ* hybridization approach that allowed examination of gene expression in mixed PKM *in vitro* cultures, which are known to contain macrophages at different stages of differentiation (19, 29, 30). Using a differential cross-screen approach coupled to RT-PCR analysis, legumain and CD63 have been previously shown to be preferentially expressed in mature macrophage and monocyte PKM subsets, respectively (31). Coupling these results to the examination of sCSF-1R expression determined that sCSF-1R was expressed by PKM mature macrophages and not monocytes (Figure 5.2 B). In contrast, both of these PKM sub-populations expressed CSF-1R (Figure 5.2 C), consistent with prior analyses (16). This also highlights the specificity of sCSF-1R and CSF-1R probes used in these experiments. Finally, apoptotic cells were added to PKM cultures at decreasing ratios and protein expression was examined by Western blot (Figure 5.2 D). Protein

concentration of native sCSF-1R decreased with decreasing ratios of apoptotic cells.

5.2.3 Soluble CSF-1R does not affect PKM viability, phagocytosis nor production of reactive oxygen intermediates in resting macrophages.

Since sCSF-1R expression increased in PKM cultures upon exposure to apoptotic cells, I was curious if sCSF-1R may be one of the soluble factors mediating responses to these inducers of anti-inflammatory homeostatic responses. To this end, I incubated PKMs *in vitro* with increasing concentrations of recombinant sCSF-1R (rsCSF-1R) known to induce dose-dependent inhibition of PKM proliferation (16, 17). Based on the contributions of CSF-1 to macrophage survival and up-regulation of phagocytic responses (13-15), I therefore examined the impact of increasing concentrations of rsCSF-1R on PKM survival under basal and oxidative conditions, as well as on the phagocytic uptake of zymosan. Unlike the effects incurred on PKM proliferation, no changes were detected in PKM survival or phagocytosis under any of the conditions tested (Figure 5.3 A). Characterization of PKM ROS production via DHR also yielded no changes at any of the rsCSF-1R concentrations tested (Figure 5.3 B). Finally, isolation of peritoneal macrophages provided *ex vivo* examination of another distinct population of goldfish macrophages. Consistent with PKM results, *ex vivo* administration of rsCSF-1R did not affect ROS production in this tissue macrophage population (Figure 5.3 B). I then wished to assess the impact of rsCSF-1R on activated macrophages. To this end, PKMs were activated with

MAF/LPS for 24 hours +/- rsCSF-1R. Interestingly, rsCSF-1R significantly decreased ROS production in activated macrophages but had no effect on phagocytosis (Figure 5.4).

5.2.4 Apoptotic cells selectively induce up-regulation of goldfish sCSF-1R expression *in vivo*, which coincides with increased macrophage numbers at an inflammatory site.

The previous chapter showed that *in vivo* administration of apoptotic cells into the goldfish peritoneal cavity resulted in a significant increase in macrophage numbers, as defined by morphological, cytochemical, and cell surface marker analyses (22). Flow-assisted *in situ* hybridization analysis of sCSF-1R and CSF-1R using gene specific probes corroborated these results and showed selective up-regulation of sCSF-1R and CSF-1R following *in vivo* administration of apoptotic cells but not zymosan (Figure 5.5). Together, these experiments indicated that up-regulation of sCSF-1R expression *in vivo* coincided with an increase in macrophage numbers that resulted from administration of apoptotic cells into the goldfish peritoneal cavity. These findings supported those observed *in vitro* where PKM also increased sCSF-1R expression following apoptotic body but not zymosan treatment (Figure 5.2 A). Conversely, there was no correlation between increased sCSF-1R expression, G-CSFR expression, and the infiltration of neutrophils into the peritoneal cavity observed during early zymosan-induced inflammatory responses. Gene expression analysis indicated selective up-regulation of G-CSFR expression in peritoneal cells from fish injected with zymosan (Figure

5.5). This up-regulation of G-CSFR expression paralleled the increase in neutrophil infiltration observed using morphological cellular analysis and Sudan Black cytochemical staining (22). However, peritoneal cells from fish injected with zymosan had a significant reduction in expression of sCSF-1R, in contrast to those from fish treated with apoptotic cells (Figure 5.5). Administration of apoptotic cells 4 hours prior to zymosan stimulation (-4h group) led to an intermediate expression phenotype similar to that of PBS-treated controls (Figure 5.5).

5.2.5 Expression of sCSF-1R throughout a time-course of acute inflammation mimics the presence of apoptotic cells.

Zymosan has been previously shown to induce an acute, self-resolving peritonitis that generally resolves within 72 hours. These kinetics, however, have not been described in fish so I measured a range of inflammatory responses within this 72 hour time period. I found that cellular infiltration rose steadily, peaking at 18 hours. Counts then dropped steadily from 24- 72 hours (Figure 5.6 A). The kinetics of cellular infiltration matched those of ROS responses. When CSF-1 expression was measured, I found responses peaked at 24 hours, dropping below basal levels at 72 hours. When apoptotic cell death was measured in this same window, I found that apoptosis levels were significantly increased at 72 hours. This was the same time point at which we found significant increases in sCSF-1R expression. When this time course was carried out further, it was found that sCSF-1R levels remained high until 10 days post-injection, then returned to basal levels (Figure 5.6 B). This data suggests that, similar to expression data found with

injected apoptotic cells, the generation of apoptotic cells *in vivo* coincides with sCSF-1R expression increases.

Over this same time period, I measured cytokines known to be involved in cellular recruitment, induction of inflammation and resolution of inflammation. I found that CXCL-8 (a chemokine involved in neutrophil recruitment) levels were high between 8 and 12 hours (Figure 5.7). This time period of expression immediately precedes the detection of neutrophil infiltration, occurring primarily at 18 hours. Two important pro-inflammatory cytokines, TNF-α 2 and IL-1β 1, also show high levels of expression early within the acute inflammatory period, dropping to basal levels between 24 and 72 hours. While no increases in IL-10, an important anti-inflammatory cytokine in mammalian systems, was detected late in the inflammatory response, a significant increase was detected at 8 hours. This likely is to control early inflammatory monocyte responses, as has been suggested in murine sepsis models (32). Finally, this data suggests that, like in mammals, zymosan peritonitis resolves within 72 hours in goldfish as well.

5.3 Discussion

Recent studies point to the conservation of the CSF-1 system between teleost fish and mammals (13, 17, 33-38). Both CSF-1 and/or its cognate receptor, CSF-1R, have been identified in a range of species and display the classic characteristics associated with CSF-1 activity. In mammals, this cytokine regulatory node is responsible for the control of macrophage numbers and contributes to the modulation of their state of activation and function. However, the breadth of its

contributions also expands into bone metabolism, atherogenesis, lipoprotein clearance, and female reproduction [(13) and references therein]. In teleost fish, the CSF-1 / CSF-1R axis has been studied primarily in the context of macrophage development and function, but is also known to be important for the development of osteoclasts and the establishment of adult pigment pattern expressed by zebrafish (13, 34-36, 39-41). The current chapter expands on the contributions of this cytokine regulatory axis to teleost biology, through characterization of the impact that sCSF-1R has on the inhibition of leukocyte inflammatory processes. Two key findings from this study present the first evidence for the regulation of teleost fish inflammation by sCSF-1R. Firstly, sCSF-1R expression was strongly induced in response to apoptotic cells. Secondly, rsCSF-1R significantly decreased ROS production in activated macrophages.

Based on the effective association of rsCSF-1R with goldfish rCSF-1, and the capacity of this soluble receptor to abrogate recombinant and native CSF-1 activity *in vitro*, it appears that this soluble receptor may inhibit PKM proliferation through competitive inhibition of CSF-1 binding to the membrane-associated CSF-1R (16, 17, 20). Notably, the ability of rsCSF-1R to regulate PKM responses *in vitro* beyond those associated with macrophage proliferation highlights the potential complexity of the CSF-1 / CSF-1R regulatory node even in this lower vertebrate. Soluble CSF-1R directly impacts macrophage respiratory burst antimicrobial responses in fish *in vitro*. The *in vivo* effects of sCSF-1R will be discussed in the next chapter.

Overall, this chapter expands our current understanding of the CSF-1 system. I show here that the contributions of this cytokine regulatory node to teleost fish biology are beyond those in macrophage hematopoiesis and function, osteoclast development, and the establishment of adult pigment patterns. A novel player, the soluble form of the CSF-1 receptor, is induced upon exposure to apoptotic cells and increases late in inflammatory processes. Early indications suggest that it may also be involved in regulating inflammatory processes, which will be examined more fully in the next chapter.

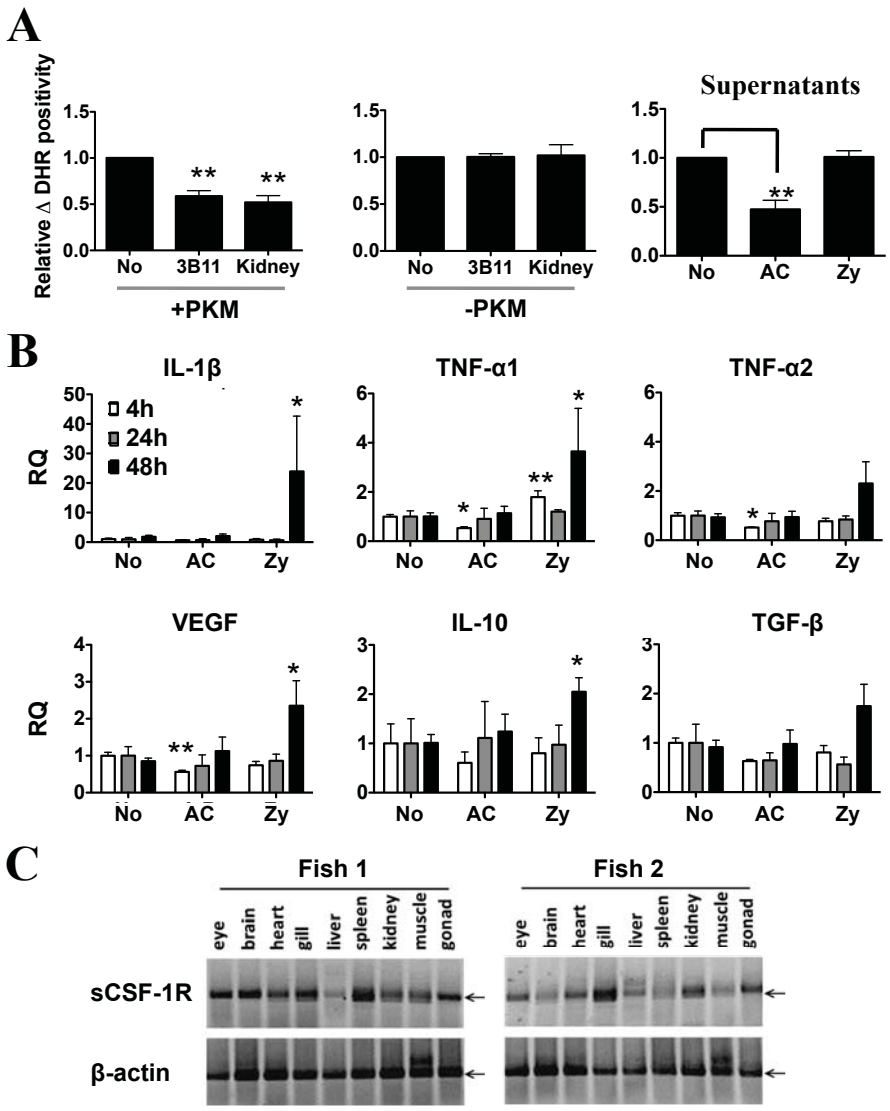

Figure 5.1. Soluble factors regulate macrophage responses to apoptotic cells.

(**A**) Primary kidney macrophage (PKM) cultures were incubated in a transwell system. Within the 0.4 μm transwell, apoptotic cells derived from 3B11 catfish B cell line or kidney leukocytes were cultured in the presence (left) or absence (right) of PKMs. Target PKMs across the transwell membrane were harvested 2 hours later and ROS production was assayed via DHR staining. For supernatants, PKMs were incubated with indicated stimuli for 24 hours. Supernatants were harvested, filter sterilized, and added to fresh PKM cultures at 50% of the culture volume. PKM ROS responses were assessed 2 hours later. (**B**) PKM cultures were incubated alone (No), with apoptotic cells (AC) or with zymosan (Zy) for the indicated time points. Cells were then harvested, RNA was extracted and converted to cDNA and levels of the indicated cytokines were assayed via Q-PCR. Expression of sCSF-1R was assessed by reverse transcriptase PCR (**C**). n=3 for A and B; * $p<0.05$; ** $p<0.01$ (One-way ANOVA; Tukey's post-hoc); error bars show SEM.

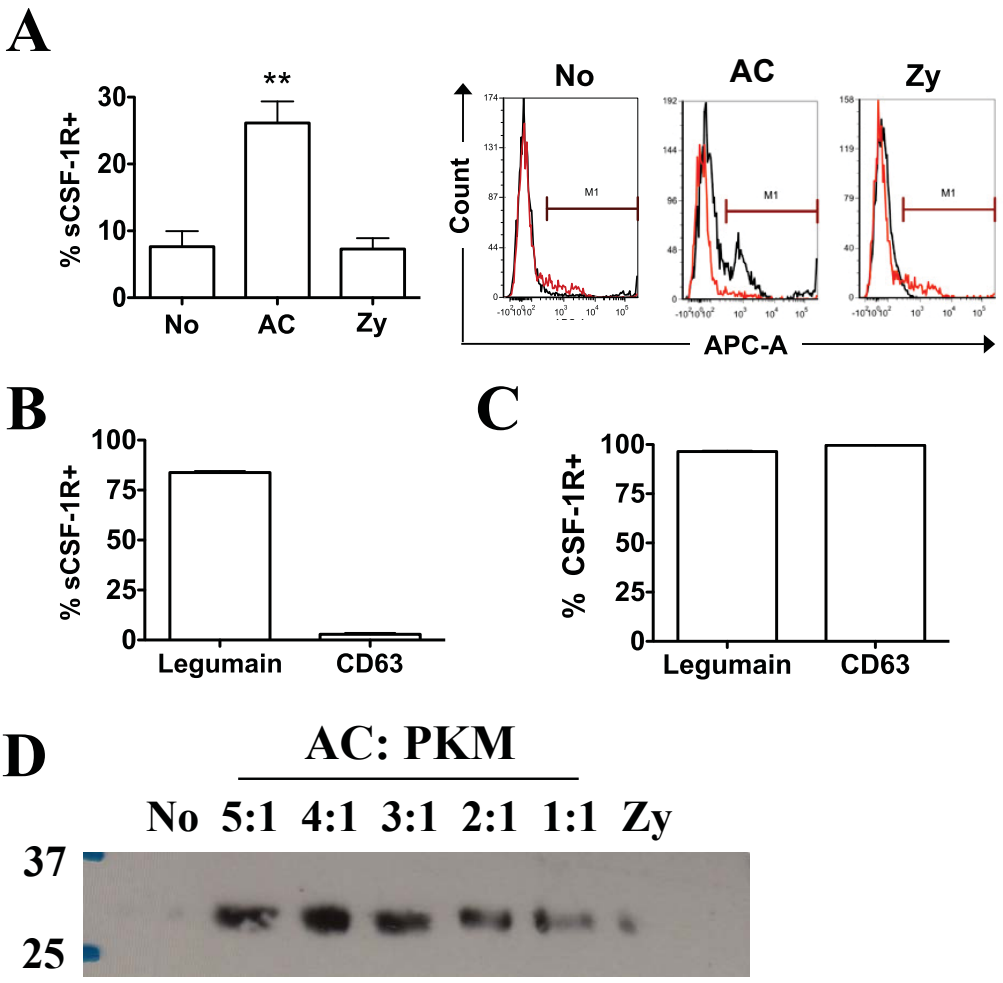

Figure 5.2. Characterization of soluble CSF-1R expression in goldfish primary kidney macrophages.

(**A**) PKM cells were incubated alone (No), with apoptotic cells (AC) or zymosan (Zy) for 2 hours. Levels of soluble CSF-1R were measured using a flow cytometry-based fluorescent *in situ* hybridization approach. Relative fluorescence of sense probe (negative control; red line) and anti-sense probe (experimental; black line). "M1" denotes positive cellular events. (**B-C**) PKM cells were cultured with apoptotic bodies for 2 hours and expression of sCSF-1R **(B)** or CSF-1R **(C)** were examined in the context of a monocyte (CD63) and a mature macrophage (legumain) PKM marker, as described in A. For A-C n=3; ** $p<0.01$ (One-way ANOVA; Tukey's post-hoc); error bars show SEM. (**D**) PKM were incubated with decreasing concentrations of apoptotic cells or zymosan for 4 hours. Supernatants were then collected and run on a Western blot.

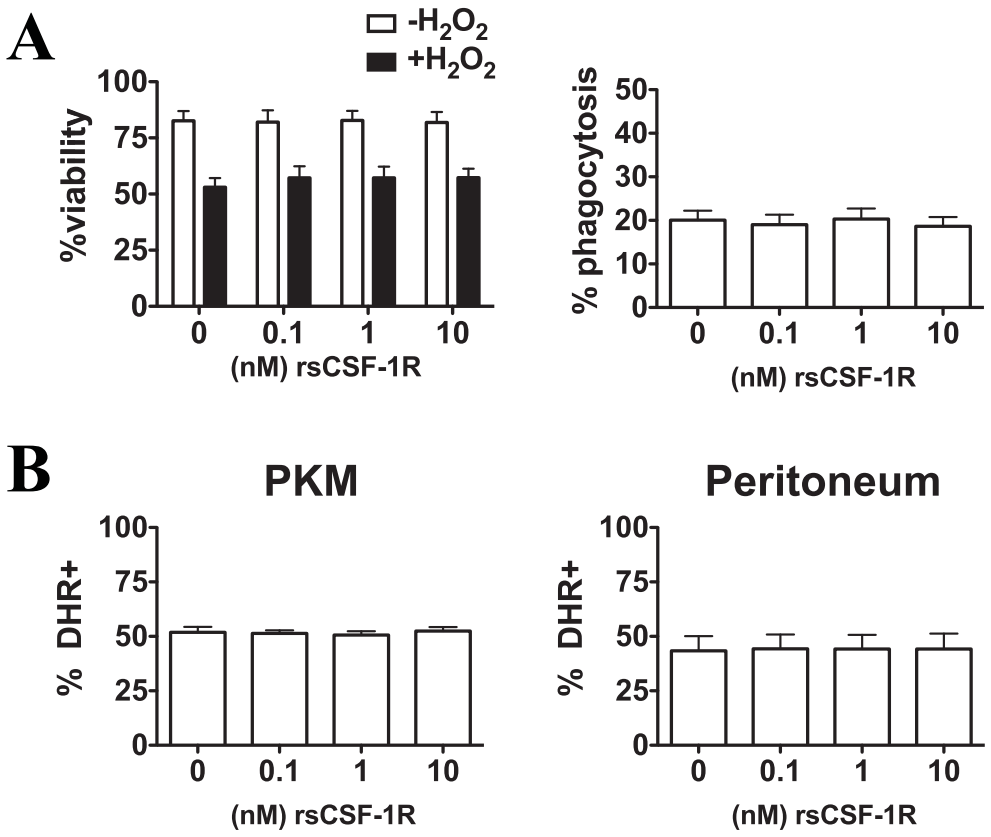

Figure 5.3. Impact of recombinant sCSF-1R on resting goldfish primary macrophages.

(**A**) To determine the impact of rsCSF-1R on various aspects of macrophage function, PKM cultures were incubated with increasing concentrations of rsCSF-1R for 24 hours. After this time point, survivability under basal and oxidative conditions, and phagocytosis were examined. PKM viability was assessed by Annexin V/ propidium iodide staining, and phagocytosis was examined using fluorescent zymosan. (**B**) To determine the impact of rsCSF-1R on the production of reactive oxygen species, goldfish macrophages derived from PKM *in vitro* cultures or the peritoneal cavity were incubated with increasing concentrations of sCSF-1R (24 hours for PKM cultures; 2 hours for *ex vivo* peritoneal macrophages). Following incubation, ROS production was measured via DHR staining. n=9; error bars show SEM.

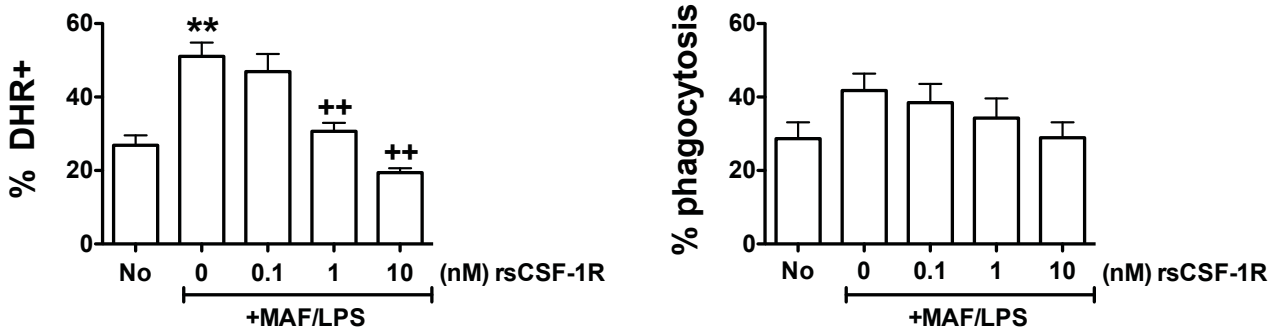

Figure 5.4. Impact of recombinant sCSF-1R on activated goldfish primary macrophages.

To determine the impact of rsCSF-1R on the production of reactive oxygen species, goldfish macrophages derived from PKM *in vitro* cultures were incubated with increasing concentrations of sCSF-1R for 24 hours in the presence of MAF/LPS. Following incubation, ROS production was measured via DHR staining and phagocytosis was examined using fluorescent zymosan. n=6; ** $p<0.01$ compared to No; ++ p,0.01compared to 0 (One-way ANOVA; Tukey's post-hoc); error bars show SEM.

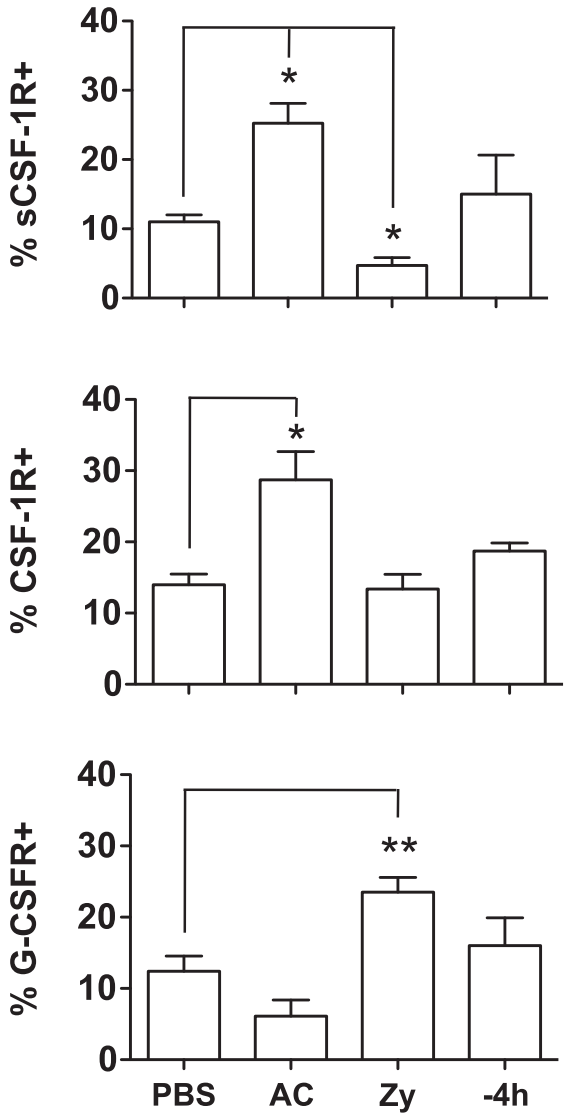

Figure 5.5. Expression of soluble CSF-1R during an inflammatory response *in vivo*.

Goldfish were injected intraperitoneally with 1x PBS, apoptotic cells (AC), zymosan (Zy) or apoptotic bodies and zymosan, or with apoptotic bodies injected 4 hours prior to zymosan administration (-4h). Goldfish were lavaged 24 hours later. sCSF-1R, CSF-1R, and G-CSFR expression was examined in peritoneal lavage cells using a flow cytometry-based fluorescent *in situ* hybridization approach. n=4; * $p<0.05$; ** $p<0.01$ (One-way ANOVA; Tukey's post-hoc); error bars show SEM.

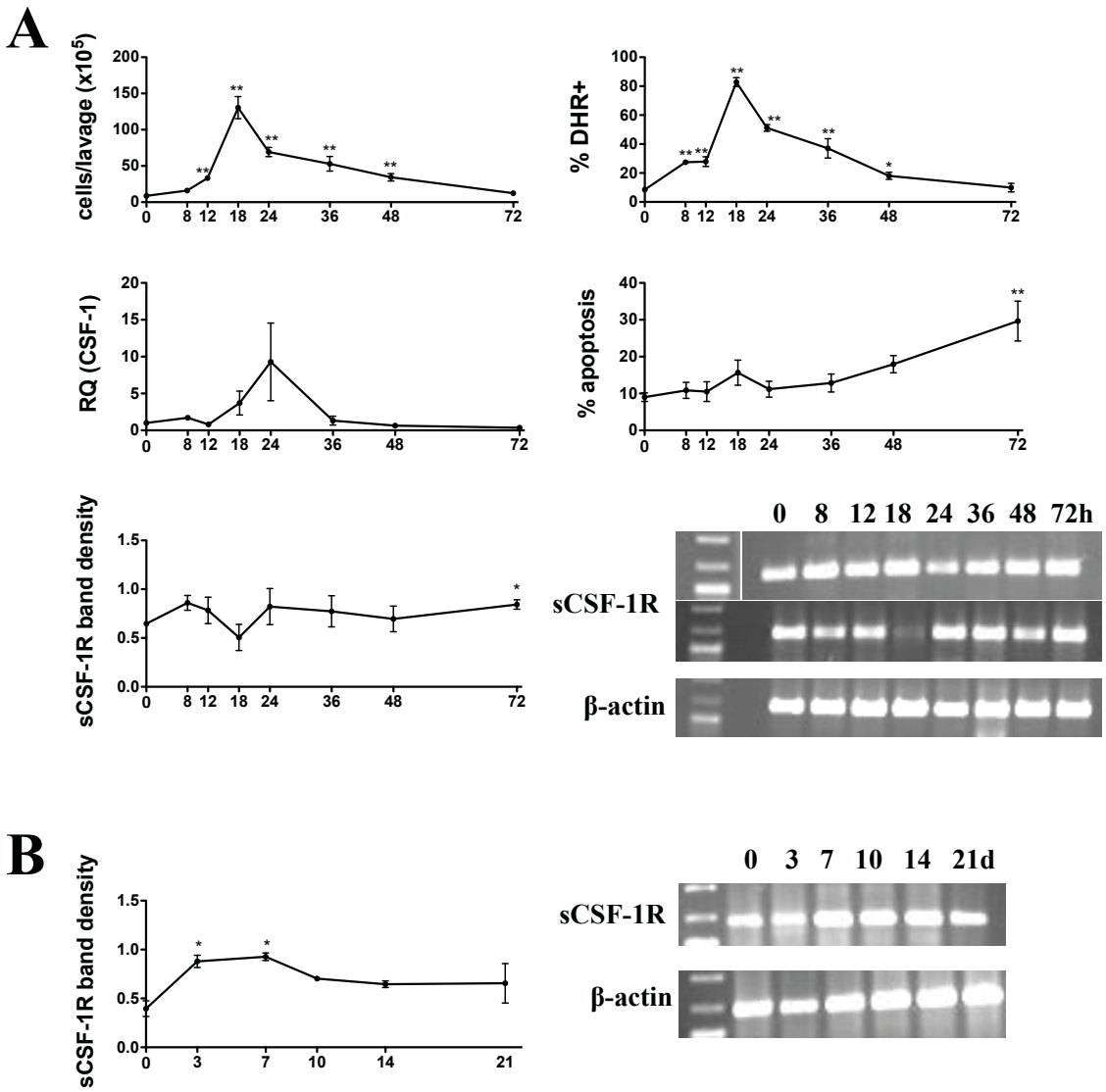

Figure 5.6. Expression of soluble CSF-1R *in vivo* matches increases in apoptotic cell death.

(A) Goldfish were injected intraperitoneally with zymosan and cells were harvested at the indicated time points. At each time point, cells were counted to determine infiltration. Viability was assessed by AnnexinV/PI staining. ROS production was measured with DHR. RNA was harvested from the remaining cells, converted into cDNA and used to profile CSF-1 and sCSF-1R expression. (B) Goldfish were injected intraperitoneally with zymosan and cells were harvested at the indicated time points. At each time point, RNA was harvested from the cells, converted into cDNA and used to profile sCSF-1R expression. For all, n=5; * $p<0.05$; ** $p<0.01$ (One-way ANOVA; Tukey's post-hoc); error bars show SEM.

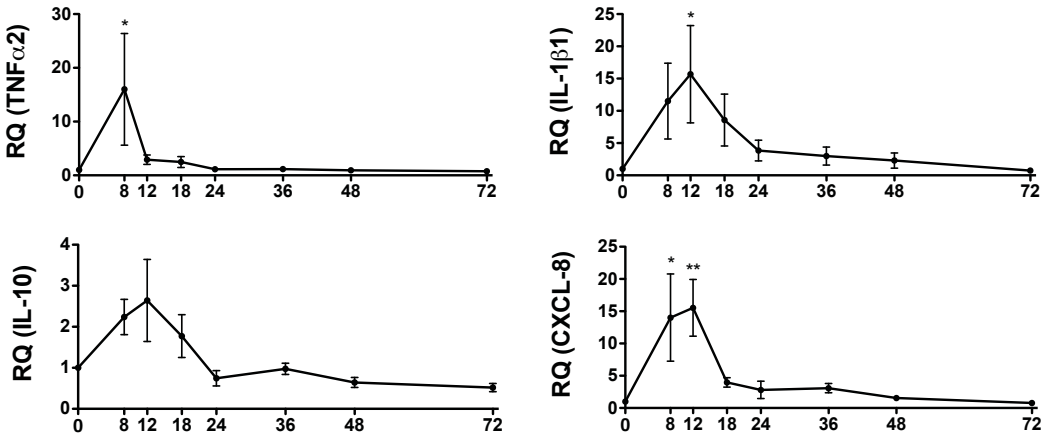

Figure 5.7. Cytokine gene expression kinetics during acute zymosan peritonitis.

Goldfish were injected intraperitoneally with zymosan and cells were harvested at the indicated time points. RNA was harvested from the harvested cells, converted into cDNA. Gene expression was determined by quantitative PCR. n=5; * $p<0.05$; ** $p<0.01$ (One-way ANOVA; Tukey's post-hoc); error bars show SEM.

5.4 References

1. Soehnlein, O., and Lindbom, L. 2010. Phagocyte partnership during the onset and resolution of inflammation. *Nature Reviews Immunology* 10:427-439.
2. Johann, A.M., von Knethen, A., Lindemann, D., and Brune, B. 2006. Recognition of apoptotic cells by macrophages activates the peroxisome proliferator-activated receptor-gamma and attenuates the oxidative burst. *Cell Death Differ* 13:1533-1540.
3. Reiter, I., Krammer, B., and Schwamberger, G. 1999. Cutting edge: differential effect of apoptotic versus necrotic tumor cells on macrophage antitumor activities. *J Immunol* 163:1730-1732.
4. Zamboni, D.S., and Rabinovitch, M. 2003. Nitric oxide partially controls Coxiella burnetii phase II infection in mouse primary macrophages. *Infect Immun* 71:1225-1233.
5. Huynh, M.L., Fadok, V.A., and Henson, P.M. 2002. Phosphatidylserine-dependent ingestion of apoptotic cells promotes TGF-beta1 secretion and the resolution of inflammation. *J Clin Invest* 109:41-50.
6. Potter, P.K., Cortes-Hernandez, J., Quartier, P., Botto, M., and Walport, M.J. 2003. Lupus-prone mice have an abnormal response to thioglycolate and an impaired clearance of apoptotic cells. *J Immunol* 170:3223-3232.
7. Bellingan, G.J., Caldwell, H., Howie, S.E., Dransfield, I., and Haslett, C. 1996. In vivo fate of the inflammatory macrophage during the resolution of inflammation: inflammatory macrophages do not die locally, but emigrate to the draining lymph nodes. *J Immunol* 157:2577-2585.
8. Fadok, V.A., Bratton, D.L., Konowal, A., Freed, P.W., Westcott, J.Y., and Henson, P.M. 1998. Macrophages that have ingested apoptotic cells in vitro inhibit proinflammatory cytokine production through autocrine/paracrine mechanisms involving TGF-beta, PGE2, and PAF. *J Clin Invest* 101:890-898.
9. Kim, S., Elkon, K.B., and Ma, X. 2004. Transcriptional suppression of interleukin-12 gene expression following phagocytosis of apoptotic cells. *Immunity* 21:643-653.
10. Maderna, P., and Godson, C. 2003. Phagocytosis of apoptotic cells and the resolution of inflammation. *Biochim Biophys Acta* 1639:141-151.
11. Stark, M.A., Huo, Y., Burcin, T.L., Morris, M.A., Olson, T.S., and Ley, K. 2005. Phagocytosis of apoptotic neutrophils regulates granulopoiesis via IL-23 and IL-17. *Immunity* 22:285-294.
12. Weigert, A., Jennewein, C., and Brune, B. 2009. The liaison between apoptotic cells and macrophages--the end programs the beginning. *Biol Chem* 390:379-390.
13. Barreda, D.R., Hanington, P.C., and Belosevic, M. 2004. Regulation of myeloid development and function by colony stimulating factors. *Dev Comp Immunol* 28:509-554.

14. Hume, D.A., Pavli, P., Donahue, R.E., and Fidler, I.J. 1988. The effect of human recombinant macrophage colony-stimulating factor (CSF-1) on the murine mononuclear phagocyte system in vivo. *J Immunol* 141:3405-3409.
15. Stanley, E.R., Guilbert, L.J., Tushinski, R.J., and Bartelmez, S.H. 1983. CSF-1--a mononuclear phagocyte lineage-specific hemopoietic growth factor. *J Cell Biochem* 21:151-159.
16. Barreda, D.R., Hanington, P.C., Stafford, J.L., and Belosevic, M. 2005. A novel soluble form of the CSF-1 receptor inhibits proliferation of self-renewing macrophages of goldfish (Carassius auratus L.). *Dev Comp Immunol* 29:879-894.
17. Hanington, P.C., Wang, T., Secombes, C.J., and Belosevic, M. 2007. Growth factors of lower vertebrates: characterization of goldfish (Carassius auratus L.) macrophage colony-stimulating factor-1. *J Biol Chem* 282:31865-31872.
18. Barreda, D.R., and Belosevic, M. 2001. Characterisation of growth enhancing factor production in different phases of *in vitro* fish macrophage development. *Fish and Shellfish Immunology* 11:169-185.
19. Barreda, D.R., Neumann, N.F., and Belosevic, M. 2000. Flow cytometric analysis of PKH26-labeled goldfish kidney-derived macrophages. *Dev Comp Immunol* 24:395-406.
20. Hanington, P.C., Hitchen, S.J., Beamish, L.A., and Belosevic, M. 2009. Macrophage colony stimulating factor (CSF-1) is a central growth factor of goldfish macrophages. *Fish Shellfish Immunol* 26:1-9.
21. Neumann, N.F., Barreda, D.R., and Belosevic, M. 1998. Production of a macrophage growth factor(s) by a goldfish macrophage cell line and macrophages derived from goldfish kidney leukocytes. *Developmental and Comparative Immunology* 22:417-432.
22. Rieger, A.M., Konowalchuk, J.D., Grayfer, L., Katzenback, B.A., Havixbeck, J.J., Kiemele, M.D., Belosevic, M., and Barreda, D.R. 2012. Fish and mammalian phagocytes differentially regulate pro-inflammatory and homeostatic responses in vivo. *PLoS ONE* - Accepted [manuscript number: PONE-D-12-21984].
23. Biswas, S.K., and Mantovani, A. 2010. Macrophage plasticity and interaction with lymphocyte subsets: cancer as a paradigm. *Nat Immunol* 11:889-896.
24. Geissmann, F., Manz, M.G., Jung, S., Sieweke, M.H., Merad, M., and Ley, K. 2010. Development of monocytes, macrophages, and dendritic cells. *Science* 327:656-661.
25. Choi, H.K., Kim, T.H., Jhon, G.J., and Lee, S.Y. 2011. Reactive oxygen species regulate M-CSF-induced monocyte/macrophage proliferation through SHP1 oxidation. *Cell Signal* 23:1633-1639.
26. Gueller, S., Goodridge, H.S., Niebuhr, B., Xing, H., Koren-Michowitz, M., Serve, H., Underhill, D.M., Brandts, C.H., and Koeffler, H.P. 2010. Adaptor protein Lnk inhibits c-Fms-mediated macrophage function. *J Leukoc Biol* 88:699-706.

27. Goodridge, H.S., Simmons, R.M., and Underhill, D.M. 2007. Dectin-1 stimulation by Candida albicans yeast or zymosan triggers NFAT activation in macrophages and dendritic cells. *J Immunol* 178:3107-3115.
28. Underhill, D.M. 2003. Macrophage recognition of zymosan particles. *J Endotoxin Res* 9:176-180.
29. Belosevic, M., Hanington, P.C., and Barreda, D.R. 2006. Development of goldfish macrophages in vitro. *Fish Shellfish Immunol* 20:152-171.
30. Neumann, N.F., Barreda, D.R., and Belosevic, M. 2000. Generation and functional analysis of distinct macrophage sub-populations from goldfish (Carassius auratus L.) kidney leukocyte cultures. *Fish Shellfish Immunol* 10:1-20.
31. Barreda, D.R., Hanington, P.C., Walsh, C.K., Wong, P., and Belosevic, M. 2004. Differentially expressed genes that encode potential markers of goldfish macrophage development in vitro. *Dev Comp Immunol* 28:727-746.
32. Latifi, S.Q., O'Riordan, M.A., and Levine, A.D. 2002. Interleukin-10 controls the onset of irreversible septic shock. *Infect Immun* 70:4441-4446.
33. Wang, T., Hanington, P.C., Belosevic, M., and Secombes, C.J. 2008. Two macrophage colony-stimulating factor genes exist in fish that differ in gene organization and are differentially expressed. *J Immunol* 181:3310-3322.
34. Chatani, M., Takano, Y., and Kudo, A. 2011. Osteoclasts in bone modeling, as revealed by in vivo imaging, are essential for organogenesis in fish. *Dev Biol* 360:96-109.
35. Crowhurst, M.O., Layton, J.E., and Lieschke, G.J. 2002. Developmental biology of zebrafish myeloid cells. *Int J Dev Biol* 46:483-492.
36. Herbomel, P., Thisse, B., and Thisse, C. 2001. Zebrafish early macrophages colonize cephalic mesenchyme and developing brain, retina, and epidermis through a M-CSF receptor-dependent invasive process. *Dev Biol* 238:274-288.
37. Honda, T., Nishizawa, T., Uenobe, M., Kohchi, C., Kuroda, A., Ototake, M., Nakanishi, T., Yokomizo, Y., Takahashi, Y., Inagawa, H., et al. 2005. Molecular cloning and expression analysis of a macrophage-colony stimulating factor receptor-like gene from rainbow trout, Oncorhynchus mykiss. *Mol Immunol* 42:1-8.
38. Williams, H., Brenner, S., and Venkatesh, B. 2002. Identification and analysis of additional copies of the platelet-derived growth factor receptor and colony stimulating factor 1 receptor genes in fugu. *Gene* 295:255-264.
39. Parichy, D.M., Ransom, D.G., Paw, B., Zon, L.I., and Johnson, S.L. 2000. An orthologue of the kit-related gene fms is required for development of neural crest-derived xanthophores and a subpopulation of adult melanocytes in the zebrafish, Danio rerio. *Development* 127:3031-3044.
40. Parichy, D.M., and Turner, J.M. 2003. Temporal and cellular requirements for Fms signaling during zebrafish adult pigment pattern development. *Development* 130:817-833.
41. Quigley, I.K., Manuel, J.L., Roberts, R.A., Nuckels, R.J., Herrington, E.R., MacDonald, E.L., and Parichy, D.M. 2005. Evolutionary diversification of

pigment pattern in Danio fishes: differential fms dependence and stripe loss in D. albolineatus. *Development* 132:89-104.

Chapter 6: The soluble form of the CSF-1 receptor contributes to the inhibition of inflammation in a teleost fish[1]

6.1 Introduction

Macrophage colony stimulating factor-1 (M-CSF or CSF-1) is the main regulator of the proliferation, differentiation and survival of macrophages (1). It also regulates key aspects of macrophage function including microbicidal activity (2, 3), cytokine (4, 5) and chemokine (6, 7) production, chemotaxis (8, 9) and phagocytosis (10, 11), which is a testament to its importance in the regulation of immunity. However, CSF-1 has also been linked to numerous pathological conditions, including but not limited to, allograft and xenograft rejection, cancer, autoimmune disorders, atherosclerosis, and obesity (4, 12-16). As such, tight regulation of the CSF-1 system is critical for proper balance between the beneficial and the potential deleterious outcomes.

CSF-1 exerts its biological effects in nanomolar concentrations and several mechanisms have evolved to regulate its actions, including receptor-mediated endocytosis, metabolic processing, and the inhibition of downstream signaling (1). CSF-1 activity is also regulated through intracellular modulation of the gene

---

[1] A version of this chapter has been previously published:

Rieger AM, Konowalchuk JD, Havixbeck JJ, Robbins JS, Smith MK, Lund JM, Barreda DR. 2013. A soluble form of the CSF-1 receptor contributes to the inhibition of inflammation in a teleost fish. *Dev Comp Immunol* 39: 438-46.

expression of both CSF-1 and its cognate receptor CSF-1 receptor (CSF-1R) (1). Most recently, a unique mechanism for the regulation of CSF-1 activity in teleost fish was identified- through the production of a soluble form of CSF-1 receptor (sCSF-1R) (17). Soluble CSF-1R decreases macrophage proliferation in a dose-dependent manner and was originally identified among primary macrophage cultures with high levels of apoptosis (17, 18). The native protein was detected in goldfish serum (17), which suggested that this protein might also play a role in systemic regulation, in addition to its role in regulating proliferation within the hematopoietic compartment.

In the previous chapter, I showed that the expression of sCSF-1R was linked to the presence of apoptotic cells. Further, sCSF-1R significantly decreased ROS responses in activated macrophages, suggesting a potential role in inflammatory control. With this in mind, in this chapter I examine the role of sCSF-1R in the regulation of teleost macrophage inflammatory responses. The main objectives of this chapter were to detail the role of sCSF-1R in regulating inflammatory processes, notably (1) cellular infiltration and chemotaxis, (2) production of reactive intermediates, (3) phagocytic capacity, and (4) production of inflammatory mediators.

6.2 Results

6.2.1 Soluble CSF-1R contributes to amelioration of goldfish leukocyte infiltration responses *in vivo*.

To determine if sCSF-1R was affecting inflammatory processes *in vivo*, I injected goldfish intra-peritoneally with both zymosan and increasing concentrations of rsCSF-1R (Figure 6.2 A). As a control, fish were also injected with zymosan with recombinant erythropoietin receptor; this recombinant protein had no effects on inflammatory processes, suggesting that the effects of recombinant sCSF-1R are due to the presence of sCSF-1R protein and not simply because a protein was added (Figure 6.1). After 24 hours, leukocytes were harvested by peritoneal lavage and counted. Intra-peritoneal administration of zymosan resulted in significant up-regulation of inflammatory ROS production by peritoneal leukocytes compared to those derived from saline-treated fish (Figure 6.2 A). Consistent with the effects observed upon co-injection of apoptotic bodies (19), co-administration with rsCSF-1R resulted in significant inhibition of zymosan-induced ROS production; a dose-dependent effect was observed in response to increasing concentrations of rsCSF-1R (Figure 6.2 A). Parallel examination of leukocyte infiltration into the peritoneal cavity further pointed to an anti-inflammatory effect for rsCSF-1R against zymosan-induced pro-inflammatory responses. The total number of infiltrating leukocytes decreased in a dose-dependent manner compared to zymosan-stimulated controls upon addition of increasing doses of rsCSF-1R (Figure 6.2 B). At a concentration of 800 ng rsCSF-1R, leukocyte numbers in the peritoneal cavity were equivalent to those of saline-treated controls. To examine the impact on individual neutrophil, lymphocyte, and monocyte/macrophage sub-populations, peritoneal exudates were characterized as previously described based on morphological, cytochemical, and flow cytometric

characteristics (19). Administration of rsCSF-1R decreased the levels of all three leukocyte subsets. However, inhibition of leukocyte infiltration was most notable for the neutrophilic subset, as evidenced by the progressive dose-dependent decrease associated with increasing concentrations of rsCSF-1R (Figure 6.2 B). Further support for the potential contributions of rsCSF-1R to the inhibition of goldfish inflammation came from evaluation of its impact on the proportions of individual cellular subsets within the peritoneal cavity of zymosan-stimulated fish. The percentage of neutrophils decreased dramatically in this zymosan-induced peritonitis model following co-administration of rsCSF-1R; a progressive dose-dependent decrease was observed in response to increasing concentrations of rsCSF-1R (Figure 6.2 C). This decrease in the proportion of neutrophils was accompanied by a parallel increase in the proportion of monocytes/macrophage and lymphocyte sub-populations within the peritoneal cavity that was most marked at 800 ng rsCSF-1R.

6.2.2 Soluble CSF-1 receptor decreases pro-inflammatory phagocytic responses similarly to apoptotic cells.

Phagocytosis of apoptotic cells is known to be a potent down-regulator of inflammatory processes. I have shown in Chapter 4 that, in mammals, both macrophages and neutrophils actively internalize apoptotic cells, leading to reduction in the production of inflammatory antimicrobial products (20). In teleost fish, however, neutrophils are not capable of internalizing apoptotic cells, leaving macrophages as the main mediators of anti-inflammatory responses. As such, I

wished to investigate further the macrophage-specific mechanisms by which apoptotic cells decrease inflammation in teleost fish. The previous data pointed to a potential key role of soluble CSF-1R in regulating cellular infiltration and inflammatory ROS production (21). I was curious, then, if sCSF-1R and apoptotic cells were intrinsically linked and able to similarly down-regulate inflammatory processes. I focused my studies on phagocytosis and the subsequent downstream processes, as these are known to be integral to both the initiation and resolution of inflammation. I found that both sCSF-1R and apoptotic cells significantly decreased the phagocytic responses to basal levels (Figure 6.3 A, left panel). These cells also had significant reduction in the production of reactive oxygen species, an antimicrobial mechanism downstream of phagocytosis (Figure 6.3 A, right panel). Interestingly, sCSF-1R seemed to have a greater impact on ROS production than apoptotic cells. When the killing capacity of these cells was assessed using a gentamicin protection assay, I found that apoptotic cells and rsCSF-1R significantly decreased zymosan-induced increases in killing capacity (Figure 6.3 C). As such, sCSF-1R appears to play an integral role in regulating antimicrobial responses of goldfish macrophages.

It has been suggested that apoptotic cells drive macrophage phenotypes from a classically activated, inflammatory macrophage (M1) towards an alternatively activated macrophage (M2) (22, 23). The phenotypic difference seems to lie largely in the balance between nitric oxide (M1) and arginase (M2) production (24, 25). These macrophage phenotypes have also been described in teleost fish, suggesting that they are highly conserved (26, 27). Since I appear to be getting a classical-type

macrophage phenotype in the zymosan peritonitis model, I investigated if either sCSF-1R or apoptotic cells were capable of driving macrophages towards an alternatively activated phenotype, similar to mammalian macrophages. While I found a significant increase in iNOS expression (both A and B) with zymosan, sCSF-1R significantly decreased iNOS B, but not iNOS A (Figure 6.4). Apoptotic cells had no significant impact on iNOS expression, though it tended to be lower (Figure 6.4). Interestingly, though sCSF-1R had a greater impact on iNOS, it had no effect on arginase expression, suggesting that sCSF-1R is impacting inflammatory antimicrobial mechanisms but may not be driving macrophages toward the alternatively activated phenotype. In contrast, apoptotic cells significantly increased arginase activity in spite of a limited effect on iNOS expression. It is possible that, after 24-hour exposure to apoptotic cells, I may be at the tipping point between classical and alternative macrophage activation. A greater time of exposure may push the responses towards a true alternatively activated macrophage phenotype.

6.2.3 Cytokine expression is differentially affected by sCSF-1R and apoptotic cells.

Since sCSF-1R and apoptotic cells both exert strong anti-inflammatory effects on phagocytosis and ROS production, I wondered if this control extended to cytokine production, another downstream process that is integral to the development and maintenance of inflammation. To this end, goldfish were injected with zymosan in the presence or absence of either sCSF-1R or apoptotic cells.

Peritoneal cells were harvested by lavage 24 hours later and RNA was extracted from the cells. Cytokine levels were then assayed by Q-PCR, using a panel of cytokines known to be important in goldfish inflammatory processes (28-31). Overall, sCSF-1R has a greater impact on inflammatory cytokine production than apoptotic cells, causing a significant decrease in the expression of TNF-α 2, IL-1β 1 and 2, IFNγ and IFNγrel (IFNγ-related), IL12p35 and CSF-1 (Figure 6.5). However, both sCSF-1R and apoptotic cells significantly decreased TNF-α 2, IFNγrel and IL-12p35, suggesting that these cytokines may be the primary targets for reducing inflammation, making them likely critical to inflammatory processes in goldfish.

Macrophages are important to both the induction and resolution of inflammation (32, 33). It has been previously shown that phagocytosis of apoptotic cells results in the production of an array of anti-inflammatory soluble factors (32-35). As such, I wanted to test the impact of sCSF-1R and apoptotic cells would have on the production of goldfish anti-inflammatory cytokines (36, 37). Unlike mammalian studies, I found little impact on the expression on TGF-β or vascular endothelial growth factor (VEGF), an important mediator of wound healing, with either sCSF-1R or apoptotic cells (Figure 6.6). However, I did find a significant increase in IL-10 expression with apoptotic cells, but not sCSF-1R, suggesting that sCSF-1R may be important in down-regulating inflammatory processes but may not directly activate anti-inflammatory mechanisms.

It has been previously reported that suppressor of cytokine signaling 3 (SOCS3) is upregulated following exposure to apoptotic cells, leading to a decrease

in inflammatory cytokines and chemokines (38). Interestingly, I found no increases with either sCSF-1R or apoptotic cells, suggesting that the observed decreases in pro-inflammatory cytokine expression in goldfish may not be regulated by SOCS3 (Figure 6.6).

6.2.4 Soluble CSF-1R affects cytokine expression in a dose-dependent manner.

Figures 6.2 and 5.4 show that sCSF-1R has dose-dependent effects on both cellular infiltration and ROS production (21). I wondered if there were also dose-dependent effects on cytokine production. To examine this, I injected goldfish with zymosan and increasing concentrations of sCSF-1R or apoptotic cells. Peritoneal cells were harvested by lavage and cytokine expression was measured from the extracted RNA. I chose to focus these studies on TNF-α 2, CSF-1, SOCS3 and IL-10 since these cytokines were differentially affected by both sCSF-1R and apoptotic cells. I found that TNF-α 2 was significantly decreased at all concentrations of sCSF-1R, suggesting that expression of TNF-α 2 may be tightly linked to the CSF-1 system (Figure 6.7). For CSF-1 and SOCS3, I found that expression tended to be increased slightly with decreasing concentrations of sCSF-1R, though this was not significant (Figure 6.7). Further, SOCS3 never significantly rose above basal levels, again suggesting that this may not be the primary mediator for decreasing the observed pro-inflammatory cytokine expression in this system. The most dramatic effect of sCSF-1R concentration was seen on IL-10 expression, where levels significantly increased with decreasing

sCSF-1R concentration (Figure 6.7). Interestingly, low levels of sCSF-1R induced IL-10 expression to levels near what was found with apoptotic cells.

6.2.5 Neutrophil chemotaxis but not ROS production is impacted by sCSF-1R.

Neutrophil infiltration is one of the hallmarks of inflammation. Figure 6.2 shows that zymosan-induced neutrophil infiltration is reduced by sCSF-1R (21). However, neutrophils are not directly affected by sCSF-1R, suggesting that the inhibition of inflammation caused by sCSF-1R relies on leukocyte cross-talk. Given the central contribution of chemokines to leukocyte recruitment, I first examined the impact of sCSF-1R on CXCL-8 and CCL-1, two important chemokines, that are known to drive neutrophil and monocyte chemotaxis, respectively. Recombinant sCSF-1R significantly decreased CXCL-8 at all concentrations tested (Figure 6.8). In comparison, CCL-1 only displayed significant decreases in expression at the highest concentration of sCSF-1R used.

Since macrophages are the primary recruiters of neutrophils to an inflammatory site, I was curious if sCSF-1R decreased the capacity of macrophages to drive neutrophil chemotaxis. To assess this, I isolated infiltrating inflammatory neutrophils from zymosan-injected fish and measured chemotaxis towards supernatants from activated macrophages treated with increasing concentrations of sCSF-1R (Figure 6.9). Neutrophil chemotaxis in a blind-well chamber decreased in a dose-dependent manner with increasing concentration of

recombinant sCSF-1R and reached similar levels to those achieved upon addition of apoptotic cells.

In Chapter 4, I showed that murine but not teleost neutrophils were able to internalize apoptotic cells, leading to decreased ROS production in neutrophils with phagocytosed apoptotic cells (20). These experiments, however, were done *ex vivo*, removing the effects of *in vivo* leukocyte cross-talk in the responses. As such, I wished to determine if exposure to soluble products *in vivo* following either apoptotic cells or sCSF-1R injection would impact neutrophil ROS. Interestingly, I found that neutrophil-specific ROS responses were reduced in goldfish injected with apoptotic cells but not with sCSF-1R (Figure 6.10 A). This is strikingly different from ROS responses found in monocyte/ macrophages, where responses are significantly reduced with both sCSF-1R and apoptotic cells (20, 21). Finally, I assessed neutrophil killing capacity with a gentamicin protection assay and found a significantly decreased ability to kill when exposed to soluble products from macrophages activated in the presence of either apoptotic cells or rsCSF-1R (Figure 6.8 B). Importantly, this data suggests that apoptotic cells are able to trigger a variety of pathways that contribute to the resolution of inflammation, as evidenced by the wide range of responses, while sCSF-1R is more targeted and likely only able to regulate responses directly controlled by the CSF-1 system.

6.3 Discussion

Inflammation is a beneficial process required for the clearance and control of pathogens. However, a loss of control of inflammatory processes can have grave

consequences for the host, including development of chronic inflammatory diseases, autoimmunity, or chronic infection (39-41). Macrophages and their central regulator, CSF-1, have been linked tightly to both the beneficial and deleterious effects of inflammation (4). As such, the CSF-1 system represents a potentially excellent target for controlling inflammatory processes.

Soluble receptors have been shown to be important and common regulators of many cytokines within the immune system, including IL-1, IL-6, IFNγ, TNF-α, GM-CSF, G-CSF and many more (42, 43). This chapter describes a novel soluble receptor- soluble CSF-1 receptor- that, to date, has only been found in teleost fish. In primary macrophage cultures, soluble CSF-1R was found at the highest levels when macrophage development needed to be tightly controlled. In the senescent phase of goldfish *in vitro* macrophage development, macrophage increase in sCSF-1R production paralleled induction of apoptotic events (17). Recombinant sCSF-1R inhibited macrophage proliferation, pointing to a potential role in hematopoiesis control (17). As I have shown here, this novel soluble product is also able to induce inflammatory control within teleost fish. Further, my data places the CSF-1 system as a primary driver behind a range of inflammatory processes in goldfish.

Chapter 4 shows that apoptotic cells significantly decrease inflammatory responses in goldfish by decreasing cellular infiltration and production of reactive oxygen species (20). While there are striking differences in the cellular infiltration responses in teleosts and mice (20), the overall outcomes following exposure to apoptotic cells is similar between these two species. Interestingly, I have also shown that sCSF-1R impacts the cellular infiltration and ROS production in a

similar manner as apoptotic cells (21). I wondered if this similarity would extend to other aspects of the inflammatory response, suggesting that sCSF-1R was a primary mediator of resolution responses in teleost fish. While I found some similarities in the effects of sCSF-1R and apoptotic cells, there were some striking differences in the responses that were induced.

Overall, soluble CSF-1R, like apoptotic cells, is an efficient regulator of inflammatory processes. This was most evident in the production of antimicrobial inflammatory mediators, where sCSF-1R reduced zymosan-induced ROS production and iNOS B expression to basal levels. This was combined with a significant decrease in expression of a number of inflammatory cytokines, notably IL-1β 1 and 2, IFNγ and IFNγrel, TNF-α 2, IL-12p35 and CSF-1. All of these cytokines have been shown to be important in the regulation of inflammatory processes in goldfish macrophages, especially phagocytosis and the production of reactive intermediates (28-31). It is probable, then, that the effects on ROS and iNOS may not be a direct one but may be due to the changes in the cytokine profiles following exposure to sCSF-1R. Further, since sCSF-1R is thought to only bind CSF-1, it is likely that these cytokines and the production of reactive intermediates are tightly linked to the CSF-1 system. However, the possibility exists that sCSF-1R may be interacting with factors other than CSF-1 to exert these effects. Interestingly, I found significant down-regulation of two pro-inflammatory cytokines- TNFα 2 and CSF-1- across a range of sCSF-1R concentrations. This suggests a high degree of sensitivity of these cytokines to sCSF-1R. It will be interesting to examine the impact of low doses of sCSF-1R across a panel of pro-

inflammatory cytokines to see if this is a general effect or if pro-inflammatory cytokines have differential levels of sensitivity to sCSF-1R.

When I studied canonical anti-inflammatory responses, I found further differences between responses to sCSF-1R and apoptotic cells. The most dramatic effect was seen on IL-10 expression. Unlike the pro-inflammatory cytokines, I found that IL-10 expression increased with decreasing concentrations of sCSF-1R. At the lowest level of sCSF-1R tested, responses were similar to those measured with apoptotic cells. This may indicate that, at low doses of sCSF-1R, there are sufficient pro-inflammatory signals remaining to induce IL-10 expression that are ablated at high levels of sCSF-1R. Alternatively, it may show IL-10 requires a threshold level of CSF-1 expression to be produced and it is not expressed below this level. Interestingly, I have yet to observe an increase in TGF-β following apoptotic cell exposure, even though this is the primary mediator of anti-inflammatory responses following phagocytosis of apoptotic cells in mammals (44). While expression and many of the functions of TGF-β are highly conserved (37, 45), it is possible that the link between TGF-β and apoptotic cells is not conserved through evolution. It is also possible that a different trigger or combination of triggers is required to induce TGF-β production following exposure to apoptotic cells in teleost fish.

Neutrophils are among the earliest leukocytes recruited into an inflammatory site and are known for their vast inflammatory and antimicrobial arsenal. Therefore, reducing the infiltration of neutrophils into an inflammatory site may represent an important mechanism to limit damage to host tissues. I show here that

both sCSF-1R and apoptotic cells significantly reduce the infiltration of neutrophils into an inflammatory site (20, 21). I was curious if this was occurring due to changes in chemotaxis or through another mechanism. Using a blind-well chemotaxis chamber, I found that neutrophil chemotaxis was significantly decreased with increasing concentrations of sCSF-1R or with apoptotic cells. Further, both sCSF-1R and apoptotic cells significantly decreased expression of CXCL-8 (also known as IL-8), the primary mediator of neutrophil chemotaxis (46). The relatively limited impact on CCL-1 also matches my infiltration data, where monocyte/macrophage infiltration was only impacted at the highest doses of sCSF-1R (21). I have previously shown that goldfish neutrophils are unable to ingest apoptotic cells and that their ROS production is not changed by soluble factors produced *ex vivo* (20). Thus, I examined if exposure to complex *in vivo* milieu could affect neutrophil-specific ROS responses. Surprisingly, I found that only apoptotic cells and not sCSF-1R resulted in decreased neutrophil ROS production, though neutrophil killing capacity was equally affected by soluble products from apoptotic cell or sCSF-1R stimulated macrophages. This suggests two things: [1.] neutrophil ROS is not controlled by the CSF-1 system; and [2.] apoptotic cells are able to affect inflammatory pathways not targeted by sCSF-1R, suggesting that these two anti-inflammatory mediators are complimentary, not redundant.

Overall, the proper control of inflammation is of outmost physiological importance for the long-term survival of an animal host. This chapter further describes a novel method of controlling inflammation- through the production of a soluble CSF-1 receptor. Soluble CSF-1R affects every aspect of a macrophage

inflammatory response examined- phagocytosis, production of inflammatory cytokines and chemokines, production of reactive intermediates, and the ability to recruit cells into an inflammatory site. This speaks to the importance of CSF-1 to inflammation and suggests that it may be an important target for inflammatory control across vertebrates.

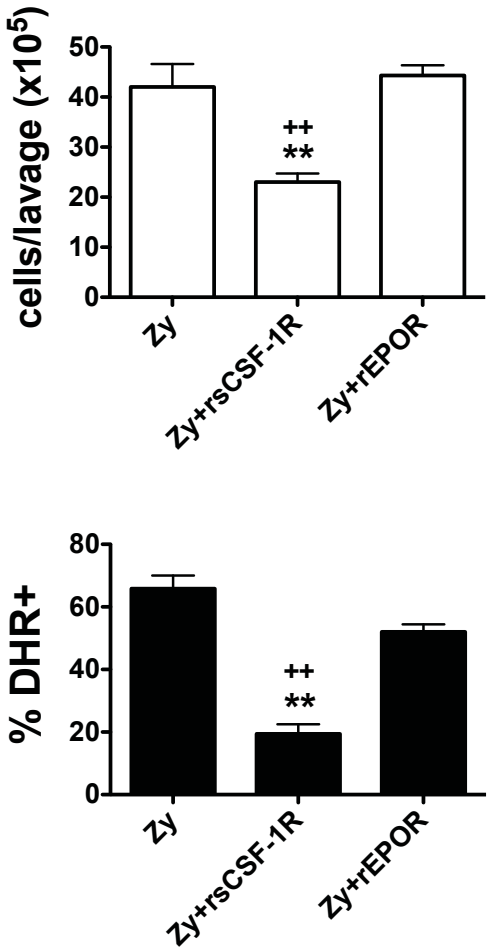

Figure 6.1. Recombinant sCSF-1R but not recombinant EPO receptor affects inflammatory processes.

Goldfish were injected intraperitoneally with zymosan (Zy), zymosan plus recombinant sCSF-1R, or zymosan with recombinant erythropoietin receptor. Cells were harvested by peritoneal lavage 24 hours later. Cells were also counted to determine levels of total leukocyte infiltration. ROS production was measured via DHR staining.. n= 3; ** $p<0.01$ compared to Zy ++ $p<0.01$ compared to Zy+EPOR (One-way ANOVA; Tukey's post-hoc); error bars show SEM.

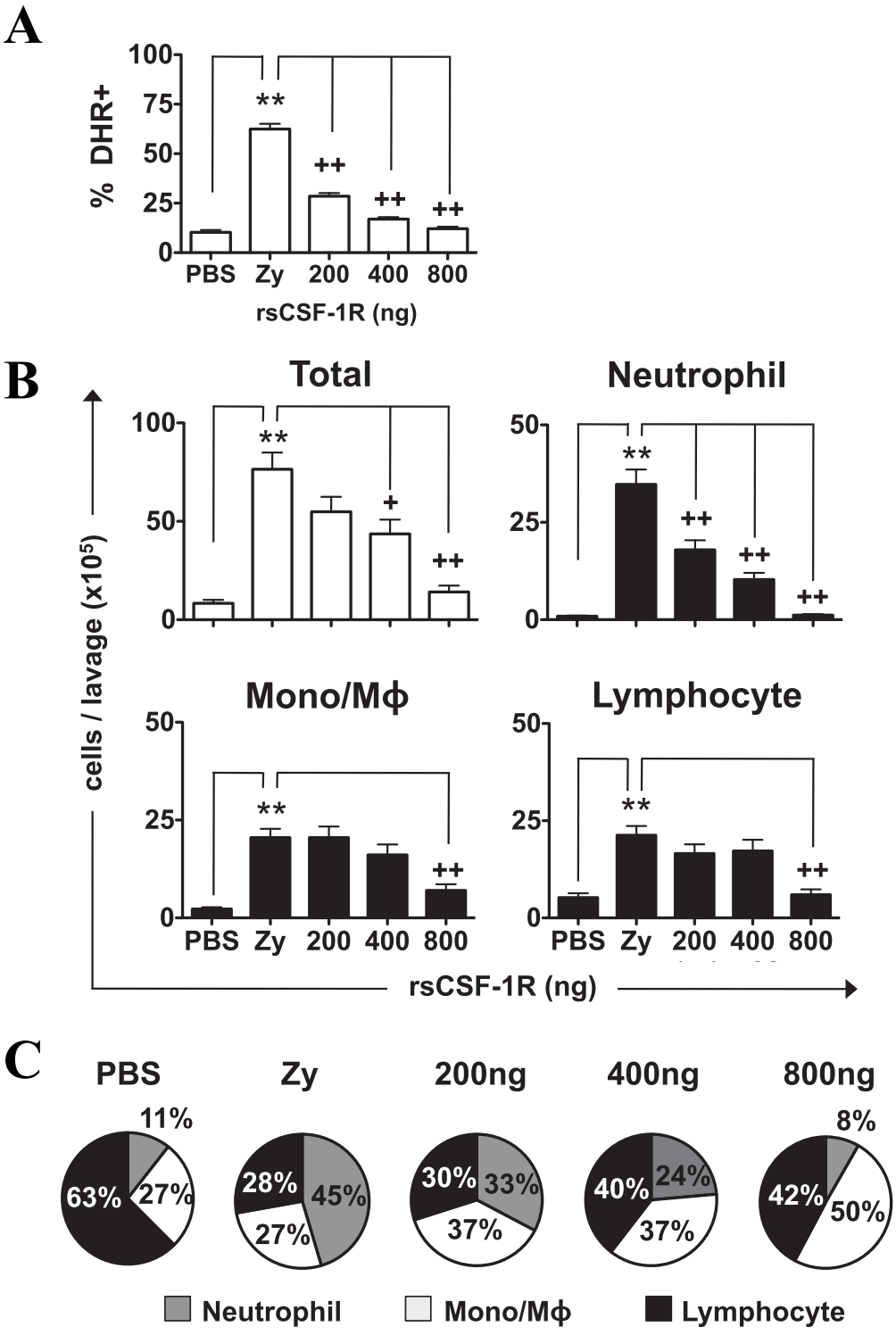
A
% DHR+
100
75
50
25
0
**
++
++
++
PBS
Zy
200
400
800
rsCSF-1R (ng)
B
Total
Neutrophil
Mono/Mϕ
Lymphocyte
cells / lavage (x10^5)
100
50
25
0
**
+
++
++
++
++
++
++
PBS
Zy
200
400
800
rsCSF-1R (ng)
C
PBS
Zy
200ng
400ng
800ng
11%
63%
27%
28%
45%
27%
30%
33%
37%
40%
24%
37%
8%
42%
50%
Neutrophil
Mono/Mϕ
Lymphocyte

Figure 6.2. Recombinant sCSF-1R affects inflammatory leukocyte infiltration *in vivo.*

Goldfish were injected intraperitoneally with PBS, zymosan (Zy) or zymosan plus the indicated amounts of recombinant sCSF-1R. Cells were harvested by peritoneal lavage 24 hours later. (**A**) ROS production was measured via DHR staining. (**B**) Cells were also counted to determine levels of total leukocyte infiltration. Total leukocytes were further broken down into cellular subpopulations based on morphology, Sudan Black staining and flow cytometric forward and side scatter parameters. (**C**) Cell proportions for each subpopulations in the total leukocyte pool were determined based on characteristics outlined in (**B**). n= 6; ** $p<0.01$ compared to PBS; + $p<0.05$ compared to Zy; ++ $p<0.01$ compared to Zy (One-way ANOVA; Tukey's post-hoc); error bars show SEM.

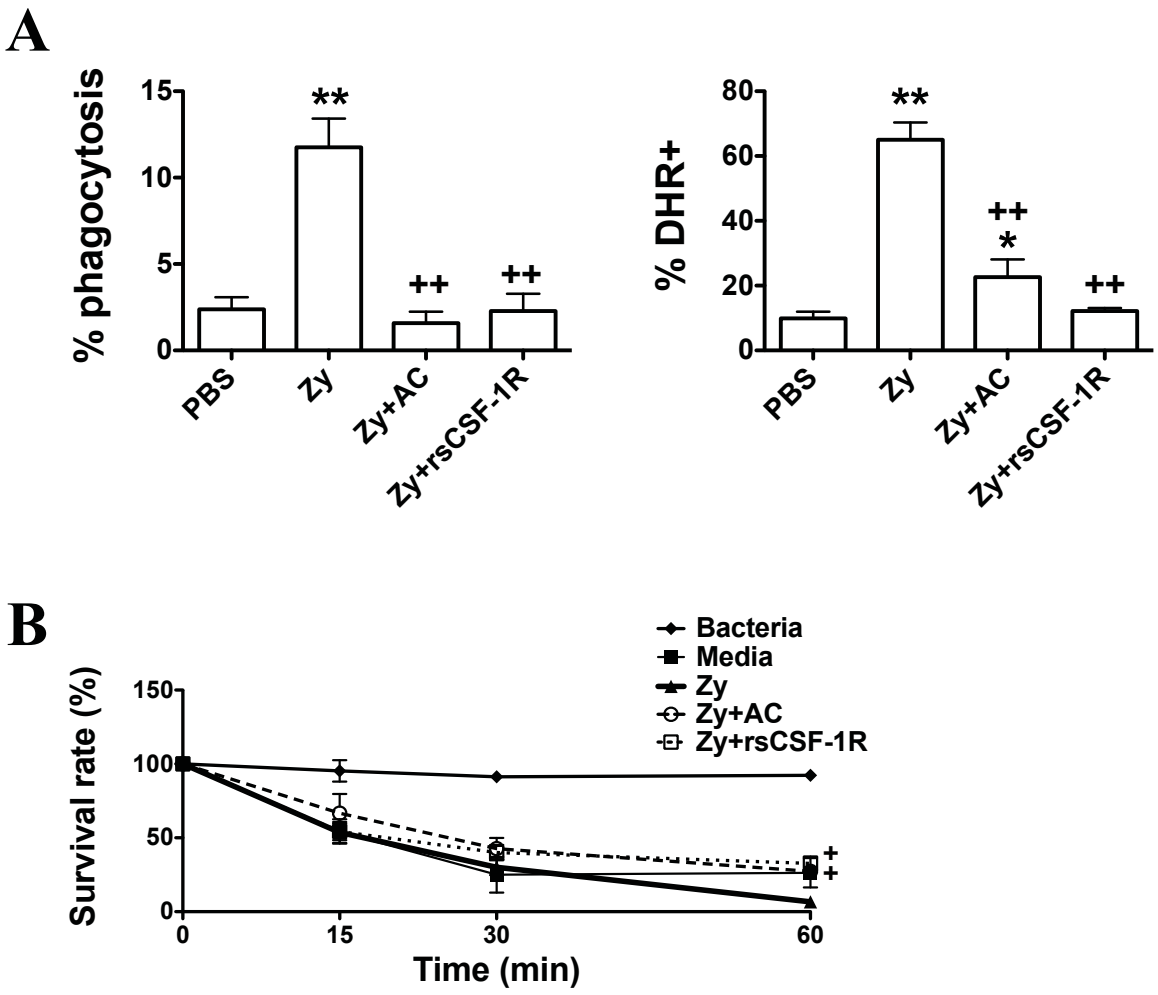

Figure 6.3. Soluble CSF-1R and apoptotic cells down-regulate pro-inflammatory phagocytic responses.

Goldfish were injected i.p. with zymosan in the presence or absence of either apoptotic cells (AC) or recombinant sCSF-1R. After 24 hours, peritoneal cells were harvested by lavage. **(A)** Cells were then incubated with zymosan-FITC particles (5:1 ratio, particle: cell) for 2 hours to measure phagocytosis. Reactive oxygen production was measured with dihydrorhodamine (DHR). Both apoptotic cells and sCSF-1R reduced phagocytic and ROS responses. n=4. **(B)** Killing capacity was measured with a gentamicin protection assay. PKMs were incubated for 2 hours with the noted stimuli. *Aeromonas veronii* was then added for 30 minutes. Cells were washed and incubated in a high dose of gentamicin for 30 minutes. At the indicated time points, cells were lysed and plated onto TSA plates. Colonies were counted 48 h later. n=6; * $p<0.05$, ** $p<0.01$ compared to PBS; + $p<0.05$, ++ $p<0.01$ compared to zymosan (One-way ANOVA; Tukey's post-hoc for A; Two-way ANOVE; Bonferroni post-hoc for B); error bars show SEM.

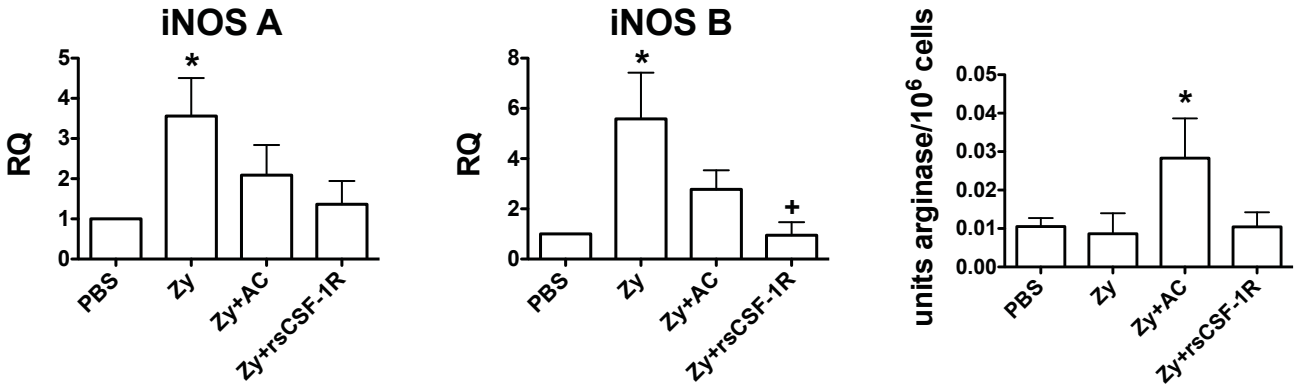

Figure 6.4. Soluble CSF-1R does not shift macrophages towards an alternative pathway phenotype.

iNOS and arginase levels were measured as indicators of classical vs. alternative macrophages, respectively. iNOS A and B levels were determined by Q-PCR. Arginase activity was determined using a standard arginase assay. n=6; * $p<0.05$, ** $p<0.01$ compared to PBS; + $p<0.05$, ++ $p<0.01$ compared to zymosan (One-way ANOVA; Tukey's post-hoc); error bars show SEM.

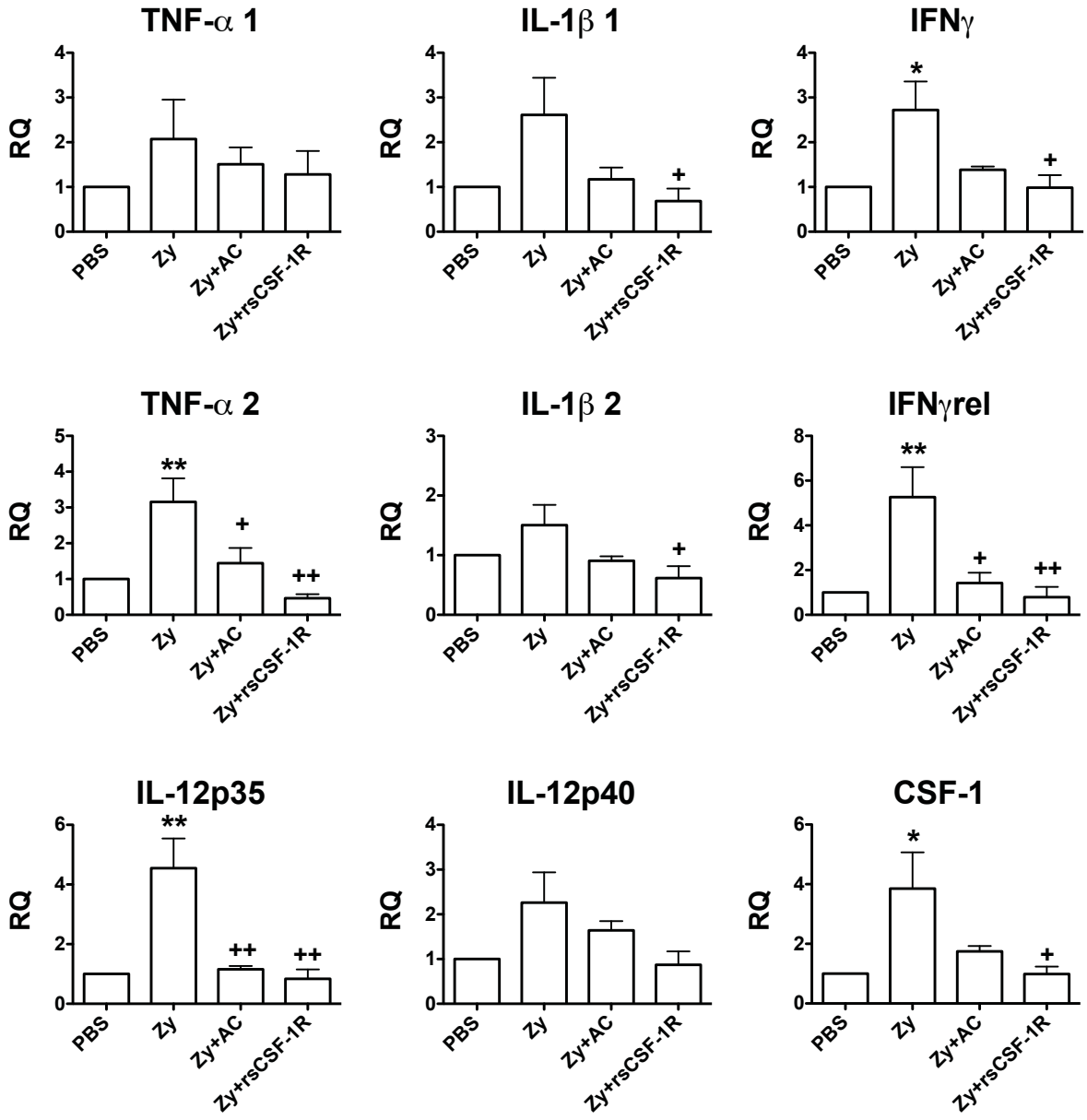

Figure 6.5. Soluble CSF-1R dramatically decreases inflammatory cytokine expression.

Goldfish were injected i.p. with zymosan in the presence or absence of either apoptotic cells (AC) or recombinant sCSF-1R. After 24 hours, peritoneal cells were harvested by lavage and RNA was extracted. Cytokine levels were measured by Q-PCR. sCSF-1R causes a general down-regulation of pro-inflammatory cytokines. n=6; * $p<0.05$, ** $p<0.01$ compared to PBS; + $p<0.05$, ++ $p<0.01$ compared to zymosan (One-way ANOVA; Tukey's post-hoc); error bars show SEM.

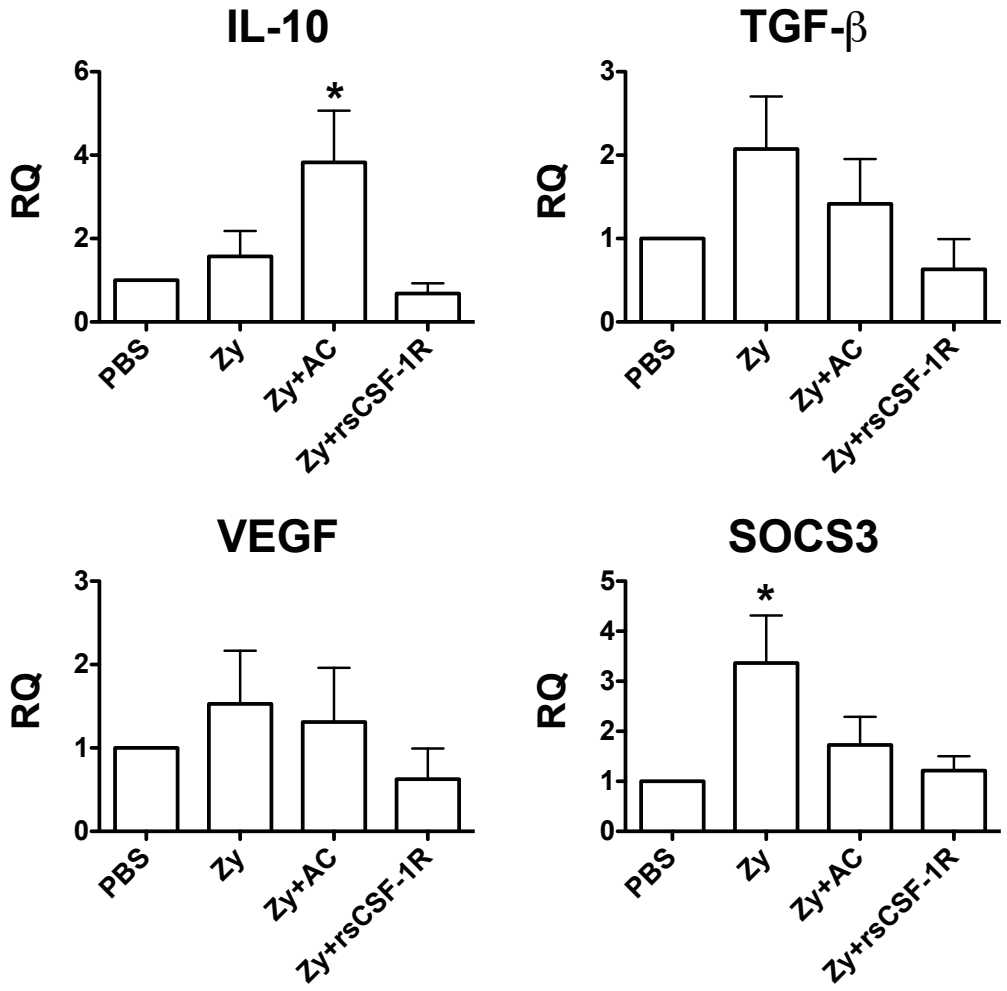

Figure 6.6. Both apoptotic cells and sCSF-1R have a limited impact on anti-inflammatory cytokine expression.

Goldfish were injected i.p. with zymosan in the presence or absence of either apoptotic cells (AC) or recombinant sCSF-1R. After 24 hours, peritoneal cells were harvested by lavage and RNA was extracted. Cytokine levels were measured by Q-PCR. n=6; * $p<0.05$, ** $p<0.01$ compared to PBS; + $p<0.05$, ++ $p<0.01$ compared to zymosan (One-way ANOVA; Tukey's post-hoc); error bars show SEM.

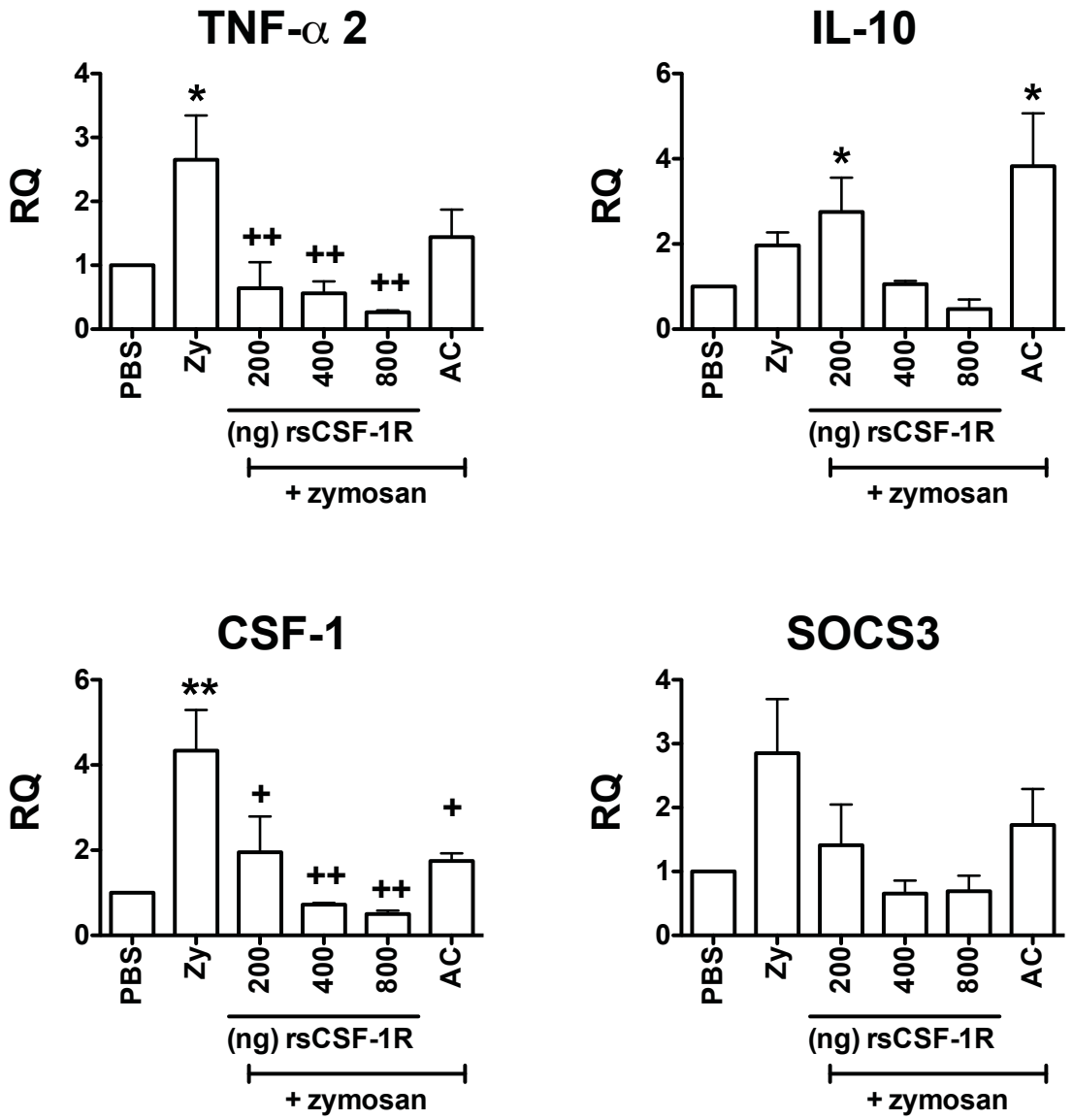

Figure 6.7. Soluble CSF-1R has dose-dependent effects on important pro- and anti-inflammatory factors.

Goldfish were injected i.p. with zymosan in the presence or absence of either apoptotic cells (AC) or recombinant sCSF-1R. After 24 hours, peritoneal cells were harvested by lavage and RNA was extracted. Cytokine levels were measured by Q-PCR. n=6; * $p<0.05$, ** $p<0.01$ compared to PBS; + $p<0.05$, ++ $p<0.01$ compared to zymosan (One-way ANOVA; Tukey's post-hoc); error bars show SEM.

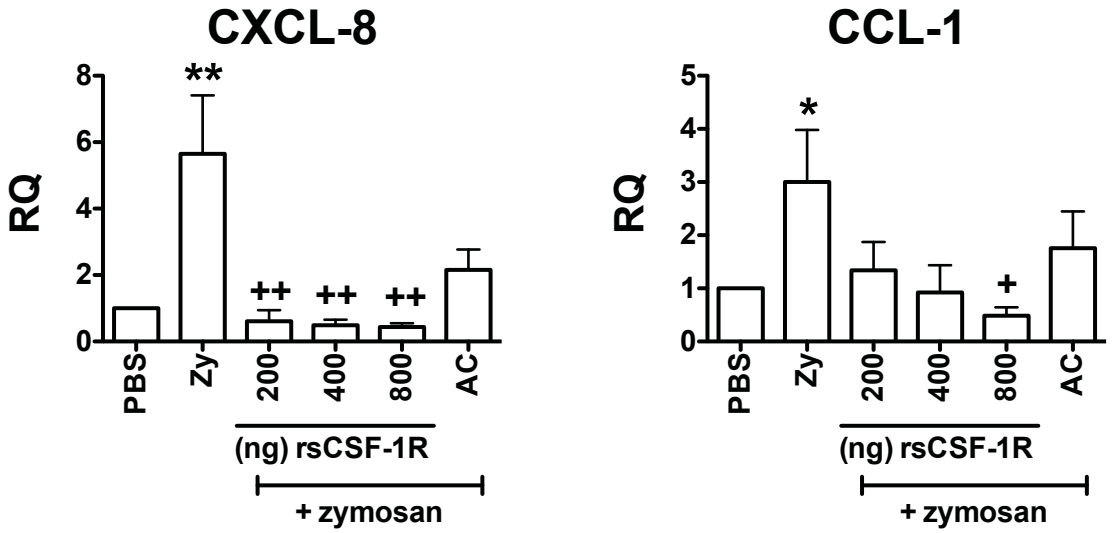

Figure 6.8. Soluble CSF-1R alters chemokine expression, especially CXCL-8.

Goldfish were injected i.p. with zymosan in the presence or absence of either apoptotic cells (AC) or recombinant sCSF-1R. After 24 h, peritoneal cells were harvested by lavage and RNA was extracted. Chemokine levels were measured by Q-PCR. n=6; * $p<0.05$, ** $p<0.01$ compared to PBS; + $p<0.05$, ++ $p<0.01$ compared to zymosan (One-way ANOVA; Tukey's post-hoc); error bars show SEM.

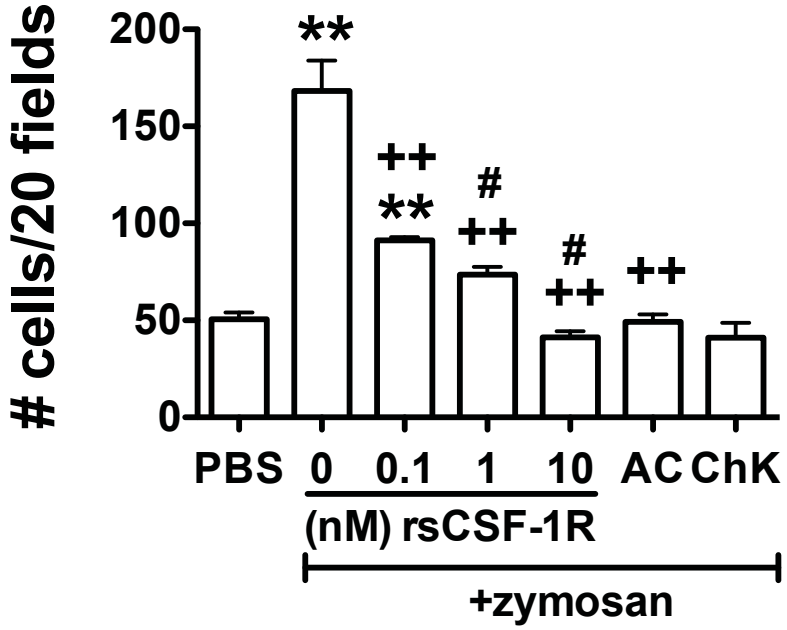

Figure 6.9. Neutrophil chemotaxis is decreased by macrophage soluble factors produced in the presence of sCSF-1R.

Goldfish PKM cultures were incubated with zymosan in the presence/absence of increasing doses of recombinant sCSF-1R or apoptotic cells. After 24 h, filtered supernatants were applied to the bottom of a blind-well chemotaxis chamber. Neutrophils isolated from zymosan-injected fish were isolated and applied to the top chamber. After 1 h, membranes were removed and neutrophil chemotaxis was counted. ChK= chemokinesis control. n=6; * $p<0.05$, ** $p<0.01$ compared to PBS; + $p<0.05$, ++ $p<0.01$ compared to zymosan; # $p<0.05$ compared to 0.1 (One-way ANOVA; Tukey's post-hoc); error bars show SEM.

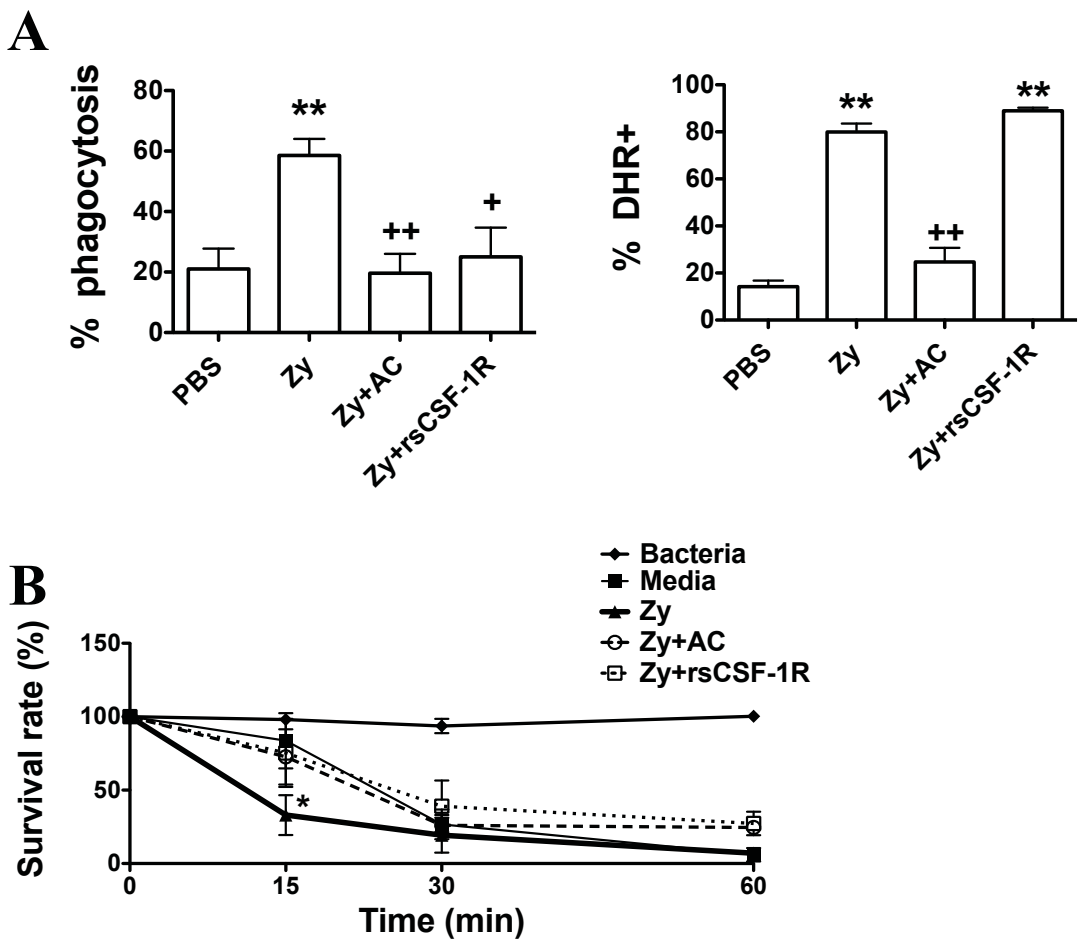

Figure 6.10. Neutrophil killing, but not ROS, responses are affected by soluble products produced by macrophages activated in the presence of sCSF-1R.

Goldfish were injected i.p. with zymosan in the presence or absence of either apoptotic cells (AC) or recombinant sCSF-1R. After 24 h, peritoneal cells were harvested by lavage and neutrophils were isolated. (**A**) Cells were then incubated with zymosan-FITC particles (5:1 ratio, particle:cell) for 2 h to measure phagocytosis. Reactive oxygen production was measured with dihydrorhodamine (DHR). Both apoptotic cells and sCSF-1R reduced phagocytic and ROS responses. n=5. (**B**) Neutrophil killing potential was assessed with a gentamicin protection assay. Neutrophils were incubated in the soluble products from PKMs activated with the with noted stimuli for 2 h. *Aeromonas veronii* was then added (100:1) for 30 min. Cells were then treated with gentamicin for 30 min and lysed at the indicated time points. n=3; * $p<0.05$, ** $p<0.01$ compared to PBS; + $p<0.05$, ++ $p<0.01$ compared to zymosan (One-way ANOVA; Tukey's post-hoc for A; Two-way ANOVA; Bonferroni post-hoc for B); error bars show SEM.

6.4 References

1. Barreda, D.R., Hanington, P.C., and Belosevic, M. 2004. Regulation of myeloid development and function by colony stimulating factors. *Dev Comp Immunol* 28:509-554.
2. O'Mahony, D.S., Pham, U., Iyer, R., Hawn, T.R., and Liles, W.C. 2008. Differential constitutive and cytokine-modulated expression of human Toll-like receptors in primary neutrophils, monocytes, and macrophages. *Int J Med Sci* 5:1-8.
3. Roilides, E., Lyman, C.A., Mertins, S.D., Cole, D.J., Venzon, D., Pizzo, P.A., Chanock, S.J., and Walsh, T.J. 1996. Ex vivo effects of macrophage colony-stimulating factor on human monocyte activity against fungal and bacterial pathogens. *Cytokine* 8:42-48.
4. Chitu, V., and Stanley, E.R. 2006. Colony-stimulating factor-1 in immunity and inflammation. *Curr Opin Immunol* 18:39-48.
5. Evans, R., Kamdar, S.J., Fuller, J.A., and Krupke, D.M. 1995. The potential role of the macrophage colony-stimulating factor, CSF-1, in inflammatory responses: characterization of macrophage cytokine gene expression. *J Leukoc Biol* 58:99-107.
6. Hashimoto, S., Yoda, M., Yamada, M., Yanai, N., Kawashima, T., and Motoyoshi, K. 1996. Macrophage colony-stimulating factor induces interleukin-8 production in human monocytes. *Exp Hematol* 24:123-128.
7. Sweet, M.J., and Hume, D.A. 2003. CSF-1 as a regulator of macrophage activation and immune responses. *Arch Immunol Ther Exp (Warsz)* 51:169-177.
8. Boocock, C.A., Jones, G.E., Stanley, E.R., and Pollard, J.W. 1989. Colony-stimulating factor-1 induces rapid behavioural responses in the mouse macrophage cell line, BAC1.2F5. *J Cell Sci* 93 (Pt 3):447-456.
9. Webb, S.E., Pollard, J.W., and Jones, G.E. 1996. Direct observation and quantification of macrophage chemoattraction to the growth factor CSF-1. *J Cell Sci* 109 (Pt 4):793-803.
10. Akagawa, K.S. 2002. Functional heterogeneity of colony-stimulating factor-induced human monocyte-derived macrophages. *Int J Hematol* 76:27-34.
11. Cheers, C., Hill, M., Haigh, A.M., and Stanley, E.R. 1989. Stimulation of macrophage phagocytic but not bactericidal activity by colony-stimulating factor 1. *Infect Immun* 57:1512-1516.
12. Kleemann, R., Zadelaar, S., and Kooistra, T. 2008. Cytokines and atherosclerosis: a comprehensive review of studies in mice. *Cardiovasc Res* 79:360-376.
13. Lewis, C.E., and Pollard, J.W. 2006. Distinct role of macrophages in different tumor microenvironments. *Cancer Res* 66:605-612.
14. Weisberg, S.P., McCann, D., Desai, M., Rosenbaum, M., Leibel, R.L., and Ferrante, A.W., Jr. 2003. Obesity is associated with macrophage accumulation in adipose tissue. *J Clin Invest* 112:1796-1808.

15. Menke, J., Rabacal, W.A., Byrne, K.T., Iwata, Y., Schwartz, M.M., Stanley, E.R., Schwarting, A., and Kelley, V.R. 2009. Circulating CSF-1 promotes monocyte and macrophage phenotypes that enhance lupus nephritis. *J Am Soc Nephrol* 20:2581-2592.
16. Rubin Kelley, V., Bloom, R.D., Yui, M.A., Martin, C., and Price, D. 1994. Pivotal role of colony stimulating factor-1 in lupus nephritis. *Kidney Int Suppl* 45:S83-85.
17. Barreda, D.R., Hanington, P.C., Stafford, J.L., and Belosevic, M. 2005. A novel soluble form of the CSF-1 receptor inhibits proliferation of self-renewing macrophages of goldfish (Carassius auratus L.). *Dev Comp Immunol* 29:879-894.
18. Barreda, D.R., and Belosevic, M. 2001. Characterisation of growth enhancing factor production in different phases of in vitro fish macrophage development. *Fish Shellfish Immunol* 11:169-185.
19. Rieger, A.M., Konowalchuk, J.D., Grayfer, L., Katzenback, B.A., Havixbeck, J.J., Kiemele, M.D., Belosevic, M., and Barreda, D.R. 2012. Fish and mammalian phagocytes differentially regulate pro-inflammatory and homeostatic responses in vivo. *PLoS ONE* - Accepted [manuscript number: PONE-D-12-21984].
20. Rieger, A.M., Konowalchuk, J.D., Grayfer, L., Katzenback, B.A., Havixbeck, J.J., Kiemele, M.D., Belosevic, M., and Barreda, D.R. 2012. Fish and mammalian phagocytes differentially regulate pro-inflammatory and homeostatic responses in vivo. *PLoS One* 7:e47070.
21. Rieger, A.M., Konowalchuk, J.D., Havixbeck, J.J., Robbins, J.S., Smith, M.K., Lund, J.M., and Barreda, D.R. 2013. A soluble form of the CSF-1 receptor contributes to the inhibition of inflammation in a teleost fish. *Dev Comp Immunol* 39:438-446.
22. Murray, P.J., and Wynn, T.A. 2011. Protective and pathogenic functions of macrophage subsets. *Nat Rev Immunol* 11:723-737.
23. Mosser, D.M., and Edwards, J.P. 2008. Exploring the full spectrum of macrophage activation. *Nat Rev Immunol* 8:958-969.
24. Edwards, J.P., Zhang, X., Frauwirth, K.A., and Mosser, D.M. 2006. Biochemical and functional characterization of three activated macrophage populations. *J Leukoc Biol* 80:1298-1307.
25. Ho, V.W., and Sly, L.M. 2009. Derivation and characterization of murine alternatively activated (M2) macrophages. *Methods Mol Biol* 531:173-185.
26. Joerink, M., Forlenza, M., Ribeiro, C.M., de Vries, B.J., Savelkoul, H.F., and Wiegertjes, G.F. 2006. Differential macrophage polarisation during parasitic infections in common carp (Cyprinus carpio L.). *Fish Shellfish Immunol* 21:561-571.
27. Joerink, M., Savelkoul, H.F., and Wiegertjes, G.F. 2006. Evolutionary conservation of alternative activation of macrophages: structural and functional characterization of arginase 1 and 2 in carp (Cyprinus carpio L.). *Mol Immunol* 43:1116-1128.

28. Grayfer, L., and Belosevic, M. 2009. Molecular characterization, expression and functional analysis of goldfish (Carassius aurutus L.) interferon gamma. *Dev Comp Immunol* 33:235-246.
29. Grayfer, L., Garcia, E.G., and Belosevic, M. 2010. Comparison of macrophage antimicrobial responses induced by type II interferons of the goldfish (Carassius auratus L.). *J Biol Chem* 285:23537-23547.
30. Grayfer, L., Hanington, P.C., and Belosevic, M. 2009. Macrophage colony-stimulating factor (CSF-1) induces pro-inflammatory gene expression and enhances antimicrobial responses of goldfish (Carassius auratus L.) macrophages. *Fish Shellfish Immunol* 26:406-413.
31. Grayfer, L., Walsh, J.G., and Belosevic, M. 2008. Characterization and functional analysis of goldfish (Carassius auratus L.) tumor necrosis factor-alpha. *Dev Comp Immunol* 32:532-543.
32. Weigert, A., Jennewein, C., and Brune, B. 2009. The liaison between apoptotic cells and macrophages--the end programs the beginning. *Biol Chem* 390:379-390.
33. Huynh, M.L., Fadok, V.A., and Henson, P.M. 2002. Phosphatidylserine-dependent ingestion of apoptotic cells promotes TGF-beta1 secretion and the resolution of inflammation. *J Clin Invest* 109:41-50.
34. Erwig, L.P., and Henson, P.M. 2007. Immunological consequences of apoptotic cell phagocytosis. *Am J Pathol* 171:2-8.
35. Erwig, L.P., and Henson, P.M. 2008. Clearance of apoptotic cells by phagocytes. *Cell Death Differ* 15:243-250.
36. Grayfer, L., Hodgkinson, J.W., Hitchen, S.J., and Belosevic, M. 2011. Characterization and functional analysis of goldfish (Carassius auratus L.) interleukin-10. *Mol Immunol* 48:563-571.
37. Haddad, G., Hanington, P.C., Wilson, E.C., Grayfer, L., and Belosevic, M. 2008. Molecular and functional characterization of goldfish (Carassius auratus L.) transforming growth factor beta. *Dev Comp Immunol* 32:654-663.
38. Tassiulas, I., Park-Min, K.H., Hu, Y., Kellerman, L., Mevorach, D., and Ivashkiv, L.B. 2007. Apoptotic cells inhibit LPS-induced cytokine and chemokine production and IFN responses in macrophages. *Hum Immunol* 68:156-164.
39. Poon, I.K., Hulett, M.D., and Parish, C.R. 2010. Molecular mechanisms of late apoptotic/necrotic cell clearance. *Cell Death Differ* 17:381-397.
40. Duffield, J.S. 2003. The inflammatory macrophage: a story of Jekyll and Hyde. *Clin Sci (Lond)* 104:27-38.
41. Soehnlein, O., and Lindbom, L. 2010. Phagocyte partnership during the onset and resolution of inflammation. *Nat Rev Immunol* 10:427-439.
42. Fernandez-Botran, R. 1991. Soluble cytokine receptors: their role in immunoregulation. *FASEB J* 5:2567-2574.
43. Heaney, M.L., and Golde, D.W. 1998. Soluble receptors in human disease. *J Leukoc Biol* 64:135-146.
44. Fadok, V.A., Bratton, D.L., Konowal, A., Freed, P.W., Westcott, J.Y., and Henson, P.M. 1998. Macrophages that have ingested apoptotic cells in vitro

inhibit proinflammatory cytokine production through autocrine/paracrine mechanisms involving TGF-beta, PGE2, and PAF. *J Clin Invest* 101:890-898.

45. Newfeld, S.J., Wisotzkey, R.G., and Kumar, S. 1999. Molecular evolution of a developmental pathway: phylogenetic analyses of transforming growth factor-beta family ligands, receptors and Smad signal transducers. *Genetics* 152:783-795.
46. Harada, A., Sekido, N., Akahoshi, T., Wada, T., Mukaida, N., and Matsushima, K. 1994. Essential involvement of interleukin-8 (IL-8) in acute inflammation. *J Leukoc Biol* 56:559-564.

Chapter 7: *Aeromonas* infections induce high levels of soluble CSF-1R expression and impact hematopoietic cell production

7.1 Introduction

Aeromonas is one of the oldest known fish pathogens, originally characterized in the 1890s (1). This highly virulent fish pathogen has had devastating effects on the fish farming industry (2). *Aeromonas* infections are characterized by the presence of fin rot, tail rot, ulcers, and hemorrhagic septicemia- leading to scale shedding, hemorrhages in the gills and anal area, exophthalmia, and abdominal swelling (3-7). However, many carrier fish do not present with external furuncles but are still capable of shedding bacteria into the environment at high rates (10^5-10^6 CFU/fish/hour) (8). In fact, it has been estimated that up to 80% of cultivated fish may carry *Aeromonas* (9), and in many cases of major die-offs in fish, *Aeromonas* species caused invasive secondary infections in fish that were immune suppressed due to adverse environmental conditions (improper handling, drastic temperature changes, poor water quality) (5-8, 10) or spawning (1).

While reports vary, depending on the classification system used, there are currently up to 24 characterized species of *Aeromonas* reported (1). The genus is characterized as being Gram-negative, oxidase- and catalase-positive, glucose fermenting rods (10) that have traditionally been divided into two groups: the psychrophilic group and the mesophilic group (1). The psychrophilic group,

typified by *A. salmonicida*, causes primarily fish diseases and is compromised of non-motile isolates that grow optimally at 22-25^{o}C (1, 10). The mesophilic group, typified by *A. hydrophila*, is composed of motile isolates that grow well at 35-37^{o}C and are commonly associated with human infections (1, 10). Other important pathogens within this group include *A. caviae, A. sobria*, and the *Aeromonas veronii* group (AVG) (*A. veronii* bv *sobria, A. veronii* bv *veronii*, and *A. allosaccharophila*) (10). Bacteria within the AVG have been characterized as 'virulent pathogens', with an LD_{50} ranging from$10^{4.07}$-10^{7} CFU/fish (11-13), depending on species of fish and site of administration.

Of the characterized aeromonads, *Aeromonas veronii* displays virulence in the greatest host range of species, including causing wound infections, diarrhea and septicemia in humans (1, 11, 14), as well as infections in fish (15), eels (16) and pigs (17). This species has been shown to produce significantly higher levels of endotoxins than other *Aeromonas* species (18). One of the important endotoxins is Act, a cytotoxic factor present in culture supernatants responsible for host cell death and damage (19). Act has been shown to induce apoptosis in epithelial cells through oxidant-dependent activation of the mitochondrial pathway (20), and is thought to be the causative cytotoxic enterotoxin that induces apoptosis in murine macrophages (21). Cell death is largely caused by the extensive generation of reactive nitrogen and oxygen intermediates within the site of infection (22).

Aeromonas veronii is protected from ROS –induced damage by the presence of KatA, an antioxidant enzyme catalase (23). This enzyme has been shown to be important for bacterial survival within oxidative conditions, as well as proliferation

and persistence within a leech host (23). Furthermore, *A. veronii* has a catalase-independent defensive mechanism against exogenous H_2O_2 during stationary-phase growth (23). It has also been shown that, though *A. veronii* interacts with macrophages, these interactions have a low rate of phagocytosis in murine macrophages that is only slightly increased by activation with high levels of IFNγ (24). This slight increase in phagocytic rates, however, was not followed by an increased rate in bacterial clearance (24), suggesting that avoidance of phagocytosis or escape/protection from downstream killing mechanisms represent immune evasion techniques employed by *A. veronii*.

The previous chapters have examined the role of macrophage-specific factors in regulating inflammatory responses induced by zymosan. In this chapter, I examine the role of macrophages and the CSF-1 axis in an *Aeromonas* infection. The main objectives of this chapter were to (1) identify the causative strain of *Aeromonas* found within the University of Alberta aquatics facility, (2) examine the expression of sCSF-1R and CSF-1 in infected fish, and (3) determine the impact of sCSF-1R on macrophage responses during an *Aeromonas* infections, including the impact on proliferation within the hematopoietic compartment.

7.2 Results

7.2.1 Isolates obtained from furuncles were typed by sequence analysis.

Goldfish naturally infected with *Aeromonas* are routinely found within the aquatic facilities at the University of Alberta, with the prevalence increasing during the spring months (spawning season) or immediately after animal shipments arrive.

Goldfish commonly present with sores on the body, mouth and oral cavity, and on their fins/tail. Sores were classified based on the level of progress- early infection fish had a raised, red area; mid infection had a red sore with a white center that had not erupted; late infection fish had larger sores that had erupted in the center (or extensive fin/tail rot) (Figure 7.1 A). When goldfish were swabbed, bacteria were only detected from the furuncles, but not from areas without sores (on infected or control fish) (Figure 7.1 B).

Bacterial clones were isolated from 6 furuncles (2 body, 1 mouth/oral cavity, 1 eye and 2 fin/tail) and expression of 16s rRNA and *gyrB* were analyzed by PCR (Figure 7.2 A). PCR products were purified and sequences were analyzed. Sequence alignments identified the isolated bacteria as *Aeromonas veronii* bv *sobria* (Figure 7.2 B).

7.2.2 Naturally infected goldfish have increased expression of sCSF-1R within the furuncle and peripheral tissues.

Furuncle, spleen, and kidney tissues were harvested from naturally infected fish. For furuncle tissue, a similarly sized piece of tissue of the same origin was harvested from an uninfected area (ie. for a body sore, a piece of muscle was removed from the uninfected side of the fish). Control spleens and kidneys were harvested from fish with no apparent sores. RNA was isolated from each tissue and the corresponding cDNA was used to analyze sCSF-1R expression (Figure 7.3 A). Furuncle, spleen, and kidney tissue of infected fish all had significant increases in sCSF-1R expression. Interestingly, no increases in CSF-1 expression were detected

in the furuncle or spleen, and a significant decrease in CSF-1 expression was found in infected kidneys (Figure 7.3 B). This suggested that *Aeromonas* might be manipulating the CSF-1 system. Further, changes to the CSF-1 system are not a general outcome of infection in goldfish, as goldfish infected with *Mycobacterium marinum* showed significant decreases in sCSF-1R expression (Figure 7.4).

7.2.3 Addition of sCSF-1R does not abrogate *Aeromonas*-induced inflammatory responses.

To determine the effects of sCSF-1R on *Aeromonas*-induced ROS production, PKM cultures were incubated with heat-killed *A. veronii* clonal isolates in the presence of apoptotic cells or sCSF-1R (Figure 7.5 A). As a control, PKM cultures were also activated with MAF/LPS or zymosan. As expected, both apoptotic cells and sCSF-1R significantly reduced ROS production in PKM cultures activated with MAF/LPS or zymosan. Interestingly, in cultures activated with *Aeromonas*, sCSF-1R had no impact on ROS responses; however, apoptotic cells still significantly reduced ROS production. This same trend was observed when PKM cultures were activated with heat-killed or live *A. veronii* clonal isolates (Figure 7.5 B). Finally, PKM cultures were activated by clonal *A. veronii* or *A. salmonicida*, in the presence of apoptotic cells or sCSF-1R (Figure 7.5 C). Of note, *A. salmonicida*-induced ROS production was intermediately affected by sCSF-1R, where ROS production was significantly higher than un-activated cells but significantly reduced compared to both *A. salmonicida* and *A. veronii* activated cells.

To assess the effects of sCSF-1R on *Aeromonas*-induced inflammation *in vivo*, heat-killed *A. veronii* was injected intraperitoneally in combination with apoptotic cells or sCSF-1R (Figure 7.6). Similar to *in vitro* experiments, sCSF-1R had no impact on *A. veronii*-induced leukocyte infiltration or ROS production. Apoptotic cells resulted in a significant reduction in both leukocyte infiltration and ROS production.

7.2.4 Induced infection with *Aeromonas veronii* isolates also results in increased sCSF-1R expression.

While intraperitoneal injection is a good method to measure the effects of sCSF-1R on *Aeromonas*-induced inflammation *in vivo*, it does not recapitulate the hypothesized mechanism of exposure of fish to *Aeromonas*. To better mimic a natural infection, a patch of scales was removed and the underlying tissue was slightly scraped. This area was then rubbed with a cotton-tip swab soaked in an *A. veronii* clonal culture. This would mimic a fish rubbing up against another fish with a sore. Bacteria from the swabbed area would also be introduced into the water, coming into contact with all the fish in the tank. Control fish were rubbed with a cotton-tip swab soaked in PBS. Fish were then harvested at the indicated time points. Representative control and infected fish are shown in Figure 7.7. Sites of infection and kidneys were harvested at each time point, RNA was isolated and sCSF-1R expression was measured from the corresponding cDNA (Figure 7.8). *Aeromonas*-infected fish tended to have higher sCSF-1R expression at both the site of infection and in the kidney, similar to naturally infected fish.

7.2.5 Goldfish with natural or induced *A. veronii* infection have significant reductions in proliferation within the hematopoietic compartment.

Goldfish with either a natural or induced *Aeromonas veronii* infection have significant, systemic increases in sCSF-1R expression. However, unlike zymosan or MAF/LPS-induced inflammation, sCSF-1R does not appear to reduce *Aeromonas*-induced inflammatory processes. Since sCSF-1R was originally described as a regulator of macrophage hematopoiesis, I was curious if the hematopoietic compartments of infected fish would be affected. To this end, infected goldfish (natural or induced) were injected intraperitoneally with BrdU. Proliferation was then measured from isolated kidney cells. Interestingly, goldfish that were infected with *Aeromonas veronii*, either naturally (Figure 7.9 A) or through an induced infection (Figure 7.9 B), showed significant decreases in kidney cell proliferation.

7.3 Discussion

Aeromonas veronii is a ubiquitous fresh water pathogen that has been found to be associated with a wide range of hosts, including vertebrates and invertebrates (1, 25). While this bacteria may have beneficial symbiotic relationships with some hosts such as the leech, *Aeromonas* is a highly virulent bacterial pathogen that has been linked to many massive die-offs in the fish farming industry, as well as to human diseases ranging from diarrhea to septicemia (25).

In this chapter, I show that *Aeromonas veronii* infection promotes systemic expression of the soluble colony stimulating factor-1 receptor (sCSF-1R) in challenged goldfish. However, unlike other pathogen models, sCSF-1R was unable to inhibit inflammation at the *A. veronii* challenge site. Instead, sCSF-1R did not decrease leukocyte infiltration or the production of reactive oxygen species (ROS). This was further supported by *in vitro* experiments with live and heat-killed *A. veronii*, suggesting this pathogen may prevent sCSF-1R-mediated down-regulation of macrophage ROS production. Importantly, while sCSF-1R did not appear to reduce inflammatory processes, the increased systemic expression of sCSF-1R in *A. veronii* infected fish appears to decrease proliferative activity among cells in the hematopoietic compartment, which is further coupled to a decrease in CSF-1 expression in kidney hematopoietic tissues. It is interesting to speculate that manipulating the CSF-1 system may represent a unique additional mechanism by which *A. veronii* promotes sustained host-derived cytotoxic responses and pathogenesis.

Currently, the mechanism behind the increase in Aeromonas-induced sCSF-1R expression is unknown. I have shown in previous chapters that sCSF-1R expression appears to be closely linked to apoptotic cell death. It has been previously reported that *A. veronii* induces cell death in murine macrophages and epithelial cells (21, 22, 24). This may be a potential explanation behind expression levels within the furuncle tissues, where there would be a high level of cell death. However, it has been recently reported that *Aeromonas*-induced cell death results in pyroptosis (programmed cell death associated with antimicrobial responses in

inflammation, leading the cells to produce cytokines, swell, and burst), and not apoptosis in macrophages (26). Specifically, cell death was induced by aerolysin and the type III secretion system (T3SS), leading to activation of caspase-1, secretion of IL-1β, and pyroptosis (26). It is currently unknown if pyroptosis will have a similar effects on sCSF-1R expression as apoptosis. However, pyroptosis is generally an inflammatory process, so it is hypothesized that this form of cell death would not induce sCSF-1R expression.

In earlier chapters, I have shown that sCSF-1R reduces phagocytosis of zymosan by goldfish macrophages. Further, sCSF-1R significantly decreases the capacity of goldfish macrophages to kill *Aeromonas veronii*. Reduced phagocytic capacity and killing has been previously reported for murine macrophages (21, 24) and leech hemocytes (27). The changes in phagocytic capacity and killing appear to be related to the type III secretion system (T3SS) (27). The T3SS has been shown to be an important virulence factor in mammals, as bacteria with a mutant T3SS have significantly reduced cytotoxic effects and decreased host mortality (27). It will be interesting to test, then, the potential for modulation of the CSF-1 system by the T3SS and related secretion products. This may represent an alternative explanation for the induction of sCSF-1R and may represent an additional mechanism by which *A. veronii* modulates macrophage responses, in addition to inducing macrophage death, as a method for evading the immune response.

Reactive oxygen species (ROS) are short-lived species generated by inflammatory cells that accumulate during inflammatory processes. ROS have potent destructive effects on both DNA and proteins, making them effective

antimicrobial mediators (28). However, these mediators also have the potential to destroy host tissue, especially under strong inflammatory conditions (28). *Aeromonas* species have been shown to induce strong ROS and nitric oxide responses (20). While this induction results in cell death and tissue destruction in the host, (20-22, 24), *Aeromonas* is relatively well protected by catalase dependent and independent mechanisms (23). This tissue damage may be an important mechanism for *Aeromonas* infection, as tissue infections in mammals generally occur after traumatic tissue injury that was exposed to infected water (29). I have shown in previous chapters that sCSF-1R is able to reduce production of ROS following activation with various inflammatory mediators. However, this does not occur with *Aeromonas*-induced ROS production, suggesting that *Aeromonas* may have developed a mechanism to modulate the effect of sCSF-1R on ROS production. It will be interesting to determine if this further contributes to *Aeromonas* colonization through subversion of host immune responses.

I also found increased expression of sCSF-1R in the kidney within both naturally infected goldfish and goldfish with an induced infection. This increase in expression appears to be linked to a decrease in the proliferative capacity within the hematopoietic compartment and to a significant decrease in CSF-1 expression. Prior to its link in regulating inflammatory processes, sCSF-1R had been characterized as potent regulator of macrophage hematopoiesis (30-33). *Aeromonas salmonicida* has previously been shown to induce changes to hematopoietic transcription factors through an undetermined mechanism (34). This included significantly decreased expression of markers of hematopoietic stem cells and

myeloid progenitors (34). Interestingly, the myeloid marker most decreased by *Aeromonas* infection (*egr1*) was greatly increased by addition of recombinant CSF-1 (34), suggesting a link between *Aeromonas* infection, the CSF-1 system, and the regulation of hematopoiesis. Further, it was hypothesized that the downregulation in hematopoietic transcription factors during an *Aeromonas* infection may result in either an arrest in commitment of monocyte/macrophage progenitors or in the reduction in mobilization of these cells from the hematopoietic organ into the periphery (34). It will be interesting, then, to determine if the increased expression of sCSF-1R has a similar impact on hematopoietic transcription factor expression, suggesting that *Aeromonas veronii* is modulating hematopoietic proliferation through modulating sCSF-1R expression. Further, if these changes do result in arrest of hematopoiesis or reduced mobilization to the periphery, it will be interesting to determine what impact this has on both [1.] the recovery from an *Aeromonas* infection; and [2.] the ability to protect against subsequent/ secondary infections. The potential also exists that the changes in proliferation observed may be due to stress, as this is a common effect of stress hormones on immune function (35). Recent data from our group has shown that following zymosan injection, proliferation is reduced for 36 hours (Havixbeck, J.J., unpublished data). As such, it seems possible that early decreases in proliferation may be due to stress. However, we hypothesis that sustained reductions in proliferation are due to the *Aeromonas* infection, and more specifically due to the enhanced expression of sCSF-1R within the hematopoietic compartment.

Overall, the data presented in this chapter suggest that *Aeromonas veronii* has evolved a mechanism by which it can modulate the CSF-1 system of teleosts. Infection with *A. veronii* results in increased sCSF-1R in local and peripheral tissues. However, the increased expression of sCSF-1R does not appear to decrease inflammatory responses, but instead reduces proliferation within the hematopoietic compartment. These effects appear to most greatly benefit the pathogen, suggesting that modulation of the CSF-1 system may represent a unique immune evasion response that impacts the host both at the site of infection, and within the hematopoietic compartment.

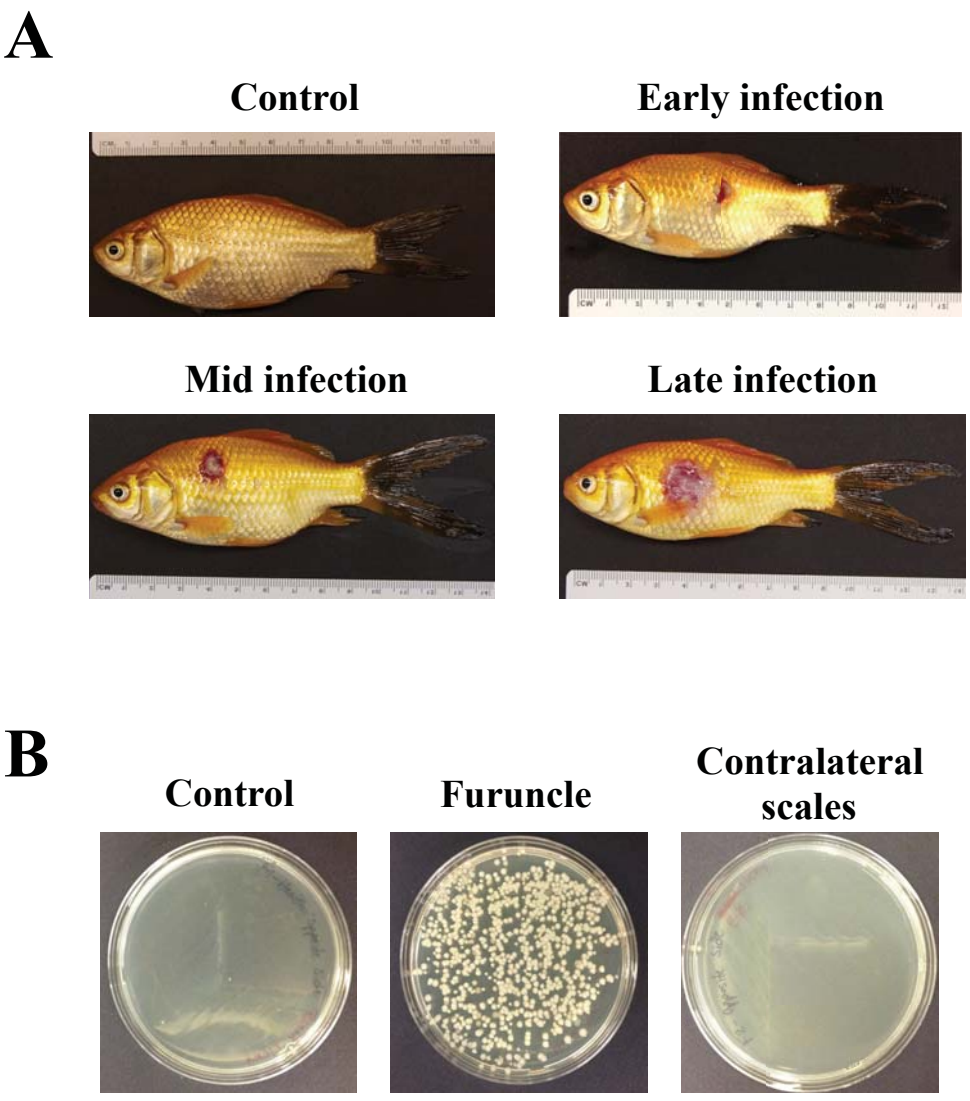

Figure 7.1. Presentation of naturally occurring *Aeromonas* infection.

(**A**) Representative images of goldfish presenting with body sores at various stages of infection. (**B**) Representative images of plates streaked from swabs of goldfish scales.

A

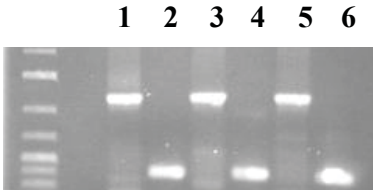

1 – 16s rRNA, Eye Furuncle Isolate
2 – gyrB, Eye Furuncle Isolate
3 – 16s rRNA, Body Furuncle Isolate
4 – gyrB, Body Furuncle Isolate
5 – 16s rRNA, Fin Furuncle Isolate
6 – gyrB, Fin Furuncle Isolate

B

Score	Expect	Identities	Gaps	Strand
926 bits(501)	0.0	501/501(100%)	0/501(0%)	Plus/Plus

```
Query  1    TCGAGCGGCAGCGGGAAAGTAGCTTGCTACTTTTGCCGGCGAGCGGCGGACGGGTGAGTA  60
            ||||||||||||||||||||||||||||||||||||||||||||||||||||||||||||
Sbjct  7    TCGAGCGGCAGCGGGAAAGTAGCTTGCTACTTTTGCCGGCGAGCGGCGGACGGGTGAGTA  66

Query  61   ATGCCTGGGGATCTGCCCAGTCGAGGGGGATAACAGTTGGAAACGACTGCTAATACCGCA  120
            ||||||||||||||||||||||||||||||||||||||||||||||||||||||||||||
Sbjct  67   ATGCCTGGGGATCTGCCCAGTCGAGGGGGATAACAGTTGGAAACGACTGCTAATACCGCA  126

Query  121  TACGCCCTACGGGGGAAAGCAGGGGACCTTCGGGCCTTGCGCGATTGGATGAACCCAGGT  180
            ||||||||||||||||||||||||||||||||||||||||||||||||||||||||||||
Sbjct  127  TACGCCCTACGGGGGAAAGCAGGGGACCTTCGGGCCTTGCGCGATTGGATGAACCCAGGT  186

Query  181  GGGATTAGCTAGTTGGTGAGGTAATGGCTCACCAAGGCGACGATCCCTAGCTGGTCTGAG  240
            ||||||||||||||||||||||||||||||||||||||||||||||||||||||||||||
Sbjct  187  GGGATTAGCTAGTTGGTGAGGTAATGGCTCACCAAGGCGACGATCCCTAGCTGGTCTGAG  246

Query  241  AGGATGATCAGCCACACTGGAACTGAGACACGGTCCAGACTCCTACGGGAGGCAGCAGTG  300
            ||||||||||||||||||||||||||||||||||||||||||||||||||||||||||||
Sbjct  247  AGGATGATCAGCCACACTGGAACTGAGACACGGTCCAGACTCCTACGGGAGGCAGCAGTG  306

Query  301  GGGAATATTGCACAATGGGGGAAACCCTGATGCAGCCATGCCGCGTGTGTGAAGAAGGCC  360
            ||||||||||||||||||||||||||||||||||||||||||||||||||||||||||||
Sbjct  307  GGGAATATTGCACAATGGGGGAAACCCTGATGCAGCCATGCCGCGTGTGTGAAGAAGGCC  366

Query  361  TTCGGGTTGTAAAGCACTTTCAGCGAGGAGGAAAGGTTGGTAGCGAATAACTGCCAGCTG  420
            ||||||||||||||||||||||||||||||||||||||||||||||||||||||||||||
Sbjct  367  TTCGGGTTGTAAAGCACTTTCAGCGAGGAGGAAAGGTTGGTAGCGAATAACTGCCAGCTG  426

Query  421  TGACGTTACTCGCAGAAGAAGCACCGGCTAACTCCGTGCCAGCAGCCGCGGTAATACGGA  480
            ||||||||||||||||||||||||||||||||||||||||||||||||||||||||||||
Sbjct  427  TGACGTTACTCGCAGAAGAAGCACCGGCTAACTCCGTGCCAGCAGCCGCGGTAATACGGA  486

Query  481  GGGTGCAAGCGTTAATCGGAA  501
            |||||||||||||||||||||
Sbjct  487  GGGTGCAAGCGTTAATCGGAA  507
```

Figure 7.2. Sequence analysis of isolated bacterial clones.

(A) Goldfish presenting with an *Aeromonas* infection were swabbed and isolated bacterial clones were analyzed for expression of 16S rRNA and gyrB. **(B)** Bands were excised and sequenced. Sequence analysis identified the bacteria to be *Aeromonas veronii* bv *sobria*.

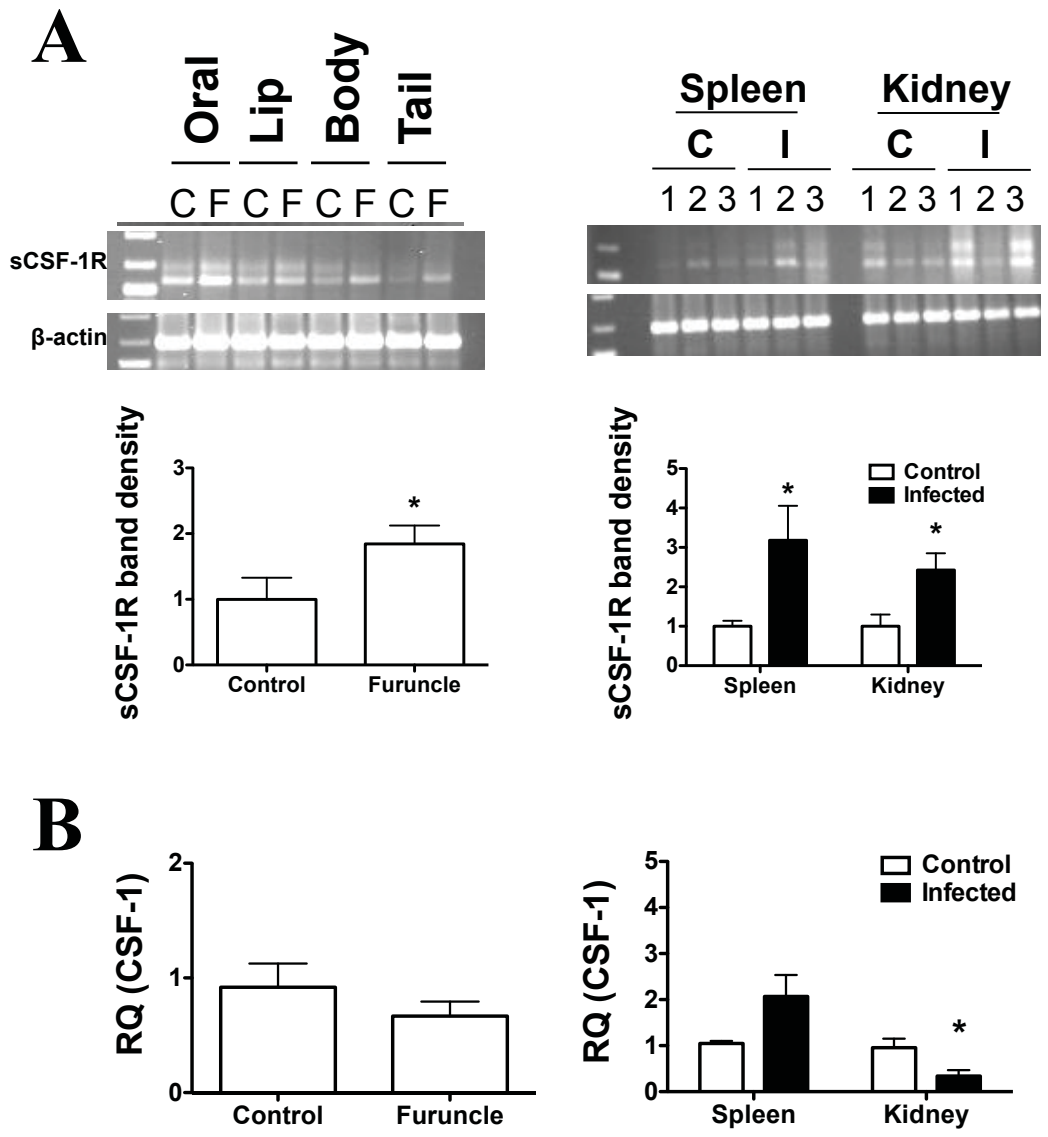

Figure 7.3. Soluble CSF-1R expression is increased in furuncle and peripheral tissues.

RNA was extracted from tissues harvested from control and naturally infected goldfish and sCSF-1R and CSF-1 expression was measured by RT-PCR and Q-PCR, respectively. n=4; * $p<0.05$, ** $p<0.01$ compared to control (Student's t-test); error bars show SEM.

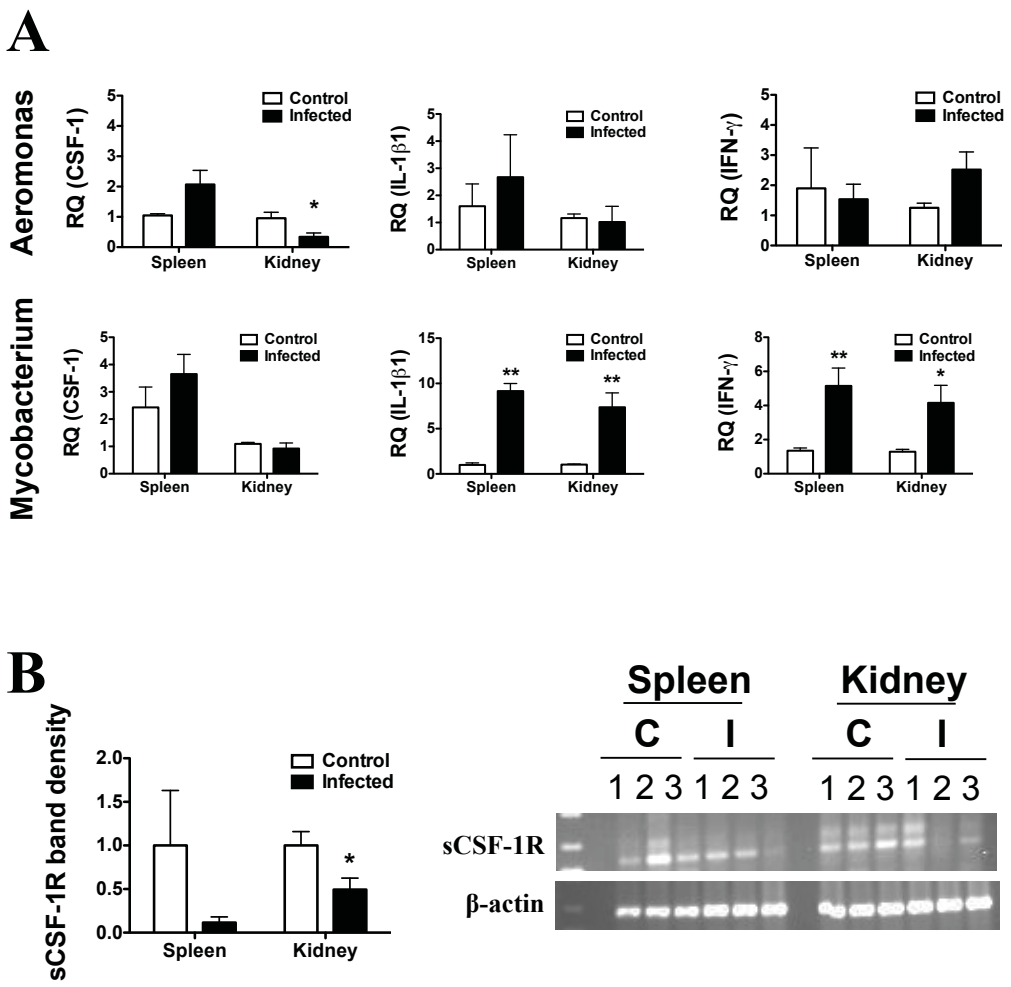

Figure 7.4. Soluble CSF-1R increases do not occur in a *Mycobacterium marinum* infection.

RNA was extracted from tissues harvested from control goldfish, naturally *Aeromonas*- infected goldfish, and goldfish with an induced *Mycobacterium marinum* infection. sCSF-1R was measured by RT-PCR. CSF-1, IL-1β1, and IFN-γ expression was analyzed by Q-PCR. n=4; * $p<0.05$, ** $p<0.01$ compared to control (Student's t-test); error bars show SEM.

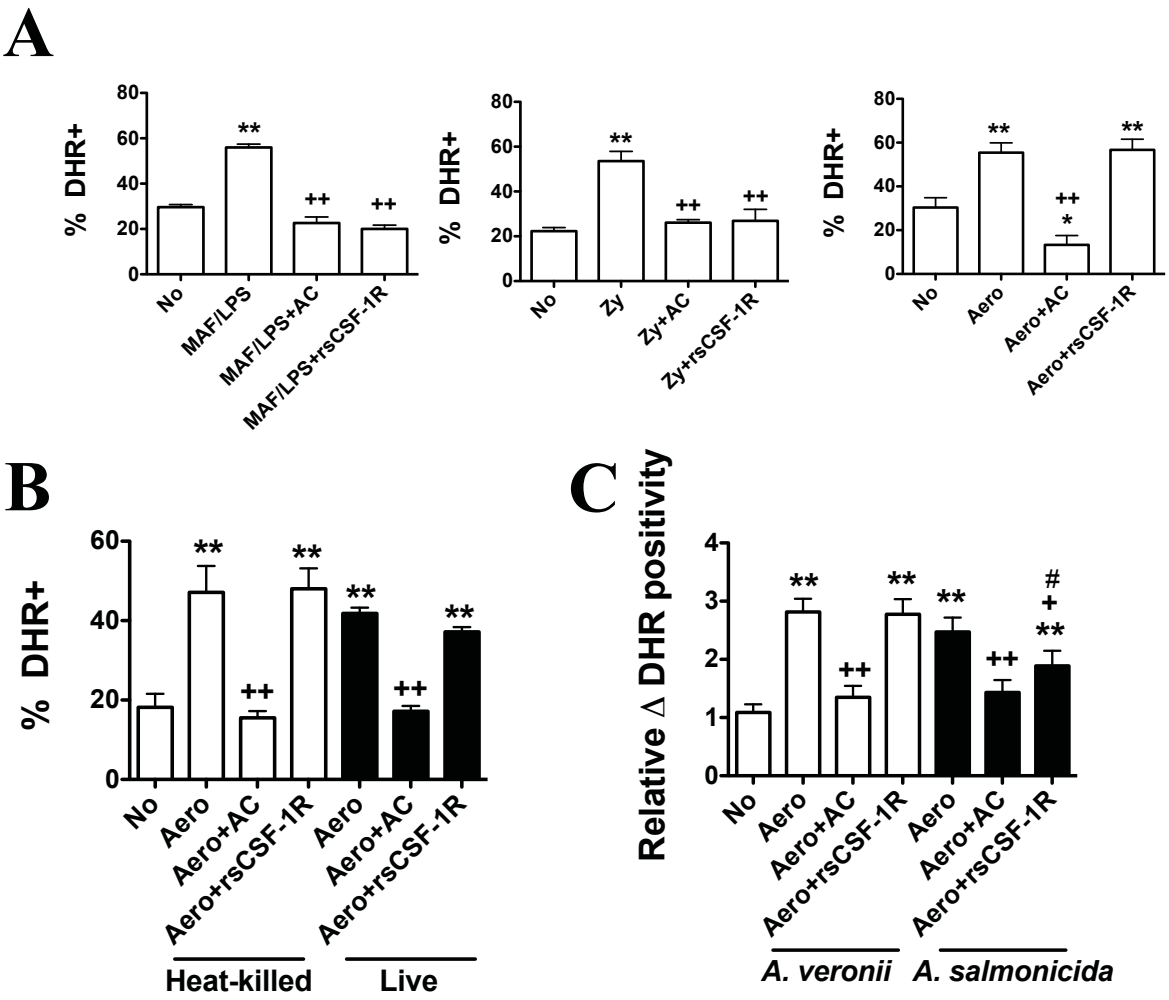

Figure 7.5. Soluble CSF-1R does not reduce *Aeromonas veronii*-induced ROS production.

(**A**) Goldfish PKM were incubated with MAF/LPS, zymosan or heat-killed *Aeromonas veronii* in the presence/absence of apoptotic cells (AC) or recombinant sCSF-1R. ROS production was measured after 2 hours. (**B**) Goldfish PKM were incubated with live or heat-killed *Aeromonas veronii* in the presence/absence of apoptotic cells (AC) or recombinant sCSF-1R. ROS production was measured after 2 hours. (**C**) Goldfish PKM were incubated with heat-killed *Aeromonas veronii* or *Aeromonas salmonicida* in the presence/absence of apoptotic cells (AC) or recombinant sCSF-1R. ROS production was measured after 2 hours. n=4; * $p<0.05$, ** $p<0.01$ compared to control; + $p<0.05$, ++ $p<0.01$ compared to Aero (One-way ANOVA; Tukey's post-hoc); error bars show SEM.

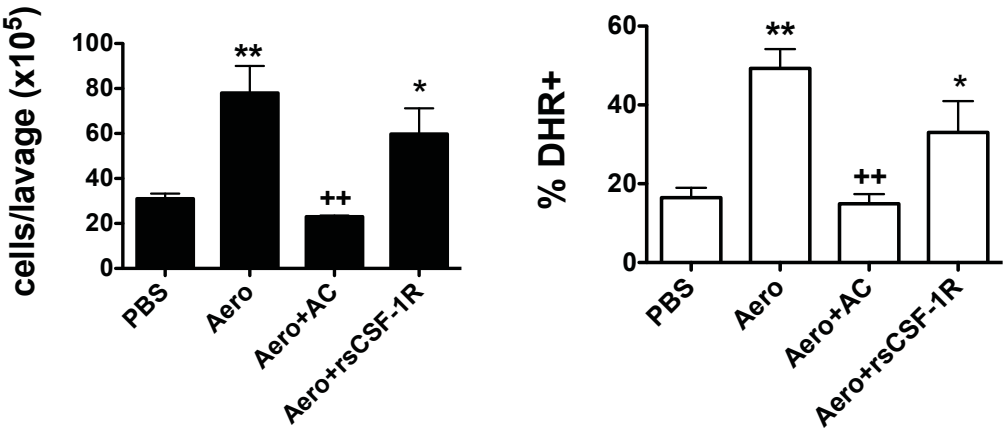

Figure 7.6. Soluble CSF-1R does not reduce *Aeromonas*-induced cellular infiltration or ROS production *in vivo*.

Goldfish were injected i.p. with heat-killed *Aeromonas veronii* in the presence or absence of either apoptotic cells (AC) or recombinant sCSF-1R. After 24 hours, peritoneal cells were harvested by lavage and counted. ROS production was measured by DHR. n=6; * $p<0.05$, ** $p<0.01$ compared to PBS; + $p<0.05$, ++ $p<0.01$ compared to Aero (One-way ANOVA; Tukey's post-hoc); error bars show SEM.

	PBS		*Aeromonas*	
Day 1				
Day 2				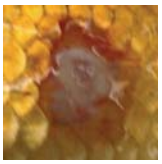
Day 4				
Day 7				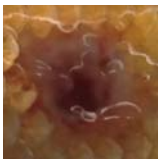
Day 10		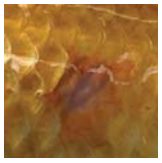		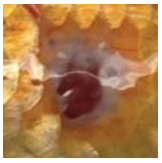
Day 14				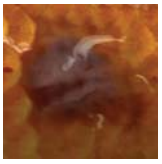

Figure 7.7. Representative images of goldfish with induced *Aeromonas veronii* infection.

Goldfish were infected with *Aeromonas veronii* by rubbing an exposed area with a swab soaked in a clonal culture. Fish were harvested at the time points indicated.

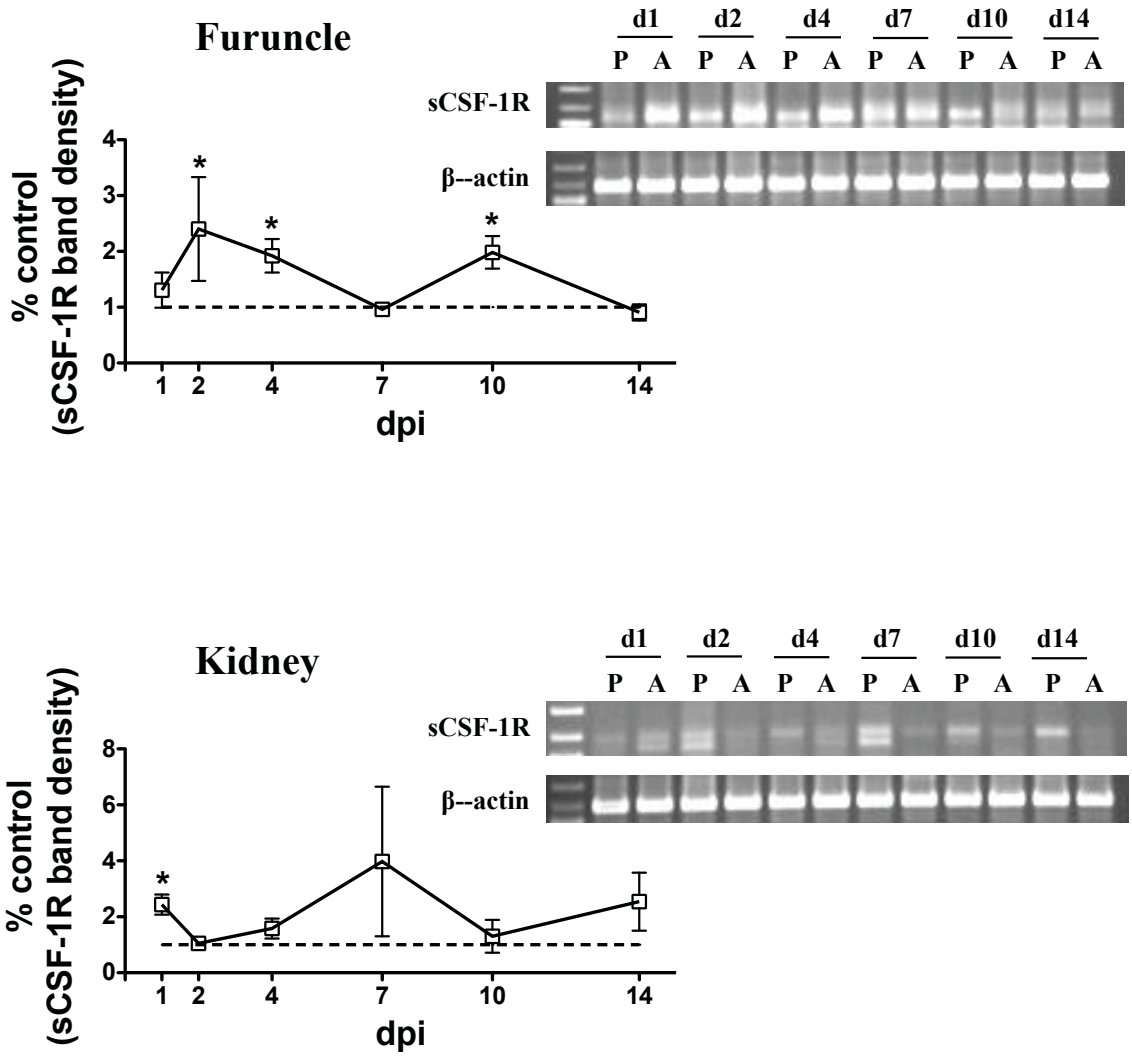

Figure 7.8. Expression of sCSF-1R in the furuncle and kidney of goldfish with induced *Aeromonas veronii* infection.

At each of the indicated time points, furuncle and kidney tissue were harvested from PBS (P) or *Aeromonas veronii* (A) infection goldfish. RNA was isolated and sCSF-1R expression was measured with the corresponding cDNA. n=3; * $p<0.05$, ** $p<0.01$ compared to PBS (One-way ANOVA; Tukey's post-hoc); error bars show SEM.

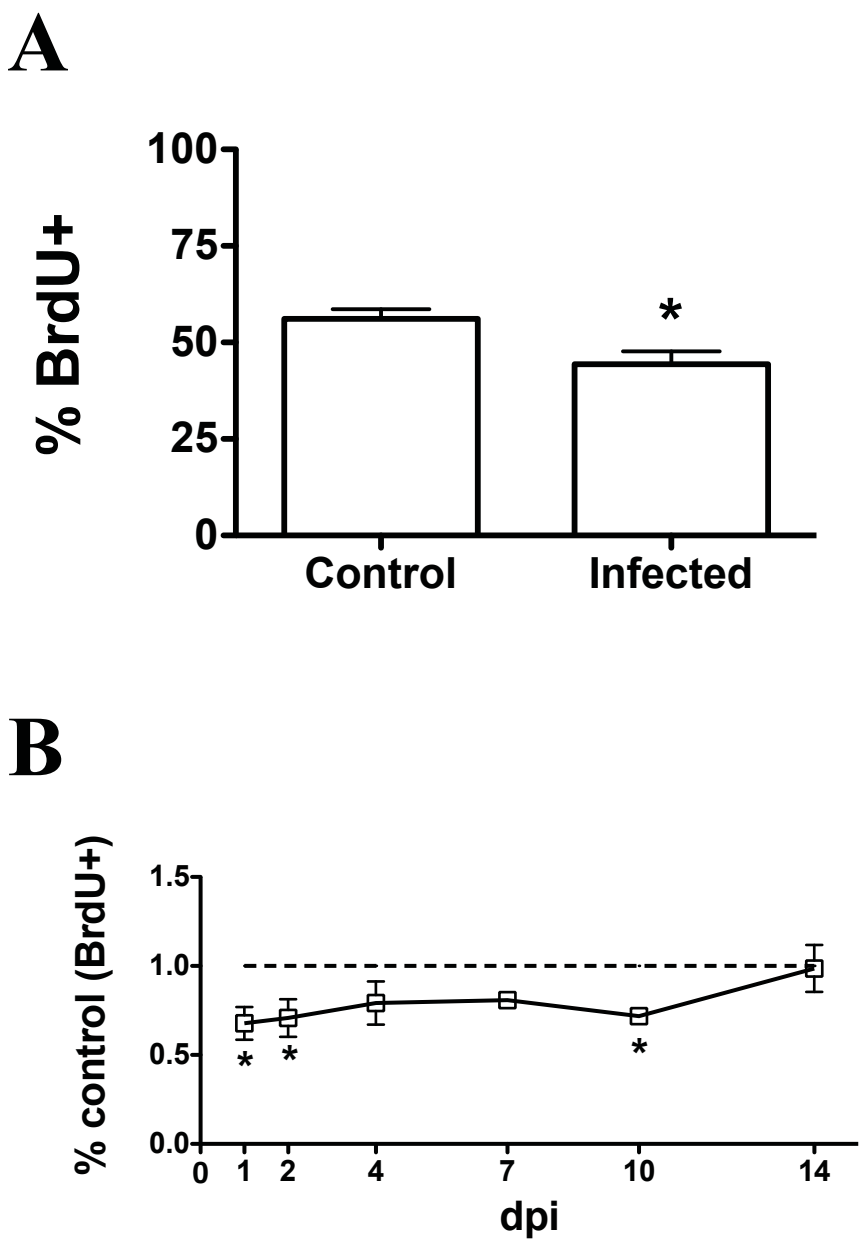

Figure 7.9. *Aeromonas* infection reduces proliferation within the kidney.

Prior to kidney harvesting, goldfish were injected i.p. with BrdU and incubated for 1 hour. Kidneys were then harvested from (**A**) naturally-infected goldfish or (**B**) goldfish with an induced infection and proliferation was measured based on BrdU incorporation. For naturally infected fish, n=8; for induced infection, n=3; *$p<0.05$ compared to control (Student's t-test for A; One-way ANOVA; Tukey's post-hoc for B); error bars show SEM.

7.4 References

1. Janda, J.M., and Abbott, S.L. 2010. The genus Aeromonas: taxonomy, pathogenicity, and infection. *Clin Microbiol Rev* 23:35-73.
2. Monette, S., Dallaire, A.D., Mingelbier, M., Groman, D., Uhland, C., Richard, J.P., Paillard, G., Johannson, L.M., Chivers, D.P., Ferguson, H.W., et al. 2006. Massive mortality of common carp (Cyprinus carpio carpio) in the St. Lawrence River in 2001: diagnostic investigation and experimental induction of lymphocytic encephalitis. *Vet Pathol* 43:302-310.
3. Joseph, S.W., and Carnahan, A. 1994. The isolation, identification, and systematics of the motile *Aeromonas* species. *Annual Review of Fish Diseases* 4:315-343.
4. Austin, B., and Autin, D. 2007. *Bacterial fish pathogens, disease of farmed and wild fish*: Springer-Praxis.
5. Bernoth, E., Ellis, A., Midtlyng, P., Olivier, G., and Smith, P. 1997. *Furunculosis Multidisciplinary Fish Disease Research*: Academic Press.
6. Hiney, M., Dawson, M.T., Heery, D.M., Smith, P.R., Gannon, F., and Powell, R. 1992. DNA probe for Aeromonas salmonicida. *Appl Environ Microbiol* 58:1039-1042.
7. Wiklund, T., and Dalsgaard, I. 1998. Occurrence and significance of atypical Aeromonas salmonicida in non-salmonid and salmonid fish species: a review. *Dis Aquat Organ* 32:49-69.
8. Noga, E. 2010. *Fish disease*: Willey-Blackwell.
9. Gustafson, C.E., Thomas, C.J., and Trust, T.J. 1992. Detection of Aeromonas salmonicida from fish by using polymerase chain reaction amplification of the virulence surface array protein gene. *Appl Environ Microbiol* 58:3816-3825.
10. Martinez-Murcia, A.J., Esteve, C., Garay, E., and Collins, M.D. 1992. Aeromonas allosaccharophila sp. nov., a new mesophilic member of the genus Aeromonas. *FEMS Microbiol Lett* 70:199-205.
11. Sreedharan, K., Philip, R., and Singh, I.S. 2013. Characterization and virulence potential of phenotypically diverse Aeromonas veronii isolates recovered from moribund freshwater ornamental fishes of Kerala, India. *Antonie Van Leeuwenhoek* 103:53-67.
12. Cai, S.H., Wu, Z.H., Jian, J.C., Lu, Y.S., and Tang, J.F. 2012. Characterization of pathogenic Aeromonas veronii bv. veronii associated with ulcerative syndrome from chinese longsnout catfish (Leiocassis longirostris Gunther). *Braz J Microbiol* 43:382-388.
13. Han, H.J., Taki, T., Kondo, H., Hirono, I., and Aoki, T. 2008. Pathogenic potential of a collagenase gene from Aeromonas veronii. *Can J Microbiol* 54:1-10.
14. Silver, A.C., Williams, D., Faucher, J., Horneman, A.J., Gogarten, J.P., and Graf, J. 2011. Complex evolutionary history of the Aeromonas veronii group revealed by host interaction and DNA sequence data. *PLoS One* 6:e16751.

15. Vega-Sanchez, V., Acosta-Dibarrat, J., Vega-Castillo, F., Castro-Escarpulli, G., Aguilera-Arreola, M.G., and Soriano-Vargas, E. 2013. Phenotypical characteristics, genetic identification, and antimicrobial sensitivity of Aeromonas species isolated from farmed rainbow trout (Onchorynchus mykiss) in Mexico. *Acta Trop* 130C:76-79.
16. Yi, S.W., You, M.J., Cho, H.S., Lee, C.S., Kwon, J.K., and Shin, G.W. 2013. Molecular characterization of Aeromonas species isolated from farmed eels (Anguilla japonica). *Vet Microbiol* 164:195-200.
17. Aires, A., Dias, C.S., Rosa, E.A., and Saavedra, M.J. 2013. Antimicrobial susceptibility of Aeromonas spp. isolated from pig ileum segments to natural isothiocyanates. *Med Chem* 9:861-866.
18. Trower, C.J., Abo, S., Majeed, K.N., and von Itzstein, M. 2000. Production of an enterotoxin by a gastro-enteritis-associated Aeromonas strain. *J Med Microbiol* 49:121-126.
19. Sha, J., Kozlova, E.V., and Chopra, A.K. 2002. Role of various enterotoxins in Aeromonas hydrophila-induced gastroenteritis: generation of enterotoxin gene-deficient mutants and evaluation of their enterotoxic activity. *Infect Immun* 70:1924-1935.
20. Krzyminska, S., Tanska, A., and Kaznowski, A. 2011. Aeromonas spp. induce apoptosis of epithelial cells through an oxidant-dependent activation of the mitochondrial pathway. *J Med Microbiol* 60:889-898.
21. Krzyminska, S., Kaznowski, A., and Chodysz, M. 2009. Aeromonas spp. human isolates induce apoptosis of murine macrophages. *Curr Microbiol* 58:252-257.
22. Krzyminska, S., Mokracka, J., Koczura, R., Cwiertnia, A., and Kaznowski, A. 2012. Aeromonas spp.-mediated cell-contact cytotoxicity is associated with the presence of type III secretion system. *Antonie Van Leeuwenhoek* 101:243-251.
23. Rio, R.V., Anderegg, M., and Graf, J. 2007. Characterization of a catalase gene from Aeromonas veronii, the digestive-tract symbiont of the medicinal leech. *Microbiology* 153:1897-1906.
24. Krzyminska, S., Kaznowski, A., and Puk, M. 2008. Interaction of Aeromonas spp. human isolates with murine macrophages. *New Microbiol* 31:481-488.
25. Janda, J.M., and Abbott, S.L. 1998. Evolving concepts regarding the genus Aeromonas: an expanding Panorama of species, disease presentations, and unanswered questions. *Clin Infect Dis* 27:332-344.
26. McCoy, A.J., Koizumi, Y., Higa, N., and Suzuki, T. 2010. Differential regulation of caspase-1 activation via NLRP3/NLRC4 inflammasomes mediated by aerolysin and type III secretion system during Aeromonas veronii infection. *J Immunol* 185:7077-7084.
27. Silver, A.C., Kikuchi, Y., Fadl, A.A., Sha, J., Chopra, A.K., and Graf, J. 2007. Interaction between innate immune cells and a bacterial type III secretion system in mutualistic and pathogenic associations. *Proc Natl Acad Sci U S A* 104:9481-9486.

28. Simon, H.U., Haj-Yehia, A., and Levi-Schaffer, F. 2000. Role of reactive oxygen species (ROS) in apoptosis induction. *Apoptosis* 5:415-418.
29. Behera, B., Bhoriwal, S., Mathur, P., Sagar, S., Singhal, M., and Misra, M.C. 2011. Post-traumatic skin and soft tissue infection due to Aeromonas hydrophila. *Indian J Crit Care Med* 15:49-51.
30. Barreda, D.R., Hanington, P.C., Stafford, J.L., and Belosevic, M. 2005. A novel soluble form of the CSF-1 receptor inhibits proliferation of self-renewing macrophages of goldfish (Carassius auratus L.). *Dev Comp Immunol* 29:879-894.
31. Hanington, P.C., Wang, T., Secombes, C.J., and Belosevic, M. 2007. Growth factors of lower vertebrates: characterization of goldfish (Carassius auratus L.) macrophage colony-stimulating factor-1. *J Biol Chem* 282:31865-31872.
32. Hanington, P.C., Hitchen, S.J., Beamish, L.A., and Belosevic, M. 2009. Macrophage colony stimulating factor (CSF-1) is a central growth factor of goldfish macrophages. *Fish Shellfish Immunol* 26:1-9.
33. Rieger, A.M., Hanington, P.C., Belosevic, M., and Barreda, D.R. 2014. Control of CSF-1 induced inflammation in teleost fish by a soluble form of the CSF-1 receptor. *Fish Shellfish Immunol*.
34. Katzenback, B.A., Karpman, M., and Belosevic, M. 2011. Distribution and expression analysis of transcription factors in tissues and progenitor cell populations of the goldfish (Carassius auratus L.) in response to growth factors and pathogens. *Mol Immunol* 48:1224-1235.
35. Webster Marketon, J.I., and Glaser, R. 2008. Stress hormones and immune function. *Cell Immunol* 252:16-26.

Chapter 8: General Discussion[1]

8.1 Overview of findings

Inflammation is a complex, biological process that occurs following activation by a noxious stimulus such as tissue injury or infection. Phagocytes are central effectors in both the induction and resolution of inflammatory programs. These cells are armed with potent antimicrobial defenses that aid in the clearance of infiltrating pathogens. They are also capable of producing a wide range of soluble mediators that instruct and shape downstream responses. However, though inflammation is generally of benefit to the host, it can also have a high cost associated with it. This includes collateral tissue damage, septic shock, and autoimmune diseases (1). As such, various mechanisms have evolved to balance these responses in order to maximize the host benefit and minimize inflammatory tissue damage.

The main focus of my Ph.D. was to characterize functional phagocyte responses that occur at inflammatory sites, where various responses are involved in the clearance of pathogens, dying or senescent cells, and in tissue repair/ wound healing. Using an *in vitro* system for culturing macrophage-lineage cells, I determined that both goldfish monocytes and macrophages were highly phagocytic

---

[1] A portion of this chapter has been previously published:

Rieger AM, Hanington PC, Belosevic M and Barreda DR. 2014. Control of CSF-1 induced inflammation in teleost fish by a soluble form of the CSF-1 receptor. *Fish Shellfish Immunol* pii: S1050-4648(14)00105-3.

(Chapter 3). Both cell types upregulated phagocytic and antimicrobial responses in a temporal fashion, dependent on the stage of differentiation (Chapter 3). However, the data presented here suggest that monocytes and macrophages may preferentially rely on different killing mechanisms: monocytes appear to favor phagolysosome fusion while macrophages have stronger, more sustained production of reactive oxygen and nitrogen species (Chapter 3). A similar dichotomy exists in mammalian macrophage-lineage cells, where it is hypothesized that maturation of macrophages leads to decreases in lysosomal proteolysis, allowing for better presentation of antigens (2). My results highlight intrinsic differences in phagocyte responses are present in teleost fish.

Mammalian macrophages are well known for their roles in both the induction and resolution of inflammatory responses. Further, mammalian macrophages are capable of internalizing both pathogenic and homeostatic/self particles, resulting in activation of vastly different macrophage responses (3, 4). In Chapter 4, I showed that teleost macrophages, similar to mammalian macrophages, downregulate inflammatory responses following exposure to apoptotic cells (5). Internalization of apoptotic cells resulted in decreased ROS production *in vitro* and *in vivo* (Chapter 4). Using a zymosan peritonitis model, I found that apoptotic cells significantly reduced infiltration of neutrophils, monocytes, and lymphocytes (Chapter 4). Interestingly, in mice, apoptotic cell addition resulted in a decrease in only the monocyte and lymphocyte populations, and not the neutrophil subset (Chapter 4), suggesting a potential role for neutrophils in the resolution of inflammatory responses. Using a purified inflammatory neutrophil population, I

found that, in mice, both neutrophils and macrophages were able to internalize apoptotic cells, resulting in decreased ROS production (Chapter 4). In goldfish, only macrophages (not neutrophils) were able to internalize apoptotic cells (Chapter 4).

Early indications suggested that responses to apoptotic cells by goldfish macrophages were partially mediated by soluble factors (Chapter 4/5). Interestingly, unlike, mammalian systems, I detected no changes in the levels of IL-10 and TGF-β (6), suggesting that a different soluble factor may be mediating these responses (Chapter 5). A candidate molecule was soluble CSF-1R. When sCSF-1R was originally characterized, the greatest levels of expression were detected in senescent macrophage cultures, where there are high levels of apoptotic cells death (7). In addition, the native sCSF-1R protein was detected in goldfish serum (7), which suggested that this protein might also play a role in systemic regulation in addition to its role in regulating proliferation within the hematopoietic compartment. When goldfish macrophages were exposed to apoptotic cells either *in vitro* or *in vivo*, expression of sCSF-1R transcript is greatly increased (approximately 3-fold) (Chapter 5) (6). *In vivo*, the expression of sCSF-1R within peritoneal cells is highest during the resolution of acute peritonitis, peaking after cellular infiltration when the levels of apoptotic cell death are highest (Chapter 5). This increase in expression is maintained following resolution of peritonitis (Chapter 5).

In vitro, addition of recombinant sCSF-1R reduced phagocytic responses, production of reactive nitrogen and oxygen species, and chemotaxis in

macrophages activated with either CSF-1 (8) or zymosan (Chapter 5/6) (6). *In vivo*, recombinant sCSF-1R exerted a potent downregulatory effect on zymosan-induced ROS production that is dose dependent (6) and reduces inflammatory ROS responses to a similar degree as found with apoptotic cells (5) (Chapter 6). I also found an *in vivo* reduction in macrophage phagocytic responses that culminates in a reduced capacity to kill bacteria (*Aeromonas veronii*) (Chapter 6).

Within an inflammatory site, macrophages are known to produce a wide range of soluble products that are important in recruiting cells and instructing responses of responding cells. As inflammatory processes resolve, there is a drive to switch off pro-inflammatory factors while increasing anti-inflammatory factors. When studying a panel of pro-inflammatory goldfish cytokines, I found that recombinant sCSF-1R greatly reduced zymosan-induced production of a wide range of cytokines, including TNF-α 2, IL-1β 1 and 2, IFNγ and IFNγrel (IFNγ-related), IL12p35, and CSF-1 (Chapter 6). The effects of apoptotic cells appear to be targeted to a more select group of pro-inflammatory cytokines (TNF-α 2, IFNγrel, and IL-12p35). Interestingly, while the presence of apoptotic cells induced a slight increase in IL-10 expression, no change was induced by sCSF-1R (Chapter 6), suggesting that sCSF-1R may be important in down-regulating inflammatory processes but may not directly activate anti-inflammatory mechanisms.

In addition to reducing inflammatory macrophage responses, recombinant sCSF-1R also dramatically decreased zymosan-induced leukocyte infiltration into the peritoneal cavity (6) (Chapter 6). Interestingly, sCSF-1R appeared to preferentially affect neutrophil infiltration, since, even at the highest doses of

recombinant sCSF-1R, lymphocytes and monocytes are present at higher levels than in control fish (6) (Chapter 6). This is unlike apoptotic cells, which targets the infiltration of all three leukocyte subsets to a similar extent (5) (Chapter 4). When I measured the *in vivo* expression of chemokines by quantitative PCR, I found that sCSF-1R dramatically reduced levels of CXCL-8, the primary chemokine involved in neutrophil recruitment, and had only a modest effect on expression of CCL-1, the recruiter of lymphocytes and monocytes (Chapter 6). Interestingly, the neutrophils that at still recruited into the inflammatory site maintain their ROS production capacity in fish injected with sCSF-1R, but not those injected with apoptotic cells (Chapter 6). However, following injection with sCSF-1R or apoptotic cells, the recruited neutrophils exhibit a reduced capacity to kill bacteria (Chapter 6).

Using an *Aeromonas* model, I found that infection, either natural or induced, resulted in significant increases in sCSF-1R expression both at the site of infection and distally in the kidney and spleen (Chapter 7). Interestingly, addition of sCSF-1R *in vitro* or intraperitoneally did not reduce *Aeromonas*-induced inflammatory responses, namely ROS production and leukocyte infiltration (Chapter 7). However, I found a significant decrease in kidney cell proliferation (Chapter 7), suggesting that *Aeromonas*-induced expression of sCSF-1R may affect the hematopoietic compartment, possibly compromising host responses to this pathogen.

Overall, my data suggests that sCSF-1R is produced at time when either [1.] CSF-1 production is high or [2.] there are high levels of apoptotic cell death. The

presence of sCSF-1R then drives the inflammatory process towards resolution by targeting inflammatory macrophage processes (Figure 8.1). Because of the mode of action of sCSF-1R (binding CSF-1 and preventing interaction with membrane bound CSF-1R), sCSF-1R can only block macrophage actions that require or are downstream of CSF-1. By understanding the macrophage actions that are controlled by sCSF-1R, we then not only gain an understanding of the role of sCSF-1R in macrophage survival, proliferation, differentiation, and regulation of immunity, we also gain a better appreciation of the varied roles of CSF-1 in immune processes. My work places CSF-1 as a central component of teleost inflammatory responses, being important in activating downstream processes that direct leukocyte responses. As a primary regulator of CSF-1 activity, sCSF-1R has become integrated at all levels of macrophage actions, from controlling proliferation and differentiation to inducing the resolution of inflammation, with the outcomes of its actions extending past macrophages.

8.2 Evolution of inflammatory control mechanisms

Responses to an inflammatory stimulus activate a complex web of interactions between phagocytes and other immune cells throughout the response, from induction to resolution (9-13). Apoptotic cell internalization has been recognized as an important switch between inflammatory and repair programs (4). All organisms have mechanisms in place to maintain integrity, both structural and physiologically, following injury or disruption. Tissue repair, wound healing, and regeneration are necessary for the long-term survival of an organism. It is therefore

reasonable to hypothesize that repair mechanisms are evolutionarily ancient. For my thesis, I have focused on the role of apoptotic cells in downregulating inflammatory responses. A comprehensive discussion of this can be found in Chapter 4. This section will focus on outcomes of apoptotic cell phagocytosis across a range of species, bringing in the impact on inflammatory control where this is currently known, to gain a wider evolutionary appreciation of this process. A summary of our current understanding can be found in Figure 8.2.

Genetic studies in *Caenhorhabditis elegans* have identified two partially conserved pathways involved in the internalization of apoptotic cells that are highly conserved (13-16). Interestingly, in *C. elegans*, apoptotic cells (called "cell corpses") are rapidly engulfed by neighboring cells and generally not by professional phagocytes (17-19). Internalized corpses, similar to mammalian phagocytes, are enclosed within a phagosome that fuses with lysosomes to form a phagolysosome (20). In *C. elegans*, this is dependent on *arl-8* expression; loss of function of this gene results in accumulation of cell corpses and decreased degradation (20). When a pathogen is sensed by *C. elegans* pattern recognition receptors, a cascade of inducible defense mediators is initiated, including antimicrobial peptides, caenopores, lysozymes, lectins, and ROS (21). The mechanisms induced are pathogen- and tissue specific (21). This split in functions suggests that phagocytes of *C. elegans* may not have the capacity to induce divergent responses to pathogenic or homeostatic particles at the level of a single cell. This, however, has not been studied yet.

Drosophila has proven to be a powerful model organism for the study of a variety of biological processes. Within their immune system, three major types of hemocytes have been identified: plasmatocytes, crystal cells, and lamellocytes (22, 23). Of these, plasmatocytes are most similar to mammalian phagocytes and are involved in phagocytosis of invading pathogens, clearance of apoptotic cells, and tissue repair/wound healing (22, 23). These cells are able to mount a number of defenses, including production of antimicrobial peptides, nitric oxide, and ROS, induce blood coagulation, and produce cytokine-like molecules (24-26). Crystal cells also participate in wound healing, involved in formation of scabs (26). Unlike *C. elegans*, phagocytosis of both pathogens and apoptotic cells is carried out by hemocytes (27, 28). Similar to mammalian macrophages, the recognition and internalization of apoptotic cells appears to involve phosphatidylserine (29). Further, current work from the Barreda lab has shown that *Drosophila* hemocytes are capable of internalizing bacteria and apoptotic cells at a single cell level (Wong, M.E., unpublished observation). Functional outcomes of phagocytosis of both apoptotic cells and pathogenic particles are currently unknown.

Lamprey, along with hagfish, are thought to be the earliest known vertebrates. Unlike invertebrates, which appear to possess only innate immune systems, lampreys possess both innate and adaptive immune systems. The lamprey adaptive immune system, however, is different from that found in higher vertebrates, consisting of lymphocyte-like cells that express somatically diversified clonal variable lymphocyte receptors (VLRs) (30). Recent work from the Barreda lab has shown that lamprey phagocytes are capable of internalizing both pathogenic

and homeostatic particles (31). Similar to goldfish, internalization of apoptotic cells significantly reduces ROS production from lamprey phagocytes (31). However, unlike goldfish, lamprey phagocytes appeared to by pre-disposed to have strong responses to the internalization of apoptotic cells, and were less responsive to the presence of zymosan (31). Internalization of a single apoptotic cell by lamprey phagocytes was able to significantly reduce responses to zymosan, even when 3-fold more zymosan was internalized (31). In goldfish, a similar downregulation in responses was only observed when the number of internalized apoptotic cells outnumbered zymosan 3:1 within an individual phagocyte (31). These data suggest that a primary method of regulating inflammatory responses in lamprey may be due to a shift in the balance of pro- and anti-inflammatory responses, with anti-inflammatory responses being favored.

During my thesis work on goldfish, I found two main mechanisms by which goldfish appear to regulate inflammatory responses. The first is through the production of a novel receptor: soluble CSF-1 receptor. This is extensively discussed in Chapters 5 and 6 and reviewed in Chapter 8, so will not be covered here. Another mechanism appears to involve leukocyte recruitment. During an acute peritonitis response, I found that neutrophils were recruited early in the response, followed by a rapid reduction in neutrophil recruitment. Since goldfish neutrophils do not appear to reduce inflammatory responses in the presence of apoptotic cells (Chapter 4), it stands to reason then that reduced recruitment is a primary mechanism whereby neutrophil inflammatory responses can be controlled.

Frogs, during metamorphosis, undergo a drastic change, involving significant amounts of apoptotic cell death in the tail and body muscle. Macrophages are known to be present in the body and tail muscles during active metamorphosis and phagocytosis apoptotic muscle cells (32). Frog macrophages are also known to be highly involved in immune defenses, providing protection against pathogens and activating adaptive immune defenses (33-35). However, currently no comprehensive work has studied frog macrophage responses when both apoptotic cell and pathogenic particles are internalized. Interestingly, in salamanders, it has recently been shown that infiltration of macrophages into a site of limb regeneration is essential to the regeneration process (36). Further, the cells recruited to the site are highly phagocytic (36).

In mice, it has been well documented that internalization of apoptotic cells by macrophages results in important changes in phenotype- the macrophages decrease production of pro-inflammatory cytokines and chemokines, reduce production of inflammatory antimicrobial factors, and increase production of anti-inflammatory mediators (3, 9, 37-42), thereby promoting the resolution of inflammatory responses. Classically, neutrophils, due to their vast armamentarium of antimicrobial defenses and short life span, have been thought to contribute only to the induction of inflammation and pathogen clearance. It is becoming clear, however, that they also actively participate in the control of inflammation. As shown in Chapter 4 and summarized in Figure 8.3, murine neutrophils are able to internalize apoptotic cells, leading to decreased ROS production (5). This appears to be a relatively newly evolved feature of neutrophils as it has only been found

noted so far in murine (5) and human neutrophils (43). Murine neutrophils are also capable of producing resolution-promoting mediators such as lipoxins from arachidonic acid, which attenuate inflammatory responses (44). This suggests that, over evolution, neutrophils have acquired the capacity to aid macrophages in the resolution of inflammation. This added complexity of phagocyte-mediated inflammatory control has the potential to increase the efficiency of resolution responses. However, as systems gain in complexity, there tend to be more points at which the system can fall apart or lose regulation. Inappropriate regulation of inflammatory responses, especially during aging, may explain the increase in diseases of affluence and extended lifespan that have a chronic inflammatory component such as cardiovascular disease, obesity, neurodegenerative diseases, and cancer (45-51).

Wound healing and tissue repair are essential for the long-term survival and growth of an organism. As shown by the candidate species outlined above, there is a varied array of responses by which phagocytes participate in the process of wound healing, following the recognition of apoptotic cells. Through evolution, these responses have become highly integrated and interdependent, leading to increasing complexity in this process. Further, it is becoming increasingly apparent that macrophage responses to pathogenic and homeostatic, self particles have been well conserved across evolution while neutrophils appear to be acquiring a capacity to actively participate in resolution events over evolution.

8.2.1 Apoptotic cells vs. exosomes

During the process of apoptosis, cells undergo a number of morphological changes including cell shrinkage and rounding, chromatin condensation, and organelle fragmentation (52). The cellular contents are then packaged up into several vesicles- the apoptotic bodies- that are then phagocytosed (53, 54). In order to be phagocytosed, these apoptotic bodies are identified by the presence of several "eat me" signals on the surface (53-55), as discussed in Chapter 1. Apoptotic bodies are just one type of extracellular vesicle released from the plasma membrane. Almost all cells release vesicles, also known as exosomes, which have a variety of physiological effects. It is important to note that the protein and lipid composition of exosomes is different from apoptotic bodies (56). Exosomes are derived from the membrane of living cells and contain various molecules, including adhesion molecules, membrane trafficking molecules, cytoskeleton molecules, heat shock proteins, cytoplasmic enzymes, signal transduction proteins, cytokines, chemokines, proteinases, cell-specific antigens, mRNA, non-coding RNAs, microRNAs, and extra-chromosomal DNA (56). Exosomes are found in plasma and other body fluids and are important for intercellular communication, especially within the immune system (56). These vesicles have been shown to mediate immune stimulation and suppression, and have been implicated in pathologies from infections, inflammation, and autoimmunity (56). Because they are derived from living membranes, exosomes are not recognized by the same "eat me" signals as apoptotic bodies. Further, exosomes tend to be much smaller in size (30-100 nm vs. 1 μm); as such the contents of exosomes tend to enter cells through either endocytosis or fusing with the plasma membrane (56). Therefore, it is

unlikely that immune suppression by exosomes or any potential roles of exosomes in resolving inflammation occur through similar mechanisms induced by apoptotic cells/bodies.

8.3 Soluble CSF-1R and self-renewing macrophages: potential for inflammatory control

When originally characterized, soluble CSF-1R was most highly expressed in progenitor cells and mature macrophages, the two populations in primary kidney macrophage cultures that are capable of self-renewal (7). While self-renewal is a common characteristic of progenitor/ hematopoietic stem cells, this feature is generally lost following terminal differentiation. However, it is becoming increasingly apparent that self-renewing macrophages exist in mammals, as well as goldfish. It is now thought that major macrophage populations derived from embryonic progenitors are able to renew independent of hematopoietic stem cells and can respond to stimuli indefinitely without loss of functional differentiation (57). Under homeostatic conditions, self-renewing macrophage populations have a low level of proliferation (57). Under stress or challenge conditions, an increased proliferative response is induced (57). This feature appears to be due to a continued induction of proliferation by CSF-1 in mature macrophages. In non-self renewing macrophages, CSF-1 generally enhances survival but no longer promotes proliferation (58). There is a strong phenotypic similarity between self-renewing macrophages in mammals and mature/ alternative pathway macrophages in goldfish- both maintain their proliferative capacity and are highly responsive to

CSF-1 (59). Interestingly, goldfish mature/ alternative pathway macrophages are also capable of producing CSF-1, in addition to sCSF-1R, allowing these cells to regulate induction and suppression of proliferative responses (60). It will, then, be interesting to determine if mammalian self-renewing macrophages have a similar, self-contained mechanism(s) of regulation.

There is increasing evidence in mammalian literature showing the need for macrophage proliferation within a site of infection (61-63). Local proliferation of tissue-resident macrophages is transient and intense, and occurs following recruitment of inflammation-associated macrophages (61). This proliferative burst is dependent on CSF-1 (62). Interestingly, it has also been shown that inflammatory macrophages recruited from bone-marrow precursors are also capable of proliferation during the resolution phase of inflammation, also in a CSF-1-dependent manner (62). Based on this, it has been hypothesized that the role of CSF-1 in the resolution of inflammation is thought be dual: [1.] re-establishing the tissue resident- macrophage population in a tightly governed manner that is restricted once normal tissue macrophage numbers has been restored (61); and [2.] maintaining the continued presence of inflammatory macrophages to control pathogens or injury (62). The dynamics of proliferation induced by CSF-1 in these two seemingly opposite types of macrophages is of critical importance, especially given the strong link to fibrosis (excessive activity of resident tissue macrophages?) and chronic inflammatory disease (excessive activity of inflammatory macrophages?). It is interesting to speculate a role of a putative sCSF-1R in this system, as a potential regulator of proliferation in these disparate

macrophage populations. Further, it will be of interest to determine if self-renewing macrophages exist *in vivo* in goldfish, and what role sCSF-1R has in regulating both the proliferation and inflammatory responses of this population.

8.4 *Aeromonas*-driven modulation of the inflammatory response: implications for host defenses

Aeromonas is a highly virulent pathogen that, depending on the bacterial species, can infect a range of hosts. In fish, infections are most prominent during times of stress, including changes in water temperature, water quality or hormone levels. In humans, infections are most common following traumatic tissue injury or in immune-compromised individuals. *Aeromonas* species possess a vast repertoire of virulence factors and host evasion strategies, which are covered in Chapter 1. One main protective mechanism appears to be induction of apoptosis in macrophages (64-66). Inducing apoptosis in members of the myeloid phagocyte family is a common virulence mechanism of several successful bacterial pathogens (67-69). When an overwhelming amount of apoptosis occurs at a site of infection, it is common for non-cleared apoptotic cells to progress to secondary necrosis (70), especially in the presence of extensive pathogen-induced macrophage apoptosis (71). Within a site of infection, this is an efficient, self-amplifying mechanism that benefits the pathogen in two distinct ways: [1.] clearance of macrophages (by apoptosis) and neutrophils (by secondary necrosis) protects the bacteria from potent anti-microbial defenses of phagocytes; and [2.] lysis of neutrophils during secondary necrosis results in release of potent molecules that increase damage and

contribute to infection associated pathology (71). During an *Aeromonas* infection, furunculation coincides with inflammation and large-scale cell death. Interestingly, there is also a significant increase in sCSF-1R expression (Chapter 7). While this may be due to the presence of apoptotic cells, its expression may amplify the protective effects of *Aeromonas*-induced macrophage apoptosis for the pathogen- macrophages within site are either undergoing apoptosis or less efficient at phagocytosing and killing *Aeromonas* due to the effects of sCSF-1R (Chapter 6). Thus, apoptosis of macrophages is likely highly beneficial to the establishment of infection and subsequent tissue infection that occurs during furunculation.

Interestingly, I also noted an increase in sCSF-1R expression within the kidney of infected fish (Chapter 7). This increase likely cannot be explained by apoptotic cell death. While it is currently unclear what is inducing this increase, the expression of sCSF-1R within the kidney coincides with a decrease in hematopoietic proliferation (Chapter 7). Previously, it has been reported that infection with *Aeromonas salmonicida* significantly alters the expression patterns of transcription factors important to myeloid cell development (72). Specifically, it was found that during infection expression of *runx1*, *cmyb*, and *egr* decreased, while expression of *pu.1* and *cjun* increased (72). *Runx1* and *cmyb* are involved in proliferation and maintenance of progenitor cells (73). *Egr* and *cjun* are important for monocyte/macrophage differentiation (74). *Pu.1* expression is necessary for myeloid fate decision (75). It has been hypothesized that these changes may shift cells within the kidney towards early myeloid committed progenitors, followed by either an arrest in commitment/progression or mobilization of myeloid cells that

are not fully differentiated (72). It will be of great interest to determine if *Aeromonas veronii* infection also results in changes to transcription factor expression. Arrest in commitment combined with decreased proliferation may allow *Aeromonas* to subvert defenses within the kidney and aid in colonization. Therefore, it will be interesting to determine if expression of sCSF-1R within the kidney contributes to *Aeromonas* colonization through the modulation of hematopoiesis, thereby subverting host immune responses.

8.5 Future Directions

8.5.1 Neutrophil-driven inflammatory control in goldfish

In Chapter 4, I showed that goldfish neutrophils did not have the capacity to internalize apoptotic cells. However, neutrophils incubated in the presence of apoptotic cells produced soluble factors that decreased ROS responses in monocytes and macrophages. It is currently unknown what these factors are. Further, though neutrophil recruitment is temporally regulated (in zymosan peritonitis, occurs between 18-24 hours), the neutrophils that remain within the peritoneum after this time reduce ROS production while still maintaining phagocytic responses. The role of these neutrophils remaining within the site is currently unknown but it is hypothesized that they play a dual role: [1.] aid in resolution of inflammation through the production of soluble factors, likely lipid mediators involved in resolution responses, such as lipoxins and resolvins; and [2.] provide protection against remaining pathogens or secondary infections that may challenge a host following an inflammatory response. This topic is currently the

focus of the Ph.D. research of a current Barreda lab student J.J. Havixbeck. I predict that, even though they lack the capacity to internalize apoptotic cells, goldfish neutrophils are highly integrated into resolution responses and aid in repair processes.

8.5.2 Does sCSF-1R promote long-term survival of *Aeromonas* within host tissue?

At the end of Chapter 7, I mentioned that fish with *Aeromonas* infections, either natural or induced, had significant decreases in proliferation. A next logical step is to determine if, similar to *Aeromonas salmonicida* infections, there is a change in transcription factor expression in *Aeromonas veronii* infected fish. This may give an indication as to which progenitor populations are being affected during an infection. To determine if these changes are due to the infection itself or to the increase in sCSF-1R expression in the kidney, goldfish will be injected with recombinant sCSF-1R into the caudal vein. Kidney proliferation and transcription factor expression can then be analyzed for changes.

Aeromonas salmonicida infections have been shown to result in long-term infection of several tissues, including the kidney, that can last for up to 2 years. To determine if sCSF-1R contributes to survival of *Aeromonas veronii* in the kidney, goldfish will be infected using the scale-scraping method. These fish will then be injected with sCSF-1R or anti-sCSF-1R antibodies early in the infection process (multiple injections between day 0 and day 7, the day the peak furunculosis). Colony forming units in the kidney will be determined on various days, from day 0

to day 56 post-infection (or later). If sCSF-1R aids in survival, it would be expected that CFUs of *Aeromonas* will increase in fish injected with sCSF-1R and decrease in fish injected with antibodies against sCSF-1R. There is a possibility, however, that the antibody raised against sCSF-1R will affect the function of membrane bound CSF-1R on resident macrophages, impeding the action of macrophages and aiding in colonization of *Aeromonas*. These studies are currently underway in the Barreda lab, being conducted by M.E. Wong. I predict that *Aeromonas* co-opts the CSF-1 system to its advantage, essentially inducing a short-term, localized, pseudo-immunocompromisation necessary for infection. By inducing high levels of sCSF-1R expression, *Aeromonas* effectively decreases the efficacy and efficiency of macrophage responses and generation, allowing *Aeromonas* to gain a foothold and overcome host defenses, leading to long-term survival within the host. In the absence of such disruption, I believe that *Aeromonas* infections would be rapidly cleared by the host.

8.5.3 Detection of sCSF-1R outside of teleosts

To date, sCSF-1R has only been identified in teleosts- goldfish and zebrafish (Lund, J.M., M.Sc. thesis 2012). Based analysis of the splice site sequence variations in the Exon4/Intron4 boundary and the presence of the hydrophilic tail, it is predicted that sCSF-1R may also exist in Japanese medaka, Xenopus, chicken, mouse, horse, gorilla, and human (Lund, J.M., M.Sc. thesis 2012). We have previously attempted to identify native sCSF-1R in mice using RACE-PCR in basal and LPS injected mice (Rieger, A.M. and Tam, J., unpublished data). These

attempts identified a potential transcript but this transcript did not have a poly-A tail. Given the significant increase in sCSF-1R infection induced by *Aeromonas*, it may be worth using a murine *Aeromonas veronii* infection model to hypothetically increase sCSF-1R expression within the mouse as well. This may aid in detection. It is also possible that, similar to phagocytic B cells, sCSF-1R plays a much more focused role in mammalian compared to piscine immune systems. As such, it is worth attempting to detect sCSF-1R within tissues that require specialized modulation of macrophage responses such as the brain or liver. Once/if sCSF-1R is found in mice and a recombinant protein is generated, it will be interesting to determine if murine sCSF-1R is also capable of modulating inflammatory responses or if it plays a more specialized role. I predict that sCSF-1R will have a limited, highly specialized role in the mammalian immune system. I think it will be localized to areas with a high density of self-renewing macrophages and will be involved in regulating the generation of these cells.

8.6 Relevance

8.6.1 To basic biology

Colony stimulating factor-1 is central to a number of processes, including survival and maintenance of macrophage-lineage cells, and in inflammatory processes. Through the study of CSF-1 and factors regulating the action of CSF-1 (ie. sCSF-1R), we will gain a better understanding of how the CSF-1 system induces inflammation and regulates phagocytes throughout an inflammatory reaction. Further, by studying the actions of CSF-1 from an evolutionary

perspective, we will gain added information on the highly conserved mechanisms of CSF-1 action, allowing identification of critical roles of this important cytokine.

8.6.2 To aquaculture

One of the greatest challenges in aquaculture is mass death caused by infections. *Aeromonas* infections are commonly associated with mass death outbreaks. As such, gaining a better understanding of mechanisms of immune evasion and modulation employed by this pathogen may lead to the development of novel strategies for disease prevention.

8.6.3 To medicine

Currently, there are a number of therapeutic inhibitors are being developed against *c-fms*, or CSF-1R. These include Ki20227 (bone metastasis), GW2580 (rheumatoid arthritis), SB1578 (rheumatoid arthritis), and PLX5622 (rheumatoid arthritis) (76-79). Other therapeutics targeting the CSF-1 system are being developed for interventions against infections, other autoimmune disorders, various cancers, and a range of inflammatory conditions (80). The potential, therefore, exists that an sCSF-1R-like therapeutic could be beneficial to a range of medically relevant diseases.

8.7 Summary

The main objective of my Ph.D. was to characterize functional phagocyte responses that occur at inflammatory sites. I specifically focused on responses that

occur at the boundary between inflammation and resolution. My research has expanded our current knowledge of inflammatory control on goldfish and mice, highlighting important roles for phagocytes in each species. Further, the identification of sCSF-1R as a central regulator of inflammation in goldfish has advanced our understanding of the importance of the CSF-1 system in inflammation and opens the door for potential applications not only to aquaculture, but to human therapeutics as well.

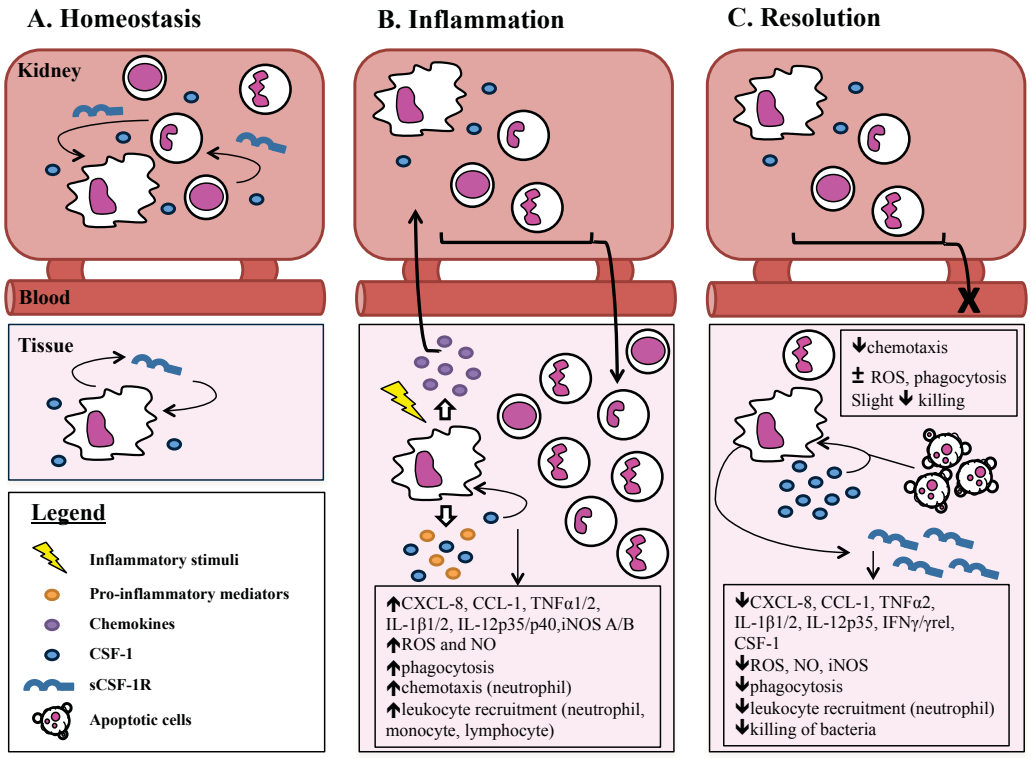

Figure 8.1. Summary of roles of CSF-1 and sCSF-1R in homeostasis, inflammation and the resolution of inflammatory processes.

(**A**) Within the kidney, the primary hematopoietic organ, a fine balance exists between CSF-1 (blue circle) and sCSF-1R (blue) to maintain the pool of progenitors and support differentiation and proliferation of monocytes and macrophages to meet the demands of the host. Within peripheral tissues, CSF-1 and sCSF-1R maintain tissue macrophages in a homeostatic state. (**B**) When tissue macrophages are triggered by an inflammatory stimuli (injury, infection), the resident tissue macrophage responds by producing increased levels of CSF-1 (blue), as well as a number of pro-inflammatory cytokines (orange circles) and chemokines (purple circles). The increased expression of CSF-1 feedback on the macrophage, resulted in the actions listed above. The other inflammatory factors produced as influence and direct the responses of both the resident tissue macrophages and the infiltrating leukocytes. (**C**) As the inflammatory process continues, the increase in CSF-1 and/or increasing numbers of apoptotic cells triggers macrophages to produce high levels of sCSF-1R. This results in the initiation of resolution events, primarily those outlined above. These actions, however, appear to be targeted largely towards macrophage-lineage cells as other phagocytes remaining in the site (neutrophils) maintain their capacity to mount ROS, phagocytic and killing responses. This would allow responses to any remaining infectious stimuli within the site while still promoting resolution of inflammation.

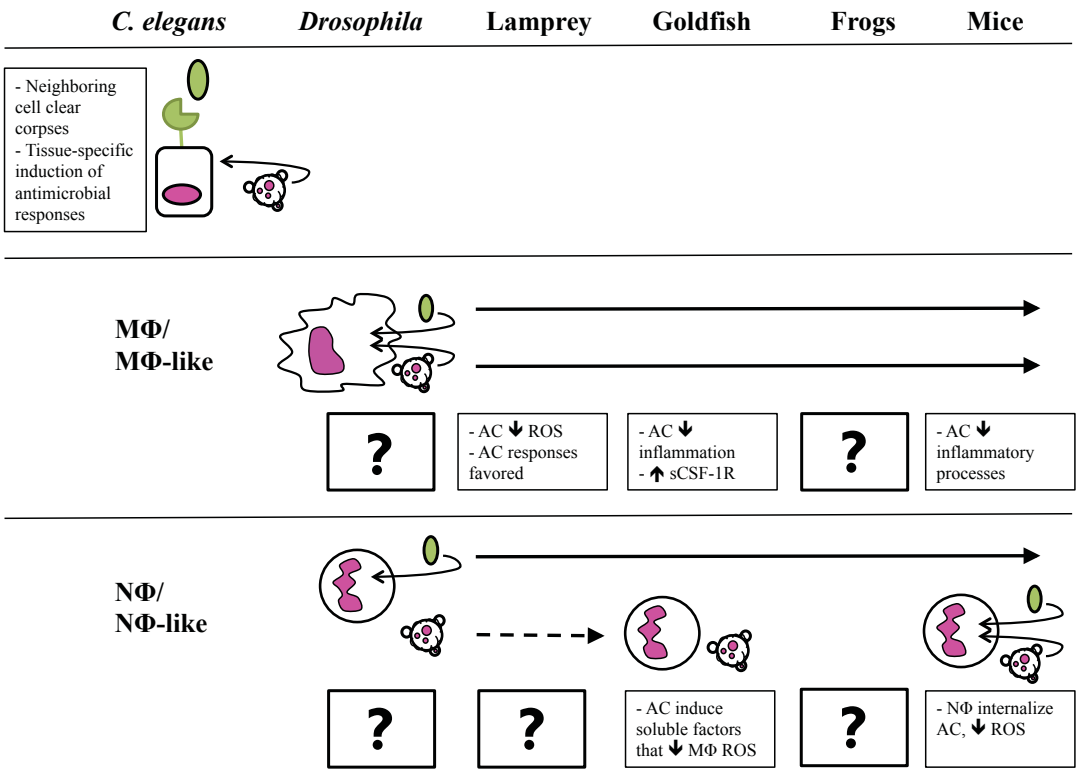

Figure 8.2. Evolution of phagocyte control of inflammation following internalization of apoptotic cells.

Apoptotic cells are thought to be an important stimulus in the switch between inflammation and resolution. The ability to recognize and clear apoptotic cells has been highly conserved across evolution. This figure highlights our current knowledge of responses to apoptotic cells in an inflammatory site across a range of species.

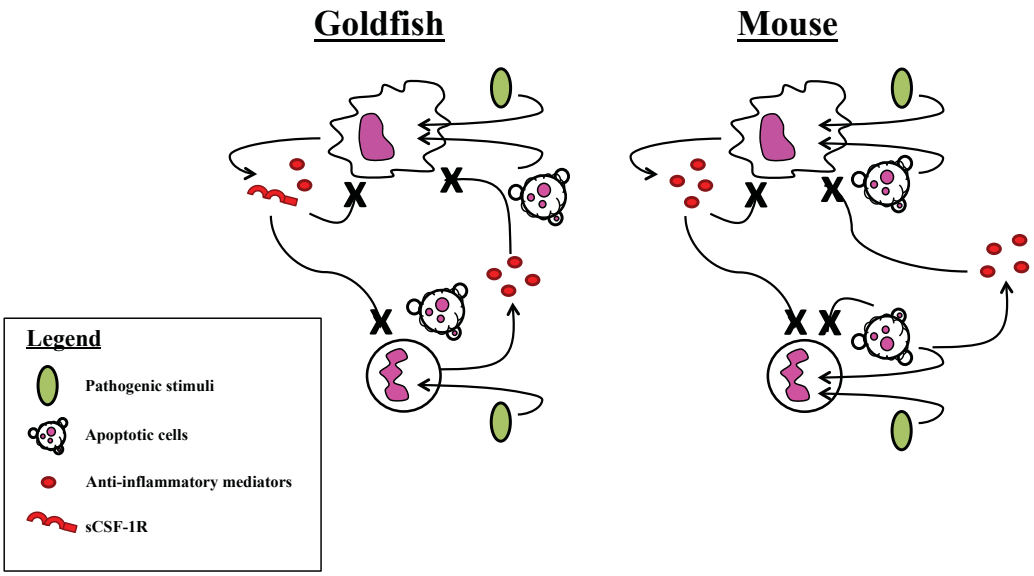

Figure 8.3. Phagocyte-driven control of inflammation by apoptotic cells.

Phagocyte responses are highly integrated throughout an inflammatory response. This figure summarizes key interactions described in the thesis. In goldfish, macrophage internalization of apoptotic cells induces a switch in the production of soluble factors from pro- to anti-inflammatory. Soluble CSF-1R is a primary anti-inflammatory factor that is upregulated. These soluble factors reduce inflammatory processes in both macrophages and neutrophils, including ROS production, phagocytosis, killing of bacteria, and production of inflammatory cytokines and chemokines. Goldfish neutrophils do not internalize apoptotic cells; however, neutrophils incubated in the presence of apoptotic cells produce soluble factor(s) that decrease ROS responses in macrophages, suggesting they may actively participate in resolution responses. In mice, both macrophages and neutrophils internalize apoptotic cells, leading to the production of a range of soluble factors that downregulate macrophage and neutrophil responses.

8.8 References

1. Okin, D., and Medzhitov, R. 2012. Evolution of inflammatory diseases. *Curr Biol* 22:R733-740.
2. Delamarre, L., Pack, M., Chang, H., Mellman, I., and Trombetta, E.S. 2005. Differential lysosomal proteolysis in antigen-presenting cells determines antigen fate. *Science* 307:1630-1634.
3. Weigert, A., Jennewein, C., and Brune, B. 2009. The liaison between apoptotic cells and macrophages--the end programs the beginning. *Biol Chem* 390:379-390.
4. Soehnlein, O., and Lindbom, L. 2010. Phagocyte partnership during the onset and resolution of inflammation. *Nat Rev Immunol* 10:427-439.
5. Rieger, A.M., Konowalchuk, J.D., Grayfer, L., Katzenback, B.A., Havixbeck, J.J., Kiemele, M.D., Belosevic, M., and Barreda, D.R. 2012. Fish and mammalian phagocytes differentially regulate pro-inflammatory and homeostatic responses in vivo. *PLoS One* 7:e47070.
6. Rieger, A.M., Konowalchuk, J.D., Havixbeck, J.J., Robbins, J.S., Smith, M.K., Lund, J.M., and Barreda, D.R. 2013. A soluble form of the CSF-1 receptor contributes to the inhibition of inflammation in a teleost fish. *Dev Comp Immunol* 39:438-446.
7. Barreda, D.R., Hanington, P.C., Stafford, J.L., and Belosevic, M. 2005. A novel soluble form of the CSF-1 receptor inhibits proliferation of self-renewing macrophages of goldfish (Carassius auratus L.). *Dev Comp Immunol* 29:879-894.
8. Grayfer, L., Hanington, P.C., and Belosevic, M. 2009. Macrophage colony-stimulating factor (CSF-1) induces pro-inflammatory gene expression and enhances antimicrobial responses of goldfish (Carassius auratus L.) macrophages. *Fish Shellfish Immunol* 26:406-413.
9. Maderna, P., and Godson, C. 2003. Phagocytosis of apoptotic cells and the resolution of inflammation. *Biochim Biophys Acta* 1639:141-151.
10. Bianchi, S.M., Prince, L.R., McPhillips, K., Allen, L., Marriott, H.M., Taylor, G.W., Hellewell, P.G., Sabroe, I., Dockrell, D.H., Henson, P.W., et al. 2008. Impairment of apoptotic cell engulfment by pyocyanin, a toxic metabolite of Pseudomonas aeruginosa. *Am J Respir Crit Care Med* 177:35-43.
11. Erwig, L.P., and Henson, P.M. 2007. Immunological consequences of apoptotic cell phagocytosis. *Am J Pathol* 171:2-8.
12. Fullard, J.F., Kale, A., and Baker, N.E. 2009. Clearance of apoptotic corpses. *Apoptosis* 14:1029-1037.
13. Fadeel, B., Xue, D., and Kagan, V. 2010. Programmed cell clearance: molecular regulation of the elimination of apoptotic cell corpses and its role in the resolution of inflammation. *Biochem Biophys Res Commun* 396:7-10.
14. Park, D., Tosello-Trampont, A.C., Elliott, M.R., Lu, M., Haney, L.B., Ma, Z., Klibanov, A.L., Mandell, J.W., and Ravichandran, K.S. 2007. BAI1 is an engulfment receptor for apoptotic cells upstream of the ELMO/Dock180/Rac module. *Nature* 450:430-434.

15. Tosello-Trampont, A.C., Kinchen, J.M., Brugnera, E., Haney, L.B., Hengartner, M.O., and Ravichandran, K.S. 2007. Identification of two signaling submodules within the CrkII/ELMO/Dock180 pathway regulating engulfment of apoptotic cells. *Cell Death Differ* 14:963-972.
16. Kinchen, J.M., and Ravichandran, K.S. 2010. Identification of two evolutionarily conserved genes regulating processing of engulfed apoptotic cells. *Nature* 464:778-782.
17. Sulston, J.E., and Horvitz, H.R. 1977. Post-embryonic cell lineages of the nematode, Caenorhabditis elegans. *Dev Biol* 56:110-156.
18. Gumienny, T.L., Lambie, E., Hartwieg, E., Horvitz, H.R., and Hengartner, M.O. 1999. Genetic control of programmed cell death in the Caenorhabditis elegans hermaphrodite germline. *Development* 126:1011-1022.
19. Zhou, Z., Hartwieg, E., and Horvitz, H.R. 2001. CED-1 is a transmembrane receptor that mediates cell corpse engulfment in C. elegans. *Cell* 104:43-56.
20. Sasaki, A., Nakae, I., Nagasawa, M., Hashimoto, K., Abe, F., Saito, K., Fukuyama, M., Gengyo-Ando, K., Mitani, S., Katada, T., et al. 2013. Arl8/ARL-8 functions in apoptotic cell removal by mediating phagolysosome formation in Caenorhabditis elegans. *Mol Biol Cell* 24:1584-1592.
21. Engelmann, I., and Pujol, N. 2010. Innate immunity in C. elegans. *Adv Exp Med Biol* 708:105-121.
22. Lanot, R., Zachary, D., Holder, F., and Meister, M. 2001. Postembryonic hematopoiesis in Drosophila. *Dev Biol* 230:243-257.
23. Hartenstein, V. 2006. Blood cells and blood cell development in the animal kingdom. *Annu Rev Cell Dev Biol* 22:677-712.
24. Lemaitre, B., and Hoffmann, J. 2007. The host defense of Drosophila melanogaster. *Annu Rev Immunol* 25:697-743.
25. Kounatidis, I., and Ligoxygakis, P. 2012. Drosophila as a model system to unravel the layers of innate immunity to infection. *Open Biol* 2:120075.
26. Wang, L., Kounatidis, I., and Ligoxygakis, P. 2013. Drosophila as a model to study the role of blood cells in inflammation, innate immunity and cancer. *Front Cell Infect Microbiol* 3:113.
27. Nonaka, S., Nagaosa, K., Mori, T., Shiratsuchi, A., and Nakanishi, Y. 2013. Integrin alphaPS3/betanu-mediated phagocytosis of apoptotic cells and bacteria in Drosophila. *J Biol Chem* 288:10374-10380.
28. Tung, T.T., Nagaosa, K., Fujita, Y., Kita, A., Mori, H., Okada, R., Nonaka, S., and Nakanishi, Y. 2013. Phosphatidylserine recognition and induction of apoptotic cell clearance by Drosophila engulfment receptor Draper. *J Biochem* 153:483-491.
29. Manaka, J., Kuraishi, T., Shiratsuchi, A., Nakai, Y., Higashida, H., Henson, P., and Nakanishi, Y. 2004. Draper-mediated and phosphatidylserine-independent phagocytosis of apoptotic cells by Drosophila hemocytes/macrophages. *J Biol Chem* 279:48466-48476.
30. Boehm, T., McCurley, N., Sutoh, Y., Schorpp, M., Kasahara, M., and Cooper, M.D. 2012. VLR-based adaptive immunity. *Annu Rev Immunol* 30:203-220.

31. Havixbeck, J.J., Rieger, A.M., Wong, M.E., Wilkie, M.P., and Barreda, D.R. 2014. Evolutionary conservation of divergent pro-inflammatory and homeostatic responses in Lamprey phagocytes. *PLoS One* 9:e86255.
32. Nishikawa, A., Murata, E., Akita, M., Kaneko, K., Moriya, O., Tomita, M., and Hayashi, H. 1998. Roles of macrophages in programmed cell death and remodeling of tail and body muscle of Xenopus laevis during metamorphosis. *Histochem Cell Biol* 109:11-17.
33. Corsaro, C., Scalia, M., Leotta, N., Mondio, F., and Sichel, G. 2000. Characterisation of Kupffer cells in some Amphibia. *J Anat* 196 (Pt 2):249-261.
34. Grayfer, L., and Robert, J. 2013. Colony-stimulating factor-1-responsive macrophage precursors reside in the amphibian (Xenopus laevis) bone marrow rather than the hematopoietic subcapsular liver. *J Innate Immun* 5:531-542.
35. Grayfer, L., De Jesus Andino, F., and Robert, J. 2014. The Amphibian (Xenopus laevis) Type I Interferon Response to Frog Virus 3: New Insight into Ranavirus Pathogenicity. *J Virol* 88:5766-5777.
36. Godwin, J.W., Pinto, A.R., and Rosenthal, N.A. 2013. Macrophages are required for adult salamander limb regeneration. *Proc Natl Acad Sci U S A* 110:9415-9420.
37. Fadok, V.A., Bratton, D.L., Konowal, A., Freed, P.W., Westcott, J.Y., and Henson, P.M. 1998. Macrophages that have ingested apoptotic cells in vitro inhibit proinflammatory cytokine production through autocrine/paracrine mechanisms involving TGF-beta, PGE2, and PAF. *J Clin Invest* 101:890-898.
38. Voll, R.E., Herrmann, M., Roth, E.A., Stach, C., Kalden, J.R., and Girkontaite, I. 1997. Immunosuppressive effects of apoptotic cells. *Nature* 390:350-351.
39. Bellingan, G.J., Caldwell, H., Howie, S.E., Dransfield, I., and Haslett, C. 1996. In vivo fate of the inflammatory macrophage during the resolution of inflammation: inflammatory macrophages do not die locally, but emigrate to the draining lymph nodes. *J Immunol* 157:2577-2585.
40. Stark, M.A., Huo, Y., Burcin, T.L., Morris, M.A., Olson, T.S., and Ley, K. 2005. Phagocytosis of apoptotic neutrophils regulates granulopoiesis via IL-23 and IL-17. *Immunity* 22:285-294.
41. Tassiulas, I., Park-Min, K.H., Hu, Y., Kellerman, L., Mevorach, D., and Ivashkiv, L.B. 2007. Apoptotic cells inhibit LPS-induced cytokine and chemokine production and IFN responses in macrophages. *Hum Immunol* 68:156-164.
42. Kim, S., Elkon, K.B., and Ma, X. 2004. Transcriptional suppression of interleukin-12 gene expression following phagocytosis of apoptotic cells. *Immunity* 21:643-653.
43. Esmann, L., Idel, C., Sarkar, A., Hellberg, L., Behnen, M., Moller, S., van Zandbergen, G., Klinger, M., Kohl, J., Bussmeyer, U., et al. 2009. Phagocytosis of apoptotic cells by neutrophil granulocytes: diminished

proinflammatory neutrophil functions in the presence of apoptotic cells. *J Immunol* 184:391-400.
44. Levy, B.D., Clish, C.B., Schmidt, B., Gronert, K., and Serhan, C.N. 2001. Lipid mediator class switching during acute inflammation: signals in resolution. *Nat Immunol* 2:612-619.
45. Hotamisligil, G.S., and Erbay, E. 2008. Nutrient sensing and inflammation in metabolic diseases. *Nat Rev Immunol* 8:923-934.
46. Libby, P., and Plutzky, J. 2007. Inflammation in diabetes mellitus: role of peroxisome proliferator-activated receptor-alpha and peroxisome proliferator-activated receptor-gamma agonists. *Am J Cardiol* 99:27B-40B.
47. Deguchi, J.O., Aikawa, M., Tung, C.H., Aikawa, E., Kim, D.E., Ntziachristos, V., Weissleder, R., and Libby, P. 2006. Inflammation in atherosclerosis: visualizing matrix metalloproteinase action in macrophages in vivo. *Circulation* 114:55-62.
48. Shimizu, K., Mitchell, R.N., and Libby, P. 2006. Inflammation and cellular immune responses in abdominal aortic aneurysms. *Arterioscler Thromb Vasc Biol* 26:987-994.
49. Libby, P. 2006. Inflammation and cardiovascular disease mechanisms. *Am J Clin Nutr* 83:456S-460S.
50. Trinchieri, G. 2012. Cancer and inflammation: an old intuition with rapidly evolving new concepts. *Annu Rev Immunol* 30:677-706.
51. Wyss-Coray, T., and Mucke, L. 2002. Inflammation in neurodegenerative disease--a double-edged sword. *Neuron* 35:419-432.
52. Green, D. 2011. *Means to an End: Apoptosis and Other Cell Death Mechanisms*. Cold Spring Harbor, NY: Cold Spring Harbor Laboratory Press.
53. Fadok, V.A., and Henson, P.M. 1998. Apoptosis: getting rid of the bodies. *Curr Biol* 8:R693-695.
54. Geske, F.J., Monks, J., Lehman, L., and Fadok, V.A. 2002. The role of the macrophage in apoptosis: hunter, gatherer, and regulator. *Int J Hematol* 76:16-26.
55. Devitt, A., Moffatt, O.D., Raykundalia, C., Capra, J.D., Simmons, D.L., and Gregory, C.D. 1998. Human CD14 mediates recognition and phagocytosis of apoptotic cells. *Nature* 392:505-509.
56. Robbins, P.D., and Morelli, A.E. 2014. Regulation of immune responses by extracellular vesicles. *Nat Rev Immunol* 14:195-208.
57. Sieweke, M.H., and Allen, J.E. 2013. Beyond stem cells: self-renewal of differentiated macrophages. *Science* 342:1242974.
58. Molawi, K., and Sieweke, M.H. 2013. Transcriptional control of macrophage identity, self-renewal, and function. *Adv Immunol* 120:269-300.
59. Barreda, D.R., Hanington, P.C., and Belosevic, M. 2004. Regulation of myeloid development and function by colony stimulating factors. *Dev Comp Immunol* 28:509-554.

60. Rieger, A.M., Hanington, P.C., Belosevic, M., and Barreda, D.R. 2014. Control of CSF-1 induced inflammation in teleost fish by a soluble form of the CSF-1 receptor. *Fish Shellfish Immunol*.
61. Davies, L.C., Rosas, M., Smith, P.J., Fraser, D.J., Jones, S.A., and Taylor, P.R. 2011. A quantifiable proliferative burst of tissue macrophages restores homeostatic macrophage populations after acute inflammation. *Eur J Immunol* 41:2155-2164.
62. Davies, L.C., Rosas, M., Jenkins, S.J., Liao, C.T., Scurr, M.J., Brombacher, F., Fraser, D.J., Allen, J.E., Jones, S.A., and Taylor, P.R. 2013. Distinct bone marrow-derived and tissue-resident macrophage lineages proliferate at key stages during inflammation. *Nat Commun* 4:1886.
63. Rosas, M., Davies, L.C., Giles, P.J., Liao, C.T., Kharfan, B., Stone, T.C., O'Donnell, V.B., Fraser, D.J., Jones, S.A., and Taylor, P.R. 2014. The transcription factor Gata6 links tissue macrophage phenotype and proliferative renewal. *Science* 344:645-648.
64. Krzyminska, S., Mokracka, J., Koczura, R., Cwiertnia, A., and Kaznowski, A. 2012. Aeromonas spp.-mediated cell-contact cytotoxicity is associated with the presence of type III secretion system. *Antonie Van Leeuwenhoek* 101:243-251.
65. Krzyminska, S., Kaznowski, A., and Puk, M. 2008. Interaction of Aeromonas spp. human isolates with murine macrophages. *New Microbiol* 31:481-488.
66. Krzyminska, S., Kaznowski, A., and Chodysz, M. 2009. Aeromonas spp. human isolates induce apoptosis of murine macrophages. *Curr Microbiol* 58:252-257.
67. Allen, L.A. 2003. Mechanisms of pathogenesis: evasion of killing by polymorphonuclear leukocytes. *Microbes Infect* 5:1329-1335.
68. Flannagan, R.S., Cosio, G., and Grinstein, S. 2009. Antimicrobial mechanisms of phagocytes and bacterial evasion strategies. *Nat Rev Microbiol* 7:355-366.
69. Bhavsar, A.P., Guttman, J.A., and Finlay, B.B. 2007. Manipulation of host-cell pathways by bacterial pathogens. *Nature* 449:827-834.
70. Silva, M.T. 2010. Secondary necrosis: the natural outcome of the complete apoptotic program. *FEBS Lett* 584:4491-4499.
71. Silva, M.T. 2010. Bacteria-induced phagocyte secondary necrosis as a pathogenicity mechanism. *J Leukoc Biol* 88:885-896.
72. Katzenback, B.A., Karpman, M., and Belosevic, M. 2011. Distribution and expression analysis of transcription factors in tissues and progenitor cell populations of the goldfish (Carassius auratus L.) in response to growth factors and pathogens. *Mol Immunol* 48:1224-1235.
73. Loose, M., Swiers, G., and Patient, R. 2007. Transcriptional networks regulating hematopoietic cell fate decisions. *Curr Opin Hematol* 14:307-314.
74. Krishnaraju, K., Hoffman, B., and Liebermann, D.A. 1998. The zinc finger transcription factor Egr-1 activates macrophage differentiation in M1 myeloblastic leukemia cells. *Blood* 92:1957-1966.

75. Burda, P., Laslo, P., and Stopka, T. 2010. The role of PU.1 and GATA-1 transcription factors during normal and leukemogenic hematopoiesis. *Leukemia* 24:1249-1257.
76. Dewar, A.L., Cambareri, A.C., Zannettino, A.C., Miller, B.L., Doherty, K.V., Hughes, T.P., and Lyons, A.B. 2005. Macrophage colony-stimulating factor receptor c-fms is a novel target of imatinib. *Blood* 105:3127-3132.
77. Ohno, H., Kubo, K., Murooka, H., Kobayashi, Y., Nishitoba, T., Shibuya, M., Yoneda, T., and Isoe, T. 2006. A c-fms tyrosine kinase inhibitor, Ki20227, suppresses osteoclast differentiation and osteolytic bone destruction in a bone metastasis model. *Mol Cancer Ther* 5:2634-2643.
78. Paniagua, R.T., Chang, A., Mariano, M.M., Stein, E.A., Wang, Q., Lindstrom, T.M., Sharpe, O., Roscow, C., Ho, P.P., Lee, D.M., et al. 2010. c-Fms-mediated differentiation and priming of monocyte lineage cells play a central role in autoimmune arthritis. *Arthritis Res Ther* 12:R32.
79. Madan, B., Goh, K.C., Hart, S., William, A.D., Jayaraman, R., Ethirajulu, K., Dymock, B.W., and Wood, J.M. 2012. SB1578, a novel inhibitor of JAK2, FLT3, and c-Fms for the treatment of rheumatoid arthritis. *J Immunol* 189:4123-4134.
80. Hume, D.A., and MacDonald, K.P. 2012. Therapeutic applications of macrophage colony-stimulating factor-1 (CSF-1) and antagonists of CSF-1 receptor (CSF-1R) signaling. *Blood* 119:1810-1820.

Appendix I: Conventional apoptosis assays using propidium iodide generate a significant number of false positives that prevent accurate assessment of cell death[1]

AI.1 Introduction

Propidium iodide (PI) is a widely utilized stain for assessing cell death, for measuring cell cycling and for determining ploidy in tumor samples. Since the advent of flow-cytometry based apoptosis assays, PI, in combination with Annexin V, has been commonly used to distinguish between live, apoptotic and necrotic cells based on differences in membrane permeability (1, 2). Intact membranes exclude PI, and thus live and early apoptotic cells are not stained as PI does not pass through the plasma membrane (1-3). Cells undergoing late apoptosis or necrosis, however, have changes in the permeability of both the plasma and nuclear membranes. In late apoptotic cells, increased permeability of nuclear pores allows even large proteins and complexes to enter the nucleus (4). In necrotic cells,

---

[1] A version of this Appendix has been previously published:

Rieger AM, Hall BE, Luong Le T, Schang LM, Barreda DR. 2010. Conventional apoptosis assays using propidium iodide generate a significant number of false positives that prevent accurate assessment of cell death. *J Immunol Methods* 358: 81-92.

Rieger AM, Nelson KL, Konowalchuk JD, Barreda DR. 2011. Modified AnnexinV/Propidium Iodide apoptosis assay for accurate assessment of cell death. *J Vis Exp* 50: pii: 2597.

mitochondrial dysfunction results in the disruption of nuclear membrane integrity (5). Therefore, in late apoptotic and necrotic cells, PI enters the cell, passes through the disrupted nuclear membrane and intercalates into DNA, causing red fluorescence in the nucleus (1-3).

Early studies that precede current flow cytometry-based assays indicated that PI does not only bind DNA but can intercalate into any double-stranded nucleic acid in the cell, which includes both DNA and dsRNA (6). For this reason, early microscopy-based PI staining protocols had an RNase treatment following fixation to remove RNA and thereby increase the specificity of the PI stain for DNA (6, 7). This step, however, has been omitted in the vast majority of studies and protocols of major developers of assays that employ flow cytometry. Since the first published Annexin V/PI staining protocol in 1995 (2), only 3 of 1019 published papers using an Annexin V/PI stain have an RNase treatment (8) and the main PI staining protocols for apoptotic cells, including Current Protocols in Immunology (9) and those of major developers of flow cytometry applications (e.g. Molecular Probes, BD Biosciences, eBioscience, Abcam, MBL international, Santa Cruz, Miltenyi Biotech, Roche Applied Science), do not include an RNase treatment. This likely stems from a lack of RNase permeability in live cells.

The ImageStream multi-spectral flow cytometer combines features of both flow cytometry and fluorescence microscopy (10). The ImageStream 100 platform (Amnis) produces six simultaneous images of each cell and images over 100 cells per second (11). In an effort to correlate Annexin V/PI staining with morphological changes associated with apoptotic events, I examined cellular death in a variety of

primary cells systems and cell lines using an ImageStream multi-spectral flow cytometer. In this appendix, I show that conventional Annexin V/PI staining results in a significant number of false positive events that greatly impacts quantification of cell death. Based on thse findings, I have developed and propose a modified Annexin V/PI protocol in which cells are fixed at a late stage in the procedure and RNase treated prior to examination. This greatly reduces the number of false positive events while having no detectable impact on Annexin V or nuclear PI stains. The modified protocol described here would be applicable to ImageStream multi-spectral and conventional flow cytometry applications, as well as microscopy and microplate-based approaches that historically rely on examination of cellular death events in unfixed cells. Importantly, these modifications are necessary to accurately quantify cell death, especially in biological systems where changes in RNA content could severely impact accurate assessment of cell death. As I show here, RNA produced during replicative viral infection (DNA or RNA virus) can be misinterpreted as cell death, leading to a belief that infected cells may actively induce cell death to contain virus spread. In fact, I found that cell viability levels in virally infected cells remains high between 6 and 24 hours. This points to an alternative conclusion: during the initial phase of infection, host defenses are overcome but cell death is not induced. Instead, high levels of viral RNA likely serve to produce high titers of infectious viral particles.

AI.2 Materials and Methods

AI.2.1 Animals

Four-to-six week old C57BL/6 female mice were maintained in a P-2-specific pathogen-free facility in the Biosciences Animal Services Centre at the University of Alberta.

Goldfish (*Carassius auratus* L.) 10–15 cm in length were purchased from Mount Parnell (Mercersburg, PA) and maintained in the Aquatic Facility of the Department of Biological Sciences, University of Alberta. The fish were held at 20^{o}C in a flow-through water system on a simulated natural photoperiod. Unlike its smaller cyprinid relative, *D. rerio*, *C. auratus* provided sufficient numbers of hematopoietic progenitors necessary for the establishment of in vitro primary macrophage cultures. Blastoderms were isolated from hatching eggs obtained from white leghorn hens (Lohmann LSL-Lite) at the Poultry Research Center, University of Alberta. Weaner pigs were obtained from the Swine Research and Technology Center, University of Alberta. All animals were maintained in accordance with the guidelines of the Canadian Council on Animal Care.

AI.2.2 Primary cells

Primary cells from four species were examined to study the relevance of these findings across a wide range of animal models. Chicken blastodermal cells were isolated from embryos after 0, 4 or 14 days of storage. Following dissection, embryonic tissue was trypsin digested for 10 minutes at 37^{o}C. Cells were then washed and allowed to settle for 2 minutes. The cells were harvested and the

isolated cells stained. Goldfish (*Carassius auratus* L.) leukocytes were isolated from kidneys. Primary kidney macrophages (PKM) were generated by seeding isolated leukocytes and culturing in 15 mL complete MGFL-15 media (MGFL-15 supplemented with 100 U/mL penicillin, 100 μg/mL streptomycin, 100 μg/mL gentamicin, 10% newborn calf serum (Gibco) and 5% carp serum) with 5 mL cell-conditioned media from previous experiments and incubated for 6-9 days at 20^{o}C (12). Naïve C57BL/6 mice were sacrificed by cervical dislocation and their spleens were harvested. Spleen tissue was passed through a tissue screen and allowed to settle for 2 minutes. The cells were harvested and washed once in $PBS^{-/-}$ (no calcium, no magnesium) and treated with ACK lysing buffer (Lonza) for 1 minute at room temperature. Cells were washed once in complete DMEM media (DMEM, 100 U/mL penicillin, 100 μg/mL streptomycin, 10% fetal calf serum; all from Gibco) and cultured at 37^{o}C/5% CO_2 for 24 hours. Spleen and lung tissues isolated from weaner pigs were diced into 1 cm^2 pieces and passed through a tissue screen in homogenizing solution (100 U/mL penicillin, 100 μg/mL streptomycin and 0.1% heparin in DMEM). The tissue was allowed to settle and the supernatant is transferred to a 51% Percoll (GE Healthcare Life Sciences) gradient and spun for 25 minutes at 300 x *g* at 4^{o}C. The interface between the solution and the pellet was collected in washed twice in complete DMEM media. Cells were then cultured for 24 hours in complete DMEM media to allow adherence of macrophage populations. After 24 hours, culture plates were washed with $PBS^{+/+}$ to remove all non-adherent cells. The remaining adherent cell population (> 90% macrophages) was cultured for another 24 hours in complete DMEM media.

AI.2.3 Cell lines

Jurkat T cells were cultured in RPMI 1640 supplemented with 100 U/mL penicillin, 100 μg/mL streptomycin, 10% fetal calf serum, 1 mM sodium pyruvate, and 1x non-essential amino acids (all from Gibco). RAW 264.7 macrophage cells were cultured in complete DMEM media. Cell lines were cultured at 37°C/5% CO_2 and passaged every 3-4 days. RAW and Jurkat cells were treated with 10 μg/mL cycloheximide (Sigma) for 24 hours prior to propidium iodide staining to induce cell death.

AI.2.4 Nuclear stains

AI.2.4.1 BrdU staining

Cells were incubated with 10 μM bromodeoxyuridine (5-bromo-2-deoxyuridine, BrdU) (BD Biosciences) for 18 hours. Cells were subsequently harvested, washed twice in $PBS^{-/-}$, and fixed with 1% formaldehyde on ice for 10 minutes. Cells were then stained following the manufacturer's protocol (BD Biosciences).

AI.2.4.2 Propidium iodide staining

Following BrdU staining, cells were washed twice in $PBS^{-/-}$ and re-suspended at $2x10^7$ cells/mL. 100 μL ($2x10^6$ cells) were transferred to 500 μL siliconized polypropylene tubes. Propidium iodide (Sigma) was then added at a final concentration of 1 μg/mL and cells were incubated for another 15 minutes at room

temperature. To ensure that false positives were not due to a specific lot of the reagent, PI staining was compared between two unique lots of PI purchased from two major distributors - Sigma and Molecular Probes (Invitrogen).

AI.2.4.3 DAPI staining

Following PI staining, cells were washed once with $PBS^{-/-}$ and re-suspended in 100 µL of 1 µg/mL 4',6-diamidino-2-phenylindole (DAPI) (Invitrogen) in $PBS^{-/-}$. Cells were incubated for 15 minutes at room temperature. Following DAPI staining, cells were washed twice with $PBS^{-/-}$ and re-suspended in 60 µL $PBS^{-/-}$.

AI.2.4.4 DRAQ5 staining

Cells were stained with a 1:600 dilution of DRAQ5 (Biostatus). Cells were subsequently incubated at room temperature for a minimum of 5 minutes before acquisition.

AI.2.5 RNase treatment to remove false positive events

Fixed and unfixed cells were treated with 0 µg/mL or 50 µg/mL (equivalent to 4 units of activity) DNase-free RNase A (Sigma) for 15 minutes at 37°C. Cells were then washed once with $1xPBS^{-/-}$ (centrifuge 393 x *g* for 10 minutes at 4°C) and stained with PI as outlined above.

AI.2.6 Modified Annexin V/PI staining protocol to reduce false positive events

Cells were harvested and washed once with $PBS^{-/-}$ and once with 1x Annexin V binding buffer (BD Biosciences). Cells were re-suspended at a final concentration of $2x10^7$ cell/mL and 100 μL ($2x10^6$ cells) was transferred into a 500 μL siliconized polypropylene tube. Annexin V-Alexa Fluor 488 (Molecular Probes) was added at a 1:20 dilution and cells were incubated for 15 minutes at room temperature. Following this, PI was added at a final concentration of 1 μg/mL and cells were stained for a further 15 minutes at room temperature. After staining, cells were washed twice with $PBS^{-/-}$ and fixed with 1% formaldehyde for 10 minutes on ice. Following fixation, cells were washed twice with $1xPBS^{-/-}$ (centrifuge 393 x *g* for 10 minutes at 4^oC) and treated with 50 μg/mL DNase-free RNase for 15 minutes at 37^oC. Cells were then washed once with $1xPBS^{-/-}$ (centrifuge 393 x *g* for 10 minutes at 4^oC), stained with DRAQ5 (1:600 final concentration) and were then analyzed by an ImageStream multi-spectral flow cytometer (Amnis).

AI.2.7 Viral infection

African green monkey (Vero) cells were maintained in DMEM supplemented with 50 U/mL penicillin, 50 μg/mL streptomycin, and 5% fetal calf serum (all from Gibco). Cells were infected with 5 plaque-forming units (PFU) per cell of herpes simplex virus type-1 (HSV-1) or vesicular stomatitis virus (VSV) (multiplicity of infection- MOI 5). Mock-infected cells were used to control for normal cell death. Cycloheximide treated cells were used to control for cell death with no viral infection. Cells were harvested at 6 and 24 hours (HSV-1) or 6 and 16 hours (VSV)

and stained using the conventional (-RNase) or modified (+RNase) AnnexinV/PI protocols. To ensure that the additional steps in the modified protocol (fixation, incubation and washes) did not skew the results, the samples stained with the conventional protocol were treated the same but received PBS during the RNase incubation step. Data was then acquired using a FACSCalibur (Becton Dickson) and an ImageStream multispectral flow cytometer (Amnis) and were analyzed as described below.

AI.2.8 Acquisition and analysis- ImageStream

Cell imagery was acquired using an ImageStream multi-spectral imaging flow cytometer (Amnis Corporation). Classifiers were set to eliminate cell debris and clusters prior to data acquisition based on low and high bright field area, respectively (11). After acquisition, a compensation matrix was applied to all data to correct for spectral overlap.

All analyses were completed on a population of spectrally compensated, single, focused cells. Using analysis features available in IDEAS® (Image Data Exploration and Analysis Software, Amnis Corporation), a mask was applied to determine the nuclear area based on DAPI, BrdU and DRAQ5 staining (11). Using this mask, the similarity feature was then applied to calculate the degree of localization of PI stain to the nucleus. Cells with a high degree of similarity between PI stain and the defined nuclear area were characterized as ‘true-positive’ PI stained cells. Cells with a low degree of similarity (PI stain largely outside of the nuclear region) were classified as ‘false-positive’ PI stained cells. For further

description of ImageStream technology and analysis features, refer to Zuba-Surma et al. (2007).

AI.2.9 Acquisition and analysis- flow cytometry

Flow cytometry data was acquired on a FACSCalibur (Becton Dickson) and analyzed using FCS express. Debris were eliminated by gating based on FSC-H and SSC-H parameters. Cell death was then analyzed based on the intensity of FL1-H (AnnexinV) and FL2-H (PI). Gates were defined based on differences in fluorescence levels between experimental and non-infected controls.

AI.2.10 Statistics

GraphPad Prism software was used to determine the significance between control and experimental groups by paired Student's t-test. Probability level of $P < 0.05$ was considered significant.

AI.3 Results

AI.3.1 Propidium iodide stains outside of the nuclear area in fixed cells.

Primary cells and cell lines were harvested, fixed and stained with DAPI, BrdU FITC, PI and DRAQ5, using standard protocols, to compare nuclear staining patterns (Figure AI.1). While DAPI, BrdU FITC and DRAQ5 all had a high degree of similarity in nuclear staining patterns, PI showed a significantly broader staining pattern that included marked staining of the cytoplasmic compartment. This pattern of staining was verified using a Zeiss LSM 510 laser scanning confocal

microscope. Using this microscope, I found that the majority of cells exhibited strong cytoplasmic staining by PI at both 40x and 63x magnification (Figure AI.1 D, E).

Since DAPI, BrdU and DRAQ5 had a high degree in similarity with respect to nuclear staining patterns, I chose to use DRAQ5 as the nuclear stain for the remainder of the experiments as it has been previously reported that DRAQ5 staining correlates very well with PI staining (13). Furthermore, DRAQ5 is highly membrane permeable (14), allowing for rapid nuclear staining of both live and dead cells (15). In contrast, BrdU only stains proliferating cells making it less amenable for this application. Finally, DRAQ5 can be excited by either 488 nm and 658 nm lasers (13) making it compatible with the optics of benchtop flow cytometers and non-UV laser scanning confocal microscopes (16). In contrast, compatibility of DAPI staining tends to be restricted by a requirement for optics not commonly found in these systems.

Results from the ImageStream multi-spectral imaging flow cytometer and laser scanning confocal microscope led us to classify PI stained cells as “true-positive” or “false-positive” based on distinct staining parameters within nuclear and cytoplasmic compartments (Figure AI.2). To ensure that false positives were not due to a specific lot of the reagent, PI staining was compared between two unique lots of PI purchased from Sigma-Aldrich and Molecular Probes-Invitrogen. No difference was found in the staining patterns derived from these two PI stains.

AI.3.2 False positive PI staining is detected in both unfixed primary cells and cell lines.

Propidium iodide has become a popular stain for assessing membrane integrity, thereby aiding in studies of viability in unfixed cells. While cytoplasmic staining of PI has been documented in fixed cells (17), this pattern of PI staining has not been studied in unfixed cells. Since PI positivity in apoptosis / necrosis assays is based upon nuclear DNA PI staining (18-20), false positive cytoplasmic PI staining would greatly affect the accuracy of quantifying cell viability. Primary cells and cells lines were harvested and stained with PI and DRAQ5 to determine the degree of similarity between the two stains in unfixed cells. Gating on the population of PI+/DRAQ5+ cells, I used the similarity feature to determine the degree of similarity between PI and DRAQ5 stains in goldfish primary kidney macrophages (Figure AI.3 A). I found that there was a sizable proportion of falsely stained PI positive in these cells, as well as in all unfixed primary cells and cell lines tested (Figure AI.3 B).

I examined and present data derived from cells isolated from a broad range of animal species that span across teleost fish, avian and mammalian animal models. The percentage of false positive PI stained cells was greater in primary cells than in the cell lines tested, ranging from 3-40% in primary cells compared 1-3% in cells lines (Figure AI.3 C). For primary cell preparations there were generally two distinct cell populations, ‘small cells’ and ‘large cells’ (Figure AI.4 A). Small cells were classified based on a nuclear: cytoplasmic ratio of greater than 0.5 while the large cells were classified based on a nuclear: cytoplasmic ratio of less than 0.5.

The false PI staining was much more pronounced in cells with a nuclear: cytoplasmic ratio less than 0.5 (Figure AI.1 B). I believe that this is associated with a lower limit in the capacity to detect cytoplasmic PI staining in cells with small cytoplasmic compartments, rather than an intrinsic inability of these cells to exhibit cytoplasmic PI staining.

AI.3.3 RNase removes false positive staining but only in fixed cells.

Previous work using microscopy has shown that RNase treatment in fixed cells prior to PI staining greatly reduces cytoplasmic PI staining (17). To determine the effect that RNase treatment had on false PI staining for unfixed cells, cells were treated for 15 minutes at 37^{o}C with 50 μg/mL (4U) DNase-free RNase A. RNase A was added prior to PI staining. In all primary cells and cell lines tested, RNase treatment had no significant effect on the percentage of false positive PI events (Figure AI.5 A). Furthermore, morphological examination showed that RNase treatment on unfixed cells did not decrease the intensity of the false cytoplasmic stain (Figure AI.5 B). However, when cells were fixed prior to RNase treatment, the percentage of false positive PI events was significantly reduced (Figure AI.5 C). It is likely that the increased membrane permeabilization that results from fixation allows RNase to pass through the cell membrane thereby increasing its capacity to target cytoplasmic RNA.

AI.3.4 Modified Annexin V/PI protocol significantly reduces the number of false positive PI events.

Annexin V and PI are commonly used stains to determine cell viability as they allow discrimination between live, apoptotic, and necrotic cells (3). However, current Annexin V/PI protocols fail to remove false positive PI staining associated with RNA staining in the cytoplasmic compartment. This presents a particularly relevant problem for flow cytometry applications, which unlike ImageStream and microscopy-based assays lack the spatial resolution to discriminate between different subcellular compartments. This results in a significant overestimation of the number of PI positive events, and thus late apoptotic and necrotic events. I therefore propose a modification to the current Annexin V/PI protocol. Following staining with Annexin V and PI as described previously (2), cells are fixed with 1% formaldehyde to 10 minutes on ice. This fixation protocol increases plasma membrane permeability thereby promoting RNase A entry. This step, however, must be completed after staining and thorough removal of excess stain to prevent entry of unbound stain into cells. Following fixation, cells are treated with DNase-free RNase A for 15 minutes at 37^{o}C. I found that this combination of incubation time and temperature optimally removes false positive staining across the broad range of primary cells and cell lines observed in this study. Results using this modified protocol are shown for representative cell types in Figure AI.6 A. Importantly, this modified protocol has no adverse effect on Annexin V staining or nuclear PI staining (Figure AI.6 B, C). Inclusion of these steps in conventional Annexin V /PI staining protocols results in significant reduction of false positive events and greatly improves the accuracy of cell death measurements.

AI.3.5 Virus infection increases dsRNA content in cells and is detected as cell death

I have shown here that false positive propidium iodide staining occurs in resting cells from species as diverse as mice and teleost fish. Since false positive PI staining is due to RNA, I hypothesized that the number of false positive events would be further exacerbated in cells that undergo increased RNA production. This could potentially compromise conclusions stemming from any cellular system where levels of RNA change at the time of analysis. Virally infected cells represent a common biological system in which apoptosis is studied and in which cellular RNA content is increased due to viral replication. To study the effects of replicative viral infection on the detection of true cell death, Vero cells were infected with an RNA virus, vesicular stomatitis virus (VSV) or a DNA virus, herpes simplex virus type-1 (HSV-1). Cell death was then assayed using the conventional (-RNase) and modified (+RNase) Annexin V/PI protocols. Results using the conventional AnnexinV/PI protocol indicated that infection with either VSV or HSV-1 led to an increase in cellular death. Other authors have speculated that this may represent an effective host defense mechanism designed to slow down viral spread by decreasing the number of cells that can yield de novo viral particles (21, 22). However, my results indicate that viral infection leads to a high percentage of false positive PI events in these cells, and that this is associated with PI-mediated staining of cytoplasmic viral RNA (Figure AI.6 D). The levels were highest at 6 hours, the time with the highest levels of viral replication. The percentage of cytoplasmic PI staining was greatly reduced with the modified

(+RNase) protocol. Overall, these results support an alternative conclusion: during the initial phase of infection viruses overcome existing host defenses, and effectively increase cytoplasmic RNA that likely serves as a platform for de novo production of infectious viral particles. Further, viral infection does not lead to induction of cellular death.

AI.3.6 Modified protocol allows multivariate dissection of cellular processes.

Current Annexin V/ PI protocols require that cells be analyzed shortly after staining because the cells are unfixed. With this modified Annexin V/ PI protocol, cells can be stored at 4^0C for up to 7 days and can also be stained with various intracellular markers, allowing further dissection of cellular processes during death. This opens the door for multivariate analysis of cellular processes (Figure AI.7). RAW cells were stained with the modified Annexin V/ PI protocol following two-hour stimulation with 250 ng/mL *E. coli* LPS (Invitrogen). After fixation and RNase treatment, cells were permeabilized and stained with NF-κB to examine the state of activation in live, early apoptotic, late apoptotic and necrotic cells, as measured by the degree of NF-κB translocation. I have found that the subsequent staining steps have no impact on Annexin V and PI staining as the percent gated cells in each quadrant does not significantly change following permeabilization and NF-κB staining. Adding this extra dimension to current Annexin V/ PI apoptosis assays will enable comprehensive analysis of live, early apoptotic, late apoptotic and necrotic cell individual populations previous limited to whole cell populations.

AI.4 Discussion

Propidium iodide is one of the most commonly used dyes for the quantitative assessment of DNA content and for determination of cell viability (23). In this appendix, I have shown that PI staining results in a sizable proportion of false positive events- up to 40%- in both primary cells and cell lines. The percent of false positive events were particularly prominent in primary cells. While RNase treatment significantly decreased the degree of false positive staining in fixed cells, it had no effect on false positive staining in unfixed cells. Thus, it required modification of conventional Annexin V/PI staining protocols and optimization of the methodology to ensure that it will be amenable to a broad range of cell types and several animal models currently used in the field today. Further, removal of PI false positive staining needed to maintain integrity of the parallel Annexin V stain. To achieve this I determined the optimal concentration of RNase, incubation time and temperature to maximally remove false positive PI staining with no effect on Annexin V staining. Finally, I applied this modified protocol to study apoptosis in a system with high levels of RNA- virally infected cells. I have shown here that, in virally infected cells, RNase treatment significantly reduces levels of cytoplasmic PI staining, indicating that in the absence of RNase treatment, PI staining is due to virally produced RNA and not cell death.

The nucleic acid composition of cells typically consists of DNA, ssRNA and dsRNA. PI has been shown to intercalate into double-stranded regions of helical nucleic acids, which includes both DNA and dsRNA (6). While most studies have focused on the DNA binding properties of PI, some studies have exploited the

binding capacity of PI to study dsRNA content in DNase-treated cells (24). These studies have shown that, under basal conditions, cells normally have low dsRNA content, with bone marrow primary cells and certain neoplastic cell lines (HeLa, L1210, HL60, ARH-77) generally having higher dsRNA content compared to other primary/ non-neoplastic cells (24, 25). This would lead to differential false positives across different cell types, consistent with results presented in this manuscript. Based on these studies it is likely that the majority of false positive events are resulting from cytoplasmic staining of dsRNA. Importantly, cellular activation and proliferation led to an increase in dsRNA abundance within the cytoplasmic compartment (24-26). As such, it is likely that false positive events are more prominent in activated and/or cycling cells, thus falsely increasing the relative gap in cell death events between activated and non-activated groups.

False positive, cytoplasmic PI staining has been previously documented by confocal microscopy on ethanol fixed tissue sections (17, 27). In the absence of RNase treatment, both the cytoplasm and nucleus stained with PI (17, 27). This has likely been overlooked in assays with unfixed cells as cytoplasmic PI staining was thought to occur only in fixed cells (28). The assumption that unfixed cells would not exhibit false positive cytoplasmic staining was supported by early flow cytometry data showing that RNase treatment of unfixed cells has no effect on the intensity of PI staining (7). However, as I have shown here, this observation was not due to a lack of false positive staining but, instead, because RNase is unable to cross the membrane of unfixed cells. Based on my work, it is clear that cytoplasmic RNA staining does occur in conventional Annexin V/PI staining protocols.

However, cells must be fixed prior to RNase treatment in order for RNase to pass through the membrane and degrade cytoplasmic RNA. For those studies employing conventional Annexin V/PI staining protocols, failure to remove cytoplasmic RNA has likely led to varying degrees of false positives, depending on the cell model used, and an overestimation of late apoptotic and/or necrotic events. More critically, my findings have important ramifications for studies that examine events in cellular models experiencing changes in RNA content. As I have shown, virally infected cells, for example, are qualified as undergoing cellular death in response to infection when conventional Annexin V/PI staining protocols are used; in fact, these cells are alive and actively producing viral dsRNA that can serve to produce additional infectious viral particles.

Importantly, these ramifications go beyond the viral infection example that I describe, and would be relevant to any cellular system where changes in RNA, especially dsRNA, occur during examination of cellular death events. Among others, these include cells undergoing genotoxic stress (29, 30), cells treated with cell cycle arrest drugs such as thymidine or hydroxyurea (25, 31), neoplastic tissue (31) or studies on embryonic cells where developmental progression is characterized by discrete changes in cellular RNA synthesis (32). The potential impact of this is shown in a recent study by Mansilla *et al* (2006). In this study, breast cancer cell lines were treated with two cell cycle arrest drugs and cell death was assayed with a conventional AnnexinV/PI assay and by caspase activation. It was concluded that the drugs induced necrotic type cell despite identification of caspase induction, which is generally associated with apoptosis (33). It is possible

that PI-mediated staining of RNA may have led to under-estimation of early apoptotic cells, which may be more consistent with the parallel caspase activation events observed. Thus, the findings presented in this appendix could have significant implications in the design, testing and use of cancer therapeutics, as necrosis and apoptosis are known to have divergent pro-inflammatory outcomes.

Using ImageStream technology, I have shown here that current apoptosis assays using PI are likely overestimating the amount of cell death due to false positive PI staining. While these false positive events can be detected by ImageStream analysis software and removed from subsequent analyses, this is not possible by standard flow cytometry. Overall, my work emphasizes the importance of addressing cytoplasmic RNA staining in those cells being examined for apoptosis and necrotic events using Annexin V/PI staining. The modified protocol that I propose increases the overall specificity of PI staining and does not compromise Annexin V or nuclear DNA staining. As such, it will allow for more accurate quantification of cell death across several platforms available today such as conventional flow cytometry. Notably, this protocol is amenable to multivariate analysis of cellular death mechanisms, setting the stage for more in depth characterization of cellular death programs. Among others, this could allow for characterization of important mediators such as cytochrome c, Bax, Bcl-2, or activated caspases in mixed live, apoptotic and necrotic populations. Parallel characterization of downstream events could also take advantage of existing intracellular cytokine stains and activation markers. These analyses will provide

detailed information in particular populations of cells and will open avenues for comprehensive analysis of mechanisms of cell death.

AI.5 Protocol

This procedure can be performed in 500 µL siliconized tubes or 6 mL polystyrene round-bottom FACS tubes. The latter is normally used when carrying out viability analysis in conjunction with other procedures. All volumes given are for 6 mL polystyrene round-bottom FACS tubes. For 500 µL siliconized tubes, reduce all volumes by 1/5.

The optimum concentration for flow cytometry analysis is 2-4 x 10^6 cells per 200 µL volume. Cell loss may result from this procedure and thus we recommend that each sample consist of 4 x 10^6 cells at the start of the procedure.

1. Cell Preparation

1. Harvest cells - refer to specific procedures for corresponding cell lines or primary cell isolations.
2. Centrifuge samples at 311 x *g* for 10 minutes at 4^{o}C and decant the supernatant.
3. Resuspend cells in 2 mL 1 x phosphate buffered saline (PBS) $^{-/-}$ (no calcium, no magnesium).
4. Centrifuge samples at 311 x *g* for 10 minutes at 4^{o}C and decant the supernatant.
5. Resuspend cells in 1 mL 1 x Annexin V binding buffer.

6. Centrifuge samples at 311 x *g* for 10 minutes at 4°C and decant the supernatant.
7. Resuspend cells in 100 µL 1 x Annexin V binding buffer.

2. Application of Annexin V/ PI Stain

1. Add Annexin V according to the manufacturer's recommendations [e.g. 5 µL Annexin V Alexa Fluor 488 (Molecular Probes, A13201)].
2. Incubate tubes in the dark for 15 minutes at room temperature.
3. Add 100 µL of 1 x Annexin V binding buffer to each reaction tube. There should be approximately 200 µL in each tube.
4. Add 4 µL of PI (Sigma, Cat# P-4864-10ML) that has been diluted 1:10 in 1 x Annexin V binding buffer (i.e. 1 µL PI with 9 µL 1 x Annexin V binding buffer). This will yield a final PI concentration of 2 µg/mL in each sample.
5. Incubate tubes in the dark for 15 minutes at room temperature.
6. Add 500 µL 1 x Annexin V binding buffer to wash the cells.
7. Centrifuge samples at 311 x *g* for 10 minutes at 4°C and decant the supernatant.
8. Resuspend cells in 500 µL 1 x Annexin V binding buffer and 500 µL 2% formaldehyde to create a 1% formaldehyde (fixative) solution. Mix tubes by gentle flicking.
9. Fix samples on ice for 10 minutes. Alternatively, samples can be stored overnight at 4°C in the dark. If the latter method is chosen, make sure to be

consistent across all tubes labeled with Annexin V/PI (including compensation controls).

10. Add 1 mL 1 x $PBS^{-/-}$ to each sample and mix gently by flicking.
11. Centrifuge tubes at 393 x *g* for 10 minutes at 4°C and decant the supernatant.
12. Repeat steps 2.10 and 2.11.
13. Resuspend pellet by flicking the tube.
14. Add 16 µL of 1:100 diluted RNase A (Sigma, R4642) to give a final concentration of 50 µg/mL. Incubate for 15 min at 37°C.
15. Add 1 mL 1 x $PBS^{-/-}$ and mix gently by flicking.
16. Centrifuge tubes at 393 x *g* for 10 minutes at 4°C.
17. Samples are now ready to be analyzed. Alternatively, samples can be used for subsequent staining steps if Annexin/PI staining is being performed in parallel with other procedures.

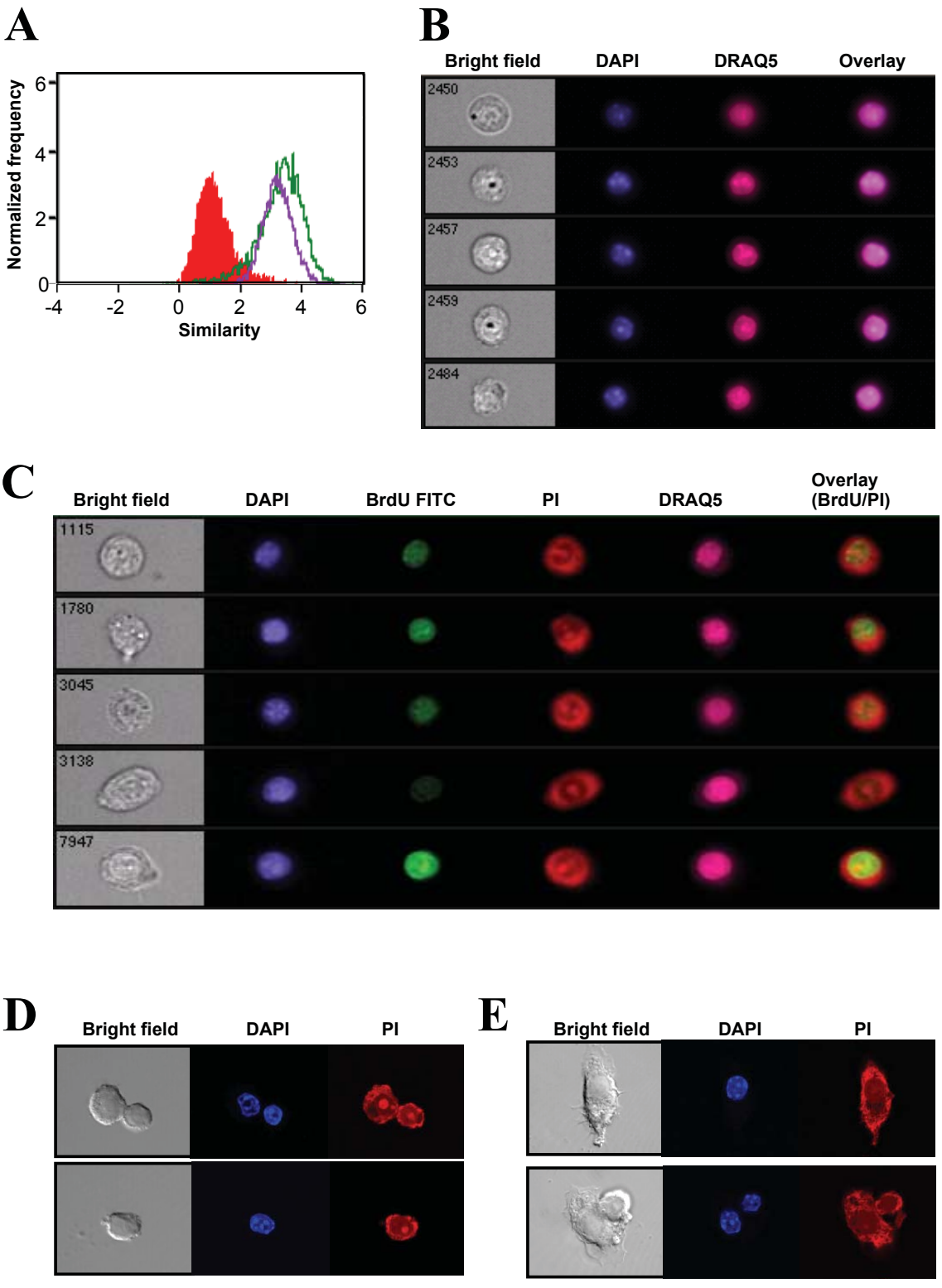
A
Normalized frequency
6
4
2
0
-4
-2
0
2
4
6
Similarity
B
Bright field
DAPI
DRAQ5
Overlay
2450
2453
2457
2459
2484
C
Bright field
DAPI
BrdU FITC
PI
DRAQ5
Overlay (BrdU/PI)
1115
1780
3045
3138
7947
D
Bright field
DAPI
PI
E
Bright field
DAPI
PI

Figure AI.1. Propidium iodide stains outside of the nuclear area.

(**A-C**) RAW cells were stained with DAPI, BrdU FITC, PI and DRAQ5 in order to compare nuclear staining patterns and imagery was acquired using an ImageStream multi-spectral flow cytometer. All imagery was collected using 40X magnification. Two independent experiments examined 10,000 cells. (**A**) Using the similarity feature (refer to Materials and Methods for description of analysis), the degree of similarity between nuclear stains was determined. Purple line: similarity between DAPI and DRAQ5; green line: similarity between DAPI and BrdU FITC; red histogram: similarity between DAPI and PI. The low similarity between DAPI and PI indicates that PI stains the cytoplasm as well as the nucleus. (**B**) Representative images showing the high degree of similarity between DAPI and DRAQ5. (**C**) Representative images showing the low degree of similarity between PI and other nuclear stains. (**D, E**) RAW cells (n=2) were stained with DAPI and PI and imaged using a Zeiss LSM 510 laser scanning confocal microscope to examine correlation with ImageStream results. Images were acquired at 40x/1.3 (F-Fluar lens) (**D**) and 63x/1.4 (Plan Apochromat lens) (**E**). Images were acquired at room temperature in Fluoromount G imaging media (Southern Biotech) with a Zeiss LSM510 camera. Data was acquired and analyzed using Zen software. Propidium iodide staining was detectable in the cytoplasm at both levels of magnification.

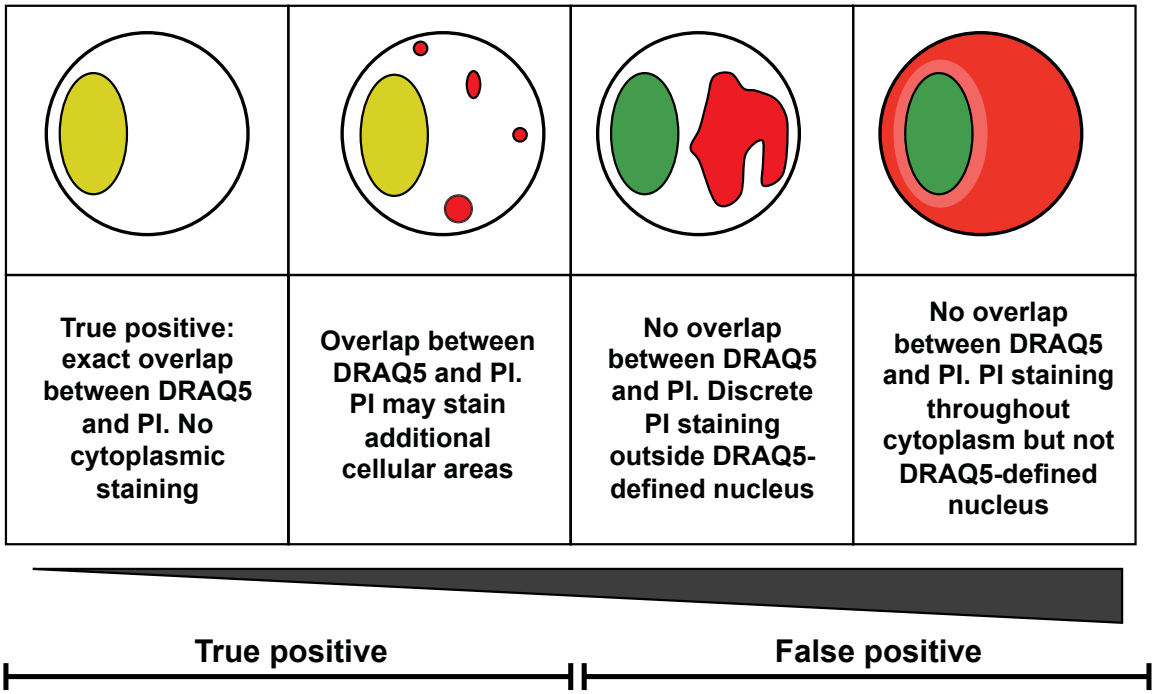

Figure AI.2. Classification of true and false positive propidium iodide staining patterns.

True positive stained cells are defined as having overlap between PI and DRAQ5 in the nuclear region. In some cases, there may be stain of additional cellular areas. False positive stained cells are classified as having no overlap between PI and DRAQ5. PI staining may be in discrete locations outside the DRAQ5 defined nucleus or throughout the cytoplasm.

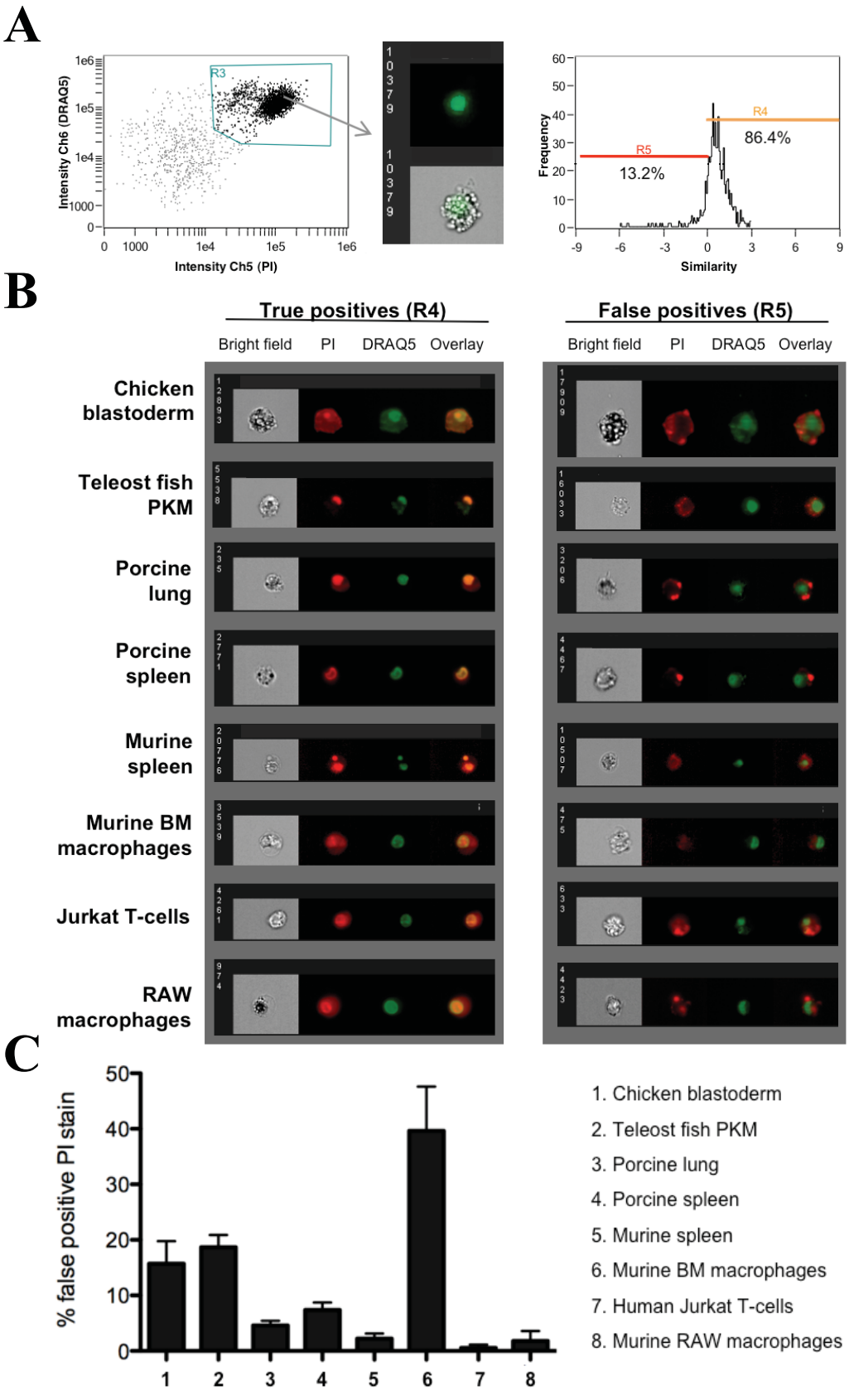
A
Intensity Ch6 (DRAQ5)
Intensity Ch5 (PI)
R3
Frequency
Similarity
R4
86.4%
R5
13.2%
B
True positives (R4)
False positives (R5)
Bright field
PI
DRAQ5
Overlay
Chicken blastoderm
Teleost fish PKM
Porcine lung
Porcine spleen
Murine spleen
Murine BM macrophages
Jurkat T-cells
RAW macrophages
C
% false positive PI stain
1. Chicken blastoderm
2. Teleost fish PKM
3. Porcine lung
4. Porcine spleen
5. Murine spleen
6. Murine BM macrophages
7. Human Jurkat T-cells
8. Murine RAW macrophages

Figure AI.3. Primary cells and cell lines exhibit false-positive PI staining.

Primary cells and cell lines were harvested and stained with propidium iodide and DRAQ5. Primary cells included chicken blastodermal cells, goldfish primary kidney macrophages (PKM), porcine lung macrophages, porcine spleen macrophages murine splenocytes and bone marrow (BM) macrophages. Cell lines included human Jurkat T-cells and murine RAW macrophages. Imagery was acquired by an ImageStream multi-spectral imaging flow cytometer. (**A**) Representative analysis shows procedure for classification of primary kidney macrophage cells into true positive (R4) and false positive (R5) populations. Using a mask that highlighted the nuclear area, based on the pixel intensity of the DRAQ5 stain (refer to Materials and Methods for description of masking strategy), the degree of colocalization between DRAQ5 and PI was determined. (**B**) All cell types tested exhibited false positive PI staining to varying degrees. To allow for easier visual determination of PI and DRAQ5 colocalization, the DRAQ5 stain was given a green pseudocolour. Areas where PI and DRAQ5 colocalize appear yellow. Cells with a high degree of colocalization were characterized as true positive. Cells with a low degree of colocalization were characterized as false positive. Chicken blastodermal cells, n=5; goldfish PKM, n=3; porcine lung and spleen macrophages, n=3; murine splenocytes and bone marrow (BM) macrophages, n=2; Jurkat T-cells, n=3; RAW macrophages, n=3; error bars show SEM.

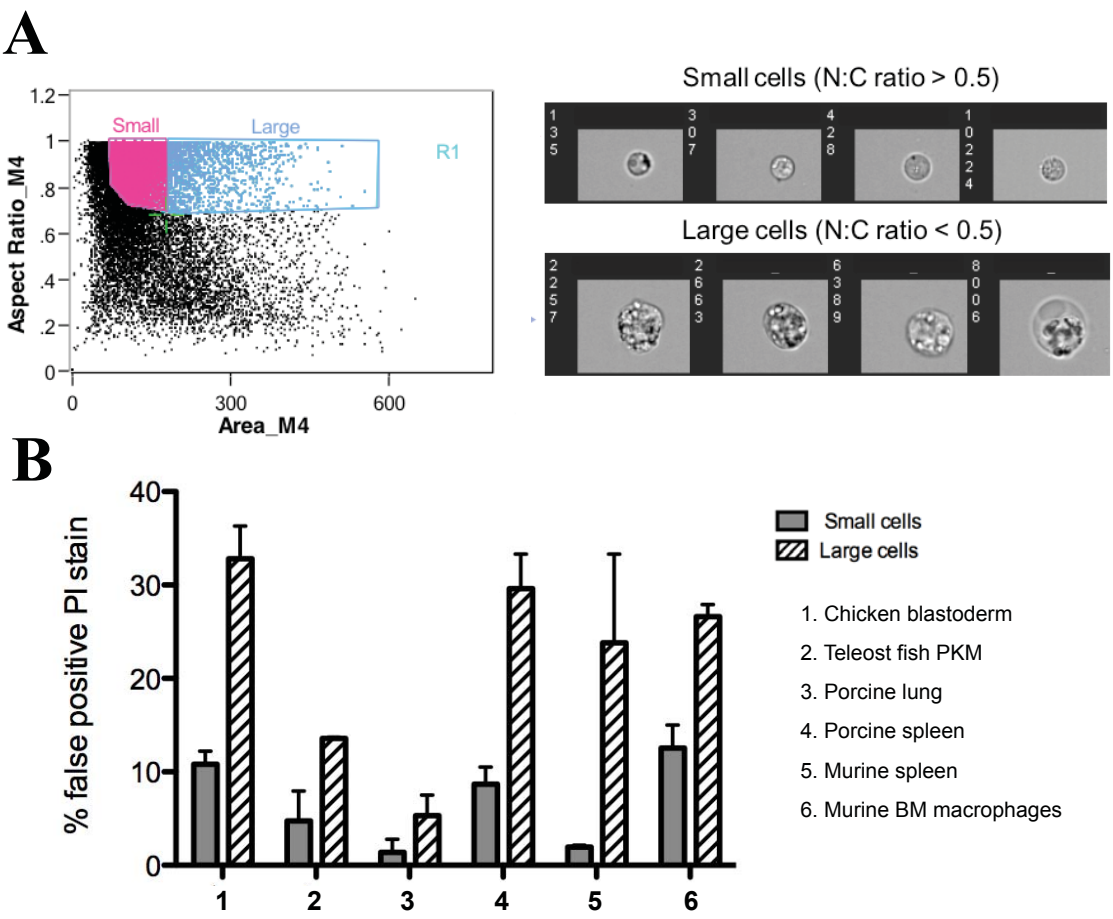

Figure AI.4. False PI stain is more readily detected in large cells with a nuclear: cytoplasmic ratio less than 0.5.

(**A**) Gated single cell populations of single cells could be divided further into small cells (pink) and large cells (blue). Small cells were classified as having a nuclear: cytoplasmic ratio greater than 0.5. Large cells were classified as having a nuclear: cytoplasmic ratio less than 0.5. (**B**) In primary cells, large cells had a greater percentage of false positive PI events compared to small cells. Cell lines were not sub-divided as cells were homogenous in size. Chicken blastodermal cells, n=5; goldfish PKM, n=3; porcine lung and spleen macrophages, n=3; murine splenocytes and bone marrow (BM) macrophages, n=2; error bars show SEM.

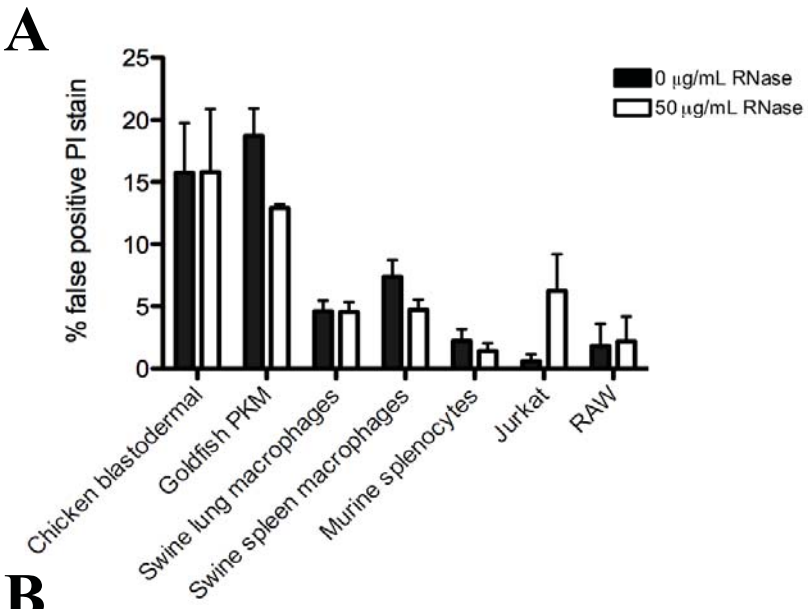
A
% false positive PI stain
25
20
15
10
5
0
0 μg/mL RNase
50 μg/mL RNase
Chicken blastodermal
Goldfish PKM
Swine lung macrophages
Swine spleen macrophages
Murine splenocytes
Jurkat
RAW

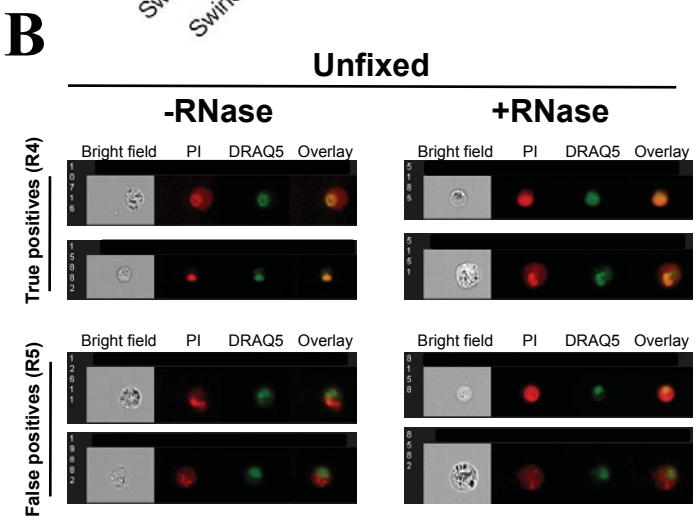
B
Unfixed
-RNase
+RNase
Bright field
PI
DRAQ5
Overlay
True positives (R4)
False positives (R5)

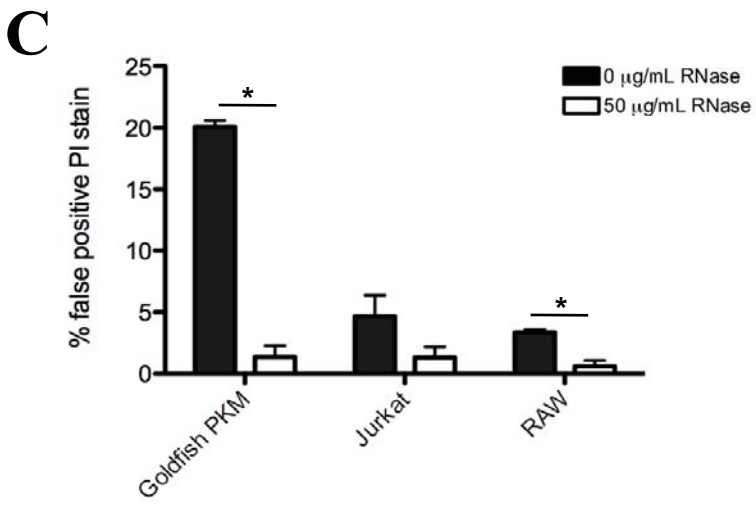
C
% false positive PI stain
25
20
15
10
5
0
0 μg/mL RNase
50 μg/mL RNase
*
*
Goldfish PKM
Jurkat
RAW

Figure AI.5. RNase treatment decreases false positive PI stain on fixed cells but not in unfixed cells.

(**A**) Chicken blastodermal cells, goldfish primary kidney macrophages (PKM), murine splenocytes, porcine lung macrophages, porcine spleen macrophages, Jurkat T-cells and RAW macrophages were harvested and treated +/- 50 μg/mL DNase-free RNase for 15 minutes prior to propidium iodide and DRAQ5 staining. Imagery was acquired by an ImageStream multi-spectral imaging flow cytometer equipped with 488nm and 658nm lasers. The percentage of true- and false-positive PI events was calculated by determining the degree of colocalization between DRAQ5 and PI. RNase treatment did not decrease the percentage of false positive PI stains in unfixed cells. Chicken blastoderm, n=4; goldfish PKM, n=3; murine splenocytes, n=2; porcine lung and spleen macrophages, n=3; Jurkat T-cells, n=3; RAW macrophages, n=3; error bars show SEM. (**B**) Representative figures from fixed and unfixed goldfish primary kidney macrophage cells treated +/- 50 μg/mL DNase-free RNase for 15 minutes prior to PI and DRAQ5 staining. (**C**) Unfixed cells continue to stain non-nuclear areas following RNase treatment. In contrast, RNase treatment of fixed cells removes cytoplasmic RNA staining. Goldfish primary kidney macrophages (PKM), Jurkat T-cells and RAW macrophage cells were harvested and fixed with 1% formaldehyde. Cells were then washed and treated +/- 50 μg/mL DNase-free RNase for 15 minutes prior to PI and DRAQ5 staining. Imagery was acquired by an ImageStream multi-spectral imaging flow cytometer. The percentage of true- and false-positive PI events was calculated by determining the degree of colocalization between DRAQ5 and PI. RNase treatment significantly decreased the percentage of false positive PI stains in goldfish PKM and RAW. n=2, *$p<0.05$; error bars show SEM.

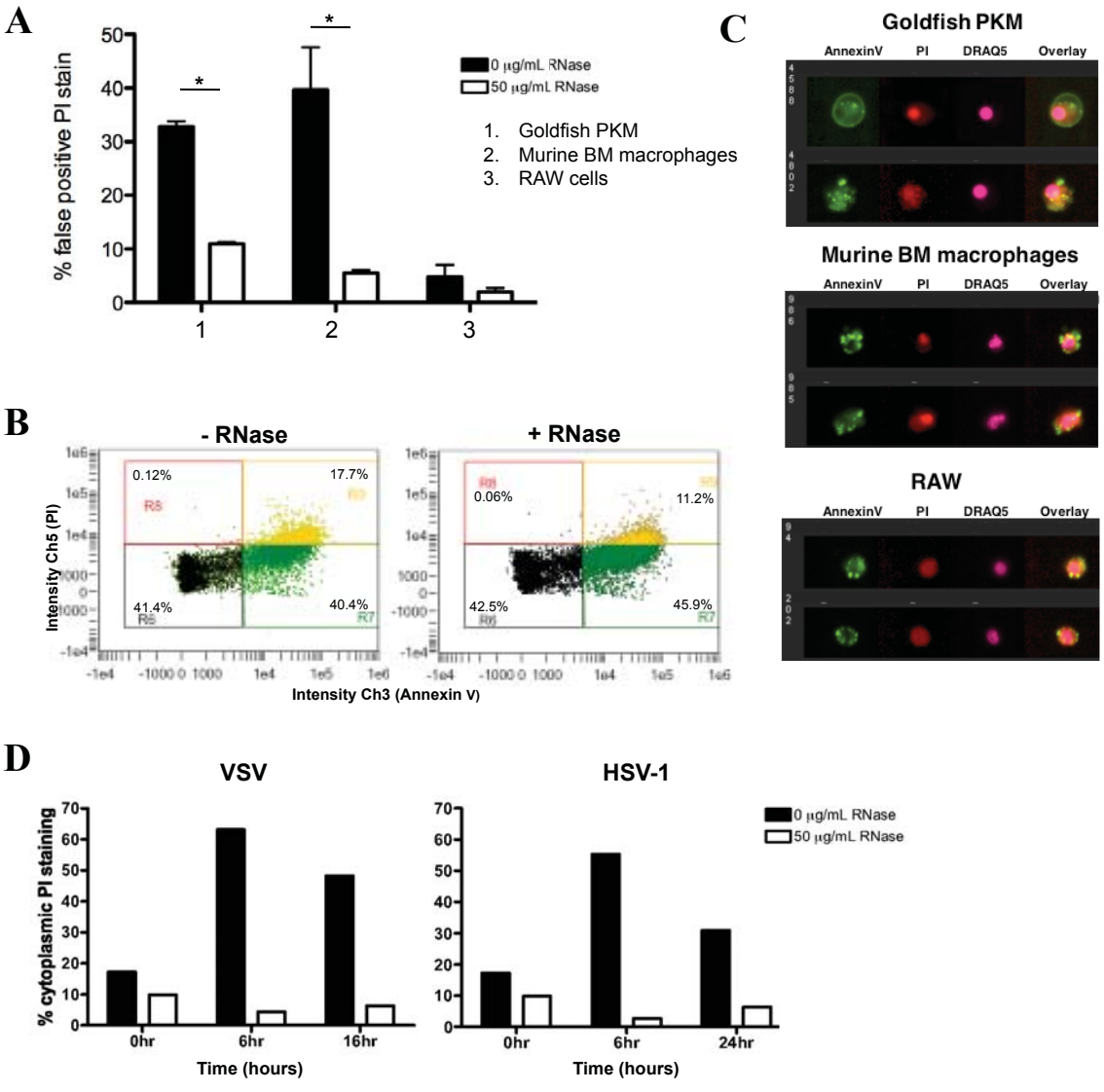
A
% false positive PI stain
0 μg/mL RNase
50 μg/mL RNase
1. Goldfish PKM
2. Murine BM macrophages
3. RAW cells
B
- RNase
+ RNase
Intensity Ch5 (PI)
Intensity Ch3 (Annexin V)
0.12%
17.7%
41.4%
40.4%
0.06%
11.2%
42.5%
45.9%
C
Goldfish PKM
Murine BM macrophages
RAW
AnnexinV
PI
DRAQ5
Overlay
D
VSV
HSV-1
% cytoplasmic PI staining
0 μg/mL RNase
50 μg/mL RNase
0hr
6hr
16hr
24hr
Time (hours)

Figure AI.6. Modified Annexin V/PI protocol significantly reduces false positive PI staining while not affecting Annexin V or nuclear PI staining.

(**A**) Goldfish PKM, murine bone marrow macrophages and RAW cells were stained with Annexin V and PI using a standard protocol. Cells were then fixed with 1% formaldehyde and treated +/- 50 μg/mL DNase-free RNase for 15 minutes according to the modified protocol. Imagery was then acquired using an ImageStream multispectral flow cytometer. RNase treatment significantly reduces the percentage of false positive PI events; n=3, *$p<0.05$; error bars show SEM. (**B**) Scatterplots depicting Annexin V/PI stain of goldfish PKM. Following RNase treatment, there was a decrease in the percentage of PI+ cells due to removal of false positive events. Note: the decrease in false positive events is shown in the context of the whole population of cells (PI+ and PI-). (**C**) Representative images of goldfish PKM, murine bone marrow macrophages and RAW cells stained using the modified Annexin V/PI protocol. Using this protocol, cytoplasmic PI staining is reduced while intensity/ pattern of Annexin V stain is unchanged. (**D**) Vero cells were infected with VSV or HSV-1 with a multiplicity of infection of 5. Cells were harvested at the indicated time points and stained using either the conventional AnnexinV/PI protocol (-RNase) or with the modified AnnexinV/PI protocol (+RNase). Viral infection increases the number of false positive PI events detected. Treatment with RNase greatly reduces the percentage of cells with cytoplasmic PI staining.

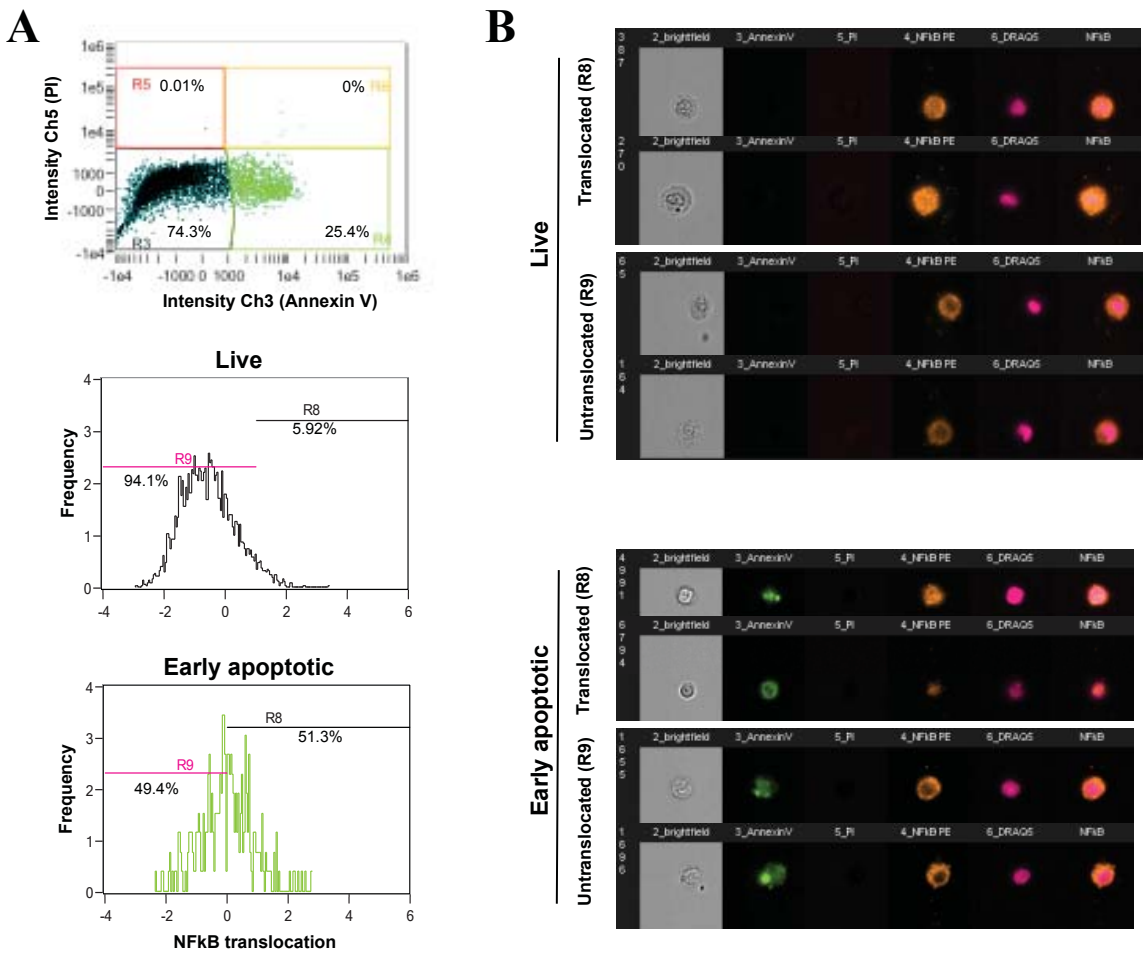

Figure AI.7. Modified protocol allows further analysis of apoptotic and necrotic populations.

RAW cells were stimulated with 250 ng/mL *E. coli* LPS for 2 hours. Cells were stained using the modified AnnexinV/ PI protocol. Following fixation and RNase treatment, cells were permeabilized for 10 minutes on ice with 0.1% saponin buffer and then stained with NFkB primary antibody followed by goat- anti-rabbit R-PE secondary antibody. Imagery was then acquired using an ImageStream multi-spectral flow cytometer. (**A**) Using the modified protocol, cellular activation (NFkB translocation) was studied in live, early apoptotic, necrotic and late apoptotic populations. We found a higher degree of NFkB translocation in early apoptotic cells than live cells. Cell counts in necrotic and late apoptotic populations were too low to analyze. (**B**) Representative images of NFkB translocated and untransloacted cells from live (top) and early apoptotic cells (bottom).

AI.6 References

1. Vermes, I., Haanen, C., and Reutelingsperger, C. 2000. Flow cytometry of apoptotic cell death. *J Immunol Methods* 243:167-190.
2. Vermes, I., Haanen, C., Steffens-Nakken, H., and Reutelingsperger, C. 1995. A novel assay for apoptosis. Flow cytometric detection of phosphatidylserine expression on early apoptotic cells using fluorescein labelled Annexin V. *J Immunol Methods* 184:39-51.
3. Darzynkiewicz, Z., Bruno, S., Del Bino, G., Gorczyca, W., Hotz, M.A., Lassota, P., and Traganos, F. 1992. Features of apoptotic cells measured by flow cytometry. *Cytometry* 13:795-808.
4. Faleiro, L., and Lazebnik, Y. 2000. Caspases disrupt the nuclear-cytoplasmic barrier. *J Cell Biol* 151:951-959.
5. Kroemer, G., Dallaporta, B., and Resche-Rigon, M. 1998. The mitochondrial death/life regulator in apoptosis and necrosis. *Annu Rev Physiol* 60:619-642.
6. Deitch, A.D., Law, H., and deVere White, R. 1982. A stable propidium iodide staining procedure for flow cytometry. *J Histochem Cytochem* 30:967-972.
7. Fried, J., Perez, A.G., and Clarkson, B.D. 1976. Flow cytofluorometric analysis of cell cycle distributions using propidium iodide. Properties of the method and mathematical analysis of the data. *J Cell Biol* 71:172-181.
8. http://apps.isiknowledge.com/summary.do?qid=17&product=UA&SID=3EdJcO897oK2Gfd6EH4&search_mode=Refine. 2009. Web of Knowledge search.
9. Muppidi, J., Porter, M., and Siegel, R.M. 2004. Measurement of apoptosis and other forms of cell death. *Curr Protoc Immunol* Chapter 3:Unit 3 17.
10. Zuba-Surma, E.K., Kucia, M., Abdel-Latif, A., Lillard, J.W., Jr., and Ratajczak, M.Z. 2007. The ImageStream System: a key step to a new era in imaging. *Folia Histochem Cytobiol* 45:279-290.
11. Henery, S., George, T., Hall, B., Basiji, D., Ortyn, W., and Morrissey, P. 2008. Quantitative image based apoptotic index measurement using multispectral imaging flow cytometry: a comparison with standard photometric methods. *Apoptosis* 13:1054-1063.
12. Barreda, D.R., Hanington, P.C., Stafford, J.L., and Belosevic, M. 2005. A novel soluble form of the CSF-1 receptor inhibits proliferation of self-renewing macrophages of goldfish (Carassius auratus L.). *Dev Comp Immunol* 29:879-894.
13. Yuan, C.M., Douglas-Nikitin, V.K., Ahrens, K.P., Luchetta, G.R., Braylan, R.C., and Yang, L. 2004. DRAQ5-based DNA content analysis of hematolymphoid cell subpopulations discriminated by surface antigens and light scatter properties. *Cytometry B Clin Cytom* 58:47-52.
14. Smith, P.J., Wiltshire, M., Davies, S., Patterson, L.H., and Hoy, T. 1999. A novel cell permeant and far red-fluorescing DNA probe, DRAQ5, for blood cell discrimination by flow cytometry. *J Immunol Methods* 229:131-139.

15. Martin, R.M., Leonhardt, H., and Cardoso, M.C. 2005. DNA labeling in living cells. *Cytometry A* 67:45-52.
16. Smith, P.J., Blunt, N., Wiltshire, M., Hoy, T., Teesdale-Spittle, P., Craven, M.R., Watson, J.V., Amos, W.B., Errington, R.J., and Patterson, L.H. 2000. Characteristics of a novel deep red/infrared fluorescent cell-permeant DNA probe, DRAQ5, in intact human cells analyzed by flow cytometry, confocal and multiphoton microscopy. *Cytometry* 40:280-291.
17. Suzuki, T., Fujikura, K., Higashiyama, T., and Takata, K. 1997. DNA staining for fluorescence and laser confocal microscopy. *J Histochem Cytochem* 45:49-53.
18. Overbeeke, R., Steffens-Nakken, H., Vermes, I., Reutelingsperger, C., and Haanen, C. 1998. Early features of apoptosis detected by four different flow cytometry assays. *Apoptosis* 3:115-121.
19. Bryson, G.J., Harmon, B.V., and Collins, R.J. 1994. A flow cytometric study of cell death: failure of some models to correlate with morphological assessment. *Immunol Cell Biol* 72:35-41.
20. Ormerod, M.G., Sun, X.M., Snowden, R.T., Davies, R., Fearnhead, H., and Cohen, G.M. 1993. Increased membrane permeability of apoptotic thymocytes: a flow cytometric study. *Cytometry* 14:595-602.
21. Everett, H., and McFadden, G. 1999. Apoptosis: an innate immune response to virus infection. *Trends Microbiol* 7:160-165.
22. O'Brien, V. 1998. Viruses and apoptosis. *J Gen Virol* 79 (Pt 8):1833-1845.
23. Riccardi, C., and Nicoletti, I. 2006. Analysis of apoptosis by propidium iodide staining and flow cytometry. *Nat Protoc* 1:1458-1461.
24. Frankfurt, O.S. 1980. Flow cytometric analysis of double-stranded RNA content distributions. *J Histochem Cytochem* 28:663-669.
25. Frankfurt, O.S. 1981. Unbalanced growth and cell death in HeLa S3 cultures treated with DNA synthesis inhibitors. *J Cell Physiol* 107:115-122.
26. Smolewski, P., Grabarek, J., Halicka, H.D., and Darzynkiewicz, Z. 2002. Assay of caspase activation in situ combined with probing plasma membrane integrity to detect three distinct stages of apoptosis. *J Immunol Methods* 265:111-121.
27. Matsuzaki, T., Suzuki, T., Fujikura, K. and Takata, K. 1997. Nuclear staining for laser confocal microscopy. *Acta Histochemica et Cytochemica* 30:309-314.
28. Invitrogen. 2006. Propidium Iodide Nucleic Acid Stain Product Data Sheet.1-5.
29. Bottger, S., Jerszyk, E., Low, B., and Walker, C. 2008. Genotoxic stress-induced expression of p53 and apoptosis in leukemic clam hemocytes with cytoplasmically sequestered p53. *Cancer Res* 68:777-782.
30. Catalano, A., Caprari, P., Soddu, S., Procopio, A., and Romano, M. 2004. 5-lipoxygenase antagonizes genotoxic stress-induced apoptosis by altering p53 nuclear trafficking. *FASEB J* 18:1740-1742.
31. Hartwell, L.H., and Kastan, M.B. 1994. Cell cycle control and cancer. *Science* 266:1821-1828.

32. Bernstein, R.M., and Mukherjee, B.B. 1972. Control of nuclear RNA synthesis in 2-cell and 4-cell mouse embryos. *Nature* 238:457-459.
33. Budihardjo, I., Oliver, H., Lutter, M., Luo, X., and Wang, X. 1999. Biochemical pathways of caspase activation during apoptosis. *Annu Rev Cell Dev Biol* 15:269-290.

Appendix II: X-FISH: the use of RNA-based probes in flow cytometry for differentiating cellular populations based on RNA expression patterns

AII.1 Introduction

Fluorescent *in situ* hybridization (FISH) allows detection of nucleic acid (both RNA and DNA) within tissues and cells. FISH has proven to be a very useful technique in the detection of mRNA expression (1), viral RNA (2, 3), telomere length determination (4), and studies of gene expression (5). While FISH is conventionally used to study expression in cells or tissues fixed on slides, this technique has been adapted to study hybridization by flow cytometry (flow-FISH) (6), a powerful technique for the detection and quantification of mRNA within cell populations (7-10). This technique has also been recently used to study gene expression within bacteria and viruses (11, 12). However, due to the time consuming nature of the technique, the limitations in sensitivity and resolution, the difficulty in maintaining cellular morphology following the required fixation steps, and issues of probe design and stability (13, 14), flow-FISH is infrequently utilized in eukaryotic cells compared to other techniques to study mRNA (e.g. real-time PCR).

One of the greatest challenges in comparative immunology is the lack of specific antibodies to differentiate between subpopulations of cells. While morphological and functional features can be used to differentiate cells, further characterization of subpopulations using unique markers has been limited. Teleost

fish, being the earliest known vertebrate to have both an innate and adaptive immune system, are a commonly used model in comparative immunology studies. While teleost fish have been shown to possess the main immune cells that are characteristic of mammalian systems (15), further sub-typing of these cells has not been possible due to a lack of reagents. As such, there is currently a great deal of interest in finding unique markers to differentiate between various leukocyte populations.

Previous studies with goldfish macrophages have identified a number of genes by PCR that are differentially expressed in the three distinct macrophage subpopulations (16-21). However, all of these studies have been performed using cell lysates of sorted populations. The protocol developed herein utilizes RNA-based markers to differentiate between leukocyte populations in mixed cultures. Importantly, this is accomplished while still maintaining cellular morphology. This technique can be applied to any cellular system to allow sensitive and specific detection of mRNA species that are differentially expressed- in cellular subsets, over time, following activation or following any treatment that affects expression. Using this technique, cells are studied as single events, allowing for robust statistical analyses not possible in lysate-based detection methods.

AII.2 Materials and Methods

AII.2.1 Animals

Goldfish (*Carassius auratus* L.) 10–15 cm in length were purchased from Mount Parnell (Mercersburg, PA) and maintained in the Aquatic Facility of the

Department of Biological Sciences, University of Alberta. The fish were held at 20^{o}C in a flow-through water system on a simulated natural photoperiod. All animals were maintained according to the guidelines of the Canadian Council on Animal Care. The University of Alberta Animal Care and Use Committee approved all protocols.

AII.2.2 Cell lines

RAW 264.7 macrophage cells and COS-1 wild type cells were cultured in complete DMEM media (DMEM supplemented with 10% heat-inactivated fetal bovine serum, 100 U/mL penicillin, and 100 μg/mL streptomycin). Thp-1 and U937 cells were cultured in complete RPMI 1640 media (RPMI, supplemented with 10% heat-inactivated fetal bovine serum, 100 U/mL penicillin, and 100 μg/mL streptomycin). Cell lines were cultured at 37^{o}C/5% CO_2 and passaged every 3-4 days.

AII.2.3 Goldfish primary kidney macrophage cultures

Primary kidney macrophages (PKM) were generated by seeding isolated leukocytes and culturing in 15 mL complete MGFL-15 media (MGFL-15 supplemented with 100 U/mL penicillin, 100 μg/mL streptomycin, 100 μg/mL gentamicin, 10% newborn calf serum (Gibco) and 5% carp serum) with 5 mL cell-conditioned media from previous experiments and incubated for 6-9 days at 20^{o}C (22, 23).

AII.2.4 cDNA synthesis

RNA was extracted from cultured cells using an RNeasy Mini kit (Qiagen). TURBO DNA-free (Ambion) was used to remove any remaining contaminating genomic DNA from the isolated RNA. First strand synthesis was completed using the Clontech SMARTScribe protocol. In brief, 2 μg of RNA was incubated with 20 μM CDS poly T primer and 5' oligo at 72^{o}C for 3 minutes. 5X first-strand buffer, dNTPs (Invitrogen), DDT and reverse transcriptase (Clontech) were then added and the reaction was incubated at 42^{o}C for 60 minutes. Heating at 70^{o}C for 15 minutes terminated the reaction. Second strand synthesis was completed using Taq: Pfu with 20 μM 5' PCR primer.

AII.2.5 PCR amplification of genes of interest and cloning

Refer to Table AII.1 for all primer sequences. Primers were designed to amplify β-actin, FcγRIIa, legumain, CD63, tumor necrosis factor (TNF)-α1 (goldfish), TNF-α (mouse) and interleukin (IL)-12p40. Optimal length of inserts for generating probes was found to be between 400-700 base pairs. Genes were elongated at 52.5^{o}C for 1.5 minutes for 35 cycles and run on a 1% agarose gel. Bands were extracted and purified using QIAquick gel extraction kit (Qiagen). Purified PCR products were cloned into pCRII-TOPO, following the manufacturer's directions (Invitrogen). TOP10 competent cells (Invitrogen) were incubated with the TOPO cloning reaction for 5 minutes on ice to transform cells. Cells were then plated directly onto pre-warmed LB-ampicillin plates (100 μg/mL) and incubated over night at 37^{o}C.

AII.2.6 Identification of positive clones

Colonies were picked from LB-ampicillin plates and PCR was preformed using M13 forward and reverse primers (vector based). Plasmids were purified from positive clones using QIAprep Spin Miniprep kit (Qiagen) and sequenced using BigDye (Applied Biosystems) to confirm the insert and to determine the orientation of the insert.

AII.2.7 Probe synthesis

Purified plasmids from positive clones were digested with BamHI for 1 hour at 37^{o}C to linearize plasmids. Linear plasmids were purified using a PCR purification kit (Qiagen). 1 μg of linear template plasmid was then incubated with T7 RNA polymerase in the presence of 25 mM RNA label mix (fluorescein-UTP: Roche; biotin-CTP: Invitrogen; digoxigenin-UTP: Roche) and 0.1M dithiothreitol (DTT) for 2 hours at 37^{o}C. Probe size was verified by running on a 1% agarose gel with RiboRuler High Range RNA ladder (Fermentas).

AII.2.8 Hybridization

Cells were harvested and fixed with 2% formaldehyde overnight at 4^{o}C. Cells were then spun down and resuspended in 70% ethanol and incubated for 15 minutes at room temperature. After washing in incomplete media (centrifuge 393 x *g* for 10 minutes at 4^{o}C), cells were resuspended in 20 mM Tris-HCl/ 2 mM $CaCl_2$ (pH 7.5) and treated with proteinase K (1 mg/mL, Sigma) for 7.5 minutes at room

temperature. Cells were then re-fixed in 2% formaldehyde for 10 minutes at 4°C and centrifuged at 393 x *g* for 10 minutes at 4°C. Cells were resuspended in a mix of formamide and 20X SSC (2:1) and 100 µL was aliquoted into 5 mL round bottom polypropylene tubes containing 400 µL hybridization buffer (5X SSC, 50% formamide, 10 mg/mL sheared salmon sperm DNA, 0.1% Tween-20 and 0.5% SDS) and probes. Tubes were mixed thoroughly and incubated in a 60°C water bath for 4 hours, with occasional mixing. After 4 hours, excess hybridization buffer without probe was added to each tube to remove unbound probe and cells were incubated further for 45 minutes at 60°C. Cells were then washed once in 2X SSC followed by 0.1X SSC (centrifuge 393 x *g* for 10 minutes at 4°C). Cells were then washed twice in 1x $PBS^{-/-}$ (centrifuge 393 x *g* for 10 minutes at 4°C) and resuspended in 1x$PBS^{-/-}$/ 2% newborn calf serum (Gibco) for staining. Samples can also be resuspended in 2% formaldehyde and stored at 4°C overnight prior to washes and staining.

AII.2.9 Detection and analysis

Hybridized cells were stained with streptavidin-PE (Invitrogen) or streptavidin-DyLight405 (Jackson ImmunoResearch Laboratories; to detect biotin-CTP labeled probes) and/or anti-FITC IgG1 DyLight488 (Jackson ImmunoResearch Laboratories; to detect fluorescein-UTP labeled probes) and/or anti-digoxigenin (Roche) followed by anti-mouse IgG1 (BD BioSciences; to detect digoxigenin-UTP probes) for 30 minutes at room temperature. Cells were then washed twice with 1x$PBS^{-/-}$/ 2% newborn calf serum (centrifuge 393 x *g* for 10

minutes at 4°C) and data was acquired using an ImageStream multi-spectral flow cytometer (Amnis) or FACSCanto II (BD Biosciences). Hybridization was analyzed based on fluorescence intensity using IDEAS 4.0 software (Amnis), FACSDiva (BD Biosciences) or FCS Express 3.0. Statistics were done using a two-tailed Students' T test (Prism).

AII.2.10 Intracellular cytokine staining

Cells were activated in the presence of GolgiPlug (BD BioSciences). Following activation, cells were fixed with 2% formaldehyde at 4°C for a minimum for 10 minutes. Cells were then washed twice with 1X $PBS^{-/-}$ containing 2% calf serum (centrifuge 393 x *g* for 10 minutes at 4°C). Cells were then permeabilized with 0.1% saponin in 1X $PBS^{-/-}$ containing 2% calf serum on ice for 20 minutes. Anti-TNF-α-PE (BD BioSciences) was then added for 30 minutes. Cells were then washed 3 times with saponin buffer (centrifuge 393 x *g* for 10 minutes at 4°C).

AII.3 Results

AII.3.1. X-FISH detects specific RNA species within the cytoplasm.

Fluorescent *in situ* hybridization is a robust technique for the detection of nucleic acids within tissues and cells. Though most FISH assays have focused on microscopy-based readouts, recent protocols have adapted this technique for use in flow cytometry. Because of the lack of protein-based markers and the wealth of information on gene expression in comparative immunology systems, I sought to

test the efficacy of FISH in providing unique markers for subpopulations of immune cells. To this end, I created a flow cytometry-based FISH that detects RNA with a high level of specificity and sensitivity in cells with minimal effect of cellular morphology.

In order to optimize the X-FISH assay, I designed probes for β-actin, a ubiquitously expressed gene. This probe was used in COS-1 cells, which have a large cytoplasmic area, giving an increased area for hybridization, as well as a good indication of the effect that the hybridization protocol has on cell morphology. COS-1 cells were hybridized with either sense or anti-sense β-actin probes (Figure AII.1 A and B). The sense probe served as a control to determine the level of background fluorescence due to unhybridized probe not removed by washes. As a control to show specificity of the probe for RNA, COS-1 cells were also pretreated with RNase A (equivalent 4 units of activity) for 15 minutes at room temperature. Hybridization with an anti-sense β-actin probe (binds complementary sense mRNA within the cell) resulted in a significant shift in fluorescence compared to both streptavidin alone or hybridization with a sense probe (95% vs. 3% and 6%, respectively; Figure AII.1 A). When cells are pretreated with RNase A, the level of fluorescence is dramatically reduced (8%), showing that the detected fluorescence is due to RNA hybridization. Importantly, using the protocol described here, sensitive hybridization is accomplished while cell morphology is maintained (Figure AII.1 B). This is necessary to detect a strong signal within the cytoplasmic compartment. As expected, the β-actin signal is localized throughout the cytoplasm in a disperse pattern.

As a next step, I wanted to ensure that this protocol was amenable to use in immune cells and could specifically discriminate between cells that had differentially expressed genes. To this end, I designed sense and anti-sense probes to FcγRIIa, an Fc-receptor expressed on human but not murine leukocytes. These probes were used to stain three myeloid cell lines: human Thp-1 and U937 monocytes and murine RAW 264.7 macrophages. As expected, I saw a significant shift in fluorescence with the anti-sense probes in the Thp-1 and U937 cell lines (Figure AII.1 C). The murine RAW 264.7 cells displayed no difference in fluorescence between sense and anti-sense probes.

AII.3.2 RNA probes match expression patterns of antibody markers.

An important criterion for this protocol is to possess a similar robustness in detection as is present for protein-based markers. As such, I wanted to test this protocol with a gene expressed in low quantities and compare this to the expression detected with an antibody to the same molecule. To this end, I activated RAW 264.7 macrophages with LPS or PMA over a 24-hour period and used both X-FISH and intracellular cytokine staining to measure TNF-α expression (Figure AII.2 A). I found similar levels of expression and kinetics of upregulation with both techniques, showing that X-FISH is not only able to detect RNA species that expressed at a low level, but is also able to sensitively detect subtle changes in expression following activation. Further, I found no difference in the staining pattern with TNF-α antibodies when the stain was done separately or in

conjunction with the X-FISH protocol, suggesting that these two techniques may be combined so long as the antibody epitope is unchanged by the fixation steps.

AII.3.3 X-FISH can distinguish between cells in mixed populations and measure changes in activation in each subpopulation.

As a final step, I wanted to test the protocol on primary cells, as primary cells are known to be generally much more sensitive and less amenable to manipulation compared to cell lines. For this, I employed a well-studied teleost primary macrophage culture – goldfish primary kidney macrophage cells (PKMs). It has been previously shown by PCR that the three subpopulations within these cultures (early progenitors, monocytes and mature macrophage) have distinct expression patterns of certain markers (21). To test this protocol, I selected CD63, a marker of monocytes, and legumain, a marker of mature macrophages. Using the X-FISH protocol, I probed PKMs that had been incubated with fluorescent zymosan with probes against legumain, CD63 and TNF-α1. I found that TNF-α1 was expressed to a significantly higher degree in cells that had internalized zymosan compared to cells that had not (Figure AII.2B). This occurred in both legumain+ mature macrophages and CD63+ monocytes. Similar to cell lines, I noticed no negative impact of the X-FISH protocol on primary goldfish macrophage cells.

AII.4. Discussion

Fluorescent *in situ* hybridization is a powerful technique for detecting nucleic acids within cells or whole tissue mounts. The protocol described here adapts this

process for use on cells in suspension and provides sensitive detection of RNA species while maintaining cellular morphology. Further, this technique can be applied to both cell lines and primary cells and can be used across a range of species.

There are a number of challenges associated with FISH assays, the most prominent being the ability to detect a signal with a high signal: noise ratio. The majority of background fluorescence with this technique is associated with unbound probe that remains within the cells following washes (24). As such, stringent washing protocols must be followed to remove unbound probe (24). In this assay, have developed here, I detected little fluorescence due to either unbound probe or non-specific staining with the secondary detection antibodies.

Another common challenge with *in situ* hybridization is optimizing fixation and permeabilization steps to avoid loss of cell morphology as well as to minimize any effects that these steps may have on signal levels and integrity of organelles (25). I found that the fixation and permeabilization steps outlined here had minimal effect on the nuclear: cytoplasmic ratios while still providing strong signal detection. This was true for not only cell lines, but primary cells as well. Maintaining the cytoplasmic size is of critical importance as loss of cytoplasm will significantly reduce the ability to detect hybridization, especially in cells such as leukocytes that may have a small nuclear: cytoplasmic ratio. Lastly, target accessibility presents a unique challenge. Within cells, RNA molecules have complex secondary structures and associated proteins that may mask or outcompete

probe binding sites (14). As such, it may be necessary design, synthesize and test multiple probes to select the best target probe (14).

While there may be many challenges associated with *in situ* hybridization, I have been able to overcome the main challenges through optimization of the X-FISH protocol. As such, X-FISH appears to hold significant potential in creating probes to differentiate between cell populations in the absence of specific protein-based markers. This technique may also be complexed with certain antibodies to provide an added layer investigation. Finally, X-FISH can be applied to any cell or tissue, irrespective of species or origin. As such, is can be easily applied to and transferred across many different comparative immunology model systems, filling a void until protein-based markers become available. Finally, as a testament to the importance of this technique across a wide range of disciplines, there are now multiple companies with commercial products similar to the technique described in this Appendix (Stellaris, EMD Millipore, eBioscience).

AII.5. Protocol

1. PCR of desired insert and ligation into vector

1. Follow established lab protocols for PCR of the gene of interest.
2. Excise band from gel and follow gel purification protocol in Qiagen kit.
3. Insert into TOPO TA cloning vector and transform bacteria, following the recommended protocol outlined by Invitrogen.
4. Isolate plasmid by mini-prep, following the Qiagen protocol.

2. Linearize plasmid

1. Digest plasmid with BamHI (cuts on opposite side of insert from T7)- Incubate in water bath at 37^{o}C for 1 hour
2. Reaction mix:

   Plasmid (~5ug)

   2 µL 10x REact 3 buffer

   3 µL BamHI

   x- µL nf-H_20 (to 20uL final volume)
3. Incubate in water bath at 37^{o}C for 1 hour
4. Purify linearized plasmid using Qiagen PCR purification kit, following manufacturers protocol.

3. Make RNA probe

1. Reaction mix:

   11 µL linear plasmid DNA

   2 µL biotin-14-CTP mix (or fluorescein-12-UTP)

   - Biotin-CTP (*Invitrogen*; *cat #: 19519-016*): Add 10mM biotin-14-CTP to 10mM dNTP mix (*Invitrogen; cat #: 18109-07*) in equal volume

   - Fluorescein-12-UTP (*Roche; cat #: 11685619910*): Use stock solution

   2 µL T7 RNA polymerase (*Invitrogen; cat #: 18033-019*)

   4 µL 5x reaction buffer (*comes with T7*)

1 µL 0.1M DTT (*comes with T7*)

= Final volume 20uL/ reaction

2. Incubate in water bath at 37^{o}C for 2 hours
3. Run on 1% agarose gel to ensure probe is present (use 5 µL RNA MW marker- tube in use at -20^{o}C; store rest at -80^{o}C)

4. Hybridization

1. Fix cells overnight in 2% formaldehyde
2. Spin down (centrifuge 393 x *g* for 10 minutes at 4^{o}C))
3. Resuspend in 1 mL 70% EtOH made with nuclease-free water and incubate 15 minutes at room temperature
4. Add incomplete media (PBS$^{-/-}$ does not work well) and centrifuge at 393 x *g* for 10 minutes at 4^{o}C
5. Resuspend in 300 µL of 20mM Tris-HCl/2mM $CaCl_2$/pH 7.5 + 0.5mg/mL proteinase K (*Sigma; cat #: P2308-10MG*) and incubate 7 minutes at room temperature (timing may vary with different cells)

   - Tris/$CaCl_2$ buffer (10 mL 1M Tris-HCl, pH 7.5; 1 mL 1M $CaCl_2$; top up to 500 mL with DEPC H_2O)

   - Dilute proteinase K 1:20 (10 mg/mL stock)
6. Fix in 2% formaldehyde for 10 minutes and centrifuge at 393 x *g* for 10 minutes at 4^{o}C

7. Resuspend cells in a 100 µL 1:2 ratio of 20X SSC (87.65 g NaCl/ 44.1 g Na-citrate (*Sigma; cat #: S1804-1KG*) in 500 mL nuclease-free H_2O) and formamide (*Fisher Scientific; cat #: BP227-500*)
8. Add 400 µL hybridization buffer

    - Hybridization buffer:

        1 mL sheared salmon sperm DNA (*Ambion; AM9680*)

        1 0mL formamide

        5 mL 20X SSC

        200 µL Tween-20 (*Fisher Scientific; cat #: BP337-500*)

        0.1 g SDS

        4 mL DEPC water

    - Add 1-2 µL probes/tube (depending on concentration) directly to tubes and mix well
9. Incubate in water bath at 60^{o}C (may vary for different probes) for 4 hours; flick every 30-60 minutes
10. Add 1 mL hybridization buffer to each tube, mix and incubate 45 minutes as above
11. Centrifuge at 393 x *g* for 10 minutes at 4^{o}C
12. Resuspend in 2x SSC, mix well, spin down (centrifuge at 393 x *g* for 10 minutes at 4^{o}C)
13. Resuspend in 0.1X SSC, mix well, spin down (centrifuge at 393 x *g* for 10 minutes at 4^{o}C)

14. Resuspend in 1x $PBS^{-/-}$(or can store overnight in incomplete media but not PBS)
15. Spin down (centrifuge at 393 x *g* for 10 minutes at $4^{o}C$) and wash in 1x $PBS^{-/-}$
16. Add secondary antibody
    - Streptavidin-PE (*Invitrogen; cat # SA1004-1* ***OR*** *Jackson; cat #: 016-100-084)*: 1 in 50 (use with biotin-14-CTP)
    - Anti-fluorescein- DyLight 488 (*Jackson; cat #: 200-482-037*): 1 in 50 (use with fluorescein-12-UTP)
17. Incubate 30 minutes at room temperature in the dark
18. Wash 2x with $PBS^{-/-}$ (centrifuge at 393 x *g* for 10 minutes at $4^{o}C$)

19. Acquire using a flow cytometer

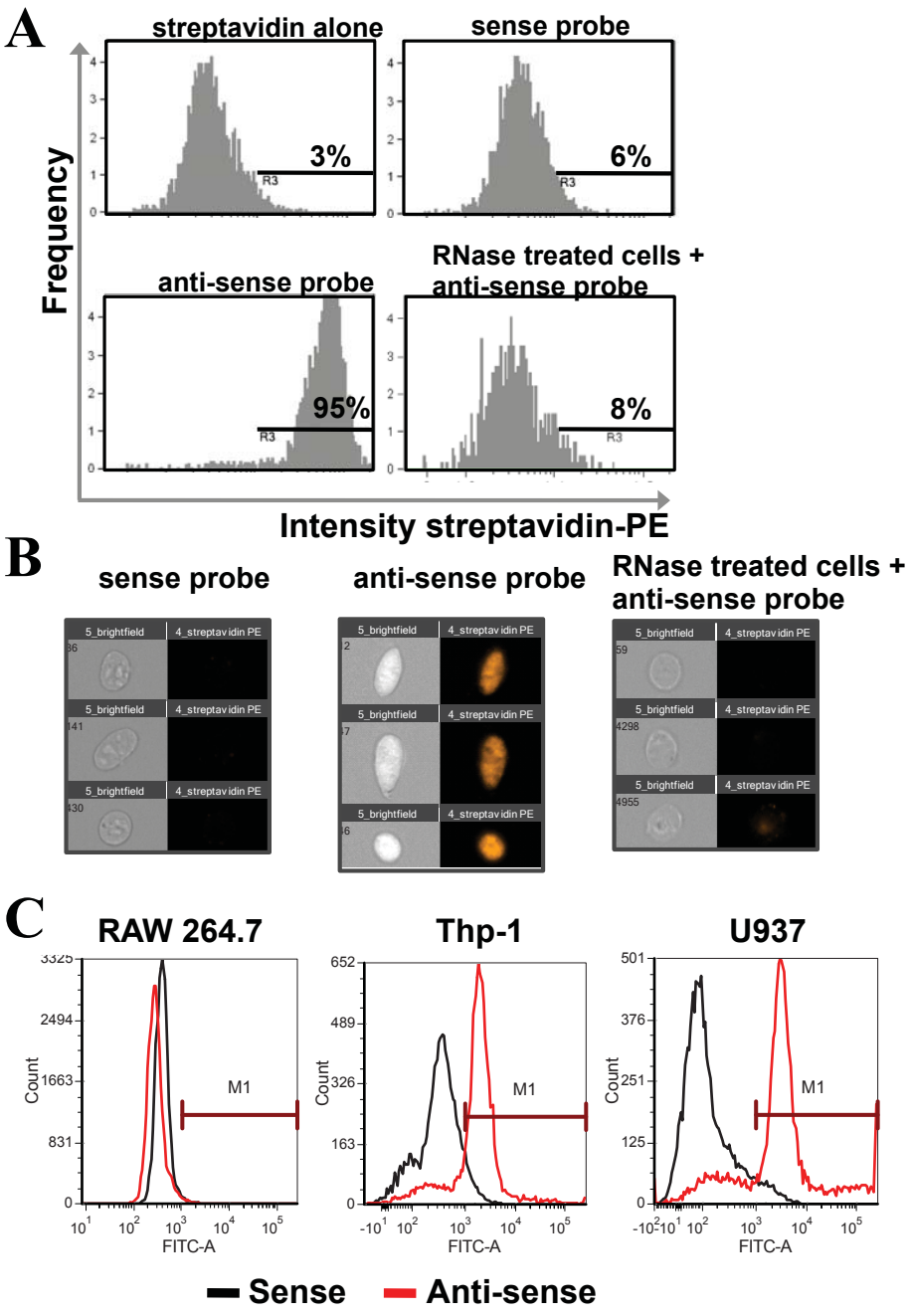
A
streptavidin alone
sense probe
anti-sense probe
RNase treated cells + anti-sense probe
3%
6%
95%
8%
R3
Frequency
Intensity streptavidin-PE
B
sense probe
anti-sense probe
RNase treated cells + anti-sense probe
5_brightfield
4_streptavidin PE
C
RAW 264.7
Thp-1
U937
Count
FITC-A
M1
Sense
Anti-sense

Figure AII.1. X-FISH detects RNA expression in the cytoplasm specifically and sensitively.

(**A**) COS-1 cells were fixed and hybridized with a probe against β-actin. Cells stained with secondary alone or sense (control) probe show limited fluorescence. Cells probed with an anti-sense probe show intense staining that is removed with RNase treatment, showing specificity for RNA. (**B**) Images acquired from an ImageStream imaging flow cytometer show β-actin signal in COS-1 cells throughout the cytoplasm. Cytoplasmic fluorescence is lost following RNase treatment. It is also important to note that COS-1 cells maintain a normal morphological appearance. (**C**) Macrophage cells lines were stained with sense or anti-sense probes against FcγRIIa, an Fc-receptor expressed on human but not murine leukocytes. Expression was detected in Thp-1 and U937 human monocyte cell line but not in RAW 264.7 murine macrophage, showing specificity of probes to target RNA.

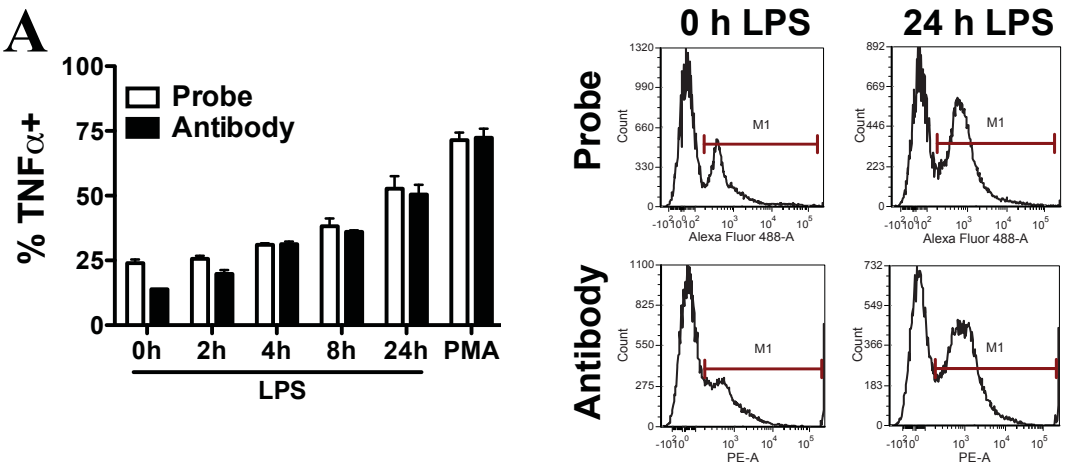
A
% TNFα+
Probe
Antibody
0h
2h
4h
8h
24h
PMA
LPS
0 h LPS
24 h LPS
Probe
Antibody
Count
M1
Alexa Fluor 488-A
PE-A

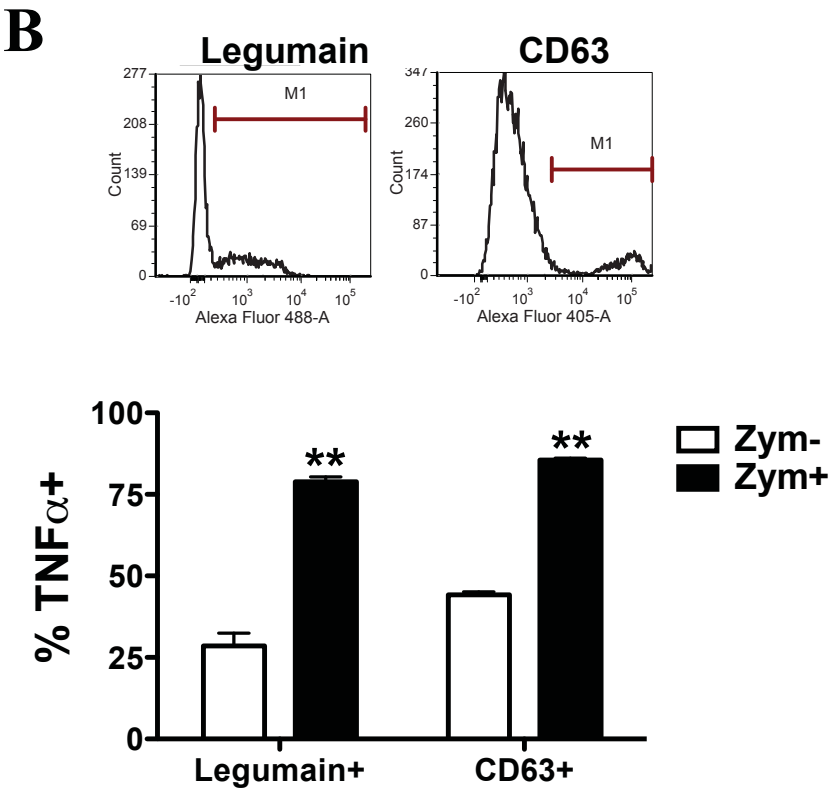
B
Legumain
CD63
Count
M1
Alexa Fluor 488-A
Alexa Fluor 405-A
% TNFα+
**
Zym-
Zym+
Legumain+
CD63+

Figure AII.2. X-FISH detects changes in cytokine expression following activation in specific cell subpopulations.

(**A**) RAW 264.7 macrophages were activated with LPS for 0-24 h. Cells were then harvested and fixed and TNF-α with either an RNA based probe using the X-FISH protocol or with an antibody through intracellular cytokine staining. Probe and antibody showed similar patterns of staining. n=4; **p<0.01; error bars show SEM. (**B**) Goldfish primary kidney macrophages were incubated with fluorescent zymosan for 2 h. Cells were then fixed and probed with legumain, CD63 and TNF-α1 probes. Both legumain+ mature macrophages and CD63+ monocytes significantly increased TNF-α1 expression following internalization of zymosan. n=4; **p<0.01; error bars show SEM.

Table AII.1. Primer sequences.

Primer	Sequence 5' to 3'
CDS poly T	AAG CAG TGG TAT CAA CGC AGA GTA TT
5' oligo	AAG CAG TGG TAT CAA CGC AGA GTA CG
β-actin fwd	ACG TTG CTA TCC AGG CTG TGC TAT
β-actin rev	GCA ATC AAA GTC CTC GGC CAC ATT
FcγRIIa fwd	CTC GAC AAG CTG CTC CCC CAA AG
FcγRIIa rev	AAT TAC AGG ATC AGT GGA ATT GGC
TNF-α (mouse) fwd	CTC CCT CTC ATC AGT TCT ATG G
TNF-α (mouse) rev	GAA AGG TCT GAA GGT AGG AAG G
Legumain fwd	TGT CGT TGC CTG TGA TTA CTG AA
Legumain rev	CCT GGT ATC CTC CCT GAC ACA
CD63 fwd	CGA CAC CTC AGC CAT CAT CA
CD63 rev	TGG CAC AGA GAT ATA CAG GAT GA
TNF-α1 (goldfish) fwd	CCT TTA CTG GAG AAA GGA CC
TNF-α1 (goldfish) rev	GAA GAA GGT CTT TCC GTT GTC G
IL-12p40 fwd	CAA CAG TGA GGG ATC CTA CC
IL-12p40 rev	TTG CAG AAT TCA TCC CTG GC
M13 fwd	GTA AAA CGA CGG CCA G
M13 rev	ACC AGC TAT GAC CAT GAT TAC

AII.5. References

1. Desmouliere, A., Geinoz, A., Gabbiani, F., and Gabbiani, G. 1993. Transforming growth factor-beta 1 induces alpha-smooth muscle actin expression in granulation tissue myofibroblasts and in quiescent and growing cultured fibroblasts. *J Cell Biol* 122:103-111.
2. Schnittman, S.M., Psallidopoulos, M.C., Lane, H.C., Thompson, L., Baseler, M., Massari, F., Fox, C.H., Salzman, N.P., and Fauci, A.S. 1989. The reservoir for HIV-1 in human peripheral blood is a T cell that maintains expression of CD4. *Science* 245:305-308.
3. Brigati, D.J., Myerson, D., Leary, J.J., Spalholz, B., Travis, S.Z., Fong, C.K., Hsiung, G.D., and Ward, D.C. 1983. Detection of viral genomes in cultured cells and paraffin-embedded tissue sections using biotin-labeled hybridization probes. *Virology* 126:32-50.
4. Moyzis, R.K., Buckingham, J.M., Cram, L.S., Dani, M., Deaven, L.L., Jones, M.D., Meyne, J., Ratliff, R.L., and Wu, J.R. 1988. A highly conserved repetitive DNA sequence, (TTAGGG)n, present at the telomeres of human chromosomes. *Proc Natl Acad Sci U S A* 85:6622-6626.
5. Lalli, E., Gibellini, D., Santi, S., and Facchini, A. 1992. In situ hybridization in suspension and flow cytometry as a tool for the study of gene expression. *Anal Biochem* 207:298-303.
6. Bauman, J.G., Bayer, J.A., and van Dekken, H. 1990. Fluorescent in-situ hybridization to detect cellular RNA by flow cytometry and confocal microscopy. *J Microsc* 157:73-81.
7. Crouch, J., Leitenberg, D., Smith, B.R., and Howe, J.G. 1997. Epstein-Barr virus suspension cell assay using in situ hybridization and flow cytometry. *Cytometry* 29:50-57.
8. Belloc, F., and Durrieu, F. 1994. Detection of mRNA species by flow cytometry. *Methods Cell Biol* 42 Pt B:59-69.
9. Childs, G.V., Lloyd, J.M., Unabia, G., Gharib, S.D., Wierman, M.E., and Chin, W.W. 1987. Detection of luteinizing hormone beta messenger ribonucleic acid (RNA) in individual gonadotropes after castration: use of a new in situ hybridization method with a photobiotinylated complementary RNA probe. *Mol Endocrinol* 1:926-932.
10. Grunwald, D. 1993. Flow cytometry and RNA studies. *Biol Cell* 78:27-30.
11. Robertson, K.L., Verhoeven, A.B., Thach, D.C., and Chang, E.L. 2010. Monitoring viral RNA in infected cells with LNA flow-FISH. *RNA* 16:1679-1685.
12. Robertson, K.L., and Vora, G.J. 2012. Locked nucleic acid flow cytometry-fluorescence in situ hybridization (LNA flow-FISH): a method for bacterial small RNA detection. *J Vis Exp*:e3655.
13. Robertson, K.L., and Thach, D.C. 2009. LNA flow-FISH: a flow cytometry-fluorescence in situ hybridization method to detect messenger RNA using locked nucleic acid probes. *Anal Biochem* 390:109-114.
14. Bao, G., Rhee, W.J., and Tsourkas, A. 2009. Fluorescent probes for live-cell RNA detection. *Annu Rev Biomed Eng* 11:25-47.

15. Miller, N., Wilson, M., Bengten, E., Stuge, T., Warr, G., and Clem, W. 1998. Functional and molecular characterization of teleost leukocytes. *Immunol Rev* 166:187-197.
16. Hanington, P.C., Barreda, D.R., and Belosevic, M. 2006. A novel hematopoietic granulin induces proliferation of goldfish (Carassius auratus L.) macrophages. *J Biol Chem* 281:9963-9970.
17. Grayfer, L., and Belosevic, M. 2009. Molecular characterization of novel interferon gamma receptor 1 isoforms in zebrafish (Danio rerio) and goldfish (Carassius auratus L.). *Mol Immunol* 46:3050-3059.
18. Grayfer, L., and Belosevic, M. 2009. Molecular characterization of tumor necrosis factor receptors 1 and 2 of the goldfish (Carassius aurutus L.). *Mol Immunol* 46:2190-2199.
19. Katzenback, B.A., and Belosevic, M. 2009. Molecular and functional characterization of kita and kitla of the goldfish (Carassius auratus L.). *Dev Comp Immunol* 33:1165-1175.
20. Walsh, J.G., Barreda, D.R., and Belosevic, M. 2007. Cloning and expression analysis of goldfish (Carassius auratus L.) prominin. *Fish Shellfish Immunol* 22:308-317.
21. Barreda, D.R., Hanington, P.C., Walsh, C.K., Wong, P., and Belosevic, M. 2004. Differentially expressed genes that encode potential markers of goldfish macrophage development in vitro. *Dev Comp Immunol* 28:727-746.
22. Neumann, N.F., Barreda, D., and Belosevic, M. 1998. Production of a macrophage growth factor(s) by a goldfish macrophage cell line and macrophages derived from goldfish kidney leukocytes. *Dev Comp Immunol* 22:417-432.
23. Neumann, N.F., Barreda, D.R., and Belosevic, M. 2000. Generation and functional analysis of distinct macrophage sub-populations from goldfish (Carassius auratus L.) kidney leukocyte cultures. *Fish Shellfish Immunol* 10:1-20.
24. Buongiorno-Nardelli, M., and Amaldi, F. 1970. Autoradiographic detection of molecular hybrids between RNA and DNA in tissue sections. *Nature* 225:946-948.
25. Behrens, S., Fuchs, B.M., Mueller, F., and Amann, R. 2003. Is the in situ accessibility of the 16S rRNA of Escherichia coli for Cy3-labeled oligonucleotide probes predicted by a three-dimensional structure model of the 30S ribosomal subunit? *Appl Environ Microbiol* 69:4935-4941.